From: [redacted]
To: Martinez, Catherine
Subject: RE: RE: RE: Donation to ACT Government schools
Date: Friday, 31 January 2020 3:33:02 PM

Hi Catherine,

Thanks again for setting up the call earlier today. David mentioned it would be good for me to liaise with Lynne who handles the media side of things – are you able to share her email address or introduce me on email if possible?

Thanks,
[redacted]

From: Martinez, Catherine <Catherine.Martinez@act.gov.au>
Sent: Friday, 31 January 2020 11:56 AM
To: [redacted]
Subject: [External Mail] RE: RE: RE: Donation to ACT Government schools

UNCLASSIFIED For-Official-Use-Only

No worries at all, David will give you a call in 10-15 minutes.

Regards
Catherine

From: [redacted]>
Sent: Friday, 31 January 2020 11:50 AM
To: Martinez, Catherine <Catherine.Martinez@act.gov.au>
Subject: RE: RE: RE: Donation to ACT Government schools

Thanks Catherine, please can we schedule a slot in?

My only concern is that we need to send our comms out asap so I really need to align with David today.

Thanks,
[redacted]

From: Martinez, Catherine <Catherine.Martinez@act.gov.au>
Sent: Friday, 31 January 2020 11:36 AM
To: [redacted]>
Subject: [External Mail] RE: RE: RE: Donation to ACT Government schools

UNCLASSIFIED For-Official-Use-Only

Hi [redacted]

David has been caught up in meetings, can he try to give you a call later a bit later?

Regards
Catherine

From: [redacted]>
Sent: Thursday, 30 January 2020 5:09 PM
To: Martinez, Catherine <Catherine.Martinez@act.gov.au>
Subject: Re: RE: RE: Donation to ACT Government schools

Thanks Catherine.

Sent from my iPhone

On 30 Jan 2020, at 4:41 pm, Martinez, Catherine <Catherine.Martinez@act.gov.au> wrote:

UNCLASSIFIED For-Official-Use-Only

Hi [redacted]

David will try to give you a call later today if that's ok. Thank you for your patience. Apologies he has been in back to back meetings today.

Regards
Catherine

From: [redacted]>
Sent: Thursday, 30 January 2020 10:15 AM
To: Martinez, Catherine <Catherine.Martinez@act.gov.au>
Subject: Re: RE: Donation to ACT Government schools

Hi Catherine,
Hope you're well.
Am I able to schedule a time to speak with David today if possible please?
Thanks,
[redacted]

Sent from my iPhone

On 29 Jan 2020, at 12:55 pm, Martinez, Catherine <Catherine.Martinez@act.gov.au> wrote:

UNCLASSIFIED For-Official-Use-Only

Good afternoon [redacted]

Thank you for your email. David will give you a call later today when he is available.

Regards
Catherine

Catherine Martinez | Executive Officer to David Matthews, Executive Group Manager
Phone: 02 6207 6641 | Email: catherine.martinez@act.gov.au
Executive Support | Business Services | Education | ACT Government
Level 6 | 220 Northbourne Avenue Braddon ACT 2612 | act.gov.au

---

From: [redacted] >
Sent: Wednesday, 29 January 2020 12:06 PM
To: Matthews, David <David.Matthews@act.gov.au>
Cc: [redacted] >; EDU, EDBSD <EDBSD.EDU@act.gov.au>
Subject: RE: Donation to ACT Government schools

Hi David,

Hope you're well. As [redacted] mentioned, we're grateful to both yourself and [redacted] for helping to make this initiative happen.

I'd be keen to discuss a couple of comms-related elements with you on the phone today, do let me know when suits and the best number to reach you on? Alternatively, feel free to call me on [redacted]

Best regards,
[redacted]

[redacted]

Email:
[redacted]

Suite 2, Level 22, Tower 3,

International
Towers,
300
Barangaroo
Avenue,
Barangaroo
NSW
2000,
Australia
<image001.jpg>

From: [redacted]>
Sent: Wednesday, 29 January 2020 11:50 AM
To: Matthews, David <David.Matthews@act.gov.au>; [redacted]>; EDU, EDBSD <EDBSD.EDU@act.gov.au>
Cc: [redacted]>
Subject: RE: Donation to ACT Government schools

Thank you David.

[redacted] who leads our PR team is going to reach out to you to run through any plans for a Dyson announcement to confirm you're aligned.

Also, we have spoken to Ken and based on storage available in the Stirling location, stock will be delivered next week.

Best regards,

[redacted]

From: Matthews, David <David.Matthews@act.gov.au>
Sent: Tuesday, 28 January 2020 8:35 AM
To: [redacted]>
Cc: [redacted] EDU, EDBSD <EDBSD.EDU@act.gov.au>
Subject: [External Mail] RE: Donation to ACT Government schools

UNCLASSIFIED For-Official-Use-Only

Thank you once again [redacted]

We don't have any immediate plans about announcements, I will seek some further advice and get back to you on this point.

I'll stay in touch.

Regards

David Matthews

From: [redacted]>
Sent: Saturday, 25 January 2020 9:01 AM
To: Matthews, David <David.Matthews@act.gov.au>
Cc: [redacted]>; EDU, EDBSD <EDBSD.EDU@act.gov.au>
Subject: RE: Donation to ACT Government schools

Thank you David and also [redacted] for putting us in contact to bring this to life.

I will work with our supply team on Monday to deploy the 400 units to the Headley Beare Centre and update yourself and Ken on an delivery times.

[redacted] looks after all of our PR so I will discuss any announcements with him and have him contact you. Will you be doing an announcement?

Once again, thank you for all your efforts and we hope the purifiers make a difference in the schools.

Best regards,

[redacted]

[redacted]

[redacted]

Suite 2, Level 22, Tower 3, International Towers, 300 Barangaroo Avenue, Barangaroo

NSW
2000

<image001.jpg>

From: Matthews, David <David.Matthews@act.gov.au>
Sent: Friday, 24 January 2020 11:40 AM
To: [redacted]>
Cc: [redacted]>; EDU, EDBSD <EDBSD.EDU@act.gov.au>
Subject: [External Mail] Donation to ACT Government schools

UNCLASSIFIED For-Official-Use-Only

[redacted]

Can I start by acknowledging the offer of a donation of 400 x Dyson

Tower Purifiers for ACT public schools. Your offer is both generous and very welcome in light of the challenges faced by our community in recent weeks.

I would also like to recognise [redacted] spontaneous efforts and active support of our schools.

As you are aware the ACT has experienced an unprecedented and prolonged smoke event associated with bushfire activities in the surrounding region. From 3 February 2020 approximately 50,000 students will be returning to school, having experienced a highly disrupted, and for some traumatic, period of their young lives. The conditions will also have exacerbated asthma and other complex medical issues experienced by a portion of our students.

We are proposing to deploy at least 2 x Dyson units to each of our 88 schools to ensure that each location will have a designated area with purified air for vulnerable children and young people. The remaining units will be distributed to schools on the basis on the level of relative vulnerability of students and local environmental conditions.

At this stage we do not envisage requiring on the ground support to install the units – but once again thank you for this generous offer. Any supporting material would be appreciated.

ACT Education would appreciate the opportunity to review any proposed public wording you may wish to use, and the timing of any announcements in relation to this generous donation.

With regard to delivery arrangements, the units can be delivered to the Headley Beare Centre for Teaching and Learning (HBCTL), Freemantle Drive, Stirling, ACT. This site is easily accessible and regularly accessed by our school based staff. The contact point at HBCTL is Ken Newman. Ken is contactable by phone on [redacted] or [redacted] and via email: Ken.Newham@act.gov.au.

Please let me know if you have any comments or queries on the above, and I would be more than happy to discuss anything further.

Thank you once again and I look forward to talking again soon.

David Matthews
Executive Group Manager, Business Services
Education Directorate, ACT Government
Office: 6207 0384 | Email: david.matthews@act.gov.au

From: Parkinson, Andrew
To: Sloane, Brenton
Cc: Larkin, Lyn; Caines, Justine; EDU Media; ICW EBM Office
Subject: Re: Dyson comment
Date: Thursday, 6 February 2020 12:49:55 PM

Happy for you to send this to EGM - BSD for clearance

Andrew Parkinson | Executive Branch Manager
Infrastructure & Capital Works | Education Directorate | ACT Government
Phone 02 6205 1289 | Mobile 0478 301 085

From: Sloane, Brenton <Brenton.Sloane@act.gov.au>
Sent: Thursday, February 6, 2020 12:23 pm
To: Parkinson, Andrew
Cc: Larkin, Lyn; Caines, Justine; EDU Media; ICW Directors Office
Subject: RE: Dyson comment

Hello Andrew,

Following on from today's event with Dyson, HerCanberra have requested a comment from the Education Directorate.

Suggest the following to come from a Directorate spokesperson:

We know that as a result of experiences over the summer across the ACT due to bushfire smoke, many families are concerned about air quality within schools.

The Education Directorate have worked with experts, including from ACT Health and the Worksafe Commissioner, and in consultation with a range of stakeholders including unions and the ACT Council of Parents and Citizens Association, to prepare clear advice for schools on how to manage air quality issues.

In addition to this, and as a result of community advocacy from Torrens Primary School [redacted], we are very pleased to accept the generous offer from Dyson Australia to distribute 400 air purifiers to ACT public schools. This distribution has already begun.

Every ACT Public School will have at least two air purifiers to ensure a designated area of purified air for vulnerable students. The remaining units will be distributed on the basis of the level of student vulnerability and local environmental conditions.

We thank Dyson Australia for their generous contribution to ACT public schools.

Cheers,

Brenton Sloane | Assistant Director
Media and Communications | Education | ACT Government
P: (02) 6205 4196| M: 0431 252 698 | E: brenton.sloane@act.gov.au
Level 6, 220 Northbourne Avenue | GPO Box 158 Canberra ACT 2601
www.education.act.gov.au | Facebook | Twitter | Instagram | LinkedIn

From: BERRY
To: [redacted]
Subject: Correspondence from Minister Berry
Date: Thursday, 2 April 2020 11:26:52 AM
Attachments: 20200402110013927.pdf

Dear [redacted]

Please see attached letter from Minister Yvette Berry.

Kind regards,

Gabriela Falzon| Adviser
620 72670

Office of Yvette Berry MLA | Member for Ginninderra
Deputy Chief Minister
Minister for Education and Early Childhood Development
Minister for Housing and Suburban Development
Minister for the Prevention of Domestic and Family Violence
Minister for Women
Minister for Sport and Recreation
Phone: +61 2 6205 0233 | Email: berry@act.gov.au
Facebook | Twitter | www.yvetteberry.com.au

I acknowledge the traditional custodians of the land, the Ngunnawal people, and pay my respect to their Elders past, present and emerging.

ACT Government

Yvette Berry MLA

Deputy Chief Minister
Minister for Education and Early Childhood Development
Minister for Housing and Suburban Development
Minister for the Prevention of Domestic and Family Violence
Minister for Sport and Recreation
Minister for Women
Member for Ginninderra

[redacted]

Dear [redacted]

Thank you for your emails of [redacted] about air quality concerns in schools. I apologise for the delay in responding.

The safety of students and staff is our highest priority. The Education Directorate worked with experts such as the ACT Chief Health Officer and the Worksafe Commissioner to develop strategies to manage exposure to poor air quality. A range of stakeholders including unions, the non-government sector, the Asthma Foundation and the Parents and Citizen Associations were also consulted to ensure the planned responses were appropriate.

I acknowledge your request for indoor and outdoor air quality monitoring stations and HEPA filtration systems at every ACT public school. As you have noted, air monitoring equipment and HEPA filtration systems are both highly technical and expensive. Additionally, indoor air quality often varies considerably from one room to another within the same building, which limits the viability and usefulness of such monitors on a large campus. Determining the suitability of outdoor air monitoring stations, locations and the viability of HEPA filtration systems requires comprehensive exploration. An increase in air quality monitoring capacity for the ACT is currently under review by ACT Health. I have received confirmation your recommendations will be considered as part of this process.

The Education Directorate developed an Air Quality and Response Guide to provide clear advice to schools. The guide included:

- a checklist to ensure schools are prepared to implement site specific air quality controls if and when necessary,
- risk assessment tools to support staff preparation and decision making across the Directorate, and
- a local incident action plan.

ACT Legislative Assembly
London Circuit, Canberra ACT 2601, Australia GPO Box 1020, Canberra ACT 2601, Australia
Phone +61 2 6205 0233 **Email** berry@act.gov.au
@YvetteSBerry YvetteSBerry yvettesberry

Each morning schools were provided with air quality guidance based on information from ACT Health to inform their operational response for that day. The advice provided four impact levels for air quality – normal conditions, minimal impact, moderate impact and high impact, with actions aligned to ensure the safety of staff and students.

The advice reminded schools to communicate anticipated impacts and controls to staff, students and the community. This included all visitors, volunteers and workers at the school that day. Key resources were also provided to schools with links to ACT Health air monitoring and quality, weather, fire danger rating and bushfire activity. In addition, the Education Directorate deployed tower air purifiers, donated by Dyson, to every ACT public school to assist in improving indoor spaces for vulnerable groups.

The ACT Government has received many enquiries about issues related to air quality this summer. This was an unprecedented event that resulted in many state and territory governments reviewing the information they provide to the public in relation to air quality. As you may have seen, the ACT Government recently agreed to the development of a dedicated Air Quality Strategy for the ACT.

Thank you for raising your concerns and sharing your expertise.

Yours sincerely

[redacted]

Yvette Berry MLA
Minister for Education and Early Childhood Development

2 APR 2020

RECORD 4

Centers for Disease Control and Prevention

Ventilation in Buildings

Updated June 2, 2021

Summary of Recent Changes

Updates as of June 2, 2021

- Added a new Frequently Asked Question on protective barriers and ventilation.

View Previous Changes

CDC recommends a layered approach to reduce exposures to SARS-CoV-2, the virus that causes COVID-19. This approach includes using multiple mitigation strategies, including improvements to building ventilation, to reduce the spread of disease and lower the risk of exposure. In addition to ventilation improvements, the layered approach includes physical distancing, wearing face masks, hand hygiene, and vaccination.

SARS-CoV-2 viral particles spread between people more readily indoors than outdoors. Indoors, the concentration of viral particles is often higher than outdoors, where even a light wind can rapidly reduce concentrations. When indoors, ventilation mitigation strategies can help reduce viral particle concentration. The lower the concentration, the less likely viral particles can be inhaled into the lungs (potentially lowering the inhaled dose); contact eyes, nose, and mouth; or fall out of the air to accumulate on surfaces. Protective ventilation practices and interventions can reduce the airborne concentrations and reduce the overall viral dose to occupants.

Reoccupying a building during the COVID-19 pandemic should not, in most cases, require new building ventilation systems. However, ventilation system upgrades or improvements can increase the delivery of clean air and dilute potential contaminants. Consult experienced heating, ventilation, and air conditioning (HVAC) professionals when considering changes to HVAC systems and equipment. Buildings that provided healthy, code-compliant indoor air quality prior to the pandemic can be improved for pandemic occupancy using less costly interventions. Below is a list of ventilation interventions that can help reduce the concentration of virus particles in the air. They represent a list of "tools in the mitigation toolbox," each of which can contribute towards a reduction in risk. Implementing multiple tools at the same time is consistent with CDC's layered approach and will increase overall effectiveness of ventilation interventions. These ventilation interventions can reduce the risk of exposure to the virus and reduce the spread of disease, but they will not eliminate risk completely.

While the list of tools can be universally applied across indoor environments, applying them to different building types, occupancies, and activities under environmental and seasonal changes can be challenging. The specific combination of tools chosen for use at any point in time can change. It will be up to the building owner or operator (with expert consultation as needed) to identify which tools are appropriate for each building throughout the year. In addition to buildings, vehicles – including public transportation such as buses, subways, trains, school buses, carpools, and rideshares – are also areas where ventilation improvements can be applied to reduce the spread of the virus and lower the risk of exposure.

Tools to Improve Ventilation

Some of the following interventions are based on the American Society of Heating, Refrigerating, and Air-Conditioning Engineers (ASHRAE) Guidance for Building Operations During the COVID-19 Pandemic [78 KB, 3 pages]. Not all interventions will work in all scenarios. Use caution in highly polluted areas when increasing outdoor air ventilation. The following tools identify ways to improve ventilation:

- Increase the introduction of outdoor air:
  - Open outdoor air dampers beyond minimum settings to reduce or eliminate HVAC air recirculation. In mild weather, this will not affect thermal comfort or humidity. However, this may be difficult to do in cold, hot, or humid weather, and may require consultation with an experienced HVAC professional.
  - Open windows and doors, when weather conditions allow, to increase outdoor air flow. Do not open windows and doors if doing so poses a safety or health risk (e.g., risk of falling, triggering asthma symptoms) to occupants in the building. Even a slightly open window can introduce beneficial outdoor air.
- Use fans to increase the effectiveness of open windows:
  - To safely achieve this, fan placement is important and will vary based on room configuration. Avoid placing fans in a way that could potentially cause contaminated air to flow directly from one person to another (see FAQ below on indoor use of fans). One helpful strategy is to use a window fan, placed safely and securely in a window, to exhaust room air to the outdoors. This will help draw outdoor air into the room via other open windows and doors without generating strong room air currents. Similar results can be established in larger facilities using other fan systems, such as gable fans and roof ventilators.
- Ensure ventilation systems operate properly and provide acceptable indoor air quality for the current occupancy level for each space.
- Rebalance or adjust HVAC systems to increase total airflow to occupied spaces when possible.
- Turn off any demand-controlled ventilation (DCV) controls that reduce air supply based on occupancy or temperature during occupied hours. In homes and buildings where the HVAC fan operation can be controlled at the thermostat, set the fan to the "on" position instead of "auto," which will operate the fan continuously, even when heating or air-conditioning is not required.
- Improve central air filtration:
  - Increase air filtration to as high as possible without significantly reducing design airflow. Increased filtration efficiency is especially helpful when enhanced outdoor air delivery options are limited.
  - Make sure air filters are properly sized and within their recommended service life.
  - Inspect filter housing and racks to ensure appropriate filter fit and minimize air that flows around, instead of through, the filter.
- Ensure restroom exhaust fans are functional and operating at full capacity when the building is occupied.
- Inspect and maintain exhaust ventilation systems in areas such as kitchens, cooking areas, etc. Operate these systems any time these spaces are occupied. Operating them even when the specific space is not occupied will increase overall ventilation within the occupied building.
- Use portable high-efficiency particulate air (HEPA) fan/filtration systems to enhance air cleaning (especially in higher risk areas such as a nurse's office or areas frequently inhabited by people with a higher likelihood of having COVID-19 and/or an increased risk of getting COVID-19). See the FAQ below on HEPA filters and portable HEPA air cleaners. (Note: Portable air cleaners that use filters less efficient that HEPA filters also exist and can contribute to room air cleaning. However, they should be clearly labeled as non-HEPA units.)
- Generate clean-to-less-clean air movement by evaluating and repositioning as necessary, the supply louvers, exhaust air grilles, and/or damper settings. See the FAQ below on Directional Airflow. This recommendation is easier to accomplish when the supply and exhaust points are located in a ceiling grid system.
- Use ultraviolet germicidal irradiation (UVGI) as a supplemental treatment to inactivate SARS-CoV-2 when options for increasing room ventilation and filtration are limited. Upper-room UVGI systems [6.1 MB, 87 pages] can be used to provide air cleaning within occupied spaces, and in-duct UVGI systems can help enhance air cleaning inside central ventilation systems.
- In non-residential settings, run the HVAC system at maximum outside airflow for 2 hours before and after the building is occupied.

The ventilation interventions listed above come with a range of initial costs and operating costs, which, along with risk assessment factors – such as community incidence rates, facemask compliance expectations and room occupant density – may affect the selection of tools. The following are examples of cost estimates for ventilation interventions:

- No cost: opening windows; inspecting and maintaining dedicated exhaust ventilation; disabling DCV controls; repositioning outdoor air dampers
- Less than $100: using fans to increase effectiveness of open windows; repositioning supply/exhaust diffusers to create directional airflow
- $500 (approximately): adding portable HEPA fan/filter systems
- $1500 to $2500 (approximately): adding upper room UVGI

Ventilation FAQs

1. Can COVID-19 be transmitted through HVAC (ventilation) systems?

The risk of spreading SARS-CoV-2, the virus that causes COVID-19, through ventilation systems is not clear at this time. Viral RNA has reportedly been found on return air grilles, in return air ducts, and on heating, ventilation, and air conditioning (HVAC) filters, but detecting viral RNA alone does not imply that the virus was capable of transmitting disease. One research group reported that the use of a new air-sampling method allowed them to find viable viral particles within a COVID-19 patient's hospital room with good ventilation, filtration and ultraviolet (UV) disinfection (at distances as far as 16 feet from the patient). However, the concentration of viable virus detected was believed to be too low to cause disease transmission. There may be some implications for HVAC systems associated with these findings, but it is too early to conclude that with certainty. While airflows within a particular space may help spread disease among people in that space, there is no definitive evidence to date that viable virus has been transmitted through an HVAC system to result in disease transmission to people in other spaces served by the same system.

Healthcare facilities have ventilation requirements in place to help prevent and control infectious diseases that are associated with healthcare environments. For more information, see the CDC Guidelines for Environmental Infection Control in Health-Care Facilities.

Non-healthcare (e.g., businesses and schools) building owners and managers should, at a minimum, maintain building ventilation systems according to state and local building codes and applicable guidelines. Ensuring appropriate outdoor air and ventilation rates is a practical step to ensure good indoor air quality.

2. How long will it take to dilute the concentration of infectious particles in a room once they are generated?

While large droplets (100 micrometers [μm] and larger) will settle to surrounding surfaces within seconds, smaller particles can stay suspended in the air for much longer. It can take several minutes for particles 10 μm in size to settle, while particles 5 μm and smaller may not settle for hours or even days. Dilution ventilation and particle filtration are commonly used to remove these smaller particles from the air. Larger particles can also be removed using these strategies, but since they fall out of the air quickly, they might not have a chance to get captured by filtration systems.

The time required to remove airborne particles from a space can be estimated using Table B.1 in the CDC's Guidelines for Environmental Infection Control in Health-Care Facilities (2003). The estimates assume the source of infectious particles is no longer present in the space. The estimates are based upon the rate that particle-free air is delivered to the room and the desired removal efficiency (99% or 99.9%). The particle-free air, measured in air changes per hour (ACH), can be uncontaminated supply air or the clean exhaust from a High Efficiency Particulate Air (HEPA) fan/filtration system [See HEPA filtration discussion below].

Although there are some highly contagious airborne diseases (like measles) where CDC provides specific guidance for 99.9% clearance wait times, the general recommendation in CDC's Guidelines for Environmental Infection Control in Health-Care Facilities is to wait to allow for a 99% reduction of any generated airborne particles before re-entering the room.

RECORD 4

In the absence of guidance specifying a longer wait period for SARS-CoV-2, the wait time associated with 99% clearance is appropriate for healthcare and other spaces. Regardless of whether the 99% or 99.9% column on Table B.1 is used, the value in the table is usually an under-estimation of the actual dilution clearance time as noted in the table's footnotes which include the following statement: "The times given assume perfect mixing of the air within the space (i.e., mixing factor = 1). However, perfect mixing usually does not occur. Removal times will be longer in rooms or areas with imperfect mixing or air stagnation." Appropriate use of Table B.1 to establish clearance times from any space requires multiplying the time in the table by a mixing factor (k) that ranges between 1 and 10. This factor represents how well the ventilation system mixes and dilutes the concentration of airborne particles within the room.

As a rule of thumb, rooms with higher airflow rates (6 ACH and higher) and good placement of supply and exhaust grilles (hospital airborne infection isolation rooms) are considered to have "good" mixing and thus a mixing factor of k = 3 is often used for these spaces. In that case, the time identified from Table B.1 should be multiplied by 3 to determine the actual clearance time prior to re-entry. Nonventilated or poorly ventilated spaces have typical values of k ranging from 8 to 10. Increased ACH generally lead to reductions in k, although k can also be reduced by the use of a fan in the space, which does not have an impact on ACH. Ultimately, wait times can be reduced by increasing ACH, reducing k, or a combination of both.

Example 1. Given: A room measuring 12 feet x 10 feet with a ceiling height of 10 feet is served with a 100% outdoor air ventilation system that delivers 65 cubic feet per minute (cfm) of supply air (Q_s = 65 cfm) and exhausts 80 cfm of air from the room (Q_e = 80 cfm). The room has average air mixing, so assign k = 5.

COVID-19

Solution: Since Q_e is larger than Q_s by 15 cfm, the heating, ventilation, and air conditioning (HVAC) system is pulling 15 cfm of air into the room from adjacent areas (i.e., the room is under negative pressure). For this example, the 15 cfm of transfer air is assumed to be free of infectious airborne particles. The clean volumetric air flow rate (Q) is the larger value between Q_s and Q_e, so Q = 80 cfm. Calculate the air changes per hour:

ACH = [Q x 60] / (room volume) = (80 cfm x 60) / (12' x 10' x 10') = 4800/1200 = 4.0 ACH

Using Table B.1 the perfect mixing wait time based on 4 ACH and a 99% reduction of airborne particles is 69 minutes.

Using the mixing factor of 5, the estimated wait time for 99% reduction of airborne contaminants in the room is 5 x 69 = 345 minutes or 5 hours and 45 minutes.

Note: Determining the true value of the mixing factor is difficult and requires special equipment to measure air flows and conduct tracer gas decay testing. Thus, conservative estimates of k are often used (as described above). Also, the addition of an air cleaning device (e.g., a portable HEPA filtration unit) within the same room will reduce the wait time. The flow rate from the air cleaning device can be added to Q determined above, which will increase the overall ACH in the room. The air movement created by the air cleaning device can also decrease the value of k. Together, the increased ACH and decreased k can help substantially reduce wait times. See Example 2 for more information, including an example of the calculations.

3. Can ventilation filters effectively capture SARS-CoV-2 viral particles?

Filters for use in heating, ventilation, and air conditioning (HVAC) systems are generally tested under procedures outlined in ANSI/ASHRAE Standard 52.2-2017-Method of Testing General Ventilation Air-Cleaning Devices for Removal Efficiency by Particle Size. This standard was developed by ASHRAE, a global society focused on building systems, indoor air quality, and sustainability in the built environment, and is available for free online viewing during the ongoing pandemic. Based on the filtration efficiency determined by the testing procedures, filters are assigned a Minimum Efficiency Reporting Value (MERV). The MERV provides a measure of the "filter efficiency" over the range of particle sizes prescribed in the test procedure. MERV values range from 1 to 16 and higher MERV values correspond to more efficient filters.

Research shows that the particle size of SARS-CoV-2 is around 0.1 micrometer (µm). However, the virus generally does not travel through the air by itself. These viral particles are human-generated, so the virus is trapped in respiratory droplets and droplet nuclei (dried respiratory droplets) that are larger than an individual virus. Most of the respiratory droplets and particles exhaled during talking, singing, breathing, and coughing are less than 5 µm in size. CDC recommends using the highest efficiency ventilation filters possible, without having detrimental effects on overall HVAC system performance. ASHRAE has similar guidance; however, they recommend a minimum filtration efficiency target of MERV 13, provided there are not substantial negative impacts on the HVAC system performance and occupant comfort. A MERV 13 filter is at least 50% efficient at capturing particles in the 0.3 μm to 1.0 μm size range and 85% efficient at capturing particles in the 1 μm to 3 μm size range. Collectively these particles are capable of remaining airborne for hours and are most associated with deep lung penetration. A MERV 14 filter is at least 75% and 90% efficient, respectively, at capturing those same particles. Efficiencies for MERV 15 and MERV 16 filters are even higher. Thus, the recommended filters are significantly more efficient at capturing particles of concern than a typical MERV 8 filter, which is only around 20% efficient in the 1 μm to 3 μm size range and is not rated for capture efficiency of the smaller 0.3 μm to 1.0 μm particles.

Increasing filtration efficiency can increase the pressure drop across the filters. This can lead to increased fan energy, reduced airflow rates, and/or issues controlling indoor temperature and relative humidity levels. Scientific developments in filter design and manufacturing have reduced the amount of the increased pressure drop and its resulting impact on HVAC operations, but not all filters have adopted the newer technology. Prior to a filtration upgrade, the specific filters under consideration should be investigated for their pressure drop ratings at the flow rate(s) of intended use and the potential impacts of that pressure drop evaluated against the capabilities of the existing HVAC system.

High-efficiency particulate air (HEPA) filters are even more efficient at filtering human-generated infectious particles than MERV 16 filters. However, outside of a few unique applications, HEPA filters are rarely used in central HVAC systems. [See the question on Portable HEPA Filtration to learn more about them and their application in protective air cleaning].

4. What is meant by "directional airflow?" How and where should it be used?

Directional airflow is a protective ventilation concept where air movement flows in a clean-to-less-clean direction. This ventilation concept is applied to areas where the "clean" environment requires a higher level of protection and/or where the "less-clean" environment has a higher risk of containing airborne contaminants (activities or occupancy by individuals with a higher risk of being infectious). Examples of "clean" spaces might include healthcare facility triage stations or rooms/corridors adjacent to higher risk activities. Examples of "less-clean" spaces might include spaces that contain known/suspect infectious persons or spaces where a known activity has increased likelihood of generating infectious airborne particles.

The creation of directional airflow can be accomplished within a particular space or between two adjacent spaces. This can be done passively, through intentional placement of supply and exhaust heating, ventilation, and air conditioning (HVAC) grilles, or by the intentional creation of pressure differentials between adjacent spaces through specification of offset exhaust and supply air flow rates. Creation of the directional airflow can also be done actively, through the use of fans exhausting through open windows, strategic placement of ductwork attached to portable HEPA filtration units, or dedicated exhaust systems (installed or portable) that generate a desired airflow by exhausting air out of windows, doorways, or through temporary ducts. In specific settings, specialized local control ventilation interventions that establish the desired airflow directions can also be used (see the NIOSH Ventilated Headboard).

Directional airflows must be evaluated carefully. Testing of the directional airflow effectiveness can be accomplished using visual tracer techniques that use "smoke tubes" or handheld "fog generators." Other tools, such electronic monitors or visual aids to monitor pressure differences can be used when directional airflow is established between two adjacent spaces. To reduce the potential for directing airflow from infectious towards non-infectious space occupants, it is important that the "clean" and "less-clean" space determinations be established using infection control risk assessment considerations.

5. What is a HEPA filter and why use a portable HEPA air cleaner?

Research shows that the particle size of SARS-CoV-2 is around 0.1 micrometer (μm). However, the virus generally does not travel through the air by itself. These viral particles are human-generated, so the virus is trapped in respiratory droplets and droplet nuclei (dried respiratory droplets) that are larger. Most of the respiratory droplets and particles exhaled during talking, singing, breathing, and coughing are less than 5 μm in size. By definition, a High Efficiency Particulate Air (HEPA) filter is at least 99.97% efficient at capturing particles 0.3 μm in size. This 0.3 μm particle approximates the most penetrating particle size (MPPS) through the filter. HEPA filters are even more efficient at capturing particles larger and smaller than the MPPS. Thus, HEPA filters are no less than 99.97% efficient at capturing human-generated viral particles associated with SARS-CoV-2.

Portable HEPA filtration units that combine a HEPA filter with a powered fan system are a preferred option for auxiliary air cleaning, especially in higher risk settings such as health clinics, vaccination and medical testing locations, workout rooms, or public waiting areas. Other settings that could benefit from portable HEPA filtration can be identified using typical risk assessment parameters, such as community incidence rates, facemask compliance expectations, and room occupant density. While these systems do not bring in outdoor dilution air, they are effective at cleaning air within spaces to reduce the concentration of airborne particulates, including SARS-CoV-2 viral particles. Thus, they give effective air exchanges without the need for conditioning outdoor air.

In choosing a portable HEPA unit, select a system that is appropriately sized for the area in which it will be installed. This determination is made based on the air flow through the unit, which is typically reported in cubic feet per minute (cfm). Many portable HEPA filtration units are assigned a Clean Air Delivery Rate (CADR) (See EPA's Guide To Air Cleaners In The Home), which is noted on a label in the operators manual, on the shipping box, and/or on the filtration unit itself. The CADR is an established standard defined by the Association of Home Appliance Manufacturers (AHAM). Participating portable air cleaner manufacturers have their products certified by an independent laboratory, so the end user can be assured it performs according to the manufacturer's claims. The CADR is generally reported in cfm for products sold in the United States. The paragraphs below describe how to select an appropriate air cleaner based on the size of the room in which it will be used. The procedure below should be followed whenever possible. If an air cleaner with the appropriate CADR number or higher is not available, select a unit with a lower CADR rating. The unit will still provide incrementally more air cleaning than having no air cleaner at all.

In a given room, the larger the CADR, the faster it will clean the room air. Three CADR numbers are given on the AHAM label, one each for smoke, dust, and pollen. The smoke particles are the smallest, so that CADR number applies best to viral particles related to COVID-19. The label also shows the largest room size (in square feet, ft^2) that the unit is appropriate for, assuming a standard ceiling height of up to 8 feet. If the ceiling height is taller, multiply the room size (ft^2) by the ratio of the actual ceiling height (ft) divided by 8. For example, a 300 ft^2 room with an 11-foot ceiling will require a portable air cleaner labeled for a room size of at least 415 ft^2 ($300 \times [11/8] = 415$).

The CADR program is designed to rate the performance of smaller room air cleaners typical for use in homes and offices. For larger air cleaners, and for smaller air cleaners whose manufacturers choose not to participate in the AHAM CADR program, select a HEPA unit based on the suggested room size (ft^2) or the reported air flow rate (cfm) provided by the manufacturer. Consumers might take into consideration that these values often reflect ideal conditions which overestimate actual performance.

For air cleaners that provide a suggested room size, the adjustment for rooms taller than 8 feet is the same as presented above. For units that only provide an air flow rate, follow the "2/3 rule " to approximate a suggested room size. To apply this rule for a room up to 8 feet tall, choose an air cleaner with an air flow rate value (cfm) that is at least 2/3 of the floor area (ft^2). For example, a standard 300 ft^2 room requires an air cleaner that provides at least 200 cfm of air flow ($300 \times [2/3] = 200$). If the ceiling height is taller, do the same calculation and then multiply the result by the ratio of the actual ceiling height (ft) divided by 8. For example, the 300 ft^2 room described above, but with an 11-foot ceiling, requires an air cleaner that can provide at least 275 cfm of air flow ($200 \times [11/8] = 275$).

While smaller HEPA fan systems tend to be stand-alone units, many larger units allow flexible ductwork to be attached to the air inlet and/or outlet (note that larger ducted units don't fall under the "room air cleaner" description and may not have a CADR rating). Using ductwork and placing the HEPA system strategically in the space can help provide desired clean-to-less-clean airflow patterns where needed. Ducted HEPA systems can also be used to establish direct source capture interventions for patient treatment and /or testing scenarios (See CDC/NIOSH discussion on Ventilated Headboard). Depending on the size of the HEPA fan/filter units and how the facility in which they are being used is configured, multiple small portable HEPA units deployed to high risk areas may be more useful than one large HEPA unit serving a combined space.

Example 2. Given: The room described in Example 1 is now augmented with a portable HEPA air cleaning device with a smoke CADR of 120 cfm (Q_{hepa} = 120 cfm). The added air movement within the room improves overall mixing, so assign k = 3.

Question: How much time is saved to achieve the same 99% reduction in airborne contaminants by adding the portable HEPA device to the room?

Solution: The addition of the HEPA filter device provides additional clean air to the room. Here, the clean volumetric air flow rate (Q) is: $Q = Q_e + Q_{hepa}$ = 80 cfm + 120 cfm = 200 cfm.

ACH = [Q x 60] / (room volume) = (200 cfm x 60) / (12′ x 10′ x 10′) = 12,000/1,200 = 10 ACH.

Using Table B.1, the perfect mixing wait time based on 10 ACH and a 99% reduction of airborne particles is 28 minutes.

Using the mixing factor of 3, the estimated wait time for 99% reduction of airborne contaminants in the room is 3 x 28 = 84 minutes. Thus, the increased ACH and lower k value associated with the portable HEPA filtration unit reduced the wait time from the original 5 hours and 45 minutes to only 1 hour and 24 minutes, saving a total of 4 hours and 21 minutes before the room could be safely reoccupied.

Adding the portable HEPA unit increased the effective ventilation rate and improved room air mixing. This resulted in over a 75% reduction in time for the room to be cleared of potentially-infectious airborne particles.

---

6. Does ultraviolet germicidal irradiation (UVGI) kill SARS-CoV-2?

Yes. Ultraviolet germicidal irradiation (UVGI), otherwise known as germicidal ultraviolet (GUV), is a disinfection tool used in many different settings, such as residential, commercial, educational, and healthcare settings. The technology uses ultraviolet (UV) energy to inactivate (kill) microorganisms, including viruses, when designed and installed correctly.

There is still a lot to learn about SARS-CoV-2 and the extent of airborne viral particles and spread. However, UVGI can inactivate viruses in the air and on surfaces.* The design and sizing of effective UVGI disinfection systems requires specific knowledge and experience.

Seek consultation with a reputable UVGI manufacturer or an experienced UVGI system designer prior to installing UVGI systems. These professionals can assist by doing necessary calculations, making fixture selections, properly installing the system, and testing for proper operation specific to the setting.

*Note: CDC's recommendation for primary surface disinfection in occupied environments is to follow the CDC/EPA guidance for surface disinfection.

---

7. What types of ultraviolet germicidal irradiation (UVGI) devices are available for cleaning and disinfection in the workplace?

Upper-room UVGI

Upper-room (or upper-air) UVGI uses specially designed UVGI fixtures mounted on walls or ceilings to create a disinfection zone of ultraviolet (UV) energy that is focused up and away from people. These fixtures disinfect air as it circulates from mechanical ventilation, ceiling fans, or natural air movement. The advantage of upper-room UVGI is that it disinfects the air closer to and above people who are in the room. Since the 1980s, UVGI systems have been widely used for control of tuberculosis (TB). The CDC guidance Environmental Control for Tuberculosis: Basic Upper-Room Ultraviolet Germicidal Irradiation Guidelines for Healthcare Settings provides information on appropriate UVGI system design, related safe operation, and maintenance. Based on data from other human coronaviruses, a UVGI system designed to protect against the spread of TB should be effective at inactivating SARS-CoV-2 and therefore prevent spread. UVGI systems usually require a few UV fixtures to be effective. For example, a rectangular-shaped waiting room with 10–30 occupants will require 2–3 upper-air UVGI fixtures. As part of system installation, care must be taken to control the amount of UV energy directed or reflected into the lower occupied space below levels recognized as safe. Reputable UVGI manufacturers or experienced UVGI system designers will take the necessary measurements and make any required adjustments to prevent harmful UV exposures to people in the space.

Potential Application: Can be used in any indoor environment; most useful in spaces highly occupied with people who are or may be sick.

In-Duct UVGI

In-duct UVGI systems are installed within a heating, ventilation, and air-conditioning (HVAC) system. These systems are designed to serve one of two purposes:

1) Coil treatment UVGI keeps HVAC coils, drain pans, and wetted surfaces free of microbial growth. These devices produce relatively low levels of UV energy. This energy is continually delivered 24 hours a day, which is why they are effective. Coil treatment UVGI devices are not designed for disinfecting the air and should not be installed for the purpose of air disinfection.

Potential Application: Can be used to reduce HVAC maintenance and improve operational efficiency within large, commercial HVAC systems or residential HVAC systems; not recommended for inactivating airborne pathogens.

2) Air disinfection UVGI systems can be effective at applying intense UV energy to inactivate airborne pathogens as they flow within the HVAC duct. HVAC air disinfection UVGI systems generally require more powerful UV lamps or a greater number of lamps, or both, to provide the necessary UVGI required to inactivate pathogens in a short period of time. Air disinfection systems are often placed downstream of the HVAC coils. This location keeps the coil, drain pan, and wetted surfaces free of microbial growth and also disinfects the moving air.

Potential Application: Can be used inside any HVAC system to disinfect infectious airborne pathogens.

Far-UV (or Far-UVC)

Far-UV is one of many emerging technologies that have become popular during the COVID-19 pandemic. While standard UVGI fixtures emit UV energy at a wavelength around 254 nanometers (nm), far-UV devices use different lamps to emit UV energy at a wavelength around 222 nm. Aside from the wavelength, a major difference between the two technologies is that standard UVGI systems are specifically designed to avoid exposing people to the UV energy, while many far-UV devices are marketed as safe for exposing people and their direct environment to UV energy. A review of peer-reviewed literature indicates that far-UV wavelengths can effectively inactivate microorganisms, including human coronaviruses, when appropriate UV doses are applied. Questions remain about the mechanisms of killing microorganisms and overall safety. Far-UV might prove to be effective at disinfecting air and surfaces, without some of the safety precautions required for standard UVGI. Far-UV devices are best viewed as new and emerging technology. Consumers considering an emerging technology such as Far-UV should read the FAQ on emerging technologies below.

8. Many new air disinfection devices are marketed for their ability to inactivate SARS-CoV-2. How can I tell if they work as advertised?

CDC does not provide recommendations for, or against, any manufacturer or product. There are numerous technologies being heavily marketed to provide air cleaning during the ongoing COVID-19 pandemic. Common among these are ionization, dry hydrogen peroxide, and chemical fogging disinfection. Some products on the market include combinations of these technologies. These products generate ions, reactive oxidative species (ROS, which are marketed using many names), or chemicals into the air as part of the air cleaning process. People in spaces treated by these products are also exposed to these ions, ROS, or chemicals.

While variations of these technologies have been around for decades, relative to other air cleaning or disinfection methods, they have a less-documented track record when it comes to cleaning/disinfecting large and fast volumes of moving air within heating, ventilation, and air conditioning (HVAC) systems or even inside individual rooms. This does not necessarily imply the technologies do not work as advertised. However, in the absence of an established body of peer-reviewed evidence showing proven efficacy and safety under as-used conditions, the technologies are still considered by many to be "emerging."

As with all emerging technologies, consumers are encouraged to exercise caution and to do their homework. Registration alone, with national or local authorities, does not always imply product efficacy or safety. Consumers should research the technology, attempting to match any specific claims against the intended use of the product. Consumers should request testing data that quantitively demonstrates a clear protective benefit and occupant safety under conditions consistent with the intended use. When considering air cleaning technologies that potentially or intentionally expose building with the intended use. When considering air cleaning technologies that potentially or intentionally expose building occupants, the safety data should be applicable to all occupants, including those with health conditions that could be aggravated by the air treatment. In transient spaces, where average exposures to the public may be temporary, it is important to also consider occupational exposures for workers that must spend prolonged periods in the space.

Preferably, the documented performance data under as-used conditions should be available from multiple sources, some of which should be independent, third-party sources. Unsubstantiated claims of performance or limited case studies with only one device in one room and no reference controls should be questioned. At a minimum, when considering the acquisition and use of products with technology that may generate ozone, verify that the equipment meets UL 867 standard certification (Standard for Electrostatic Air Cleaners) for production of acceptable levels of ozone, or preferably UL 2998 standard certification (Environmental Claim Validation Procedure (ECVP) for Zero Ozone Emissions from Air Cleaners) which is intended to validate that no ozone is produced.

9. Can carbon dioxide (CO_2) monitors be used to indicate when there is good ventilation?

Carbon dioxide (CO_2) monitoring can provide information on ventilation in a given space, which can be used to enhance protection against COVID-19 transmission. Strategies incorporating CO_2 monitors can range in cost and complexity. However, greater cost and complexity does not always mean greater protection.

Traditionally, CO_2 monitoring systems are expensive, require extensive knowledge to accurately install and set up, and require sophisticated control programs to effectively interact with the building heating, ventilation and air-conditioning (HVAC) systems in real time. They were not designed to protect building occupants from disease transmission. Developers of whole-building CO_2 monitoring equipment/software for HVAC system operations have been around for decades, with the technology most often applied in the pursuit of energy savings. As the current pandemic response has progressed, this technology has been marketed as a potential tool for providing an indication of building ventilation efficacy, leading to questions about whether monitoring indoor CO_2 concentrations can be used as a tool to help make ventilation decisions.

In some well-designed, well-characterized, well-maintained HVAC environments, the use of fixed CO_2 monitors can be informative. When used, these monitors are often incorporated into demand-controlled ventilation (DCV) systems that are designed with a primary intent of maximizing energy efficiency through reductions in outdoor air delivery. However, guidance throughout the pandemic has been to exceed minimum ventilation whenever possible, in addition to masking, physical distancing, enhanced filtration, and other intervention-focused considerations. From the beginning of this pandemic's response, both CDC and ASHRAE have advised to deactivate DCV systems and operate the ventilation systems at maximum airflows, within the safety limitations of the equipment.

Fixed-position CO_2 monitors measure CO_2 concentration as an indicator of the number of people in the space. As the CO_2 concentration increases, the HVAC DCV system increases the amount of outdoor air ventilation in the space to dilute CO_2 (and vice versa). The number of CO_2 sensors, the placement of those sensors, and their calibration and maintenance are collectively a large and complex issue that must not be overlooked. For example, the CO_2 concentration measured by a fixed, wall-mounted monitor may not always represent the actual concentrations in the occupied space. If air currents from the room HVAC, or even make-up air from windows, flows directly over this monitor location, the corresponding concentration measurements will be artificially low. If the room has good air mixing, the measured concentration should approximate the true concentration, but rooms are rarely well mixed, particularly in older buildings with aging ventilation systems (or none at all). Also, if an elevated CO_2 concentration results in an air flow increase to one room, that air may be "stolen" from other rooms on the same HVAC system. This may result in elevated CO_2 concentrations in those other spaces which the HVAC system is unable to control.

Limited information exists regarding a direct link associating CO_2 concentrations to a risk of COVID-19 transmission. Changes in CO_2 concentrations can indicate a change in room occupancy and be used to adjust the amount of outdoor air delivered. However, CO_2 concentrations cannot predict who has SARS-CoV-2 infection and might be spreading the virus, the amount of airborne viral particles produced by infected people, or whether the HVAC system is effective at diluting and removing viral concentrations near their point of generation. As a simple example, a small room with three occupants will have the same level of CO_2 (and hence the same outdoor air ventilation rate controlled by the DCV system) whether no one has SARS-CoV-2 infection or whether one or more people are infected with the virus. Ventilation based on CO_2 measurements cannot recognize the increased risk of transmission in the second scenario.

A more modest, cost-efficient, and accurate use of CO_2 monitoring is the use of portable instruments combined with HVAC systems that do not have modulating setpoints based on CO_2 concentrations. The CO_2 meter can be purchased for under $300 and its measurements can be collected/logged near the breathing zones of occupied areas of each room. Under this approach, the HVAC outdoor air dampers could be set to introduce more outdoor air than code requires (as recommended by CDC and ASHRAE) and the resulting CO_2 concentrations in rooms at the real-world occupancy levels documented using a calibrated, handheld portable CO_2 meter. This documentation will be the CO_2 concentration benchmarks for each room under the HVAC operating conditions and occupancy levels.

One potential target benchmark for good ventilation is CO_2 readings below 800 parts per million (ppm). If the benchmark readings are above this level, reevaluate the ability to increase outdoor air delivery. If unable to get below 800 ppm, increased reliance on enhanced air filtration (including portable HEPA air cleaners) will be necessary. Once the benchmark concentrations are established, take periodic measurements and compare them to the benchmarks. As long as the ventilation airflow is unchanged (outdoor air or total air) and the occupancy capacity is not increased, future portable CO_2 concentrations that are 110% of the benchmarks indicate a potential problem that should be investigated. Under the pandemic response, a pragmatic application of portable CO_2 measurement tools is a cost-effective approach to monitoring building ventilation.

---

10. Should indoor temperature and humidity be used to help reduce the risk of COVID-19 transmission?

For COVID-19, the first steps in reducing the indoor concentrations of the virus are wearing face masks, physical distancing, and reducing occupancy levels. Improved ventilation is an additional prevention strategy. For ventilation systems, increasing outdoor air above the code minimum requirements, increasing total ventilation, and increasing filtration efficiencies are more effective at controlling infectious disease transmission than controlling indoor temperature and humidity. However, the use of temperature and/or humidity to reduce the risk of disease transmission should be considered on a case-by-case basis, taking into account the building enclosure, heating, ventilation, and air-conditioning (HVAC) system capabilities, level of control and/or building automation, local COVID-19 transmission rates, any unique clinical features of the occupants, and local climate.

Both temperature and humidity can influence the transmission of infectious diseases, including COVID-19, but that influence has practical limitations. Research on the impact of temperature has shown that SARS-CoV-2, the virus that causes COVID-19, is sensitive to elevated temperatures, with over 99.99% inactivation in only a few minutes at 70°C (158°F). However, this temperature is far outside the limits of human comfort and could damage some building materials. While temperatures lower than 70°C (158°F) are also effective, the required exposure time for inactivation increases as the temperature decreases. So, elevated temperatures offer the potential for decontamination of SARS-CoV-2 virus in the air or on surfaces, but the use of increased temperature solely for decontamination is not generally recommended and is not realistic for occupied spaces. Another important consideration is that when the temperature in a space is elevated, the corresponding relative humidity level decreases.

Current evidence is not persuasive that humidity significantly reduces transmission of SARS-CoV-2 beyond the level resulting from good ventilation and filtration. Some research studies have shown that the survival of viruses, including human coronaviruses, may be reduced when the relative humidity is in the 40–60% range. However, the reductions are modest and there are outliers to these findings. Consequently, neither ASHRAE nor CDC recommends introducing humidification for the sole purpose of limiting transmission of COVID-19. While not affecting transmission, there are peer-reviewed studies that suggest preventing excessive dryness in the air could help maintain the effectiveness of the human body's immune system.

Some HVAC systems can actively control both temperature and humidity. However, the majority of HVAC systems do not have dedicated humidification capabilities. Some dehumidification happens during warmer months as a byproduct of cooling humid warm air below its dew point and causing water to condense out of the air. Less common is the ability to limit low humidity by introducing water vapor into the dry supply air.

Most existing residential and commercial buildings located in cold climates are not constructed to resist the corrosion and excessive moisture accumulation that can result from long-term, whole-building humidification. If additional winter humidification is used to maintain comfort and prevent excessive dryness of nasal and ocular membranes, first analyze the building enclosure to verify that condensation and moisture accumulation will not become a problem. ASHRAE

Standard 160 (Criteria for Moisture-Control Design Analysis in Buildings) provides guidance for hygrothermal analysis of building enclosures. For commercial buildings that are properly constructed to allow for long-term humidification, and which have humidification capabilities already installed, there is no reason not to humidify the air to comfortable levels during the winter months.

In residential settings, portable in-room humidifiers may be used for sensory comfort and to reduce excessively low relative humidity levels. In these instances, use a humidifier with a built-in humidistat and control the relative humidity level near 40%. Higher humidity levels are not necessarily better and may lead to localized mold growth, mildew, and other long-lasting indoor air quality issues. Maintenance and cleaning of portable humidification systems is very important. Change the water in the humidifier daily and maintain and clean the humidifier in accordance with manufacturer recommendations.

11. Can fans be used to decrease the risk of COVID-19 transmission indoors?

Yes. While fans alone cannot make up for a lack of outdoor air, fans can be used to increase the effectiveness of open windows, as described in the CDC list of ventilation improvement considerations. Fans can also be used indoors to improve room air mixing. Improved room air mixing helps distribute supplied clean air and dilute viral particle concentrations throughout the room, which reduces the likelihood of stagnant air pockets where viral concentrations can accumulate. As with all fan use during the COVID-19 pandemic, take care to minimize the potential to create air patterns that flow directly across one person onto another:

- Avoid the use of the high-speed settings
- Use ceiling fans at low velocity and potentially in the reverse-flow direction (so that air is pulled up toward the ceiling)
- Direct the fan discharge towards an unoccupied corner and wall spaces or up above the occupied zone.

Fans can also enable clean-to-less-clean directional airflow. Such applications should be evaluated closely to avoid unintended consequences and only adopted when supported by a safety risk assessment.

12. Will using protective barriers interfere with improved ventilation?

Barriers can physically separate spaces that are next to each other. When used for infection control, the barrier is intended to prevent someone on one side of the barrier from exposing a person on the other side of the barrier to infectious fluids, droplets, and particles. Whether a barrier interferes with improved ventilation depends on how it is installed. Protective barriers can sometimes help improve ventilation, but they can sometimes hinder ventilation too. Sometimes they have no effect on ventilation.

Protective barriers can assist with improved ventilation when used to facilitate directional airflows or desired pressure differentials between clean and less-clean spaces. The barrier can be aligned with the intended airflow to help direct it towards a desired location, such as an HVAC return air grille or a portable air cleaner inlet. Example scenarios for this type of barrier deployment include those where there is a known source of potentially infectious aerosols, such as a dental operatory or COVID-19 testing station.

Alternatively, the barrier might be placed between two areas to better isolate one side of the barrier from the other. In this configuration, the barrier can also assist the HVAC design scheme in establishing a desired pressure differential between the adjacent spaces. If necessary, small pass-through openings or a retractable panel incorporated into the barrier can allow transfer of physical objects from one side to the other. Examples where this type of barrier application might be applied include a receptionist’s desk or a ticket booth.

When not carefully installed, barriers can sometimes hinder good ventilation. Barriers can unintentionally interrupt the airflow distribution within a space, thus allowing a concentration build-up of human-generated or other aerosols that may remain suspended in the air for minutes to hours. In this case, people could be exposed to higher concentrations of infectious aerosols than they would without the barriers in place. The larger the barrier, the greater the likelihood that this may occur. To reduce this likelihood, ensure that barriers are correctly positioned for the anticipated occupancy and that they are no larger than necessary to prevent direct transfer of respiratory droplets that could "spray" directly from one person onto another.

Any time barriers are deployed, airflow distribution testing with tracer "smoke" or handheld fog generators should be conducted. This testing can assist in evaluating airflow distribution within the occupied spaces. If stagnant air pockets are seen to occur, barrier redesign or reorientation can help to minimize the occurrence. Airflow distribution modifications such as adjusting the positioning of supply air louvers or the discharge of portable air cleaners can also assist in eliminating the development of stagnant air pockets.

The Clean Air in Buildings Challenge helps building owners and operators improve indoor air quality and protect public health. Create your clean indoor air action plan today.

Previous Updates

Updates from Previous Content

As of March 23, 2021

- Simplified language in the overall list of tools to improve ventilation.
- Added three new Frequently Asked Questions (FAQs) on the usefulness of carbon dioxide monitors to inform ventilation decisions, the usefulness of temperature and relative humidity to control the spread of COVID-19, and the use of fans indoors.
- Expanded the FAQ on emerging technologies to include more products available on the market.
- Added additional information with simple calculations to the FAQ on portable HEPA air cleaners to help consumers choose appropriate units for their spaces.

Last Updated June 2, 2021

Yapp, Phillip

From:	Mitchell, BethL
Sent:	Friday, 16 July 2021 5:13 PM
To:	Banda, Ajay; Yapp, Phillip
Subject:	FW: Airflow Research FYI
Attachments:	Jay et al 2019 Energy and Buildings.pdf; Human Thermal Sensation & Comfort - Zhang et al.pdf

OFFICIAL

FYI.

Phil, Ajay is managing a project to install these at Theodore.

Cheers

Beth Mitchell | Director – Asset Strategies, Sustainability and Environment

Phone: +61 2 6207 8364 | Fax: +61 2 6205 9333 |Email: bethl.mitchell@act.gov.au
Infrastructure and Capital Works | Education| ACT Government
Level 4 220 London Circuit | GPO Box 158 Canberra ACT 2601 | www.det.act.gov.au

---

From: Sam Rochaix <sam@airius.com.au>
Sent: Friday, 16 July 2021 10:48 AM
To: Mitchell, BethL <BethL.Mitchell@act.gov.au>
Subject: Airflow Research FYI

Great to chat earlier,

Please see attached research Beth.

I will send you through the proposals for Theodore shortly.

Kind regards,

Sam Rochaix
Regional Sales Director (AU, NZ & SE Asia)

AIRIUS Airflow Reinvented   THE CLEAN AIR COMPANY

Airius Asia Pacific Pty Ltd | The Clean Air Company
A: PO Box 1812 | Byron Bay | NSW | 2481
P: +61 (0) 2 8034 0598
M: +61 (0) 406 585 402

E: sam@airius.com.au
W: www.airius.com.au | www.thecleanaircompany.com.au

Connect on LinkedIn

Energy & Buildings 193 (2019) 92–98

Contents lists available at ScienceDirect

Energy & Buildings

journal homepage: www.elsevier.com/locate/enbuild

Fanning as an alternative to air conditioning – A sustainable solution for reducing indoor occupational heat stress

Ollie Jay[a,b,*], Roman Hoelzl[a,c], Jana Weets[a,c], Nathan Morris[a], Timothy English[a], Lars Nybo[e], Jianlei Niu[f], Richard de Dear[f], Anthony Capon[b,d]

[a] The University of Sydney, Thermal Ergonomics Laboratory, Exercise and Sport Science, Faculty of Health Sciences, NSW 2141, Australia
[b] The University of Sydney, Charles Perkins Centre, NSW 2006, Australia
[c] Technische Universität München, Institute of Ergonomics, Boltzmannstraße 15, 85748 Garching, Germany
[d] The University of Sydney, Sydney School of Public Health, Faculty of Medicine and Health, NSW 2050, Australia
[e] Section for Human Physiology, Faculty of Sciences, University of Copenhagen, Denmark
[f] The University of Sydney, School of Architecture, Design and Planning, NSW 2006, Australia

ARTICLE INFO

Article history:
Received 21 August 2018
Revised 20 March 2019
Accepted 22 March 2019
Available online 23 March 2019

Keywords:
Convection
Climate
Energy conservation
Evaporation
Occupational heat stress

ABSTRACT

We assessed whether increasing airflow with an electric fan is similarly effective as decreasing air temperature with air cooling (AC) in preventing heat-related reductions in productivity, and elevations in body temperatures and discomfort in a warm/humid indoor environment. In 48 experimental trials, we compared the reduction in the human heat stress response of sixteen participants during 135 min of intermittent arm ergometry at a fixed heart rate of 110 beats min^{-1}, from a simulated tropical environment (HOT; 30 °C, 70%RH; wind < 0.2 m s^{-1}) to that observed with either a, (i) 7 °C reduction in air temperature (AC; 23 °C, 70%RH, wind < 0.2 m s^{-1}); or (ii) facilitated airflow (FAN; 30 °C, 70%RH, wind $= 4.2$ m s^{-1}). Cumulative work was similarly improved (+11%) by FAN compared to AC. Likewise, reductions in rectal temperature, thermal sensation, and thermal discomfort were similar with the two different cooling strategies. Sweat losses in the FAN trial were higher compared to AC but lower than HOT without fanning. In conclusion, fanning offers an effective method for alleviating thermal stress and preventing productivity losses for workers exposed to environmental heat. Moving air instead of chilling it may require a little more sweating, but it can save electricity and hence lower greenhouse gas emissions compared to AC.

1. Introduction

Progressive increases in global temperatures [12] have already exerted disproportionately negative effects on the health and well-being of people in densely populated low-income countries with tropical climates. These impacts are particularly evident in indoor working environments [22] where goods destined for consumers in high-income countries are often manufactured in factories without air conditioning or any other effective cooling systems in place [5,35].

In hot occupational environments that require elevated physical activity, manual work intensity must be reduced to mitigate rising body temperatures and excessive heat-related elevations in heart rate [18,27] that occur following a cutaneous vasodilation [33], as well as thermal discomfort [10] and dehydration [37]. Indeed, the World Health Organisation (WHO) has recommended that work intensity should be maintained at a level that does not permit heart rate to exceed, on average, 110 beats min^{-1} [38]. However, worker salaries in many developing countries are typically tied to absolute daily productivity [20], so factory employees must work longer hours during the hottest months of the year in order to receive the same income without experiencing excessive heat-related strain/discomfort [17]. Currently, workers in countries such as Bangladesh, Cambodia, India, Pakistan and Viet Nam are estimated to lose ~1–4% of daylight work hours per year due to extreme heat, with these losses projected to rise to ~15–20% of daylight working hours over the next 70 years [16,19] if greenhouse gas emission rates continue along the "business as usual" trajectory. It therefore seems inevitable that from legal, ethical and business perspectives better cooling systems must be used on a large scale as global temperatures continue to rise [11].

Cooling air with air conditioning is currently the most effective cooling strategy for mitigating worker heat stress [9] with the indoor temperature set-point in many tropical countries typically

* Corresponding author at: Dr. Ollie Jay, Thermal Ergonomics Laboratory, Faculty of Health Sciences, University of Sydney, 75 East St, Lidcombe, NSW 2141, Australia.
E-mail address: ollie.jay@sydney.edu.au (O. Jay).

https://doi.org/10.1016/j.enbuild.2019.03.037
0378-7788/

~23 °C [21], with air velocity typically < 0.2 m s^{-1} [6]. Yet the immediate and downstream environmental impacts of air conditioner use are enormous in terms of greenhouse gas emissions [5] and the worsening of current [24] and future heat-related weather extremes [26]. The electricity demands required to support such intensive use of air conditioning, even with future advances in energy efficiency, would also likely contribute substantially to emerging energy crises in numerous countries/regions [5].

An air conditioner cools a person by increasing dry heat loss through lowering air temperature and thus widening the temperature gradient between the skin and the surrounding environment. However one of the two principal dry heat loss components, convection, can also be augmented without lowering air temperature, provided it is lower than skin temperature (~35 °C [13]), by simply increasing the rate at which air flows across the skin surface [8]. Moreover, greater convective flow can also accelerate the rate at which sweat evaporates from the skin surface, thus enhancing latent heat loss [15]. Theoretically therefore, in many situations/conditions blowing air across the skin of a worker with a device such as an electric fan can yield a similar physical, physiological and perceived cooling effect as cooling the air, and likewise moderate heat-related reductions in work performance at a fixed heart rate, but with a much lower electricity requirement/cost and concomitant environmental impact.

The aim of the present study was to assess the efficacy of electric fan use for mitigating heat-related reductions in work output, and elevations in body temperatures and thermal discomfort without exceeding an average heart rate of 110 beats min^{-1} [38] in a hot simulated workplace (30 °C, 70% relative humidity) in comparison to the cooling benefits observed with the reduction in air temperature typically obtained with air conditioner use (i.e. 23 °C). It was hypothesized that given the comparable improvement in dry heat loss between an increase in air velocity from 0.2 to 4.2 m s^{-1} (at 30 °C), and a decrease in air temperature from 30 °C to 23 °C (with 0.2 m s^{-1} air velocity), the cooling benefits with fan use at 30 °C, 70%RH, in terms of a greater work output at a fixed heart rate and a lower thermal strain and discomfort, would be similar to those observed with a reduction in air temperature of 7 °C.

2. Methods

2.1. Participants

Sixteen participants (5 females, 11 males) with a mean ± SD age of 26 ± 5 years and body mass of 73.1 ± 11.5 kg were recruited to participate in the study. Females were tested during their follicular phase (between 2 and 8 days into the menstrual cycle) or were taking oral contraceptive [36]. All participants were healthy and without a history of respiratory, metabolic, cardiovascular disease, or diabetes. Each participant voluntarily provided written informed consent prior to commencing the study. The study received prior approval from the University of Sydney Human Research Ethics Committee conforming to the principles set forth in the Declaration of Helsinki, 2013. All trials were completed in a climate chamber in the Thermal Ergonomics Laboratory at the University of Sydney, New South Wales, Australia. In order to minimise any potential differences in heat acclimatisation status among participants, all data collection took place in the Australian summer months (December 2016 to February 2017 [$n = 12$]; and December 2017 to January 2018 [$n = 4$]). All trials for each participant were conducted within 4 weeks and separated by a minimum of 24 h.

2.2. Fixed heart rate experimental model

A fixed heart rate experimental model (Fig. 1) was used in order to assess the effective cooling attributable to the two different environmental modifications in the present study: an increase in radiative and convective heat loss secondary to a reduction in operative temperature (Air Cooling (AC) trial), and a greater convective and evaporative heat loss due to an increase in air velocity without any change in air temperature (HOT-FAN trial). The increase in skin surface heat loss and parallel reduction in skin temperature serves to diminish the requirement for increases in skin blood flow mediated by a cutaneous vasodilation. The greater volume of oxygenated blood that can be subsequently delivered to the working musculature at a fixed heart rate enables the generation of a higher work output on the arm ergometer. Any differences in work output can thus be directly attributed to differences in skin surface heat loss.

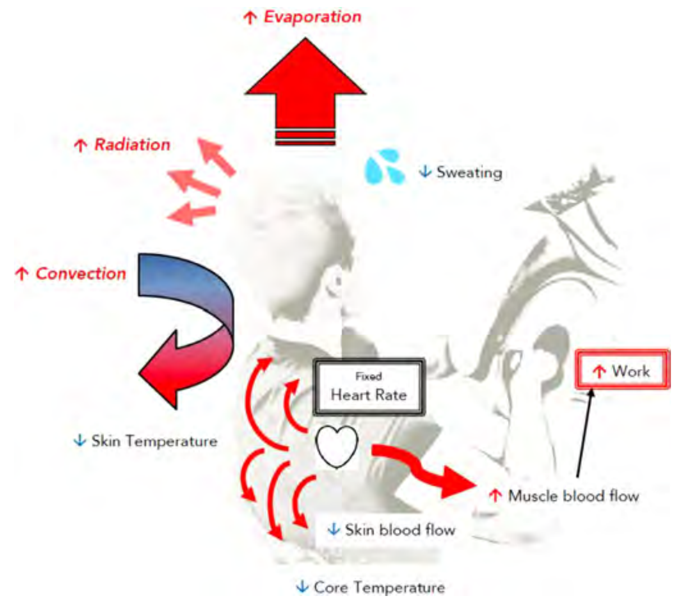

Fig. 1. A description of the link between modifications of skin surface heat loss and measured external work using a fixed heart rate experimental model.

2.3. Protocol

Preliminary session: Each participant completed a preliminary trial to become familiar with the experimental protocol and procedures. In order to mitigate any learning effects in the cognitive tasks, each participant completed five alternate repetitions of the d2 test and word recall test separated by 30 s. After, each participant completed 10 min of arm ergometry in order to determine the approximate resistance required to initially elicit the target HR of 110 beats min^{-1}.

Experimental session: Each participant completed three experimental trials presented in a counterbalanced order on separate days. On two occasions environmental conditions were regulated to mimic the mean summer indoor conditions previously measured (personal communication: Prof. Tord Kjellstrom) in a textile factory in Viet Nam (30 °C, 70%RH), with (1) 4.2 m/s of air flow (measured with a hot wire anemometer; (VelociCalc 9535, TSI Inc, Shoreview MN, USA) blowing air from an 18-inch diameter electrical fan (45 cm Moretti High-Speed Fan, Australia) placed a distance of 1 m diagonally behind the participant (HOT-FAN; Fig. 2), or (2) with still air (< 0.2 m/s) on another occasion (HOT-NO FAN). On a third occasion, ambient temperature within the chamber was regulated at 23 °C, 70%RH with still (< 0.2 m/s) air (AC).

Upon arrival, the participant donned a standardized clothing ensemble consisting of a cotton t-shirt, shorts, socks and running shoes, and was instrumented. Following 15 min of baseline rest in

Fig. 2. Photograph of experimental set-up.

a neutral environment, the participant entered the chamber and was weighed. The trial then commenced with thermal sensation and thermal comfort assessed, followed by the cognitive tasks (d2 test and word recall test), which required a total of 10 min, and then 20 min of seated arm ergometry (Angio 917,902, Lode, Netherlands) with the external workload constantly adjusted to maintain a fixed heart rate of 110 beats min^{-1}. This 30-min cycle (10 min cognitive task followed by 20 min of physical work) was repeated a total of 4 times with the last work bout followed by a final 10-min cognitive test and a final body mass measurement, resulting in a total trial length of 130 min.

2.4. Instrumentation

Rectal temperature (T_{re}) was measured using a Mon-a-therm general-purpose thermistor probe 400TM (Covidien, Mansfield, MA, USA) that was self-inserted to 12 cm beyond the anal sphincter. Skin temperature was measured using wireless iButtons (DS1921H, Maxim Integrated Products Inc., San Jose, CA, USA) secured to the chest, shoulder, thigh and calf using hypoallergenic surgical tape [23]. Mean skin temperature (T_{sk}) was estimated using a 4-point weighted mean according to Ramanathan [32]. Heart rate (HR) was monitored using a Polar RS 400 watch with chest strap (Polar Electro Oy, Kempele, Finland). Whole body sweat loss (WBSL) was estimated from pre- and post-trial body mass (±2 g) measurements [4] using a platform scale (Mettler, Germany).

Participants were asked to rate their thermal sensation (TS) using a bipolar 200 mm scale ranging from “very cold” (0 mm), through “neutral” (100 mm), to “very hot” (200 mm), and thermal discomfort (TD) using the same scale ranking from “not uncomfortable” (0 mm) through “slightly uncomfortable” (40 mm) and “uncomfortable” (80 mm) to “very uncomfortable” (120 mm). Word recall test performance assessing short-term memory was evaluated using the percentage of correctly recalled words from a total of 15 words presented in 2-s intervals on a computer screen. Performance of the “d2 test”, evaluated attention/scanning speed by asking participants to identify on a page any letter “d” with two dots above it or below it, in any order, among surrounding distractors such as a “p” with two dots, or a “d” with one or three marks. Responses were assessed using the percentage of correctly identified and marked “d2s” on a page of a total of 14 rows consisting of 56 d2s each (total = 784 d2s) [2].

2.5. Statistical analysis

Cumulative physical work output for the entire trial and WBSL were assessed using a one-way repeated measures analyses of variance (ANOVA) employing the independent variable of “condition” (3 levels: HOT-FAN, HOT-NO FAN, AC). A two-way repeated measures with the independent variable of condition and “time” (9 levels: baseline (BL), and then at the end of each alternating bout of work [W1, 2, 3 and 4] and then rest [R1, 2, 3 and 4]) was used to assess the dependent variables of HR, T_{re}, T_{sk}, TS, and TD, as well performance in the d2 and word recall tests. All two-way ANOVAs included a Mauchly’s test for sphericity and applied a Greenhouse–Geisser correction factor if required. If a significant main effect or interaction was observed, post-hoc comparisons were conducted using a Holm-Sidak multiple comparisons test. A critical alpha level error of 0.05 was maintained throughout. All statistical analyses were conducted using GraphPad Prism Version 7.0 for Windows (Graphpad Software, La Jolla, CA, USA).

3. Results

3.1. Work output

Cumulative work output (Fig. 3A–D) was altered by condition ($p < 0.001$), with more work completed in the AC (269 ± 92 kJ; $p < 0.001$) and HOT-FAN (261 ± 92 kJ; $p = 0.001$) trials relative to the HOT-NO FAN trial (236 ± 84 kJ), but similar work output between AC and HOT-FAN ($p = 0.46$). Notably, 14 of 16 participants performed more work in the HOT-FAN trial relative to the HOT-NO FAN trial (Fig. 3B), and 13 of 16 participants performed more work in the AC trial compared to the HOT-NO FAN trial (Fig. 3C). Yet, only 9 of 16 participants completed more work in the AC trial compared to the HOT-FAN trial (Fig. 3D).

3.2. Heart rate

By design, HR was similar throughout between all trials ($p = 1.00$), with mean HR 109 ± 2 beats min^{-1} in AC, 109 ± 2 beats min^{-1} in HOT-FAN, and HR 109 ± 2 beats min^{-1} in HOT-NO FAN.

3.3. Core and mean skin temperature

While T_{re} increased from baseline once physical work began ($p < 0.001$), the change in T_{re} was influenced by condition ($p = 0.036$) (Fig. 4A) with greater rises in T_{re} observed in the HOT-NO FAN trial during and after the fourth bout of physical work compared to both the HOT-FAN (W4: $p = 0.007$; R4: $p = 0.008$) and AC trials (W4: $p = 0.012$; R4: $p = 0.010$).

Skin temperature was higher ($p < 0.001$) throughout the HOT-NO FAN trial compared to the HOT-FAN and AC trial by ~1.5 °C and ~2.0 °C respectively (Fig. 4B). However, at all but one time point (W2) T_{sk} was ~0.5 °C higher in the HOT-FAN trial ($p < 0.028$) compared to AC.

3.4. Whole body sweat loss

Cumulative whole-body sweat losses (Fig. 3C) were altered by condition ($p < 0.001$), with WBSL greater in the HOT-NO FAN trial (724 ± 283 g) compared to HOT-FAN (645 ± 259 g; $p = 0.038$) and AC trials (564 ± 260 g; $p < 0.001$). WBSL was also greater in the HOT-FAN trial compared to the AC trial ($p = 0.038$). Converted into whole-body sweat rates (in g h^{-1}), values were 322 ± 130,

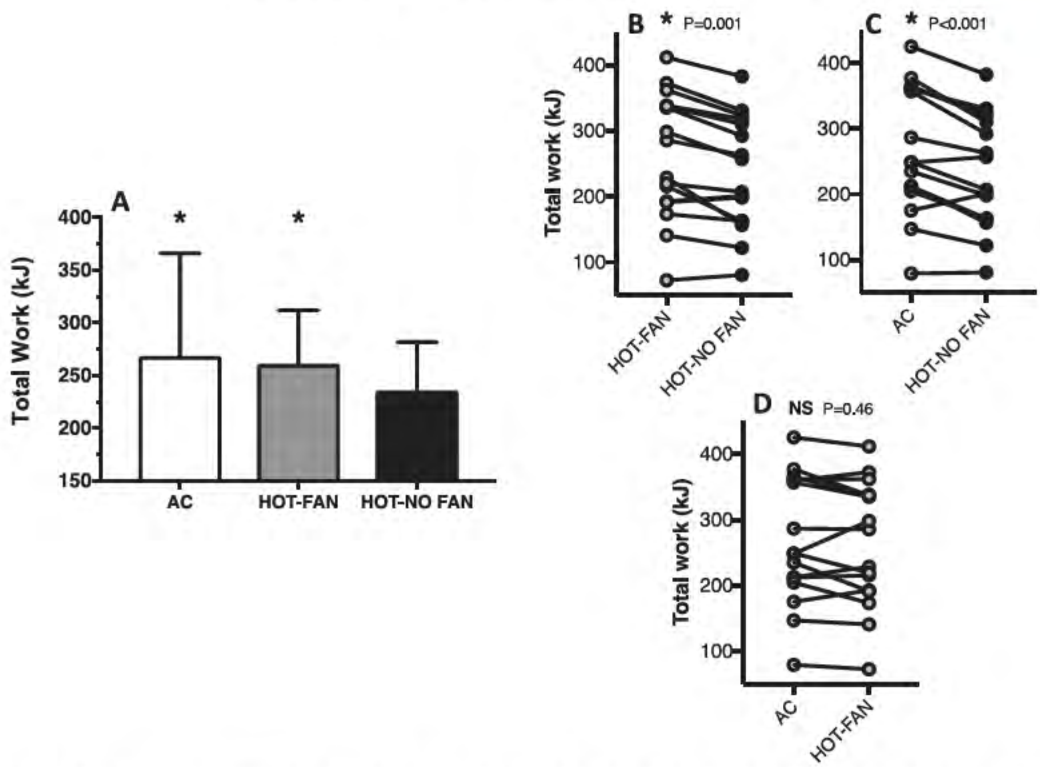

Fig. 3. (A–D) Mean total work (A) performed throughout the entire experimental protocol in the hot still air (HOT-NO FAN; black bar), hot with fan use (HOT-FAN; grey bar) and air conditioned (AC; white bar) trials. Error bars are SD. Panels B–D report individual data [$n = 16$] for each condition. Asterisk (*) different to the HOT-NO FAN condition ($p \leq 0.001$).

287 ± 119, and 251 ± 119 g h^{-1} in the HOT-NO FAN, HOT-FAN and AC trials respectively.

3.5. Thermal sensation and discomfort

A greater level of thermal discomfort (Fig. 5A) was reported in the HOT-NO FAN compared to the HOT-FAN and AC trials ($p < 0.001$). Moreover, as trial time progressed a gradual alteration in thermal discomfort was observed ($p = 0.007$) with a greater level of discomfort reported in the AC trial during the third ($p = 0.002$) and fourth ($p = 0.004$) bout of physical work compared to the HOT-FAN trial.

A main effect of condition ($p < 0.001$) was observed for thermal sensation (Fig. 5B), with TS cooler in HOT-FAN and AC trials compared to HOT-NO FAN ($p < 0.001$), but a similar TS observed between HOT-FAN and AC trials throughout ($p = 0.28$).

3.6. Cognitive performance

Performance in the d2 test was not different between conditions ($p = 0.52$) but declined with trial time ($p = 0.035$). The mean number of correct answers was 83 ± 13%, 83 ± 12% and 82 ± 14% in the HOT-NO FAN, HOT-FAN and AC trials respectively. Similarly, word recall test performance was not different between conditions ($p = 0.58$) or altered by trial time ($p = 0.58$), with the mean number of correctly recalled words 9 ± 2, 10 ± 2 and 10 ± 2 in the HOT-NO FAN, HOT-FAN and AC trials respectively.

4. Discussion

An increase in convective flow using a simple electric fan in conditions corresponding to a typical hot occupational environment in South East Asia (30 °C, 70%RH) yielded improvements in cumulative work output, thermal sensation and discomfort at a fixed heart rate of 110 beats min^{-1}, that were all at least equivalent to those resulting from a ~7 °C reduction in air temperature. Despite the greater work output with fan use at 30 °C, 70%RH, skin temperatures were ~1.5 °C lower than without fanning and participants were less dehydrated.

Forcing air across the skin is a much less electricity-intensive cooling strategy than chilling air. In the present study we used an air temperature of 23 °C as a reference condition (air cooling trial) as this is the typical indoor temperature set-point employed in air conditioned places in many SE Asian countries [21], albeit not with the slightly elevated air movement that sometimes accompanies indoor air conditioning. Moreover, it should be noted that 70% RH is very much at the upper humidity limit for thermal comfort at 23 °C [1] and a true air-conditioned environment would likely be at a lower relative humidity. The ambient conditions of 30 °C, 70%RH were chosen to mimic the mean summer indoor conditions in many occupational settings. The electricity requirement of the fan used in the present study was 55 W, which is approximately 30-times lower than the wattage required using central air conditioning to cool a 90 m^3 working space with 6 occupants with a sedentary rate of metabolic heat production with no additional heat from machinery and equipment. Even if each occupant is targeted with an individual fan, this basic and rather conservative estimate suggests that the electricity requirements and associated CO_2 emissions for convectively cooling each individual could still be one-fifth of air conditioning. In view of the projected dramatic rise of potential air conditioner use with global warming in heavily populated countries such as India, China, Indonesia, Viet Nam, Thailand and Bangladesh [5], advocacy of convective cooling as an effective alternative that is cleaner, has lower capital and operating costs, and contributes negligibly to peak demand problems on electricity infrastructure, would seem to be judicious. Indeed,

RECORD 5

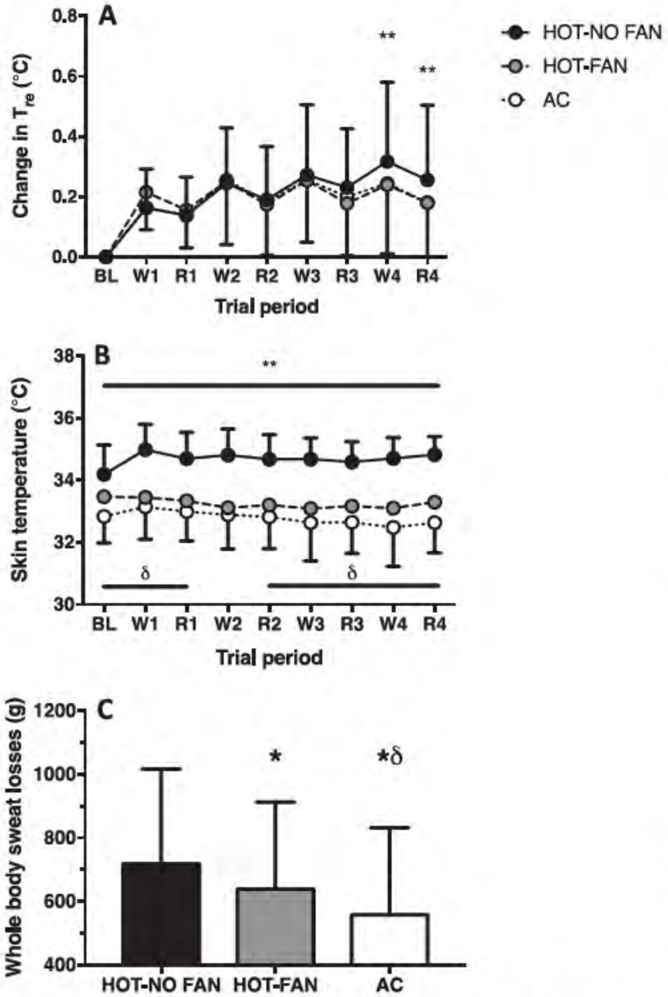

Fig. 4. (A–C) Mean change in rectal temperature (A), and mean skin temperature (B) during baseline (BL), four work (W1-4) and four rest (R1-4) periods; and whole body sweat loss (C) throughout the entire trial in the HOT-NO FAN (black), HOT-FAN (grey) and AC (white) trials. Error bars are 95% CIs. Asterisk (*) different to HOT-NO FAN. Double asterisk (**) both AC and HOT-FAN different to HOT-NO FAN. Delta (δ) different to HOT-FAN.

moving rather than chilling air may be cleaner still if the energy demands required to generate convective flow are met using renewable means (e.g. solar power). It is unclear whether other low-energy cooling strategies, such as cooling vests, may elicit a similar effect on work output in the same setting. However, it is usually necessary to regularly replace the cooling stimulus (e.g. ice/cold packs) to prevent a diminished efficacy of conductive skin contact cooling, and relatively large-scale refrigeration/freezing is still required to individually equip a workforce with such cooling garments.

A greater amount of work at a fixed heart rate was possible in the HOT-FAN and AC trials compared to the HOT-NO FAN condition, presumably due to a lower physiological requirement to deliver blood to the skin surface and therefore a greater availability of blood to deliver oxygen to working muscles. While skin blood flow was not measured, the blunted rise in skin temperature in the HOT-FAN and AC trials likely led to a lower locally mediated cutaneous vasodilation [25]. In both cases elevations in skin temperature were mitigated by a greater dry heat loss, augmented by a greater convective heat transfer coefficient in the HOT-FAN trial, and a greater temperature gradient between skin and air enhancing heat loss by both convection and radiation in the AC trial. In the case of the HOT-FAN trial, skin temperature rises would have been further blunted by enhanced sweat evaporation secondary to a higher evaporative heat transfer coefficient. Despite the greater metabolic rate associated with higher work rates in the HOT-FAN trial and AC trials, the rate of dehydration, indicated by whole-body sweat losses, was lower in both trials compared to the HOT-NO FAN trial. In both trials higher rates of internal heat production would have been offset by greater non-evaporative heat loss (i.e. convection and/or radiation) requiring less evaporation, and therefore sweating to attain heat balance. Moreover, the greater convective flow across the skin with fan use would have also increased evaporative efficiency resulting in the evaporation of a greater proportion of secreted sweat compared to a relatively still environment [3].

The rise in rectal temperature was slightly blunted (~0.1 °C) by either fan use or air cooling towards the end of the 135-min trial, despite a greater internal heat production associated with a higher work output. Moreover, the environment was perceived to be cooler and less uncomfortable in both the HOT-FAN and AC trials compared to the HOT-NO FAN trial. Notably, these subjective sensations were at least as cool and comfortable with fan use at 30 °C than without fan use at 23 °C. The slightly greater level of discomfort reported in the AC trial relative to the HOT-FAN trial may be attributable to a greater wettedness since a more complete evaporation of secreted sweat on the skin surfaces exposed to greater air flow would be expected with fan use and therefore a lower local skin wettedness despite a higher whole-body sweat rate [7]. Again, it should be noted that in a truly air-conditioned environment air velocity may be elevated in some areas, and relative humidity would likely be lower, relative to the present AC trial such that these differences may not be observed in a real-world setting. No differences in cognitive performance were observed between trials using the tasks selected to assess short-term memory (word recall) and attention/scanning speed (d2 test). Recent evidence suggests that while minimal to no influence of the heat

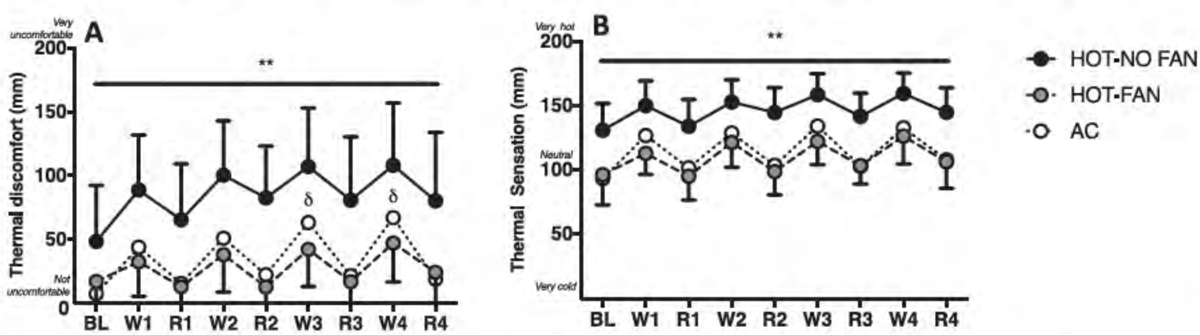

Fig. 5. (A,B) Mean thermal discomfort (A) and thermal sensation (B) scores at baseline (BL) and during the four work (W1-4) and four rest (R1-4) periods in the HOT-NO FAN (black), HOT-FAN (grey) and AC (white) trials. Error bars are 95% CIs. Asterisk (*) different to HOT-NO FAN. Double asterisk (**) both AC and HOT-FAN different to HOT-NO FAN. Delta (δ) AC different to HOT-FAN.

is observed on simple cognitive tasks, the performance of combined cognitive and complex motor tasks may be impaired [31]. Whether heat-related decrements in these more complex tasks are improved by convective flow, if indeed they are ecologically relevant to a particular occupational setting, is yet to be determined.

The fixed heart rate experimental model employed in the present study was chosen above other fixed physiological parameters for several reasons; indeed, if sweat rate was the fixed variable then work output may have declined with fan use. A fixed heart rate seems to be most consistent with how exercise (and thus work) output is self-regulated with an increasing heat load. Rather than simply accepting ever increasing body temperatures, work output tends to be selected to maintain a stable cardiovascular load [14,29,30]. Variables such as sweat rate only indirectly determine self-selected work output secondarily throughout alterations in cardiovascular load, and only after reaching a critical level of dehydration [34]. Practically speaking, heart rate is also easily measured with good accuracy. The average heart rate limit of 110 beats min^{-1} employed in the present study was based on a recommendation from a WHO scientific report for working conditions of heat stress [38] for workers conducting physical activity for a complete work day, and not 130 min. As the authors of the report suggest, several factors including worker age and physical condition must also be considered when choosing an appropriate target heart rate. Future studies employing activities that engage larger muscles groups (e.g. treadmill walking) and different clothing properties for similarly shorter durations might require a higher target heart rate limit as the combined heat stress might elicit average heart rates exceeding 110 beats min^{-1} with little or even no work performed. For future studies using the arm ergometry model employed in the present study, within-subject comparisons might be better performed using a fixed change in heart rate from thermoneutral rest, as participants with low resting heart rates require quite a high work output to achieve 110 beats min^{-1} which can prove quite difficult due to local muscular fatigue.

A major limitation for using the horizontal movement of air mass to induce convective flow across the skin in some occupational environments is the potentially hazardous disturbance of particulate matter or gases causing ocular and/or respiratory distress. However for jobs that require the worker to be seated, the recent development of personal comfort systems composed of a user-controlled chair with built-in low-energy fans individually targeting the back of the torso and upper legs [28] may provide a safe alternative to the use of pedestal and floor fans or inducing high levels of environmental mass flow. The efficacy of these devices for cooling seated but physically active workers in hot occupational environments would require experimental verification. Other future research directions include the assessment of the impact of clothing, which may vary considerably between different countries and cultures, upon the cooling effect of moving air instead of chilling it. Moreover, while the upper ambient temperature tested in the present study was based on in-situ environmental measurements, the potentially diminishing benefit of convective cooling at higher air temperatures, particularly those over 35 °C when increases in dry heat loss with greater air flow become dry heat gain, need to be determined with different humidity levels. Even at the same ambient temperature as the present study, greater level of humidity would also limit the observed benefit of fanning. Collectively, while the present study demonstrates proof-of-concept for fan use as an alternative cooling strategy to air cooling, applications will ultimately be limited depending on the environment, as well as clothing of the individual. While the fixed heart rate method is based on the notion that workers will naturally self-regulate work output to attain a stable cardiovascular load [14], it is possible that if self-pacing was permitted in the present study the differences in work output would have been eliminated; however this would have presumably occurred at the expense of a greater physiological and perceptual strain. Finally, fanning within spaces that are still air-conditioned also has the potential to drastically reduce net HVAC energy demands. The greater convective and evaporative heat loss for a given air temperature (< 35 °C) with more air movement means that the same net cooling effect can be achieved with less air cooling. The high air speeds used in the present study would likely induce thermal discomfort at lower air temperatures but augmented air movement up to ~1 m s^{-1} [1] should still elevate the upper air temperature at which thermal discomfort for a particular workload occurs.

In conclusion, compared to no fan use in conditions representative of a typical hot occupational environment in South East Asia (30 °C, 70%RH), the use of a simple electric fan yielded equivalent improvements in work output (~11%) at a fixed average heart rate (of 110 beats min^{-1}) to a ~7 °C reduction in air temperature. In parallel, reductions in skin temperature, thermal sensation, and the rate of dehydration, as well as improvements in thermal comfort with fan use compared to no fan use at 30 °C, 70%RH were all similar to a 23 °C, 70%RH environment. Cognitive performance of tasks selected to assess short-term memory and attention/scanning speed were similar in all conditions.

Funding

This study was funded by a University of Sydney Bridging Grant.

Declaration of interests

None.

References

[1] ANSI/ASHARE, Standard 55: 2017, Thermal Environmental Conditions for Human Occupancy, ASHRAE, Atlanta, 2017.
[2] M.E. Bates, E.P. Lemay Jr., The d2 test of attention: construct validity and extensions in scoring techniques, J. Int. Neuropsychol. Soc. 10 (2004) 392–400.
[3] V. Candas, J.P. Libert, J.J. Vogt, Influence of air velocity and heat acclimation on human skin wettedness and sweating efficiency, J. Appl. Physiol. 47 (1979) 1194–1200.
[4] S.N. Cheuvront, R.W. Kenefick, CORP: improving the status quo for measuring whole body sweat losses, J. Appl. Physiol. 123 (2017) 632–636.
[5] L.W. Davis, P.J. Gertler, Contribution of air conditioning adoption to future energy use under global warming, P. Natl. Acad. Sci. USA 112 (2015) 5962–5967.
[6] R.J. DeDear, G. Brager, Developing an adaptive model of thermal comfort and preference, ASHRAE Trans. 104 (1998) 145–167.
[7] T. Fukazawa, G. Havenith, Differences in comfort perception in relation to local and whole body skin wettedness, Eur. J. Appl. Physiol. 106 (2009) 15–24.
[8] A.P. Gagge, Y. Nishi, Heat exchange between human skin surface and thermal environment, sect. 9, in: Handbook of Physiology, American Physiological Society, Bethesda, MD, 1977, pp. 69–92.
[9] F. Golbabaei, A. Mazloumi, S.M. Khani, Z. Kazemi, M. Hosseini, M. Abbasinia, S.F. Dehghan, The effects of heat stress on selective attention and reaction time among workers of a hot industry: application of computerized version of Stroop test, J. Health Saf. Work 5 (2015) 240–246.
[10] R.T. Gun, G.M. Budd, Effects of thermal, personal and behavioural factors on the physiological strain, thermal comfort and productivity of Australian shearers in hot weather, Ergonomics 38 (1995) 1368–1384.
[11] S. Hallegatte, Strategies to adapt to an uncertain climate change, Global Environ. Change 19 (2009) 240–247.
[12] J. Hansen, M. Sato, R. Ruedy, K. Lo, D.W. Lea, M. Medina-Elizade, Global temperature change, Proc. Natl. Acad. Sci. USA 103 (2006) 14288–14293.
[13] J.D. Hardy, E.F. Dubois, The technique of measuring radiation and convection, J. Nutr. 15 (1938) 461–475.
[14] N. Junge, R. Jørgenson, A.D. Flouris, L. Nybo, Prolonged self-paced exercise in the heat–environmental factors affecting performance, Temperature 3 (2016) 539–548.
[15] G.P. Kenny, O. Jay, Thermometry, calorimetry, and mean body temperature during heat stress, Compr. Physiol. 3 (2013) 1689–1719.
[16] T. Kjellstrom, Impact of climate conditions on occupational health and related economic losses: a new feature of global and urban health in the context of climate change, Asia Pac. J. Public Health 28 (2016) 28S–37S.

[17] T. Kjellstrom, I. Holmer, B. Lemke, Workplace heat stress, health and productivity—an increasing challenge for low and middle-income countries during climate change, Global Health Action 2 (2009) 2047.
[18] T. Kjellstrom, R.S. Kovats, S.J. Lloyd, T. Holt, R.S. Tol, The direct impact of climate change on regional labor productivity, Arch. Environ. Occup. Health 64 (2009) 217–227.
[19] T. Kjellstrom, B. Lemke, M. Otto, Climate conditions, workplace heat and occupational health in South-East Asia in the context of climate change, WHO South East Asia J. Public Health 6 (2017) 15–21.
[20] T. Kjellstrom, M. Otto, B. Lemke, O. Hyatt, D. Briggs, C. Freyberg, L. Lines, Climate Change and Labour: Impacts of Heat in the Workplace, in: M. Mckinnon, E. Buckle, K. Gueye, I. Toroitich, D. Ionesco, E. Mach (Eds.), United Nations Development Agency (UNDP), 2016.
[21] A.G. Kwok, J. Reardon, K. Brown, Thermal comfort in tropical classroms/discussion, ASHRAE Trans. 104 (1998) 1031.
[22] K. Lundgren, K. Kuklane, C. Gao, I. Holmer, Effects of heat stress on working populations when facing climate change, Ind. Health 51 (2013) 3–15.
[23] W.D. van Marken Lichtenbelt, H.A.M. Daanen, L. Wouters, R. Fronczek, R.J.E.M. Raymann, N.M.W. Severens, E.J.W. Van Someren, Evaluation of wireless determination of skin temperature using iButtons, Physiol. Behav. 88 (2006) 489–497.
[24] G.A. Meehl, C. Tebaldi, More intense, more frequent, and longer lasting heat waves in the 21st century, Science 305 (2004) 994–997.
[25] C.T. Minson, L.T. Berry, M.J. Joyner, Nitric oxide and neurally mediated regulation of skin blood flow during local heating, J. Appl. Physiol. 91 (2001) 1619–1626.
[26] C. Mora, B. Dousset, I.R. Caldwell, F.E. Powell, R.C. Geronimo, C.R. Bielecki, C.W. Counsell, B.S. Dietrich, E.T. Johnston, L.V. Louis, M.P. Lucas, M.M. Mckenzie, A.G. Shea, H. Tseng, T. Giambelluca, L.R. Leon, E. Hawkins, C. Trauernicht, Global risk of deadly heat, Nat. Clim. Change 7 (2017) 501–506.
[27] D.S. Moran, A. Shitzer, K.B. Pandolf, A physiological strain index to evaluate heat stress, Am. J. Physiol. 275 (1998) R129–R134.
[28] W. Pasut, H. Zhang, E. Arens, Y.C. Zhai, Energy-efficient comfort with a heated/cooled chair: results from human subject tests, Build Environ. 84 (2015) 10–21.
[29] J. Périard, M.N. Cramer, P. Chapman, C. Caillaud, M.W. Thompson, Cardiovascular strain impairs prolonged self-paced exercise in the heat, Exp. Physiol. 96 (2011) 134–144.
[30] J. Périard, S. Racinais, Self-paced exercise in hot and cool conditions is associated with the maintenance of %VO_{2peak} within a narrow range, J. Appl. Physiol. 118 (2015) 1258–1265.
[31] J.F. Piil, J. Lundbye-Jensen, S.J. Trangmar, L. Nybo, Performance in complex motor tasks deteriorates in hyperthermic humans, Temperature 4 (4) (2017) 420–428.
[32] N.L. Ramanathan, A new weighting system for mean surface temperature of the human body, J. Appl. Physiol. 19 (1964) 531–533.
[33] L.B. Rowell, Cardiovascular aspects of human thermoregulation, Circ. Res. 52 (1983) 367–379.
[34] M.N. Sawka, S.N. Cheuvront, R.W. Kenefick, Hypohydration and human performance: impact of environment and physiological mechanisms, Sports Med. 45 (2015) S51–S60.
[35] M. Sivak, Will AC put a chill on the global energy supply? Am. Sci. 101 (2013) 330–333.
[36] J. Słomko, P. Zalewski, The circadian rhythm of core body temperature (Part I): the use of modern telemetry systems to monitor core body temperature variability, Pol. Hyperb. Res. 55 (2016) 79–83.
[37] V. Venugopal, J.S. Chinnadurai, R.A. Lucas, T. Kjellstrom, Occupational heat stress profiles in selected workplaces in India, Int. J. Environ. Res. Public Health 13 (2015) E89.
[38] World Health Organization, Scientific group on health factors involved in working under conditions of heat stress, Health Factors Involved in Working Under Conditions of Heat Stress; Report of a WHO Scientific Group, World Health Organization, 1969.

Title
Human thermal sensation and comfort in transient and non-uniform thermal environments

Author
Zhang, H.

Publication Date
2003-09-01

Peer reviewed

Human Thermal Sensation and Comfort in Transient and Non-Uniform Thermal Environments

by

Hui Zhang

B.E. (Tsinghua University) 1983
M.E. (Tsinghua University) 1986

A dissertation submitted in partial satisfaction of the

requirement for the degree of

Doctor of Philosophy
in

Architecture

in the

GRADUATE DIVISION

of the

UNIVERSITY OF CALIFORNIA, BERKELEY

Committee in charge:

Professor Edward A. Arens, Chair
Professor Gail S. Brager
Professor Boris Rubinsky
Specialist Charlie Huizenga

Fall 2003

Title

Human Thermal Sensation and Comfort

in Transient and Non-Uniform Thermal Environments

by

Hui Zhang

The dissertation of Hui Zhang is approved:

Chair 12/9/03
Date

12/9/03
Date

12/11/03
Date

12/11/03
Date

University of California, Berkeley

Fall 2003

Abstract

Human Thermal Sensation and Comfort

in Transient and Non-Uniform Thermal Environments

by

Hui Zhang

Doctor of Philosophy in Architecture

University of California, Berkeley

Professor Edward A. Arens, Chair

Most existing thermal comfort models are only applicable only in uniform, steady-state thermal environments. This thesis presents results from 109 human subject tests that were performed under non-uniform and transient conditions in the UC Berkeley Controlled Environmental Chamber. In these tests, local body surfaces of the subjects were independently heated or cooled while the rest of the body was exposed to a warm, neutral or cool environment. Skin temperatures, core temperature, thermal sensation and comfort responses were collected at one- to three-minute intervals. Based on these tests, we have developed predictive models of local and overall thermal sensation and comfort:

- Local thermal sensation for 19 body parts
- Local thermal comfort model for 19 body parts
- Overall sensation model
- Overall comfort model

A separate set of tests was carried out in an automobile in a climate-controlled wind tunnel at the Delphi Harrison facility in Lockport, NY. These tests simulated conditions found in vehicles during both hot and cold weather. The subjects' body temperatures, thermal sensation and thermal comfort were measured similarly to those in the UCB chamber tests. The results of the Delphi tests were primarily used for model validation. The validation results show that the models predicted the actual sensation and comfort votes well.

The models will be useful for designing and evaluating non-uniform and transient environments in buildings, vehicles, and outdoors.

TABLE OF CONTENTS

1. Introduction 1

2. Background 3

2.1 Physical basis of thermal sensation 5
2.1.1 Thermoreceptors 5
2.1.2 Hypothalamus thermoregulation 8
2.2 Models of thermal sensation in stable asymmetrical conditions 10
2.2.1 Weighting factor approach 10
2.2.2 EHT and Piste 14
2.3 Models of dynamic thermal sensation 16
2.4 Sensation and comfort 22
2.5 Need for human subject tests 25

3. Objectives 27

4. Methods 29

4.1 General description of the experiment 29
4.2 Experimental Facility 30
4.2.1 Controlled Environmental Chamber 30
4.2.2 Local warm- and cold-air supplies 31
4.2.3 Pre-conditioning bath 32
4.2.4 Air sleeves for local cooling and heating 34
4.2.4.1 General air-sleeve design 36
4.2.4.2 Leotard 37
4.2.4.3 Air-sleeve design for different body parts 38
4.3 Measurement 45
4.3.1 Skin Temperature Measurement 45
4.3.1.1 Skin Temperature Measurement Sites 45
4.3.1.2 Thermocouples 48
4.3.1.2.1 Calibration of the thermocouples 49
4.3.1.2.2 Data acquisition 50
4.3.2 Core temperature measurement 50
4.3.2.1 Wireless Sensor Pill 50
4.3.2.2 Discussion of core measurement methods 52
4.3.3 Thermal sensation and comfort 53
4.3.3.1 Seven-point sensation scale and Bedford's comfort scale 53
4.3.3.2 Sensation and comfort scales used in our tests 55
4.4 Test description 58
4.4.1 Test procedure 58
4.4.2 Types of tests 59

4.4.2.1 Single body part cooling and heating test 59
4.4.2.2 Multiple segment cooling and heating test 62
4.4.2.3 Whole-body step-change tests 63
4.4.2.4 Neutral-condition tests 64
4.4.2.5 Taking Infrared video images 65
4.4.2.6 Delphi Wind Tunnel tests 66
4.5 Human subjects 72
4.5.1 UCB subjects 72
4.5.2 Body composition information 73
4.5.3 Subjects' clothing 74
4.5.4 Metabolic level of subjects 75
4.5.5 Delphi subjects 75
5. Test Results, Physiological and Subjective Responses 77

5.1 Introduction 77
5.2 Stable/uniform environments 79
5.2.1 Neutral-conditions tests 79
5.2.1.1 Skin temperature set points 80
5.2.1.1.1 Experimental results 80
5.2.1.1.2 Comparison with values in the literature 82
5.2.1.2 Sensation and comfort in neutral conditions 84
5.2.1.3 Responses over time 88
5.2.2 Cold-condition tests 91
5.2.2.1 Skin temperature distribution 92
5.2.2.2 Thermal sensation and comfort distribution 94
5.2.2.3 Responses over time 96
5.2.3 Warm-condition tests 98
5.2.3.1 Skin temperature distribution 98
5.2.3.2 Thermal sensation and comfort distribution 100
5.2.3.3 Responses over time 102
5.3 Stable/non-uniform environments 104
5.4 Correlating skin temperature and local sensation: stable environments 105
5.5 Transient/non-uniform environments 106
5.5.1 Cooling and heating of a single body part 107
5.5.1.1 A typical test sequence 111
5.5.1.2 Relative influence of body parts on overall sensation and comfort 113
5.5.1.2.1 Most influential group 116
5.5.1.2.2 Least influential group 127
5.5.1.2.3 Moderately influential group 141
5.5.1.2.4 Breath intake air: warming vs. cooling 153
5.5.1.2.5 Statistical significance of the three groups 158
5.5.1.2.6 Correlating skin temperature and its rate of change with local sensation 160
5.5.1.3 Core temperature responses 161
5.5.1.3.1 Local cooling in warm environment 161
5.5.1.3.2 Local heating in cold environment 165
5.5.1.3.3 Local cooling in cold environment 167
5.5.1.4 Sensation voting behavior during transients 169
5.5.1.5 Comfort vote overshooting during heat stress removal 173
5.5.2 Effects of cooling and heating multiple body parts 177

5.5.2.1 Chest cooling + hand cooling........178
5.5.2.2 Neck cooling + foot cooling........180
5.5.2.3 One-hand heating + one-hand cooling........182
5.5.2.4 Core temperature responses in multiple thermal application........186
5.5.3 Repeatability of sensation and comfort votes........187
5.5.4 Changing the order of body parts undergoing local cooling........190
5.5.5 Cooling one hand or foot does not affect the other hand or foot........190
5.6 Transient/uniform environments (whole-body step-change tests)........194
5.6.1 Skin temperature, sensation, and comfort........194
5.6.2 Core temperature responses in whole body step-change processes........199
5.7 Additional physiological and subjective observations........200
5.7.1 Hand and finger temperatures........200
5.7.1.1 Hand and finger skin temperatures in stable environment........200
5.7.1.2 Hand motion increases hand and finger temperatures........203
5.7.2 Hand skin temperature recovery speed after local cooling........205
5.7.3 Local skin temperature and its impact on heat loss........210
5.7.3.1 Face and forehead........210
5.7.3.2 Back of the head........211
5.7.3.3 Neck........212
5.7.3.4 Lower arm and upper arm........213
5.7.3.5 Hand........214
5.7.3.6 Whole body, legs, and feet........216
5.8 Overall summary of test results........218
5.9 Database........224
6. Model Development........225

6.1 Brief overview of the models........226
6.1.1 Local thermal sensation model........229
6.1.2 Local thermal comfort model........232
6.1.3 Overall thermal sensation model........237
6.1.4 Overall thermal comfort model........239
6.2 Local thermal sensation model........240
6.2.1 Static local sensation model........240
6.2.1.1 Logistic function........240
6.2.1.2 Impact of whole-body thermal state on local thermal sensation........244
6.2.1.2.1 Experimental observations........244
6.2.1.2.2 Experimental observations by other researchers........246
6.2.1.2.3 Mathematical description........248
6.2.1.3 Regression results........249
6.2.1.4 Body builder impact........253
6.2.1.5 Analysis of the regression results........253
6.2.1.6 Adaptation........254
6.2.2 Dynamic model for local sensation in transient conditions........258
6.2.3 The complete local thermal sensation model........262
6.2.4 Local thermal sensation model validation........264
6.2.5 Use of mean skin temperature ($\overline{T}_{skin}$) and $\frac{dT_c}{dt}$........269
6.3 Local thermal comfort model........273
6.3.1 Results from literature and our tests........273
6.3.2 Key hypotheses for the local comfort model........283

6.3.3 Mathematical description ... 285
6.3.4 Regression results ... 294
6.3.5 Analysis of the regression results ... 298
6.3.6 Discussion ... 303
6.3.7 Validation of the local thermal comfort model – the saddle model ... 305
6.4 Overall thermal sensation model ... 310
6.4.1 Proposing an integration model involving weighting factors ... 311
6.4.2 Regression results ... 315
6.4.3 Analysis of the regression results ... 316
6.4.4 Overall sensation model validation ... 318
6.4.4.1 Validation using Delphi test data ... 318
6.4.4.2 Validation using UCB stable-condition tests ... 321
6.4.5 Discussion of the overall sensation model ... 324
6.5 Overall thermal comfort model ... 326
6.5.1 Process of developing the overall thermal comfort model ... 327
6.5.2 Validation of the model ... 331
6.5.2.1 Validation using Delphi test data ... 332
6.5.2.2 Validation using UCB steady-state-tests ... 334
6.5.3 Discussion of the overall comfort model ... 339
7. Conclusion ... 343
7.1 New sensation and comfort models ... 343
7.2 Limitations ... 345
7.2.1 Local sensation model during exercise ... 345
7.2.2 Skin wettedness and discomfort ... 346
7.3 Implications for thermal environmental control ... 347
7.4 Suggestions for Future Work ... 348
7.4.1 Future studies ... 348
7.4.2 Recommendations for experimental methods ... 352
8. References ... 354
9. Appendices ... 363
9.1 Appendix 4.1 – Selection of a method to cool/heat local skin temperature ... 363
9.2 Appendix 4.2 - Skin temperature measurement sites ... 369
9.3 Appendix 4.3 – Comparison of three core temperature measurements ... 378
9.4 Appendix 4.4 - Test conditions ... 385
9.5 Appendix 4.5 – A paper accepted for the SAE Technical Paper Series ... 389
9.6 Appendix 5.1 – Database ... 390
9.7 Appendix 6.1 - Adaptation model ... 392
9.8 Appendix 6.2 - Core temperature prediction model ... 398
9.9 Appendix 6.3 – Body composition influences on local sensation ... 403
9.10 Appendix 6.4 – Skin temperature data smoothing ... 405
9.11 Appendix 6.5 – A paper for the European Journal of Applied Physiology ... 409
9.12 Appendix 7.1 – Implications for air-conditioning ... 410

LIST OF FIGURES

Figure 2.1. Frequencies of discharge of thermoreceptors (Zotterman 1953).
Figure 2.2 General properties of thermoreceptors (Hensel 1981)
Figure 2.3 Hypothalamus and thermoregulation (Benzinger, Pratt et al. 1961)
Figure 2.4 Skin temperature measurement points (Hagino and Hara 1992)
Figure 2.5 EHT piste (Wyon 1989)
Figure 2.6 Zone-like piste proposed by Nilsson (Nilsson 2003)
Figure 2.7 Face Skin Temperature Measurement Points (Taniguchi et al. 1992)
Figure 4.1 The controlled environmental chamber setup
Figure 4.2 Local cold- and warm-air supplies
Figure 4.3 Jacuzzi to precondition subjects' thermal states
Figure 4.4 Skin temperature distribution after cooling with an air sleeve
Figure 4.5 Design details of the air sleeve
Figure 4.6 Thermal manikin measuring leotard clothing insulation value
Figure 4.7 Breathing air sleeve
Figure 4.8 Head air sleeve
Figure 4.9 Neck air sleeve
Figure 4.10 Face air sleeve
Figure 4.11 Use goggles in a test
Figure 4.12 Chest air sleeve
Figure 4.13 Back and pelvis air sleeves
Figure 4.14 Arm air sleeve
Figure 4.15 Hand air sleeve
Figure 4.16 Leg air sleeve
Figure 4.17 Foot air sleeve
Figure 4.18 Twenty-two skin temperature measurement locations
Figure 4.19 Subject wearing thermocouples and leotard during a test
Figure 4.20 Thermocouple, calibration, and data-acquisition system
Figure 4.21 Ingestible thermometer pill and recorder (HTI Technologies, Inc.)
Figure 4.22 Thermal sensation and comfort scales
Figure 4.23 Delphi Harrison Thermal Systems Climatic Wind Tunnel
Figure 4.24 Car in the Wind Tunnel during Delphi Wind Tunnel tests
Figure 4.25 Human subject tests in the Delphi Wind Tunnel
Figure 4.26 A sample of sensation and comfort questionnaires (Delphi)

Figure 4.27	Measuring height and body fat of a subject
Figure 5.1	Data used to represent different environmental conditions
Figure 5.2	Skin temperatures under neutral conditions
Figure 5.3	Comfort votes under neutral conditions
Figure 5.4	Thermal sensation under neutral conditions
Figure 5.5	Thermal sensation and comfort under neutral conditions
Figure 5.6	Core and mean skin temperature over time under neutral conditions
Figure 5.7	Local skin temperature over time under neutral conditions
Figure 5.8	Skin temperature distribution in a cold environment
Figure 5.9	Additional skin temperature distributions in a cold environment
Figure 5.10	Thermal sensation and comfort under cold conditions
Figure 5.11	Local skin temperature over time in a cold environment
Figure 5.12	Sensation, comfort, core temperature over time in a cold environment
Figure 5.13	Skin temperature distribution in a warm environment
Figure 5.14	Thermal sensation and comfort under warm conditions
Figure 5.15	Local skin temperature over time in a warm environment
Figure 5.16	Sensation, comfort, core temperature over time in a warm environment
Figure 5.17	Skin temperature, local and overall thermal sensation in one test
Figure 5.18	Skin temperature, overall sensation and comfort in one test
Figure 5.19	The three groups of body parts
Figure 5.20-1	Back and overall thermal sensation during back cooling
Figure 5.20-2	Chest and overall thermal sensation during chest cooling (a)
Figure 5.20-3	Chest and overall thermal comfort during chest cooling (a)
Figure 5.20-4	Chest and overall thermal sensation during chest cooling (b)
Figure 5.20-5	Chest and overall thermal comfort during chest cooling (b)
Figure 5.20-6	Pelvis and overall thermal sensation during pelvis cooling
Figure 5.20-7	Pelvis and overall thermal comfort during pelvis cooling
Figure 5.21	Pelvis and overall thermal sensation during pelvis cooling in the cold
Figure 5.22-1	Chest and overall thermal sensation during chest heating
Figure 5.22-2	Chest and overall thermal comfort during chest heating
Figure 5.22-3	Back and overall thermal sensation during back heating
Figure 5.22-4	Back and overall thermal comfort during back heating
Figure 5.23	Right foot skin temperature after cooling
Figure 5.24-1	Foot and overall thermal sensation during foot cooling (a)
Figure 5.24-2	Foot and overall thermal sensation during foot cooling (b)

Figure 5.24-3 Foot and overall thermal sensation and comfort during foot cooling (a)
Figure 5.24-4 Foot and overall thermal sensation and comfort during foot cooling (b)
Figure 5.24-5 Hand and overall thermal sensation during hand cooling
Figure 5.24-6 Hand and overall thermal comfort during hand cooling
Figure 5.25-1 Foot and overall thermal sensation during foot cooling in the cold
Figure 5.25-2 Foot and overall thermal comfort during foot cooling in the cold
Figure 5.25-3 Hand and overall thermal sensation during hand cooling in the cold
Figure 5.26-1 Hand and overall thermal sensation during hand warming
Figure 5.26-2 Hand and overall thermal comfort during hand warming
Figure 5.26-3 Foot and overall thermal sensation during two-feet warming
Figure 5.26-4 Foot and overall thermal comfort during two-feet warming
Figure 5.27-1 Head and overall thermal sensation during head cooling
Figure 5.27-2 Face and overall thermal sensation during face cooling
Figure 5.27-3 Face and overall thermal sensation and comfort during face cooling
Figure 5.27-4 Neck and overall thermal sensation during strong neck cooling
Figure 5.27-5 Neck and overall thermal sensation during mild neck cooling
Figure 5.27-6 Neck and overall thermal comfort during strong neck cooling
Figure 5.27-7 Neck and overall thermal comfort during mild neck cooling
Figure 5.27-8 Upper and lower arm and overall thermal sensation during arm cooling
Figure 5.28-1 Neck and overall thermal sensation during neck cooling in the cold
Figure 5.28-2 Neck and overall thermal comfort during neck cooling in the cold
Figure 5.29-1 Face and overall thermal sensation during face warming
Figure 5.29-2 Face and overall thermal comfort during face warming
Figure 5.30 Breathing and overall thermal comfort during breath intake air warming
Figure 5.31-1 Breathing and overall thermal sensation during breath intake air cooling
Figure 5.31-2 Breathing and overall thermal comfort during breath intake air cooling
Figure 5.31-3 Overall thermal sensation and comfort for three local cooling applications
Figure 5.32-1 Core temperature and overall sensation during local cooling (a)
Figure 5.32-2 Core temperature and overall sensation during local cooling (b)
Figure 5.32-3 Core temperature and overall sensation during local cooling (c)
Figure 5.32-4 Core temperature and overall sensation during local cooling (d)
Figure 5.33-1 Core temperature and overall sensation during local warming (a)
Figure 5.33-2 Core temperature and overall sensation during local warming (b)
Figure 5.34 Core temperature and overall sensation during local cooling in the cold
Figure 5.35 Sensation voting behavior during transients

Figure 5.36 Kuno effect during strong face cooling removal
Figure 5.37 Kuno effect during mild face cooling
Figure 5.38 Kuno effect during mild back cooling removal
Figure 5.39 Kuno effect during hand heating
Figure 5.40-1 Local and overall thermal sensation during chest and hand cooling
Figure 5.40-2 Local and overall comfort during chest and hand cooling
Figure 5.41-1 Local and overall thermal sensation during neck and foot cooling
Figure 5.41-2 Local and overall comfort during neck and foot cooling
Figure 5.42-1 Skin temperatures of both hands after removing the local stimuli
Figure 5.42-2 Left and right hand thermal sensation
Figure 5.42-3 Overall, left, and right-hand thermal sensations
Figure 5.42-4 Local sensation and comfort
Figure 5.43 Core and overall thermal sensation in a multiple test
Figure 5.44 Local and overall sensations and comfort vote repeatability comparison
Figure 5.45 Left and right foot sensations during right-foot cooling
Figure 5.46 Left and right hand sensations during left-hand cooling
Figure 5.47-1 Left and right hand sensations during left-hand cooling
Figure 5.47-2 Left and right hand comfort during left hand cooling
Figure 5.48 Skin temperature changes in (warm to slightly cool) step-change
Figure 5.49 Skin temperature changes in (slightly cool to warm) step-change
Figure 5.50 Skin temperature, sensation in step-change test
Figure 5.51 Sensation and comfort in step-change tests
Figure 5.52 Core temperature responses in a step-change test
Figure 5.53 Hand skin temperatures in slow motion during hand cooling
Figure 5.54 Hand skin temperature recovery speed
Figure 5.55. Recovery of hand skin temperature after local cooling
Figure 5.56 Low pressure device (Stanford University, 2002)
Figure 5.57 Head skin temperature distribution in different environments
Figure 5.58 Back of head skin temperature in cold and warm environments
Figure 5.59 Neck skin temperature in cold environment
Figure 5.60 Upper and lower arm skin temperature in different environments
Figure 5.61 Hand skin temperature in warm and cold environments
Figure 5.62 Skin temperatures a few minutes after moving
Figure 5.63 Whole body skin temperature distributions (IR-images)
Figure 5.64 Leg and foot skin temperature distribution in a cool environment

Figure 6.1 A flow chart to show models developed and their relationships
Figure 6.2 Logistic local sensation model
Figure 6.3 Asymmetrical logistic model
Figure 6.4 Overall body thermal state impact on local sensation
Figure 6.5 Static local sensation model
Figure 6.6 Dynamic local sensation model
Figure 6.7 Local sensation and local comfort linear model
Figure 6.8 Hand sensation and comfort (Mower 1976)
Figure 6.9 Shifts at maximum comfort due to overall sensation
Figure 6.10 Asymmetrical shifts and maximum comfort
Figure 6.11 Local thermal comfort model
Figure 6.12 Overall sensation model
Figure 6.13 Relationships between sensation and skin temperature (Gagge el al.1967)
Figure 6.14 Skin temperature vs. sensation (Fiala 2002)
Figure 6.15 Slopes and upper and lower limits of logistic functions
Figure 6.16 Local sensation feels warmer when the whole body is colder
Figure 6.17 Whole body thermal state modifications on local sensation
Figure 6.18 Adapting temperature (Kenshalo 1970)
Figure 6.19 Proposed adaptive model
Figure 6.20 Validation for Delphi Wind Tunnel summer tests (driver)
Figure 6.21 Validation for Delphi Wind Tunnel winter tests (driver)
Figure 6.22 Overall sensation vs. comfort (Gagge et al., 1967)
Figure 6.23 Hand comfort depends on whole body thermal status (Cabanac 1969)
Figure 6.24 Local comfort vs. local skin temperature (Attia and Engel 1981)
Figure 6.25 Local comfort (Issing and Hensel 1982)
Figure 6.26 Local thermal for foot (Issing and Hensel 1982)
Figure 6.27 Local comfort vs. local sensation and whole body thermal states
Figure 6.28 The local thermal comfort model
Figure 6.29 Logistic function acts on the linear function
Figure 6.30 Logistic function acts on the linear function to create saddle
Figure 6.31 Local sensation and local comfort when the whole body is neutral
Figure 6.32 Possible three shapes to present local sensation and local comfort
Figure 6.33 Breathing local thermal comfort model
Figure 6.34 Hand local thermal comfort model
Figure 6.35 3-D presentations of local comfort (our model and Issing and Hensel)

Figure 6.36 Validation of the thermal comfort model by Delphi Wind Tunnel test data
Figure 6.37 Predictions and actual votes of right and left foot (Delphi)
Figure 6.38 Proposed three models for predicting weights
Figure 6.39 Linear relationships to calculate the weights
Figure 6.40 Examples of integration models for back, face, and hand
Figure 6.41 Actual votes vs. prediction – validation of the overall sensation model
Figure 6.42 Sensation distribution in stable conditions (UCB tests)
Figure 6.43 Validation of the overall sensation model in stable conditions (UCB tests)
Figure 6.44 Overestimate from the all-body-part weighting method (a)
Figure 6.45 Overestimate from the all-body-part weighting method (b)
Figure 6.46 Validation of the integration comfort model for Delphi PRE dataset
Figure 6.47 Validation of overall comfort model for Delphi All4 test dataset
Figure 6.48 Validation of overall comfort model for Delphi All1 test dataset
Figure 6.49 Validation of overall comfort model for Delphi All2 test dataset
Figure 6.50 Validation of overall comfort model for Delphi All3 test dataset
Figure 6.51 Validation of overall comfort model for UC Berkeley cold test
Figure 6.52 Validation of overall comfort model for UC Berkeley warm tests
Figure 6.53 Validation of overall comfort model for UC Berkeley slightly cool tests
Figure 6.54 Validation of overall comfort model for UC Berkeley slightly warm tests
Figure 6.55 Underestimation of the overall comfort of Rule 1 for Delphi datasets
Figure 7.1 Another hypothetical overall comfort model
Figure A4.1.1 Possible alternatives to control local skin temperature
Figure A4.1.2 Uneven surface temperature of an electrical fabric
Figure A4.1.3 Phase change material surface temperature during phase change process
Figure A4.1.4 Back skin temperature distribution
Figure A4.1.5 Design process of local skin temperature control
Figure A4.2.1 Skin temperature distributions (Houdas and Ring, 1982)
Figure A4.2.2 Fifteen locations to get a mean skin temperature (Winslow et al. 1936)
Figure A4.2.3 Twenty locations of Hardy/DuBios (Hardy and DuBois 1938)
Figure A4.2.4 Seven and twelve locations of Hardy and DuBois (Mitchell 1969)
Figure A4.2.5 Five measurement sites (Houdas 1982)
Figure A4.2.6 Fourteen measurement sites used by Olesen (Olesen 1984)
Figure A4.3.1 Comparison of core temperature measurements (a)
Figure A4.3.2 Comparison of core temperature measurements (b)
Figure A5.1.1 Constructing a new dataset based on the database

Figure A6.1.1 Skin temperature adapting thresholds for each body part
Figure A6.1.2 The adaptation model for the back
Figure A6.2.1 Cycling of esophageal temperature set point (Cabanac et al. 1976)
Figure A6.2.2 Changing esophageal temperature at rest (Pandolf et al. 1988)
Figure A6.2.3 Measuring core temperature with a CorTemp pill in a 24-hour circle
Figure A6.2.4 Proposed core temperature set point model
Figure A6.4.1 Small noise signal in skin temperature measurement
Figure A6.4.2 Dominant small noise signals in derivative of skin temperature
Figure A6.4.3 Skin temperature before and after smoothing
Figure A6.4.4 Derivative after wavelet smoothing
Figure A6.4.5 Smoothing of the derivative after wavelet smoothing

LIST OF TABLES

Table 4.1.	Chamber and bathtub temperatures for tests (0.32 clo, 1 Met)
Table 4.2	ASHRAE sensation scale
Table 4.3	The Bedford scale
Table 4.4	Single-body-part cooling and heating tests
Table 4.5	Multiple-body-part cooling and heating tests
Table 4.6	Whole-body step-change tests
Table 4.7	Neutral-Condition tests
Table 4.8	Infrared video image tests
Table 4.9	Delphi Test Conditions
Table 4.10	Delphi Wind Tunnel test procedure
Table 4.11	Subject information (UC Berkeley chamber tests)
Table 4.12	Subject information (Delphi Wind Tunnel tests)
Table 5.1	Skin temperatures in neutral stable condition (our tests and Olesen 1973)
Table 5.2	Skin temperature in a cold stable condition
Table 5.3	Skin temperature in a warm condition
Table 5.4	Correlation (r) between local skin temperature and local sensation
Table 5.5.	Ratio $\frac{\Delta S_{overall}}{\Delta S_{local}}$ produced by a local cooling/heating
Table 5.6	Ratio $\frac{\Delta C_{overall}}{\Delta C_{local}}$ produced by a local cooling/heating
Table 5.7	Correlation (r) between local skin temperature and local sensation
Table 5.8	Correlation (r) between derivative of skin temperature and local sensation
Table 5.9-1	Hand and finger temperatures in a cold environment (a)
Table 5.9-2	Hand and finger temperatures in a cold environment (b)
Table 5.9-3	Hand and finger temperatures in a warm environment
Table 5.9-4	Hand and finger temperatures in a neutral environment
Table 6.1	Regression coefficients for the local sensation model
Table 6.2	Regression coefficients for the dynamic local sensation model
Table 6.3	Regression coefficients for the local thermal comfort model
Table 6.4	Regression coefficients for the overall sensation model
Table 6.5	Residuals of overall sensation model validation (UCB data)
Table A4.1.1	A back skin temperature distribution

Table A4.4.1 Test conditions
Table A5.1.1 A brief description of each file in the database
Table A6.1.1 Adapting thresholds for each body part
Table A6.1.2 Coefficients for adaptation model for each body part
Table A6.3.1 Average values for body builder information from our tests
Table A7.1 Additional regression for whole body thermal sensation

ACKNOWLEDGMENTS

Because of the challenge of this project, my supervisors, Professor Ed Arens (chair of my dissertation committee), and Specialist Charlie Huizenga worked closely with me throughout, from designing experiment apparatus to developing the thermal sensation and comfort models. They gave me countless, priceless ideas and suggestions. Without their supervision and encouragement, this project could not have been completed. In the text, "we" refers to our three-person research team.

I would like to thank student Danni Wang for her help in programming the subjective thermal questionnaire, smoothing the thermocouple-measured data, and participating in project discussions. I also would like to thank students Mingyu Shi for answering questions about statistics and using S+, Gwelen Paliaga for giving ideas about the experimental setup and measurement methods, and Keke Chen for help in smoothing the thermocouple measured data. The author would like to thank Fred Bauman for helping with test-chamber maintenance, Tengfang Xu in particular for his continuing encouragement and the ideas he gave to me during discussions, answering my questions about statistics, Clifford Federspiel and Professor Barbara Mellers for the advices about statistics.

Great appreciation goes to the 27 human subjects who participated in the tests.

I would like to thank the chair of my qualifying exam committee, Professor Gail Brager, and other members of the qualifying exam committee and the dissertation committee, Professor Boris Rubinski, Professor Cris Benton, Dr. Rick Diamond, for their encouragement and comments for my study.

This work was supported through the National Renewable Energy Laboratory (NREL) by the U.S. Department of Energy, Office of FreedomCAR and Vehicle Technologies (OFCVT). I appreciate the support of NREL project team members Rom McGuffin, John Rugh, and Rob Farrington. Delphi Harrison contributed in-kind support to make the wind tunnel testing possible. I wish to thank Taeyoung Han, Lin-Jie Huang, Greg Germaine, and the volunteer subjects from

Delphi Harrison. I am also very grateful to James Demmel for financial support under the National Science Foundation Information Technology Resource Grant.

Thank you to Nan Wishner and Dariush Arasteh for editing assistance.

I would like to thank my husband, Xiaoping Zhu, for his support and patience. Without his support, it would have been impossible to finish this project.

Thanks also to my two daughters, Molly and Megan, for their understanding and for diverting me from constantly working on this thesis.

Most of all, I would like to thank my father, Zhongyao Zhang, and my mother, Yaqing Gao. They taught me to be persistent – not to turn away from difficulties, but to face them and overcome them.

1. INTRODUCTION

There is a very old and simple experiment described by English philosopher John Locke in his 1690 *Essay Concerning Human Understanding*. A person places one hand in a basin of warm water and the other in a basin of cool water. After a short time, both hands are placed together in a third basin of water, which is at an intermediate temperature. The hand previously in warm water feels cool and the hand previously in cool water feels warm even though they are actually at the same temperature.

This thesis studies the subjective perception of thermal *sensation* in many individual local parts of the human body, and how it correlates with physiological parameters. It intends to quantify human perceptions of thermal conditions, including the phenomenon observed by Locke regarding local thermal sensation in non-uniform and transient conditions.

The thesis also addresses perceptions of thermal *comfort*. For both sensation and comfort it proposes predictive models for both the individual body parts, and for the body as a whole.

People are probably more often exposed to spatially non-uniform (asymmetrical, we use 'non-uniform' and 'asymmetrical' interchangeably) and transient (time-varying) temperatures than to thermal environments that are uniform and stable. We experience transient and non-uniform temperature conditions when moving between spaces – e.g., from indoors to outdoors, from sun to shade, from the outdoors to a parked car and then starting its air conditioner, and when occupying spaces with widely varying temperatures, e.g., an office that has large windows. In some cases, the variation in temperature is experienced as pleasant. A person who is feeling warm inside a building may , for example, enjoy a cool breeze from natural ventilation that cools exposed parts of the body. In other cases the variation is a source of discomfort. A person with cold feet is unlikely to be comfortable even if all the other body segments are pleasant.

There are currently no models of human sensation and comfort for non-uniform, transient thermal environments. This thesis reports on human subject tests undertaken both to observe the phenomena involved and to obtain data sufficient to develop models that predict local and overall thermal sensation and comfort in transient and non-uniform conditions.

The thesis is divided into seven chapters.

- Chapter 1 provides an introduction of the thesis.
- Chapter 2 describes the background.
- Chapter 3 states the objective for our work.
- Chapter 4 describes the experimental method and setup.
- Chapter 5 is subdivided and presents our observations and analysis of human physiology and subject responses during the tests
- Chapter 6 describes the predictive models we developed.
- Chapter 7 includes applications of the models, conclusions, and future work.
- Several appendices present supporting information regarding detailed description of the test conditions, the skin temperature measurement location for the human subject tests, the comparison of three different core temperature measurement, a database developed for data analysis of this study, the skin temperature adaptation model, the core temperature prediction model, the influence of "body builder" on local sensation, and three published papers.

2. BACKGROUND

The existing research on human thermal sensation and comfort has generally focused on steady-state, uniform conditions. Although a few studies have focused on asymmetrical conditions -- i.e., when some parts of the body are exposed to different conditions than others, the test conditions for asymmetrical conditions are either not complete (e.g. the test conditions only representing particular vehicle environments), or the human body conditions, such as metabolic level or clothing insulation, are limited. Other studies have focused on transient conditions – e.g., movement from an environment at one temperature to another environment at a different temperature (step-change conditions). The environments tested were uniform; so there is no special asymmetry. Although a few predictive models have been developed for either asymmetrical or transient conditions, there are currently no models that address human responses to simultaneous asymmetrical and transient thermal conditions.

Most human-subject studies in this field have evaluated the thermal sensation of subjects using voting scales that rate thermal sensation of the entire body (e.g., -3 cold to +3 hot with zero at the center of the scale representing "neutral" condition). Studies rarely address local thermal sensation, i.e., the thermal experience of individual body parts. Moreover, very few studies have addressed the distinction between sensation and comfort; it is possible for part or all of the body to feel a sensation that might be rated as "warm" or "cool" but might be either comfortable or uncomfortable, depending on the context. The issue of comfort is most significant in asymmetrical and transient thermal conditions.

For more than 30 years, two models have been most commonly used to evaluate thermal sensation: Fanger's PMV (Predicted Mean Vote) model (Fanger 1972), and Gagge's two-node model with its indices of TSENS (Thermal Sensation) and DISC (Thermal Discomfort) obtained from ET* (effective temperature) and skin wetness (Gagge, Stolwijk et al. 1970). Both are based on data from experiments conducted under uniform, steady-state thermal conditions (Nevins, Rohles et al. 1966; McNall, Jaax et al. 1967; Fanger 1972; Rohles and Wallis 1979). The two models are very effective for evaluating indoor environments that are uniform, stable, and close to thermal neutrality, and have been extensively used for that purpose. They do not attempt to model asymmetrical and/or transient thermal conditions.

Researchers did not begin to study asymmetrical thermal environments until the 1980s. At that time there was a resurgence of interest in natural ventilation in buildings, and in new localized air-conditioning systems that permit individuals to control heating or cooling within their local work spaces (e.g. under-floor heating and cooling (Bauman, Johnston et al. 1991), desk-top heating and cooling (Bauman, Carter et al. 1998)). In addition, the development of new thermally resistant glass and window products drew attention to the human experience of asymmetrical conditions. The greatest push for study of these types of conditions came from the automobile industry because of the extreme asymmetries and transients experienced in vehicle interiors.

Current indoor environment standards address asymmetrical conditions in building environments by establishing acceptable ranges for each type of temperature variation in space. ASHRAE *Standard* 55-1992 prescribes several limits for vertical and horizontal air temperature differences, radiant temperature asymmetry, draft air speed, and temperature change over time (ASHRAE 1992). However, these are based on fairly limited laboratory tests.

The automobile industry's efforts to study the complex thermal environments in vehicles resulted in the creation of a number of different models. Some are based on the PMV or the two-node model. The industry has also relied on the equivalent homogeneous temperature (EHT) model (Wyon, Larsson et al. 1989), which establishes temperature ranges for different areas of the body.

The following sections provide a brief summary of the physiological bases and the most important models.

2.1 Physical basis of thermal sensation

2.1.1 Thermoreceptors

When we perceive warmth or coolth, we do not actually sense the temperature of the room's air or surfaces directly, but rather our nerve endings, the thermoreceptors which send signals to the hypothalamus at the base of the brain when stimulated. The thermoreceptors are the sensors that signal the conditions of the space around us and permit us to feel those conditions as thermal sensations.

Early sensory investigators, Blix (1884) in Sweden, Goldscheider (1884) in Germany, and Donaldson (1885) in America, reported that some spots on the skin register warmth or cold when touched with small (punctate) warm and cold stimulators. Warm sensations can be elicited only from warmth receptors and cold sensations only from cold receptors. Dallenbach (Dallenbach 1927) explored the skin with a small-tipped cool metal probe and found that much of the skin's surface produces no sensation of cold when touched by the cold probe. He tested 100 spots on a square centimeter of skin on the forearm in great detail, examining each square millimeter with a cold and a hot stimulus. Only about 20 of the spots tested registered "hot" sensation and another 20 registered "cold" sensation.

Human beings can perceive different gradations of cold and heat, ranging from cold to cool to indifferent to warm to hot. Three different types of sensory organs –cold receptors, warmth receptors, and pain receptors – allow the body to discriminate gradations in thermal sensation. The relative degrees of stimulation of the nerve endings determine the person's perception of the intensity of thermal sensation. Each receptor is activated in a specific range (Figure 2.1). At high temperatures perceived as painfully hot, warmth receptors are inactive, and pain receptors are simulated. The same is true for cold temperatures. Thermoreceptors are located mainly in the periphery of the body and in the hypothalamus, but are also found in places such as the spinal cord, abdominal viscera, and in or around the great veins in the upper abdomen and thorax.

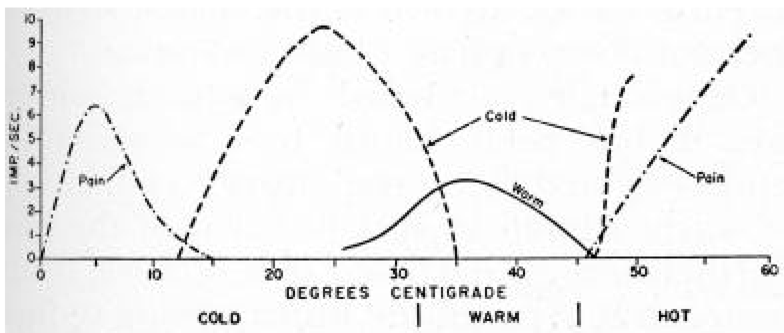

Figure 2.1 Frequencies of discharge of a cold receptor, a warmth receptor, and a pain nerve fiber at different temperatures (Guyton 1971). (The responses of the cold and warmth receptors are modified from Zotterman (Zotterman 1953).

The characteristics of thermoreceptors determine thermal sensation and comfort responses. A thermoreceptor adapts to a great extent. When it is subjected to an abrupt change in temperature, it is strongly stimulated at first, but this stimulation fades rapidly during the first minute following the temperature change, and then progressively more slowly as illustrated in Figure 2.2 until it reaches a steady response rate. Thermoreceptors respond to steady temperature states at this lower rate. As a result of this property of thermoreceptors, a person feels much colder when the temperature of the skin is actively falling than when the temperature remains at the same level. This explains the extreme sensation of coolth or warmth felt when a person enters a cold pool or a hot tub. When explaining his subjects' overreaction during down-step transient exposures (moving from a warm to cool environment), de Dear (de Dear et al., 1993) called it "overshoot".

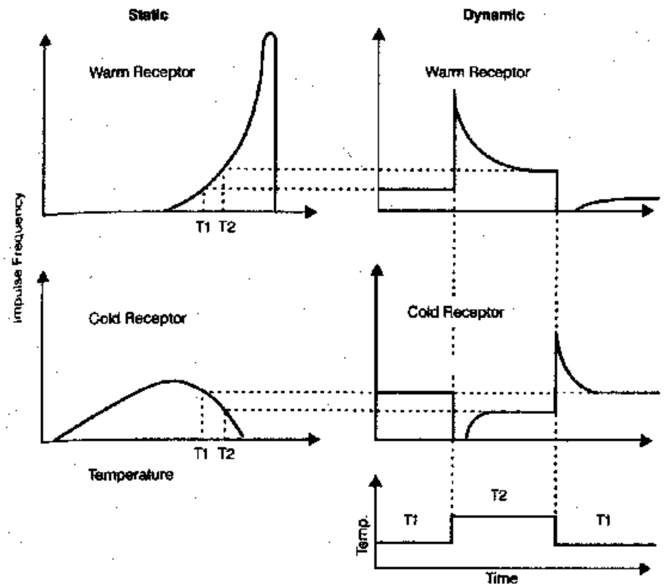

Figure 2.2 General properties of thermoreceptors. Static and dynamic responses of warm and cold receptors to constant temperature and temperature changes as given by Hensel (Hensel 1981)

Gagge (Gagge, Stolwijk et al. 1967) conducted an experiment in which subjects moved between rooms at neutral and uncomfortable temperatures. Subjects evaluated their thermal condition as "comfortable" after entering the neutral room but before skin temperature had sufficiently recovered to warrant a change in thermal sensation to the neutral conditions. Gagge calls this phenomenon "anticipation." De Dear performed up-step tests (de Dear, Ring et al. 1993) and found that when subjects experienced a step change from a cold to a warm environment, their instantaneous thermal sensation upon entering the second environment approximated the final steady-state value for that environment. This suggests that the dynamic response of thermoreceptors to changes in temperature is capable of anticipating the body's steady-state response to a new thermal environment well before the body's heat content has time to alter significantly.

The thermoreceptors are located in the intracutaneous region at an average depth of 0.15 to 0.17 mm for cold receptors and 0.3 to 0.6 mm for warmth receptors (Bazett and McGlone 1930; Bazett, McGlone et al. 1930). These depths suggest that the layer of cold receptors is immediately beneath the epidermis, and the site of warmth receptors is within the upper layer of the dermis. The number of cold thermoreceptors far exceeds the number of warmth receptors. In general, there are about 10 times more cold receptors than warmth receptors in skin (Guyton 2002).

2.1.2 Hypothalamus thermoregulation

The hypothalamus consists of several divisions, two of which control thermoregulation: the anterior and posterior nuclei. Benzinger described these areas as the "two centers" of thermoregulation, as shown in Figure 2.3 (Benzinger, Pratt et al. 1961).

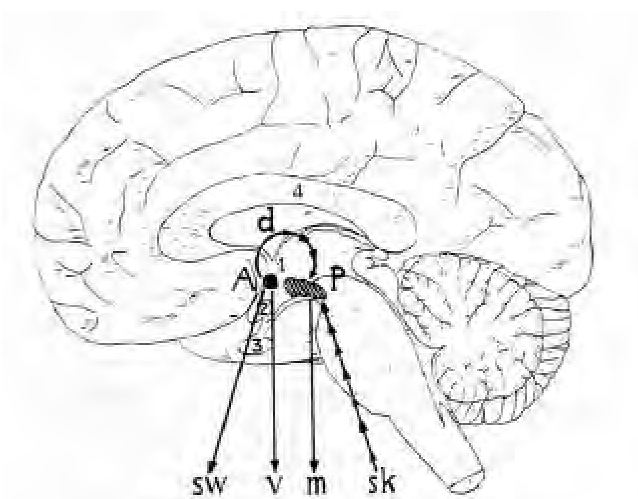

Figure 2.3 Hypothalamus and thermoregulation (Benzinger, Pratt et al. 1961)

The anterior hypothalamus (A), described as the "heat loss center," provides thermoregulation when the body is too hot. It combines the function of temperature sensor and controller; any rise in temperature above the set point of the anterior hypothalamus causes it to send out efferent nerve impulses to initiate the body's heat loss mechanisms of vasodilatation (v) and sweating (sw). The set point is normally 37 °C but is raised during exercise or fever.

The posterior hypothalamus (P) or "heat maintenance center" provides defense against cold. Keller and Hare (Keller and Hare 1932) show that after destruction of the heat maintenance center, the heat loss functions (of the heat loss center) remain intact; therefore, we know that the heat loss function is independent from the heat maintenance function. The heat maintenance center mainly receives temperature signals (sk) from the skin sensors. The resulting efferent responses are vasoconstriction and shivering (m).

The heat loss center was shown by Benzinger as having an impact on the heat maintenance center; that is, when the heat loss center temperature increases, shivering and vasoconstriction catalyzed by the heat maintenance center are depressed. This is shown by the partial loop "d" from point A (the anterior hypothalamus) to P (the posterior hypothalamus) in Figure 2.3.

McIntyre (McIntyre 1980) suggests that the two centers inhibit each other, meaning that two-way activity passes through the partial loop at d on Figure 2.3. In other words, a person who has an elevated core temperature will sweat because of the activity of the heat loss center; if his skin temperature is lowered by cooling, the posterior hypothalamus will be stimulated, inhibiting the anterior hypothalamus so that sweating diminishes or stops. Similarly, the elevated temperature of the anterior hypothalamus will prevent shivering.

This theory regarding the heat loss and heat maintenance centers gives us some background about work that has been done on the brain's interpretation of thermal signals and gives a general sense of how the brain might interpret thermal signals to create sensation and comfort.

2.2 Models of thermal sensation in stable asymmetrical conditions

2.2.1 Weighting factor approach

Ingersoll (Ingersoll, Kalman et al. 1992). A model developed for General Motors applied Fanger's PMV model individually to three different body parts: head, torso, and feet. It first uses the two-node model (Gagge et al., 1971) to predict physiological data for the three body parts individually, and then applies the PMV calculation to the three body parts. The calculated PMV for each body part is weighted by its respective surface area, and a single, average PMV is derived. There are two key problems with this approach. First, PMV was developed to represent the whole body, based on regressions of temperature and subjects' indications of the thermal sensation of the whole body. Applying whole-body thermal sensations to individual body parts assumes that each of the body parts has exactly the same effect on thermal sensation as the whole body, which may not be true. Second, the two-node model was also developed to represent the whole body, and contains no way to account for differences in the thermal sensation of individual body parts. Using the two-node model on individual body parts imposes the same thermal control strategy and set points on each body part. It also does not address heat exchange that occurs between body parts as a result of blood flow.

Matsunaga (Matsunaga, Sudo et al. 1993). Instead of simulating the temperatures of individual body parts and predicting their thermal comfort individually, the model of Isuzu

Motors uses an average equivalent temperature (AET) to calculate PMV. The AET is a surface-area-weighted average for three regions of the human body: head (0.1), abdomen (0.7), and feet (0.2). The equivalent temperature for each body region is calculated from thermal manikin measurements and defined as the temperature of a uniform enclosure in which a thermal manikin segment with realistic skin surface temperatures would lose heat at the same rate as human beings in a real environment. Because it is averaged, the AET can only evaluate the thermal environment of the entire driver or passenger compartment of a vehicle. Although the AET-based PMV value for the entire environment might indicate overall comfort, localized areas of discomfort could still exist.

Kohri (Kohri, Kataoka et al. 1995). This model, developed for Mitsubishi Motors Corporation, applies the two-node model to 11 body parts (corresponding to the body parts of their thermal manikin) to calculate standard effective temperatures (SET*) for these body parts in the vehicle environment. The SET* includes the effects of convection, radiation, and evaporation on the body. The problem with this approach is as noted above. Applying the two-node model to individual body parts ignores the heat transfer between body parts caused by blood flow.

KSU clothing model (Jones and Ogawa 1992). This model, developed by Kansas State University, combines a two-node model with a clothing model developed at Kansas State. In order to overcome the limitation that the two-node model cannot predict human physical responses and thermal comfort in asymmetrical environments which often appear in vehicle environment, the KSU clothing model divides skin into many small sections. The dividing of the skin into more smaller sections allows the model to look at the local impacts of the uneven environment and the uneven clothing insulation. The core is not divided, so the model does not account for variations in core temperature as a result of the differences among the different areas of skin; thus, the model does not account for heat exchanges between body parts or differences in thermal regulation of different body parts.

The Ford sensation model (Brown and Jones 1997). This subjective response model is based on regression analysis of human subjective data collected at Kansas State University. The whole-body thermal comfort rating was based on a nine-category combined sensation and comfort rating scale which is similar to Bedford's scale, ranging from cold (1), cold/cool (2), cool (3), cool/comfort (4), comfort (5), warm/comfort (6), warm (7), hot/warm (8), to hot (9). The Ford model divides the body into sections to simulate physical parameters such as skin temperature and skin wetness. However, the subjective thermal comfort votes are for the whole body, not for individual body parts. Because the authors did not present the details of their thermal comfort model for reasons of confidentiality, it is difficult to determine the connection between their subdivision of the body for skin temperature and skin wetness and the use of a whole-body thermal comfort votes to obtain the prediction.

Hagino and Hara (Hagino and Hara 1992). The authors of the Nissan Motor Co. model criticize Matsunaga's AET method. They argue that applying the AET to determine PMV only permits evaluation of the thermal environment of the entire passenger compartment. Although the PMV for the entire environment might indicate overall comfort, localized areas of discomfort could still exist because of solar radiation through the windows or direct exposure to airflow from the air-conditioner vents.

Hagino and Hara therefore performed a series of human subject measurements to determine the relationship between subjects' votes about their local thermal sensations and their votes about whole-body thermal sensations. The studies involved a mockup of a typical car body in an environmental chamber equipped with a solar simulator. The airflow rates and discharge air temperature were changed. Six males participated in a total of 72 tests in which skin temperatures were measured and local thermal sensations surveyed for 19 body locations. The 19 locations comprised the 12 points identified by Hardy-Dubois (referred in (Mitchell and Wyndham 1969)) for skin temperature, with the addition of seven points on the arms and legs, which were exposed to different local thermal conditions (see Figure 2.4).

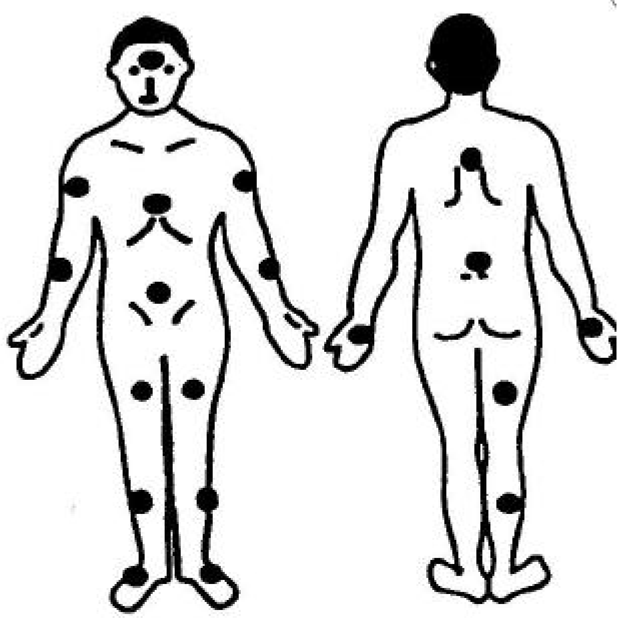

Figure 2.4 Skin temperature measurement points (Hagino and Hara 1992, Nissan Motor Co.)

When they compared the whole-body Thermal Sensation Votes (TSVs) and area-weighted average TSVs for the 19 body locations, the average TSV shifts toward more neutral values than does the whole-body TSV. This means that the area-weighting does not accurately predict whole-body sensation.

Because the setup of the experiment was similar to a vehicle environment, which mainly affects the sensation from forehead, arm (receives solar radiation), thigh and foot on the window side, the authors found that the whole body thermal sensation votes were governed by the local sensations from these areas:

TSV[whole body] = 0.42 TSV[forehead] + 0.38 TSV[upper arm on window side] + 0.2 TSV [thigh on the window side] + 0.28 TSV[instep on window side] + 0.42.

Because the test conditions focused on these specific body parts, it is only appropriate for conditions in vehicle passenger compartments.

2.2.2 EHT and Piste

Total and individual body part heat losses have been expressed in terms of Equivalent Homogeneous Temperature (EHT) (Wyon, Larsson et al. 1989). The EHT is defined as the temperature in a uniform reference environment where the heat loss from a person or a body part is the same as his/her heat loss in an actual (non-uniform) environment with same clothing and activity level. The air temperature and the mean radiation temperature are equal in the uniform reference environment. There is no thermal gradient and no air movement, and the humidity is constant. EHT is derived from the heat loss of a human body in an environment, as measured by a thermal manikin. For example, if one part of the body is exposed to air movement, the heat loss from that body part to the environment may be greater because of the air movement. Therefore, the EHT for that body part will be lower than for the rest of the body.

Wyon (Wyon, Larsson et al. 1989) also developed the concept of the "piste," a representation of the acceptable temperature range for each individual body part based on its EHT value (Figure 2.5). Between the upper and lower temperature limits is the ideal profile. Several researchers have used the piste concept in studies, and two EHT pistes are found now in the literature, in addition to Wyon's: Bohm et al. (Bohm, Browen et al. 1990), and Wahl (Wahl 1995). However, the piste developed for each study only applies to steady-state conditions and the clothing and metabolic conditions tested. So, although the piste defines acceptable temperature ranges in asymmetrical environments, its use is limited to the specific conditions tested in the studies where it was applied.

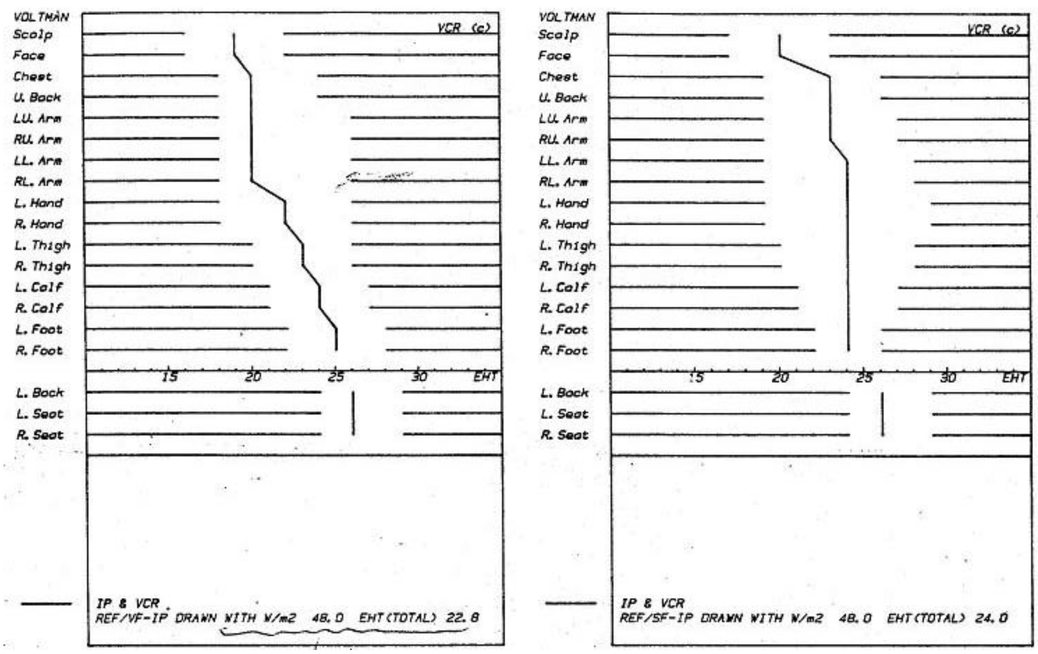

Figure 2.5 EHT piste and the ideal profiles for a driver in winter (left) and summer (right) (Wyon 1989)

Nilsson (Nilsson 2003) suggested comfort zones for the 16 body parts (Figure 2.6) by replacing the three lines (upper and lower limits and the ideal profile) in the piste with three zones (cold but comfortable, neutral, hot but comfortable),. The paper is very brief and does not provide information that explains how the three zones are defined. The details will be included in his thesis (personal communication).

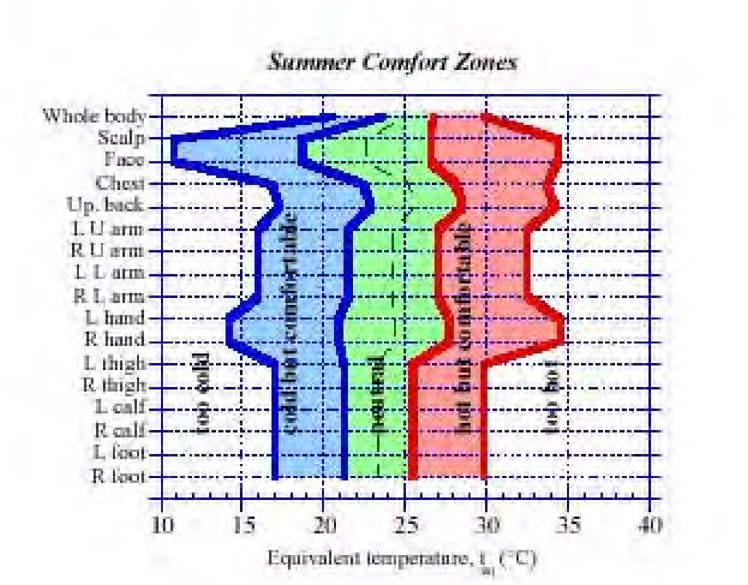

Figure 2.6 Zone-like piste proposed by Nilsson (Nilsson 2003)

2.3 Models of dynamic thermal sensation

In contrast to thermal sensation models for steady-state conditions, dynamic thermal sensation models include a derivative that corresponds to sensations experienced in transient (changing) conditions.

The dynamic response to transient conditions is correlated to the responses of the body's thermal receptors, which respond differently to static and dynamic conditions. Under steady-state conditions, the thermoreceptors sense a static signal to the brain; this signal is based on skin temperature and core temperature. When conditions change, the thermoreceptors send not only the static signal based on skin and core temperature but also a dynamic signal based on the rate of change in both temperatures (the derivative). Hensel (Hensel 1982) proposed that warm and cold sensations can be expressed as a function of the temperature (T_{skin}) of the skin, the rate of change (dT_{skin}/dt) of skin temperature, and the stimulation area (F).

$$\text{Thermal Sensation} \rightarrow f(T_{skin}, dT_{skin}/dt, F)$$

Ring and de Dear (1991) developed a skin thermal sensation model based on humans' ability to instantaneously detect changes in the thermal environment from the cutaneous thermoreceptors. Following Hensel (Hensel 1981), they developed a skin receptor impulse frequency model based on the properties of the thermoreceptors. In the model, the thermoreceptor response has a static and dynamic part; the response of the thermoreceptor to a sudden step change in skin temperature (T) yields a peak dynamic portion which decreases quickly in a few seconds until it reaches the static portion. The static portion is proportional to T and the dynamic portion is proportional to dT/dt. Ring and de Dear also applied findings from the work of Ivanov et al. (Ivanov, Konstantinov et al. 1982; Ivanov, Konstantinov et al. 1986) that the same thermoreceptor can give different responses to the same stimulus, depending on whether the stimulus is applied to the epidermis or to the subcutaneous tissue. This is accounted for in the model by distributing the depth of the thermoreceptors throughout the cutaneous tissue.

$$R(x,t) = K_s\, T(x,t) + K_d\, \partial T(x,t)/\partial t \quad \text{(Hz)}$$

where K_s and K_d are the proportionality constants for the static and dynamic parts respectively (Hz/K). Term x is the depth of the thermoreceptor and term t represents time.

The thermoreceptors in different parts of the body have different thermal sensitivities. To connect the thermoreceptor response frequency (equation shown above) to thermal sensitivity, de Dear et al. (de Dear, Ring et al. 1993) developed a Dynamic Thermal Stimulus Model (DTS) by assigning different thermal sensation Area Summation Factors (ASFs) to different regions based on thermal sensitivities (Stevens, Marks et al. 1974; Hensel 1981). The ASFs are larger for warmth and cold thermoreceptors in sensitive skin regions (5 for thermoreceptors in face, neck, and hand) and smaller for those in less sensitive regions (1 and 2 for the rest of the body) in the model. The DTS is the sum of all impulses accumulated from skin, multiplied by the appropriate ASF.

$$DTS = \sum ASF_i R_i = \sum ASF_i (K_{s,i} T_{skin,i} + K_{d,i} dT_{skin,i}/dt)$$

where term i represents different regions of the body.

The receptor model provides a detailed model for skin but applies only to skin. There is no information such as core temperature included to represent the whole body thermal state. For the dynamic responses, the derivatives of the skin temperature provide good information. However, for the static response, when the whole body is warm or cold, the same local skin temperature can result in a different subjective thermal perception. So local skin temperature alone does not provide enough information to define the whole body thermal state.

Taniguchi et al. (Taniguchi, Aoki et al. 1992). The authors found that in a vehicle environment the average temperature of face skin, and its change over time, is related to whole-body thermal sensation votes. The relationship is as follows:

$$TSV = 0.81 (T_{sk} - 33.9) + 39.1\, deltaT_{sk}.$$

where TSV is the overall thermal sensation vote

T_{sk} is the average face skin temperature (°C)

$deltaT_{sk}$ is the rate of change of average face skin temperature (°C/s)

The average face temperature was obtained from 7 measured data points on the face, shown in Figure 2.7.

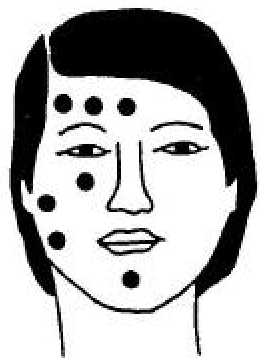

Figure 2.7 Face Skin Temperature Measurement Points (Taniguchi et al. 1992, Toyota Central Research and Development Labs.)

Taniguchi's tests were conducted in a vehicle environment. Only a limited number of body parts (e.g., face) were exposed to the transient thermal conditions, so sensation is only correlated with those body parts. The application of the model from this study is limited because only a selected number of body parts was studied.

Wang (Wang and Peterson 1992; Wang 1994). Wang developed a model to predict thermal sensation in transient conditions. She proposed that transient thermal sensation is composed of two parts: static and dynamic.

$$\text{Thermal Transient Sensation} = U_0 + \Delta U$$

The static term U_0 comes from Fanger's PMV model. The transient term is obtained by regression analysis based on the subjective thermal sensation votes during temperature ramp changes by Griffiths and McIntyre (Griffiths and McIntyre 1974) and the predicted heat loss from the author's physiology model, which is a 6-segmented (head, trunk, arms, hands, legs, feet), two layer (core and skin) model. (The thermoregulation equations and the coefficients of the physiology model are mostly from Gagge (Gagge et al. 1970), Fanger (Fanger 1972), and Stolwijk (Stolwikj 1971)). The output of the thermal transient sensation model is Bedford's sensation and comfort scale (it is not clear how the static sensation term U_0 from Fanger is converted to the Bedford's scale). The transient term ΔU is based on the rate of heat storage in the skin.

Fiala's sensation model (Fiala 1998; Fiala 2002). Fiala assembled a large amount of pre-existing human subject test data and by regression obtained a transient thermal sensation model in spatially uniform conditions that uses skin temperature, skin temperature change rate, and tympanic temperature as input variables. The author found that the derivative of the core temperature is not significantly related to the whole body thermal sensation. The human subject responses that he used for the regressions are from the literature (Gagge et al. 1967, Gagge et al. 1969, Nevins et al. 1966, Rohles 1970, McNall et al. 1967). He obtained the human subject physiology data (skin temperature, skin temperature change rate, and head core temperature) by simulation with his heat-transfer model. Because Fiala's model uses many data sources which cover many test conditions for his regression analysis, his model is widely applicable.

Both Wang and Fiala's models address transient but uniform environments.

Guan (Guan, Hosni et al. 2003; Guan, Hosni et al. 2003). Guan developed a transient thermal sensation model. The model includes a transient component, which is a function of the rate of heat gain. The steady-state component is a function of the difference between actual skin temperature and neutral skin temperature.

The author conducted human subject test by putting subjects in a car and surveyed their local and overall sensations. The physiological parameters (skin temperature and heat loss) of the subjects were simulated using a model developed by Jones and Owaga (Jones and Owaga 1992). The model is a "segmented two-node model" which divides the skin and clothing into 17 segments, while keeping the core as a single node. By regression analysis between the subjective sensation and the predicted physiological parameters, the author provided transient thermal sensation prediction model.

The author emphasizes that there is a second-order anticipation effect in determining transient thermal sensation. That is the body and mind detect the change in the rate of heat gain. Therefore, the rate of heat gain is included in his model to represent the dynamic term.

All three authors (Wang, Fiala, Guan) used their own models to predict human physiological responses and correlated them with the subjective thermal sensation votes to develop prediction models. The regression correlations are therefore specific to their own models.

Frank (Frank, Raja et al. 1999) showed that skin and core temperature have equal weighting for predicting thermal sensation in uniform conditions. The skin and core temperatures were independently altered. The skin temperature was maintained by two water mattresses which were put one above and one below the human subjects (from feet to the shoulders). The water temperature was set at 14, 34, and 42 °C. The core temperature was cooled by infusion of cold intravenous fluid. The subjective thermal sensation was assessed by using a 10-point scale (0 = "the coldest you've ever been;" 5="neutral, neither cold nor warm;" and 10 = "the hottest you've ever been."). The results show that the skin temperature has relatively greater contribution to thermal sensation (the relative contributions of core and skin temperature is 1:1) than to autonomic thermoregulation (3:1 for vasomotor changes and 3.6:1 for metabolic heat production). The skin temperature provides input equal to core temperature towards thermal sensation.

The models summarized above each have a piece of the whole picture; they either address dynamic conditions without addressing asymmetrical conditions (e.g., Fiala, Wang, de Dear and Ring) or they address asymmetrical conditions (e.g., EHT) but without addressing dynamic conditions.

2.4 Sensation and comfort

To evaluate *sensation*, researchers often ask subjects to rate their perceptions using a 7-point ASHRAE voting scale that covers a range of warm and cool sensations with the mildest sensations (e.g., “slightly cool –1” and “slightly warm +1”) near the center of the scale (more information about thermal comfort scales is given in Chapter 1.7.3). Researchers typically interpret all votes between –1 (slightly cool) and +1 (slightly warm) as “*comfortable*.” This is the basis of Fanger’s PPD (Predicted Percentage of Dissatisfied) model which is based on actual PMV.

Another way to evaluate thermal comfort is to ask the subjects’ thermal *preference*: I would prefer to be warmer, I would prefer to be colder, I would prefer no change. Preferring no change is considered as comfortable, or perhaps more precisely as “ideal”.

The comfort zone specified in ASHRAE Standard 55-1992 is based on 90-percent acceptance by subjects of thermal conditions (or 10-percent dissatisfaction) (ASHRAE 1992) based on the whole body heat balance. It assumes that another 10-percent would simultaneously be dissatisfies due to local discomfort. Fanger (Fanger 1972) related the predicted percent dissatisfied (PPD) to the predicted mean vote (PMV) and defined dissatisfaction as any vote other than –1, 0, +1. The PMV model and PPD model are the bases of ISO Standard 7730 (ISO, 1994).

Subjects who cast votes other than –1 or +1 on thermal comfort scales may not necessarily feel uncomfortable.

de Dear and Brager (de Dear and Gail 2001, Brager and de Dear 2000) challenged the ASHRAE standard by proposing an adaptive comfort standard, broaden findings from field studies that the range of thermal comfort in naturally ventilated buildings is much wider than indicated by the ASHRAE standard. The adaptive standard is based on subjects' "preference" rather than the traditional assumption that "neutral thermal sensation" is the optimum thermal condition.

In thermally asymmetrical environments, we cannot evaluate thermal comfort using neutral thermal sensation (votes within +1 and –1 on ASHRAE thermal sensation scale) because different body parts may feel comfortable in the context of the conditions that the rest of the body is experiencing. For example, a warm hand will likely be perceived as pleasant when the whole body is cold, and vice versa. Cabanac et al. (Cabanac 1972) put human subjects in baths with water temperatures of 23°, 28°, 33°, 38°, and 40° C; while in the bath, the subjects put their hands in a glove containing water whose temperature the subject could adjust according to preference. The authors found that subjects preferred warm glove temperatures when their internal temperatures were cold (hypothermic) and cold glove temperatures when their internal temperatures were warm (hyperthermia).

Just as asymmetrical thermal conditions permit some body parts to feel comfortable in the context of the different conditions to which other body parts are exposed, transient conditions can also result in perceptions of comfort based on the relative differences between the changing conditions. For example, when ambient conditions change from hot to cold, a person whose body is warm may feel cool but comfortable, at least initially, in the new cold conditions. For a subject experiencing hypothermia, a warm hand is experienced more comfortable than a hand at "neutral" temperature (defined as an environment in which subjects feel neither warm nor cool and thermoregulatory responses are minimal). Similarly, a subject experiencing both asymmetrical and transient conditions – e.g., in a naturally ventilated warm room through which a cool breeze passes, may feel very comfortable if his/her body is slightly warm.

Many researchers believe that thermal pleasure is associated with the partial relief of thermal discomfort. When a body's heat stress is eliminated, maximum comfort is experienced – in other words, subjects feel a stronger sense of comfort in this transient, asymmetrical thermal state than under uniform, stable, neutral conditions. Kuno (Kuno 1995) suggests that deliberately inducing and then easing thermal stress produces maximum thermal comfort. He gives the Japanese open-air spa (a hot bath in the cold outdoors) as an example of a situation designed for this purpose; spa-goers can repeatedly experience pleasurable thermal sensation by submerging their bodies in hot water and then exposing their chests and shoulders to the cold air to release the heat. In other words, in transient conditions, we do not necessarily seek neutral conditions as the most comfortable. Cabanac, Attia, and Mower (Cabanac 1969; Mower 1976; Attia and Engel 1981; Attia 1984) tested people's pleasure when cold and warm thermal stimuli were applied to the hand, forehead, and neck. Their tests demonstrate that subjects in a hypothermic state experienced pleasure when warm sensation was applied to these areas, and subjects in hyperthermic state experienced pleasure when cold was applied to these areas. In short, a varied thermal environment appears to be experienced as more pleasant than a uniform one.

The experiences of different body parts integrate to form an overall thermal sensation and perception of comfort. No study exists that explains how the body integrates the thermal sensations of different body parts to achieve an overall sense of comfort or discomfort. What we do know is that thermal sensitivities are different for different body parts and are also different depending on whether body parts are exposed to heat or cold. Applying a 20.3 cm^2 thermode, Stevens (Stevens 1979; Stevens and Choo 1998) found that the sensitivity of body parts to cold follows this order, from most to least sensitive: lower back, upper back, chest, abdomen, upper arm, calf, forearm, thigh, cheek, and forehead.. He (Stevens, Marks et al. 1974) also found that the sensitivity of body parts to warmth follows this order, from most to least sensitive: calf, thigh, upper arm, forearm, back, shoulder, abdomen, chest, cheek, and forehead. We do not know how the thermal sensation of individual body parts influences the body's overall thermal sensation.

2.5 Need for human subject tests

Nearly all the commonly used comfort indices and prediction models were developed from experiments in which subjects were exposed to homogeneous environments (Nevins, Rohles et al. 1966; McNall, Jaax et al. 1967; Fanger 1972; Rohles and Wallis 1979). These tests generally lasted at least three hours in order for the subjects to reach thermal equilibrium, and therefore to represent exposure to a stable environment.

Although Hagino and Hara (Hagino and Hara 1992), Taniguchi et al. (Taniguchi, Aoki et al. 1992), and Guan et al. (Guan, Hosni et al. 2003; Guan, Hosni et al. 2003) studied the human subjective sensation in asymmetrical automobile environments, the environmental conditions are limited to the automobiles. Each body part was not individually controlled; several body parts experienced the cooling or heating simultaneously. No comfort information was provided. No skin and core temperatures were measured in the tests and only Guan had transient involved. These data does not allow us to develop a general prediction model.

There exist step-change tests of transient uniform conditions (de Dear, Ring et al. 1993); (Gagge, Stolwijk et al. 1967; Gagge, Stolwijk et al. 1969). However they cannot be used to create a general sensation/comfort model. The physiological parameters of skin and core temperatures were not measured in any of the tests. The tests surveyed subjects' thermal sensation only, and did not examine their perceptions of thermal comfort. Nagano (Nagano et al. 2002) measured skin (no body core) temperature during down-step change from warm to neutral environment. The sensation and comfort questions are for the whole body and no body parts are evaluated. All the above whole body step-change tests do not address conditions with local asymmetry.

Because the relationship between sensation and comfort is very different in transient and asymmetrical environments than in uniform, stable conditions, information is needed regarding both sensation and comfort in order to predict sensation and comfort in transient, asymmetrical conditions. We need both skin temperature measurement covering local body parts and the core temperature measurement in order to develop detailed sensation and comfort models. There are no experimental data that can be used for this purpose. Our study of human subjects in asymmetrical and transient conditions must be designed to remedy this gap in the experimental literature.

3. OBJECTIVES

Our goal is to quantify subjective and physiological responses of humans to transient, asymmetrical thermal conditions and to develop local and whole-body thermal sensation and comfort prediction models for these conditions.

The thermal sensation models that predict subjective perception in transient conditions link the sensation with the physiological parameters (skin, core temperatures, rate of change of skin temperature) as described in Chapter 2.3. Some models (Hensel 1982, Ring and de Dear 1993, Taniguchi, Aoki et al. 1992) used skin temperature and the its rate of change as input parameters. The Fiala model (Fiala 1998, 2002) includes the core temperature as well to represent the whole-body thermal state. He also found that the derivative of the core temperature is not significantly related to sensation. Wang (Wang and Peterson 1992, Wang 1994) proposed to use heat storage in the skin as an alternative way to represent for the derivative of the skin temperature. Based on these models and the analysis about the static and dynamic characteristics of the thermoreceptors, we propose to develop a local sensation model of the form in Eq. (3.1). The local sensation model is a function of skin and core (or mean skin) temperatures and their rates of change. The skin and core temperatures represent the response to the stable condition, the derivatives represent the transient feature. There will be a distinct model for each body part, so that together they capture the asymmetry feature. Therefore, the entire model should predict sensation and comfort in asymmetrical and transient conditions.

$$Local\ Sensation = f(T_{skin}, \frac{dT_{skin}}{dt}, T_{core}, \frac{dT_{core}}{dt}) \qquad \text{Eq. (3.1)}$$

where:

$T_{skin,i}$ represents local skin temperature of one body part;

Term i in our case is from 1 to 19, corresponding to the body parts: head, face, neck, breathing zone, chest, back, pelvis, left and right upper arms, left and right lower arms, left and right hands, left and right thighs, left and right lower legs, left and right feet;

Term t is time,

$dT_{skin,i}/dt$ is the derivative of skin temperature;

T_{core} is the body core temperature; and

dT_{core}/dt is the derivative of the body core temperature.

Skin temperature represents local skin thermal conditions. Body core temperature represents the whole-body thermal status.

Local comfort is then predicted as a function of local sensations and the average of all the body's local sensations. The overall sensation model (whole-body thermal sensation) integrates the local sensations to provide an overall evaluation for the whole body. The overall comfort model (whole-body thermal comfort) integrates the local comfort to give an evaluation of the whole-body thermal comfort. So these models are linked to the skin and core temperatures in an indirect way.

By correlating subjective perceptions with physiological parameters, the sensation and comfort models can have broad application. For example, clothing insulation level is not a limitation. It can be different, because it would result in increased or decreased skin and core temperatures, which are inputs to the proposed sensation and comfort models. Guan Guan et al. 2003) explained the advantage of correlating the physiology responses with sensation and the disadvantage of correlating the environmental parameters with the thermal sensation.

4. METHODS

4.1 General description of the experiment

We performed 109 human subject tests in the Controlled Environmental Chamber at the University of California (U.C), Berkeley from January to mid-August, 2002. Each test lasted from three to four hours. The chamber was controlled to specific temperature ranges from 20 to 32 °C. To create transient, non-uniform environments, we applied cooling or heating separately to 19 individual body parts (local step-change) until they approached steady state condition. We studied the following individual body parts: head, face, neck, breathing, chest, back, pelvis, left and right upper arms, left and right lower arms, left and right hands, left and right thighs, left and right lower legs, left and right feet.

We administered a questionnaire to assess subjects' local and overall sensation and comfort via a computer screen. The questions were repeated at a varying time step, from 1 to 3 minutes, throughout the step change. Meanwhile, we measured the subjects' skin temperature at 28 locations and body core temperature. The subjects wore a leotard and performed work at a computer during the tests.

The human subject test was approved by the U.C. Berkeley Committee for the Protection of Human Subjects (C.P.H.S).

We also performed a series of tests in a car in the Delphi Wind Tunnel. In these tests, subjects' skin and core temperatures were measured along with subjective perceptions of sensation and comfort for the whole body and individual body parts. The measurement and voting methods were very similar to those employed in the environmental chamber tests. The subjects' temperatures were measured prior to entering the automobile and then under a variety of air-conditioning conditions within the automobile. Results from the wind tunnel tests were mainly used to validate the predictive models of thermal comfort and sensation in asymmetrical transient conditions, developed based on the data from the environmental chamber studies as well as some data from the literature. The primary difference between the environmental chamber and wind tunnel tests was that, in the wind tunnel tests, the subjects controlled the car air conditioning settings. In the environmental chamber tests, test conditions were controlled by the researchers.

4.2 Experimental Facility

4.2.1 Controlled Environmental Chamber

The layout of the controlled environmental chamber is shown in Figure 4.1. The room is divided into three sections separated by partitions. Half of the room is used as the test station, which includes a computer for the subjects to work on and to use in responding to the thermal questionnaire, and a set of outlets to supply cold and warm air to individual body parts. The researcher's station includes a chair, a table, and a computer showing the data from the 28 thermocouples measuring the subject's skin temperature. In the third area of the room, a Jacuzzi bathtub (40 x 40 x 40 in) is installed; this tub is used to precondition each subject's whole-body thermal status before the tests begin.

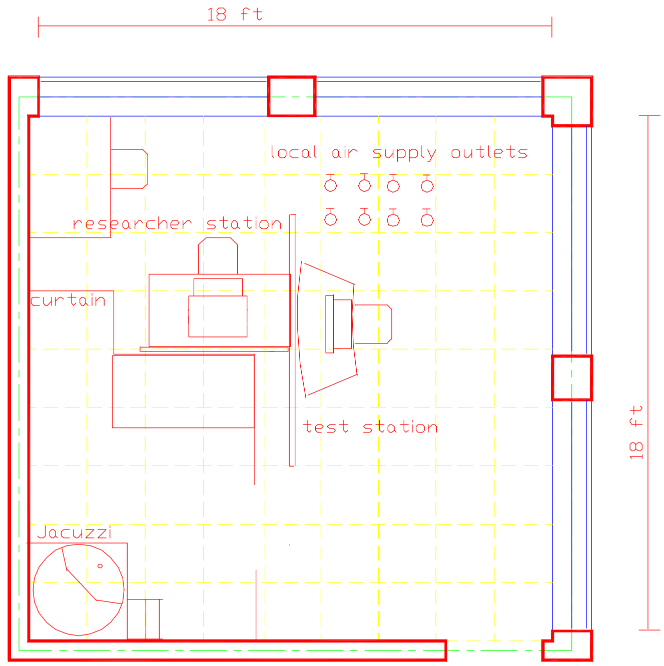

Figure 4.1 The controlled environmental chamber setup

4.2.2 Local warm- and cold-air supplies

The chamber has two air sources to provide cooling or heating to air sleeves (described below) surrounding different segments of the subjects' bodies.

The chamber has a separately controlled cold-air source, located in the floor plenum. This source has two lines: one connects to the local cold-air supply outlets, and the other connects to an electrical heater installed in the line leading to the local warm-air supply outlets. Valves installed near the outlets are used to control the airflow volume as required. Flexible ducts connect the air outlets to the air sleeves (Figure 4.2). The flexible ducts are supported by ropes hanging from the ceiling so they move easily in response to the movement of subjects connected to the air sleeves. The length of the ropes is adjustable so the height of the air sleeves can be changed to accommodate each subject.

Figure 4.2 Local cold- and warm-air supplies (valves, flexible warm and cold air ducts to connect to air-sleeves)

4.2.3 Pre-conditioning bath

Before each test began, we asked the subject to stay in the Jacuzzi for 15 minutes (Figure 4.3). The purpose of using the Jacuzzi is bring the human subjects rapidly to the designated thermal status for the given test (warm or cold conditions). We set the chamber temperatures to cover the following thermal sensations: slightly cool, cool, neutral, slightly warm, and warm. Using the two-node model, we calculated the room temperature required for each of these sensations, and the corresponding average skin temperature (Table 4.1). Then we set the water temperature equal to the average skin temperature.

Figure 4.3 Jacuzzi to precondition subjects' thermal states.

Table 4.1 Chamber and bathtub temperatures for tests (0.32 clo, 1 Met)

Body Thermal Status	Ambient Temperature °C)	PMV (two-node)	Tskin (two-node)	Bathtub Temperature C)
Neutral	26.9	0	34.5	34.5
Slightly warm	29.4	1	35.3	35.3
warm	31.8	2	35.6	35.6
Slightly cool	24.5	-1	32.9	32.9
Cool	22.1	-2	31.6	31.6

Normally it takes two to three hours for people to reach stable thermal status in new ambient thermal conditions in a laboratory experiment. Sitting in warm water in the Jacuzzi for 15 minutes can raise or lower subjects' core temperatures up to 0.4°C. The Jacuzzi is a very effective way to eliminate the difference in thermal status of subjects arriving for the tests, as caused by: the subjects' mode of arrival (some came by bicycle; some walked), the different ambient weather conditions as the seasons changed during the testing period (January to August), and the timing of the tests, which took place in the morning, afternoon, or evening. Because it was impossible to control subjects' thermal status at the time of arrival, the Jacuzzi provided a means of rapidly bringing subjects to the required stable body core temperature to begin the tests.

We installed a 250-W lamp heating on top of the Jacuzzi; the lamp was turned on when subjects emerged from the tub. The lamp's purpose was to compensate for evaporative heat loss, at which it was effective. However, the subjects' core temperatures did increase after leaving the Jacuzzi. This increase was due primarily to the increased exertion of putting on the leotard and having the thermocouples applied. The increase was unavoidable, but the period of sitting in the Jacuzzi provided consistent pre-test conditions.

The 15-minute Jacuzzi's time was based on trial observations, which showed that body core temperature stabilized within 15 minutes. If subjects remained longer in the warm water, the core temperature tended to increase; we did not test the long-term response to cold water.

4.2.4 Air sleeves for local cooling and heating

We used air sleeves to cool or heat individual areas of subjects' bodies. Using air for this purpose has major advantages:

1. Cooling and heating by air does not disturb the normal non-uniformity of skin temperature, which varies considerably even within a single body part. Skin temperature near superficial veins is, for example, significantly higher than in other areas because local vasoconstriction has less effect there. Skin temperature within a body part varies naturally. When we cool the skin using air, this natural variation is preserved. If a water suit is used, the skin temperature is closer to constant because the conductance to the water is so high. Figure 4.4 shows skin temperature distribution of a leg after cooling.

Figure 4.4 Skin temperature distribution after cooling with an air sleeve

2. For the body parts covered by the leotard and socks, air cooling/heating produces no sense of wind or turbulence. Thus heat is transferred without a sense of contact with a heavy material (water suit, electric heater, phase change material). The air sleeves give the sensation of still air conditions under light clothing.

3. For the face, hands, and breathing (which were not covered by the leotard or socks), people are accustomed to the feeling of skin being cooled or warmed by air movement, since these segments are normally unclothed.

4. The sleeves are easy put on and control, easy to fabricate; a tailor helped us sew sleeves for different body parts. Finally, as noted above, our environmental chamber had easily accessible and controllable warm- and cold-air supplies for use with the air sleeves.

Other options that we considered, including phase-change material, electric fabric, and different air cooling/heating ideas, are described in Appendix A.1

4.2.4.1 General air-sleeve design

The air sleeve is made of spinnaker cloth used for sail boats. This fabric is wind proof and very light.

Because the heat capacity of air is low, a large volume of airflow is necessary to keep the air temperature uniform as it traverses the length of the sleeve. To ensure uniform air supply and return and to prevent local spot heating or cooling near the sleeve entrance and exit, we designed a manifold that disperses the air around the circumference of the sleeves. A diagram in Figure 4.5 shows the details.

Supply air is introduced to an inlet manifold which has two layers. The outer layer is spinnaker cloth, and the inner layer is made up of mesh fabric. A baffle of spinnaker cloth in front of the air-supply entrance prevents air from blowing directly on subjects' skin and creating spot heating or cooling. The supply air inflate the manifold, and is then forced uniformly through the inner circle of mesh into the air sleeve.

The outlet of the air sleeve is designed in the same way as the entrance. The mesh material in the inner layer of the manifold permits the air to pass uniformly into the outlet after travelling over the subject's skin. A Velcro belt allows adjustment of the sleeve length. Before the human subject tests started, we repeatedly tested the sleeve design.

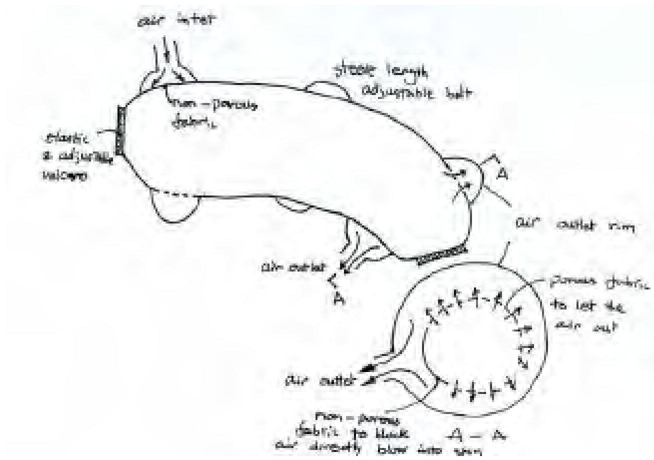

Figure 4.5 Design details of the air sleeve

4.2.4.2 Leotard

We were concerned that the large volume of airflow in the air sleeve might cause movement of subjects' skin hair, creating a sensation of moving air that would affect the subjects' perceptions of thermal comfort. To completely eliminate movement of skin hair, we had the subjects wear a leotard. The leotard fabric is thin and elastic, fits skin closely, and does not offer much insulation. As mentioned above, trial tests revealed no perceptible air motion for body parts wearing a leotard and connected to an air sleeve. The borders of each body part to be studied are defined by Velcro sewed on the leotard. The Velcro connects to the air sleeve, confining cooling and heating to specific areas of the body.

The leotard also prevents movement of the wires attached to the thermocouples that measure skin temperature. The 28 thermocouples are grouped into seven groups; each group is placed inside a 3/8-inch-diameter flexible tube. The seven tubes all emerge from the leotard at the back of the neck, sending the thermocouple data to the data acquisition board, which is hung in a basket near the subject. The subjects reported that after putting on the leotard, they were unaware of the thermocouples and wires.

A thermal manikin was used to measure the leotard clothing insulation level; Figure 4.6 shows the manikin test and clothing insulation data. The overall insulation value of the leotard (with a pair of cotton socks) is 0.32 clo (clo is the unit of measure of clothing insulation value. 1 clo = 0.155 m^2 K/Watt) . The high clo levels for back and chest are because of the air gap between the skin and the leotard in those areas. The clo value for socks is 0.51. The clo values affect only the rate of cooling/heating change because the skin temperature is measured under the clothing. This reduction in the cooling/heating rate seems unlikely to have affected our test results as our subjects reported very strong local cooling/heating sensations during cooling/heating of the back and chest areas.

head	0	l. hand	0
chest	1.10	r. hand	0
back	0.59	l. thigh	0.22
pelvis	0.28	r. thigh	0.22
l. u. arm	0.30	l. l leg	0.26
r. u. arm	0.30	r. l. leg	0.26
l. l. arm	0.22	l. foot	0.51
r. l. arm	0.22	r. foot	0.51

Figure 4.6 The thermal manikin measuring the clothing insulation value of the leotard, with insulation values (clo) listed.

4.2.4.3 Air-sleeve design for different body parts

Thirteen parts of the subjects' bodies were individually heated or cooled. For the limbs, we tested only one side of the body on the assumption that sensation for left and right sides is symmetrical. Research has shown that breathing zone air intake has a special influence on perceived thermal discomfort and indoor air quality (Berglund and Cain 1989, Fang et al., 1998, Toftum et al. 1998, Toftum et al. 2002), so we studied cooling of the breath intake air separately. We studied cooling of the neck separately from cooling of the head because the upper back and back of the neck are sensitive to draft (Fanger and Christensen 1986, Fanger, Melikov et al. 1988). We also examined cooling of the face separately from cooling of the rest of the head (hereafter termed 'head'). Although people often experience cooling of both face and head together in daily life, there are times when the face is cooled without much cooling reaching the head.

The subsections below describe the air sleeves designed for cooling of each body part/area of study, with examples of the use of each sleeve. When in use, all air sleeves are connected to the warm- and cold-air supplies shown in Figure 4.1 above.

Breathing zone

The edge of the sleeve for cooling breath intake is made of soft, thick, fuzzy material that comfortably seals against facial skin (Figure 4.7, left). During the experiments, we use a single layer of surgical tape to ensure no air leakage between the sleeve and the skin. An elastic band around the back of the subjects' heads holds the sleeve in place at the nose and mouth.

The sleeve fabric is very light, and the sleeve is attached using Velcro to a bar that is, in turn, suspended from the ceiling by a rope whose height is adjustable; this arrangement prevents the sleeve from pulling in any way on the subject's head or restricting his/her movement (Figure 4.7, right). The subject can clearly see the computer screen.

Figure 4.7 Breathing air sleeve

Head

Before attaching the head air sleeve, a thick, fuzzy band is first wrapped around the head to prevent air leakage to the face and neck regions (Figure 4.8 left). The band is adjustable, using Velcro, to accommodate the head circumference of each subject. Above the fuzzy band, Velcro attaches the air sleeve, which is connected to the supply air inlets. The air outlet extends to the side.

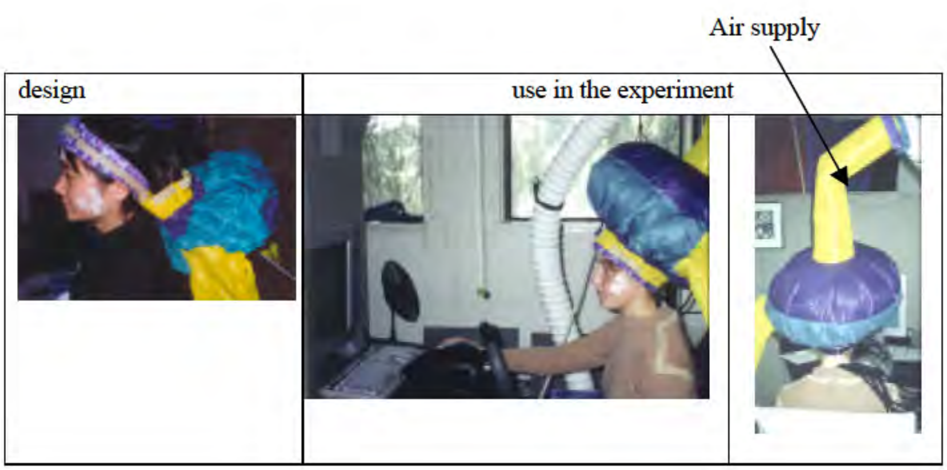

Figure 4.8 Head air sleeve

Neck

Since the leotard did not cover the neck, the neck sleeve is all impervious nylon spinnaker cloth. The Neck is cooled by conductive contact between the nylon air sleeve and the skin, which avoid any air movement on the back of neck (Figure 4.9).

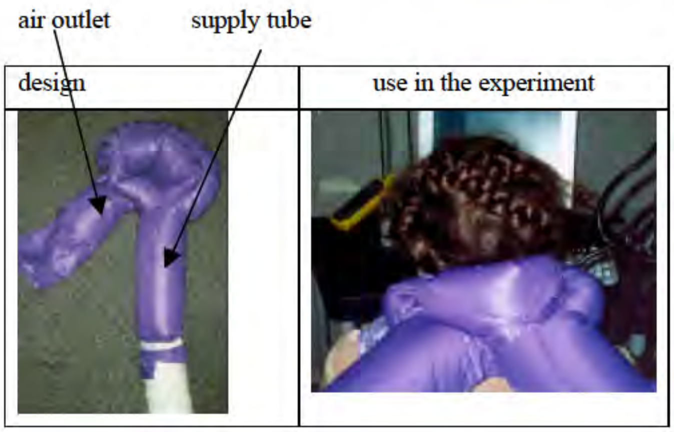

Figure 4.9 Neck air sleeve

Face

A clear curved sheet of plastic attached to the outlet of the air sleeve conducts the air to the face without blocking the subject's field of view (Figure 4.10).

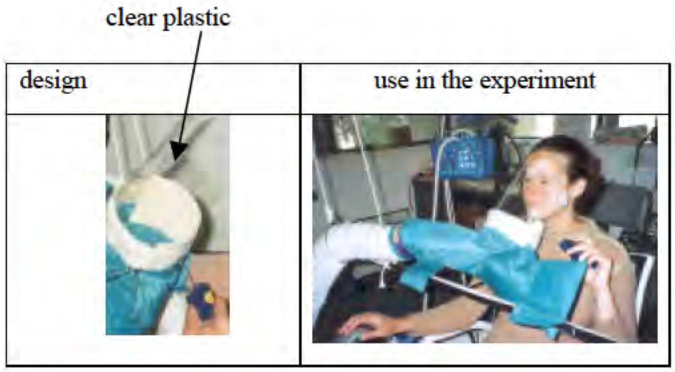

Figure 4.10 Face air sleeve

We were concerned that air movement from the face air sleeve might irritate the subjects' eyes, so we prepared goggles for eye protection if necessary. Only one subject, who wore contact lenses, felt uncomfortable with air blowing on the face (Figure 4.11).

Figure 4.11
Use goggles in a test

Chest

The supply air manifold and the sleeve cover the chest area when this area is being studied. A soft, fuzzy layer of fabric prevents air leakage at the neck. Figure 4.12 shows the chest air sleeve.

Figure 4.12 Chest air sleeve

Back and pelvis

To test thermal effects on the back and pelvis areas, a nylon mesh chair was customized. Separate polyethylene foam enclosures around the back and seat of the chair provide ducting and connections for the air supply. The mesh surface uniformly distributes air toward the subject. Velcro is attached to the chair surface around the perimeter of the mesh panels. It connects to the air sleeve, which, in turn, is attached to the subject's leotard. The back and pelvis air sleeves are shown in Figure 4.13.

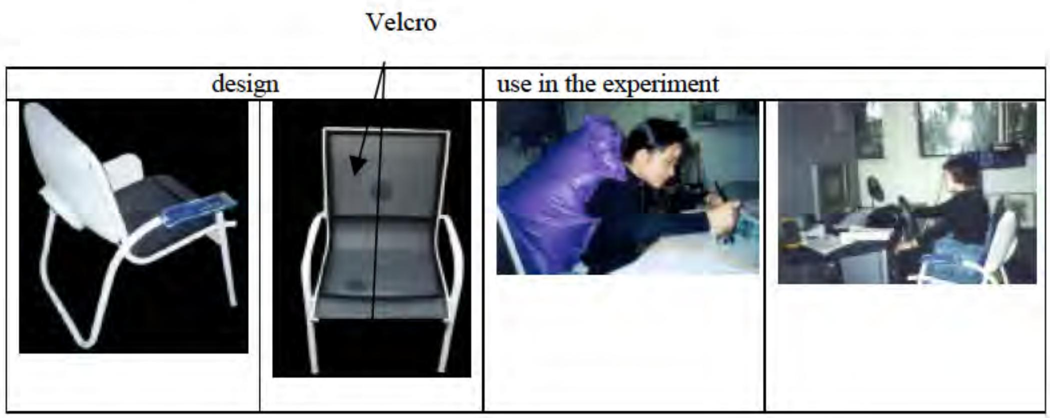

Figure 4.13 Back and pelvis air sleeves

Arm

The issues related to design of the arm air sleeve are described above in the section "General air sleeve design ." The arm sleeve is shown in Figure 4.14.

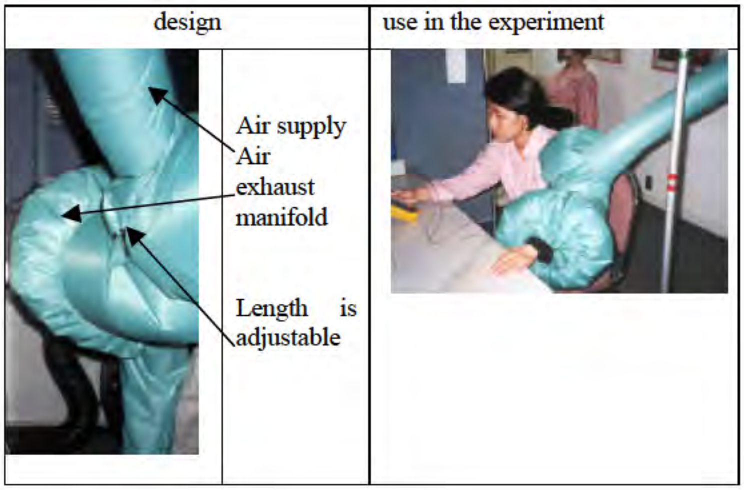

Figure 4.14 Arm air sleeve

Hand

The entrance and exhaust manifolds are visible in the photo of the hand air sleeve, Figure 4.15.

Figure 4.15 Hand air sleeve

Leg

The leg air sleeve is sewn in an L-shape that matches the leg posture of a sitting subject. Fuzzy material is used between the legs to block radiant and conductive heat transfer to the other leg. The leg air sleeve is shown in Figure 4.16.

Figure 4.16 Leg air sleeve

Foot

To heat or cool the foot, air is supplied from a bottom manifold and comes through nylon mesh that supports the foot. The air sleeve encloses the manifold and the foot. The air exhausts upward. The foot air sleeve is shown in Figure 4.17.

design	use in the experiment
	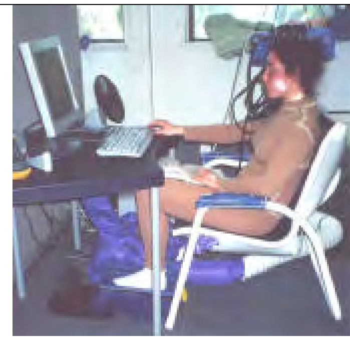 Cooling on right foot. The left foot is supported by another mesh stool for comfort.

Figure 4.17 Foot air sleeve

4.3 Measurement

4.3.1 Skin Temperature Measurement

4.3.1.1 Skin Temperature Measurement Sites

Skin temperature was measured using 28 thermocouples. We chose skin temperature measurement locations based on four considerations:

- Separate measurements are made for each of the 19 body segments studied (shown in Figure 4.18 without any highlight). These skin temperatures are used for local thermal sensation regression analysis.

- The measurement sites include the seven locations normally used in the literature to calculate mean skin temperature (forehead, belly, left forearm, left hand, left thigh, left calf, and left instep, shown in Figure 4.18 with dark highlights). Mean skin temperature is necessary to represent the whole-body thermal state in our regression analysis. Use of these seven locations also permits us to compare our results with those of other studies, since these locations are commonly used. The thermocouples for the 19 body parts include six locations needed for calculating the mean skin temperature, except one on the left calf. We added one thermocouple there.

- We put two additional thermocouples in locations which have special interest to us: finger and back neck.

These 22 locations are shown in Figure 4.18.

- Six additional thermocouples are placed in specific locations for the areas of the body being tested in each test, e.g., lower back and upper back. Typically, each test entailed three local cooling or heating applications. We normally put two additional thermocouples in each of these three locations, to measure detailed local skin temperature of those body parts.

Our selection of the seven locations monitored to determine mean skin temperature is described in Appendix 4.2 with a review of relevant literature.

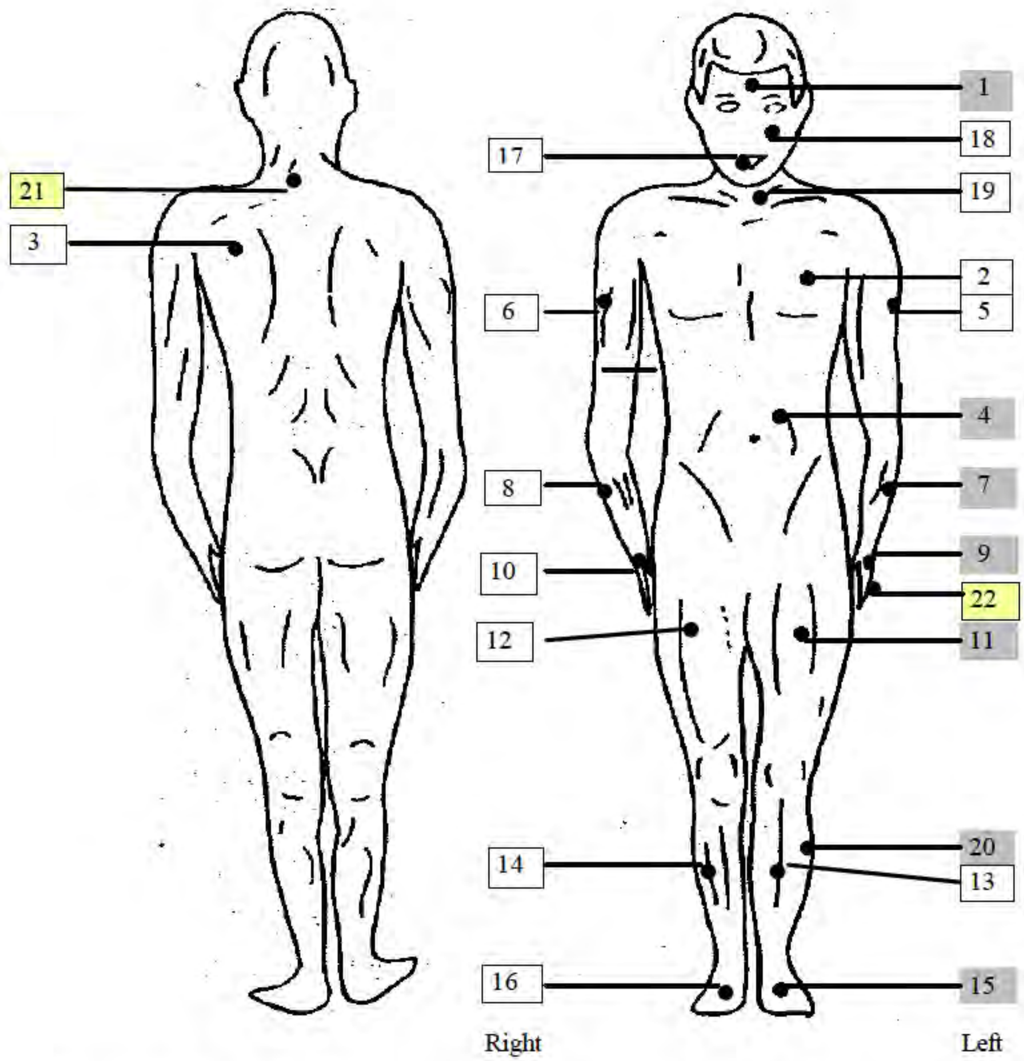

Figure 4.18 Twenty-two skin temperature measurement locations

Number 1 – 19: Local skin temperature for 19 segments studied

Seven sites to get mean skin temperature (Hardy/DuBois)

Additional local skin temperatures of interest

4.3.1.2 Thermocouples

The thermocouples used are made of the thinnest thermocouple wire available (28 gauge) from Omega (Figure 4.20). This thin, flexible wire ensures good contact with skin, is not easily broken (because it is not stiff), and is not perceived by the subjects wearing the leotard. In addition, the thin-wire thermocouples have a rapid response times, which is necessary because for the rapid, transient conditions being studied. The thermocouple is soldered to a copper plate with a diameter of eight millimeters (mm) and a thickness of 0.15 mm. Berg (Berg 1974) examined the capacity and conductance of skin and compared the response times of bare skin and skin covered by a 0.15-mm copper plate. He found that the response times from the two are very close, and that the thermal resistance of the metal plate is negligible.

The thermocouple is connected to the copper plate with a solder joint; because this connection is easily broken, we added a very small amount of polyurethane rubber glue to reinforce the joint. The thin wire and copper plate ensure collection of high-quality transient skin temperature measurement data.

We examined whether we should add atop the thermocouple in order to ensure that the thermocouple is not influenced by the environmental temperature when reading skin temperature. This question involves a tradeoff. If too much insulation is added, then the local skin temperature is increased; if too little insulation is added, the thermocouple might be disproportionately influenced by the air temperature. This question is particularly critical in our test because the air sleeves involve high rates of convection at the skin. We did a finite-element analysis of the heat transfer through and around a thermocouple to see how much insulation is needed between the thermocouple and ambient air so that the thermocouple reading represents only skin temperature, uninfluenced by air temperature. The simulation results show that one layer of tape plus one layer of leotard provides sufficient insulation to ensure that the thermocouple is not influenced by air temperature. The leotard covers the entire body (except the head, neck, hands, and feet). Because the leotard covers the entire body, it does not create any local spot heating directly below the thermocouple as would be the case if we put more insulation on the back of the thermocouple itself, but does insulate the thermocouple against the air.

The thermocouples were taped on the subjects' skin with surgical tape, which allows air to penetrate so the skin can breathe. Figure 4.19 shows a test subject wearing thermocouples.

Figure 4.19 Subject wearing thermocouples and leotard during a test

4.3.1.2.1 Calibration of the thermocouples

The thermocouples were calibrated with a Dry-Well Calibrator (Model 9105) produced by Hart Scientific. The calibration was performed for air temperatures of 10, 15, 20, 25, 30, 35, and 40°C. The dry-well temperature stability is ±0.02°C. The calibrator accuracy is 0.1°C, with resolution of 0.01°C (Figure 4.20).

4.3.1.2.2 Data acquisition

The data-acquisition system was set up using LabView software. During the tests, we observe skin temperatures on a computer screen (Figure 4.20). The thermocouple temperatures are recorded every 5 seconds.

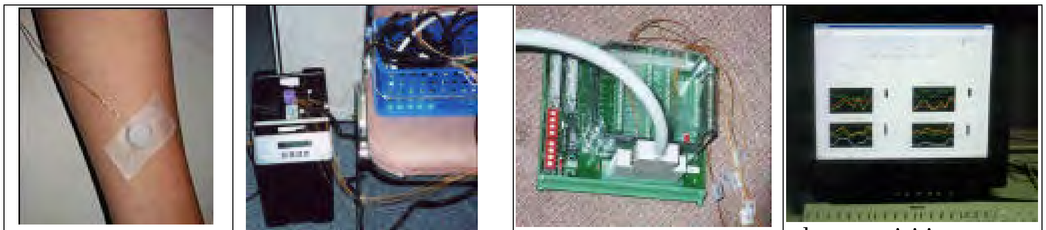

a thermocouple	calibration dry-well	data acquisition units	data acquisition display

Figure 4.20 Thermocouple, calibration, and data-acquisition system

The two thermocouple data-acquisition units are located in a basket suspended near the subject. The basket's position can be lifted or lowered and moved forward or backward by means of lines attached to a bar mounted near the ceiling. Because this suspension system moves easily, the basket and TC wires do not hinder subjects' movement.

4.3.2 Core temperature measurement

4.3.2.1 Wireless Sensor Pill

We used a wireless sensor in the form of a pill to measure subjects' core temperatures. Each subject swallowed a CorTemp™ thermometer pill (from HTI Technologies, Inc.) when s/he arrived for the test session. A recorder (CTC-2000) tied around the subject's waist recorded, displayed, and stored temperature data at 20-second intervals. After each test, the data were transferred to a computer for analysis.

The CorTemp™ pill was originally developed for use by the National Aeronautics and Space Administration (NASA) to monitor astronauts for dangerously low or high body core temperatures (http://www.htitech.com/CTSensor htm). Each silicone-coated capsule contains a telemetry system, a microbattery, and a quartz-crystal temperature sensor (Figure 4.21). Inside the gastrointestinal tract, the crystal sensor vibrates at a frequency in direct proportion to the body temperature surrounding it, producing an electromagnetic flux that is magnified by the sensor electronics and transmitted through the body to the recorder.

Each pill is 23 mm long and 9 mm in diameter. The pill's accuracy is ± 0.1 °C, and resolution is 0.01°C. The associated recorder is 4.72 x 2.23 x 0.98 inches.

The CorTemp™ pill's sensors are calibrated by the company using a National Institute of Standards traceable RTD, a frequency counter, a bath with stability of ±0.01 °C, and a three-point (35, 45, 40 °C) calibration and test process. The company's calibration and test results show that most sensors are accurate to between 0.03 and 0.05 ºC. Sensors that do not pass calibration are calibrated a second time by the company; if they fail on the second calibration, they are discarded.

Using a mercury thermometer and water in the Jacuzzi bathtub, we verified readings for a few pills; all were within 0.05°C.

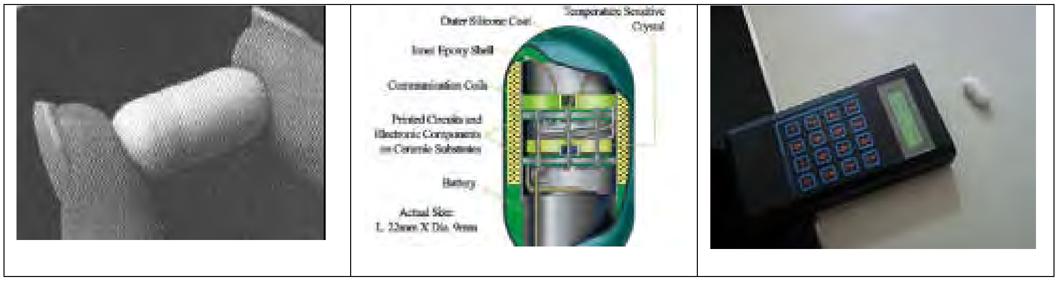

Figure 4.21 HTI Technologies, Inc. ingestible thermometer pill and associated recorder

The advantage of CorTemp™ is that it is accurate, unintrusive, and continuously measures body core temperature. A potential disadvantage is that the pill moves along through the digestive tract (it is ultimately eliminated by bowel movement). If the variation of temperature inside the body is small, this changing of the pill's location will not result in significant error (personal communication with M. Ducharme at the 5th International Meeting on Thermal Manikin and Modeling, 2003). It is known however that internal temperature varies between organs depending on metabolism and blood flow. The liver is typically the warmest organ (Segre 2002). To avoid this potential inaccuracy, we had subjects swallow the pill at the same time shortly prior to the test with warm water (about 40 minutes before they started the first votes).

During the tests we also periodically used an infrared ear thermometer to measure subjects' ear temperatures.

4.3.2.2 Discussion of core measurement methods

In research, body core temperature is commonly monitored through rectal, esophageal, tympanic, and ear measurements. Rectal measurements tend to be high relative to readings from other locations, and there is a also delay in retrieving rectal readings. Esophageal readings are more representative of the actual body core temperature. Tympanic and ear measurements are more reflective of temperature at the hypothalamus thermoregulatory center.

To compare results from the pill and tympanic and ear methods, we measured core temperature simultaneously using the pill, a thermocouple to the tympanic membrane, and an infrared ear thermometer (manufactured by Braun Company). The comparison results are presented in Appendix 4.3.

4.3.3 Thermal sensation and comfort

4.3.3.1 Seven-point sensation scale and Bedford's comfort scale

The two most widely used scales for evaluating thermal sensation and comfort are The American Society of Heating, Refrigeration, and Air-Conditioning Engineers (ASHRAE) seven-point sensation scale, and Bedford's sensation and comfort scale are.

The ASHRAE seven-point scale, shown in Table 4.2, has been widely used for thermal sensation assessment in both laboratory and field studies (Rohles 1970, Schiller, Arens et al. 1988).

Table 4.2 ASHRAE sensation scale

value	description
3	hot
2	warm
1	slightly warm
0	neutral
-1	slightly cool
-2	cool
-3	cold

McIntyre (McIntyre 1980) explains why a seven-point (versus three- or 25-point) scale is appropriate for psychological measurement. When people are presented with a set of stimuli that vary in one dimension only, the number of stimuli that can be unambiguously identified is relatively small. Subjects can identify about six different tones and five degrees of loudness without error. Along with McIntyre, Miller (Miller 1956) investigated this range, which he called the "span of absolute judgment." For several different types of stimuli, Miller found that people cannot generally deal with more than about seven levels of sensation without confusion. Because the temperature range for automobiles can be exceptional large in both the warm and cold directions, automobile thermal comfort studies have used scales of nine and more points.

Bedford's (Bedford 1936) well-known scale of sensation and comfort (Table 4.3) conflates warmth and comfort but does at least address the issue of comfort. Bedford's scale has also been applied to both field and laboratory studies (Bedford 1936; Lewis, Meese et al. 1983).

Table 4.3 The Bedford scale

value	description
3	much too warm
2	too warm
1	comfortably warm
0	comfortable
-1	comfortably cool
-2	too cool
-3	much too cool

Comfort is not necessarily dependent only on sensation; perceptions of comfort may also have to do with expectation, adaptation to conditions, and other factors. Thus, information about sensation alone is not sufficient to evaluate a subject's comfort; direct questions must also be asked about comfort level. Because of the complexity of assessing comfort transient conditions in an asymmetrical environment, we asked subjects separate questions about both thermal sensation and comfort.

4.3.3.2 Sensation and comfort scales used in our tests

The sensation scale used in our tests covers a range from “very cold” to “very hot.” It is a continuous scale; subjects can identify any place along the scale as corresponding to their perceptions (Figure 4.22). Internally, the scale is translated to the numerical values, i.e., “very cold” is –4, “cold” is –3, “cool” is –2, “slightly cool” is –1, “slightly warm” is 1, “warm” is 2, “hot” is 3, and “very hot” is 4. Our scale is thus very similar to the ASHRAE seven-point thermal sensation scale, with “very cold” and “very hot” added to encompass thermal possibilities similar to the extreme conditions found in automobile studies, as referenced below, and studies covering wider sensation range, such as the one carried out by Goto (Goto et al., 2002) examining thermal sensations corresponding to different levels of activity. The transience and asymmetry of conditions in our tests are greater than is typically found in “ normal” environments, such as offices.

A study by Kansas State University for Ford Motors added the gradation “cold/cool” between “cold” and “cool” and “hot/warm” between “hot” and “warm” to expend the scale to nine points (Guan 2003). The scale is similar to Bedfords’ sensation and comfort scale: cold, cold/cool. Comfort/cool, comfort, warm/comfort, hot/warm, hot. A Toyota study expended the scale to 11 points, adding “slightly hot” between “warm and hot,” “slightly cold” between “cool” and “cold,” and the two extremes of “very hot” and “very cold” (Taniguchi, Aoki et al. 1992). A study by Nissan used the same nine points that we use in our study (Hagino and Hara 1992).

In addition to Bedford's combined comfort and sensation scale, some studies have applied a specific comfort scale. Hagino (Hagino and Hara 1992) used a seven-point comfort scale: +3 (very comfortable), +2 (comfortable), +1 (slightly comfortable), 0 (neutral), (-1) slightly uncomfortable, (-2) uncomfortable, (-3) very uncomfortable.

Our study uses the comfort scale as shown in Figure 4.22, which ranges from very uncomfortable (-4) to very comfortable (+4). In the middle we break the scale, between "just uncomfortable (-0)" and "just comfortable (+0)," which forces subjects to make a broad determination about whether their perceived state falls in the overall category of "comfortable" or "uncomfortable."

In our tests, the sensation and comfort questionnaires address both the *whole body* and the specific *body parts* being heated or cooled in each specific test. The questionnaires appear at designated time intervals (1 – 3 minutes) on the computer screen facing the subjects in the test chamber. The intervals are designed so that, when fast transient conditions are being studied, questions appear on the screen at one-minute intervals, right after the application of the local thermal stimulus and its removal. After five minutes, the time interval grows longer until, for the longest tests, it reaches three minutes. Each time the questionnaires appears, it includes five questions. The first addresses overall sensation and the second addresses overall comfort. If the test in progress entails local cooling or heating applications, the third question addresses local sensation , i.e., the sensation in the body part that is receiving a local thermal stimulus application or removal. The fourth question is about local thermal comfort, and fifth question could be either sensation or comfort for a body part different than that being heated or cooled. The purpose of adding the fifth questionnaire is to distract the subjects' attention from the body part that is actually being heated or cooled. Prior to any application of local cooling or heating, the questionnaire also includes five questions each time it appears on the screen. The first and second question address whole-body thermal sensation and comfort, and the remaining three questions address randomly selected specific body parts.

Each question appears on the subject's screen separately and disappears after being answered; thus, the subjects cannot see the other questions or the history of responses while answering the questions each time.

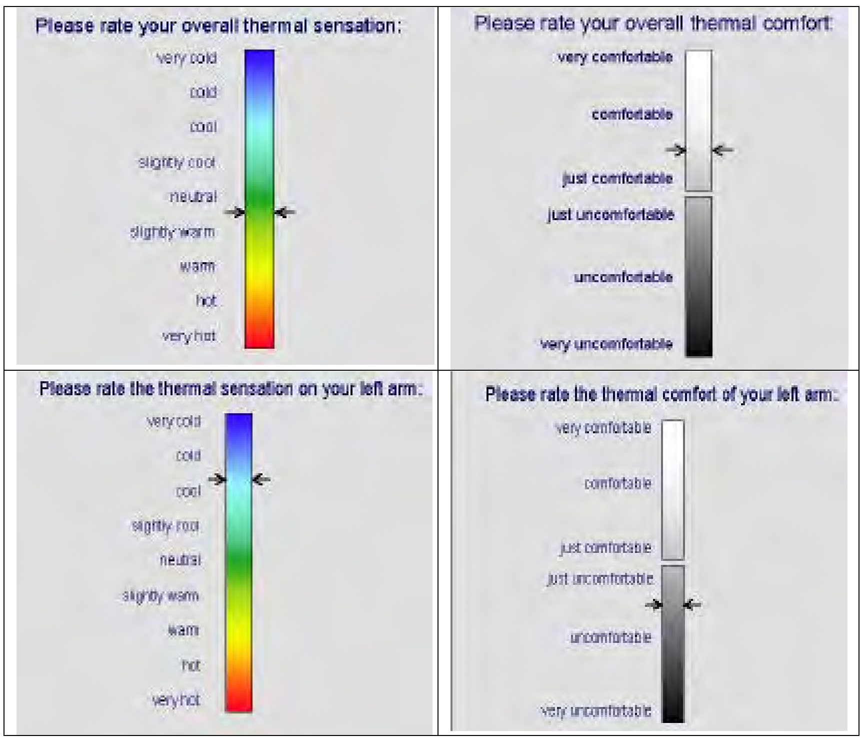

Figure 4.22 Thermal sensation and comfort scales

4.4 Test description

4.4.1 Test procedure

Each test takes three to four hours. Upon the subject's arrival, s/he first swallows the core temperature measurement pill with warm water and then spends 15 minutes in the Jacuzzi to precondition his/her overall body temperature. The temperature of the Jacuzzi is pre-adjusted according to the test of the day, as described earlier. After the subject leaves the Jacuzzi, the researcher places the 28 thermocouples at the different sites on the subject's body, as explained earlier. After the thermocouples are placed, the subject puts on the leotard described earlier and then sits on the chair in front of the computer and begins to answer the thermal questionnaires as they appear on the computer screen. Meanwhile, the data acquisition program collects readings from the 28 skin- temperature thermocouples, and the recorder takes body core-temperature data.

After about 60 minutes, the first local cooling or heating is applied to one body part through an air sleeve. The thermal comfort questionnaires are administered as described above, depending on the test being done. After 10 to 20 minutes (depending on the body part being heated or cooled, section 4.4.2.1) of local cooling or heating, the thermal stimulus is removed. A 30-minute recovery period follows, and then a local thermal stimulus is applied to another body part, and the subject answers thermal sensation and comfort questions for the new body part being heated or cooled as well as for the entire body. This procedure repeats three times -- i.e., three body parts are heated or cooled. Then the test for that day is complete, and the subject is paid. Normally the measurement time continues for more than 3 hours. The entire test (starting from the arrival of a subject) takes four hours.

For tests that entail heating or cooling for multiple rather than single body parts, two or three body parts are heated or cooled simultaneously. The entire test is complete after two multiple sets of heating/cooling to multiple body parts.

During whole-body step-change tests, the subject's whole body moves between two different environments: warm – slightly cool – warm, slightly cool – warm – slightly cool.

The first environment was the controlled environmental chamber's anteroom, followed by the test chamber described above. The subjects carried the basket with the data acquisition system with them as they walked from one room to the other. The computer with the thermal sensation and comfort questionnaires was put on a movable cart, and moved between the two rooms as well.

The "Types pf tests" section below gives additional detail about the testing.

4.4.2 Types of tests

We performed six different types of tests for this project. Below is a brief summary for each type of the tests. A detailed description of the conditions for each of the 109 tests is given in Appendix 4.4.

4.4.2.1 Single body part cooling and heating test

To test heating or cooling of a single body part, we set the chamber at a specific temperature (based on the two-node model). The correspondences among the bathwater, room, and desired skin temperature are shown in Table 4.1, section 4.2.3. The supply air temperature was determined based on trial and error, assessing the subjects' responses to the degree of temperature. Because we could only perform a limited number of tests, we aimed for relatively strong sensations of temperature change to ensure that a large of range of temperature change was experienced.

After a subject responded to the initial thermal questionnaire for one hour, the first cooling or heating stimulus was applied to a single body part. Eleven body parts were given local cooling or heating applications: head, face, breathing, neck, back, chest, pelvis, arm, hand, leg, and foot.

The duration of the local heating or cooling differed. For most body parts, the heating or cooling continued for 10 minutes. For extremities, durations were longer: 15 minutes for leg and arm, respectively and 20 minutes for hand and foot, respectively. The durations were chosen based on trial tests that showed that, for most body parts, subjective votes stabilized with 10 minutes, but a longer period of time was required before votes stabilized for extremities, especially hands and feet.

We performed 70 local cooling tests and only eight local heating tests. We emphasized cooling to address our sponsor's primary interest in vehicle cooling. Situations that cause local cooling are more common in real buildings, such as using a localizes personal control system, occupying in a naturally ventilated building, cooling of lower extremities caused by the air temperature stratification, working in a workplace near a big cold window in winter. People are more sensitive to cooling than heating because we have more cold thermoreceptors and they are located more superficial than warm thermoreceptors. The eight tests in which there was local heating of a cold whole body were primarily performed to provide comparisons for the cooling tests. For these tests, the chamber was set at temperatures between 16 and 20 °C. Three tests

RECORD 5

were also conducted in which there was local cooling of a cold whole body tests. No tests were carried out on local heating of a warm whole body. These tests are summarized in Table 4.4.

Table 4.4 Single-body-part cooling and heating tests

<table>
<tr><th>Test</th><th>Example</th></tr>
<tr><td>
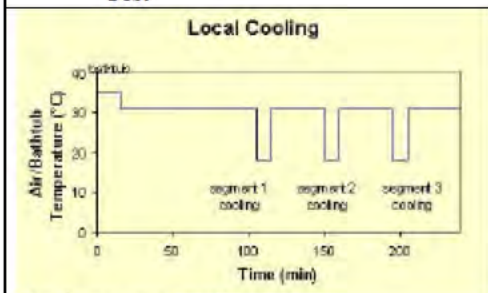

single segment cooling in warm environment (67 tests)
</td><td rowspan="3">

</td></tr>
<tr><td>
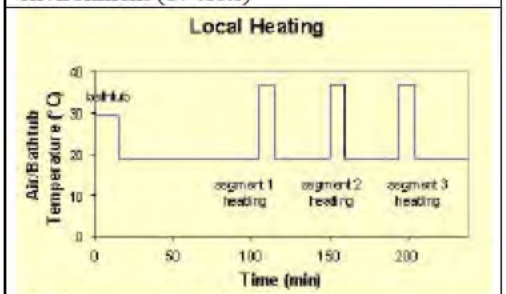

single segment heating (8 tests)
</td></tr>
<tr><td>
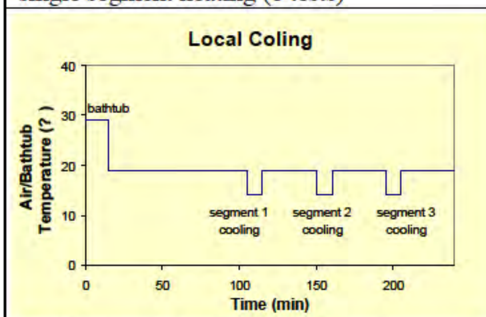

single segment cooling in cold environment (3 tests)
</td></tr>
</table>

4.4.2.2 Multiple segment cooling and heating test

The purpose of the multiple cooling/heating tests was to examine the impact of multiple signals on overall sensation. The results help define how the body integrates more than one signal.

It was impossible to include all the combinations of body parts, so we chose the combinations that are relevant in automobile interiors. Therefore, we also call these tests the "practical combination tests". For example, we chose face and chest cooling with arm heating because this is similar to the conditions in a car when air-conditioning is on while the sun shines on the arm. The duration of multiple cooling/heating was 20 minutes. We performed 17 of these combination tests, summarized in Table 4.5.

Table 4.5 Multiple-body-part cooling and heating tests

Test	Example
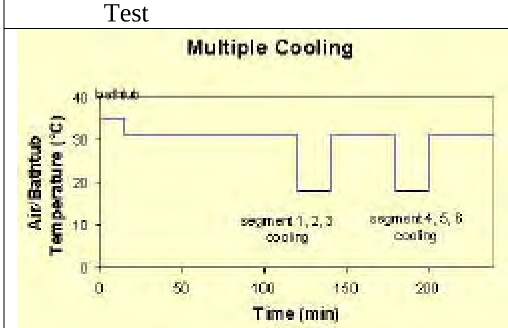 multiple segment cooling (10 tests)	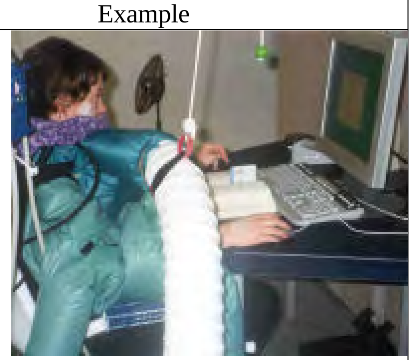
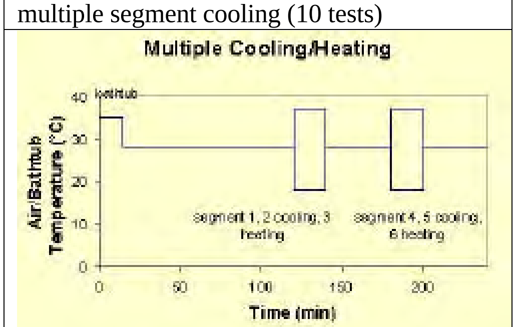 multiple segment cooling/heating (7 tests)	

We consider the period before the application of the first local heating or cooling or multiple cooling/heating to be stable conditions. This period represents a stable warm or cold environment depending on the chamber air temperature.

4.4.2.3 Whole-body step-change tests

The time frame for the whole-body step-change tests is different from that for the local cooling and heating tests. During the whole-body step-change tests, the subjects moved between two environments, remaining in each for 60 minutes.

There were five whole-body step-change tests: two in which the subjects moved from slightly cool to warm to slightly cool environments, and three in which subjects moved from warm to slightly cool to warm environments (Table 4.6).

Table 4.6 Whole-body step-change tests

<table>
<tr><th>Test</th><th>Example</th></tr>
<tr><td>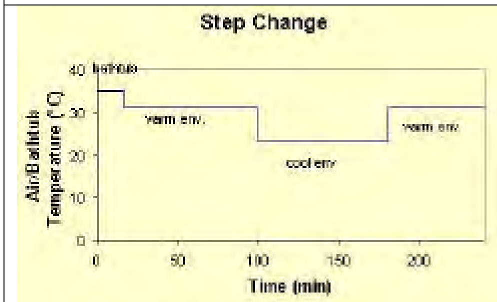

whole body step change: warm – sl. cool – warm (3 tests)</td><td rowspan="2">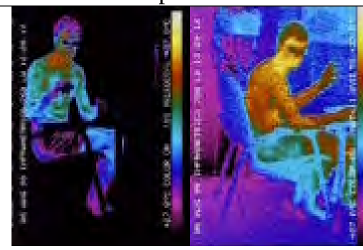</td></tr>
<tr><td>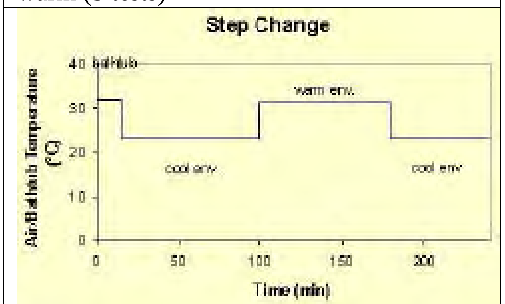

whole body step change: sl. cool – warm – sl. cool (2 tests)</td></tr>
</table>

4.4.2.4 Neutral-condition tests

The neutral condition tests have three purposes.

First, they provide local skin temperature set points needed to develop thermal sensation and comfort prediction models. Second, we want to understand subjective evaluation of thermal comfort in neutral conditions and to use it as a baseline reference when developing comfort model. Finally they permit us to observe core, skin temperatures, sensation and comfort responses under neutral condition in order to compare with results from warm- and cold-stable and transient condition tests. We cannot, however, determine core temperature set points from these tests because people’s core temperatures change too much depending on factors such as the time of day, and, for women, where they are in the menstrual cycle. Nonetheless, the behavior of core temperature in neutral conditions provides important information for understanding the core temperature responses during cold and warm transient conditions.

For neutral-conditions tests, the chamber air temperature is slightly cooler than neutral air temperature and four heat lamps (250 x 4 = 1,000 W) are mounted on the ceiling. The four lamps are aimed at the subjects from about three meters away, so the radiation is fairly uniform. People could control the power output of the four heating lamps by turning a voltage-controller that was put on the table. Subjects were instructed to change the heat-lamp output to maintain neutral conditions. We put a sheet of foil on the floor to reflect heat to lower body parts and ensure that the environment is relatively uniform. The subjects continuously voted for 2 hours. Table 4.7 shows a subject in the test chamber during a neutral-condition test and the time and temperature conditions of the tests.

Table 4.7 Neutral-Condition tests

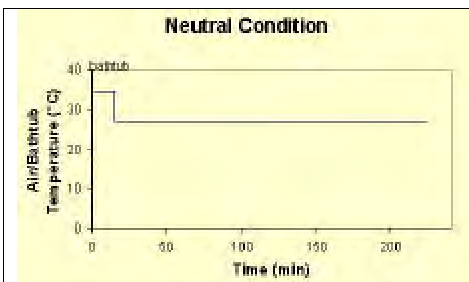 neutral condition (5 test)	 

4.4.2.5 Taking Infrared video images

During approximately one week, we took infrared images during the application of heating and cooling to body parts and also during whole-body step-change tests. Our purpose was to visually observe the transient skin temperature distributions during body-part cooling applications and whole-body step-change tests. Table 4.8 shows typical infrared video images for hand in a cool environment, foot after right foot cooling (the subject was sitting on a chair). The IR-images for step-change tests were shown in Table 4.6.

Table 4.8 Infrared video image tests

Local cooling and whole body step change tests	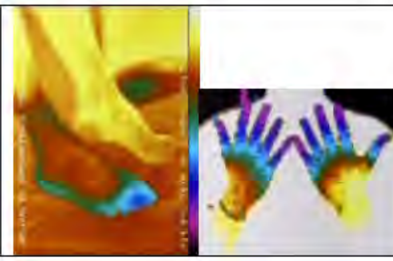

4.4.2.6 Delphi Wind Tunnel tests

We performed an entirely separate set of tests in a real vehicle in a wind tunnel. Delphi Harrison Thermal Systems gave us access to their climate-controlled wind tunnel facility in Lockport New York (Figure 4.23) for a two-week testing period, between July 22 to August 1, 2002. We used data from the Delphi tests to validate our model's accuracy in automotive environments.

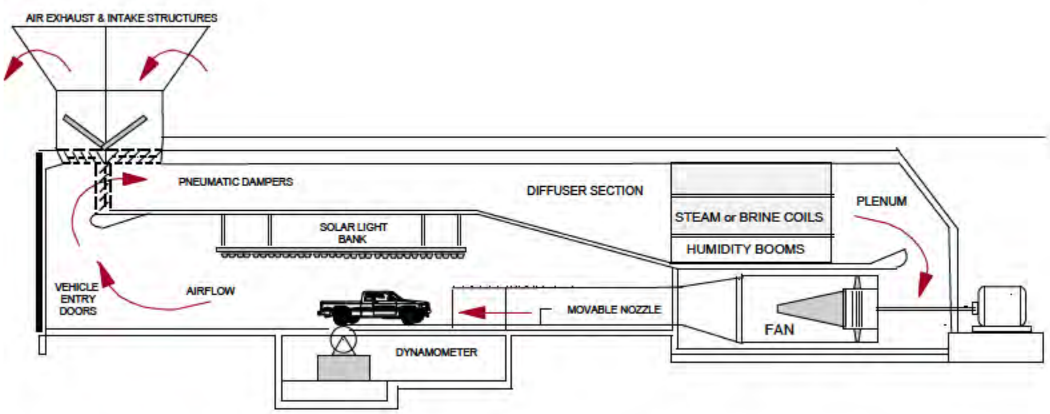

Figure 4.23 Delphi Harrison Thermal Systems Climatic Wind Tunnel

The tests were separated into two groups, the first for summer conditions and the second for winter conditions. The ambient air temperatures covered an extreme range (from - 23.3°C in winter to 43.3°C in summer), and were done both with and without solar radiation. Table 4.9 describes the test conditions.

Table 4.9 Delphi Test Conditions

				Test Description		
Ride #	**Date**	**Actual Start Time**	**Test Group**	**Ambient**	**Solar**	**PreCondition**
1	22-Jul-2002	15:07:46	pm	30.0 degC	No	5 min
2	23-Jul-2002	10:44:35	am	30.0 degC	No	5 min
3	23-Jul-2002	15:30:12	pm	37.8 degC	No	5 min
4	24-Jul-2002	10:10:39	am	37.8 degC	No	5 min
5	24-Jul-2002	14:27:48	pm	37.8 degC	Yes	5 min
6	25-Jul-2002	10:24:53	am	37.8 degC	Yes	5 min
7	25-Jul-2002	14:22:14	pm	43.3 degC	Yes	5 min
8	26-Jul-2002	10:24:59	am	43.3 degC	Yes	5 min
9	29-Jul-2002	15:19:22	pm	-6.7 degC	No	5 min
10	30-Jul-2002	10:12:05	am	-6.7 degC	No	5 min
11	30-Jul-2002	15:06:49	pm	-17.8 degC	No	5 min
12	31-Jul-2002	10:13:10	am	-17.8 degC	No	5 min
13	31-Jul-2002	15:14:35	pm	-17.8 degC	Yes	5 min
14	1-Aug-2002	10:06:11	am	-17.8 degC	Yes	5 min
15	1-Aug-2002	15:04:35	pm	-23.3 degC	No	**10 min**
16	2-Aug-2002	9:27:34	am	-23.3 degC	No	**10 min**

Test procedure: During the tests, the car (full size SUV, Chev/Tahoe, 2002 model year) was first placed in the wind tunnel and allowed to equilibrate (sock). Figure 4.24 shows the car in the Wind Tunnel during the test. The lights on the ceiling simulate solar radiation. Four subjects stood outside of the car wearing harnessed connecting thermocouples on the skin to a data acquisition system in the wind tunnel control room. The subjects remained outside the car for five or ten minutes and then entered the car and began voting their thermal sensation and comfort perceptions. The first vote was called the PRE vote, prior to starting of the car's engine and air conditioning. All body parts were voted on. Next, the subjects started the car and turned on the air-conditioning system. They could adjust the air-conditioning according to their preferences.

Under winter test conditions, the subjects used the air conditioning to warm their bodies. Under summer conditions, the subjects used air conditioning to cool their bodies. Once the car was started, the subjects voted a second time (t=0) vote. The subjects continued to vote every two minutes for 40 minutes. The test procedure is described in Table 4.10.

Figure 4.24 Car in the Wind Tunnel during Delphi Wind Tunnel tests

Table 4.10 Delphi Wind Tunnel test procedure

Hot Tunnel Time	**Event**
t = -90	**Begin Blowdown (No Solar, 10mph wind, hood and doors open.)**
t = -60	**Begin Soak (Close car). Participants arrive / begin to instrument w/ TCs. Take CorTemp pill if needed.**
t = -5	**Participants begin to pre-condition (if necessary) under solar lights**
t = 0	**Connect TCs and step into car. Begin test and log objective data every 10 seconds.**
t = 45	**Test end. 30mph, Recirc, for 30 minutes; 30mph, OSA for 7.5 minutes; Idle OSA for 7.5 minutes**
Cold Tunnel	
t = -180	**Begin Soak**
t = -60	**Participants arrive and begin to instrument w/ TCs. Take CorTemp pill if needed**
t = -5	**Participants begin to pre-condition (if necessary) at side of vehicle.**
t = 0	**Connect TCs and step into car. Begin test and log objective data every 10 seconds. Controls set to Def, M1, FH**
t = 3	**Switch to Heater, FH, High Blower**
t = 45	**Test end. 30 mph for 30 minutes & 50 mph 10 minutes, Idle for 10 minutes**

Measurements: The human subject and environmental measurements for the wind tunnel tests were as similar as possible to those taken in the environmental chamber at U.C. Berkeley. For the wind-tunnel tests, 28 thermocouples were taped on the subjects' skin (Figure 4.25). Each subject swallowed a Core-Temp™ pill before the tests began. The subjective survey included both the local and overall sensations and comfort, although the questions were given to the subjects on paper; each time a set of questions was completed, the page was turned so that the subjects could not see their previous votes. The questions were nearly identical to the questions used in the environmental chamber. The sensation scale covers the range from very cold to very hot (very cold, cold, cool, slightly cool, neutral, slightly warm, warm, hot, very hot). The comfort scale is from "just comfortable" to "very comfortable", and "just uncomfortable" to "very uncomfortable". Subjects voted their perceptions for the different body parts in alternating groups. Each data set includes votes for half of the body parts and for the whole body. Groups 1 includes overall, face, chest, back, right lower arm, right foot, right calf, right hand. Group 2 includes overall, face, chest, left upper arm, left foot, left thigh, left hand, pelvis. The body parts monitored were the same as in the U.C. Berkeley tests. An example of the voting pages used for the wind tunnel tests is shown in Figure 4.25. Wind tunnel environmental conditions and car interior conditions (dry bulb temperature, relative humidity, solar radiation, and wind speed) were recorded. The subjects wore normal office clothing.

Figure 4.25 Human subject tests in the Delphi Wind Tunnel

The difference between the sensation and comfort scales used in Delphi Wind Tunnel tests and the UC Berkeley environmental chamber tests is that the sensation and comfort scales are not continuous in Delphi Wind Tunnel tests. When the subjects made their votes, they had to choose the votes in 1 unit increase (as shown in Figure 4.26). While in the environmental chamber tests, the scales are continuous (see Figure 4.22).

In order to do the validation, the subjective data is grouped into five data sets. The first dataset is called the PRE dataset. The votes were cast once the subject entered the car and before the engine and air conditioning were started. The votes are for every body part.

While the air-conditioning was operating (transient thermal conditions), winter test data is divided into data sets All2, which includes group 1 body parts, and All4 which includes group 2 body parts. The summer test data is divided into data sets All1, which includes group 1 body parts, and All3 which includes group 2 body parts.

	Thermal Sensation									Comfort							
										uncomfortable				comfortable			
										very			just	just			very
Overall	very cold 1	cold 2	cool 3	slightly cool 4	neutral 5	slightly warm 6	warm 7	hot 8	very hot 9	1	2	3	4	6	7	8	9
Head	very cold 1	cold 2	cool 3	slightly cool 4	neutral 5	slightly warm 6	warm 7	hot 8	very hot 9	1	2	3	4	6	7	8	9
Chest	very cold 1	cold 2	cool 3	slightly cool 4	neutral 5	slightly warm 6	warm 7	hot 8	very hot 9	1	2	3	4	6	7	8	9
Back	very cold 1	cold 2	cool 3	slightly cool 4	neutral 5	slightly warm 6	warm 7	hot 8	very hot 9	1	2	3	4	6	7	8	9
Arms	very cold 1	cold 2	cool 3	slightly cool 4	neutral 5	slightly warm 6	warm 7	hot 8	very hot 9	1	2	3	4	6	7	8	9
Legs	very cold 1	cold 2	cool 3	slightly cool 4	neutral 5	slightly warm 6	warm 7	hot 8	very hot 9	1	2	3	4	6	7	8	9
Feet	very cold 1	cold 2	cool 3	slightly cool 4	neutral 5	slightly warm 6	warm 7	hot 8	very hot 9	1	2	3	4	6	7	8	9
										very			just	just			very
										uncomfortable				comfortable			

Figure 4.26 A sample of sensation and comfort questionnaires (Delphi)

4.5 Human subjects

This human subject test was approved by the Committee for the Protection og Human Subjects, University of California at Berkeley

4.5.1 UCB subjects

Twenty-seven subjects, 15 female and 12 male, participated in the UCB chamber tests. We used the same subjects repeatedly. Table 4.11 shows key data for each subject and the number of tests in which each participated. Each test represents an entire three- to four-hour testing period (rather than a single application of heating or cooling).

Table 4.11 Subject information (UC Berkeley chamber tests)

ID	gender	age	Height (cm)	weight (kg)	body fat (%)	waist circ. (cm)	neck circ. (cm)	Hip circ. (cm) (Female)
1	F	43	161	55.6	24	79.0	34.0	90.5
2	F	27	160	51.2	20	67.0	31.0	91.0
3	F	40	173	55.2	17	67.5	31.0	89.0
4	M	20	173	70.0	17	83.0	37.5	
5	M	43	180	72.0	13	82.0	36.0	
6	F	25	165	77.2	41	89.0	34.0	110.0
7	F	24	149	49.8	19	70.0	32.0	90.5
8	M	27	172	67.0	16	75.0	38.0	
9	F	47	166	78.0	39	91.0	38.0	109.0
10	M	29	174	68.4	16	75.0	37.0	
11	F	21	162	72.0	40	95.0	35.0	108.0
12	F	21	169	65.0	28	75.0	34.0	96.0
13	F	21	164	59.0	29	73.5	31.0	99.0
14	F	42	153	60.0	49	88.0	36.0	106.0
15	F	24	167	77.0	33	73.0	32.0	101.0
16	M	34	173	75.8	19	91.0	38.0	
17	F	24	176	71.2	29	72.0	36.0	99
18	M	40	179	81.2	19	93.0	39.5	
19	F	25	155	58.4	26	73.0	32.0	90.0
20	M	28	173	69.0	20	77.0	37.0	
21	F	29	174	81.4	41	88.9	32.0	110.0
22	M	37	170	70.0	22	77.0	38.0	
23	M	30	177	75.8	23	84.5	39.0	
24	M	51	181	80.0	17	93.0	38.0	
25	M	33	169	68.0	20	75.0	32.0	
26	M	40	170	68.5	20	75.0	31.0	
27	F	34	163	47.5	17	65	30	89

4.5.2 Body composition information

Because human thermoregulation is influenced by the individual body composition, e.g., height, weight, and body fat (Zhang, Huizenga et al. 2001), we measured body composition information for this test.

We used a scale (Tanita brand) to measure body weight and fat (Figure 4.27) using the bioelectrical impedance analysis (BIA) method. BIA is based on a person's height, weight, strength, and the speed at which a low-level electrical signal passes through their muscle and fat.

Hodgdon and Beckett (Hodgdon and Beckett 1984; Hodgdon and Beckett 1984) provides a method to calculate body fat based on circumferences of certain body parts (neck and waist for male and neck, waist, and hip for female). We also measured these circumferences. The Tanita scale results and the circumference method results are very close. The body fat values from both methods are listed in Table 4.11.

Figure 4.27 Measuring height and body fat of a subject

4.5.3 Subjects' clothing

During the tests at the U.C. Berkeley environmental chamber, the male subjects wore shorts inside the leotard, and the female subjects wore briefs and bra. A pair of cotton socks covered the feet. In the whole-body step-change tests and the IR-image tests, the subjects did not wear the leotard and the socks because there was no strong air supply as in the local heating/cooling test, so there was no need to protect the skin from strong air movement. In addition, our results for these tests could more easily be compared with results from tests in the literature because, in most previous step-change studies, subjects wore only briefs or shorts (Gagge, Stolwijk et al. 1967; de Dear, Ring et al. 1993). The subjects did not wear the leotard and the socks in the IR-image tests so that skin temperatures would be visible.

4.5.4 Metabolic level of subjects

Most of our subjects played computer games during the environmental chamber tests. A few played a driving game that was installed for the test. The metabolic activity involved in playing the computer driving game is similar to the activity from driving a real car, about 1.1 met (1 met = 58 W/m^2). The paper "Using a Driving Game to Increase the Realism of Laboratory Studies of Automobile Passenger Thermal Comfort," attached as Appendix 4.5 and slated for publication in 2003 as a Society of Automobile Engineering (SAE) technical series paper, describes this issue in detail.

4.5.5 Delphi subjects

Seventeen subjects participated in the 64 human subject tests, 15 males and 2 females. They are engineers who work in the Delphi company. Except Subject 13 who participated once, all the rest participated 4 tests. Subjects 1 – 4 participated in 4 afternoon summer tests, Subjects 5 – 8 participated in 4 morning summer tests, Subjects 9 – 13 participated in 4 afternoon winter tests, and Subjects 14 – 17 participated in 4 morning winter tests. Data describing each subject is provided in Table 4.12.

Table 4.12 Subject information (Delphi Wind Tunnel tests)

ID	gender	age	Height (cm)	weight (kg)	body fat (%)	waist circ. (cm)	neck circ. (cm)	Hip circ. (cm) (Female)
1	M	37	191	87	17	87	38	
2	M	43	188	109	32	110	42.5	
3	M	45	180	67	12	79.5	37	
4	M	26	178	88	25	99	37	
5	M	26	178	93	26	97	41	
6	M	39	180	87	19	87	39	
7	M	25	175	79	21	88	38	
8	M	32	185	79	17	87	39	
9	M	36	175	81	25	91.5	38	
10	M	41	180	85	23	91	40	
11	F	29	158	50	24	66	30	89
12	M	32	178	67	13	74	38	
13	F	43	160	60	31	66	33	91
14	M	47	183	79	16	93	39	
15	M	43	188	109	32	110	42.5	
16	M	53	173	77	24	90	38	
17	M	41	175	71	17	79	37	

5. TEST RESULTS, PHYSIOLOGICAL AND SUBJECTIVE RESPONSES

5.1 Introduction

This chapter presents the skin and core temperatures measured under a variety of environmental conditions in our human subject tests, along wit their associated thermal sensation and comfort responses.

The environmental conditions were:

- stable and spatially uniform warm, neutral, and cold
- stable and asymmetrical
- transient and asymmetrical, as follows:
  - warm overall environment with application of local cooling to 19 body parts (face, head, breathing, neck, chest, back, pelvis, left and right upper arms, left and right lower arms, left and right hands, left and right thighs, left and right lower legs, and left and right feet)
  - cold overall environment with application of local heating to the same 19 body parts as above
  - cold overall environment with application of local cooling to 19 body parts,
  - multiple cooling/heating simultaneously to several body parts (face, chest, hand, upper arm, lower arm, thigh, lower leg, foot, neck)
- transient but uniform resulting from whole-body step changes between warm and slightly cool environments.

The data used for the above conditions are visually presented in Figure 5.1, which represents skin temperature (solid line) and votes (circle, triangle, squares) during a local cooling/heating test. The circle represents data for stable/uniform environments, the triangle represents data for stable/asymmetrical environments, and the squares represent data forn transient/asymmetrical environments. The data for the transient/uniform environments are obtained from whole-body step-change tests and are not presented in this figure.

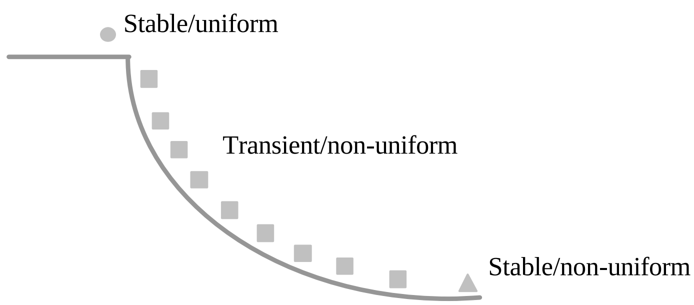

Figure 5.1 Data used to represent different environmental conditions

The experimental results are presented in the following order :

- stable and spatially uniform warm, neutral and cold tests
- stable and asymmetrical tests
- transient and asymmetrical tests
- transient, uniform whole-body step-change tests

The main findings of the experiments are:

1. In stable conditions, local sensation has a high correlation with local skin temperature. In transient conditions, this correlation is reduced, but the correlation between the local sensation and the rate of change of local skin temperature increases significantly.
2. Some body parts have much more influence on overall thermal sensation than others.
3. In response to neutral conditions, subjects voted that they were 'comfortable' (2 on the voting scale), but not 'very comfortable' (scales above 2). Only during heat-stress removal did subjects vote that they experienced maximum comfort (3 or 4 on voting scale).

4. Under neutral conditions, subjects' core temperature variation is small, within 0.1° C. Local cooling applied to one part of a warm body induces an immediate core-temperature increase. Local heating applied to one part of a cold body makes the core temperature drop.
5. Subjects felt comfortable with cooling of the breath intake air, but uncomfortable with heating of breath intake air.
6. In cold environments, flexing the hand increases hand (especially finger) skin temperature significantly. In warm or neutral environments, the influence of such movement on skin temperature is small.

5.2 Stable/uniform environments

Understanding human physiological responses and subjective perceptions in stable conditions is a starting point for understanding responses and perceptions in more complex transient conditions. Thus, we focus first on stable condition results.

5.2.1 Neutral-conditions tests

There are three purposes of neutral condition tests. 1. They provide skin temperature set points for each body part. The skin temperatures under neutral condition are set points for the proposed thermal sensation and comfort models. 2. The thermal comfort votes under neutral conditions are also needed to develop the comfort model. 3. Finally, the human responses under stable, neutral conditions provide basic information that can be used to compare responses in warm and cold conditions, and during transients.

The details of the neutral-conditions tests are presented in the Method (Chapter 4.4.2.4). The chamber was set up slightly cooler than the neutral temperature. The subjects adjusted the radiation heat from four 250 Watt heat lamps to make themselves comfortable.

5.2.1.1 Skin temperature set points

5.2.1.1.1 Experimental results

The average skin temperature from seven of the neutral-conditions tests is shown in Figure 5.2. (In the eighth test, the subject did not wear the leotard so that we could take IR photographs, and so the skin temperatures from this test were not included in calculating average values). The general locations of the thermocouples are also indicated on this figure (the exact measurement locations are shown in Figure 4.18).

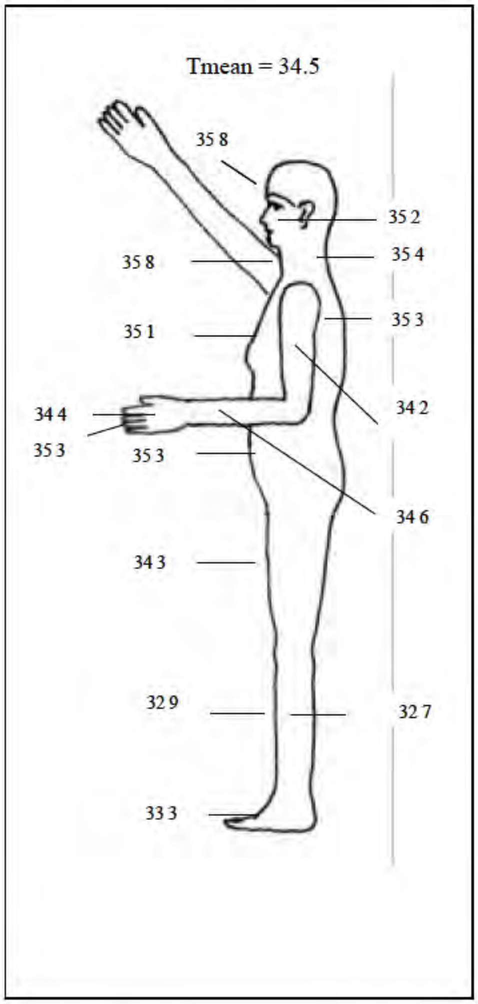

Figure 5.2 Skin Temperatures (°C) under Neutral Conditions

The skin temperature distribution in Figure 5.2 shows that under neutral conditions, there is a 3 °C difference from the coldest area, the calf, to the warmest areas, the front neck and forehead. The front neck thermocouple is located right between the two carotid arteries where the temperature is 0.4 °C higher than at the back of the neck. Cheek skin temperature is about 0.6 °C lower than forehead skin temperature. The highest skin temperature is for the head region, ranging from 35.2 to 35.8 °C.

The second highest skin temperatures are in the chest, back, and pelvis, the trunk region, ranging from 35.1°C for the chest to 35.3°C for the back and pelvis.

The skin temperatures of the upper extremities (arm and hand) and thigh are third highest; all are above 34°C. The lower arm (34.6°C) is warmer than the upper arm (34.2°C), and the finger (35.3°C) is 0.9°C warmer than the hand (34.4°C). The upper and lower arm thermocouples were located on the lateral side of the arm. The lower arm is warmer than the upper arm because of the greater insulation provided by the muscle and fat of the upper arm. This is true unless the body is cold and the blood vessels constrict. The finger has a higher skin temperature than the hand because there are more blood vessels near the fingertip than on the middle of the back of the hand, where the hand thermocouple was located. The finger thermocouple was on the back of the finger, close to the fingernail. When vasoconstriction occurs, finger temperature drops dramatically and may become the lowest temperature in the body.

The lowest skin temperature under neutral conditions is found in the lower leg and foot, ranging between 32.7 and 33.3°C. The shin skin temperature is slightly higher than the calf skin temperature because the shin temperature was measured in the front where there is less insulation than on the calf; calf skin temperature was measured on the lateral side. The foot is not normally the coldest in our test because less clothing insulation is provided by the leotard (0.32) than by the cotton sock (0.6) worn by the subjects.

5.2.1.1.2 Comparison with values in the literature

Our skin temperature data from Figure 5.2 is also shown in Table 5.1 to permit easy comparison with values found by Olesen and Fanger, who measured skin temperature at 14 locations while subjects were exposed to neutral conditions (data also presented in Table 5.1) (Olesen and Fanger 1973). Comparing the two tables, we can see that our skin temperatures are significantly higher than those recorded by Olesen. Our mean skin temperature is 34.5°C, 1°C higher than the mean skin temperature found by Olesen. Our skin temperature values are also higher than those shown by Houdas (Houdas and Ring 1982) (Appendix 4.2), whose values are similar to Olesen's.

One likely reason for the difference is that our subjects wore the leotard, while the subjects in Olesen's tests wore loose office clothing. Skin temperature in both studies was measured by thermocouples taped on the skin. For Olesen's subjects, air convection under the loose clothing might influencing the thermocouple; it would be insulated from this layer of air by only the layer of tape holding the thermocouple to the skin. In contrast, the leotard used in our experiment conforms to the body, so there is no air gap between the thermocouple/tape and the leotard. The effect of the air is felt through both the leotard and the layer of tape, effectively a double layer of insulation.

Because we set the room temperature slightly lower than neutral and used adjustable radiative heat sources to allow the subjects to create the neutral environment, our neutral conditions are a combined result of a slightly lower air temperature and a slightly higher radiation temperature. As a result, our subjects are breathing air that is slightly cooler than the neutral temperature felt on skin from the heat lamps. Because they are breathing cooler-than-neutral air, our subjects might generate more body heat to balance the heat loss through breathing than would be the case in Olesen's experimental setup, which did not use radiative heat sources. This could also cause a higher skin temperature.

Table 5.1 Local skin temperatures (°C) in neutral stable condition
(from our tests and Olesen and Fanger 1973)

Segment	Skin temperature (°C) – our tests	Skin temperature (°C) – Olesen and Fanger
forehead	35.8	34.2
cheek	35.2	
front neck	35.8	
back neck	35.4	
chest	35.1	34.5
back	35.3	34.4
abdomen	35.3	34.9
upper arm	34.2	33.5
lower arm	34.6	32.7
hand	34.4	33.5
left finger	35.3	
thigh	34.3	33.7
shin	32.9	32.6
calf	32.7	32.2
foot	33.3	32.2
mean7	34.53	33.5
average	34.45	33.38

The "mean7" in Table 5.1 represents the mean skin temperature based on the 7-location calculation method (Appendix 4.2), while "average" refers to the average of the skin temperatures from all body parts (from the forehead to the foot) listed in Table 5.1.

5.2.1.2 Sensation and comfort in neutral conditions

The comfort and sensation evaluation in neutral condition is demonstrated by several examples shown in Figure 5.3. The time series shown in these figures start from the subjects' arrival to the end of the neutral condition measurement. Normally it took about a hour between their arrival until they started to vote. During that time a subject performed the activities described in the Chapter 4: staying in the bathtub for 15 minutes, helping with the tapes for the thermocouples, and putting on the leotard. The votes continued for 2 hours. Steady state occurred in the last one and half hours of data.

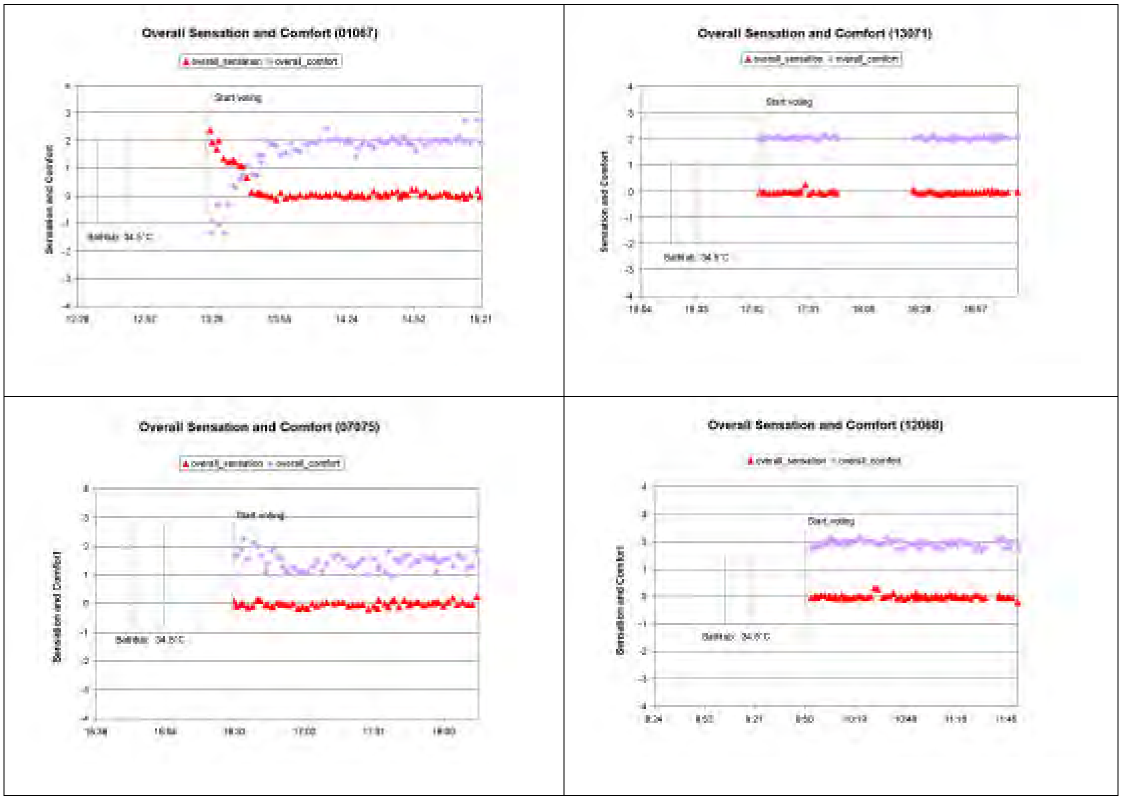

Figure 5.3 Comfort votes under neutral conditions (01067, 13071, 07075, 12086)

The subject's sensation and comfort votes stabilized after about half an hour. Once sensation stabilizes, it varies only slightly. One important observation is that the subjects evaluated the neutral environment as "comfortable" (2 on the comfort scale). They hardly ever evaluated the environment as "very comfortable" (4 on the comfort scale).

The "very comfortable" votes are recorded only during transient conditions when thermal stress is suddenly removed, which we will show in later sections when presenting the transient results. This finding matches McIntyre's statement: "When the body is at a neutral temperature, it is not possible to produce positively pleasant conditions" (McIntyre 1980). Thermal pleasure is associated with the partial relief of thermal discomfort. Thermal stimuli were perceived as very pleasant only when the subject has been under thermal stress and the perceived stimuli tend to restore homeostasis. When the subject in example Test 01067 sits down and starts to vote (time 13:26), he feels warm (sensation 2.5) because of his higher metabolic level resulting from the activities as described earlier; he also feels discomfort (comfort –1.5). As his metabolic level decreases, his sensation gradually decreases and comfort gradually increases. This process is not a sudden stress removal, which explains the absence of "very comfortable" votes.

When overall sensation is neutral, local sensation may vary. The average sensations at the end of the eight neutral-conditions tests are shown in Figure 5.4. The figure shows that head (head, face, neck, breath), arm, and hand feel slightly warm when overall sensation is neutral while foot, leg, and trunk (chest, back, and pelvis) feel slightly cool. The foot feels the coolest, and face, hand, and breath feel warmer than other areas.

The foot may be cool because of temperature stratification (average 0.6 °C between the heights of 0.1 and 1.1 m), and/or because the foot normally receives less circulation than the rest of the body. Unlike hands, feet do not move much when sitting, so they typically receive less blood circulation than hands.

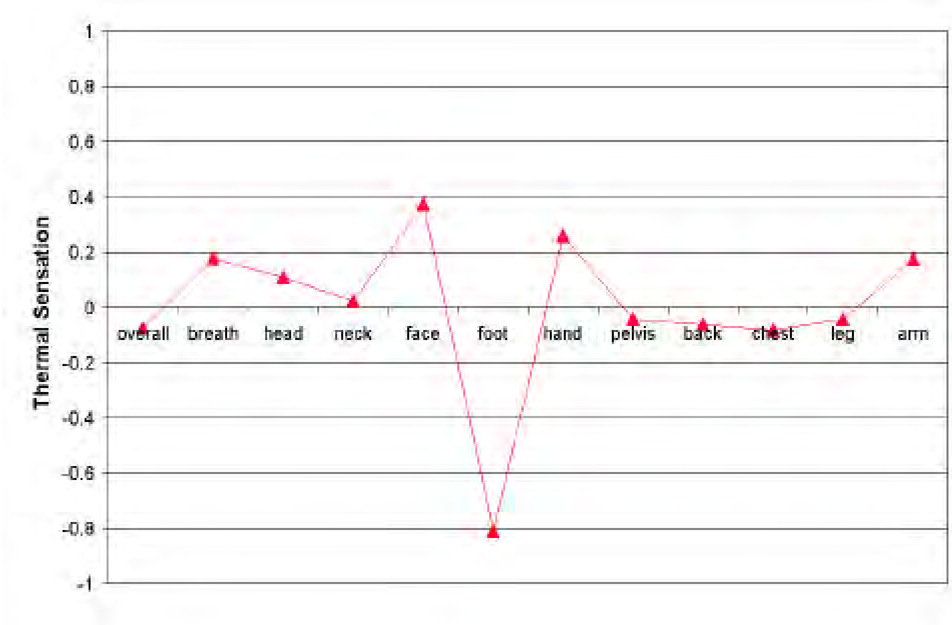

Figure 5.4 Thermal sensation under neutral conditions (8 tests)

The air temperature stratification existed throughout all the 109 tests. The stratification affects the local skin temperature. Because our goal is to correlate subjective responses with skin and core temperatures, and we measured the local skin temperatures and local sensation and comfort throughout the entire test, it is not necessary for the subject to be immersed in a very uniform environment.

Although we did not survey thermal comfort of every body part in each test, one example from test 07075 illustrates the correspondence between thermal comfort and sensation (Figure 5.5).

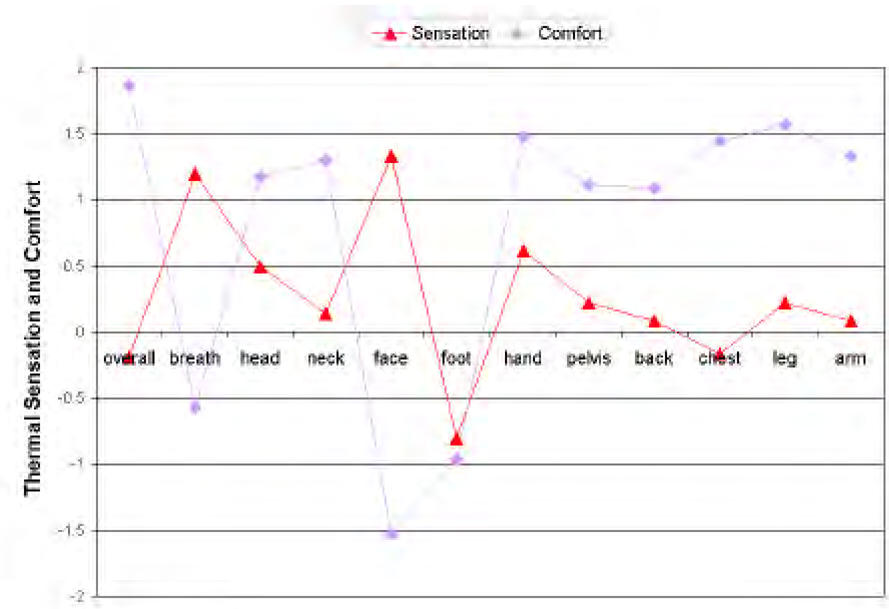

Figure 5.5 Thermal sensation and comfort under neutral conditions (07075)

Figure 5.5 shows that the subject feels uncomfortable with warm face, warm breath intake air, and cold feet.

It is interesting to notice that "overall" sensation is slightly cool, but the only two local "slightly cool areas" are the foot and chest. This suggests that the overall sensation is very sensitive to cool sensation in individual body parts.

5.2.1.3 Responses over time

A. Mean skin and core temperatures: time to reach stability

Under our test conditions, following the bathtub and the activities described earlier, the mean skin and core temperatures reached steady state in a half hour within four tests and one hour in four tests. Figure 5.6 shows one example (01067).

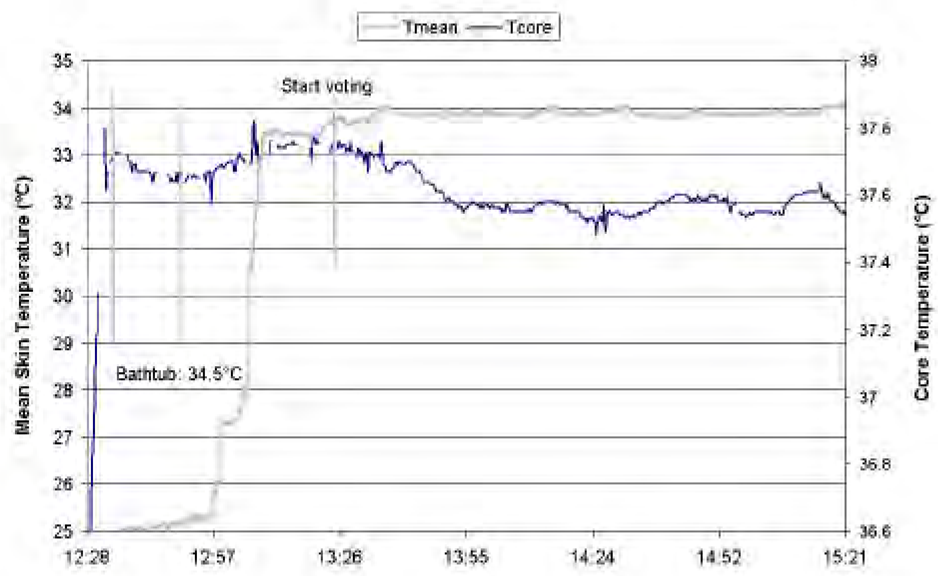

Figure 5.6 Core and mean skin temperature over time under neutral condition (01067)

In this example the core temperature stabilizes one-half hour after the subject starts voting. The mean skin temperature reaches steady state sooner, about 10 minutes after the subject starts to vote.

Nagano (Nagano et al. 2002) shows that people's mean skin temperature, sensation, and comfort reached stable conditions in 20 minutes after a step-change move from a hot to a neutral environment. Goto (Goto et al., 2002) examined sensation and comfort responses during and after three activity levels (20, 40, 60% relative work load). The authors found that after 15 minutes of the up-step and down-step activities, the sensation and comfort had reached steady-state values. No skin and core temperature were measured. The 20% relative work load corresponds to walking at a slow pace or standing and performing light work such as filing.

The above observations and the literature support our experimental procedure of having the subject stabilize for 40 to 60 minutes before the first application of the local cooling/heating, then provide 30 minutes to let the body recover after the first thermal stimulus is removed and before the next thermal stimulus is applied.

After the core temperature reaches the steady state, the variation is within 0.05 °C during the following one-and-half-hour test. In general, the core temperature variation is small once it reaches steady state in a neutral environment. It is within 0.1°C for all 8 neutral condition tests. This small variation observed in neutral-conditions tests is not found during local cooling tests, which are described later. During local cooling, core temperature is very active as the body controls the overall rate of heat loss.

B. Hand and foot skin temperature changes in neutral condition

The skin temperatures for locations such as head, chest, back are stable in neutral conditions. However, the hand and foot skin temperatures tend to change frequently, even under neutral conditions. Figure 5.7 represents an example from test 01067. Four local skin temperatures are shown in this figure: forehead, chest, foot, and the 4th finger. From this figure, we see that the forehead and chest skin temperatures are stable, but the finger skin temperature varies about 2°C and foot about 1°C. The hand skin temperature also fluctuates 1°C (not shown in the figure). This variation means that for some locations, especially the finger, we will need to average skin temperatures over time when correlating sensation and comfort.

The reason why the skin temperatures of hand, finger, and foot vary even in neutral conditions is that cutaneous vascular response is very sensitive to the body thermal state. The blood flow is controlled by variations in the size of the arterioles. This control is extremely sensitive (Brooks et al., 1996) because the blood flow varies to the fourth power of the radius. Wenger (Wenger et al. 1975) showed that as core temperature increases one degree from its set point, the finger blood flow increased three times. When dilatation and constriction happen, they happen first in the hand, foot, and finger.

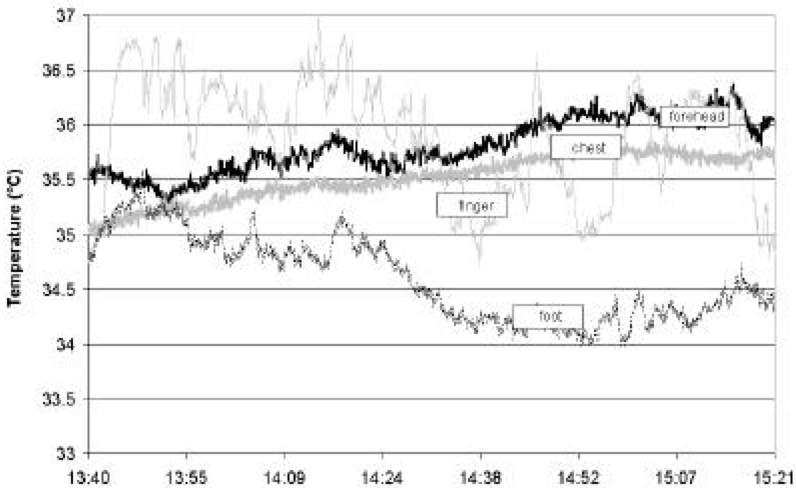

Figure 5.7 Local skin temperature change over time under neutral condition (01067)

5.2.2 Cold-condition tests

During our tests under cold conditions, the chamber temperature was between 16 and 20°C. In general the subjects' sensation votes were below cool (–2).

5.2.2.1 Skin temperature distribution

Skin temperature varies widely across the body as a whole and even within many individual body parts under cold conditions.

Because air temperatures were not exactly the same in all of the cold-conditions tests, the skin temperature measurements cannot be averaged. The skin temperature distribution at the end of a two-hour exposure for one test (21083, room air 15.6 °C) is shown in Table 5.2. Figure 5.8 shows an IR image of temperature distribution from a different cold test as a visual illustration of skin temperature distribution. Because subjects did not wear the leotard (men with shorts only and women with briefs and bras) when the IR images were taken, the absolute temperatures in the table and IR image do not match.

Table 5.2 Local skin temperatures in a cold stable condition (°C) (21083)

Segment	Skin temperature (°C)
forehead	30.7
cheek	27.7
front neck	33.5
back neck	34.5
chest	30.9
back	32.4
abdomen	28.7
upper arm	24.7
lower arm	27.3
hand	23.1
left finger	21.1
thigh	27.0
shin	26.5
calf	24.3
foot	21.4
mean7	27.0
average	26.8

Figure 5.8 Skin temperature distribution in a cold environment

From Table 5.2 and Figure 5.8 we see that temperature among different body parts varies by more than 12 °C in cold conditions. The finger is the coldest. The foot is slightly warmer than the finger, followed by the hand. The warmest place is the front of the neck.

The cheek, which might be considered the extremity of the head, is 3 °C lower than the forehead. Its temperature is close to the lower arm and thigh skin temperatures. The shin skin temperature is 5 °C warmer than the foot skin temperature. The hand is nearly 2 °C warmer than the foot. Because of the greater insulation provided by cutaneous fat, calf skin temperature is 2 °C cooler than the shin skin temperature.

Hand and finger skin temperatures are greatly increased by hand movements (typing in this study) in a cold environment. The effect of hand motion on hand and skin temperature changes is described in Chapter 5.7.1.2.

Figure 5.9 shows additional images of skin temperature distributions in cold environments, for a few body parts. These images show that forehead, neck, and armpit are at the same (warmer) level, and hand and foot are the coldest body parts. The toes are the coldest area of the foot.

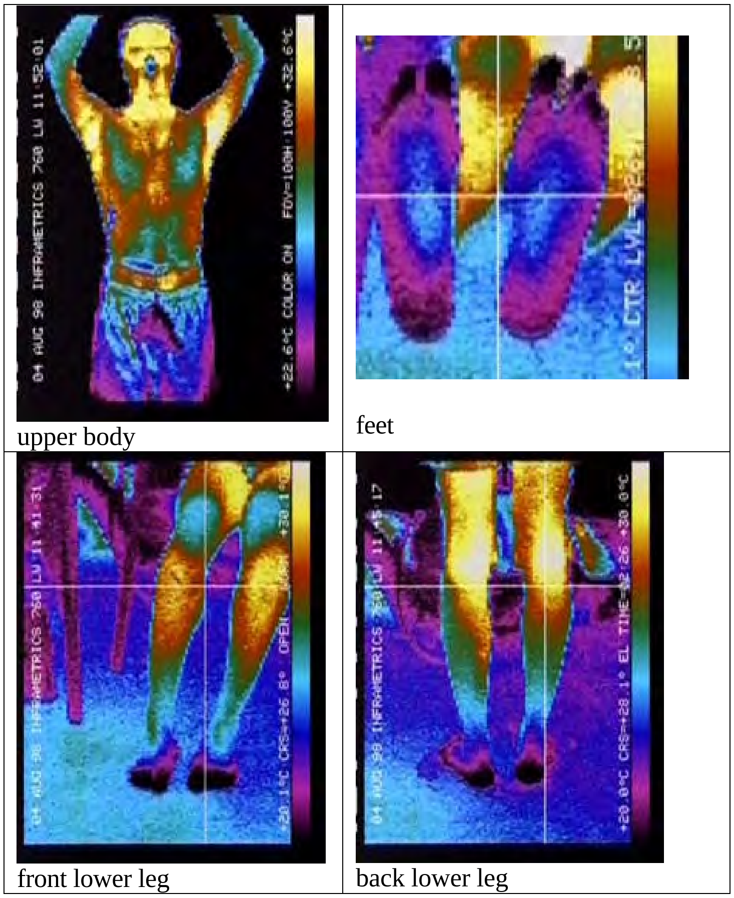

Figure 5.9 Additional skin temperature distributions in a cold environment

5.2.2.2 Thermal sensation and comfort distribution

Sensation

We have seen that skin temperature varies widely under cold conditions. Figure 5.10 shows the average thermal sensation distribution from five cold-condition tests that have overall sensation values less than –2.6. In general, local sensation matches the skin temperature distribution (see Table 5.2). There is a large variation in local sensation. The head region feels warmest (around slightly cool, between –0.5 and –1.5), and the trunk is second warmest (near cool, –2). The extremities feel cold, with the hand and foot the coldest (between cold and very cold, –3.5). The overall sensation is cold (–3.15).

It appears that the head region sensations have little impact on the overall sensation in cold environment. The differences between overall sensation and the head region sensations are the largest of all body parts. With a range of local sensation from –0.7 to –3.5, the overall sensation (–3.15) is closer to the coldest sensations. The areas of coldest sensation (hand, foot, and arm) appear to have a strong influence on overall sensation.

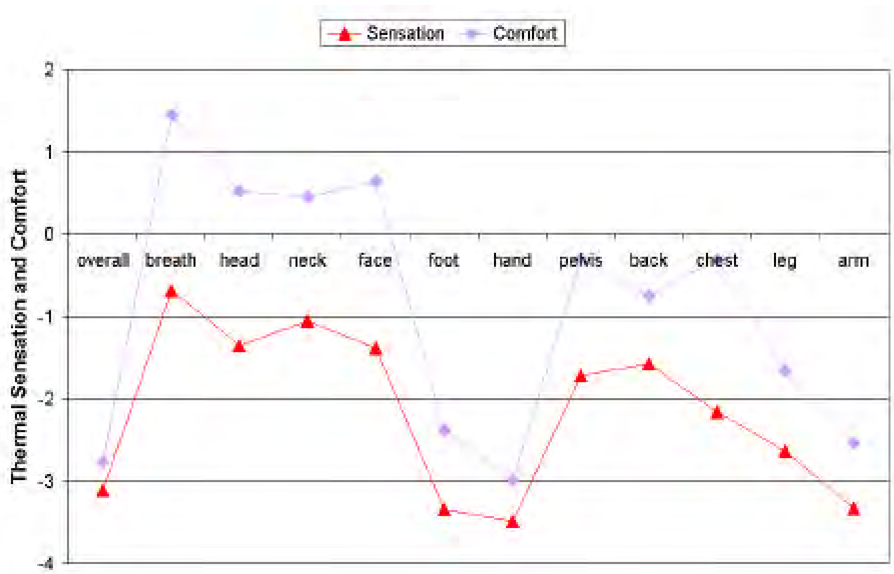

Figure 5.11 Thermal sensation and comfort under cold conditions (overall sensation near –3, 5 tests)

Comfort

The corresponding comfort votes (Figure 5.10) show that head region is perceived as comfortable even though the whole body is cold (-3.15) and the votes for all other body parts are negative. This indicates that people are happy with a cool head.

Overall comfort (–2.8), like local sensation, is very close to the least comfortable votes (–3 and –2.6). This suggests areas of extremely uncomfortable feeling have a strong influence on the perception of whole-body comfort. When we examine data from the Delphi Wind Tunnel tests (described in Chapter 6.5), we find the same phenomenon. We conclude that overall comfort can be said to be complaint-driven; that is, any local discomfort strongly influences overall comfort. This finding contributes to the development of the overall comfort model, discussed in Chapter 6.

It is interesting to note that although the sensation recorded for the back is warmer than that of the chest, subjects evaluated the back as more uncomfortable than the chest. This suggests that people are more sensitive to a cold back than to a cold chest.

In cold, the greatest local discomfort occurs for cold hands, followed by the feet and the arms.

5.2.2.3 Responses over time

Skin

For the subject whose skin temperature distribution is shown in Table 5.2, her skin temperature changes over time are shown in Figure 5.11. The forehead, cheek, chest, back, and pelvis temperatures remained very stable during the two-hour cold test. The hands and feet continuously decreased. Unlike the hand, the fingers reached their minimum skin temperature after about one hour of exposure. After that point, finger skin temperatures didn't decrease further.

The hand and finger skin temperatures fluctuated at 10:33 AM for 20 minutes. A possible explanation is arteriovenous anastomoses (AVA) action in the hand and finger. AVA periodically opens (flushes) anastomoses to send more blood to hand and finger in order to protect skin from cold-induced injury.

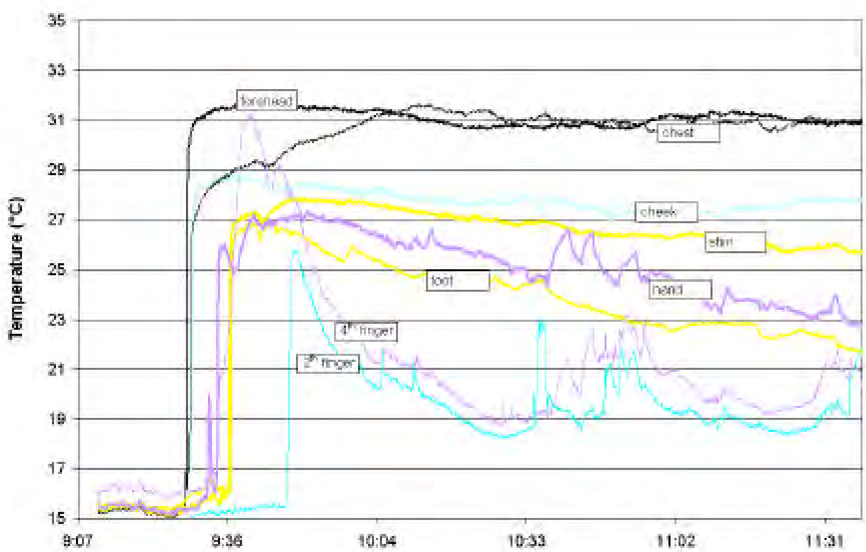

Figure 5.11 Skin temperature over time in a cold environment (21083), $T_{\text{room air}}$ = 16°C

Sensation and comfort, core temperature

For the same test illustrated in Figure 5.11 for the skin temperature (21083), we see in Figure 5.12 that the overall sensation and comfort stabilized after about one half hour. In Figure 5.11, we saw that the forehead and back skin temperatures remained stable, but not the hand and foot skin temperatures which decreased continuously during the entire test. So the overall sensation and comfort seem to follow the temperature of the forehead and back, but not the hand and foot. Core temperature was maintained and in fact went up during the two hours of cold exposure.

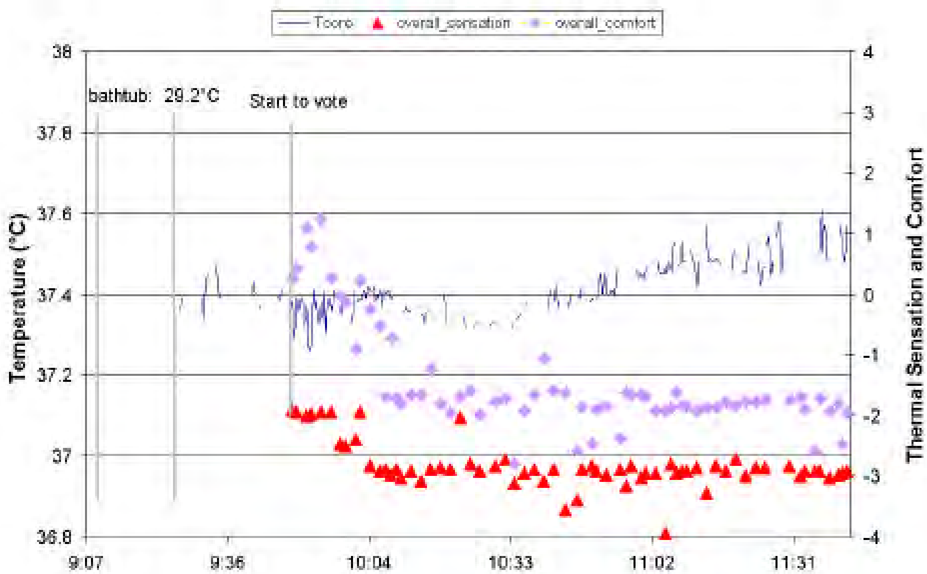

Figure 5.12 Sensation, comfort, and core temperature over time in a cold environment (21083), $T_{room\ air}$ = 16°C

5.2.3 Warm-condition tests

5.2.3.1 Skin temperature distribution

In the warm-conditions tests, the environmental temperature was held within 30 and 32°C. In these warm and hot environments, the range of skin temperature throughout the body (between 34 – 36.8 °C) is much smaller than in a cold environment (skin temperature between 21.1 – 34.5°C, Table 5.2) and in neutral environment (skin temperature between 32.7 – 35.8,

Table 5.1). Table 5.3 is from test 04098 in which the subject wore the leotard and socks. The room air temperature is 30.3 °C. The IR image in Figure 5.13 is from a warm-conditions test (room air = 30°C) in which the subject only wore shorts to permit the image to be taken. This image is included as a visual representation of skin temperature distribution under warm conditions. As with the IR image in cold environment (Figure 5.8), because subjects did not wear the leotard and the socks when the IR images were taken, the absolute temperatures in the table and the IR image do not match.

Table 5.3 Local skin temperatures in a warm condition (04098)

Segment	Skin temperature (°C)
forehead	36.5
cheek	36.3
front neck	36.8
back neck	36.1
chest	36.1
back	36.3
abdomen	36.2
upper arm	36.4
lower arm	36.1
hand	36
left finger	36.7
thigh	35.6
shin	34.4
calf	34.1
foot	36.4
mean7	35.7
average	35.8

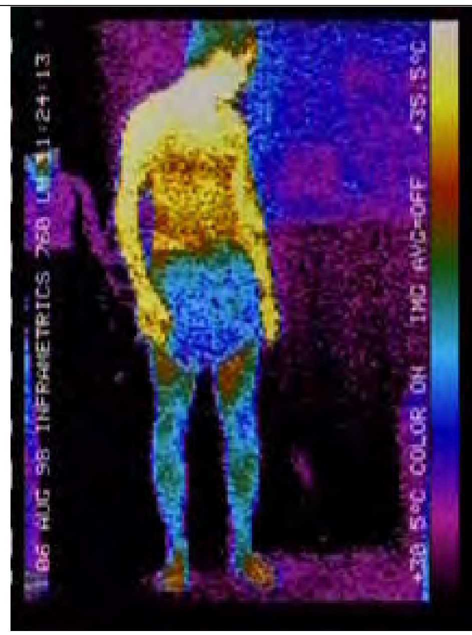

Figure 5.13 Skin temperature distribution in warm environment

The difference between forehead and cheek skin temperatures is only 0.2 °C. The difference between the trunk areas (chest, back, and abdomen) is 0.2 °C. The temperatures of the upper extremities, including upper and lower arm, hand, and finger, are all close to the trunk skin temperature. In fact, all the local skin temperatures above the pelvis are within 0.8 °C (which is the difference between hand and front neck temperatures). The finger temperature is warmer than the hand temperature because the finger vessels are well dilated. The foot skin temperature is higher than the shin and calf.

The lower extremities (thigh, lower leg, and foot) are colder than the areas above the pelvis. This can be easily seen in the IR-image shown in Figure 5.13. The legs and feet are cooler than arms and hands because they do not move frequently as the hands and arms. (Section 5.7.1.2 describes in detail test involving hand motion, which shows in detail how movement increases finger and hand skin temperatures).

5.2.3.2 Thermal sensation and comfort distribution

Sensation

Sensation distribution for 10 warm-conditions tests in which the overall average sensation is above 2, is shown in Figure 5.14.

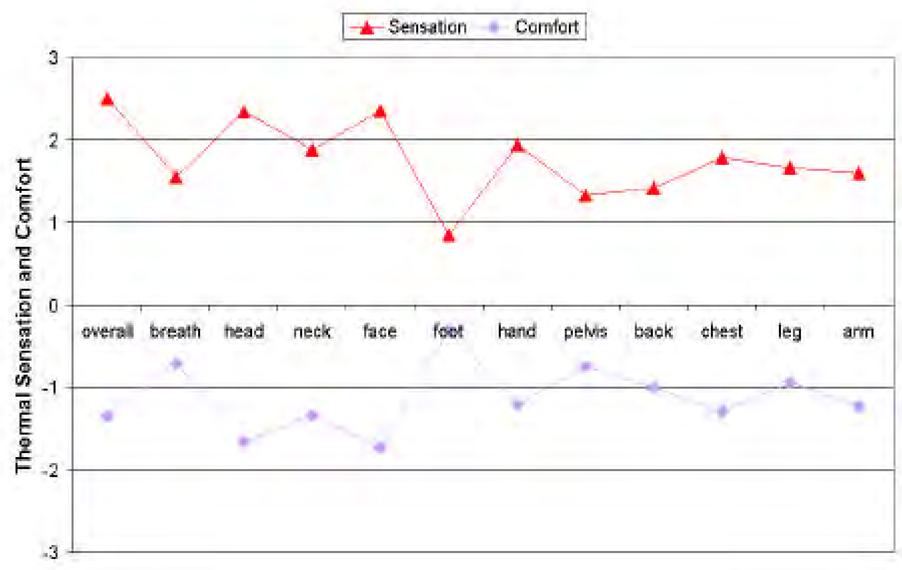

Figure 5.14 Thermal sensation and comfort under warm conditions (overall sensation between +2 and +3, 10 tests)

Again we see that the head region feels warmer than the rest of the areas of the body except breathing. In fact, the head region feels the warmest in the test results for all three conditions, overall neutral, overall warm (overall sensation >2), and overall cold (overall sensation <-2.6). From these data, we conclude that the head tends to always feel warmer than the rest of the body. Breathing has the warmest sensation in a cold environment and a cooler sensation than the other areas of the head (head, face, and neck) in a warm environment. These results imply that breathing is not sensitive to ambient air temperature. We did not examine the role of humidity in these experiments.

An interesting observation of Figure 5.14 is that the overall sensation is closer to the head and face sensations, rather than those of the rest of the body. The head region seems to have the most influence on the overall whole body thermal sensation. This is opposite to the results in cold environment (shown in Figure 5.10). When the whole body is cold, the head region feels the warmest and seems to have the least influence on the overall sensation. This difference indicates that a person is more sensitive to the warm feeling of the head than the cold feeling of the head. This observation will contribute to the regression results of the overall sensation model described in Chapter 6. The regression results will show that the weights for all 4 head parts are asymmetrical, much bigger for warm local sensations than for cold local sensations.

In a warm environment, hands feel warmer than most other body parts except the head. When the body is warm, the blood vessels of the hand are well dilated in order to release heat. The more the dilation, the higher the local skin temperature, and the warmer the local body part feels. This is different from the hand sensation when the whole body is cold (Figure 5.10). When the body is cold, the hand is the most constricted and therefore feels the coldest. The foot conversely feels the coolest in a warm environment, perhaps because of the stratification of the chamber, which had a temperature difference of about 0.6°C between head and ankle level in these tests, and perhaps also by less muscular movement in the foot, as stated earlier. Whether the foot would feel coolest without stratification of chamber air is unknown. When overall sensation is warm, the back is less warm than the chest. This relationship is reversed from the cold condition where the back feels warmer (but more uncomfortable) than the chest.

Comfort

The comfort votes also shown in Figure 5.14 correspond to the thermal sensation votes. The greater the sensation, the greater the discomfort. Sensation and comfort are almost symmetrically distributed. The head area is the least comfortable, and the foot feels the most comfortable of any area of the body.

5.2.3.3 Responses over time

Skin

The skin temperature changes of several body parts during a warm test (21094) are shown in Figure 5.15. The room air temperature was 31.5°C.

Unlike the continuously decreasing skin temperatures of the lower leg, foot, hand, and fingers in in cold environment (Figure 5.11), the skin temperatures for all body parts are very stable in this warm environment (including the hand, foot, and finger). During the 80 minute test, the skin temperature for all body parts remained the same 15 minutes after the subject did his first vote (14:19), except for the shin, which lowered 0.5°C. Unlike in the cold environment, the finger temperature was higher than the hand, the foot was higher than the shin (the insulation of the leotard with the socks is 0.32, and the insulation of the cotton sock 0.51), the forehead and cheek are close. The temperature differences between all body parts are much smaller comparing with the differences in cold tests, within 2°C.

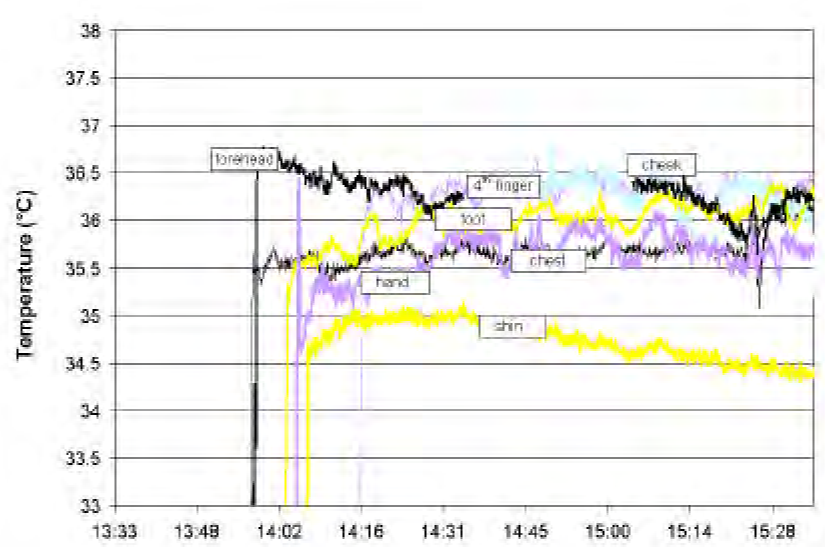

Figure 5.15 Skin temperature over time in a warm environment (21094), $T_{room\ air}$ = 31.5°C

Sensation and comfort, core temperature

The sensation and comfort reached the steady-state after 32 minutes of the first votes (Figure 5.16). The core temperature was very stable, changing only 0.07°C during the entire test.

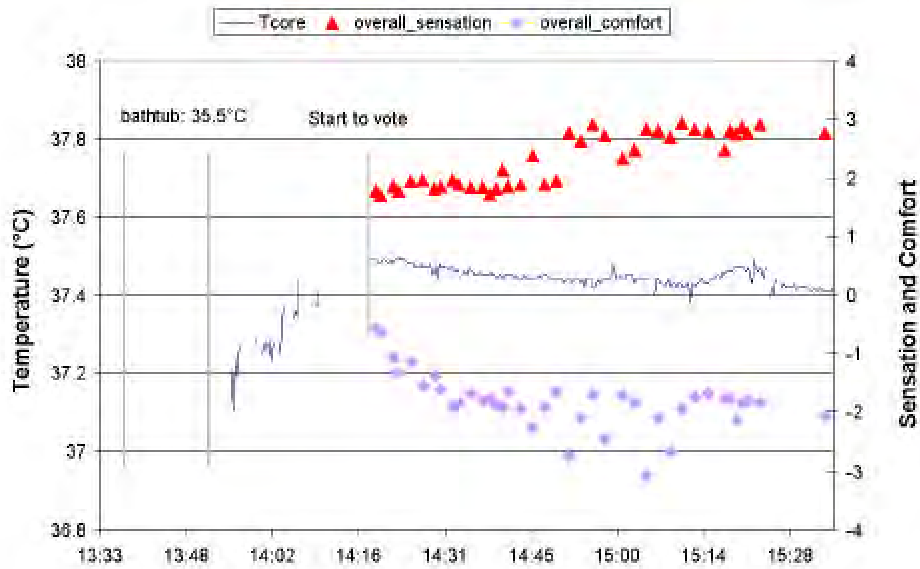

Figure 5.16 Sensation, comfort, and core temperature over time in a warm environment (21094), $T_{room\ air}$ = 31.5°C

5.3 Stable/non-uniform environments

We consider that our subjects' votes and physiological data had stabilized by the end of each local heating or cooling application (as presented by the triangle in Figure 5.1). We could not do separate tests for stable and asymmetrical conditions for budgetary reasons, so we extended the local cooling and heating treatments until the rates of change in skin temperature were low, and sensation and comfort votes were not changing. The heating and cooling application times varied because some body parts (e.g. chest and back) reached their stable state much more quickly than the others (e.g., extremities). The final vote for each application was used together with the coincident physiological measurements to develop the stable asymmetrical sensation and comfort models. Some of these votes will be shown in Chapter 6 where the models are discussed.

5.4 Correlating skin temperature and local sensation: stable environments

During stable conditions, the local sensation is well correlated with local skin temperature. Table 5.4 shows the correlations between local sensation and local skin temperature. Data are from both uniform and asymmetrical stable conditions (represented by the circle and the triangle shown in Figure 5.1).

Table 5.4 Correlation (r) between local skin temperature and local sensation

back	chest	pelvis	face	head	breath	neck	thigh	lower leg	foot	upper arm	lower arm	hand
.86	.82	.52	.79	.75	.37	.72	.63	.38	.6	.81	.83	.79

Most correlations are above 0.6. The high correlations indicate that local skin temperature is a variable to predict local sensation, which will be described in Chapter 6.

The low correlation for breath is probably due part to the fact that we correlate cheek skin temperature with breath sensation. It is possible that breath sensation is independent of a body surface temperature – e.g. the breath air temperature might be the most appropriate. We made an early decision to use a physiological temperature, and for this the cheek is a skin temperature to the breathing zone.

It is the relatively low correlation for pelvis as subjects change their posture slightly, variable geometry causes changes in airflow around the skin and radiation exchange between the upper thighs and the torso.

The low correlation for the lower leg is unclear. It might be caused by the fact that we cooled the entire leg and asked the sensations for the thigh and the lower leg separately. The sensation for the lower leg might be contaminated by the sensation from the thigh. The subject may notice the thigh sensation more than the lower leg sensation so the thigh sensation would be less contaminated.

5.5 Transient/non-uniform environments

The simplest example of transient thermal conditions is when the whole body experiences the same environmental change, as when traveling from one space to another. This is called a whole-body step change. In this case, no asymmetry of thermal conditions is involved. We discuss whole-body step changes in section 5.6.

When transient and asymmetrical thermal conditions are present at the same time, the combinations of possible temperatures of different body parts and their changes are unlimited. In order to simplify our study of these types of conditions, we first look at a single body part subjected to local cooling and heating tests. Then we examine a selected number of transient, asymmetrical-conditions tests where multiple body parts were studied, including tests when there is simultaneous asymmetry for both cooling and warming.

5.5.1 Cooling and heating of a single body part

We applied local cooling or heating to 19 individual body parts (head, face, breathing, neck, back, chest, pelvis, left and right upper arms, left and right lower arms, left and right hands, left and right thighs, left and right lower legs, and left and right feet). The rest of the environments were warm, near neutral, or cold.

In general, the test results showed that:

1. Local body sensation and comfort are strongly influenced by the local skin temperature. During local cooling/heating tests, the local skin temperature changes significantly, and so does the local sensation and comfort.

2. Upon the application of local cooling and heating and their removal, there is an immediate jump in sensation and comfort votes, more abrupt than the skin temperature change. This jump is correlated with the derivative of the skin temperature, which is the greatest upon the sudden change of an environment. The thermoreceptors in the skin react to dynamic change of skin temperature much more stronger than to steady state skin temperature (Chapter 2 section 2.1.1).

   These sudden changes in sensation and comfort are much stronger for cooling than for heating. We see this in the frequent overshooting of subjects' sensation and comfort votes during cooling, but less so during the heating process. This can be explained by the fact that humans have more cold than warm thermoreceptors, and the location of the cold thermoreceptors is more superficial than that of the warm thermoreceptors (Chapter 2, section 2.1.1).

3. When local cooling is applied to a warm body, the body core temperature immediately increases. When local heating is applied to a cold body, the body core temperature decreases. The precise responses observed by the CorTemp™ pill provide us ample justification to use the derivative of the core temperature in addition to $\frac{dT_{skin}}{dt}$ for the prediction of local sensation in transient environment. The above three findings directly contribute to the local sensation model which will be described in Chapter 6.

4. Local sensation and local comfort are closely correlated. That observation will permit us to predict local comfort based on local sensations (will be shown in the local comfort model, Chapter 6)

5. The subjects evaluate thermal neutral conditions as ‘comfortable’ (+2), but rarely ‘very comfortable’ (+3 and +4). The ‘very comfortable’ votes occur during the process of thermal stress removal (e.g. removing a local cooling stimulus). We call this phenomenon the ‘Kuno effect’ based on a paper by Kuno (Kuno 1995). The Kuno effect refers to the strongly pleasant feelings that are associated with the removal of a heat stress. This effect is apparent in some tests but not others. The Kuno effect directly contributes to the local comfort model.

6. Body parts can be categorized in three groups that reflect the degree to which local sensation influences overall sensation: most influential, least influential, and moderately influential. Each group has its own thermal function.

Local sensations from the most influential body parts have a strong impact on overall body sensation, especially when local cooling is applied. It is important to keep these most influential body parts thermally comfortable in order to ensure overall thermal comfort. The range in their local skin temperature is smaller than that of the other two groups, especially when compared to the least influential group. The skin temperatures of the body parts in the least influential group fluctuate widely and rapidly in response to the body's thermoregulation needs, and the local sensations of these body parts have very little influence on overall sensation. The moderately influential body parts exhibit behavior that falls between that of the other two groups.

These results allow us to assign weightings for the whole-body integration model. That will be described in Chapter 6. The difference in range of the skin temperature for each body part will be reflected in the local sensation model. For the least influential body parts, since the typical skin temperature change is large, the logistic curve that predicts local sensation based on local skin temperature will be shallower. For the most influential body parts, the curve will be steeper. We will also show this result in Chapter 6.

7. Our human subjects show a clearly positive response to cooling of breath intake air and a clearly negative response to heating of breath intake air. Cooling of breath intake air produced responses unlike those for other segments. During strong breath cooling both local and overall sensation dropped to 'cold', but both breathing comfort and overall comfort increased. In contrast, when the environment was cold, application of local heating was perceived as comfortable for every other body part except breath intake air. This finding will be seen in the larger weight for the warm side and smaller weight for the cold side of breathing in our overall sensation model.

The asymmetrical effect of local warm or cold sensations on overall sensation is also observed to a lesser extent in other body parts. Our subjects in general showed a preference for a cool head, so the weights for the warm side of the face, head, neck are larger than the weights for the cold side because people are more sensitive to the heating of those areas. For pelvis and feet, the subjects show a warmth preference.

8. Adaptation appears in some tests. After the removal of local cooling or heating, the local skin temperature does not recover to the level that existed before the local cooling or heating; however, the local sensation and comfort return to or sometimes even exceed the original level. This phenomenon can be explained by adaptation, which refers to a change in skin temperature set point. The difference between skin temperature and its set point determines sensation. For example, after a local cooling is removed, the local skin temperature set point has adapted to a lower value. The recovering skin temperature will be stable at a lower temperature for a length of time. During this time, the local sensation feels the same as it did with the higher skin temperature before the local cooling application. Since the differences between the local skin temperature and the set point before and after the local stimulus are the same, the local sensation will also be the same.

We will demonstrate these findings through representative examples from our human subject tests.

Most of our asymmetrical, transient tests focused on cooling in a warm environment. Because of budget constraints, we performed only a limited number of tests in which local heating was applied in a cold environment, and very few tests in which local cooling was applied in a cold environment. No test was done for local heating when the whole body is warm. The main purpose of the cold-environment tests was to gather information for comparison with the warm-environment tests. So the results shown for the colder conditions are less extensive.

5.5.1.1 A typical test sequence

Each test normally involves three local cooling/heating applications. There are 30 minutes between two local cooling/heating applications to allow the body to return to a stable state. We call this process “recovery”. The following figures give two examples of complete test sequences:

Figure 5.17 shows the local skin temperatures, local and overall sensations for a test with three-sequential local cooling applications (head, hand, pelvis). The same cooling air produces different local skin temperature decreases and different levels of local sensation. The three local cooling applications produce obviously different influences on *overall* sensation (with pelvis more than head, hand the smallest). We are not going to give a detailed analysis of this here. Later sections will provide the analysis for the response of each body part to local cooling/heating.

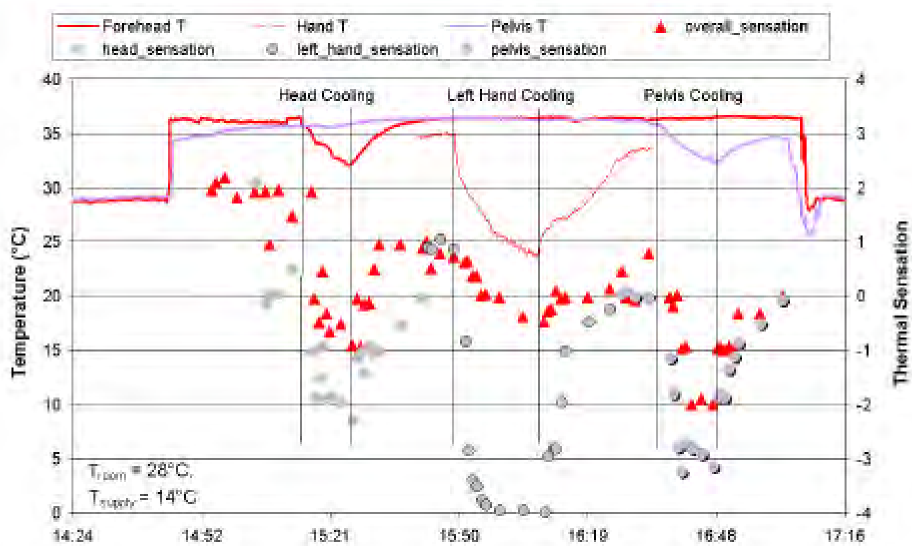

Figure 5.17 Skin temperature, local and overall thermal sensation for three local cooling applications in one test (13016)

Figure 5.18 shows results from another test in which the same three body parts were warmed while in a cold environment. This figure presents local skin temperatures and overall sensation and comfort. The results show that heating of the pelvis has a much greater effect on enhancing overall comfort than heating of the head or the hand. This suggests that heating of seats in vehicles is an effective way to increase passenger comfort when the ambient temperature is cold. The figure also includes a finger temperature measurement on the warmed hand. The variation of the hand temperature is high, but the finger is even more so.

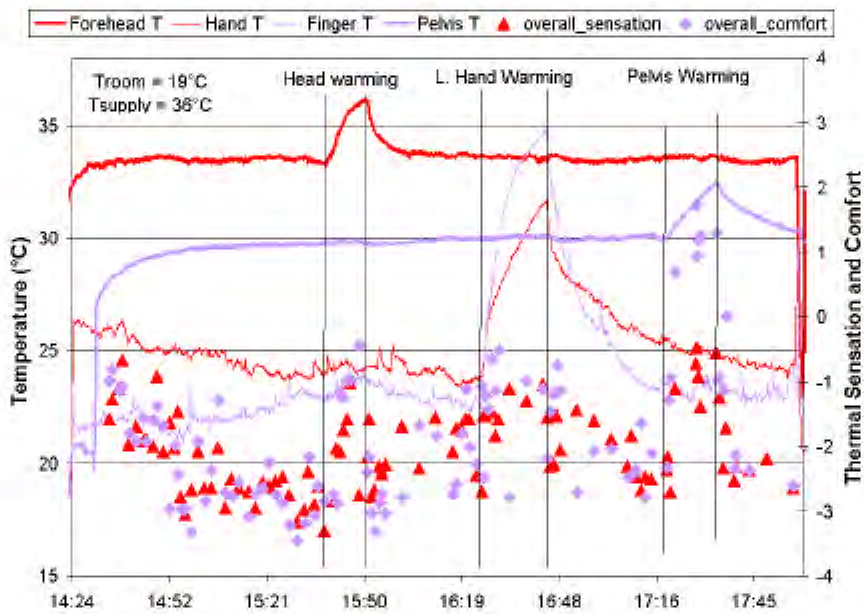

Figure 5.18 Skin temperature, overall sensation and comfort for three local heating applications in one test (07086)

5.5.1.2 Relative influence of body parts on overall sensation and comfort

We applied cooling and heating to each individual body part (e.g. chest, back, face, hand) and surveyed thermal sensation and comfort for the individual body part and the whole body during the entire cooling/heating and recovery process. As mentioned above, we found that body parts can be divided into three groups – most influential, least influential, and moderately influential – based on their influence on whole-body sensation. The most influential group shows that the overall sensation closely follows the local sensation during the cooling/heating and a recovery process. The least influential group shows a big gap between the local and the overall sensations. The moderately influential group shows an intermediate impact of local cooling/heating on the overall sensation. The following sections describe the three different levels of influences on the overall sensation from local cooling/heating and recovery process using a large number of examples, which cover many test conditions.

The most influential group consists of the back, chest, and pelvis. Sensation from these body parts has the dominant impact on overall sensation, especially during application of local cooling. The most influential body parts do not experience large skin temperature changes (compared to the temperature changes of the least influential body parts). Therefore, their heat loss is relatively constant unless evaporation happens. The main function of these body parts seems to be registering thermal sensation rather than adjusting heat loss. When these body parts are cooled, the whole body feels a similar level of coolness. When they feel “very cold,” overall sensation is also “very cold.”

The least influential group includes the hand and foot. The body parts in this group have two features. One, their skin temperatures fluctuate widely and rapidly to adjust the whole body’s heat loss and satisfy the body’s thermoregulation needs. Hands and feet are major areas through which the body releases heat when it is hot because the blood vessels in these extremities have the capacity to dilate significantly. When the body is cold, the blood vessels in these areas constrict to reduce heat loss. Therefore, skin temperatures in hands and feet respond very sensitively to the whole body thermal state. The second feature of the least influential body parts is that local sensations from these parts have very small influence on overall body sensation. It appears that the main responsibility of the hand and the foot is to adjust body heat loss rather than to contribute to whole-body thermal sensation. The two features of these body parts make this group ideal for adjusting the body’s heat loss.

All areas of the head (face, neck, breathing, and head) and arms and legs belong to the moderately influential group. The behavior from this group falls between the two groups above.

When the body parts in the moderately influential group are exposed to local cooling, their sensation contributes to the whole- body sensation but not as dominantly as the sensations of the most influential group. Subjects tolerate much more local cooling in the moderately influential body part group than the most influential group. The skin temperature change for this group is greater than for the most influential group but much less than for the least influential group. The three groups are illustrated in Figure 5.19.

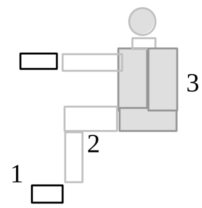

Figure 5.19 The three groups of body parts

The distinction among the three groups is most evident in the cooling test results. For local heating, it appears that the body parts in the most influential group are dominant, and the body parts in the least influential group are the least important in influencing overall sensation. The responses of the moderately influential group (which comprises the areas of the head) are less clear. Subjects rate head cooling as less severe than chest or back cooling and in general experience a slightly cool head as pleasant. However, the head region appears more sensitive to local heating, to the extent that it might be classified as 'most influential' in response to the application of heat. We did not perform enough heating tests to make a clear judgment about the moderately influential group's response to heating; therefore, we categorize the groups according to the results observed from cooling.

The subsections below describe the skin temperature and local and overall thermal sensation and comfort responses for the three groups of body parts.

5.5.1.2.1 Most influential group

This section describes examples of responses of the most influential body parts to local cooling applied under warm environmental conditions (subsection A) and cold environmental conditions (subsection B). The section includes some examples of local heating of most influential body parts.

Local cooling

A. Starting from warm

Back and Chest: Figure 5.20-1 and Figure 5.20-2 show the dominant impact on overall sensation that results from cooling of the back and the chest. The physiological cooling is seen in the reduced local skin temperatures. We see that the overall sensation followed the back or the chest sensation closely during the cooling of the back and the chest, and during their recoveries. The supply air temperature was relatively low, 14°C, and skin temperature was reduced about 4°C in both examples.

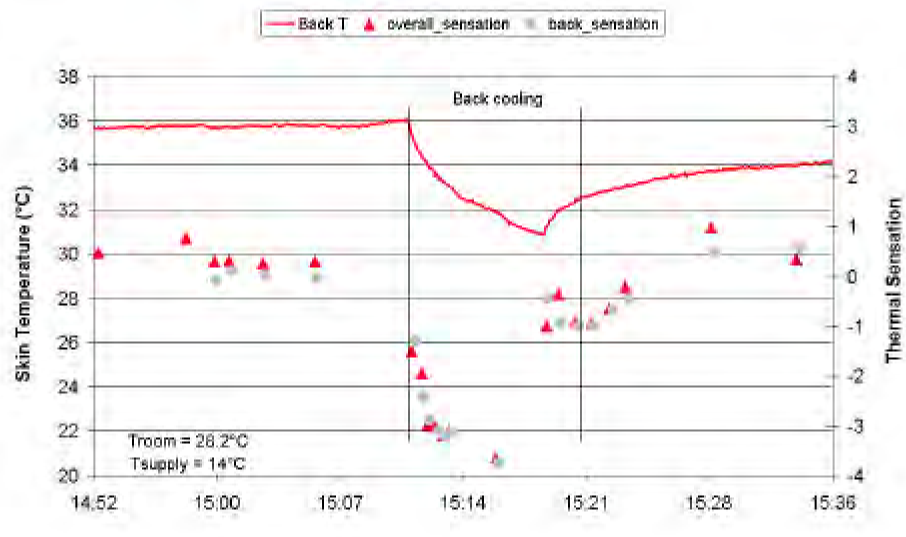

Figure 5.20-1 Back and overall thermal sensation during back cooling (03001)

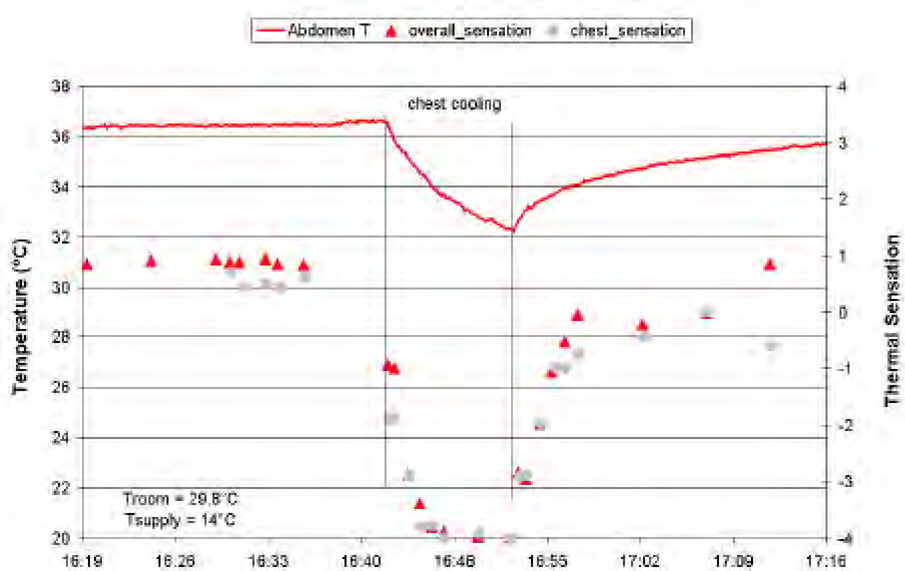

Figure 5.20-2 Chest and overall thermal sensation during chest cooling (13037)

Figure 5.20-3 shows the comfort votes from the test shown in Figure 5.20-2. The overall comfort tracked the local chest comfort closely down to 'very uncomfortable', and recovered at the same rate when the chest cooling was removed.

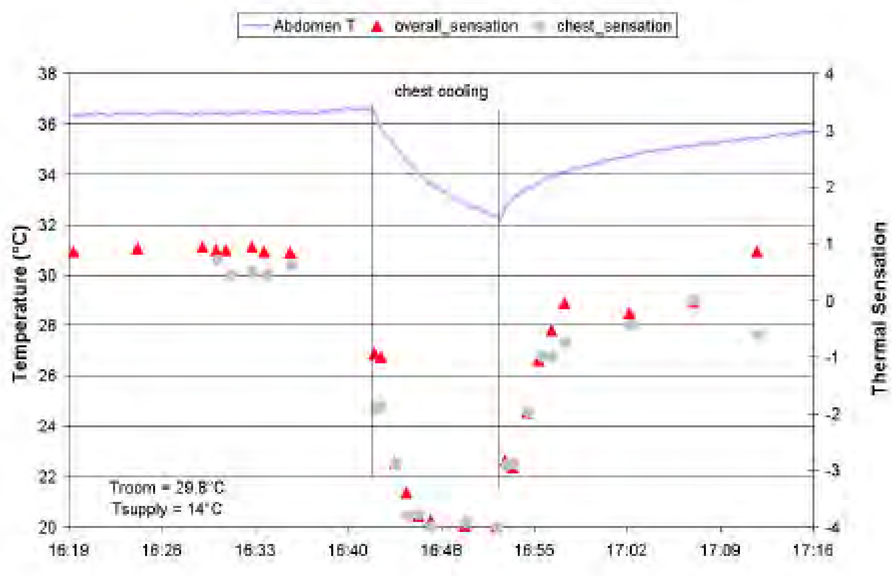

Figure 5.20-3 Chest and overall thermal comfort during chest cooling (13037)

The next example shows that even with very mild cooling of the chest, chest sensation continues to dominate overall sensation (in Figure 5.20-4). In this test we cooled the chest with air at 28°C, which was very close to the room temperature of 30°C. The chest skin temperature was reduced less than 2°C, but the subject felt both chest and overall sensation lowered about 1 scale unit during cooling, and both raised about 1 scale unit during recovery.

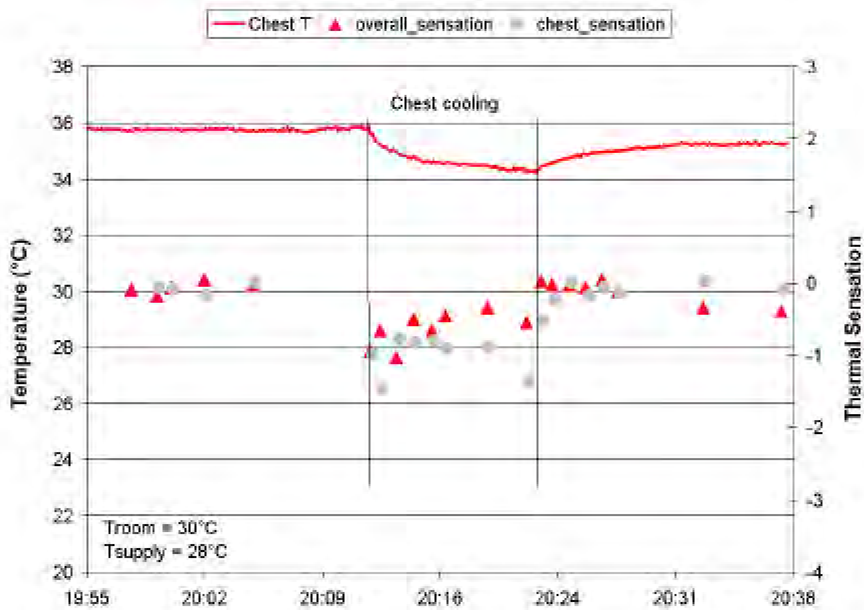

Figure 5.20-4 Chest and overall thermal sensation during chest cooling (09022)

The comfort votes in Figure 5.20-5 show the chest is very sensitive to cooling. One degree of movement towards cool sensation in the chest is perceived as more than one degree of decrease in comfort level.

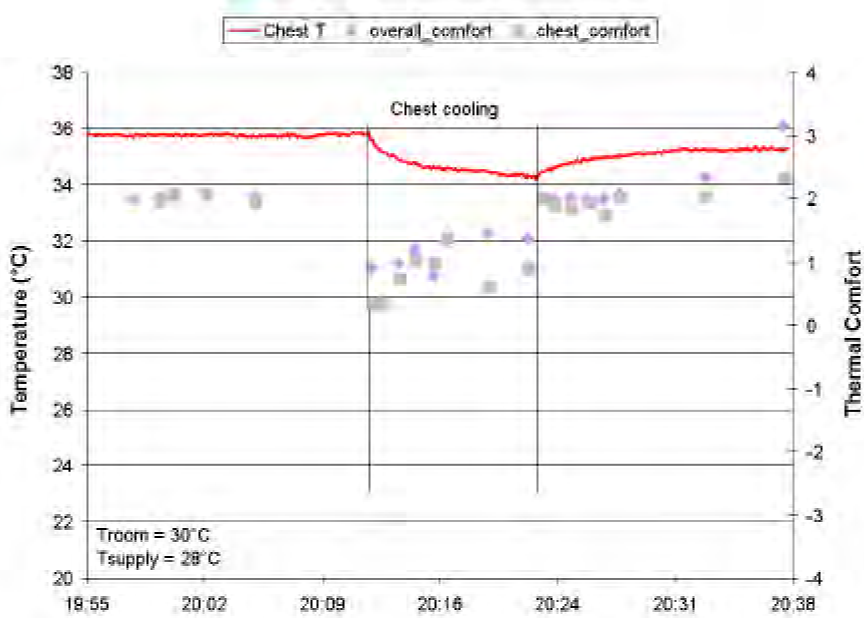

Figure 5.20-5 Chest and overall thermal comfort during chest cooling (09022)

Pelvis: Cooling of the pelvis also has a strong influence on overall sensation and comfort, as shown in Figure 5.20-6 and Figure 5.20-7. The supply air temperature was moderately cool (23°C). The skin temperature was cooled about 2°C. The overall sensation and comfort were basically the same as the pelvis sensation and comfort during the entire cooling and recovery process.

The sensation and comfort votes match well. In this example, the cooling rate was uncomfortable. With the removal of the cooling, the skin temperature increased, so did the local sensation and comfort. The good correlation between sensation and comfort is shown throughout all the examples presented in this chapter. That is why in developing the models, the local sensation is linked with the local skin temperature, while the local comfort is linked with the local sensation. The local comfort is indirectly correlated with the body physiological states.

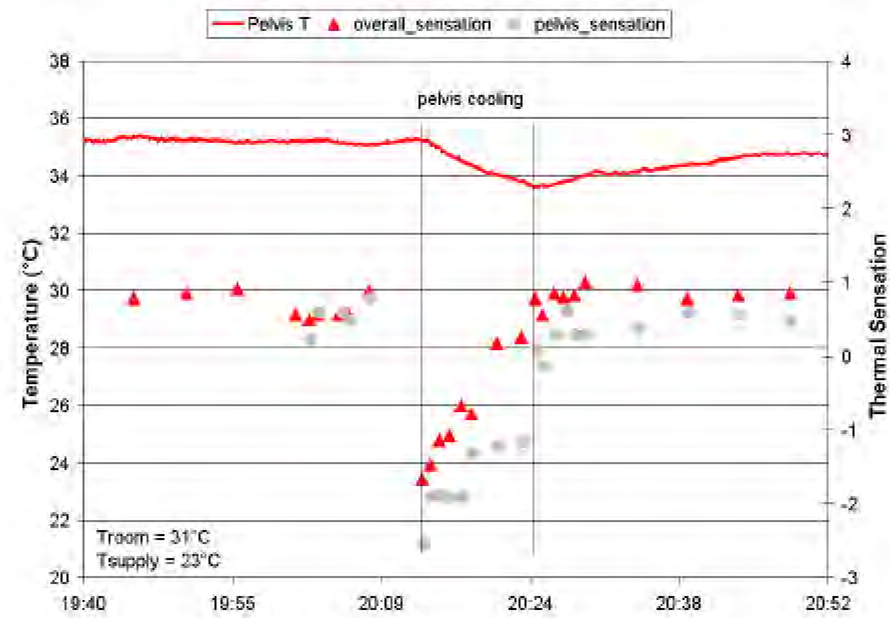

Figure 5.20-6 Pelvis and overall thermal sensation during pelvis cooling (18066)

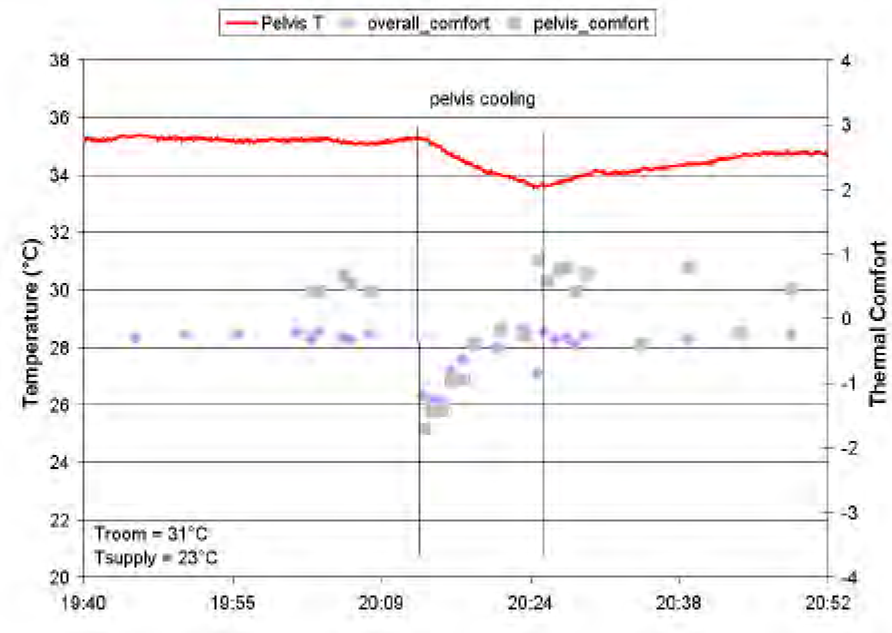

Figure 5.20-7 Pelvis and overall thermal comfort during pelvis cooling (18066)

Comparing the two chest cooling examples (tests 13037 and 09022), we can suggest that gentle cooling of the most influential body parts is a most effective way to cool people. A slight cooling of body parts that are in the most influential group would produce a significant overall cooling effect at a low expenditure of energy. One would have to be careful to avoid overcooling.

B. Starting from cold

As stated earlier, we had fewer tests for cold environments. Therefore, we only show a limited examples from the cold environmental condition tests.

<u>Pelvis:</u> In general when the body is cold, heat loss is small when local cooling is applied because the temperature difference between the skin and the environment is smaller. When the

blood vessels of the body are constricted in response to a cold environment, blood vessels in individual body parts cannot constrict further much in response to local cooling. However, in this example, the supply air temperature was low (14°C). There still existed a large temperature difference between the pelvis skin temperature (29.2°C) and the cooling air. So the skin temperature was lowered 3°C (Figure 5.21). The figure shows that the pelvis sensation cooled significantly and so did the overall sensation.

At the removal of the pelvis cooling, both overall sensation and comfort showed an overshoot. The overshooting was associated with a large positive derivative of the local skin temperature. The overshooting disappeared within 3 – 4 minutes.

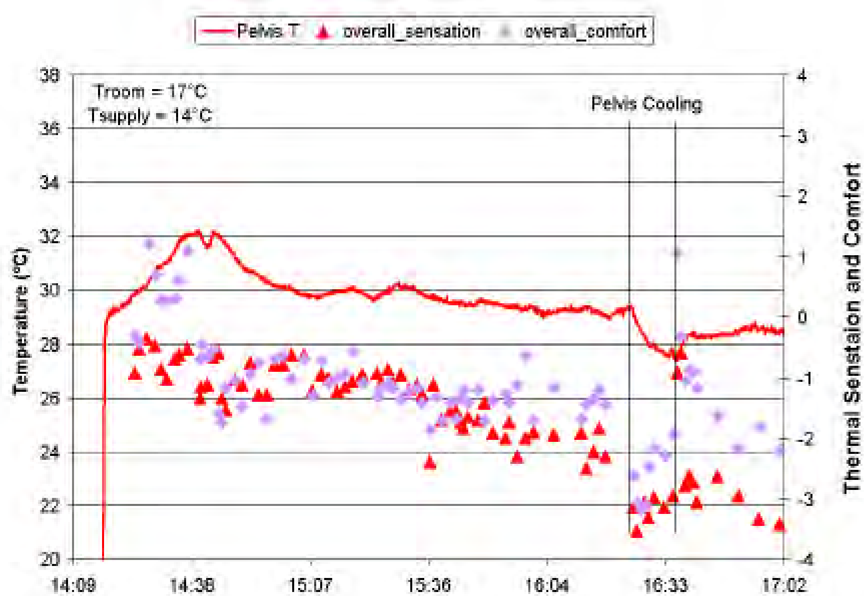

Figure 5.21 Pelvis and overall thermal sensation during pelvis cooling in a cold environment (17084)

Local heating

Heating of the chest and back have a much larger impact on overall sensation than does heating of body parts like the arm or the hand. However, the chest and back do not influence overall sensation as strongly when heated as they do when cooled. When heat was applied to the chest and back, overall sensation did not reach the same level as the chest or back sensations. Local and overall comfort both increased with local heating.

<u>Back and Chest:</u> In the following two examples, the room was cold at 17.5°C. The warm supply air was 36°C for chest and 35°C for the back. The chest skin temperature increased about 4°C and the back skin temperature increased about 3°C. The chest and the overall sensations changed 5 and 3 scale units respectively. The chest and the overall comfort changed 5 and 2 scale units respectively. For the back warming, the local and the overall sensations changed 4 and 1.5 scale units. The same variations were shown for the local and the overall comfort. Results are presented in Figure 5.22-1 and 5.22-2 for the chest and Figure 5.22-3 and 5.22-4 for the back.

After the local heating was removed, both the chest and the back skin temperatures did not recover to the level that had existed before local heating. They were about 1°C higher. However, the sensation and comfort went back to the original levels or lower. The colder sensation and reduced comfort may be caused by adaptation. Although the skin temperature became stable at a higher level after the local heating was removed, the reference set point for skin temperature perception may also have been raised due to adaptation. That can explain why the sensation value was not increased. We will discuss more about adaptation in Appendix 6.1.

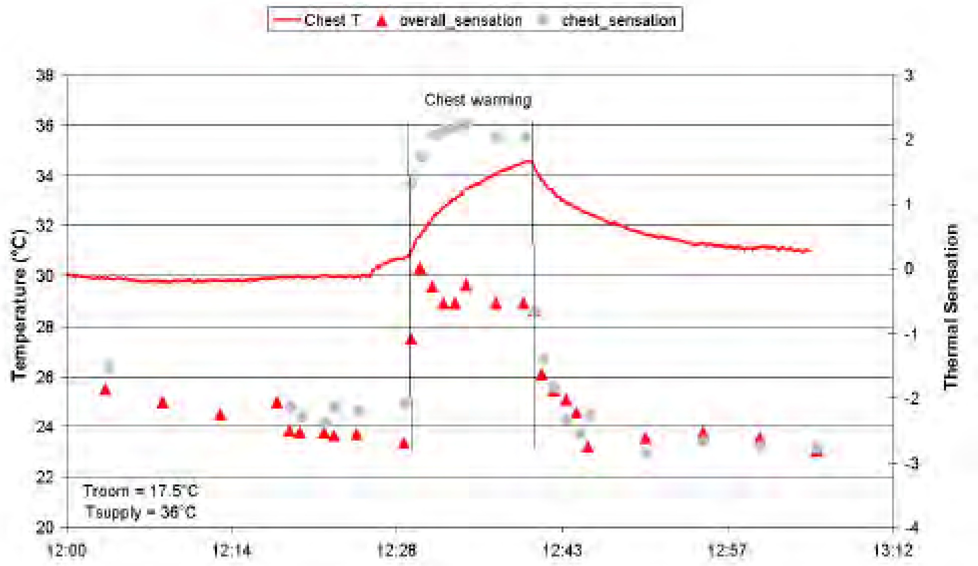

Figure 5.22-1 Chest and overall thermal sensation during chest heating (23089)

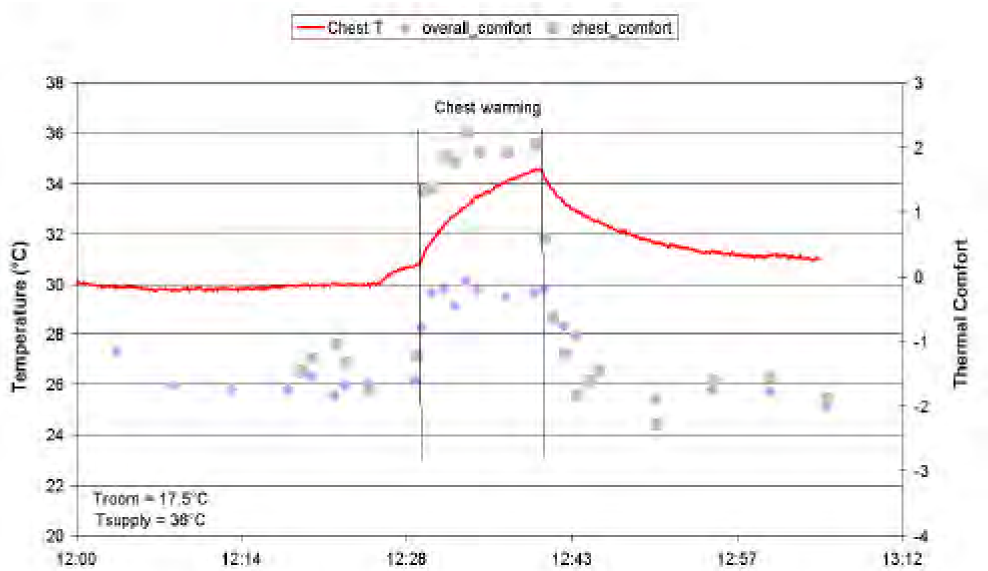

Figure 5.22-2 Chest and overall thermal comfort during chest heating (23089)

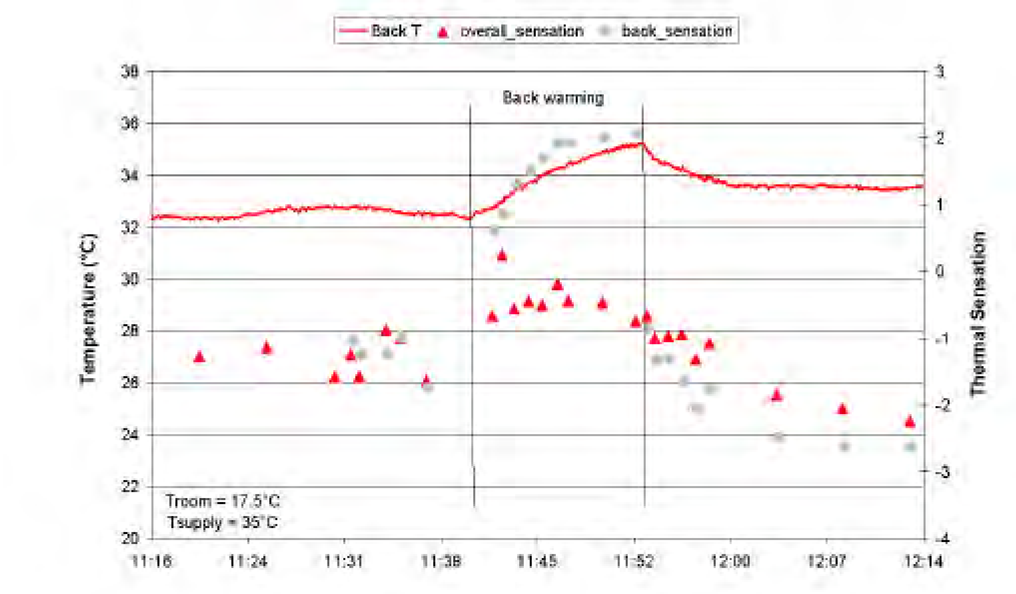

Figure 5.22-3 Back and overall thermal sensation during back heating (23089)

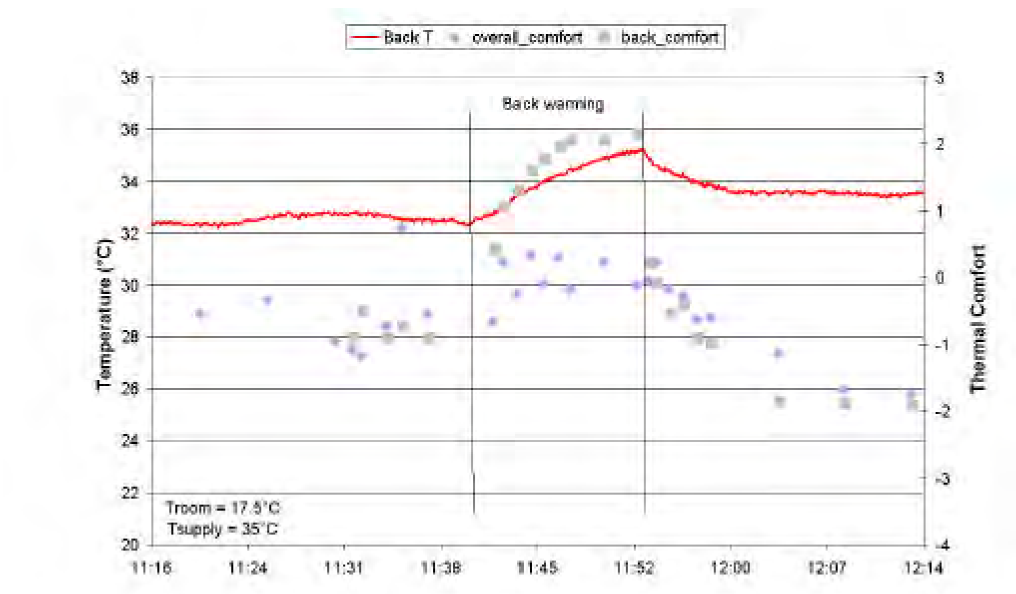

Figure 5.22-4 Back and overall thermal comfort during back heating (23089)

5.5.1.2.2 Least influential group

The least influential group includes hands and feet whose impact on overall sensation is small. The skin temperature of these body parts varies widely, which enables them to perform thermoregulation functions for the body.

The subsections below present examples of the least influential body parts' responses to local cooling under warm environmental conditions (subsection A) and cold environmental conditions (subsection B). We also give a small number of examples of responses to local heating.

Local cooling

This section presents results for local cooling of body parts in the least influential group.

A. Starting from warm

<u>Foot:</u> During the foot cooling test, skin temperature is reduced greatly along with local sensation. However, local sensation does not contribute to overall sensation.

Figure 5.23 is an IR image of the skin temperature variation after cooling the right foot. The cooling supply air temperature was 18°C. The toes are at the coldest end of the scale. Vasoconstriction allows the cooled foot to be near 8°C cooler than the uncooled foot.

Figure 5.23 Right foot skin temperature after cooling (scale from 25 – 35°C)

Figure 5.24-1 to Figure 5.24-4 present examples of foot skin temperature, sensation, and comfort during foot cooling under various test conditions.

In the examples shown in Figure 5.24-1 and Figure 5.24-2, the room air temperatures were 28 and 26 respectively. The cooling air temperature was low, 14°C. The skin temperature reduction was large, 8 and 6 °C respectively.

The foot felt cold during cooling in both examples, reached –3 at the end, and basically recovered after the cooling was removed. However, the influence on the overall sensation was very small, almost no change during the entire process. These two figures are typical for hand and foot cooling. They demonstrate that hands and feet belong to the least-influential groups.

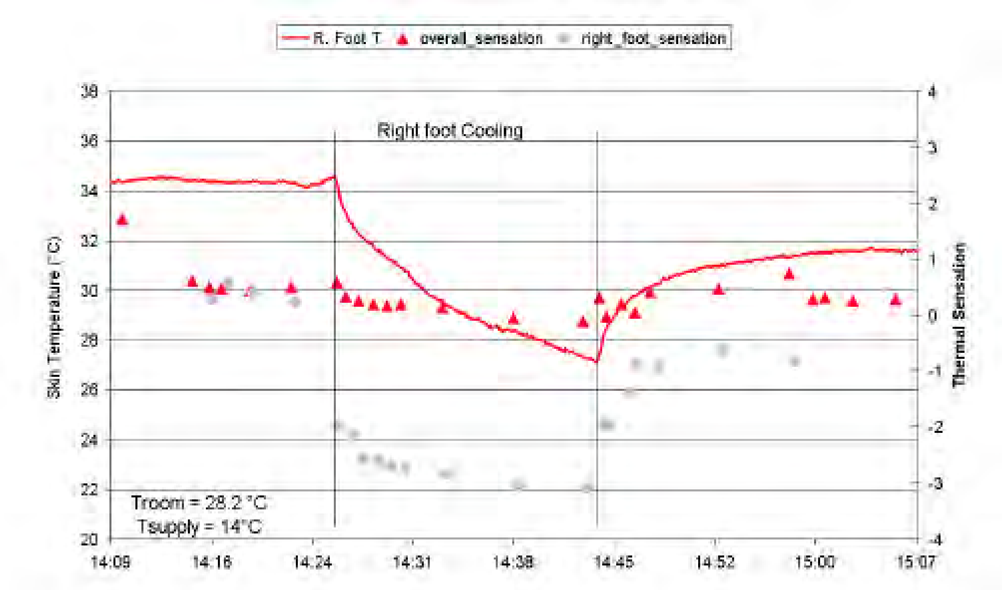

Figure 5.24-1 Foot and overall thermal sensation during foot cooling (03001)

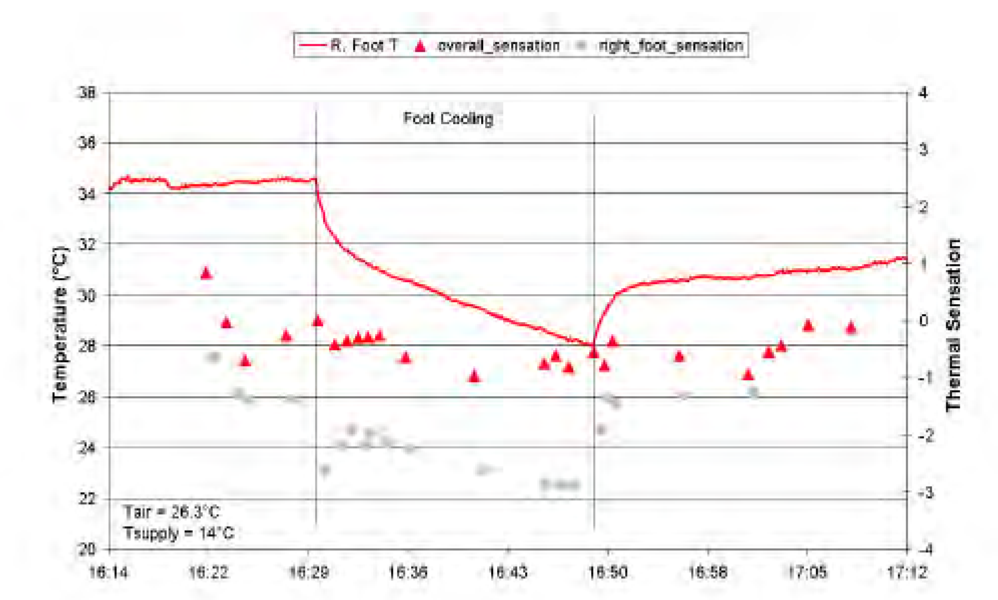

Figure 5.24-2 Foot and overall thermal sensation during foot cooling (04002)

The difference between the two figures is that the foot sensation shows quick overshooting in one of the tests (at 16:29 in 04002). Some examples show overshooting and some don't. The non-overshooting example (03001) also shows a large drop upon the cooling application. A discussion about the different vote patterns will be presented in section 5.3.1.4. Both examples show that the foot skin temperature did not recover to the original temperature that it had before cooling was applied to the foot. After recovery from cooling, the foot skin temperature became stable about 3°C lower than its original pre-cooling value. That indicates that a full recovery of foot skin temperature needs time.

Like overall sensation, overall comfort was not influenced by the foot cooling (see Figure 5.24-3). The foot comfort changed more than 1 scale unit during the entire cooling and recovery process. However, the overall comfort change was minimal.

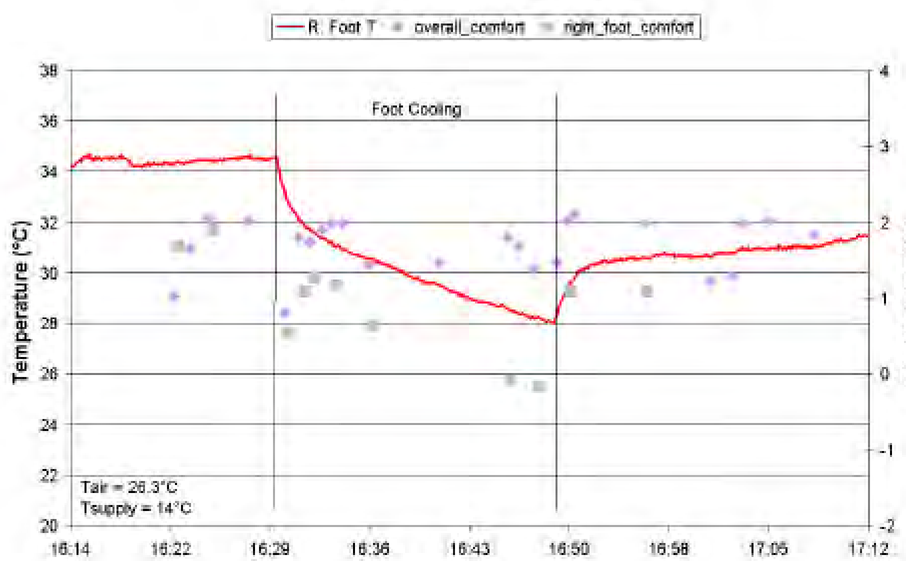

Figure 5.24-3 Foot and overall thermal sensation and comfort during foot cooling (04002)

Figure 5.24-4 (Test 16049) shows that even when people are hot (room air temperature 31°C, sensation votes near hot, +3), adding foot cooling still does not create much influence on overall sensation and comfort.

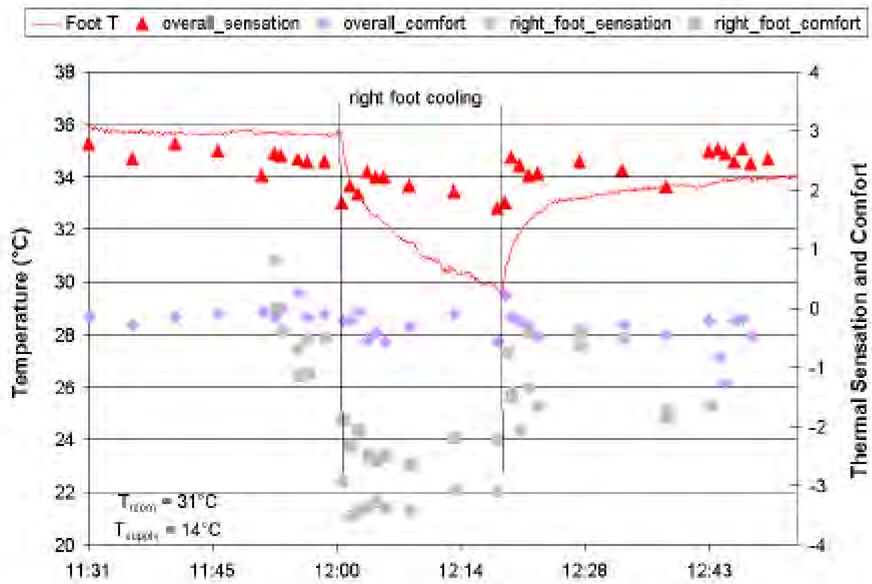

Figure 5.24-4 Foot and overall thermal sensation and comfort during foot cooling (16049)

All four examples demonstrate that whether people feel neutral, slightly warm, or hot, adding foot cooling does significantly influence overall sensation.

Hand: Hand cooling does not contribute much to overall sensation (Figure 5.24-5). In this example, the room air temperature is 28°C and the subject's local and the overall sensations are slightly warm (+1). With the cooling application of the 14°C cold air, the hand skin temperature reduces more than 10°C; finger skin temperature reduces more than 15°C. The hand felt very cold during the cooling application. However, the overall sensation felt only 1 scale unit cooler. With removal of the hand cooling, the hand sensation rose from very cold (-4) to neutral

(0). The overall sensation only felt about 0.5 scale unit warmer. After about 20 minutes, and hand and finger skin temperatures, hand and overall sensation had all recovered.

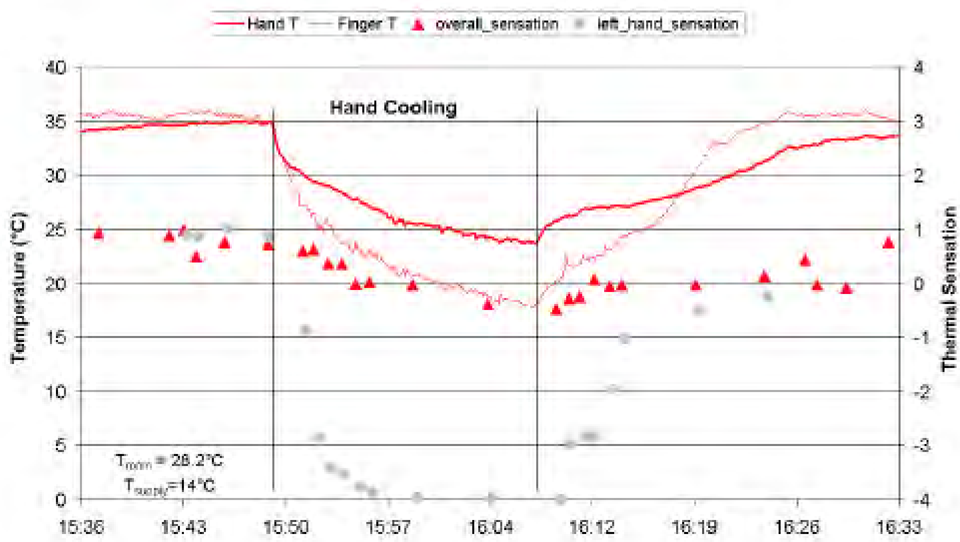

Figure 5.24-5 Hand and overall thermal sensation during hand cooling (13016)

The impact of hand cooling on overall comfort is shown in Figure 5.24-6 for the same example as shown in Figure 5.24-5. Because the hand cooling was quite severe in this case, overall comfort is reduced significantly. Hand comfort decreased, because of the cold stimulus and the constriction of blood vessels in response. Figure 5.24-5 shows that finger temperature was about 6 °C lower than hand skin temperature during the local cooling because fingers constrict the most when cold. When the cooling air is as cold as 14 °C, the finger temperature is close to the pain-receptor threshold of 18 °C.

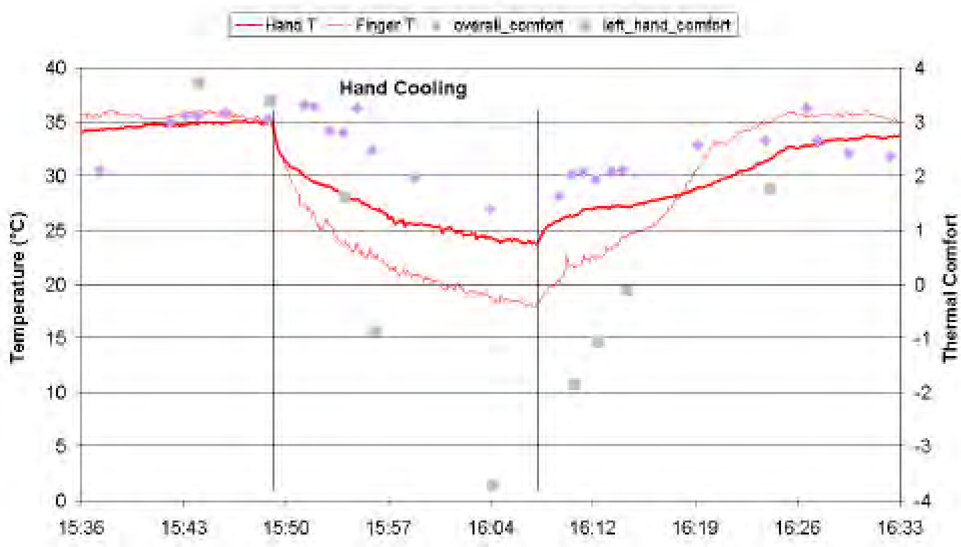

Figure 5.24-6 Hand and overall thermal comfort during hand cooling (13016)

B. Starting from cold

<u>Foot:</u> When the body is cold, vasoconstriction takes place. The constriction is especially stronger for the extremities, such as hands and feet. When local cooling is applied to a vasoconstricted extremity, the heat loss is small because the temperature difference between the skin and the environment is small. Therefore, the skin temperature change is smaller. For example, the foot skin temperature decreased only 2.5°C when the body was cold and the identical 14°C foot cooling was applied (Figure 5.25-1). This decrease is much smaller than the decrease that was observed when a warm foot was cooled (6 – 7°C in Figure 5.24-1 to Figure 5.24-4).

The corresponding changes in local sensation and comfort are also smaller. With the same cold supply air (14°C), the local sensation and comfort reduces only 1 scale unit, while when the body was warm, the reduction in local sensation and local comfort were 2 to 3 scale units.

Because of the smaller skin temperature change, the derivative of skin temperature upon the cooling application is small. Therefore, unlike when the body was warm (Figure 5.24-1 to Figure 5.24-4), the local sensation and comfort show no sudden change.

In the same example, we see that overall sensation (Figure 5.25-1) and comfort (Figure 5.25-2) were not influenced by foot cooling in cold environment. An interesting thing is that when we removed the cooling, both local and overall sensation and comfort showed quick overshooting responses. The overshooting is caused by the positive derivative of the foot skin temperature during cooling removal. From the increased sensation and comfort we see that the contribution of the dynamic skin temperature change on sensation and comfort is large. The sensation is increased more than 2 scale units over the value that existed before local cooling.

We put the chest skin temperature in Figure 5.25-2 for comparison purpose. In the cold environment and during local cooling, the chest skin temperature was very stable.

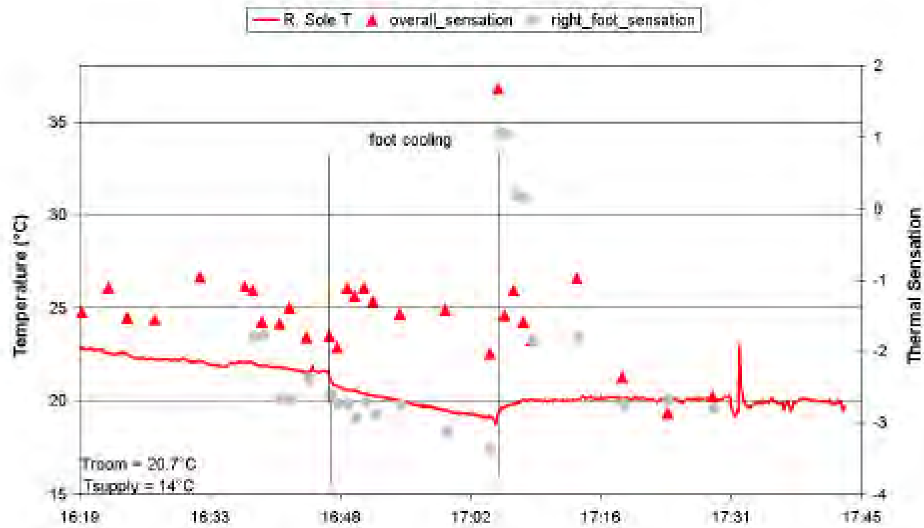

Figure 5.25-1 Foot and overall thermal sensation during foot cooling in cold environment (23082)

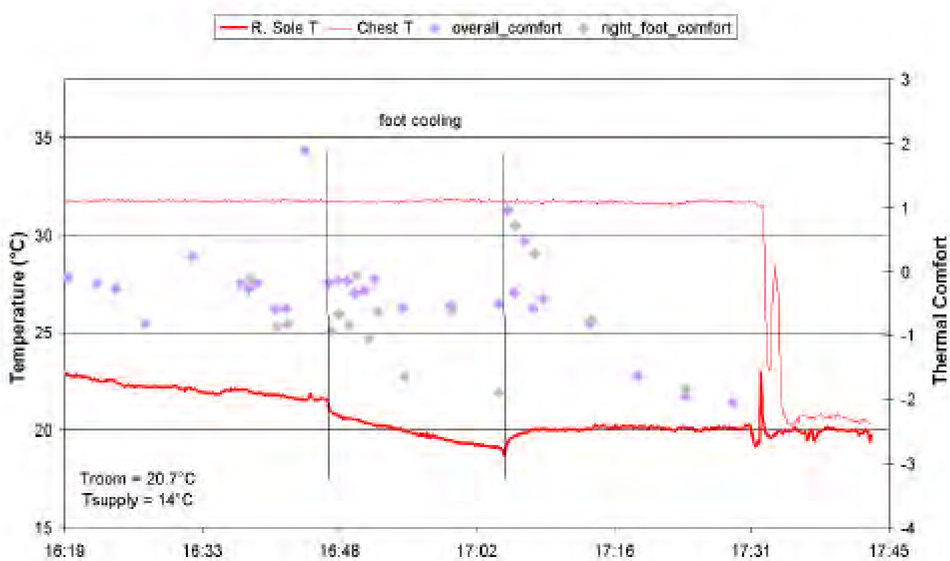

Figure 5.25-2 Foot and overall thermal comfort during foot cooling in cold environment (23082)

Hand: Similar to the foot cooling in a cold environment, cooling a cold hand further reduces the skin temperature (4°C, Figure 5.25-3) much less than cooling a warm hand (12°C,

Figure 5.24-5), because the hand blood vessels are already constricted. The corresponding hand sensation does not change much because before the cooling, the hand felt very cold already. Again we see no overshooting phenomenon because the hand skin temperature change is small and the derivative is small.

This example shows that cooling of a cold hand did not influence the overall sensation at all.

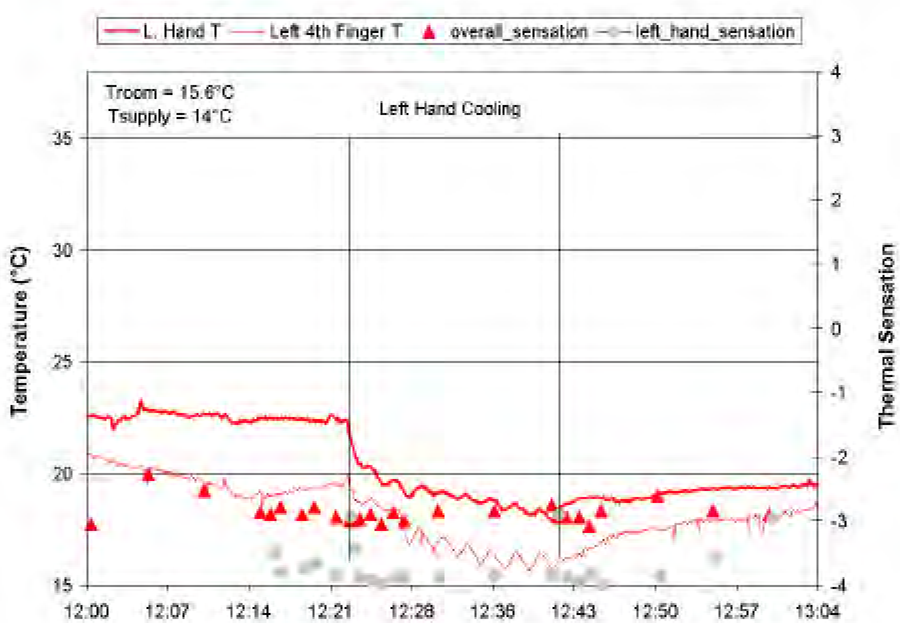

Figure 5.25-3 Hand and overall thermal sensation during hand cooling in cold environment (21083)

Figure 5.25-3 also shows physiological fluctuations in hand and finger skin temperatures. These fluctuations may be caused by shunting (vasodilation induced by exposure to cold, also called AVA action as explained in Chapter 5.2.2.1). Shunting is an attempt to protect tissue from injury. The following example is given by McIntyre (McIntyre 1980). If a hand is put in water at 18°C, the blood flow in the hand falls to about five percent of its normal value. Reducing the water temperature further has little effect until the temperature approaches 0°C. At that point, the intense vasoconstriction is relaxed every few minutes, allowing warm blood to flow through the hand and fingers to protect them from cold injury. This phenomenon is also known as cold-induced vasodilation (Lewis 1930). During vasodilation, heat loss from the hand may be considerable; however, this defense mechanism gives priority to the prevention of local injury. This thesis does not provide further information about the consequences of the AVA effect on sensation and comfort. The phenomenon shown in Figure 5.25-3 can be used to refine thermophysiological models.

Local heating

Hand: Figure 5.26-1 and 5.26-2 show the hand and finger skin temperatures, local and overall sensation, and comfort when heat was applied to a cold hand. The finger skin temperature increased the most, from 23 °C to 35 °C, and the hand skin temperature increased from 24 °C to 31 °C. The example shows that although the whole body is cold, significant vasodilation happens locally during local warming. The hand warmth sensation increased significantly too. Therefore, the local sensation and local skin temperature have a high correlation.

Although hand skin temperature, sensation (from –3 to + 3.5) and comfort (between –2 and +2) change significantly in a cold environment, hand warming has a small influence on overall sensation, 1 scale unit. The influence on overall comfort is bigger, about 1.5 units comfort scale.

Upon hand warming, the local comfort rose from uncomfortable (-2) to above comfortable (+2). However, because of the strong local heating, the hand comfort started to decrease when sensation reached hot (+3). When the whole hand experiences heating, for a cool (-2) whole body, a hot hand sensation (+3) is considered uncomfortable. This observed behavior contributes to the local comfort model in Chapter 6. As the local sensation approaches the extreme scale values for local heating applied to a cold body or for local cooling applied to a warm body, discomfort occurs. This result matches Cabanac's finding that for a hyper- or hypo-thermic person, extreme hand cooling or heating was perceived as very uncomfortable (Cabanac 1969) (presented in Chapter 6, Figure 6.21).

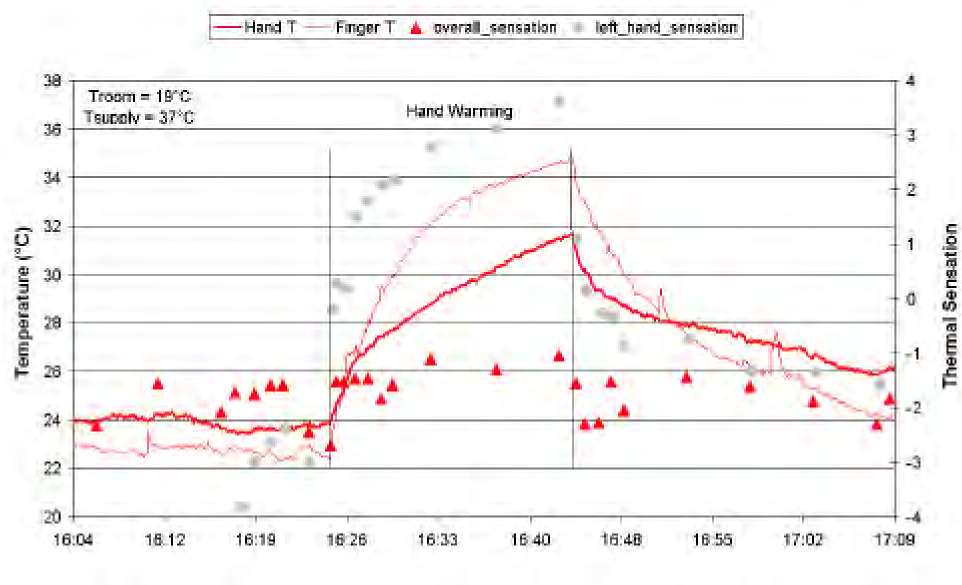

Figure 5.26-1 Hand and overall thermal sensation during hand warming in cold environment (07086)

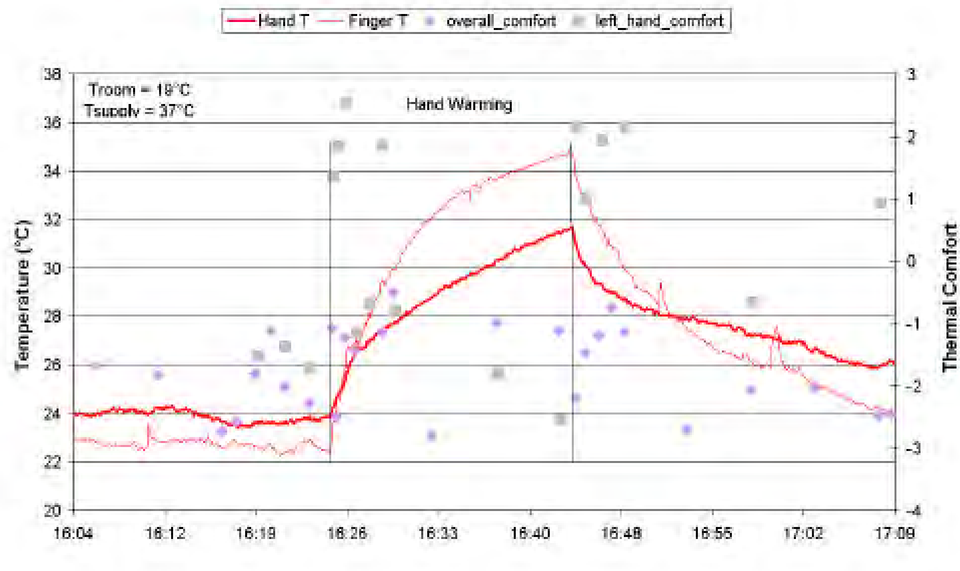

Figure 5.26-2 Hand and overall thermal comfort during hand warming in cold environment (07086)

<u>Two feet:</u> Application of heat to both feet under cold conditions produced a strong sensation of comfort (Figure 5.26-3 and 5.26-4). On this test sequence, heat was applied three times to three different body parts: neck, two feet, breathing zone air. The two-feet warming and the breathing zone warming produced the strongest local sensations. However, only the two-feet warming had a strong influence on the subject's overall sensation (triangles in Figure 5.26-3). The influence from the heating of the other two body parts was small. As for comfort, the breathing zone warming was perceived as uncomfortable with a 1 unit reduction in local comfort scale. Only the two-feet warming enhanced the overall comfort significantly (diamonds in Figure 5.26-4). In order to compare the responses of the two-feet warming with the other two warming applications, Figure 5.26-3 and 5.26-4 show the overall sensation and comfort covering all three local warming processes. Because sensation and comfort votes are same for the left and right foot, the two feet are not represented separately in the figure. We did not test warming a single foot, so we cannot compare the difference between the two-feet warming and one-foot warming.

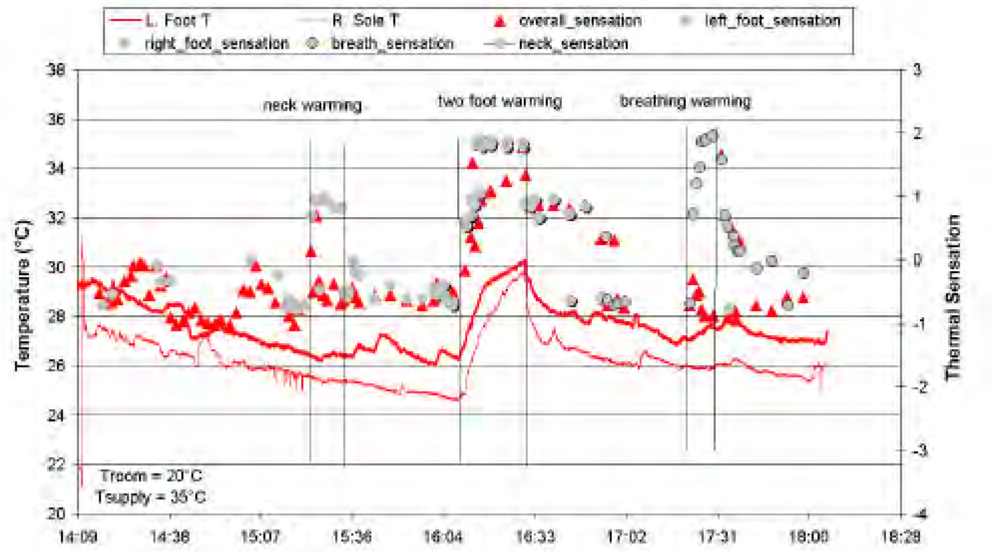

Figure 5.26-3 Foot and overall thermal sensation during two-feet warming in cold environment (26090)

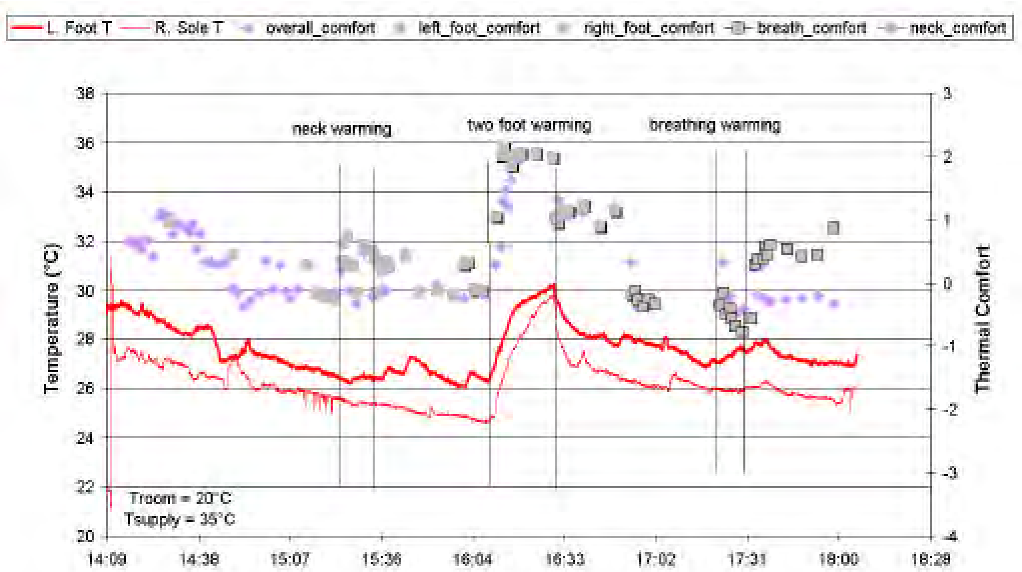

Figure 5.26-4 Foot and overall thermal comfort during two-feet warming in cold environment (26090)

The strong influence of foot heating on overall sensation will be represented by a larger weight for the warming side and a smaller weight for the cooling side of the foot sensation, in determining overall sensation in the overall sensation model (Table 6.5 in Chapter 6.4.2).

5.5.1.2.3 Moderately influential group

This section illustrates the responses to local cooling and heating of moderately influential body parts.

The main feature of the moderately influential group is that although local sensation does not so strongly affect overall sensation as to make local and overall sensation identical, the influence of the moderately influential body parts on overall sensation is nonetheless substantial. Unlike the other two groups whose local and overall comfort decreases in response to substantial local cooling, our test results show that some of the moderately influential body parts respond to the same rates of local cooling with increased comfort levels. For example, all the breathing zone air cooling, face cooling, and mild neck cooling increased perceived comfort. The reason is that the body parts in this groups are not as sensitive as those in the most influential/dominant group, but also do not experience as much vasoconstriction as the hands and feet, and therefore do not suffer significantly reduced local comfort when they are cooled.

Local cooling

This section presents results from applications of local cooling to body parts in the moderately influential group. The first series of results (subsection A) are for application of cooling to individual body parts under warm environmental conditions. The second series of results (subsection B) are for applications of cooling to individual body parts under cold environmental conditions. We conclude with selected examples of responses to local heating.

A. Starting from warm

<u>Head and Face:</u> Figures 5.27-1 through 5.27-3 show the responses of head and face to local cooling under warm environmental conditions.

The first example (13016, Figure 5.27-1) demonstrates that head cooling creates a moderate influence on overall sensation. The forehead skin temperature was cooled 4°C, which is similar to the temperature decrease experienced during the chest and back cooling discussed earlier, but much smaller than the temperature decreases experienced during hand and foot cooling.

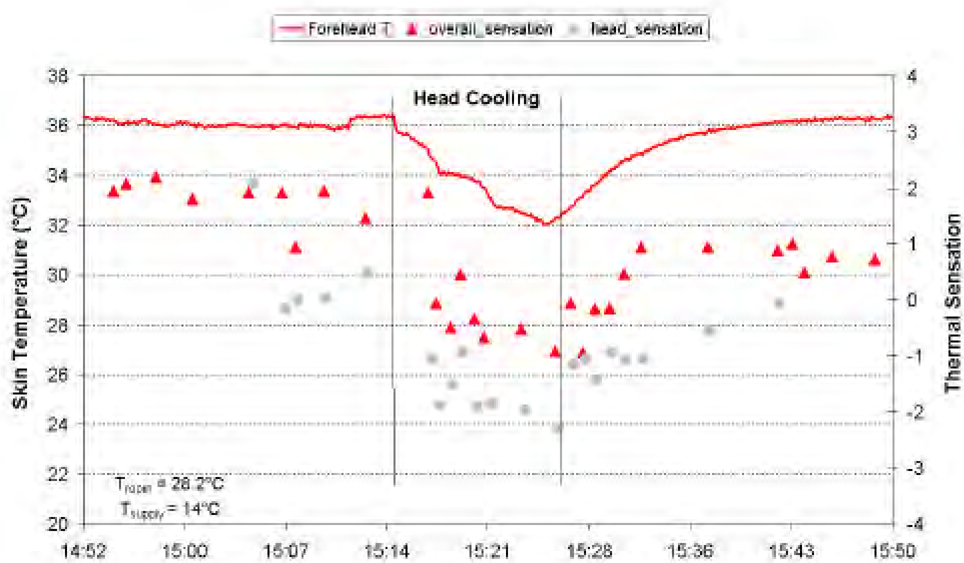

Figure 5.27-1 Head and overall thermal sensation during head cooling (13016)

Figure 5.27-2 shows face cooling results. Face skin temperature decreased by about 5 °C. Face sensation decreased from slightly warm (1) to cool (-2) while overall sensation decreased from slightly warm (1) to neutral (0). Both local and overall sensation votes reflected these final values immediately after application of cooling to the face.

After the removal of cooling, both local and overall sensations showed an overshooting pattern to levels that were higher than the sensations registered before the application of face cooling. After 10 more minutes, both overall and face sensations returned to the original values noted before face cooling. Both the sudden sensation drop with the cooling application and the overshooting with the local cooling removal are from increased thermoreceptor signals caused by rapid rate of temperature changes at the receptor. This voting behavior is typical for face cooling: at the start of face cooling, votes for both face and overall sensation immediately reached their final values. Upon removal of the cooling, votes for both sensations showed a transient overshooting response but quickly returned to their original pre-cooling values. The face skin temperature recovered to its original value in about 10 minutes as well.

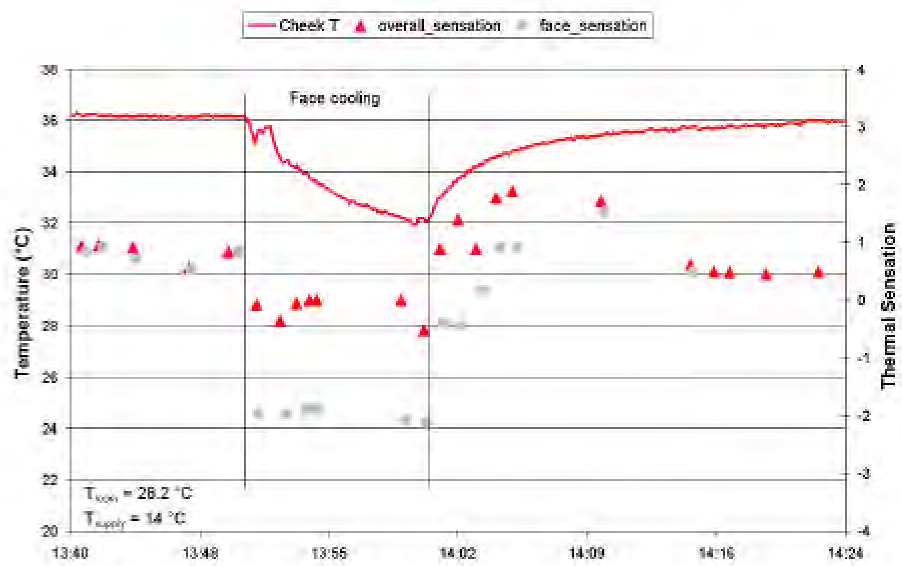

Figure 5.27-2 Face and overall thermal sensation during face cooling (03001)

Figure 5.27-3 shows the comfort responses for test 03001 (Figure 5.27-2). Before and after application of cooling to the face, both face and overall sensation are between neutral and slightly warm (between 0 and 1), but the comfort vote was at just comfortable (+0). Both overall and face comfort increased to comfortable (+2) during application of cooling to the face although the face sensation was rated at cool (–2) and overall sensation was 0 (neutral). These results imply that subjects find face cooling pleasurable. When face cooling ceased, overall comfort immediately reduced from comfortable (+2) to just comfortable (+0). Face comfort showed a short period of positive response (overshooting) above comfortable (+2) after removal of local cooling but quickly (in three minutes) reduced to just comfortable (+0).

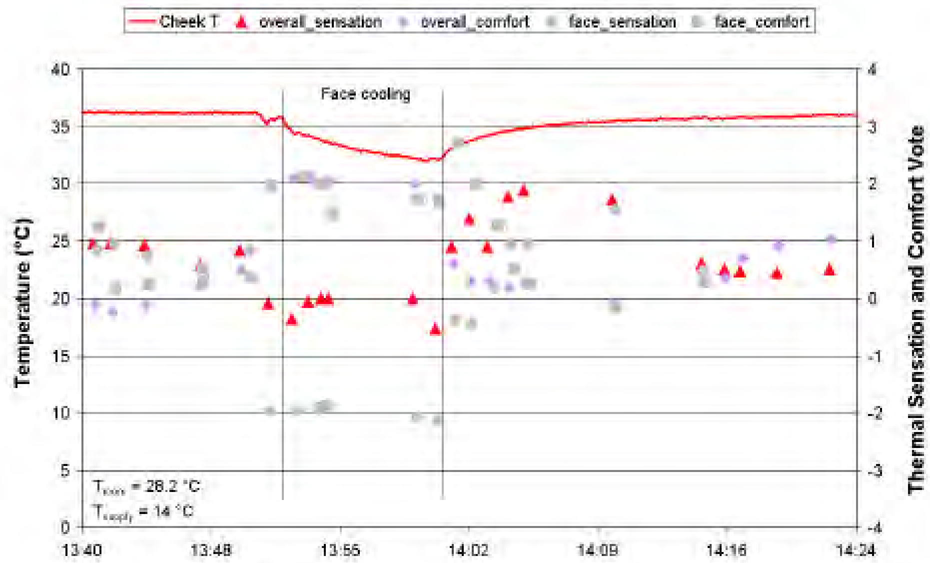

Figure 5.27-3 Face and overall thermal sensation and comfort during face cooling (03001)

<u>Neck:</u> Test 13030 is an example with strong (14°C supply air) neck cooling, and test 04072 is an example with mild (23°C) neck cooling. Both tests (Figure 5.27-4 and 5.27-5) show that neck cooling has a moderate influence on the overall sensation. After application of local cooling to the neck under warm environmental conditions (Figure 5.27-4), the front neck skin temperature reduced 2°C, probably the smallest reduction in all the strong local cooling applications. The front neck thermocouple is located between the two carotid arteries, which may explain why the skin temperature was lowered the least. Skin temperature recovered to its pre-cooling value in ten minutes. The back neck skin temperature reduced 2°C in the mild neck cooling process (Figure 3.27-5). The smaller skin temperature reduction seen here will be reflected in the local sensation model, where the logistic curve will be steeper, represented by a bigger regression coefficient for the local skin temperature (Chapter 6, Table 6.1).

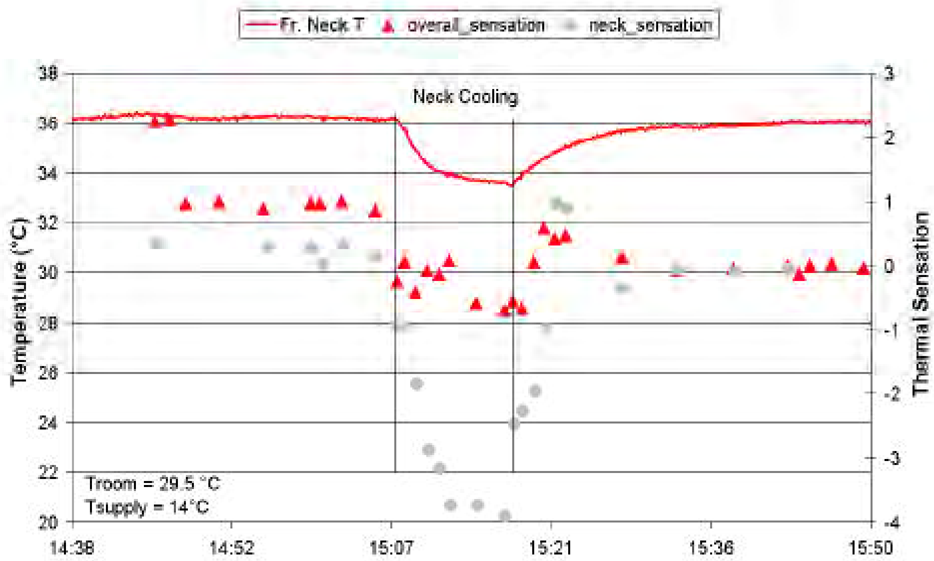

Figure 5.27-4 Neck and overall thermal sensation during strong neck cooling (13030)

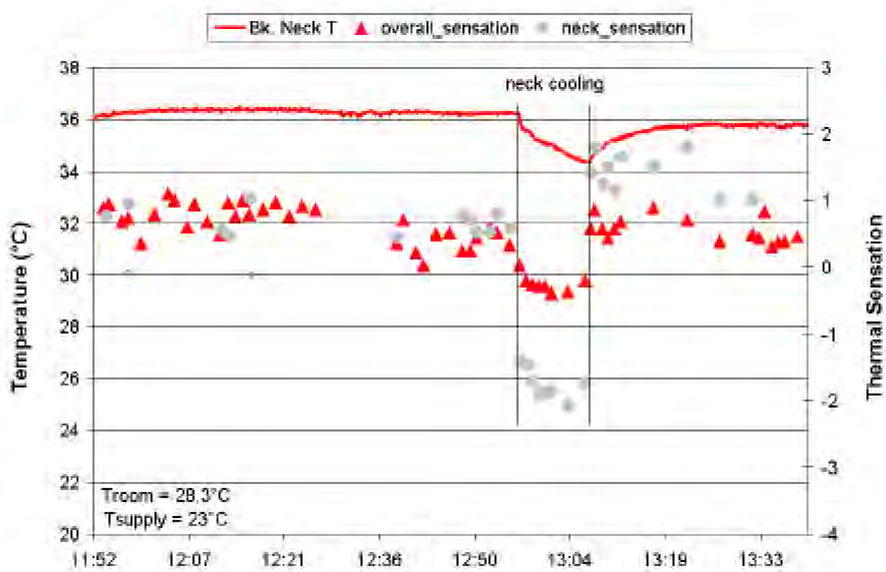

Figure 5.27-5 Neck and overall thermal sensation during mild neck cooling (04072)

Overall comfort is slightly increased when the neck is cooled, but neck comfort decreases significantly in strong neck cooling (13030, Figure 5.27-6). This indicates that the subject did not find neck cooling pleasurable, even in a warm environment. When neck cooling was removed, both local and overall comfort increased.

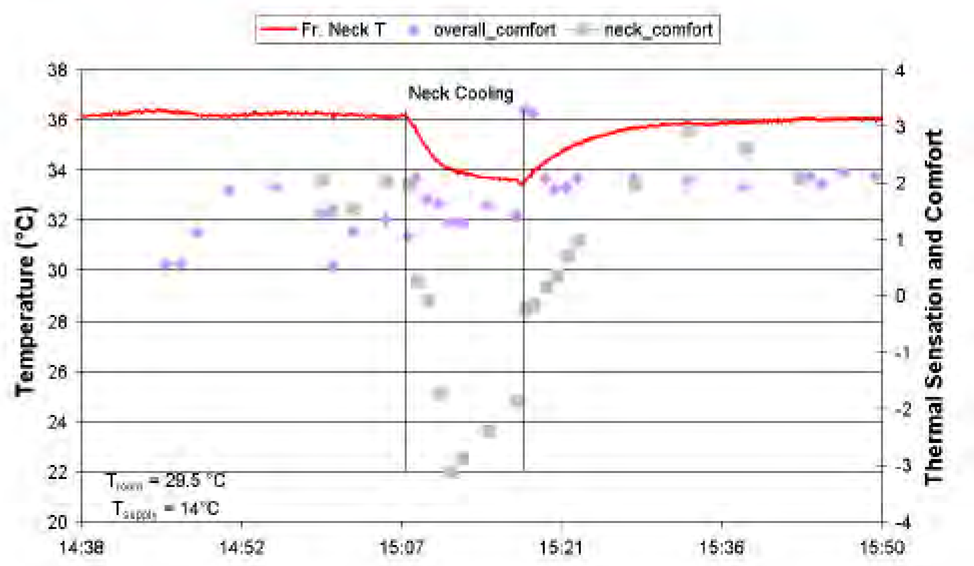

Figure 5.27-6 Neck and overall thermal comfort during strong neck cooling (13030)

When the cooling was not as severe, an increase in the comfort level was perceived (Figure 5.27-7).

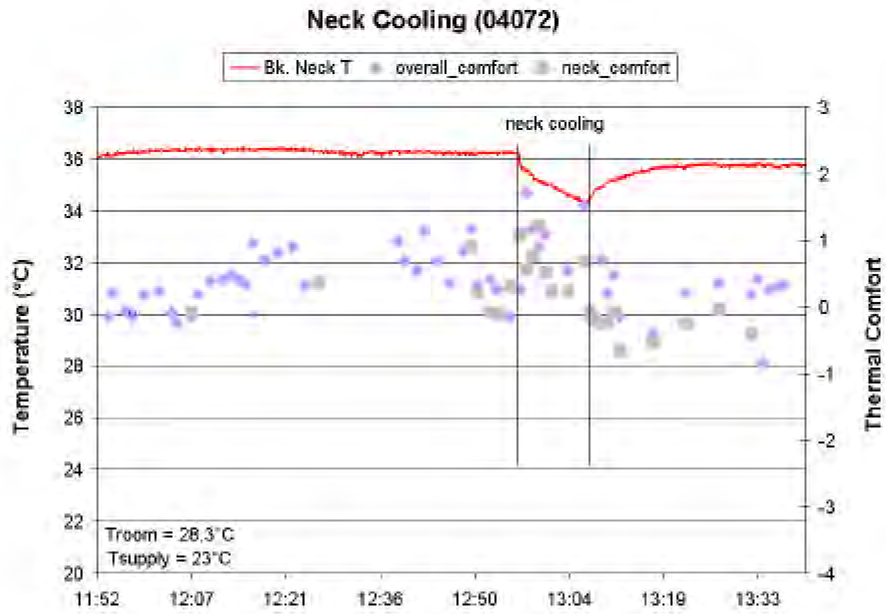

Figure 5.27-7 Neck and overall thermal comfort during mild neck cooling (04072)

<u>Right Arm:</u> Figure 5.27-8 shows that the influence of arm cooling on overall sensation is smaller than the influence of the sensations of body parts in the most influential group and greater than the influence of sensations of body parts in the least influential group.

We applied the cooling to the entire arm, but we asked the local sensation and comfort separately for the upper and lower arms. The results are also shown separately.

During cooling, the upper arm skin temperature is reduced slightly more than the lower arm. In general, the skin temperatures from the upper and lower arms are close. The sensation of the upper arm changes more than the lower arm. One possibility is that the upper arm is closer to torso and lower arm is closer to hands. In the most influential group (e.g. chest), the smaller skin temperature change corresponds to larger local sensation change. In the least influential group (e.g. hand), the skin temperature change is large. Therefore, with the same skin temperature reduction in the upper arm and lower arm, the local sensation felt cooler for the upper arm than for the lower arm. Another possibility is that the area of the upper arm is bigger than the lower arm. Thermal sensation is based on area summation (Stevens and Marks et al. 1974, Helsel 1981). We conducted 12 arm cooling tests; half showed that the upper arm felt cooler, and half showed no difference.

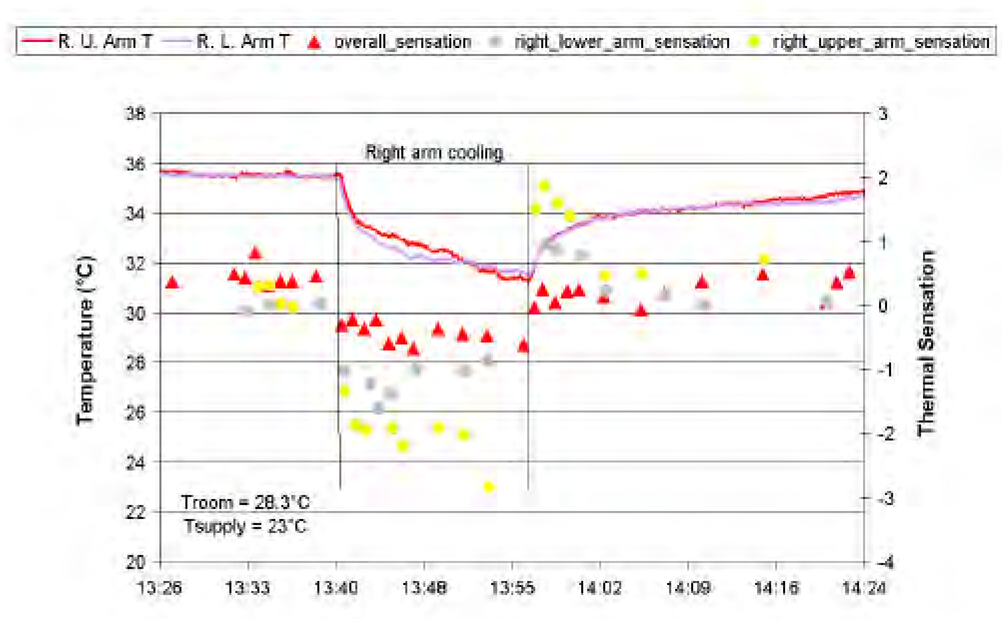

Figure 5.27-8 Upper and lower arm and overall thermal sensation during arm cooling (04072)

B. Starting from cold

<u>Neck:</u> Figure 5.28-1 shows that back neck skin temperature decreased 3°C with application of local cooling to a cold body. In a cold environment (room air temperature was 15.6°C), the neck skin temperature were well maintained (near 34°C). With the cooling application, neck sensation drops very significantly. This is different from the result applying hand cooling in a cold environment (Figure 5.25-3). In the same cold environment, the hand felt

very cold before adding the hand cooling. Applying the hand cooling did not make the hand feel much colder.

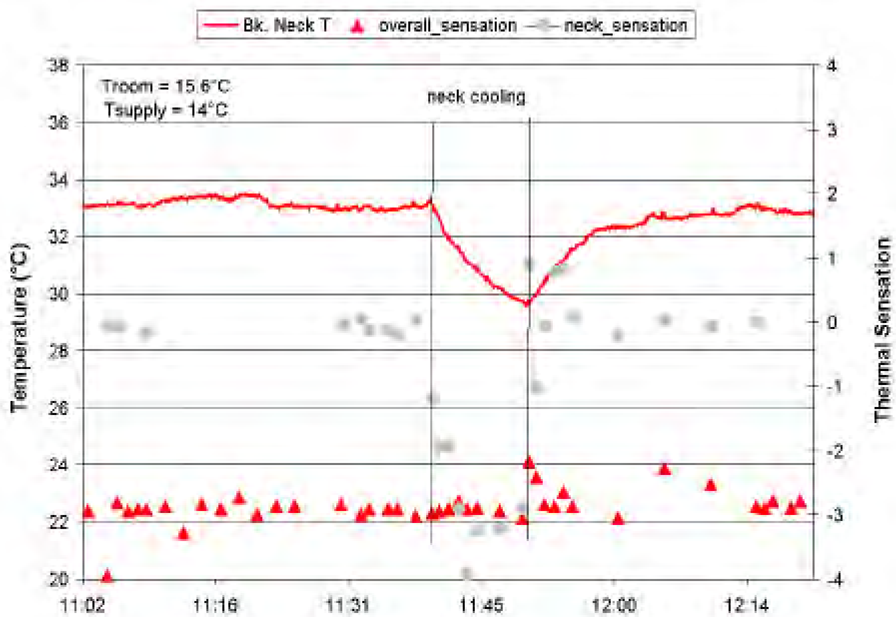

Figure 5.28-1 Neck and overall thermal sensation during neck cooling to a cold body (21083)

Because the neck is the warmest part of the body in the cold environment, the neck comfort level was high before cooling. Figure 5.28-2 shows the neck comfort results for a neck-cooling test (21083). Neck comfort changed significantly when cooling was applied. Compared with the responses of other body parts that were exposed to cooling under cold environmental conditions, neck comfort and sensation decreased the most. This result shows that subjects especially dislike neck cooling in a cold environment.

Based on our grouping, the neck is in the moderately influential group so the cooling of the neck should have certain influence on the overall sensation and comfort. However in this case, the influence from neck on overall was small because the room was cold and the subject already felt cold (-3) before the neck cooling began.

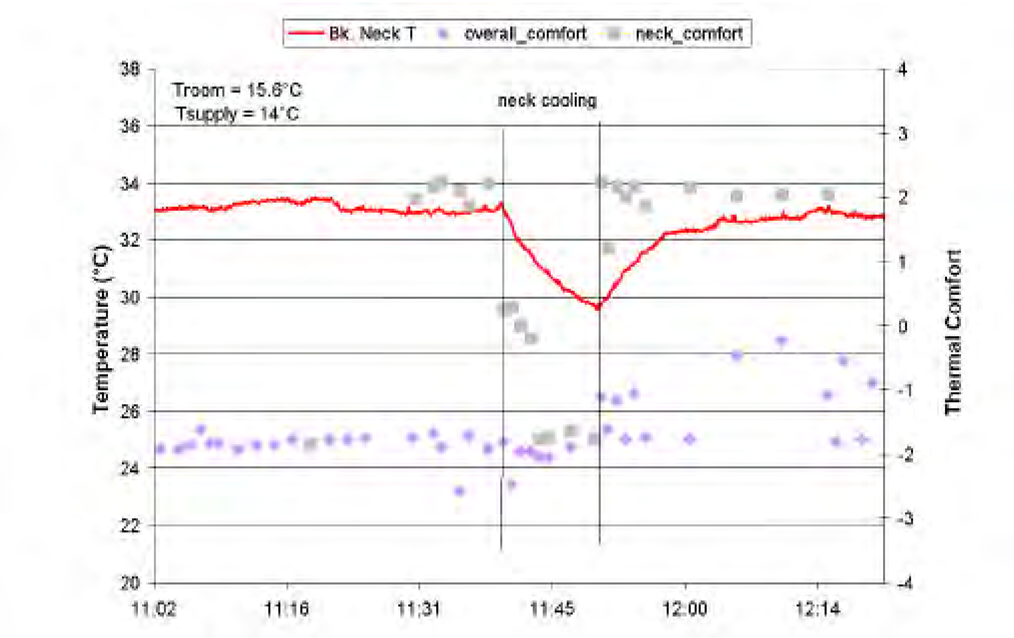

Figure 5.28-2 Neck and overall thermal comfort during neck cooling to a cold body (21083)

Local heating

Face: Figure 5.29-1 shows an example of increased face and overall sensation in response to face warming. The increase in face sensation votes were large, 3 scale units, the increase on overall sensation was more than 1 scale unit. The cheek skin temperature was warmed 4°C, and the forehead skin temperature nearly 3°C.

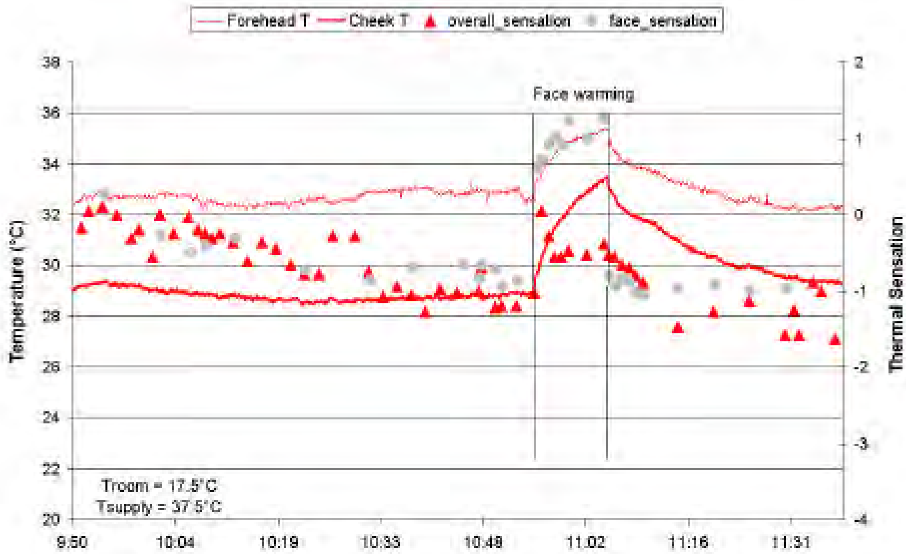

Figure 5.29-1 Face and overall thermal sensation during face warming (23089)

Figure 5.29-2 shows face comfort responses to face warming and recovery. The variation was more than 2 scale units.

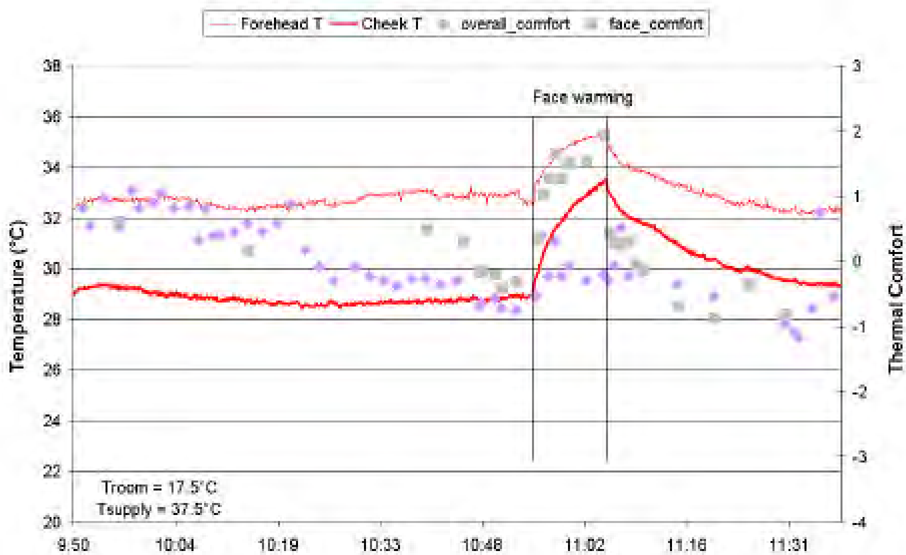

Figure 5.29-2 Face and overall thermal comfort during face warming (23089)

5.5.1.2.4 Breath intake air: warming vs. cooling

Our subjects responded positively to cooling of breath intake air and negatively to heating of breath intake air. Its influence on overall sensation and comfort are moderate. We discuss it separately because research has shown that breathing zone air intake has special influence on perceived thermal discomfort and indoor air quality. Berglund (Berglund and Cain 1989) and Fang (Fang et al., 1998,) have shown that cool and dry air is perceived as less stuffy and more acceptable than warm and humid air. Toftum (Toftum et al. 1998) discussed upper limits for air humidity for preventing warm respiratory discomfort. We examined the influence of breathing-zone air intake on thermal sensation and comfort.

Warming: In our tests, subjects exposed to warm breath intake air showed a strongly negative response. Of all the local heating tests under cold environmental conditions, the tests in which breath intake air was warmed were the only ones in which subjects' local and overall comfort decreased. For all the other local warming tests in a cold environment, local and overall comfort increased in response to local warming.

In test 27091 (Figure 5.30), the room air was 20°C and warm air for local heating was 37.5°C. Before application of local heating, the subject's overall sensation was very cold (–3) and overall comfort was low, between uncomfortable and very uncomfortable (-3). Breathing sensation was between slightly cool and cool (near -1.5) and breathing comfort was on the comfortable side, between 1 and 1.3. Local comfort declined significantly right after the application of heating and gradually reached –2.5 (Figure 5.30). The skin temperature shown in the figure was measured on the chin.

Overall comfort showed an increase with the application of warming to the breath intake air. However, when breath warming stopped, overall comfort increased again. The removal of the breath warming was apparently experienced as pleasurable.

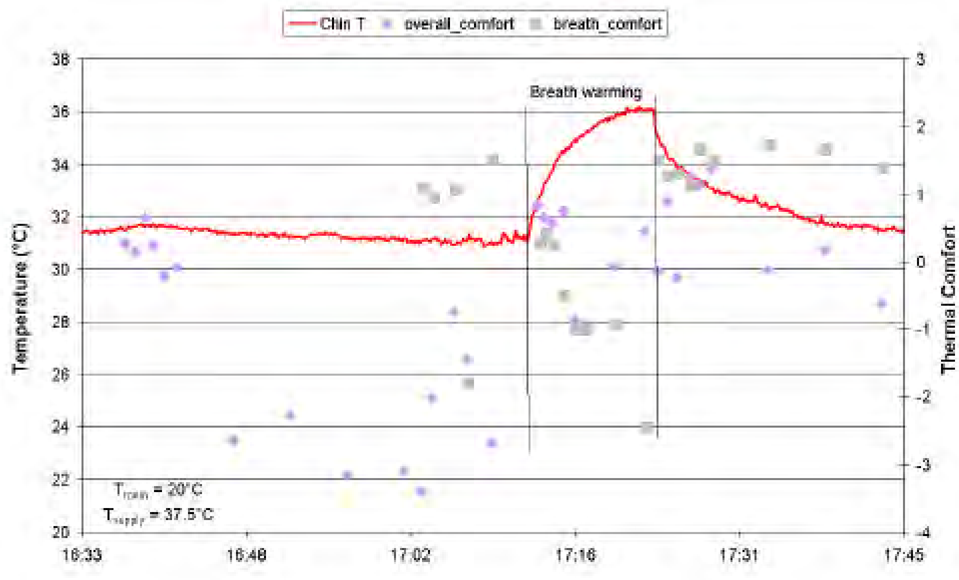

Figure 5.30 Breathing and overall thermal comfort during breath intake air warming (27091)

We performed a total of three tests in which breath intake air was heated. The other test shows a very similar pattern of comfort votes: breathing comfort declined significantly when air at 36.7 °C was applied to heat the breath, and increased significantly when this heating was removed (23088, 26090).

<u>Cooling:</u> Cooling of breath intake air produced dramatically different results than heating. Figure 5.31-1 shows a test in which breath intake air was cooled and overall sensation declined from warm (2) to neutral (0), while local sensation declined from neutral (0) to cool (–2).

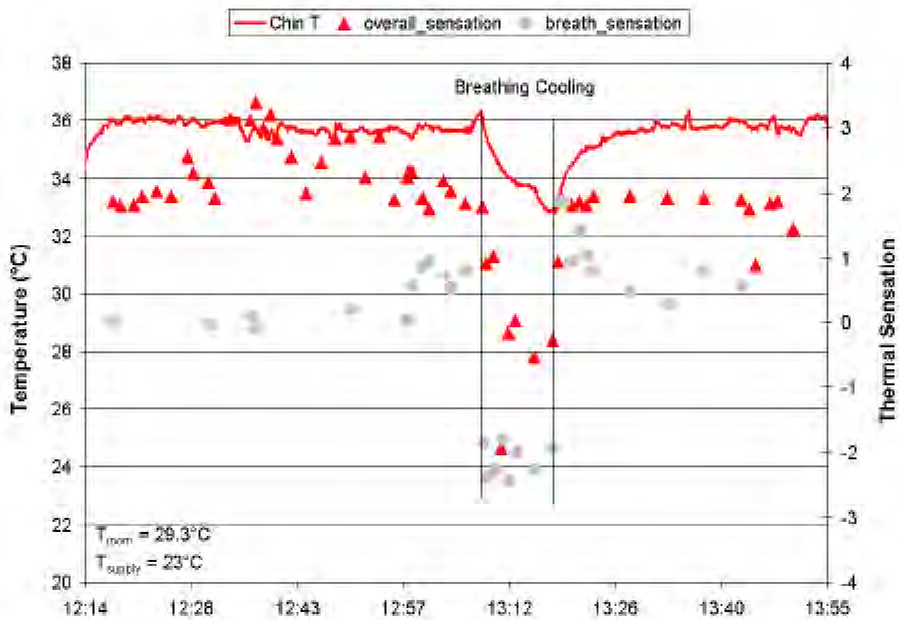

Figure 5.31-1 Breathing and overall thermal sensation during breath intake air cooling (21073)

The corresponding overall comfort greatly increased (Figure 5.31-2) from uncomfortable (–2) to above just comfortable (+0). With breath cooling, both breathing and overall sensations became cooler, and both comfort levels increased. When breathing cooling stopped, sensations became warmer and comfort levels decreased.

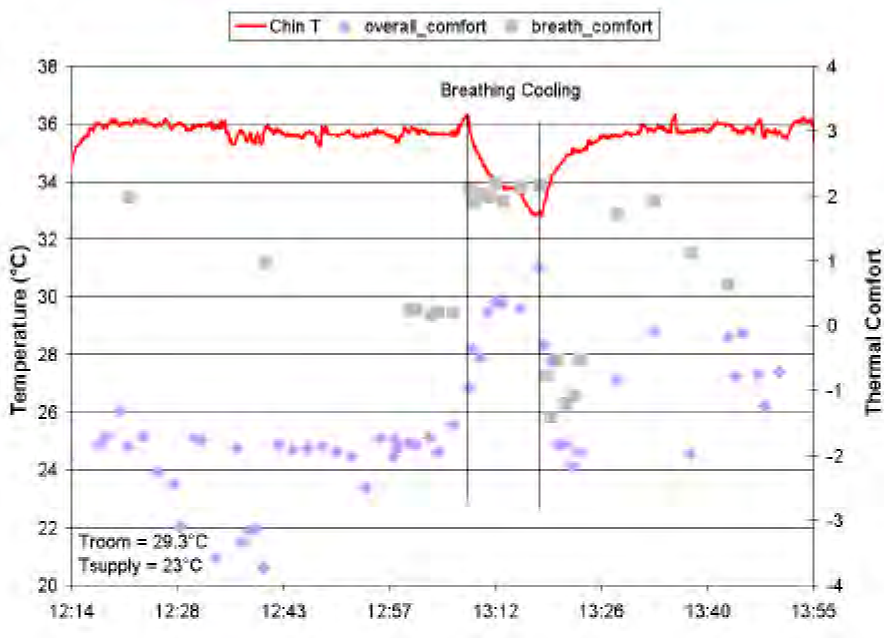

Figure 5.31-2 Breathing and overall thermal comfort during breath intake air cooling (21073)

Figure 5.31-3 shows that people are more comfortable with breathing cooling than two other local cooling treatments in the same test. The room air temperature was 30 °C and the supply air temperature was very mild, 28 °C. Breathing cooling is the only cooling treatment that showed positive comfort responses. In this example, leg cooling did not create any influence on the overall sensation, while chest cooling was considered excessive and so had a negative impact on the overall comfort. The chin skin temperature is not presented here because there was a problem with its reading. The two skin temperatures are for chest and shin.

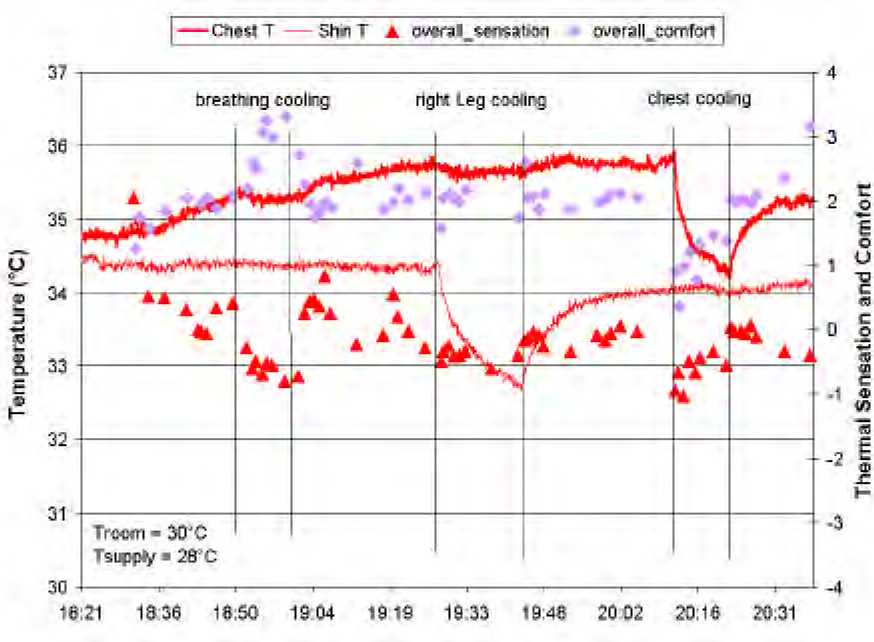

Figure 5.31-3 Overall thermal sensation and comfort for three local cooling applications in one test (09022)

We have showed that in general people are happy with a slightly cool head. The cool head helps to keep a cool brain. The reason that people are happy with the breathing zone air cooling and don't like breath warming might be correlated with the fact that breathing zone air is related with selective brain cooling. Cabanac (Cabanac 1997) concluded from human subject tests that upper airway convective-evaporative heat loss does contribute to cooling the brain.

5.5.1.2.5 Statistical significance of the three groups

Table 5.5 shows ratio of the overall sensation change over local sensation change, $\frac{\Delta S_{overall}}{\Delta S_{local}}$, for the three groups. The overall and local sensations used to calculate the changes ($\Delta S_{overall}, \Delta S_{locall}$) are before and at the end of each local cooling/heating application (represented by the circle and the triangle in Figure 5.1). The bigger the ratio, the larger the influence of local sensation on overall sensation.

The table shows the average of the ratio, standard deviation, and the number of tests used in the calculation. The differences between the most and the least influential groups, the moderately and the least influential groups are highly significant (two-tailed t-test, p<0.001). The difference between the most and the moderately influential groups is also significant (p<0.005). The significant level is lower than the difference between the other two groups.

Table 5.5 Ratio $\frac{\Delta S_{overall}}{\Delta S_{local}}$ produced by a local cooling/heating

	Highly influential	Moderately influential	Least influential
mean	0.72±0.3 (36)*	0.51±0.4 (111)	0.12±0.3 (36)

* In 0.72±0.3 (36), 0.72 is the average ratio, ±0.3 is the standard deviation, and 36 is the sample size (number of tests).

.

Table 5.6 shows the ratio of overall comfort change over local comfort change. The differences are calculated using the overall and local comfort before and at the end of each local cooling/heating application. Again, the table presents the average of the ratio, standard deviation, and the number of tests.

The differences between the most and the least influential groups, the moderately and the least influential groups are highly significant (p<0.001). The difference between the most and the moderately influential groups is also significant (p<0.05), but less so than the differences between the other two groups.

Table 5.6 Ratio $\frac{\Delta C_{overall}}{\Delta C_{local}}$ produced by a local cooling/heating

	Highly influential	Moderately influential	Least influential
mean	0.83±0.43 (61)*	0.68±0.52 (151)	0.35±0.34 (56)

* In 0.83±0.43 (61), 0.83 is the average ratio, ±0.43 is the standard deviation, and 61 is the sample size (number of tests).

The two tables show that at the p level of $p<0.05$ all three groups are significantly different for both sensation and comfort.

5.5.1.2.6 Correlating skin temperature and its rate of change with local sensation

The correlations between local skin temperature and local sensation for local body parts in transient conditions are presented in Table 5.7. The data are from local cooling/heating transient processes (represented by squares in Figure 5.1).

Table 5.7 Correlation (r) between local skin temperature and local sensation

back	chest	pelvis	face	head	breath	neck	thigh	lower leg	foot	upper arm	lower arm	hand
.56	.53	.45	.64	.55	.05	.58	.58	.22	.34	.66	.57	.74

Most of the correlations between the local skin temperature and the local sensation are between 0.5 and 0.6. They are much smaller than the values in stable environments (Table 5.4). During transient process, the dynamic signal from the thermoreceptors caused by the rate of change of skin temperature causes local sensation to have a high correlation with the derivative of the local skin temperature, as shown in Table 5.8. The correlations are around 0.5. In stable conditions, the derivative of skin temperature is zero, so there is no correlation between the two.

Table 5.8 Correlation (r) between derivative of local skin temperature and local sensation

back	chest	pelvis	face	head	breath	neck	thigh	lower leg	foot	upper arm	lower arm	hand
.58	.55	.47	.59	.47	.54	.56	.46	.43	.57	.56	.35	.58

5.5.1.3 Core temperature responses

At the beginning of the Chapter 5, we saw that when core temperature reached steady state in neutral conditions, it is very stable (within 0.1 °C, Chapter 5.2.1.3). The subsections below describe core temperature responses during transient conditions, for local cooling of single body parts in warm and cold environments, and local heating in a cold environment. Through examples, we will show: that in warm environment when local cooling is applied, the core temperature responds with an immediate increase – the opposite direction as the local cooling. In a cold environment, the core temperature responds with an decrease when local warming is applied, also in the opposite direction as the local heating. The scale of this decrease is less compared to the scale of increase when applying local cooling to a warm body. In cold environment when local cooling is applied, the core temperature is very responsive, fluctuating up to 0.8 °C up and down.

In each of the following examples, we show the core responses during one entire test in order to see its continuous response.

5.5.1.3.1 Local cooling in warm environment

Body core temperature increases almost immediately in response to local cooling of body parts, especially when the body parts belong to the most influential/dominant group (back, chest, pelvis). Whether the rapid response is caused by vasoconstriction or by shivering is unclear.

Hensel (Hensel 1981) listed the thresholds for shivering, vasomotor, and sweating from different studies (Baum et al. 1976, Cabanac and Massonet 1977, Cunningham et al. 1978). There is only one threshold for both vasoconstriction and vasodilation. When the core temperature is above the threshold, vasodilation happens; when the core temperature is below the set point, vasoconstriction occurs. Therefore, vasomotor action takes place continuously in response to the body's thermal state. Sweating and shivering have two different core set points, the threshold for sweating being higher than that for shivering. Sweating and shivering do not happen until the core temperature reaches their thresholds. Therefore, it is likely that the immediate increase in core temperature is a result of vasoconstriction.

Figures 5.32-1 through 5.32-4 show examples of body core temperature response to local cooling while the subject is in a warm environment. The overall thermal sensation is included in order to indicate the transient processes. In these figures, we see that whenever local cooling was applied, overall sensation decreased while core temperature increased. The maximum increase was almost 0.2°C during the pelvis cooling in test 13016. The increase in tests 06006 and 11013 was about 0.1°C. For test 18043, the increase was less than 0.1°C. When local cooling was removed, overall sensation increased while core temperature decreased.

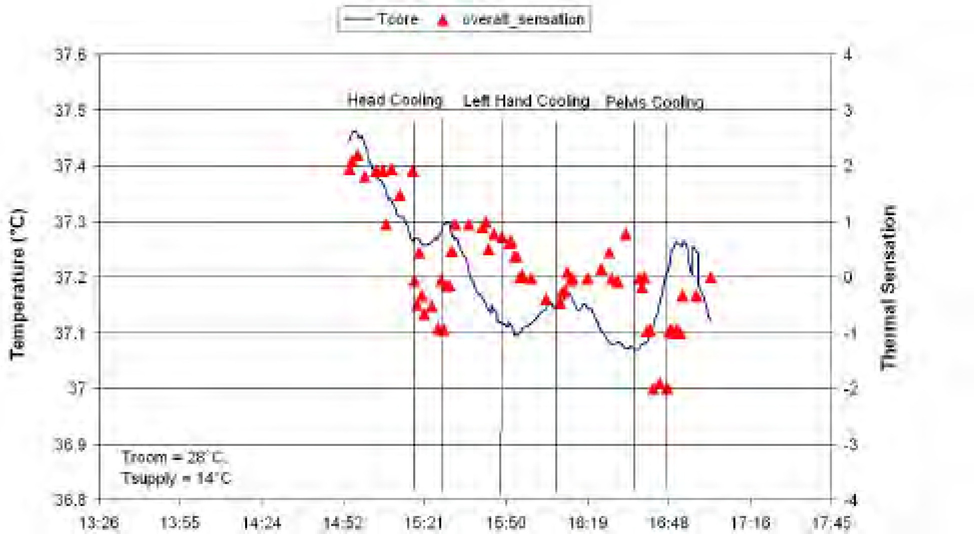

Figure 5.32-1 Core temperature and overall sensation during local cooling (13016)

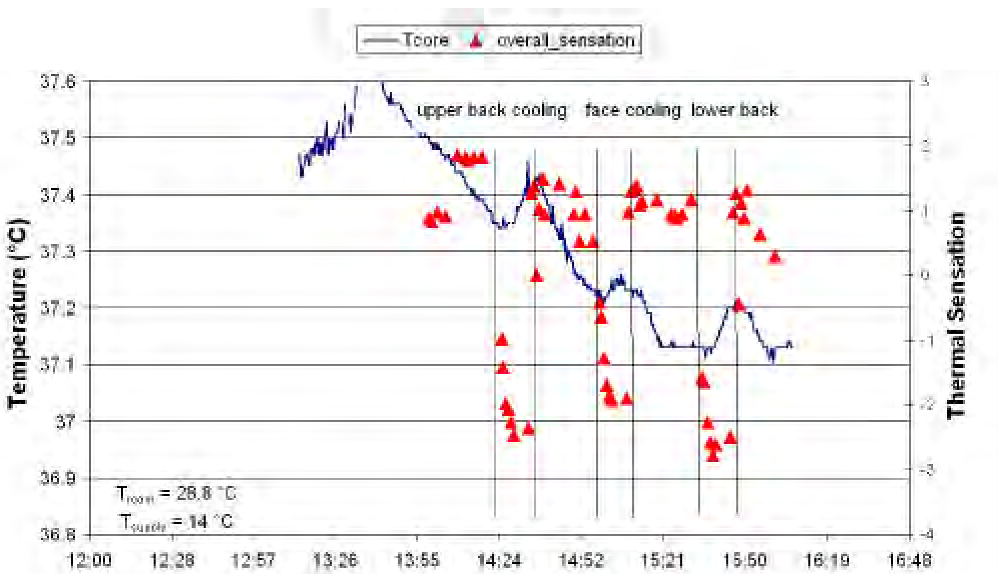

Figure 5.32-2 Core temperature and overall sensation during local cooling (06006)

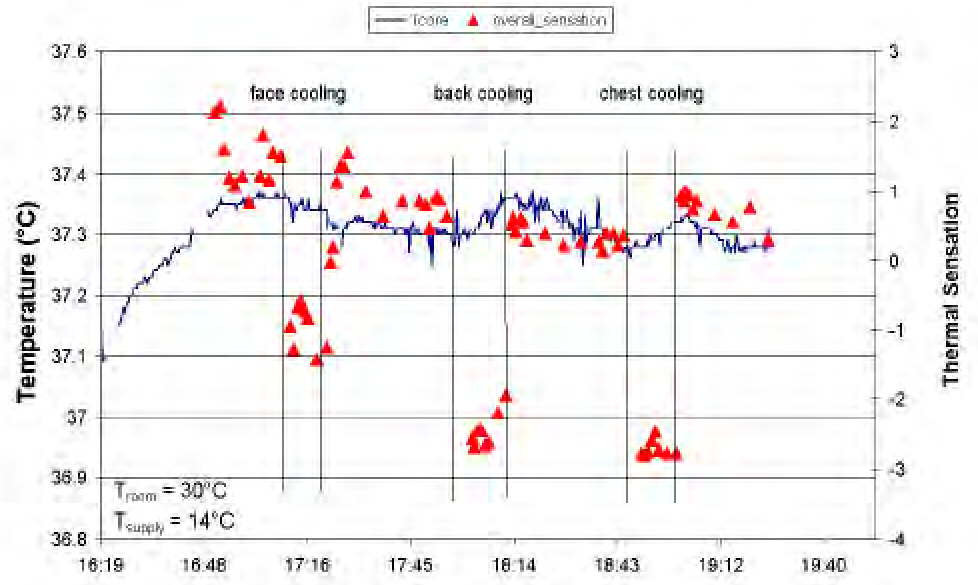

Figure 5.32-3 Core temperature and overall sensation during local cooling (18043)

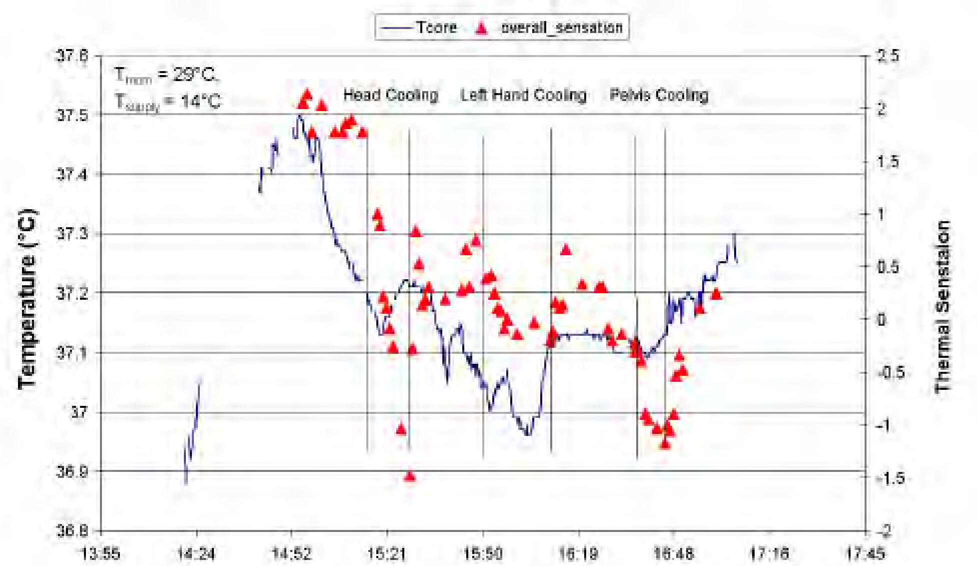

Figure 5.32-4 Core temperature and overall sensation during local cooling (11013)

5.5.1.3.2 Local heating in cold environment

The results shown in Figures 5.33-1 and 5.33-2 are from tests in which local heating was applied in cold environmental conditions. The chamber air temperature was approximately 20°C in these tests and the local heating air temperature was approximately 38 °C.

During application of local heating when the body is cold, the response is exactly opposite to that of local cooling when the body is warm. While the overall sensation increases, most of the core temperatures show a decrease. Before application of local heating the body employs vasoconstriction to maintain core temperature in the cold environment. When the body senses the application of heat, it relaxes its effort to maintain core temperature, and the core temperature begins to decrease.

In test 23089 (Figure 5.33-1), the core temperature lowered at the onset of face heating, increased for a few minutes and then decreased at chest cooling, and rose at the removal of the heating stimuli. The core temperatures dropped nearly 0.2°C upon the heating application. However, the core temperature responses to back warming and its removal are not clear. It looks almost opposite to what we would expect, rising at the warming and lowering at its removal. The author does not have an explanation for this.

In test 07084 (Figure 5.33-2), core temperature showed an obvious reduction (0.2°C) when warming was applied to the pelvis. The reduction (0.1°) during head warming is not clear because there is no obvious decrease shown. The reduction could have been a result of core fluctuation, which does occur. What is clear is that there is no increase in core temperature corresponding to head warming. Unlike the response of core temperature to hand cooling (Figure 5.32-1 and 5.32-4) where it showed an increase, during hand warming, the core temperature remained flat, with no increase and no decrease. It indicates that the core temperature responses to hand warming are not as strong as to hand cooling.

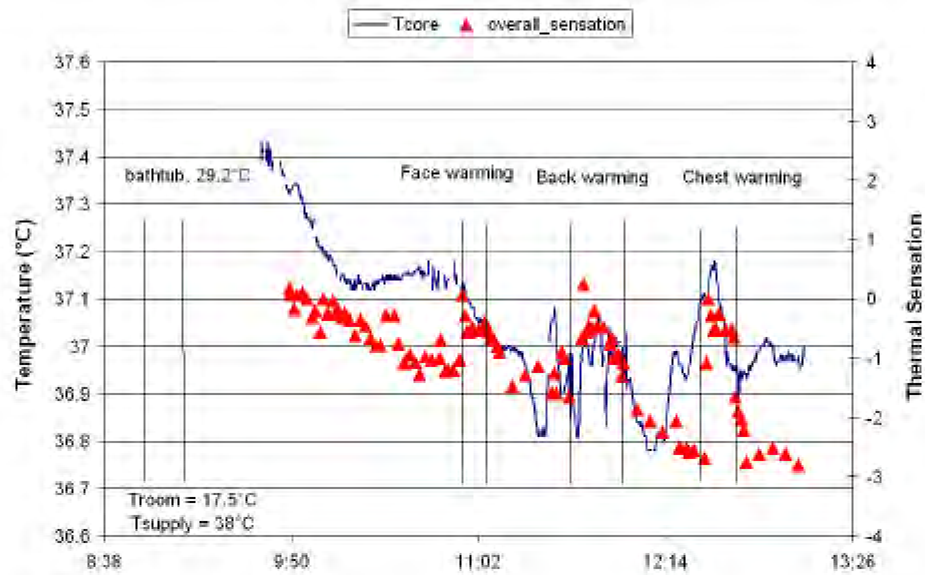

Figure 5.33-1 Core temperature and overall sensation during local warming (23089)

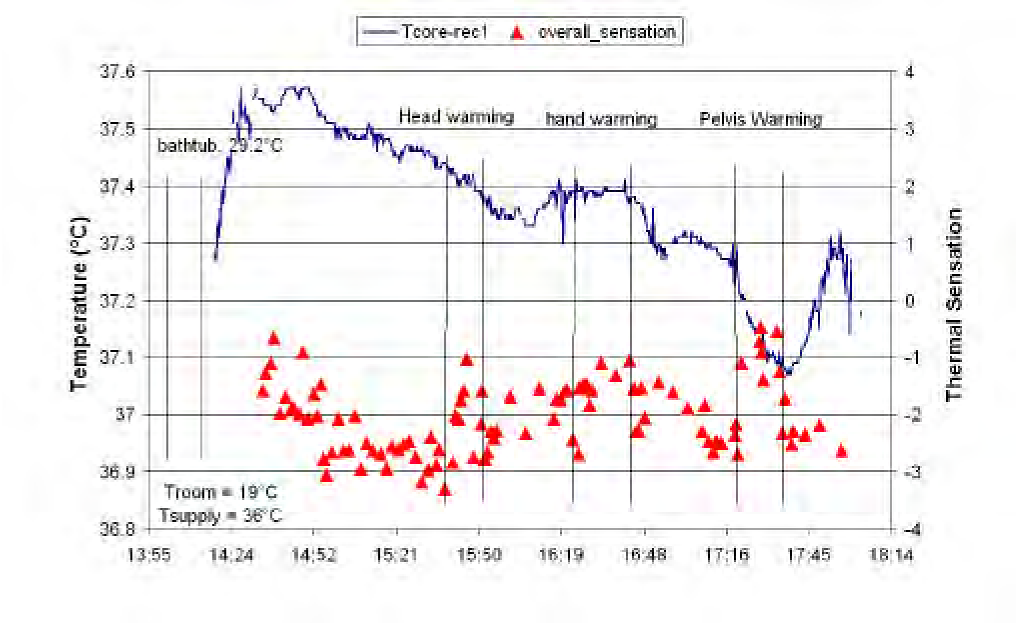

Figure 5.33-2 Core temperature and overall sensation during local warming (07086)

5.5.1.3.3 Local cooling in cold environment

We saw earlier that in a two-hour exposure to a cold environment (air temperature at 16°C), core temperature was maintained and even increased about 0.2°C (Figure 5.12 in section 5.2.2.3). The figures below show what happens to core temperature when local cooling is applied to the body in a cold environment.

The test whose results appear in Figure 5.34 last four hours. The chamber air temperature was 20.7 °C. The local supply air temperature was 14 °C.

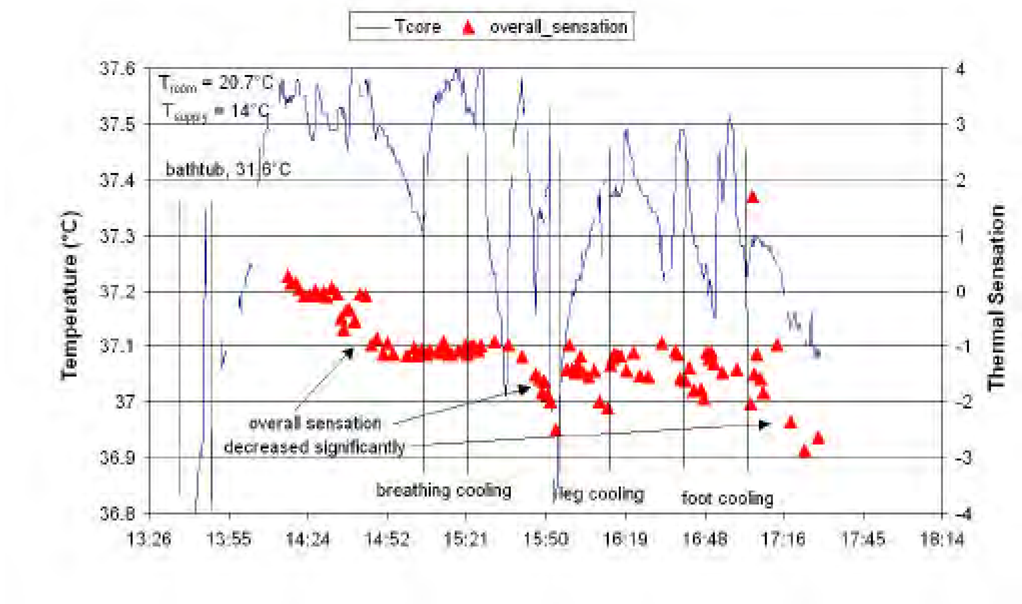

Figure 5.34 Core temperature and overall sensation during local cooling in a cold environment (23082)

The figure shows that the core temperature varied widely in an irregular fashion, changing by 0.8 °C during the test.

It is difficult to say whether the core temperature increased initially in response to local cooling because the core temperature in general fluctuated dramatically during the test. However, the three points at which overall sensation moved strongly downward all correspond to the times when the core temperature was also decreasing dramatically. This suggests that in a cold environment, the whole body feels cold when the core temperature decreases. This response is different from the core temperature decrease that occurs during body surface heating, which represents a "relaxation" of the body's effort to maintain core temperature in cold conditions.

5.5.1.4 Sensation voting behavior during transients

From the examples presented so far in this chapter, we know that people normally respond with initial jumps in sensation and comfort upon the application and the removal of a thermal stimulus. These jumps are due to the strong reaction of thermoreceptors to changes in their temperature. Without this sensitivity to dynamic changes, sensation would follow skin temperature, and produce a more gradual voting pattern. These sudden jumps will be quantified in the dynamic local sensation model (Chapter 6) by a coefficient applied to the derivative of the skin temperature.

After the initial jump, the votes sometimes change more, sometimes less. The main four types of voting behavior (quick overshooting, longer overshooting, flat pattern, and gradual pattern) observed in our tests are described in Figure 5.31 by three examples. (The sensation responses shown closely match the comfort responses).

The 'quick overshooting' response (Figure 5.35 A) shows a sharp change in sensation votes right at the step-change application (applying or removal of the thermal stimuli). The sharp sensation change can be 2 to 3 scale units and larger than the votes after the overshooting.

'Longer overshooting' responses to the thermal stimuli continue for 5 – 8 minutes and gradually reach a maximum before declining (Figure 5.35 B). The maximum or the minimum vote can be 1 to 2 scale units different from the stable votes.

In the 'flat pattern', the first vote upon the application of a thermal stimulus is the same as the rest of the votes (also shown in Figure 5.35 B), even as the skin temperature continuously changes.

In the ‘gradual pattern’, after an initial jump when a thermal stimulus is applied, the sensation votes continuously increase or decrease along with the changing skin temperature. They do not drop off later (Figure 5.35 C). This dynamic sensation response is less than that of the other three types of voting behavior.

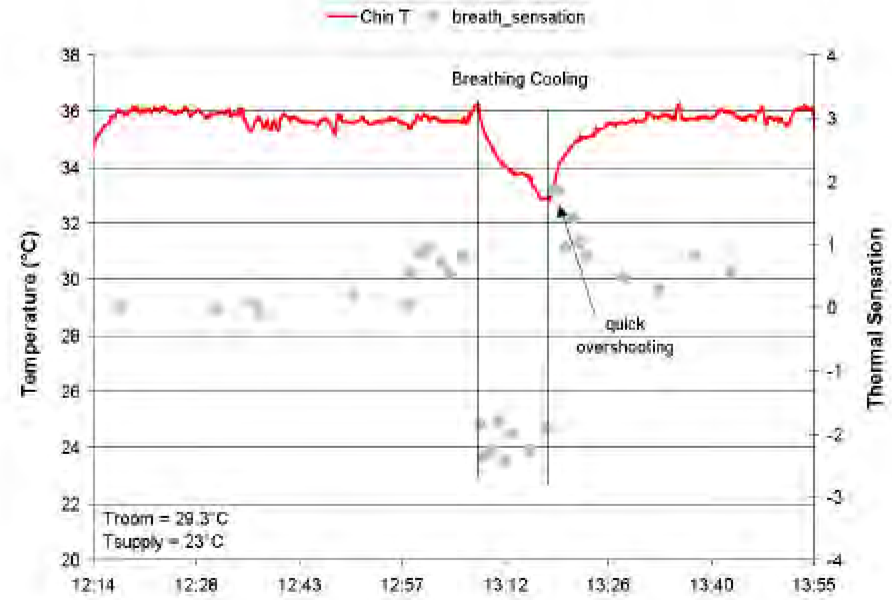

A. quick overshooting, breath cooling (21073)

Figure 5.35. Sensation voting behavior during transients (continued on next page)

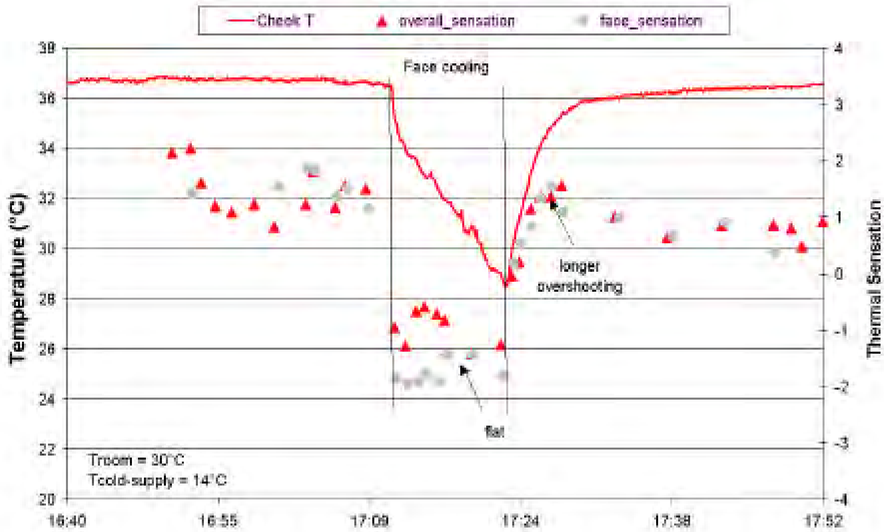

B. longer overshooting and flat pattern, face cooling (18043)

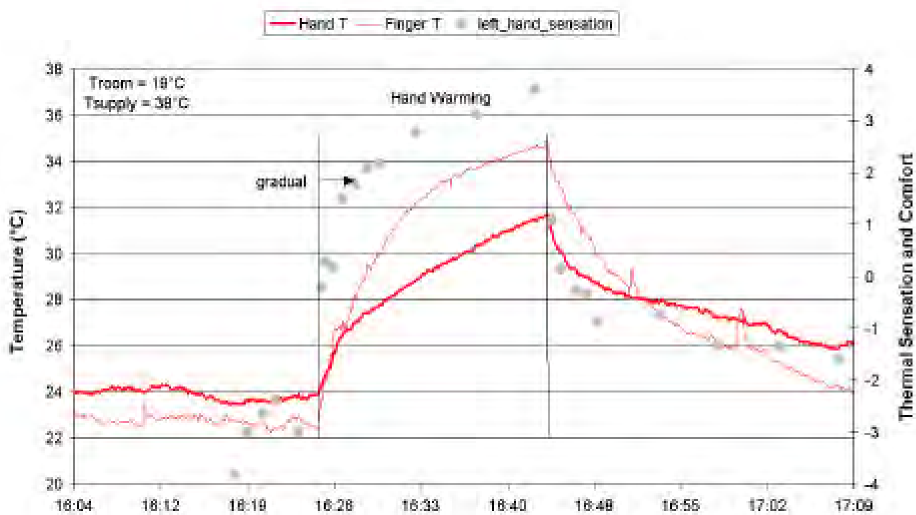

C. gradual pattern, hand warming (07086)

Figure 5.35. Sensation voting behavior during transients

Face sensation and comfort votes normally show a strong overshooting pattern. The face is very responsive to both cooling and its removal. The reason for this responsiveness might be that the thermal receptors in the face are usually directly exposed to the air and these receptors are "trained" to send strong signals in response to environmental change. However, the hand's thermoreceptors are also generally exposed to the air, and the hand sensation and comfort responses do not show a strong tendency to overshoot. The reason might be that the hand is the primary body part used for touch and holding things, so the hand's thermoreceptors might be accustomed to a wide range of thermal and comfort sensations, and the brain conditioned to minimize its reaction to these sensations.

Most of the responses during local heating exhibit the gradual pattern. The reason may be that during heating, only warm thermoreceptors are activated. Warm thermoreceptors are located deeper in the skin than cold thermoreceptors and therefore they may receive stimulation more slowly than the cold thermoreceptors that are nearer the surface of the skin. They are also more sparsely distributed in the skin, but it is not clear to us whether that would have an effect on the rate of sensation response.

Overshooting seems to be a personal variable. Some subjects exhibited overshooting in almost every response to local cooling. Other subjects did not exhibit any overshooting responses at all. Because overshooting is caused by the dynamic response of thermoreceptors, the variation among subjects might indicate that thermoreceptors are responding more actively to environmental changes for some people than for others. This variation might relate to subjects' age or the degree to which they are accustomed to being indoors or outdoors. We did not detect obvious relationships. This needs further study beyond this thesis.

5.5.1.5 Comfort vote overshooting during heat stress removal

Our subjects evaluated neutral environments as comfortable. ‘Neutral’ refers to the body thermal state when the thermal sensation vote is zero. As described in Chapter 4.4.2.4, we set up a slightly cool environment and provided heat lamps which subjects adjusted to make them feel neutral (sensation vote is zero). Under this neutral condition, our subjects’ comfort votes hardly ever went above 2 (Figure 5.3). However, during transients when applying local cooling to a warm body or a local heating to a cold body, or when removing these thermal stimuli, when the action is to remove the heat and cold stresses, the perceived comfort ratings are high, often above 3 (scale 2 is ‘comfortable’, scale 4 is ‘very comfortable’, refer to Figure 4.22). So it is heat stress removal that produces the more pleasant and comfortable feeling. We call this very comfort response as “Kuno effect”. It lasts several minutes. The overshoot in comfort votes is analogous to the overshoot in sensation votes. In the Chapter 2 (Background) and section 5.2.1.2, we saw that many researchers believe that the partial relief of discomfort is perceived as very comfortable (Cabanac 1979, Kuno 1995, McIntyre 1980, Mower 1976, Attia 1981, Attia 1984). Our test results, together with those in the literature, support the local thermal comfort model that we will describe in Chapter 6.

Here we show several examples of the Kuno effect. During our cooling tests, when the whole body was warm, applying strong local cooling (supply air temperature 14°C, high air flow rate) did not produce overshoot comfort votes. The local cooling was too cold for creating a very pleasant feeling. This overshoot pattern only happened in certain tests – heating when the whole body was cold, cooling with mild air temperature (23°C air supply) when the whole body was warm, removal of strong local cooling, and strong local cooling to breath and face.

Figure 5.36 shows the overshoot comfort votes after strong face cooling removal. As the strong cooling stress was removed, the comfort votes overshot, reaching ‘very comfortable’ (+4). The Kuno effect lasted for 4 minutes.

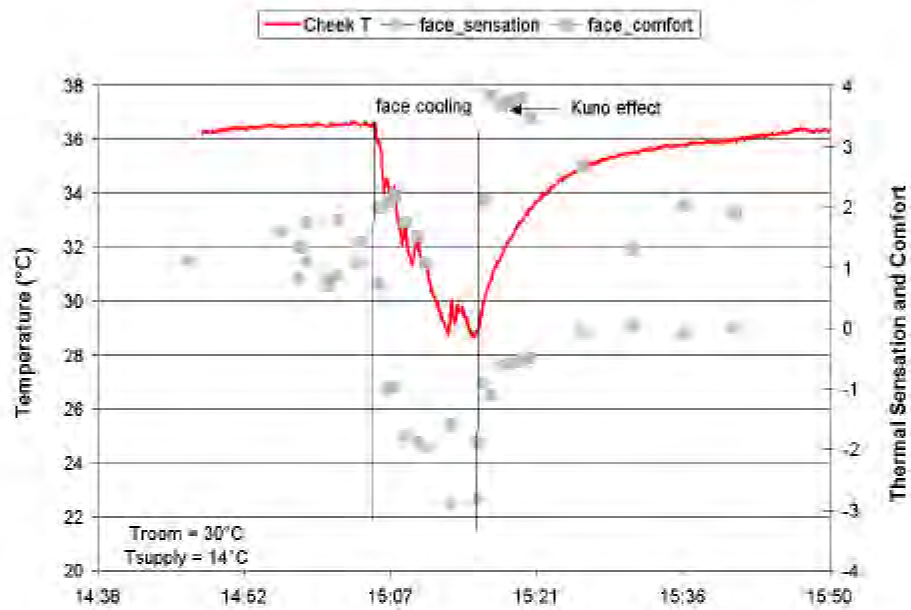

Figure 5.36 Kuno effect during strong face cooling removal (13037)

Next figure (Figure 5.37) shows that adding mild face cooling in a warm environment creates a ‘very comfortable’ feeling in both face and overall comfort. The ‘very comfortable’ feeling lasted about 3 minutes. Then it went back to a ‘comfortable’ level. Before adding the face cooling, the subject felt warm (overall sensation near 2).

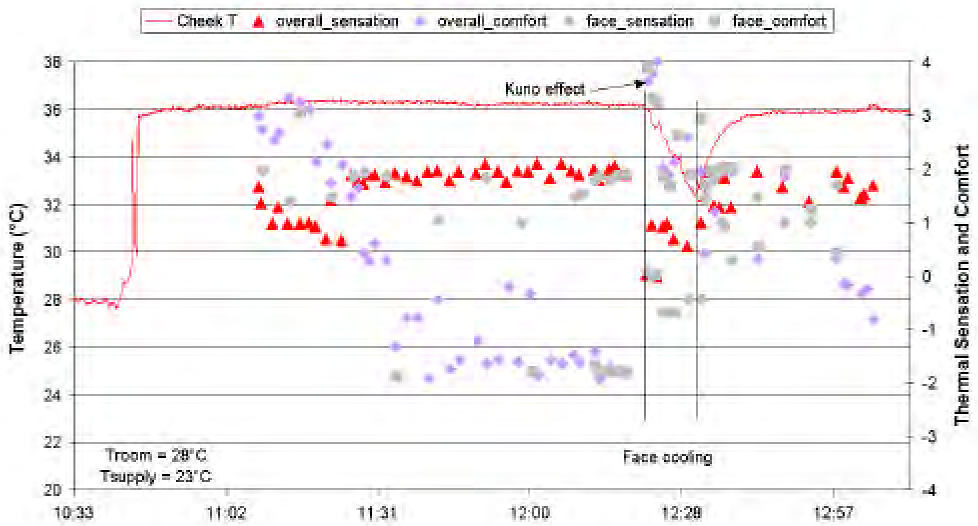

Figure 5.37 Kuno effect during mild face cooling (10063)

Unlike the example showing in Figure 5.37 which shows a 'very comfortable' vote resulting from applying mild face cooling, adding mild back cooling only produced one-minute's 'very comfort' feeling and then the comfort votes quickly dropped because the back is very sensitive to over cooling. When the mild back cooling was removed, the subject showed an overshoot (comfort votes reach to 4, Figure 5.38). This feeling lasted for 5 minutes. As the heat stress was taken away, the comfort level was lowered.

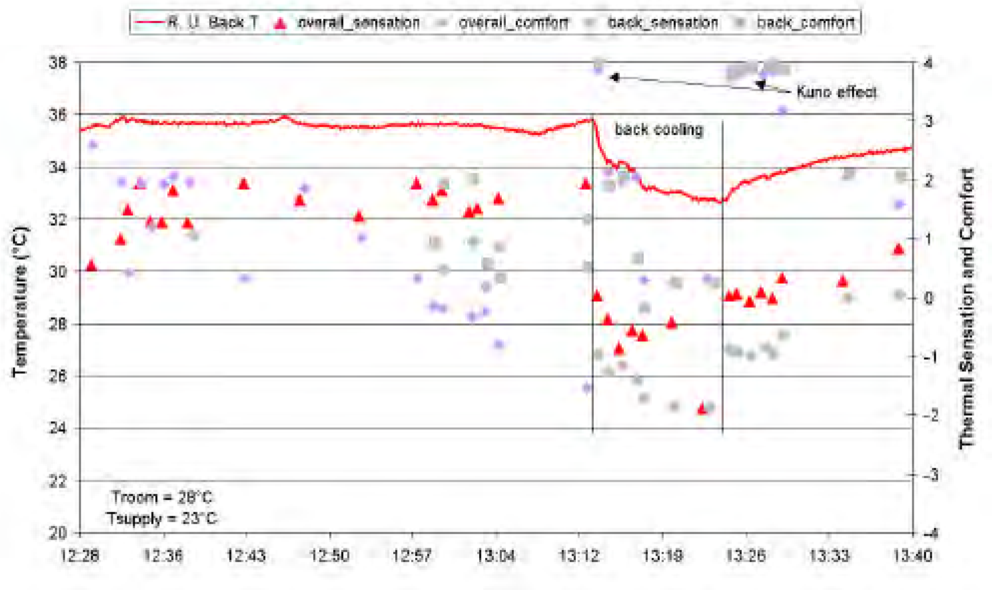

Figure 5.38 Kuno effect during mild back cooling removal (10063)

Figure 5.39 shows a Kuno effect during hand heating. The perceived comfort was 'very comfortable' at the application of the hand heating. It lasted 3 minutes after which the high supply air temperature (37°C) caused a 'very hot' sensation and discomfort.

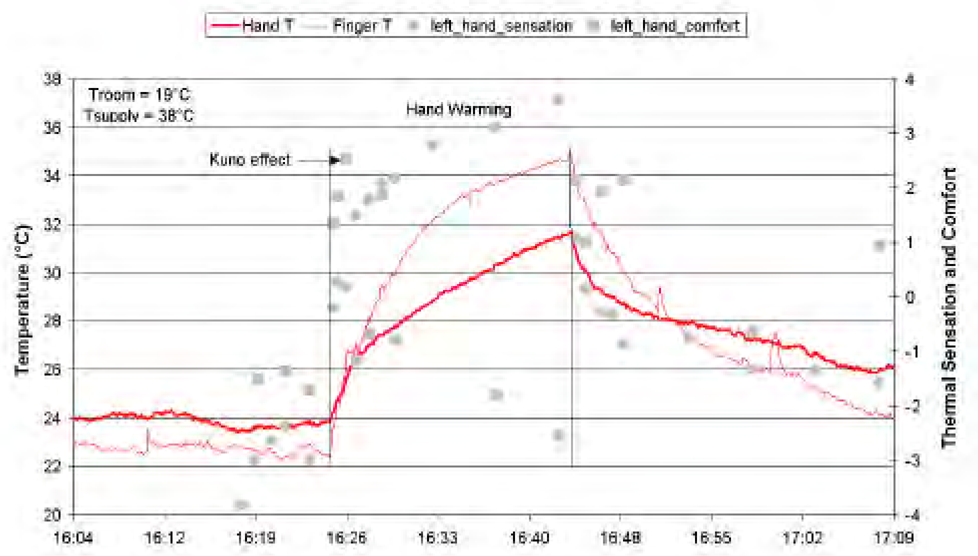

Figure 5.39 Kuno effect during hand heating (07086)

The above examples show that subjects feel very comfortable during thermal stress removal. In our tests, we did not have a way to maintain the thermal stress while applying the local cooling/heating, so the Kuno effect did not last long. As the local cooling/heating was continuously applied, the thermal stress was gradually removed, and the Kuno effect gradually disappeared.

5.5.2 Effects of cooling and heating multiple body parts

This section investigates how the body overall sensation and comfort respond to signals from multiple body parts. Understanding this is needed for modeling how combinations of body parts are perceived.

There is an unlimited number of combinations of body parts to which local cooling and heating could be applied. We selected combinations such as simultaneous cooling of chest and hand that correspond to asymmetrical conditions commonly experienced in the passenger compartment of a car, because the results of our study and our models will first be used to design air-conditioning systems in vehicles.

Because multiple body parts are cooled simultaneously in these tests, we used cooling air at a temperature of 23°C, which is not as cold as the temperature of the air used for cooling of single body parts (14°C). Because more body parts experienced the thermal stimulus, the response was expected to be strong even with mild cooling temperatures.

In general, the findings from cooling individual body parts also apply to the tests where multiple body parts are cooled. For example, the chest is dominant in determining overall sensation in both types of tests, and the neck is in the moderately influential group in both cases.

The examples of multiple-body-part cooling tests below highlight key results.

5.5.2.1 Chest cooling + hand cooling

Figure 5.40-1 shows the results of combined cooling of chest and hand. Although the hand skin temperature was 3°C lower than the chest skin temperature during cooling, the subject reported that the chest felt cooler than the hand . From having applied to single body parts, we knew that hand cooling does not have much effect on overall sensation, but that chest cooling virtually dictates overall sensation. In this case with simultaneous chest and hand cooling, we see again that overall sensation is also dictated by chest sensation. The results look almost as if there were no hand cooling at all.

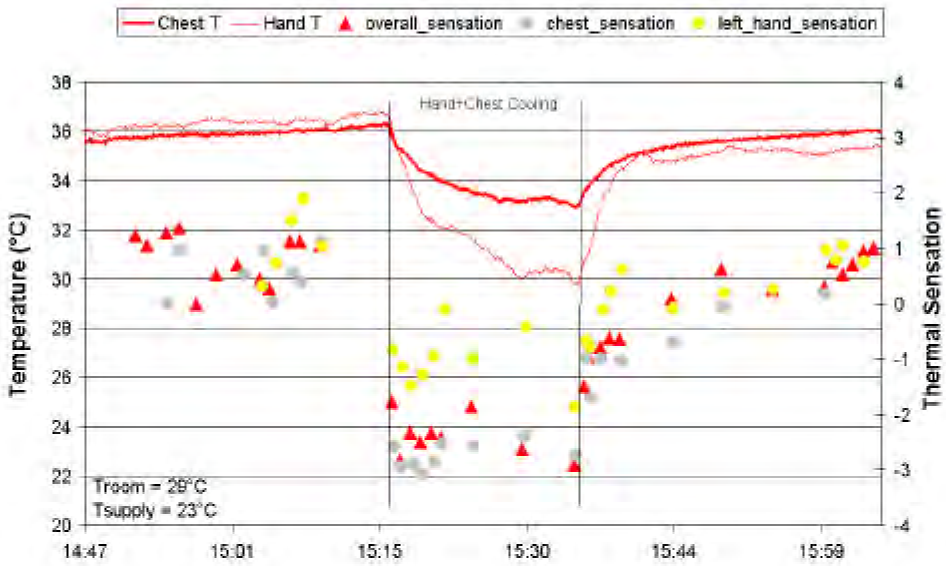

Figure 5.40-1 Local and overall thermal sensation during chest and hand cooling (19055)

Both the chest and overall *comfort* votes in Figure 5.40-2 decreased while hand comfort increased, confirming the earlier finding that experience of the hand has no impact on overall comfort.

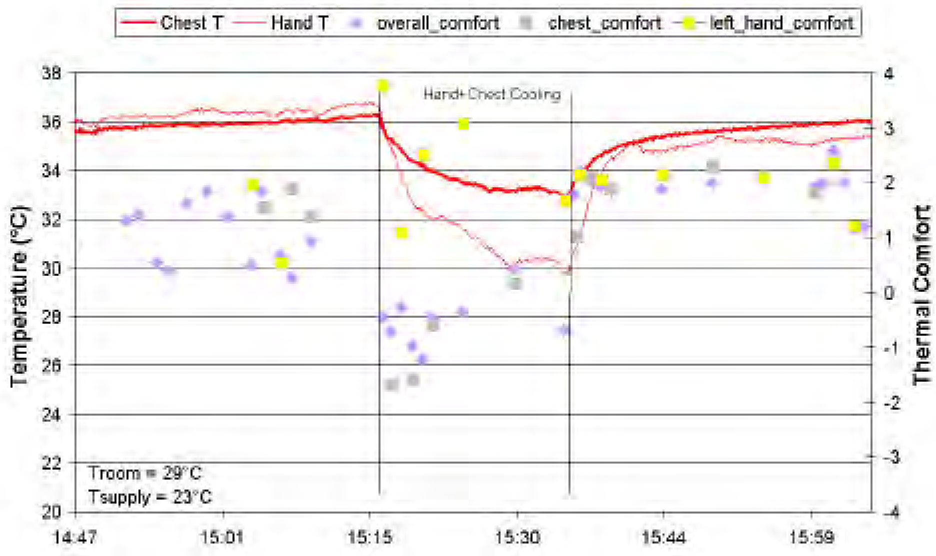

Figure 5.40-2 Local and overall comfort during chest and hand cooling (19055)

5.5.2.2 Neck cooling + foot cooling

When the neck and foot were cooled simultaneously, overall sensation remained different from both local sensations (Figure 5.41-1). Neither the neck nor the foot belong to the most influential/dominant group of body parts; even in combination, these two body parts do not sufficiently influence overall sensation to make it identical to local sensation.

Neck skin temperature recovered much faster than foot skin temperature. In fact, the foot did not return to its original pre-cooling level. Forehead skin temperature was not decreased by neck cooling.

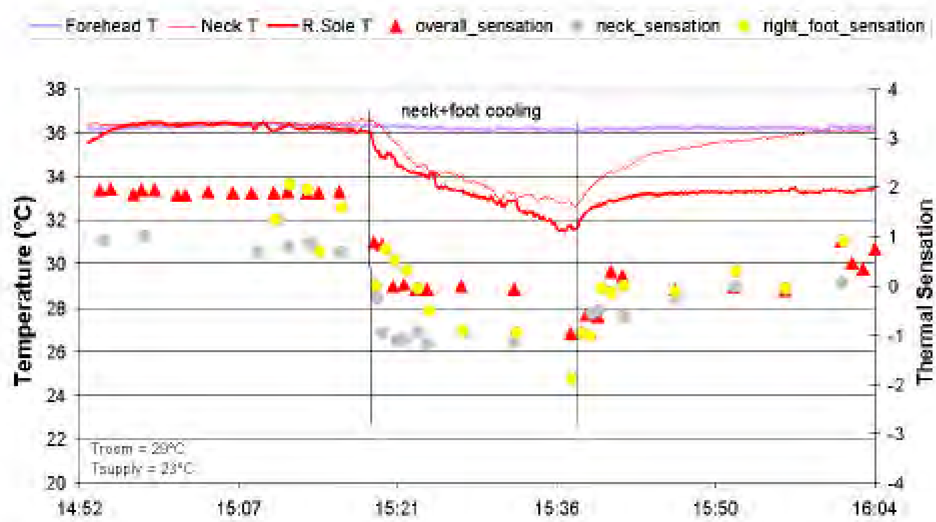

Figure 5.41-1 Local and overall thermal sensation during neck and foot cooling (13057)

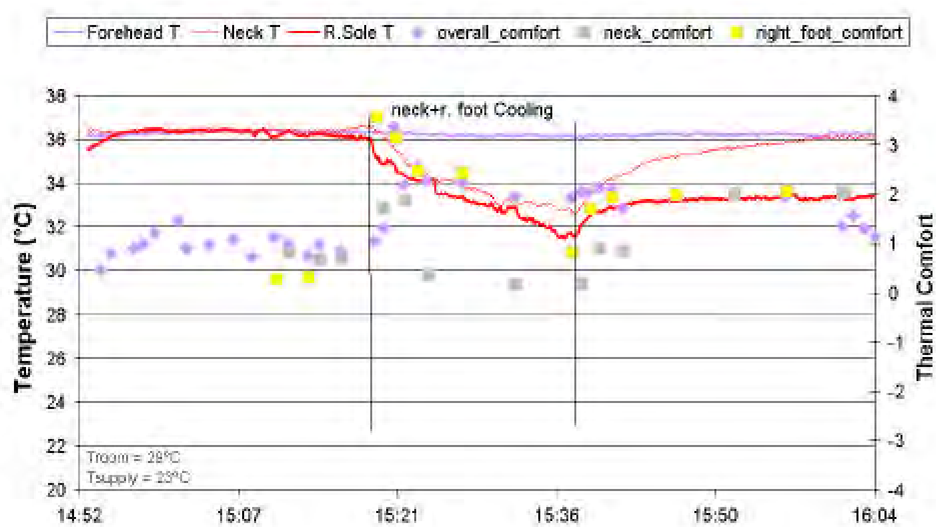

Figure 5.41-2 Local and overall comfort during neck and foot cooling (13057)

The comfort responses for this test are presented in Figure 5.41-2. It is interesting to see that in this case, where the temperature of the cooling air is milder than in the single-body-part tests, the initial overall and foot comfort votes were positive when cooling was applied. This is different from the reaction to strong local cooling. When strong local cooling (14°C supply air) had been applied, the local and the overall comfort mostly decreased.

In this test, neck comfort first increased and then decreased. The comfort votes for all three areas – foot, neck, and overall – exhibited overshooting responses during the cooling application, but not in the recovery process.

5.5.2.3 One-hand heating + one-hand cooling

In a warm test (room air temperature 30 °C), one hand was heated and one hand was cooled. The overall sensation was about slightly warm (+1) before application of heating and cooling. The left hand was heated (at 38 °C) and the right hand was cooled (20 °C) simultaneously. After 20 minutes, both stimuli were removed. An IR-image (Figure 5.42-1) shows the warm and the cold hands after the heating/cooling was removed. The following observations are made:

1. Derivatives of skin temperature on hand sensation

After 20 minutes of right hand cooling and left hand heating, the left hand temperature was much higher than the right hand temperature. When we removed the heating and cooling stimuli, the right hand felt warmer and left hand felt colder (Figure 5.42-2), even though the right hand skin temperature was lower than the left hand skin temperature (Figure 5.42-1 and Figure 5.42-2). We know that during transient conditions, both the skin temperature and its rate of change (derivative) contribute to thermal sensation. Upon removal of the right hand cooling and left hand heating, the right hand was experiencing a positive derivative and sent a positive signal while the left hand was experiencing a negative derivative and therefore send a negative signal. Because the local sensation can be sent to follow the derivative signals in transient conditions, we show that the dynamic signal is larger then the static signal (represented by the skin temperature) in transient conditions.

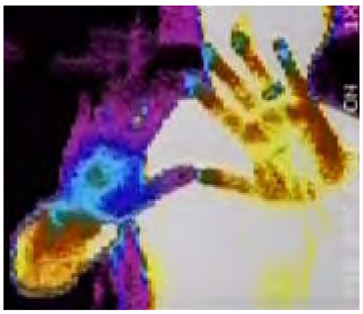

Figure 5.42-1 Skin temperatures of both hands after removing the local cooling and heating stimuli

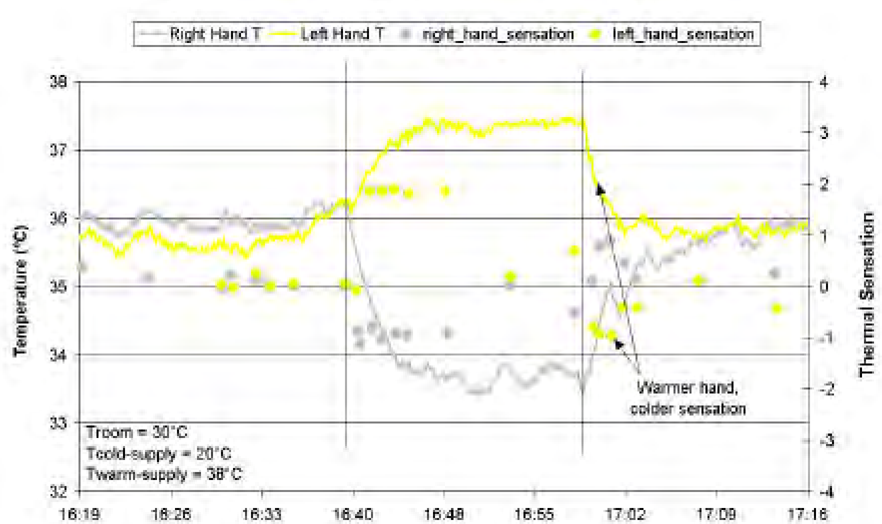

Figure 5.42-2 Left and right hand thermal sensation during right-hand cooling and left-hand heating (04098)

2. Possible thermal adaptation

It is possible that after the right hand had been cooled and the left hand heated, the right hand had adapted to a lower skin temperature and the left hand to a higher skin temperature. When both thermal stimuli were removed and both hands were exposed to the ambient temperature of the room, the hand that had adapted to a lower temperature (right hand) felt warmer, and the hand that had adapted to a higher temperature (left hand) felt cooler. This is exactly what John Locke observed in 1690 (described in the Introduction, Chapter 1) about hand sensations after putting them into buckets of different temperature water. More about thermal adaptation is presented in Appendix 6.1.

3. Overall sensation tracking the sensation of cooling

The overall sensation was warm (+1.9) before the application of hand heating and cooling. The heating made the left hand feel +1.9 scale units warmer, while the cooling made the right hand feel –1.1 scale units cooler. The overall sensation felt –0.8 scale units cooler. When the heating/cooling stimuli were removed, the cooling removal made the left hand feel +1.3 scale units warmer, while the heating removal made the left hand feel –1.6 scale units cooler. Again the overall sensation followed the cooling sensation, -0.5 scale units cooler.

Why does overall sensation seem to be following the cooling sensation? One possible reason is that the body is more sensitive to cooling than heating. Another possible explanation is the relative difference between local and overall sensations. During the entire test (as shown in Figure 5.42-3), the overall sensation was on the warm side. When cooling and heating were applied, the overall, left hand, right hand thermal sensations were 1.9, -0.9, 1.9. Not only was the cooling opposite to the slightly warm whole body sensation, but the difference was also larger (2.8) vs. the difference between the heated hand and the overall sensation (zero). Therefore, the body noticed more of the cooled hand. When the thermal stimuli are removed, the phenomenon is similar. The overall and the right hand sensations were close (around 0.7), but the left hand felt slightly cool, -0.8. The difference between overall and the left hand was larger, 1.5. So again the body part with the larger difference from the overall (or from the rest of the body) sensation influences the overall sensation more. This analysis supports the sun-burst shaped overall sensation model (described in Chapter 6).

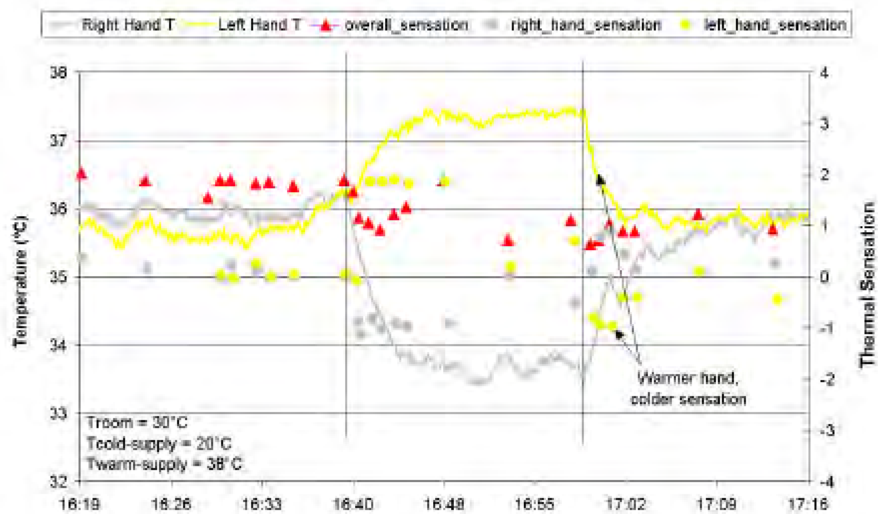

Figure 5.42-3 Overall, left, and right-hand thermal sensations during right-hand cooling and left-hand heating (04098)

4. Subject clearly distinguishes sensation and evaluates comfort

During this application of cooling and heating to the hands and their removal, the hand sensations were dramatically different. Because the overall body was warm, the feeling of cooling activated an enhanced sense of comfort for the hand being cooled. While the right hand was being cooled and the left was being heated, the comfort vote for the hand being cooled was higher than the vote for the hand being heated. When the heating and cooling stimuli were removed, the heated hand felt cooler and the cooled hand felt warmer because of the dynamic effect. In this situation also, the comfort vote for the cooler hand was higher than the one for the warmer hand. As the result, we see from Figure 5.42-4 that both hand comfort votes increased with a decrease in local sensation, even with dynamic involvement. This example demonstrates that the subject could clearly distinguish the sensations and comfort levels of the two hands.

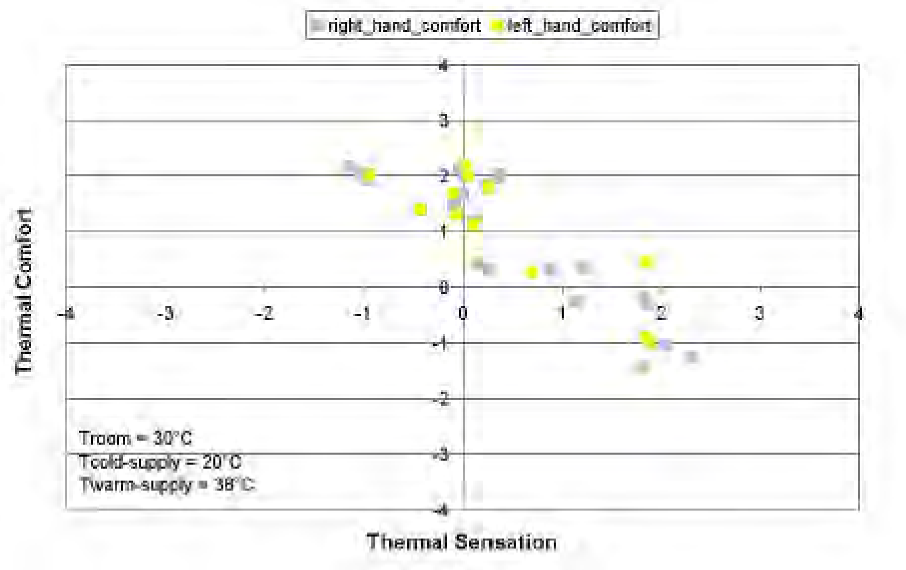

Figure 5.42-4 Local sensation and comfort during right hand cooling and left hand heating (04098)

5.5.2.4 Core temperature responses in multiple thermal application

This example describes the reaction of the body core temperature to multiple cooling and heating signals. In this example, both cooling and heating stimuli were applied; cooling stimulus was applied to face and chest and heating stimulus was applied to an arm. The core temperature responded with an increase (Figure 5.43) that was similar to the core temperature response to cooling a single body part (Figure 5.32-1 to 5.32-4). During one multiple application, the core temperature increased nearly 0.3°C. During another multiple application, the core temperature increased almost 0.2°C. It is not clear whether this core temperature response was a result of more body parts experiencing cooling than heating or because humans have more protective functions for cold than for warmth.

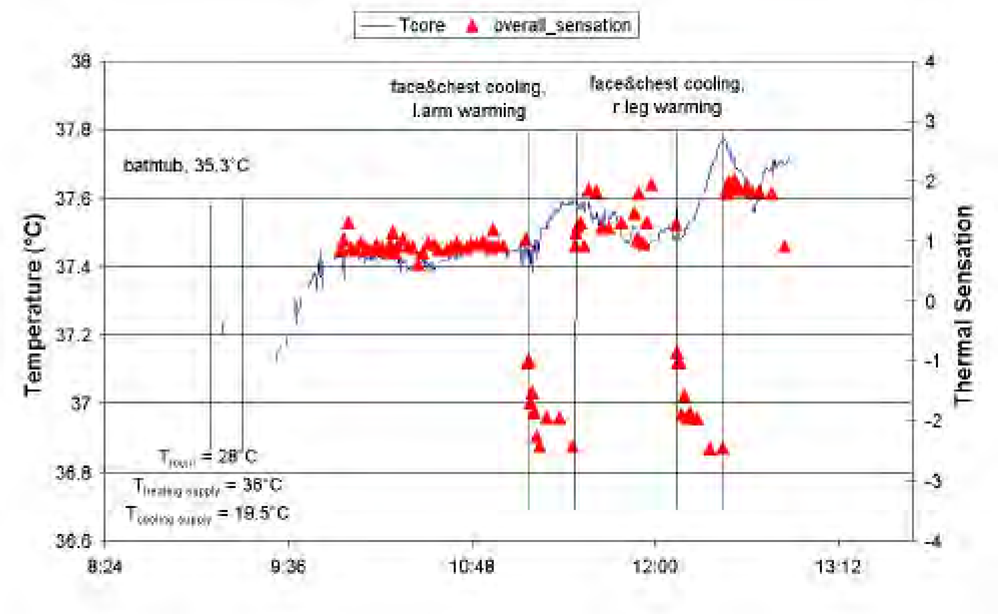

Figure 5.43 Core and overall thermal sensation during a multiple cooling/heating test (21095)

Summarizing what we have seen from the above examples about multiple-body-part cooling and heating, we conclude that what we found for the single-body-part cooling/heating (such as the three groups with differing level of influence, the core temperature responses, sensation and comfort responses to skin temperature and its derivatives) remain the same.

5.5.3 Repeatability of sensation and comfort votes

We performed tests to verify the repeatability of sensation and comfort votes in our study. These tests involved application of local cooling to the same subject under the same conditions. We found that the votes in the two tests match very closely. One example is described below for illustrative purposes.

A single subject participated in both tests 13037 and 13044. The two tests were basically the same, with local cooling applied to the face, back, and chest in a warm environment. The results show that the subject's thermal sensation and comfort vote patterns were consistent. Because the room temperature in one test was 0.8 °C higher than in the other, the actual values of the votes were slightly different, but the differences were small.

Figure 5.44 shows the votes for the two tests side by side. The comparisons include overall sensation and comfort as well as local sensations.

Test 13037	Test 13044
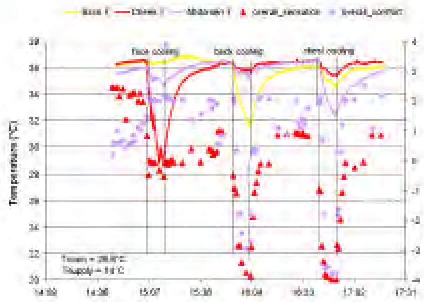 overall sensation and comfort, entire test	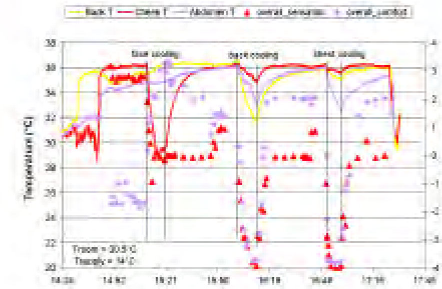 overall sensation and comfort, entire test
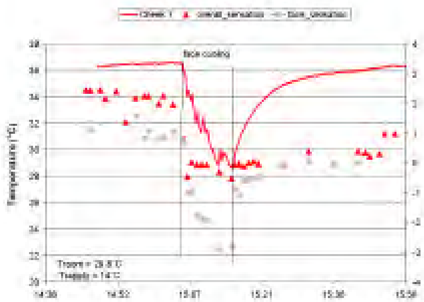 face and overall sensations, face cooling	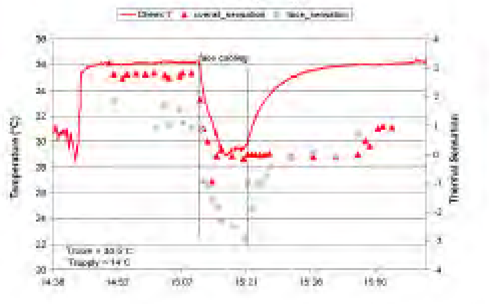 face and overall sensations, face cooling
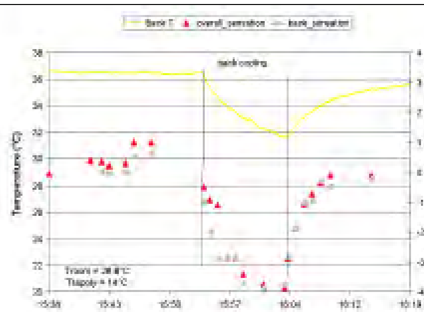 back and overall sensation, back cooling	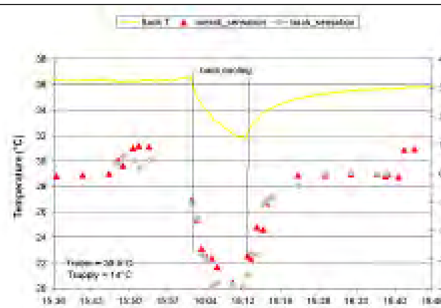 back and overall sensation, back cooling

Figure 5.44 Local and overall sensations and comfort vote repeatability comparison (continued on next page)

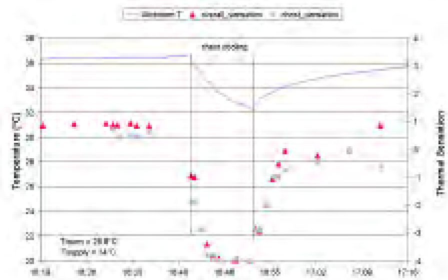

chest and overall sensation, chest cooling

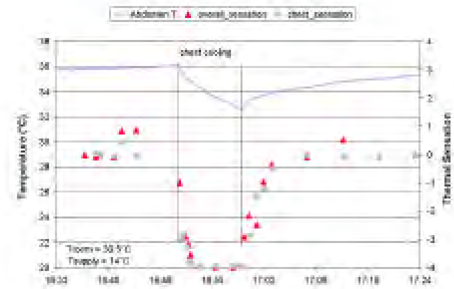

chest and overall sensation, chest cooling

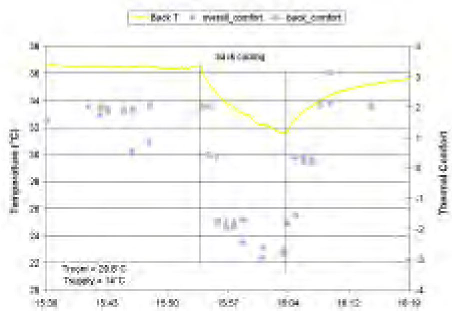

back and overall comfort, back cooling

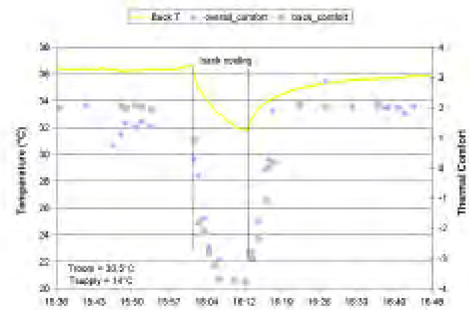

back and overall comfort, back cooling

Figure 5.44 Local and overall sensations and comfort vote repeatability comparison

5.5.4 Changing the order of body parts undergoing local cooling

During each test we normally applied cooling to three body parts. We investigated whether the order in which body parts were cooled affected subjects' thermal sensation and comfort votes. We found that the order did not affect subjects' votes.

5.5.5 Cooling one hand or foot does not affect the other hand or foot

We also investigated whether cooling or heating of one hand or foot influenced the other hand or foot. Do subjects compare the sensations of their two hands and feet when they evaluate the sensation of one hand or foot? If they do assess sensation comparatively, we hypothesize that heating or cooling of one hand or foot would make the other feel cooler or warmer, respectively.

We found that people do not compare sensations between hands or between feet. The following test results support this conclusion.

Figure 5.45 shows the sensation of the left foot during cooling of the right foot. The cooling effect was strong as evidenced by the decrease of 6 °C in skin temperature. Sensation in the right foot changed from 1 (slightly warm) to –3 (cold) as a result of cooling. Sensation in the left foot sensation showed no change.

Figure 5.45 Left and right foot sensations during right-foot cooling (04002)

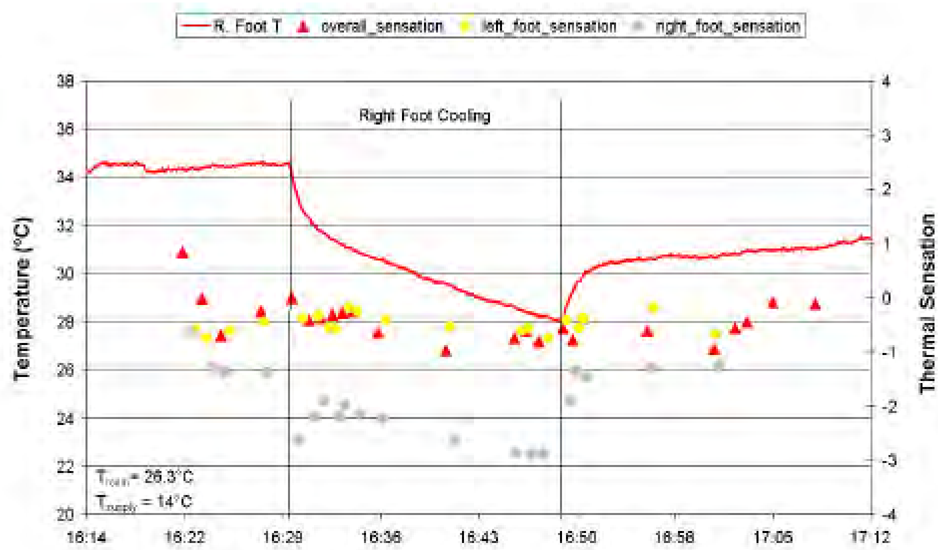

Figure 5.46 shows the right hand sensation during cooling of the left hand. Left hand sensation changed from hot (3) to between slightly cool and cool (–1.5). The right hand sensation showed little change.

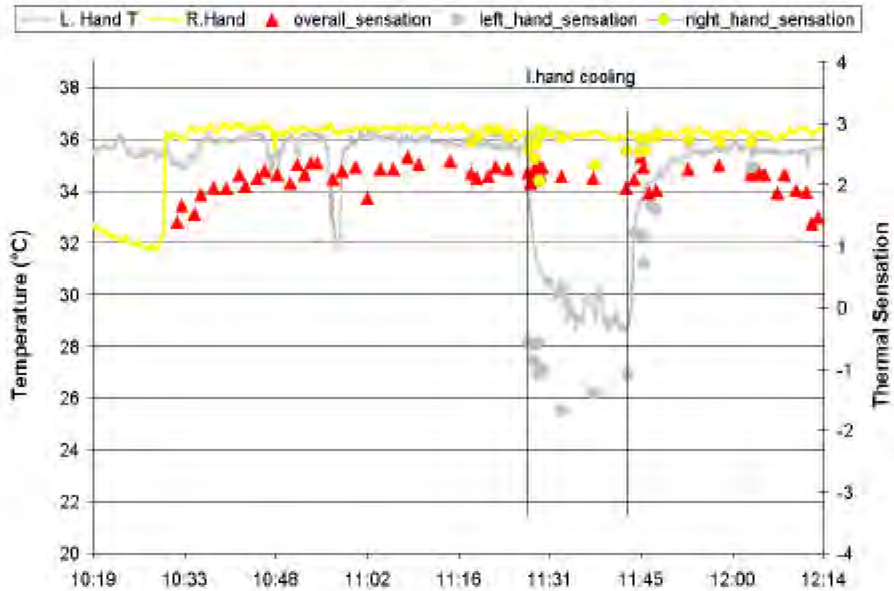

Figure 5.46 Left and right hand sensations during left-hand cooling (23108)

The figure also shows the right hand skin temperature to determine whether, when one hand is cooled, the other experiences vasoconstriction. Because we see that the right hand skin temperature was not influenced by cooling of the left hand, we know that the blood vessels did not constrict in the hand that was not being cooled. When one hand was experiencing cooling, it constricted, but the other hand was not influenced at all.

The left hand cooling test result (18066) is shown in two figures. Figure 5.47-1 shows that the right-hand skin temperature and sensation were unchanged, and Figure 5.47-2 shows that the right-hand comfort was unchanged as the left hand was cooled.

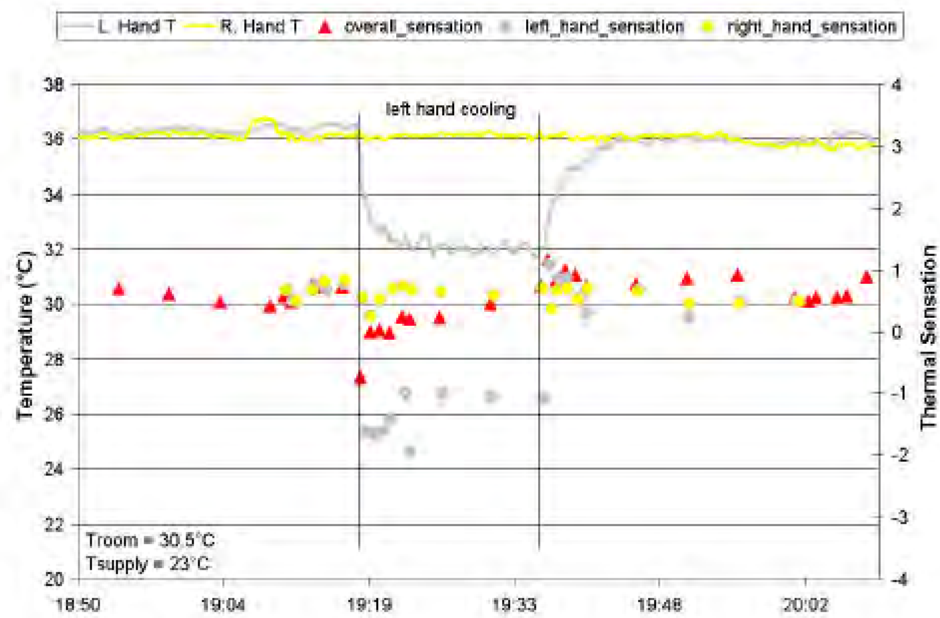

Figure 5.47-1 Left and right hand sensations during left-hand cooling (18066)

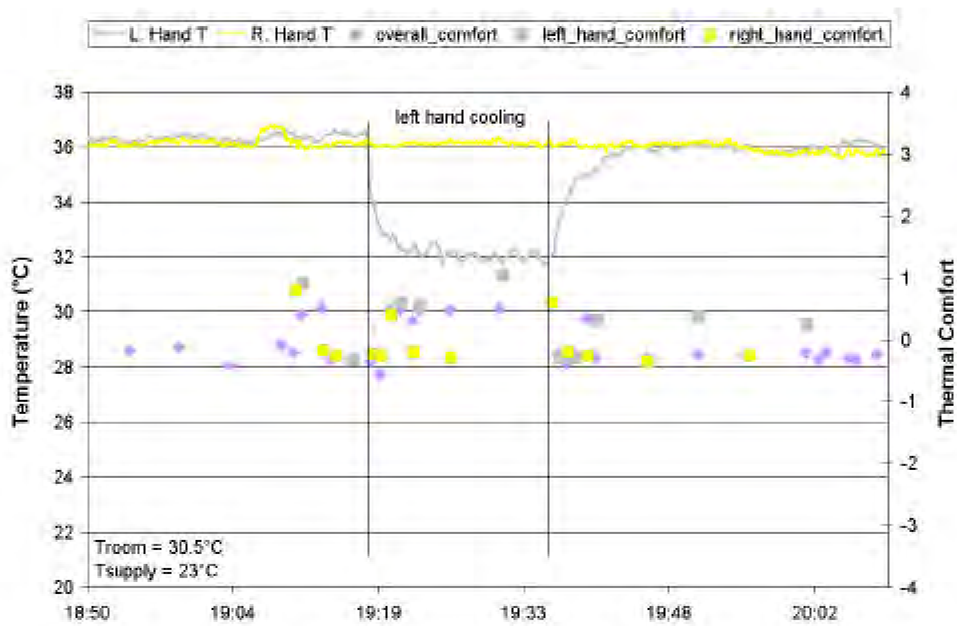

Figure 5.47-2 Left and right hand comfort during left hand cooling (18066)

Finally, we investigated the influence of cooling one arm on the other arm (04072) and found the same results: skin temperature, sensation, and comfort were unaffected in the arm that was not cooled.

5.6 Transient/uniform environments (whole-body step-change tests)

This section examines skin and core temperature changes in relation to sensation and comfort votes during tests in which the whole body moved from one environment to a different one.

5.6.1 Skin temperature, sensation, and comfort

The changes of skin temperature with time are shown by a series of IR skin temperature images taken during one of the step-change tests (04104). In this test, the subject made two moves, one from warm to slightly cool environment (we call it 'down-step', Figure 5.48), one from slightly cool to warm environment ('up-step', Figure 5.49). In color, these images show that after the down-step move, the body skin temperature quickly decreased, especially the hand and the lower arm. After 20 minutes, the head was the warmest. At the end of this down-step move, the hand and fingers were the coldest, while neck was warmest. The second warmest place was the forehead.

After the up-step move, the head skin temperature quickly recovered, followed by the shoulders, then the lower arm and the hands. At the end of this second move, the upper body skin temperature basically recovered, but not the lower extremities.

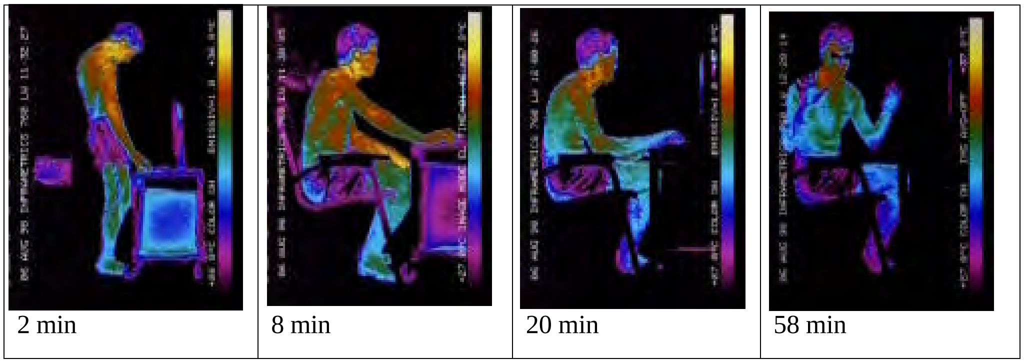

Figure 5.48 Skin temperature changes in (warm to slightly cool) step-change (04104)

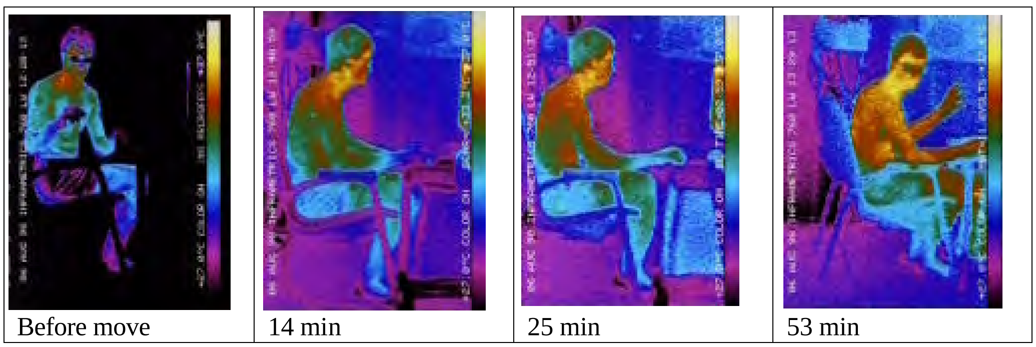

Figure 5.49 Skin temperature changes in (slightly cool to warm) step-change (04104)

Figure 5.50 shows the values of the skin temperatures for a few body parts during the entire test. This figure also shows that after the up-step move, most of the upper body skin temperature recovered, except shin and foot skin temperature. The shin temperature was about 1°C lower, and the foot 5°C lower, than the values from before the first down-step move. The time marks are located in the figure corresponding to the IR-images time series. The gap in voting near the end of the first period in the 30°C environment occurred when detailed IR-images were being taken.

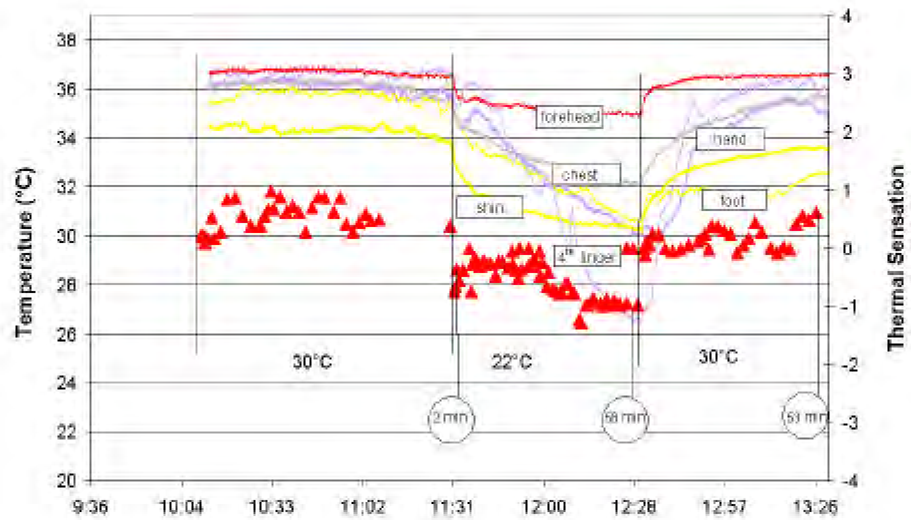

Figure 5.50 Skin temperature, sensation in step-change test (04104)

Although the skin temperatures kept changing after the down-step and the up-step moves, basically the overall sensation votes (triangles) did not change much within either environment. That means the dynamic response of the thermoreceptors was strong enough to make the first vote similar to the last votes, even though the skin temperatures were very different at these times. The figure shows a small overshooting right after the down-step move. There is no overshooting shown for the up-step move. These responses are very similar to the results from de Dear's step-change study (de Dear, Ring et al. 1993), where the authors found the overshooting in the down-step change, but not in the up-step change. Nagano (Nagano et al., 2002) did step-change tests from hot to neutral environments (34 and 37 °C to 25 and 28 °C), and reported that the subjects felt much cooler just as they stepped to the lower air temperature environment, then returned to a warmer level.

There was an abrupt decrease in sensation 30 minutes after the down-step move to the slightly cool environment. At this time, the sensation votes decreased for 15 minutes from neutral (0) to slight cool (-1). After that, the votes were stable. About the time when the sensation started to decrease, the 4th finger temperature also began to decrease rapidly. It may indicate that finger temperature is sensitive in responding whole body thermal state. When the body is cold, it constricts the blood vessels. Fingers are at the end of extremities and they reflect the vasoconstriction more obvious than other body parts.

During the whole body step-change, overall sensation and comfort correlate very well. Here we show two examples (Figure 5.51). In the example test 04104, during the period when the sensation was decreasing from neutral towards slightly cool, the overall comfort level was also lowered accordingly, from 'comfortable' (2) to 'just uncomfortable' (-0). The clear correspondence between overall sensation and comfort is also shown in example 17107. Moving from the hot environment (34.3°C) to the neutral environment (26.3°C), the overall sensation showed an overshooting towards neutral sensation, as did the overall comfort – an overshooting towards a higher comfort level. The variation seen in the comfort votes in the first period of test 04104 may be due to transient effects caused by putting on the thermocouple harness and leotard.

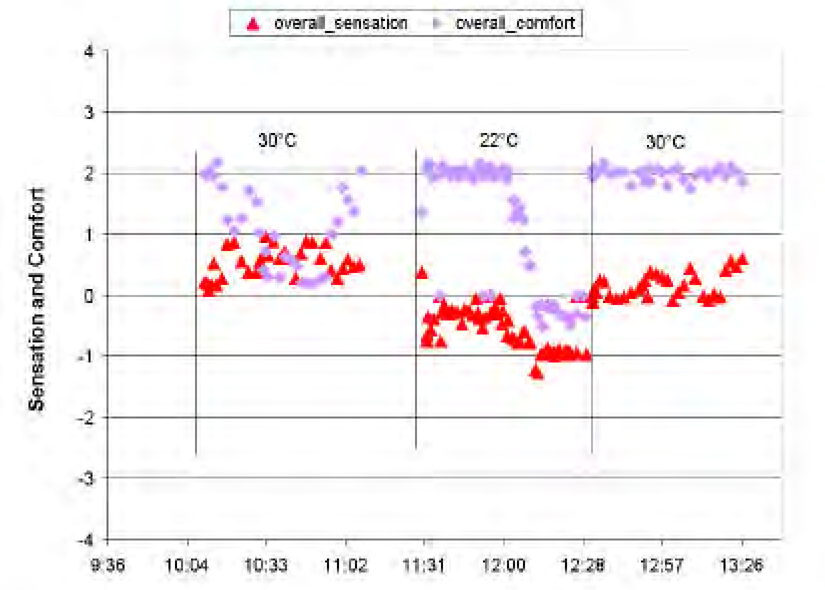

Test 04104

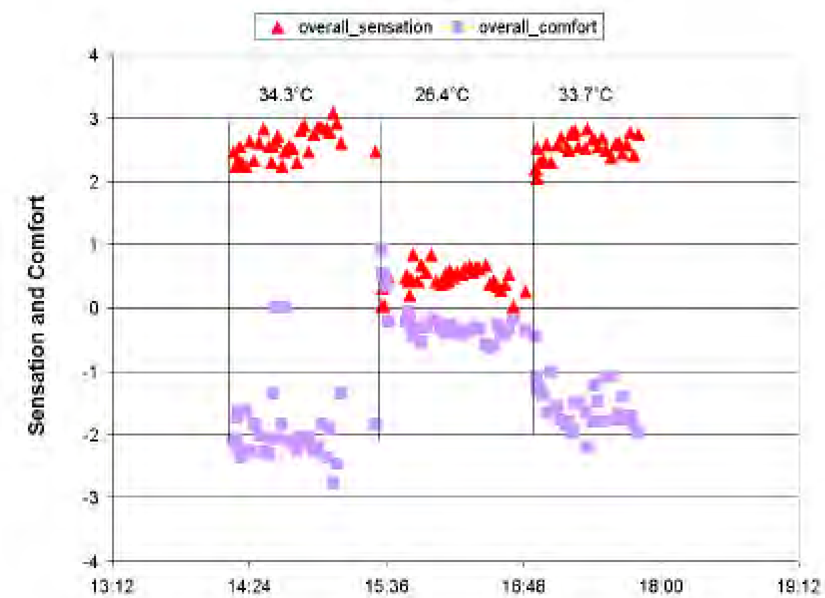

Test 17107

Figure 5.51 Sensation and comfort in step-change tests (04104, 17107)

5.6.2 Core temperature responses in whole body step-change processes

In general the core temperature during whole body step-change tests reacts similarly to that of local cooling/heating applications: increasing when stepping down to a slightly cooler environment, and decreasing when stepping up to a warm environment. The speed of increase and decrease is not as great as for local cooling/heating tests, because the air temperatures of the two environments in the whole body step-change tests were much milder than the supply air temperature in the local cooling/heating tests. Here we show one example (Figure 5.52): the core temperature stopped decreasing after the subject moved to a slightly cool environment (22°C), and decreased again after the subject moved back to the warm environment (31°C).

The core temperature decrease that occurred in the first period, before the down-step, happened in almost all the tests. It is caused by reduced metabolism after the subject sits in the chair and starts to vote. It is not a reaction to the environment change.

Figure 5.52 Core temperature responses in a step-change test (16109)

5.7 Additional physiological and subjective observations

The information provided in this section did not directly contribute to the subsequent model development in Chapter 6. I include it in this thesis because it helps explaining skin temperature responses in various environments, and may have potential value on human thermal physiology modeling and heat loss analysis.

5.7.1 Hand and finger temperatures

In neutral and warm environments, the differences in skin and finger temperatures between the left and right hands are small. However, when the environment is cold, the left hand, and especially the left fingers, have much higher skin temperatures than the right hand and fingers. One possible reason is that when people are cold, the blood vessels of the hand are quite constricted, and hand skin temperature is very low. Movement of the hand in these circumstances promotes blood circulation and therefore increases skin temperature significantly. In our tests, subjects accessed the internet on a computer, an activity similar to sedentary work in a normal office. The right hand was used primarily for holding and clicking the computer mouse, a very immobile activity. The left hand was much freer, with more finger motion. So the left hand and finger skin temperatures were higher.

The subsection below illustrates the impact of hand motion on hand and finger skin temperatures.

5.7.1.1 Hand and finger skin temperatures in stable environment

This section will present the hand and finger skin temperatures in neutral, cold, and warm stable environments.

Table 5.9-1 lists the skin temperatures of the left and right hands and fingers in a cold environment.

Table 5.9-1 Hand and finger temperatures
in cold environment, 15.7 °C (Test 21083)

Body part	Skin temperature (°C)
left hand	23.1
right hand	23.3
left palm	24.6
right palm	24.4
left 4th finger	21.1
right 4th finger	17.8
left 2nd finger	20.3

Table 5.9-1 shows that the left 4th finger temperature is more than 3°C warmer than the temperature of the right 4th finger. The right hand is restricted by the posture of clicking a computer mouse, while the left hand is free and involves more digital activity using the computer key board. The hand motion test results shown in Figure 5-53 indicate that even very slow movement of the hand can increase skin temperature about 1.5 °C. Finger temperature is very sensitive to motion, especially in a cold environment.

The left fingers are warmer than the right fingers in most of our other cold-environment tests as well. Table 5.9-2 shows another example, for a test in which the room temperature is 19 °C, warmer than in the test shown in Table 5.9-1. The difference between left and right 4th fingers is about 2 °C.

Table 5.9-2 Hand and finger temperatures
in cold environment, 19 °C (Test 23099)

Body part	Skin temperature (°C)
left hand	24.6
right hand	24.1
left palm	26.3
right palm	24.1
left 4th finger	21.1
right 4th finger	19.3

In tests conducted under warm conditions, left and right finger temperatures are close (Table 5.9-3), with the left finger temperatures slightly higher. In warm and hot environments, the blood vessels of both hands are well dilated, so finger motion does not cause much difference in the skin temperature.

Table 5.9-3 Hand and finger temperatures
in warm (30°C) environment (Test 04104)

Body part	Skin temperature (°C)
left hand	36.02
right hand	36.05
left palm	36.7
right palm	36.6
left 4th finger	36.4
right 4th finger	36.2

Table 5.9-4 shows an example of a test conducted under neutral conditions. The hand and finger temperature differences between left and right are small, 0.5 °C and 0.7 °C, respectively. Although the differences are small, they are slightly larger than the differences observed in warm environments.

Table 5.9-4 Hand and finger temperatures
in neutral environment (Test 07075)

Body part	Skin temperature (°C)
left hand	34.08
right hand	33.6
left palm	34.3
right palm	35.4
left 4^{th} finger	35.4
right 4^{th} finger	34.7

5.7.1.2 Hand motion increases hand and finger temperatures

The test shown in Figure 5.53 was specifically designed to investigate the influence of hand motion on hand skin and finger temperature. For this test, the subject was seated in a room with air temperature at 18.4°C. Skin temperature was measured for the 2^{nd} and 4^{th} fingers, the palm, and the back of both hands. An equal volume of cold air (14°C) was applied to both of the subject's hands. After 30 minutes, when both hands felt cold, the left hand began a very slow motion, opening and closing over a two-second cycle. The hand movement in this test was very gentle, and the closed position of the hand was very loose so that nothing was touching the thermocouple on the palm of the moving hand. Twenty minutes later, the left hand stopped moving, and the right hand began the same slow movement, continuing for 20 minutes and then stopping. The left hand then repeated the same motion again for 10 minutes until the end of the test.

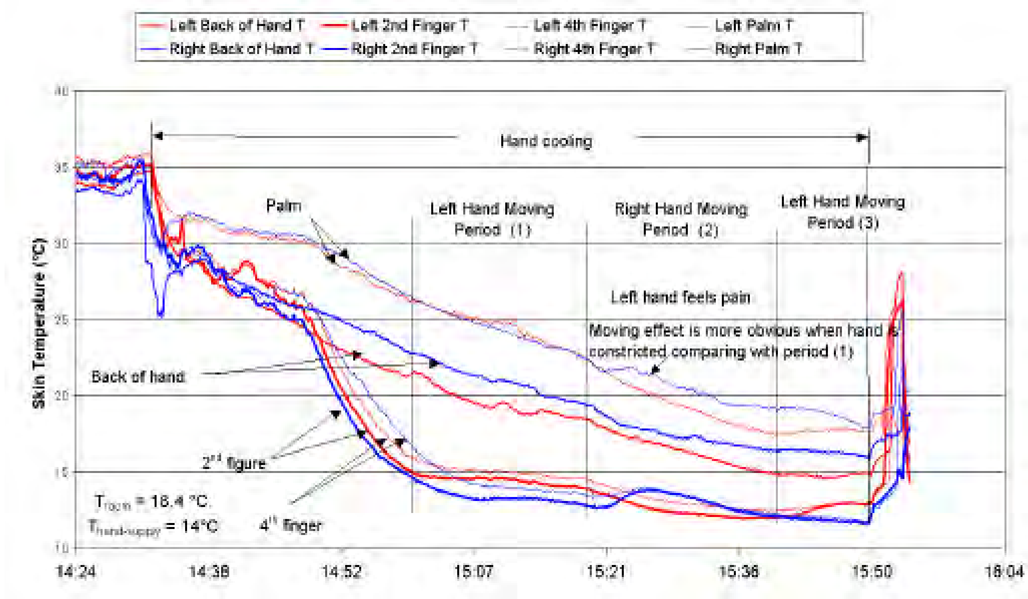

Figure 5.53 Hand skin temperatures in slow motion during hand cooling

We observe:

(1). While the hands were being cooled, the palms were the warmest, and the fingers the coldest. The temperatures of the backs of the hands were between those of the palms and fingers. The temperature difference between the palm and the finger was as great as 12°C at times.

(2). During period 1 when the left hand was moving, the temperature of the left hand 2nd finger stopped decreasing after two minutes of movement, but the 4th finger temperature stopped decreasing almost immediately. The finger temperature differences between the two hands were very small before the left hand began moving. After the left hand finished its first period of movement, the difference between the left and right hand fingers reached 1.1 °C.

(3). During period 2, the left hand ceased moving and the right hand began moving; left hand finger temperatures immediately started to decrease at this point, and the right hand finger temperatures started to increase. The right hand was strongly vasoconstricted when it began moving, and the slow movement greatly increased its finger temperatures; we see an a greater rise in the beginning of period 2 than occurred in period 1. A similar pattern is seen for palm temperatures; the right hand palm showed an increase during period 2 when the right hand began moving, but the left hand palm temperature did not increase during period 1 when the left hand was moving. The left hand was not as cold when it began moving in period 1 as was the right hand when it began moving in period 2.

(4). The increase in period 3, when the left hand started its slow motion again and the right hand stopped moving, are more similar to those from period 2 than from period 1; the temperatures of the left hand fingers and palms began to increase.

(5). Hand movement did not influence skin temperature on the back of the hand. There is very little muscle on the back of the hand, and the blood that causes the increase in finger and palm skin temperatures is presumably sent to the working muscles in the fingers and palms.

5.7.2 Hand skin temperature recovery speed after local cooling

Hand skin temperature recovery speed

Hand skin temperature recovery speed strongly depends on the whole-body thermal state. When the whole body is warm, blood is actively pumped into a cold hand in order to release heat from the hand. After the cooling is removed, the hand skin temperature quickly recovers to its original before-cooling. When the whole body is cool, blood is not so actively pumped to the hand, so hand skin temperature recovers slowly.

This phenomenon is demonstrated in Figure 5.54. The skin temperature changes are presented for several body parts normalized form. The thick gray line represents the hand skin temperature recovery process when the body is warm. The room air temperature was at 31.5°C, and the subject's overall sensation was between warm (+2) and hot (+3). The supply cooling air was 18°C. The thin gray line represent for a nearly neutral body. The room air temperature was 25°C. The subject's overall sensation was near neutral (0). The supply cooling air was 23 °C, not as cold as the previous condition.

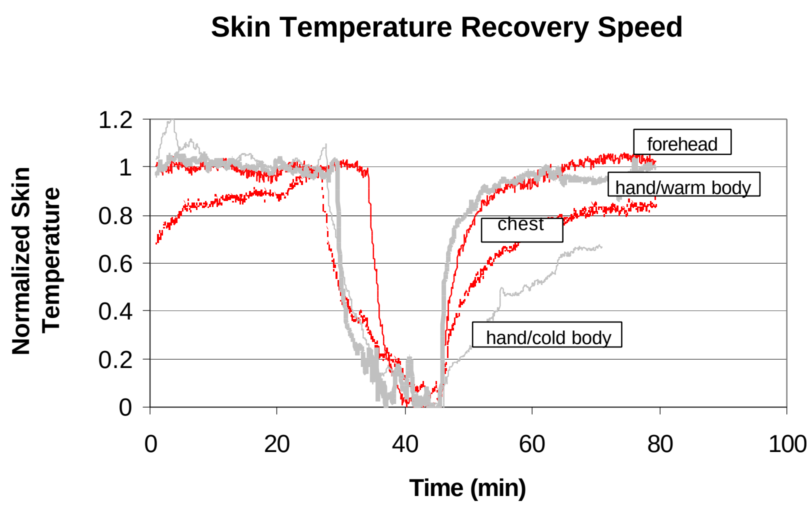

Figure 5.54 Hand skin temperature recovery speed

When the body was not warm (the thin gray line), after the hand cooling, the skin temperature did not recover to its original pre-cooling skin temperature after 30 minutes. However, when the body was warm (the thick gray line), after the removal of hand cooling, it took only about five minutes for the hand to recover to close to its original skin temperature, although the supply cooling air was cooler (18°C) in this test than in the previous test (22°).

The skin temperature recovery speeds for forehead and chest are included from different tests in order to compare them with the hand skin temperature recovery speeds. For these two local cooling tests, the room air temperature was 28°C, and the local supply air temperature 23 °C. Subjects' overall sensations was slightly warm (+1).

In general, the forehead skin temperature had the fastest recovery speed because of the larger blood supply to the head. We see that the hand skin temperature recovery speed from a warm body is as fast as the forehead skin temperature recovery speed. The recovery speed from the hand is also faster than the chest, which normally has a relatively high recovery speed.

Figure 5.55 shows a series of IR images taken after a hand cooling was removed to visualize the fast recovery process. The test is the same one as presented by the thick gray line in Figure 5.54 – the hand cooling test in the warm environment. In the test the left hand was cooled and the right hand wasn't. The first image (0 minutes) was taken right after the hand cooling was removed. We see that the left hand skin temperature was basically recovered to be similar as that of the right hand in five minutes.

0 minute | 2 minutes | 5 minutes

Figure 5.55 Recovery of hand skin temperature after local cooling

The hand's contribution to overall thermoregulation

The subject's thermal sensation votes have indicated that hand cooling does not have much impact on overall sensation (as described in the least influential group in section 5.5.1.2.2). Thus, because the blood vessels of the hand actively constrict and dilate without influencing overall thermal sensation, the hand is an ideal candidate to contribute to the body' thermoregulation. When the body is hot, the blood vessels of the hand are well dilated to permit heat to be released. When the body is cold, the blood vessels of the hand are constricted.

The blood vessels of the hand constrict rapidly, however, and, once the hand is cold, it no longer contributes to heat release. So to employ the hand for maximum heat-release benefit, we need to regulate its exposure to cold.

Consider the following example: When you are hot and place your hands in cold water at the beach, you feel an immediate release of heat stress. But the cooling of the cold water quickly makes the hand cool and vasoconstricted. After that, the function of losing heat cannot satisfied. From our test results shown above, we know that when the overall body is hot, hand skin temperature recovers very fast. So when we are at the beach as described above, to maximize heat removal, we should remove our hands from the cold water soon after the blood vessels of the hand constrict so that the warm body quickly pumps the heat to the cold hand in order to produce vasodilation and release heat. Once the hand is warm again, we can reapply cooling to remove the heat.

This might be a good strategy for car air conditioning; once conditioned air has cooled the hand so that the blood vessels are constricted and no longer release heat from the body, cooling of the hand should be avoided to allow the blood vessels of the hand to relax and dilate, at which point they could be cooled again to remove additional heat from the body. This cooling-recovery-cooling pattern will maximize the hand's contribution to regulating heat loss. Another advantage is that this process avoids activating pain receptors when strong constriction happens. Vehicle air conditioning could be designed to cool passengers' hand following a pattern of application and removal in order to maximize the hand's thermoregulation function.

Craig Heller and Dennis Grahn have designed and built a glove-like device (Figure 5.56) that creates a vacuum to prevent constriction of blood vessels while the hand is cooled by a cold control surface. The device is used by athletes to remove heat during exercise, heat being major reason for muscle fatigue.

They put great effort into finding the right cooling temperature. When the contact surface is too cold, the vacuum effect is not sufficient to keep the vessels dilated. It is possible that the cooling-recovery-cooling pattern noted above for hands could be applied in Heller's work to maximize heat removal from the body during exercise.

Figure 5.56 Low pressure device to help the heat loss from the hand (Department of Biological Science, Stanford University, 2002)

5.7.3 Local skin temperature and its impact on heat loss

The IR images in the subsections below show skin temperature distributions, which is relative within each image. Because the intention of the images is to show the relationships among skin temperatures in different areas of the body, the temperature ranges for these images have not been held constant .

5.7.3.1 Face and forehead

Figure 5.57 shows that the face, like all body parts, exhibits a greater variation in skin temperature when cold. The nose and cheeks, (the "extremities" of the head) are the coldest (see Figure 5.57 Cold). Therefore, in cold conditions, it is not necessary to cover the cheeks to save heat unless the temperature is so extreme that the pain receptors are activated (15°C skin temperature is considered the cold pain threshold). The forehead is the warmest, so in cold temperatures, putting on a hat conserves energy.

As people feel warmer, skin temperature variation decreases. In neutral conditions, the face is quite uniform except for the cool nose, (Figure 5.57 Neutral). In warm conditions, all areas of the face are warm, including the nose (Figure 5.57 Warm). When people are very hot, the cheek is warmer than the forehead because sweating occurs on the forehead and evaporation reduces the forehead skin temperature (Figure 5.57 Hot). (Note: Each picture is on a different scale, so the gray levels are not comparable among images).

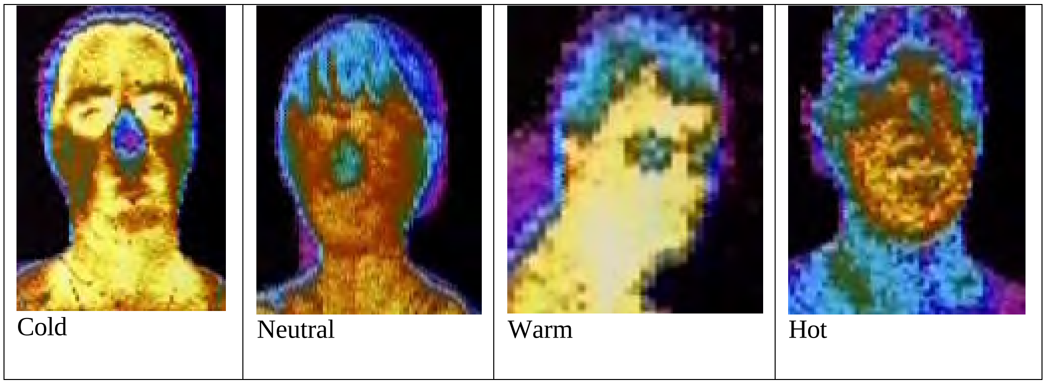

Figure 5.57 Head skin temperature distribution in different environments

Forehead and neck rank first in terms of sweat production. Randall (Randall 1946) found that the number of functional sweat glands on the forehead is about 20 times the number in the cheek. The number of functional sweat gland in the cheek is very small, the smallest one of many other skin areas (see Table 7.3). Because the cheek can be dilated and yet does not sweat much, the cheek is the warmest place on the head in warm conditions.

5.7.3.2 Back of the head

The photos in Figure 5.58 are of the same person in a warm environment and in a cold environment, respectively. The warm-environment image shows that when a person is warm, his hair is also quite warm. This subject is a 30-year-old Hispanic male with thick hair. He appears bald in the IR image because his head is warm. We can see the subject’s full hair in the cold image as well; when the subject is cold, the back of his head is not warm.

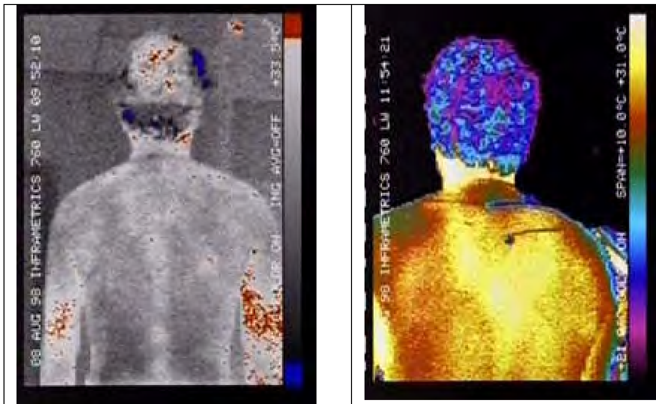

Warm | Cold

Figure 5.58 Back of head skin temperature in cold and warm environments

These two images show that when a person is hot, he releases heat not only from the face, but also from the back of the head, even with substantial hair. The entire head loses heat in order to keep the brain cool in warm conditions. We know that to maintain brain function, about 15 percent of a person's blood is constantly being supplied to the head. Because there is not much insulating tissue outside the skull, the head is usually warm. However, from this example we see that when a person is cold, the temperature of the back of his head is not warm. This may indicate that the head skin itself does dilate and constrict according to the body's thermoregulation needs.

5.7.3.3 Neck

The neck has the highest skin temperature of any body part when a person is cold. In the IR images taken in a cold environment the warm neck is very noticeable, like a bright belt (Figures 5.55). This justifies turning up jacket collars or putting on a scarf in cold weather.

(Zipping up the collar of a jacket also restricts the pumping effect of the air through the opening of the collar, which removes heat from the larger torso area).

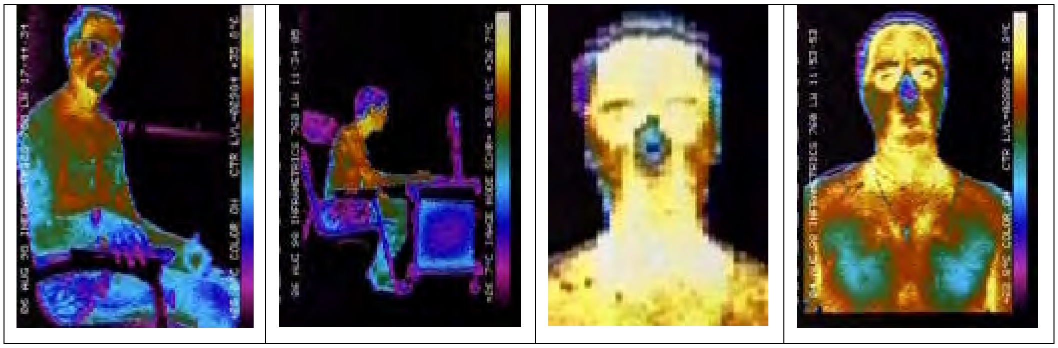

Figure 5.59 Neck skin temperature in cold environment

5.7.3.4 Lower arm and upper arm

When people are hot, the blood vessels of their outer extremities are dilated. Often the lower arm skin temperature is higher than the upper arm skin temperature (for the lateral side of the arm where we recorded arm skin temperature measurements).   Figure 5.60 Warm shows this temperature pattern. We also see this phenomenon in Table 5.3, which gives skin temperature distributions in warm environments. Part of the reason for this difference of temperature between the upper and lower arm is that there is more muscle and fat in the upper arm, so it is more insulated. This explains why it is effective to roll up one's sleeves to expose the lower arm to release heat when a person is warm. There are more sweating glands in forearm than the upper arm as well (Table 7.2, Kuno 1956, Table 7.3, Randall 1946).

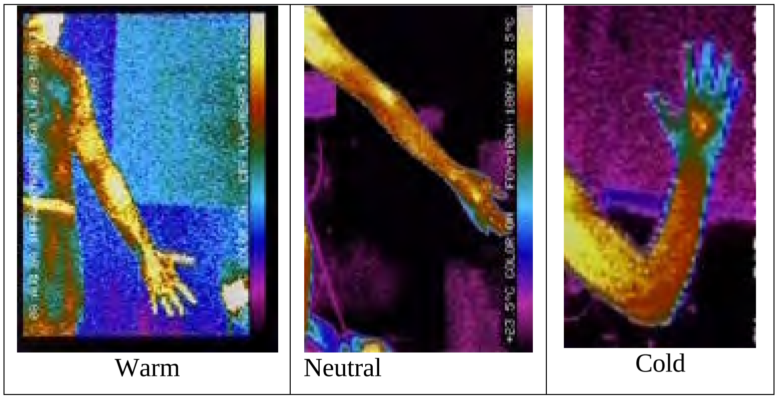

Figure 5.60 Upper and lower arm skin temperature in different environments

However, the skin temperature difference between upper and lower arm is not the same when people are cold and the blood vessels of the arm are constricted (see Figure 5.60 Cold). In this situation, the lower arm skin temperature is lower than that of the upper arm. The temperature of the most distal extremity, finger, is the coldest under these conditions.

Under neutral conditions, the temperatures of the hand, lower arm, and upper arm are not significantly different. Figure 5.60 Neutral shows upper arm slightly warmer than the lower arm in neutral conditions, and Table 5.1 shows that the upper arm (34.2°C) is slightly cooler than the lower arm (0.4°C) in neutral conditions.

5.7.3.5 Hand

The hand is probably the most active body part in responding to the body's thermoregulation requirements. In warm conditions, the hand is fully vasodilated (Figure 5.61 Warm 1, 2 & 3), and the fingertips are the warmest areas of the hand (Figure 5.61 Warm 1). However, the hand is also very sensitive to cooling. When the body feels slightly cool, the blood vessels of the hand constrict. A hand whose blood vessels are well constricted has a skin temperature variation in the range of 8 °C (Figure 5.61 Cold). When the hand is cold, it ceases to lose much heat.

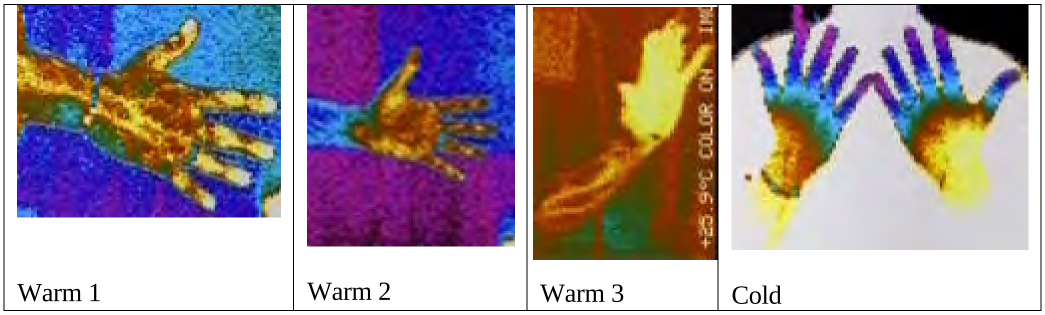

Figure 5.61 Hand skin temperature in warm and cold environments

The hand is very sensitive to the body's overall thermal state. Figure 5.62 shows an example from a whole-body step-change test. The photograph was taken a few minutes after the subject moved from a warm environment (30°C) to a slightly cool (22.6 °C) environment. Although the rest of the upper body temperature has not changed much yet, the blood vessels of the hand are already well constricted.

Figure 5.62 Skin temperatures a few minutes after moving from a warm to a slightly cool environment (18105)

For more information about hand and finger skin temperatures and the effect of hand motion on hand temperature, please see section 5.7.1.2.

5.7.3.6 Whole body, legs, and feet

In general, the upper extremities are warmer than the lower extremities. We see this in images shown in Figure 5.63 which show warm, neutral, and cool bodies, and in the skin temperature distributions presented in Table 5.1, 5.3, and 5.4 for neutral, cold, and warm environments. Normally, the toes are the coldest area of the lower extremities.

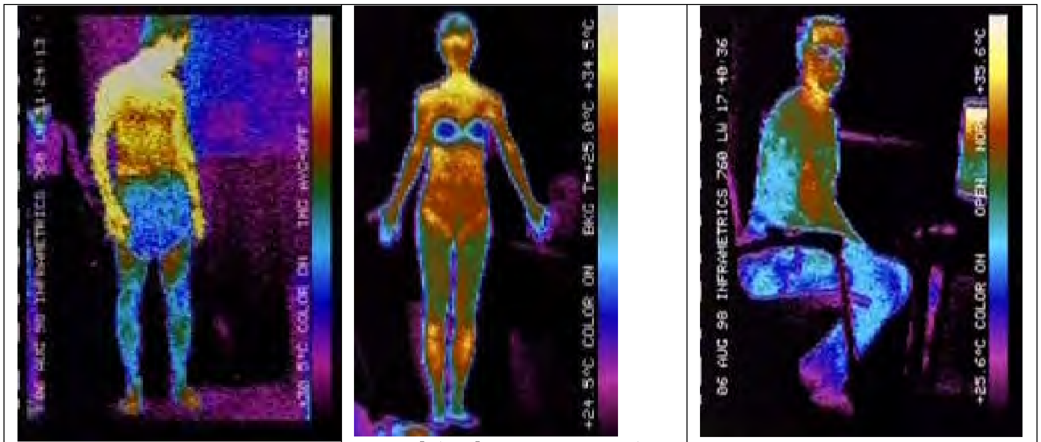

warm (scale: 30.5–35.4 C) | neutral (scale: 24.5–34.5 C) | cool (scale: 35.6– 35.6 C)

Figure 5.63 Whole body skin temperature distributions in warm, neutral, and cool environment

During our tests, the subjects sat in a chamber similar to a normal office and used a computer in a manner similar to normal office activity. Therefore, the subjects' responses are likely to be similar to the responses of people in an office environment. Our results suggest that people in office settings are, in general, likely to have colder lower extremities. This could be caused by 1. the stratification of air temperatures in a space, and 2. the absence of activity involving the legs and feet during typical office activities.

The distributions of leg and foot temperatures in a cool environment (20°C) are shown in Figure 5.64, which shows that in a cool environment, the feet are much colder than the legs, and the toes are the coldest (more than 10°C lower than the leg).

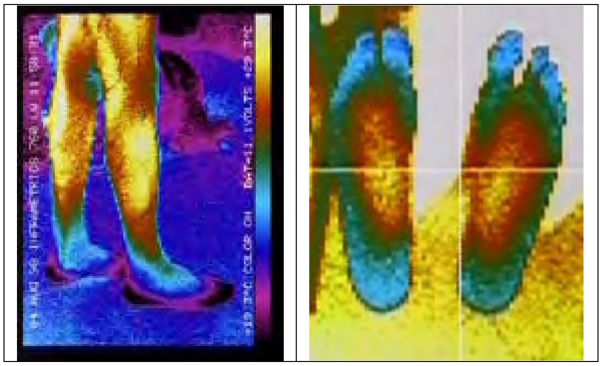

Figure 5.64 Leg (scale 19 – 29°C) and foot (scale 14 – 24 °C) skin temperature distribution in cool environment

The time that we saw warmer toes than feet, warmer feet than legs, is after a subject took a warm bath. The phenomenon is similar to a warm fingertips when people are warm (Figure 5.57 Warm 1). At these times the toes and fingers are well dilated and their temperatures are the warmest.   In the same way, the feet and hands are warmer than the legs and arms, respectively.

5.8 Overall summary of test results

The following 11 points summarized the main findings of all the tests.

1. In stable environments, local sensation is well correlated with local skin temperature. Most of the correlations are between 0.6 and 0.8 (Table 5.4).

2. Local skin temperature, rate of its change, and local sensation in transient environments: In transient environments, the correlations between local skin temperature and local sensation are reduces to around 0.5 (Table 5.7). The correlation between derivative of local skin temperature and local sensation is high, around 0.5 (Table 5.8).

3. Three body groups: The body parts can be grouped into three groups in terms of the influence on the overall sensation, the most influential group (dominant group, chest, back, and pelvis), the least influential group (hand and foot), and the moderately influential group (head, face, neck, breathing zone, upper and lower arms, thigh, lower leg). The differences between the three groups are statistically significant. For sensation, the significant level is at $p<0.005$ (Table 5.5). For comfort, the significant level is better than $p<0.05$ (Table 5.6).

If one wears a shirt in cold weather, no matter how warm the gloves he wears, one would still feel cold. Conversely, if one puts on a warm jacket, one would feel fine even without any gloves. Kayaking in a cold weather, one wears a warm jacket and shorts. Yet one feels perfectly fine. There is a Chinese saying: if the chest and back are warm, the whole body is warm. Those areas hold the high priority in keeping the whole body thermally comfortable. Certain body parts, the least influential body parts, do not influence the overall body sensation.

Just as the primary functions of hand and foot are different, the three groups of the body parts serve their own thermal purposes.

The local sensation from the dominant group directly impacts the overall thermal sensation. Those segments' skin temperatures change relatively little while their changes invoke the overall sensation change. Therefore, their heat loss is relatively constant. The main function of those segments seems to be 'sensing' the thermal sensation, not for adjusting the heat loss. It is important to keep these segments thermally comfortable.

The opposite of the dominant group is the least influential group, or heat loss group. The skin temperature fluctuates greatly in order to satisfy the thermoregulation needs. The large skin temperature variation allows the segments to adjust the heat loss. In many animals, such as bears, paws are the primary body parts through which heat is lost in addition to the effects of evaporative cooling through the tongue and breathing or panting. Like them, the human hands and feet are also major places to lose heat when the body is hot because they can be well dilated. However, when the body is cold, they constrict and will not lose heat any more. Another important feature about hands and feet is that their thermal sensation changes dramatically with the dilation and constriction, however, their sensations do not contribute to the overall sensation much, unless severe local uncomfortable feeling occurs. These two features make the group an ideal place for thermoregulation.

All the parts in the head region belong to the middle group, which produce significant impacts on overall sensation, but are not as sensitive as the segments in the dominant group which are very sensitive to cooling. In fact head segments are very happy with cooling. In general human prefers a cool brain (cool head). In severe a hot environment or during exercise, the brain applies a selective brain cooling function (Cabanac 1995, Cabanac 1998). In serving thermoregulation purpose, head segments are far less constricted than the hands and feet so the entire head acts as a heat sink. It drains the heat from the body.

The groups reflect the fact that thermal sensitivity for different body parts are different and that the impact from different segments to the overall sensation is also different. The highly influential group will have higher weighting factors in the whole body integration model. The least group will have smaller weighting factors. We will see the regression results in the overall sensation model (Chapter 6).

4. Core temperature responses

Summarizing what we saw about core responses in different test conditions, we reached these findings.

a) In neutral conditions, the core temperature is very stable. The fluctuation is within 0.1 °C.

b) In warm environments, when applying local cooling, the core temperature responds with an immediate increase.

c) In cold environments, when applying local heating, the core temperature responds with a decrease. The magnitude of decrease is smaller than the increase that happens with local cooling.

d) In cold environments, when applying cooling, the core temperature becomes very active. It fluctuates up to 0.8 °C.

e) Core temperature can maintain itself without dropping during a two-hour period of exposure to a cold (15.6 °C) environment. The subjective sensation was between cold (–3) and very cold (–4).

These five observations point out two general features of core temperature: 1) core temperature tries to maintain its set point and 2) core temperature is more cold- protective than warm-protective. The measured core temperatures provide rich and precise information. This information will be used to establish more relations about thermoregulation responses in the future.

5. Stronger response to cooling than heating

Our body responds to cooling much more strongly than heating. Evidence includes: sensation overshooting to cooling, but not to heating; discomfort due to local cooling applied to a warm body, but no discomfort due to local heating of a cold body in our test range except for breathing heating; the overall sensation lowered the same level as the local sensation by cooling of dominant segments, but much less than the local sensation by local heating; much more active core temperature responses to cooling than to heating.

The results of sensation responding to cooling more strongly than to heating is also well explained by the features of the thermoreceptors. We know that the number of cold thermoreceptors is much larger than the warm thermoreceptors, and the depth of the cold thermoreceptors is closer to the surface of the skin than the warm thermoreceptors. Those features contribute the stronger response to cooling than to heating.

Richard de Dear tested human thermal sensation during step-changes in ambient temperature. Immediate sensations that were reported in a suddenly warmer temperature closely resembled the later steady-state response to the new environment, while initial subjective reactions to temperature down-steps were typically twice the magnitude of their up-step counterparts (de Dear, Ring et al. 1993). This heightened subjective sensitivity to temperature down-steps also demonstrates the more sensitive response to cooling.

Candas (Candas 2002) tested human subject transient exposures from neutral to both PMV = +1.5 and PMV = -1.5. The responses and his model predictions show that the discomfort is much higher resulting from cooling transients compared to warming transients.

6. Sensation, comfort, and thermoreceptors in transient conditions

When applying and removing local cooling/heating stimuli, the skin temperature changes gradually. However, most of the sensation and comfort votes show a large sudden change. That indicates the dynamic signal (proportional to the derivative of the skin temperature) plays a large role in the transient thermal exposures. The derivative of skin temperature is the largest at the outset of thermal stimuli.

In the Chapter 2 (Background), we stated that the source of sensation comes from the thermoreceptors and thermoreceptors show the static and dynamic features. The dynamic signal is much larger (10 – 50 times) than the static signal during transient. The voting behavior shown in transient conditions is well explained by these characteristics of the thermoreceptors.

7. Kuno effect

Under neutral condition, people's comfort votes rarely reached above 2 (comfortable). The very comfortable votes (3 or 4) mostly happened during the local cooling removal (heat stress removal). This finding matches the findings by Cabanac, Mower, Issing, and Attia. This finding also serves the base for the proposal of the saddle local comfort model (Chapter 6).

8. Preference breathing cooling

Our human subjects show a preference for breathing cooling and uncomfortable feeling toward breathing heating.

This is also directly beneficial to the brain cooling. In general, no matter what temperature the air breathed in, the exhaled air is saturated and at the body temperature. The heat exchange by breathing is caused mainly by evaporation. So when people are happy breathing cool air, part of the reason is that the humidity is low in the cool air. The humidity might be an even more important factor for breathing than the air temperature, which was not examined in our tests.

9. Hand motion increases finger skin temperature significantly in cold environment

Comparing the relatively freer left hand keyboard motion to clicking a computer mouse with the right hand, the left hand finger temperature can be 3°C warmer than the right hand finger in a cold environment. The extra motion increases blood circulation, which enhances skin temperature. This phenomenon indirectly explains why in an office environment people's feet tend to feel cool. Besides possible air temperature stratification, non-moving feet is also part of the reason.

10. Subjective perception repeatability

A few repeat tests for local cooling show that the subjects' thermal sensation and comfort votes repeat very well.

11. Cooling/heating of extremities on one side has no influence on those on the other side

Since a human being is symmetrically produced with extremities, we tested whether cooling/heating the extremity on one side would influence the extremity on the other side. We found that there is no influence on extremity skin temperature, as well as the sensation and comfort.

5.9 Database

A database is has been developed which includes skin temperature, derivative of skin temperature, core temperature, derivative of core temperature, sensation and comfort for 19 body parts and the overall whole body. The database allows us easily subtract datasets in order to carry out the regressions analysis to develop models. The detailed description of the database in provided in Appendix 5.1.

6. MODEL DEVELOPMENT

Based primarily on the data gathered from our 109 experiments with human subjects in the U.C. Berkeley environmental chamber, we developed four models to predict local and overall thermal sensation and comfort in asymmetrical, transient conditions:

1) A local sensation model for each of 19 body parts (head, face, neck, breathing zone, chest, back, pelvis, left and right upper arms, left and right lower arms, left and right hands, left and right thighs, left and right lower legs, left and right feet),
2) A local comfort model for each of 19 body parts,
3) An overall thermal sensation model
4) An overall thermal comfort model

As described in Chapter 4 (Methods), we measured skin temperature at 28 locations and core temperature during each test. We asked sensation and comfort questions for 19 local body parts and for the overall whole body. This Chapter describes how we correlate the human subjective sensation and comfort votes with the skin and core temperature measurements and develop the models by regression analysis.

The modeling approach is to predict sensation and comfort based on the skin and core temperatures and their rates of changes. In the Chapter 2 (Background) we stated that people sense warm and cold only through thermoreceptors (Blix 1884, Goldscheider 1884, Dallenback 1927). The thermoreceptors sense the temperatures of their surrounding tissue and send signals. When discussing about thermal sensation, McIntyre (MyIntyre 1980) said, “a person cannot actually sense air temperature directly. All he can sense is the temperature of his own nerve endings, which are situated below the surface of the skin. It must be possible, therefore, to predict a person's sensation of warmth and comfort entirely from a knowledge of his physical state…mean skin and deep body temperature". As described in the Background (Chapter 2), there are other models which link the sensation with the skin, core temperatures, and the derivative of the skin temperature (Fiala 1998, Ring and de Dear 1991, Taniguchi, Aoki et al. 1992). Based on these studies, we hypothesize that it is possible to correlate the subjective perceptions with the skin and core temperatures.

In our models, the local sensation is the function of local skin and the mean skin or the core temperatures. From the experimental data (Chapter 5), we know that sensation and comfort are closely correlated. Our local comfort model is a function of local and the whole-body sensations. So comfort is indirectly linked with the skin and core temperatures.

6.1 Brief overview of the models

The four models are based on the physiological and subjective parameters measured in our tests: skin and core temperature and their rates of change, and perceptions of local and overall sensation and comfort. The local sensation and comfort models were developed based on the data from our experiments as well as data from the literature; from the patterns observed in these data, we proposed rational mathematical models and then performed regression analysis of the subjective parameters as a function of the physiological parameters.

For development of the model for local sensation, we first modeled local thermal sensation under stable conditions and then, based on these results, added transient data to develop the model for predicting local thermal sensation under transient conditions.

Based on the local and overall whole body sensation and comfort votes of the human subject tests, we performed regression analyses to arrive at the integration (overall sensation and comfort) models. The integration models were developed based on the patterns observed in our data only as there is very little information in the literature on this topic.

The flow chart in Figure 6.1 shows the models that were developed and the their relationship.

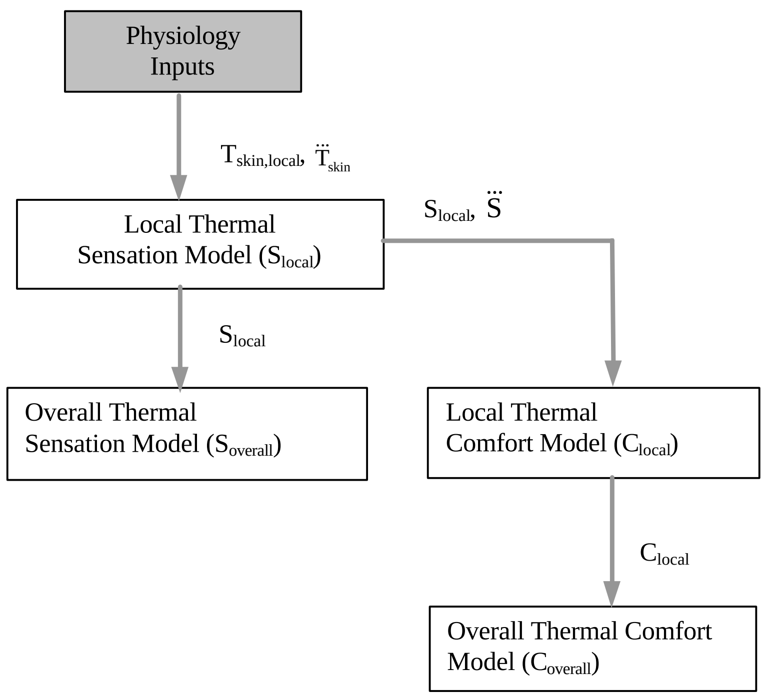

Figure 6.1 A flow chart to show models developed and their relationships

The models were validated using data from Delphi Wind Tunnel tests. The Delphi tests cover extreme test conditions (Chapter 4 Method), and the asymmetries and transients are higher than a normal building environment. Good validation results would give one confidence that the models can be applied to the less extreme environmental conditions found in buildings – such as perimeter zones affected solar radiation and air movement from windows.

Each of the models uses a different form of mathematical equation. The local sensation model is based on a logistic linear function, the local comfort model on a "saddle" shaped function, and the overall sensation model on a sunburst-shaped weighting factor equation; the overall comfort model is rule-based. We will first give an overview of these four models. The details of the mathematical concepts underlying each model are given in section 6.3 and after.

Our approach was to propose rational models and then apply regression analysis to the experimental data to obtain the model coefficients. By carefully choosing rational models, our hope is that as more data becomes available in the future, we can improve the coefficients without changing the basic form of the models. Another advantage is that a rational model with a relatively simple mathematical form makes it easier to understand the relationships between various body temperatures and comfort.

Although it is not the focus of this study, we did find that an adaptation model to adjust the set points of local body skin temperature is necessary. Based on the literature we proposed a model, which is presented in section 6.2.1.6. We did regression analysis based on our experimental data and obtained the coefficients for the models of each body part. Because this is not the main focus, we put the regression results in Appendix 6.1. As more data available in the future, the regression coefficients can be modified.

This section describes the logic of the models; details of their development follow in subsequent sections.

6.1.1 Local thermal sensation model

Local thermal sensation is well represented by a logistic function of local skin temperature (Figure 6.2). As the local skin temperature gets further away from the local skin temperature set point, the sensation reaches the sensation scale limits (+4 and –4).

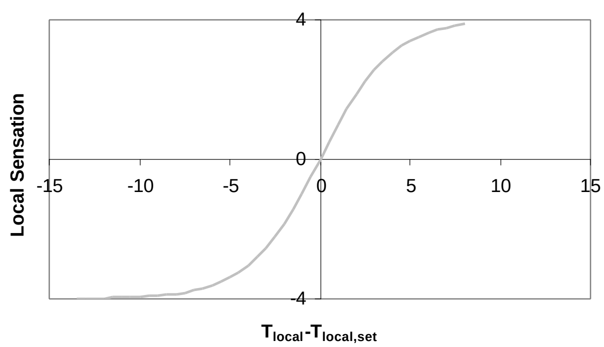

Figure 6.2 Logistic local sensation model

The rate of reaching the limit on the warm side is greater than on the cold side because the range of skin temperature change on the warm side is much smaller. Therefore, the slope of the logistic curve is asymmetrical, steeper on the warm side and more gradual on the cold side (Figure 6.3).

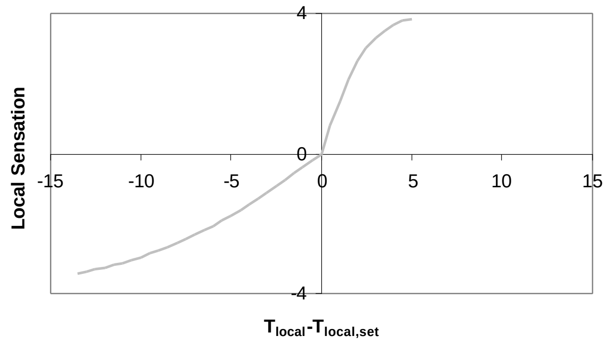

Figure 6.3 Asymmetrical logistic model

Local sensation is influenced by the overall body thermal state. If a local part is warmer than the rest of the body, its local sensation will be relatively warmer than it would be (for the same local skin temperature) if the rest of the body were warmer. This is a feature associated with the asymmetry of local thermal sensations, that is when the local sensation is different from the overall sensation. In our model, local sensation is influenced by the difference between local and overall sensation.

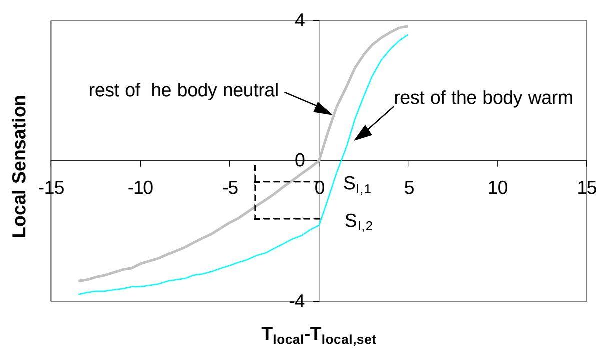

Figure 6.4 Overall body thermal state impact on local sensation

In Figure 6.4, both $S_{i,1}$ and $S_{i,2}$ represent the I segment sensation. With the same local skin temperature, a neutral body has a higher local sensation, $S_{i,1}$; warmer whole body feels a colder local sensation, $S_{i,2}$.

The final model of local thermal sensation in a static, asymmetrical environment is presented as a group of contours representing overall body thermal states (Figure 6.5). The local sensation is a function of local skin temperature and a parameter representing overall body thermal status – either core temperature or mean skin temperature. This effect can be explained by the adaptation in skin temperature. When the whole body is cooler, the local skin temperature must be relatively cooler to have a neutral (zero) sensation.

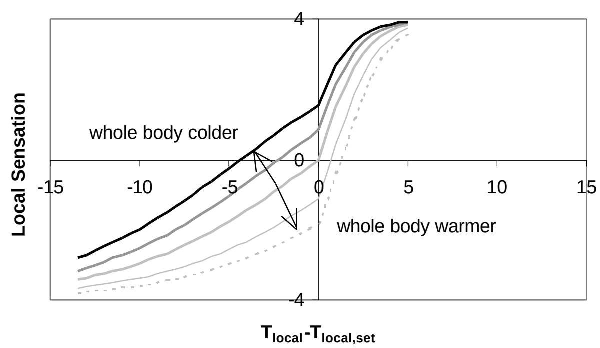

Figure 6.5 Static local sensation model

The foregoing applies to steady state conditions. A transient term is added to predict local thermal sensation in transient conditions. An example from our experiment is shown in Figure 6.6. Instead of following the logistic curve which represents the sensation under stable condition, the votes (diamonds) jump significantly upon the cooling application and its removal. This jump is caused by the activation of thermal receptors which send strong signals when the body experiences a sudden temperature change. It explains the sudden warm feeling that occurs when people enter a warm room, before either body core and skin temperature have raised to a steady-state level. The transient term is a function of the rate of change of the skin temperature. The faster the skin temperature changes, the stronger the transient thermal sensation is.

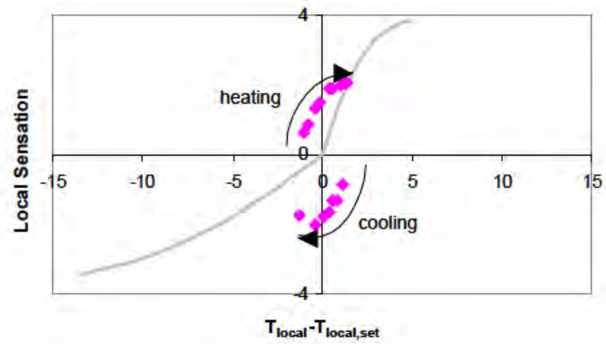

Figure 6.6 Dynamic local sensation model

6.1.2 Local thermal comfort model

The hotter or colder people are, the more uncomfortable they feel. This relationship is illustrated in Figure 6.7

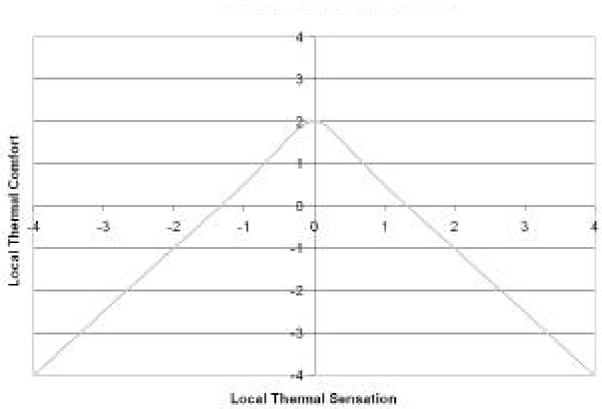

Figure 6.7 Local sensation and local comfort linear model

Mower (1976) demonstrated that during hyperthermia or hypothermia, cold or warm stimuli (respectively) to the hand were experienced as very pleasant (Figure 6.8). In neutral conditions, the stimuli were never been perceived as very pleasant. Two important things were demonstrated. First, the sensation at which the maximum comfort occurs shifts to the left or right based on the overall body thermal state. In other words, when the internal temperature is high or the whole body is warm, the cold or cool stimuli are perceived as pleasant; when the whole body is cold, the warm stimuli are perceived as pleasant. Second, the magnitude of the comfort is higher when the thermal stimuli remove the heat stress or relief the discomfort. Both Kuno and Cabanac (Kuno 1995; Cabanac, Guillaume et al. 2002) believe that it is the reduction or removal of stress that creates pleasure. Great pleasant occurs when discomfort disappears.

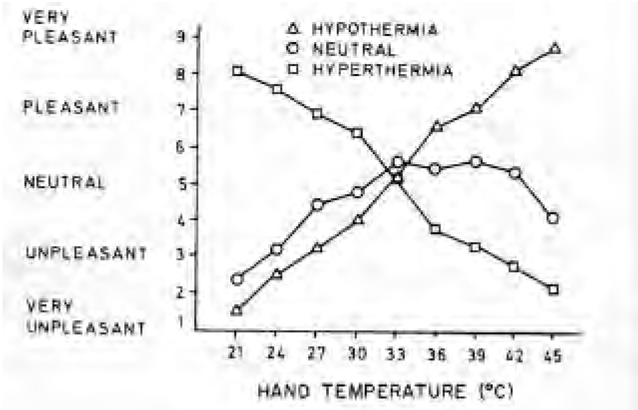

Figure 6.8 Hand sensation and comfort when whole body is hypothermia, neutral, and hyperthermia (Mower 1976)

We interpret the "pleasant" in Mower's figure the same as "comfort". Cabanac (1969) refers the same pleasant scale used in his study as the "thermal comfort".

Our proposed model is shown in Figure 6.9. The magnitude of maximum comfort increases when overall thermal status is warm or cold.

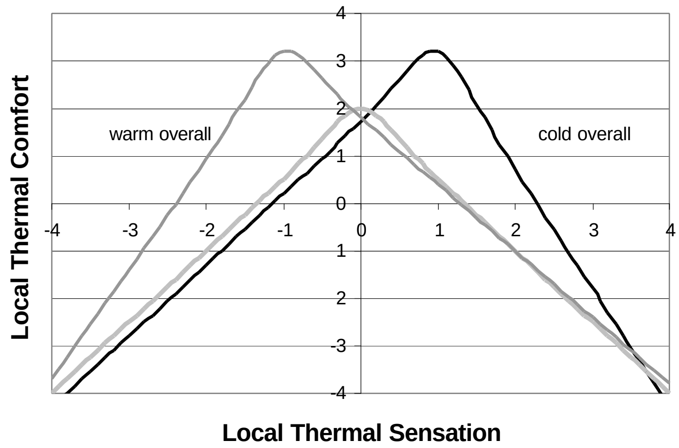

Figure 6.9 Shifts at maximum comfort due to overall sensation

Some body parts experience relatively different levels of maximum comfort by local cooling or heating when the whole body is warm or cold. For example, breathing cool air is very pleasant when the body is hot, while in general people do not like to breathe warm air even when the body is cool. This creates an asymmetric shift to the left or right (Figure 6.10). In Figure 6.10, we see different maximum comfort levels when the middle curve moves towards warm and cold overall sensation, as well as the unequal shifts at which the maximum comfort happens.

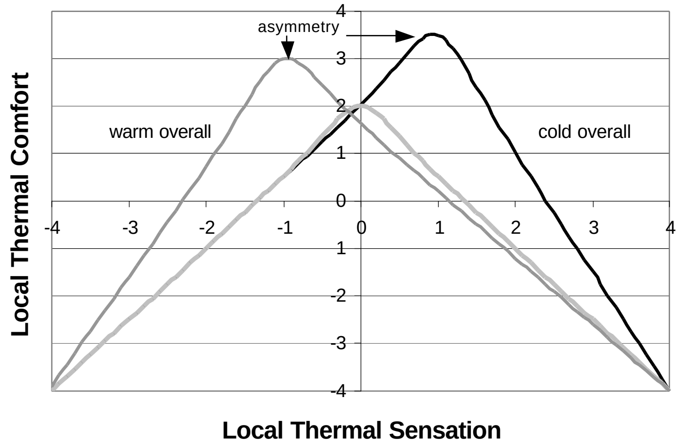

Figure 6.10 Asymmetrical shifts and maximum comfort

The local comfort is a function of both local sensation and overall sensation. The final local comfort model is represented as a group of curves representing overall whole body thermal state. When the overall body is warm, a cool local sensation is perceived as more comfortable than if the overall body was neutral or cool. When the overall body is cool, a warm local sensation is perceived as more comfortable than if the overall body was neutral or warm.

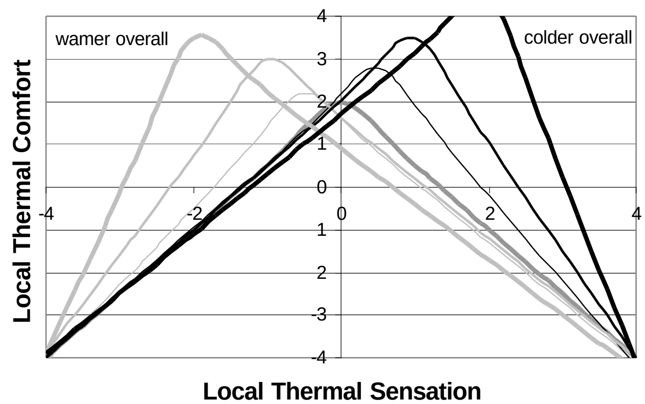

Figure 6.11 Local thermal comfort model

6.1.3 Overall thermal sensation model

Overall sensation is modeled as a weighted average of the local sensation. The following three considerations are the basis when developing the overall sensation model.

1) For some body parts (e.g. chest, back), the weights are larger than for other body parts (e.g. hand, foot). This could be due to segment size or sensitivity.

2) For one segment, the weightings for the warm side (local sensation (S_l) – mean sensation (S_{mean}) >= 0) and for cold side (S_l – S_{mean} < =0) are not necessarily equal. S_{mean} is a simple average of all segments. One segment may be more important to determine cold sensation than warm sensation.

3) The weight for any one body part is a function of difference between the local sensation and the overall sensation. This assigns larger weights to the local sensation when local sensation is opposite to or further away from the sensations of the rest of the body (e.g. a cold hand contrasted to a warm body). This relationship shows the importance of local asymmetry.

Summarizing above features, the model is presented in Figure 6.12.

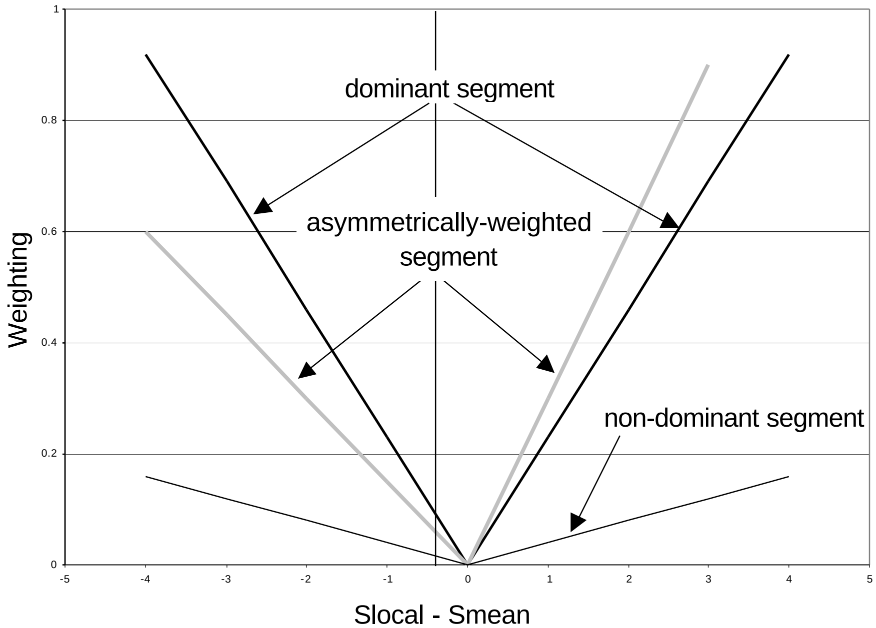

Figure 6.12 Overall sensation model

Figure 6.12 reflects the three features of the overall model. One segment (back) is more dominant than the others. As the difference between local sensation and the mean sensation of the body increases, the weighting becomes larger. The weighting for some body parts (e.g., face) is different on the warm and cold sides.

Overall sensation as a weighted average of the above weights and the local sensations.

$$Overall\ Sensation = \frac{\sum weight_i\ S_{local,i}}{\sum weight_i} \qquad \text{Eq. (6.1)}$$

6.1.4 Overall thermal comfort model

Overall comfort is determined from local segment comfort and is a complaint-driven model. It is best derived by a set of rules. These rules show that discomfort has a decisive impact on the overall comfort.

Rule 1: Overall comfort is the average of the two minimum local comfort votes unless Rule 2 applies.

Rule 2: If the following criteria are met:

- the second lowest local comfort vote is >–2.5
- the subject has some control over his/her thermal environment

  or the thermal conditions are transient

then overall comfort is the average of the two minimum votes and the maximum comfort vote.

Note: if both hands or both feet comprise the two most uncomfortable body parts, ignore the second lowest hand or foot comfort value, and use the third lowest local comfort vote as the second lowest vote in Rule 1 and Rule 2.

This model can be considered as a Boolean weighted model. It assigns weights of 0 or 1 to the local comfort and calculates the average.

The following subsections describe the development of the models in detail.

6.2 Local thermal sensation model

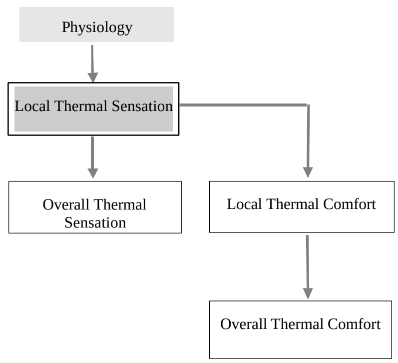

6.2.1 Static local sensation model

6.2.1.1 Logistic function

Our bodies generate heat by a variety of metabolic mechanisms, fueled by food and drink. The body dissipates approximately 85 percent of its heat through the skin and the rest by respiration and excretion under normal environmental conditions (e.g., when not extremely hot or performing vigorous exercise). Therefore, skin is the principal organ for dissipating heat.

Within certain limits when skin temperature is not very low or very high, the correlation between skin temperature and thermal sensation is close to linear. Figure 6.13 shows that overall sensation is roughly a linear function of mean skin temperature between 29 and 34°C (transcribed from a figure by McIntyre (McIntyre 1980) using data from Gagge (Gagge, Stolwijk et al. 1967)). As skin temperature moves above or below that, the linear relationship disappears, and thermal sensation starts to level off.

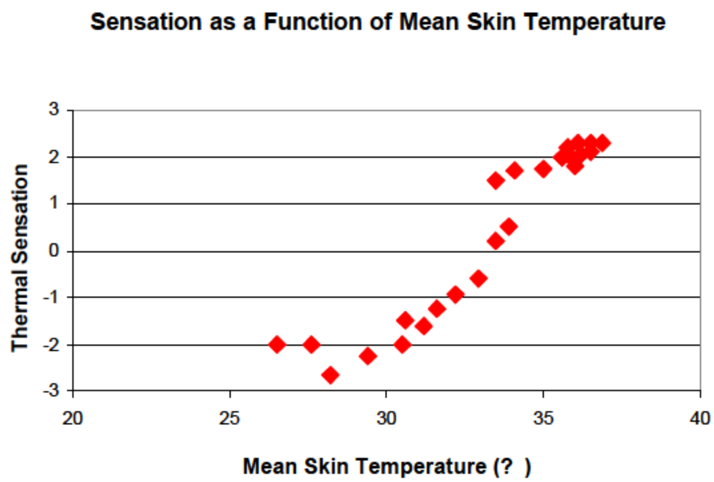

Figure 6.13 Relationships between sensation and skin temperature (Gagge, Stolwijk et al. 1967)

Fiala (Fiala 2002) developed a physiological model to predict mean skin temperature and used data from early thermal sensation studies carried out by Nevins (Nevins, Rohles et al. 1966), McNall (McNall et al. 1967), Gagge (Gagge et al.1969), and Rohles (Rohles 1970). The relationship between Fiala's predicted mean skin temperature and subjective sensation votes that he gathered from the literature is shown in Figure 6.14. The relationship is linear when the mean skin temperature is between 3°C below and 1°C above its set point, but beyond those points, the relationship approaches the scale limits exponentially. The set point of the mean skin temperature is the value when sensation is neutral (zero in the thermal sensation vote).

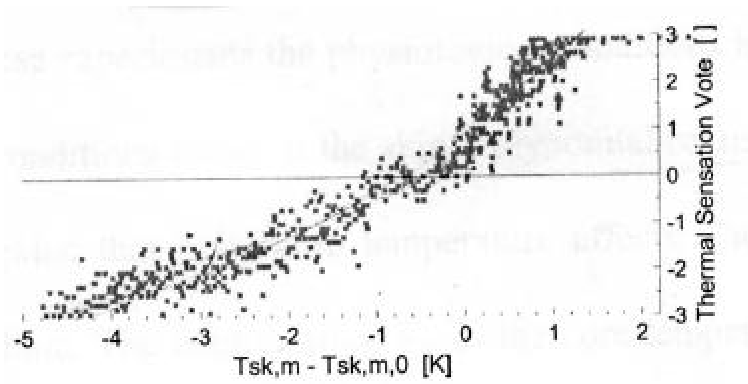

Figure 6.14 Skin temperature vs. sensation (Fiala 2002)

To cover the entire range of skin temperature change, including the extremes, we propose that local sensation is a logistic function of local skin temperature, presented as the difference between the local skin temperature and its set point. The set point for a body part is the local skin temperature when the sensation of that body part feels neutral (local sensation is zero). The logistic function is presented in Eq. (6.2). It exhibits the features shown in Figure 6.15. It shows a linear relationship in the middle but levels off when skin temperature goes high or low.

$$\text{Local Sensation } = 4\left(\frac{2}{1+e^{-C1(T_{skin\ local}-T_{skin\ local\ set})}}-1\right) \qquad \text{Eq. (6.2)}$$

In this equation, the number "4" defines the sensation range, from very cold (-4) to very hot (+4). When local skin temperature ($T_{skin,local}$) is much lower than its set point ($T_{skin,\ local,\ set}$), the exponential term $e^{-C1(T_{skin,local}-T_{skin,local,set})}$ is large and the term $\frac{2}{1+e^{-C1(T_{skin,local}-T_{skin,local,set})}}$ approaches zero. Therefore, the local sensation approaches its lower limit of –4 (very cold). When the skin temperature is much higher than its set point, the exponential term $e^{-C1(T_{skin,local}-T_{skin,local,set})}$ is close to zero and the term $\frac{2}{1+e^{-C1(T_{skin,local}-T_{skin,local,set})}}$ approaches a value of 2. The corresponding local sensation approaches its high limit, +4 (very hot). The term -$C1(T_{skin,local}-T_{skin,local,set})$ determines the slope of the logistic function. When C1 has a larger value, the logistic curve is steeper. The coefficient C1 is different for different body parts. For some body parts (such as chest and back), a small skin temperature decrease induces a large cooling sensation, so the slope is steep, and C1 has a large value. For body parts like the hand, the skin temperature change range is quite large, and the slope is therefore much more gradual, so C1 is smaller. Figure 6.15 shows the logistic curves for C1 as 1 and 0.5.

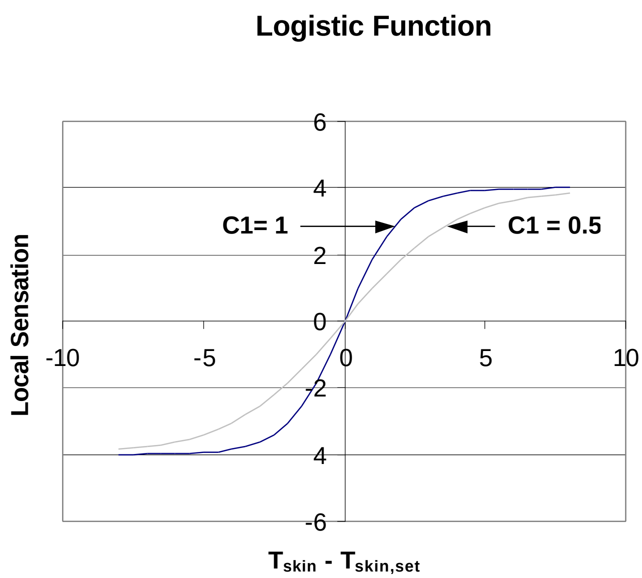

Figure 6.15 Slope and upper and lower limits of logistic functions

6.2.1.2 Impact of whole-body thermal state on local thermal sensation

6.2.1.2.1 Experimental observations

Local sensation is influenced not only by local skin temperature but also by overall thermal state. In our tests, we found that a body part with the same local skin temperature feels relatively warmer when the rest of the body is colder and colder when the rest of the body is warmer. Figure 6.16 shows examples of this phenomenon. The solid circles in the graphs are from cold-conditions tests when room air temperature is between 14 and 20°C.; the whole body is cold in these tests. The open triangles are data from warm-conditions tests when the room air temperature is between 28 and 32°C; the whole body is warm in these tests.

Except for hands and feet, we see a clear separation of local sensation in relation to warm or cold whole-body thermal states. For body parts with the same skin temperature, local sensation is much warmer during the cold tests when the whole body is cold and much colder during the warm tests when the whole body is warm.

The trend when $T_{local} - T_{local,set} > 0$ is unclear. Because our project prioritized cooling tests, we performed only a few local heating tests when the body was cold. Therefore, the number of solid circles on the warm side of the figure is very small. The open triangles on the warm side represent data gathered during removal of local cooling, which do not show a clear pattern. When $T_{local} - T_{local,set} < 0$, we see a gradual change in local sensation as skin temperature gets colder.

As described in Chapter 5.3, we consider that subjects' votes and physiological data had stabilized by the end of one local cooling/heating application and these data are used in this section to develop the stable condition local sensation model.

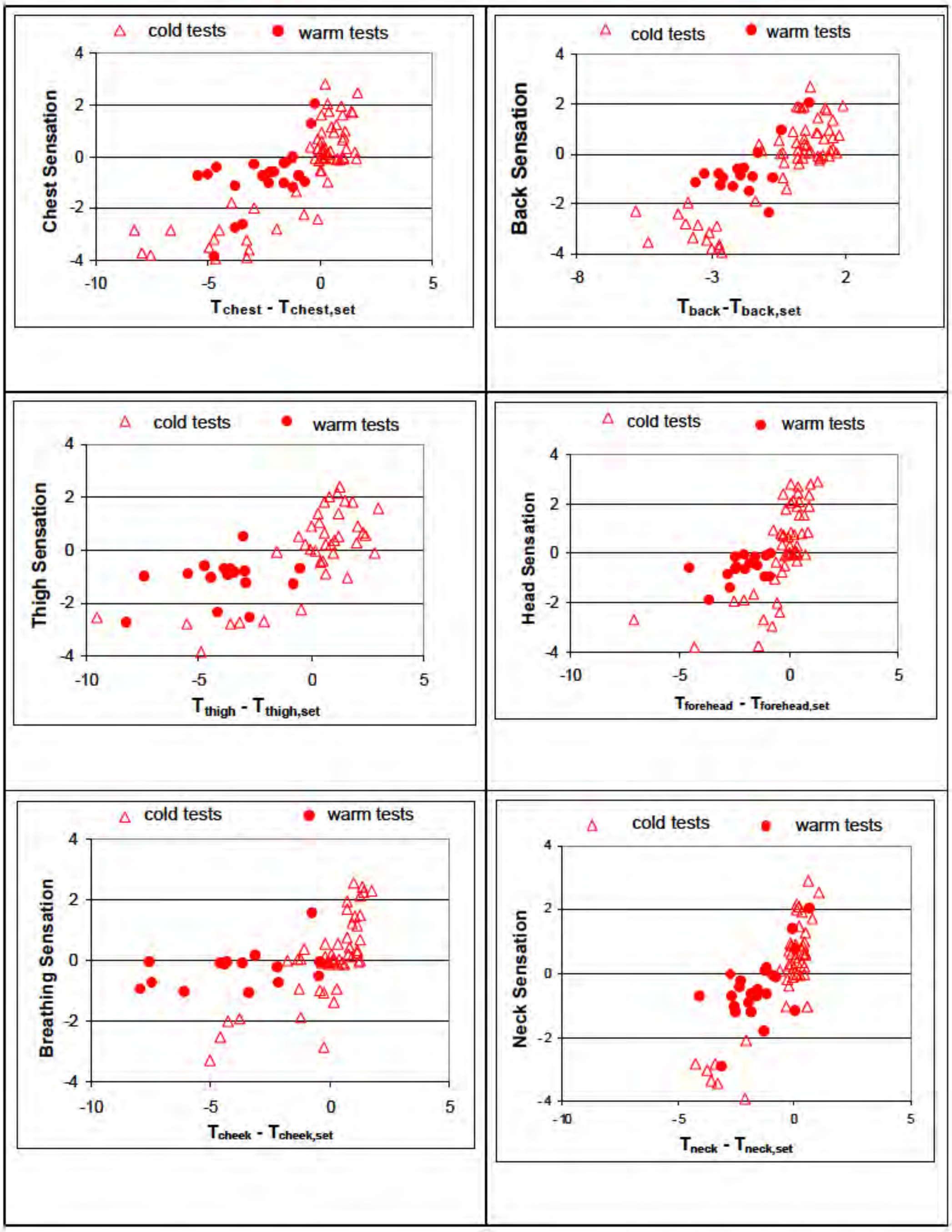

Figure 6.16 Local sensation feels warmer when the whole body is colder with same local skin temperature

This phenomenon is more evident in the head region and trunk regions and less evident in the extremities. The differences result in different regression coefficients for different body segments.

6.2.1.2.2 Experimental observations by other researchers

The observations showing local sensation modified by the relative difference between local and overall sensation can be explained in the following way as well: a local thermal stimulus usually produces a local reaction. That is, if you put your left hand in cold water, it will vasoconstrict more than your right hand and feel cold. However, this effect is modified by the temperature of the rest of the body. A person in a warm environment shows little constriction when putting a hand in cold water and therefore feels less cold. Conversely, a cold person putting his hand in warm water does not show an increase in blood flow to the hand (Bader and Mead 1949), (Hellon 1963), (Rapaport, Fetcher et al. 1949) and therefore feels less warm. In order to cool the hand to a given low temperature when the subject is in a warm environment, a colder stimulus has to be applied than would be necessary in a neutral or cool environment. As a result, the hand will feel colder when cooled in the warm environment. Similarly, to raise the hand skin temperature to a given level in a cool environment, a warmer stimulus has to be applied than would be necessary in a warm environment. This strong heating makes the hand feel warmer than it would in a warm environment.

Figures 6.17 (Hildebrandt, Engel et al. 1981, Issing and Hensel, unpublished, from Hensel 1982) support our observations shown in Figure 6.16, that local sensation feels warmer when the whole body is cold, colder when the whole body is warmer, with the same local skin temperature. The air temperature in the figures represents the overall body thermal state; that is, high air temperature indicates a warm overall state and low air temperature indicates a cold overall state. The horizontal axis is the thermode temperature, which represents local skin temperature. In these figures, we see that when the air is cold, 12°C or 15°C, local thermal sensation is warmer compared to local thermal sensation at the same local skin temperature when the air is hot (40°C or 45°C). The two figures also show that within a certain local skin temperature range, local sensation and skin temperature exhibit a nearly linear relationship. The linear relationship seems covering larger local skin temperature ranges in these examples, which may be caused by the area of a thermode, which is much smaller than a whole local body part.

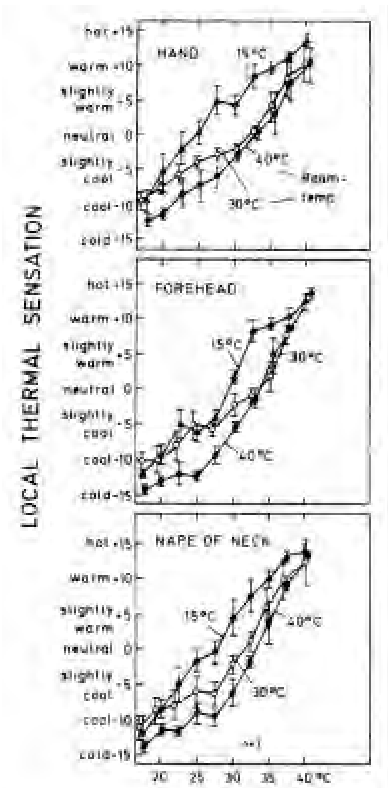

(Hildebrandt, Engel et al. 1981)

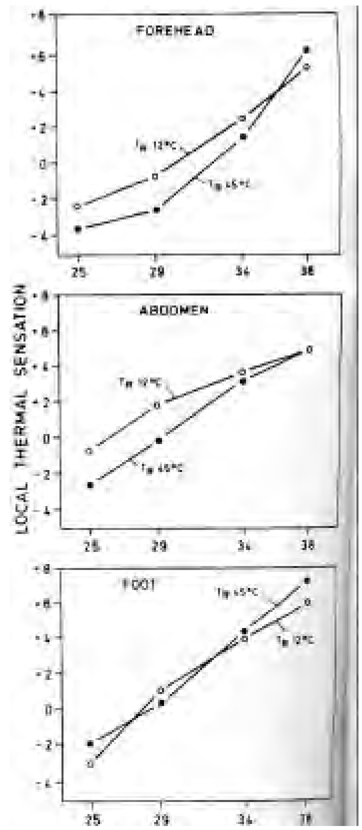

From K. Issing and H. Hensel, unpublished, copied from (Hensel 1982)

Figure 6.17 Whole body thermal state modifications on local sensation (horizontal axis is the thermode temperature, which represents local skin temperature)

6.2.1.2.3 Mathematical description

From the above analysis, we see that local sensation can be represented by a logistic function, but modified by the overall thermal state. Eq. (6.1) presents the logistic mathematical description. Now we need to incorporate a modification term representing the whole body thermal state into Eq. (6.2). The whole body thermal state can be presented by either ($\overline{T}_{skin}$ – $\overline{T}_{skin,set}$) or (T_{core} – $T_{core,set}$). $\overline{T}_{skin}$ is the mean skin temperature. T_{core} is the body core temperature. In our study, we used mean skin temperature, ($\overline{T}_{skin}$ – $\overline{T}_{skin,set}$), to represent the whole body thermal state. In section 6.2.5 we will explain why we chose the mean skin temperature instead of the core temperature to represent the whole body thermal state.

Since the exponent in Eq. (6.2), $-C1(T_{skin,local} - T_{skin,local,set})$, controls the slope of the logistic function, we need to incorporate the whole body thermal state into this part of the equation. From our own test data and the literature, we know that for a given local skin temperature, as the overall body is cooler the local sensation is warmer. The comparison between the local and the whole body thermal states is described as ($T_{skin,local}$ – $T_{skin,local,set}$) – ($\overline{T}_{skin}$ – $\overline{T}_{skin,set}$). Therefore, we can add a modification term –K1[($T_{skin,local}$ – $T_{skin,local,set}$) – ($\overline{T}_{skin}$ – $\overline{T}_{skin,set}$)] into the exponent section, $-C1(T_{skin,local} - T_{skin,local,set})$, to account for the modification from the whole body.

Our proposed model is,

$$\text{Local Sensation}_{\text{static}} = 4\left(\frac{2}{1+e^{-C1(T_{skin,local}-T_{skin,local,set})-K1\left[(T_{skin,local}-T_{skin,local,set})-(\overline{T}_{skin}-\overline{T}_{skin,set})\right]}}-1\right)$$

Eq. (6.3)

where term $-K1[(T_{skin,local} - T_{skin,local,set}) - (\bar{T}_{skin} - \bar{T}_{skin,set})]$ (alternatively written as $-K1[(T_{skin,local} - \bar{T}_{skin}) - (T_{skin,local,set} - \bar{T}_{skin,set})]$) represents the modifying effect of whole-body thermal status on local sensation. The difference between local and overall sensation is represented by the difference between local and mean skin temperatures. The difference between the local skin and mean skin set points, $(T_{skin,local,set} - \bar{T}_{skin,set})$, provides a reference. When the difference between local and mean skin temperatures equals the difference of their set points, then the contribution from whole-body thermal sensation is zero.

The entire modification $-K1[(T_{skin,local} - T_{skin,local,set}) - (\bar{T}_{skin} - \bar{T}_{skin,set})]$ is based on the relative difference between local and overall sensation. The bigger the value, the larger the impact of this difference on local sensation, and the further away of the curve from the base curve $(T_{skin,local} - \bar{T}_{skin} = T_{skin,local,set} - \bar{T}_{skin,set})$. The coefficient K1 is different for different body parts. For the same body part, it is also different for $T_{skin,local} - T_{skin,local,set} <= 0$ and $T_{skin,local} - T_{skin,local,set} >= 0$, the cold and the warm sides. The different K1 values for cold (left) and warm (right) sides are responsible for the different degrees of steepness on the two sides as seen in Table 6.1. The base-curve is represented by a thick gray line in the figures shown in the table.

Although we did not use core temperature, we did develop a model to predict core temperature as a function of time of day and gender (see Appendix 6.2).

6.2.1.3 Regression results

The regression results for local sensation (13 body parts, left and right extremities are not distinguished) in a stable asymmetrical thermal environment are shown in Table 6.1. The coefficients (C1 and K1) are listed separately for local skin temperature when it is higher or lower than its set point. The right figure represents the subjects' actual votes (horizontal) vs. the model's predictions (vertical). The ideal prediction should follow a 45°C line. The square of the correlation, R^2, is presented in the last column.

The regressions were performed after adjusting for the subjects' adaptive set points using the model as described in Appendix 6.1. Larger adjustments are made for the cold tests when the body has adapted to a cold skin temperature.

Table 6.1. Regression coefficients for Eq. (6.3) – local sensation model in asymmetrical environment

Body part (temperature measurement location)	$T_{skin,local} - T_{skin,local,set} < 0$		$T_{skin,local} - T_{skin,local,set} >= 0$		Actual vs. predicted votes,	R^2
	C1	K1	C1	K1		
Back (upper back)	0.3	0.1	0.7	0.1	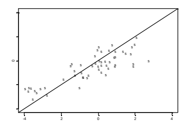	0.66
Chest (upper chest)	0.35	0.1	0.6	0.1	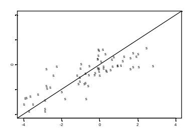	0.67
Face (cheek)	0.15	0.1	0.7	0.1	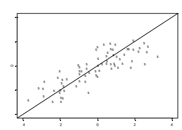	0.70
Hand (back of hand)	0.2	0.15	0.45	0.15	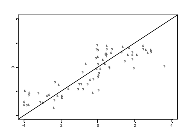	0.74
Foot (top of foot)	0.25	0.15	0.26	0.15	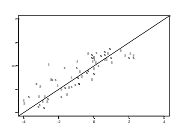	0.76
Neck (front neck)	0.4	0.15	1.25	0.15	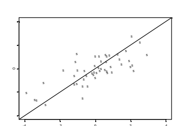	0.63

Table 6.1 (continued) Regression coefficients for Eq. (6.3) – local sensation model in asymmetrical environments

Body part (temperature measurement location)	$T_{skin,local} - T_{skin,local,set} < 0$		$T_{skin,local} - T_{skin,local,set} >= 0$		Actual vs. predicted votes,	R^2
	C1	K1	C1	K1		
Breath (cheek)	0.1	0.2	0.6	0.2	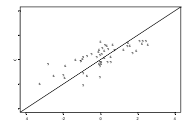	0.58
Head (forehead)	0.38	0.18	1.32	0.18	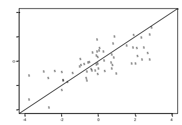	0.55
Pelvis (thigh)	0.2	0.15	0.4	0.15	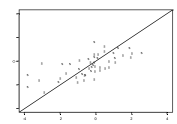	0.50
Lower arm (lateral side of lower arm)	0.3	0.1	0.7	0.1	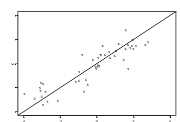	0.81
Upper arm (lateral side of upper arm)	0.29	0.1	0.4	0.1	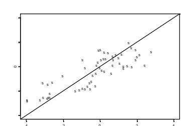	0.72
Lower leg (front shin)	0.29	0.1	0.4	0.1	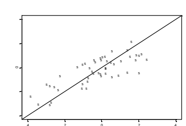	0.62
Thigh (front thigh)	0.2	0.11	0.29	0.11	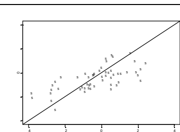	0.50

6.2.1.4 Body builder impact

Subjects' gender, age, and body fat ratio affect local sensation. Information about body build is not incorporated in the thermal sensation models, but I examined its influence on local sensation. Regression results with body build information incorporated are presented separately in Appendix 6.3.

6.2.1.5 Analysis of the regression results

The relationship between sensation and skin temperature on the warm side is much steeper than on the cold side. This is reflected in the magnitudes of the regression coefficients. We see that for each body part, the coefficient for the warm side is much larger than the coefficient for the cold side. The larger coefficients make a steeper logistic curve and therefore correspond to a smaller skin temperature change.

The coefficient C1 represents the base curve (when the skin temperature difference between local and mean is the same as the difference between their set points) with no adjustment for the overall body thermal state. The C1 values for the most influential/dominant body parts are bigger than those for the least influential/least dominant body parts. The bigger value corresponds to a steeper curve and a smaller change in local skin temperature produces a larger change in local thermal sensation. The C1 value for the least influential body parts is smaller, corresponding to a shallow curve. The shallow curve implies that a change in local skin temperature produces a smaller change in thermal sensation. We can see this for the regression results for back and chest and for hand and foot. For the cool side ($T_{skin,local} - T_{skin,kicak,set}$<0), the coefficients of C1 for the back and chest are 0.3 and 0.35 respectively; for the hand and foot, the coefficients are both 0.2. The coefficient C1 for the neck is also large, 0.4. The reason is that the front neck skin temperature does not change much because it was measured between the two carotid arteries. That is, the front skin temperature change range is small, which corresponds to a large change in local sensation.

For breathing, we use cheek skin temperature as the variable. Although cheek skin temperature may not reflect the temperature of breath intake air well, the cheek is the closest physical location to the breath intake temperature. The breathing intake air should correlate the breath sensation the most. In the near future, we will conduct a regression analysis between these two variables (this is addressed in the Future Work section in Chapter 7).

6.2.1.6 Adaptation

Skin adaptation to temperature is an aspect of human physiology similar to other sensory adaptations, e.g., eyes to darkness, tongue to taste, and ears to noise. Using noise as an example, consider that we are often unaware of the noise level in our environment; only when this level exceeds a certain threshold (e.g., construction work in a building) do we become conscious of it. Similarly, if background noise should suddenly cease (e.g., an electricity failure, turning off of an exhaust fan) we then become acutely aware of the absence of familiar sound. Most of the time we accept background noise subconsciously as part of our surroundings (Hopkinson 1963).

Adaptation entails a shift of reference set points. When part or all of the body is subjected to a change in environmental conditions, the sensation caused by the change soon ceases, partially because the set point has been shifted toward the changed environmental condition and partially because of the disappearance of the dynamic sensory signal. Stevens tested human responses to warmth and cold by applying thermal stimuli to the forearm (Stevens and Stevens 1960) and found that neutral skin temperature set points change with repeated stimulation. A heat stimulus presented toward the end of an experimental session usually elicited a smaller estimate of warmth than the same stimulus presented near the beginning of a session. This adaptation (sometimes called sensory fatigue) shifted the set point for the forearm from 31.6 to 33 °C.

Adaptation happens within one to two minutes (Hensel 1979) or even within seconds for temperatures slightly above or below normal skin temperature (Haber 1958). The skin can adapt to temperatures between 29 and 37°C (Kenshalo 1970) though wider ranges, particularly towards the cold end, have been reported (McIntyre 1980).

When a local area of skin has adapted to a temperature, the skin temperature can fluctuate within a range of temperatures extending to either side of the adaptation temperature without producing any temperature sensation. This is called the neutral zone. When the ambient temperature is changed sufficiently above or below the neutral zone, then the skin cannot maintain neutral sensation, and a persistent sensation of warmth or coolness is perceived (Haber 1958).

Kenshalo's (Kenshalo 1970) study supports Haber's finding. He first applied a thermal stimulus (14.4 cm^2) to the dorsal surface of the forearm for 45 minutes to have the surface adapted to a temperature from 28 to 40 °C. Then he applied a thermal stimulus to test the temperature at which a temperature sensation was just noticeable. Figure 6.18 shows the adapting temperature (horizontal axis) and a thermal stimulus (temperature difference from the adapting temperature, vertical axis) when a change in skin temperature is perceived. The solid curve represents for the warm and cold thresholds. The dotted line represents for the thresholds when a change in sensation was perceived.

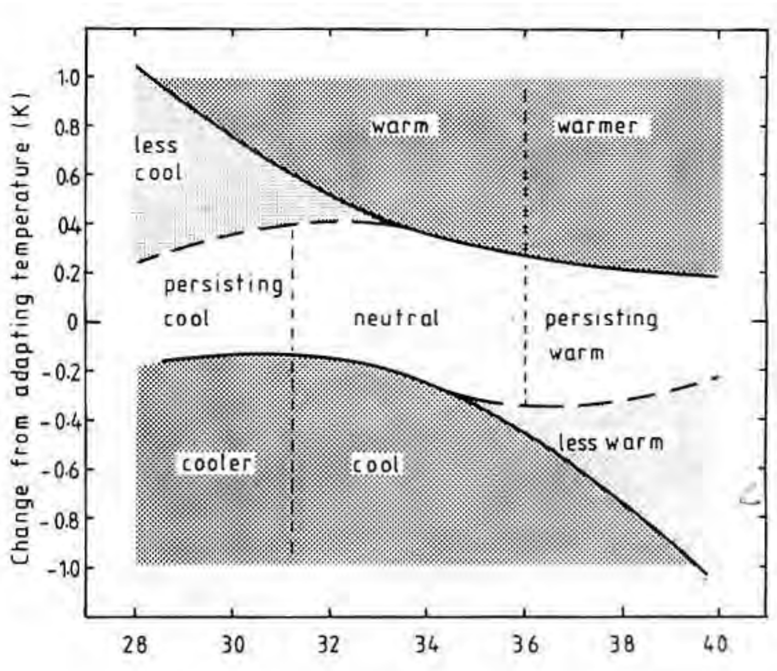

Adapting temperature (°C)

Figure 6.18 Just noticeable changes in forearm skin temperature as a function of the adapting temperature. Warm and cool thresholds are shown by the solid curve; the dotted curve is the thresholds for a change in sensation, after McIntyre (1980), original figure from Kenshalo (1970)

There is a neutral zone through which the skin temperature can be changed without producing any temperature sensation. Above and below the neutral zone, a persisting warm or cool is felt.

The range of the neutral zone changes depending on the size of the thermal stimulator and location of body parts (McIntyre 1980). In this figure with the area of 14.4 cm^2 stimulation on the forearm, the neutral zone covers 31 – 36 °C.

The adaptation model calculates the adapting thresholds. Based on Kenshalo's study and the results from other researchers as described, we proposed an adaptation model as shown in Figure 6.19. It is a logistic function. The horizontal axis represents skin temperature (T_{skin}), the vertical axis represents the adapting threshold (adapting set points, $T_{skin,set,ad}$). The curve in the figure represents the adapting threshold. Above the curve, a warm sensation is felt, below the curve, a cool sensation is felt.

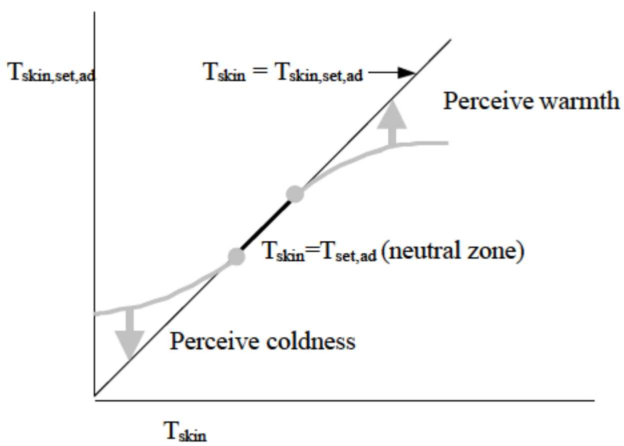

Figure 6.19 Proposed adaptive model

There is a neutral zone as represented by a straight line within two points in the curve. Same as Kenshalo, in this zone, the skin temperature equals the adapting threshold so the difference between the skin temperature and its adaptive set point is zero (following the 45° line), and sensation is neutral. The two points are the limits of the neutral zone. Beyond them, the skin temperature thresholds still adapt, but to a level less than the skin temperature change. In these two regions, there exists a difference between skin temperature and its adaptive threshold so a cool or warmth sensation exists. These regions are similar to the regions of "persisting cool" or "persisting warm" in Kenshalo study (Figure 6.18).

As for the two limits of the neutral zone, we applied skin temperatures measured under neutral conditions from our tests and the data provided by Olesen and Fanger (Olesen and Fanger 1973). The skin temperature in our tests is about 1°C higher than the skin temperature measured by Olesen and Fanger. Since both skin temperature were obtained when people felt neutral, we know that the two skin temperatures belong to the neutral zone. Whether they are the limits of the neutral zone is unclear. Because currently there is no information available, we assume that the two skin temperature values are the limits of the neutral zone. In the future, as more data available, we can modify the limits.

The process of determining the coefficients of the adaptation model for each individual body part is presented in Appendix 6.1. The results listed in Table 6.1 include the effect of the adaptation adjustment. To use the regression results in Table 6.1, it is necessary to first find the adaptive set point. The adaptive set point can by found by using the previous two minutes' average skin temperature, finding the adaptive set point for that temperature in Table A6.3.1 of Appendix 6.1, and applying the adaptive set point to the skin set points in Table 6.1.

6.2.2 Dynamic model for local sensation in transient conditions

The local sensation model in transient conditions is described as follows:

$$\text{Local Sensation} = \text{Sensation}_{static} + \text{Sensation}_{dynamic} \quad \text{Eq. (6.4)}$$

The static portion ($\text{Sensation}_{static}$) of the equation is the steady-state model as presented in Table 6.1. A dynamic portion ($\text{Sensation}_{dynamic}$) is added to the steady state model to predict local sensation in transient conditions. In order to perform the regression analysis to derive this dynamic portion, we first predicted the static portion of thermal sensation based on local skin and mean skin temperatures. Then we subtracted the static model's predicted votes from the actual votes during transient test conditions and performed the regression between the residuals with the rates of change of skin temperature and core temperature. This resulted in the dynamic portion of the local sensation model (Table 6.2). The reason that we used the derivative of core temperature instead of mean skin temperature is explained in Chapter 6.2.5.

The regression is separated into two parts for positive and negative derivatives of skin temperature. A positive derivative means that the body part is experiencing local heating, and a negative derivative means that the body part is experiencing local cooling. We know that people respond to cooling and heating differently, and the response to cooling is much stronger than the response to heating. This is confirmed in our test data. To capture the difference, we performed the regressions separately for positive and negative derivatives, and the regression coefficients are provided for the positive and negative derivatives of skin temperature separately. In the models shown in Table 6.2, $dT_{local\ skin}/dt^{(+)}$ is used when $dT_{local\ skin}/dt>=0$, the local skin temperature is increasing, $dT_{local\ skin}/dt^{(-)}$ is used when $dT_{local\ skin}/dt<=0$, local skin temperature is decreasing.

When the derivative of skin and core temperature is zero, the body is in a steady-state condition. The dynamic portion is zero, and the local sensation is predicted by the steady- state model.

Table 6.2 Dynamic model as a function of the derivatives of skin and core temperatures

Segment	Regression Equation of Dynamic Section ($dT_{back}/dt^{(-)}$ unit, °C/second)	Actual vs. Predicted Sensation	R^2
Back	$Sensation_{dynamic} = 88\ dT_{back}/dt^{(-)} + 192\ dT_{back}/dt^{(+)} - 4054\ dT_c/dt$ (Without the dynamic term, R2=0.22)	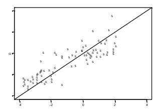	0.73
Chest	$Sensation_{dynamic} = 39\ dT_{chest}/dt^{(-)} + 136\ dT_{chest}/dt^{(+)} - 2135\ dT_c/dt$	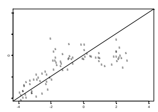	0.61
Face	$Sensation_{dynamic} = 37\ dT_{face}/dt^{(-)} + 105\ dT_{face}/dt^{(+)} - 2289\ dT_c/dt$	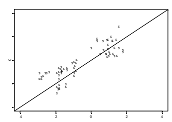	0.74
Hand	$Sensation_{dynamic} = 19\ dT_{hand}/dt^{(-)} + 46\ dT_{hand}/dt^{(+)}$	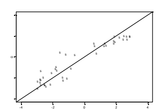	0.90
Foot	$Sensation_{dynamic} = 109\ dT_{foot}/dt^{(-)} + 162\ dT_{foot}/dt^{(+)}$	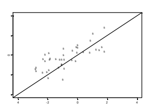	0.55
Neck	$Sensation_{dynamic} = 173\ dT_{foot}/dt^{(-)} + 217\ dT_{foot}/dt^{(+)}$ (Small change, larger coefficient – different from hand. We can show the figure too)	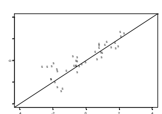	0.80
Breathing	$Sensation_{dynamic} = 68\ dT_{cheek}/dt^{(-)} + 471\ dT_{cheek}/dt^{(+)}$	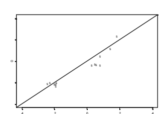	0.92
Head	$Sensation_{dynamic} = 543\ dT_{forehead}/dt^{(-)} + 90\ dT_{forehead}/dt^{(+)}$	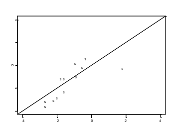	0.64

Table 6.2 (continued) Dynamic model as a function of the derivatives of skin and core temperatures

Segment	Regression Equation of Dynamic Section ($dT_{back}/dt^{(-)}$ unit, °C/second)	Actual vs. Predicted Sensation	R^2
Pelvis	$Sensation_{dynamic} = 75\ dT_{thigh}/dt^{(-)} + 137\ dT_{thigh}/dt^{(+)} - 5053\ dT_c/dt$	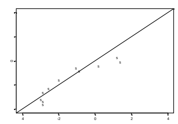	0.86
Lower Arm	$Sensation_{dynamic} = 144\ dT_{larm}/dt^{(-)} + 125\ dT_{larm}/dt^{(+)}$	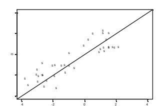	0.77
Upper Arm	$Sensation_{dynamic} = 156\ dT_{uarm}/dt^{(-)} + 167\ dT_{uarm}/dt^{(+)}$ (R2=0.74)	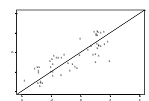	0.74
Lower Leg	$Sensation_{dynamic} = 206\ dT_{lleg}/dt^{(-)} + 212\ dT_{lleg}/dt^{(+)}$ (R2=0.85)	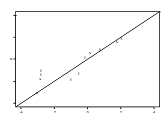	0.85
Thigh	$Sensation_{dynamic} = 151\ dT_{thigh}/dt^{(-)} + 263\ dT_{thigh}/dt^{(+)}$	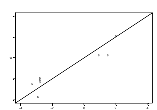	0.94

During a sudden environmental change, these derivatives, especially the one for skin temperature, can be very large. Therefore the dynamic sensation contribution is large. This explains the overshooting response shown in our test results (presented in Chapter 5). The large dynamic sensation contribution also explains the sudden warm or cold feeling when people move between very different environmental conditions (e.g., entering an air-conditioned room from the warm outdoors).

We saw in Chapter 5 that the core temperature responds to local cooling, especially of most influential body parts, with an immediate increase. This is reflected in the negative coefficients for the derivative of the core temperature for the three highly influential segments (back, chest, and pelvis). The negative coefficient for the derivative of the core temperature also appear for face. For other segments, the influence of the derivative from core temperature is not significant and therefore the coefficients are zero.

6.2.3 The complete local thermal sensation model

The complete local sensation model for a body part under transient condition is presented in Eq. (6.5).

$$S_{local} = 4\left(\frac{2}{1 + e^{-C1(T_{skin,local} - T_{skin,local,set}) - K1\left[\left(T_{skin,local} - \dddot{T}_{skin}\right) - \left(T_{skin,local,set} - \dddot{T}_{skin,set}\right)\right]}} - 1\right) + C2_i \frac{dT_{skin,local}}{dt} + C3_i \frac{dT_{core}}{dt} \qquad \text{Eq. (6.5)}$$

It combines the steady state and dynamic local thermal sensation models. When the derivatives of skin and core temperatures are zero, the model predicts thermal sensation in steady state conditions. This equation is provided for every body part.

Our approach is similar to the approach applied by Fiala (Fiala 2002) in developing a sensation prediction model. Both models predict the whole body thermal sensation in transient condition from skin and core temperatures and their derivatives.

Fiala found that the derivative of the core temperature is not significant, so the dynamic term is calculated by the derivative of the skin temperature only. Fiala's model is as follows:

$$DTS = 3\tanh\left[a\left(T_{mean} - T_{mean,set}\right) + g + \left(0.11\frac{dT_{mean}}{dt}^{(-)} + 1.91e^{-0.681t}\frac{dT_{mean}}{dt}^{(+)}_{\max} \right)\left(1+g\right)^{-1} \right]$$

where a is 0 and 1.08 for mean skin temperature above and below its set point, ($\overline{T}_{skin}$ - $\overline{T}_{skin,\,set}$) < 0 and ($\overline{T}_{skin}$ - $\overline{T}_{skin,\,set}$) > 0, respectively; d$\overline{T}_{skin}$ /dt$^{(+)}$ = 0 for d$\overline{T}_{skin}$ /dt > 0 and d$\overline{T}_{skin}$ /dt$^{(-)}$ = 0 for d$\overline{T}_{skin}$ /dt < 0. g is calculated by:

$$g = 7.94e^{\left(\frac{-0.902}{(T_{hy} - T_{hy,set}) + 0.4} + \frac{7.612}{(T_{meann} - T_{mean,set}) - 4} \right)}$$

Where DTS represents for thermal sensation under transient condition (Dynamic Thermal Sensation), T_{hy} represents for the hypothalamus temperature.

The difference between the two models is that Fiala's model predicts thermal sensation for the entire body in a uniform environment, and our model predicts local sensation in a potentially asymmetrical environment. Fiala's model was developed based on the subjects' votes in early studies carried out at Kansas State University (Gagge et al. 1967, Gagge et al. 1969, Nevins et al. 1966, Rohles et al. 1966, Rohles 1970, McNall et al. 1967), which did not involve physiological measurements; instead, he used his physiology model to predict skin and core temperatures from environmental variables measured in the tests. Fiala's regression analysis is therefore based on the votes of human subjects and simulated skin and core temperatures. The correlations are therefore specific to Fiala's physiology model. Our rational model has the ability to express the logical relationships among variables more explicitly.

In our tests we gathered both physiological data (skin and core temperature) and subjective perceptions (sensation and comfort votes), so the model stands alone and is not subject to any physiology model

6.2.4 Local thermal sensation model validation

The Delphi Wind Tunnel test data were used to validate the local sensation models. The Delphi Wind Tunnel test included summer and winter tests. Summer test conditions included air temperature 30, 37.8, 43.3 °C, with and without solar radiation. Winter test conditions included air temperature –6.7, -17.8, -23.3 °C, with and without solar radiation.

The validation was conducted using the data from the period after the subjects went inside the car and started the air-conditioning. This is the most transient period. The validation was conducted for the summer and winter tests separately, each includes 8 tests, and 8 different drivers.

So far the validation was carried out only for the front driver, who experienced more air temperature and flow-rate asymmetry and transients than other passengers. The summer test validation is presented in Figure 6.20, winter in Figure 6.21. The figures show the actual votes (horizontal) to the predictions (vertical). The validation R^2 and the standard deviation of residuals (STDEV) are also included.

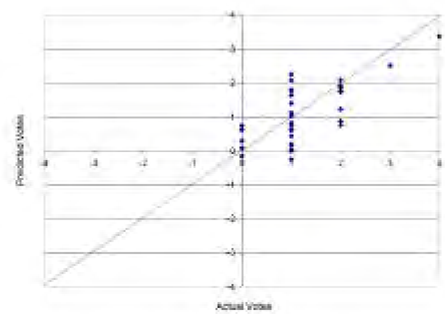

Back, R^2 = 0.34, STDEV=0.68

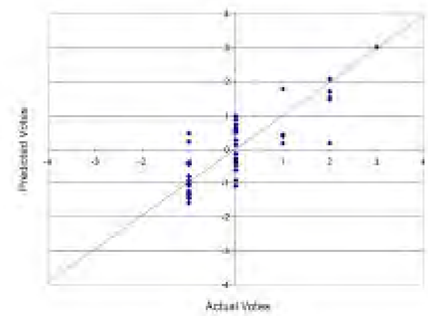

Chest, R^2 = 0.65, STDEV=0.63

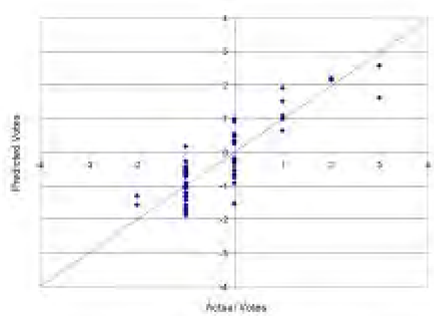

Face, R^2=0.70, STDEV=0.58

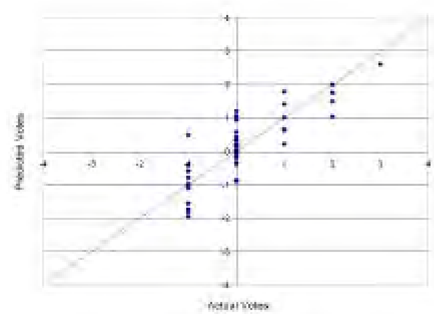

Lower arm, R^2=0.65, STDEV=0.57

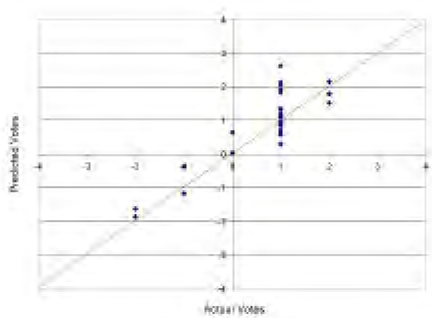

Foot, R^2=0.66, STDEV=0.55

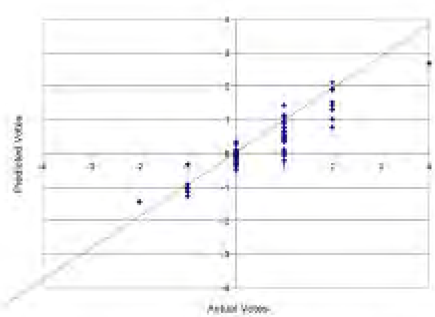

Lower leg, R^2=0.74, STDEV=0.45

Figure 6.20 Validation for Delphi Wind Tunnel summer tests (driver) (continued on next page)

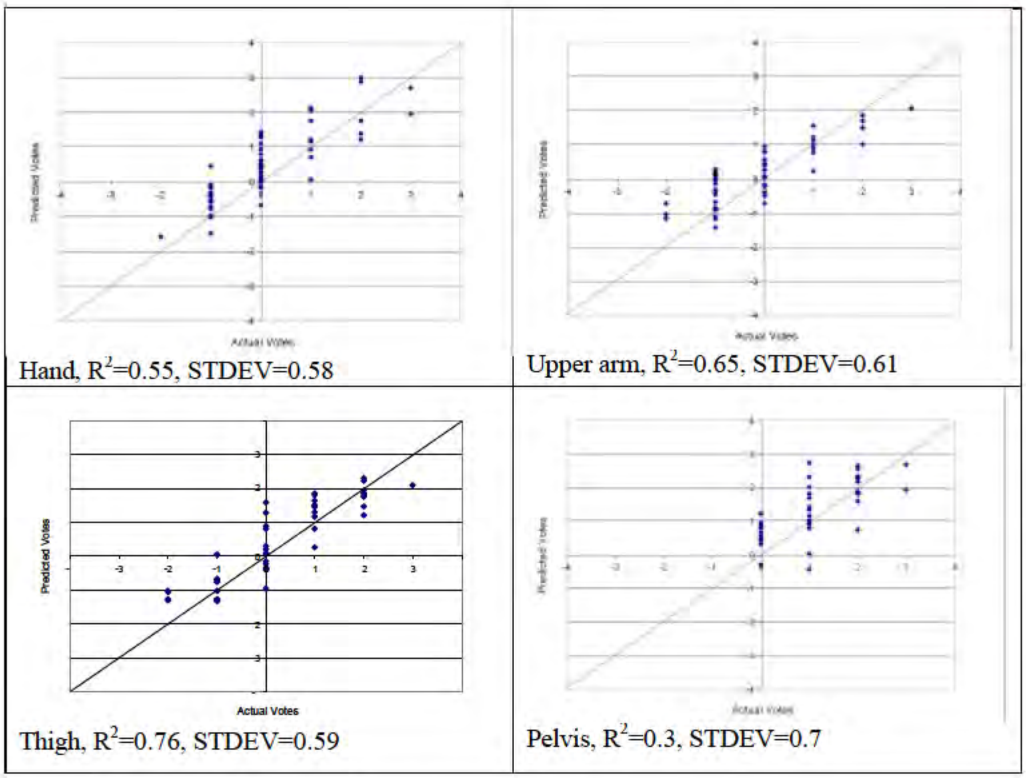

Hand, R^2=0.55, STDEV=0.58

Upper arm, R^2=0.65, STDEV=0.61

Thigh, R^2=0.76, STDEV=0.59

Pelvis, R^2=0.3, STDEV=0.7

Figure 6.20 Validation for Delphi Wind Tunnel summer tests (driver)

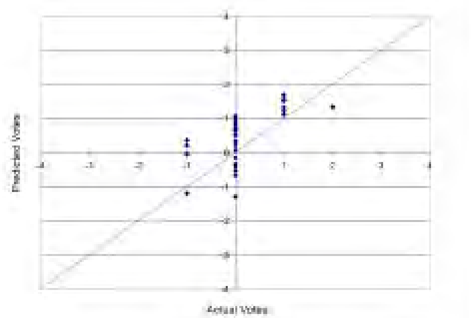

Back, R^2 = 0.32, STDEV=0.61

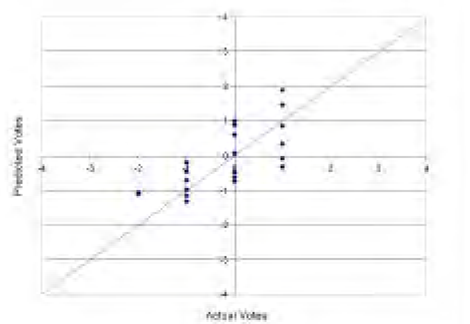

Chest, R^2 = 0.36, STDEV=0.75

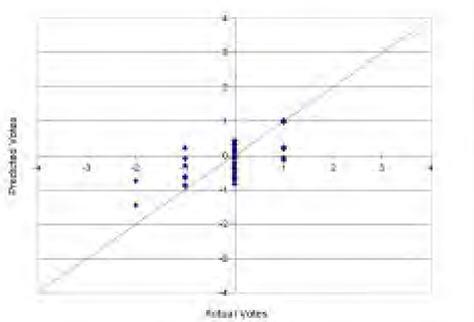

Face, R^2=0.40, STDEV=0.62

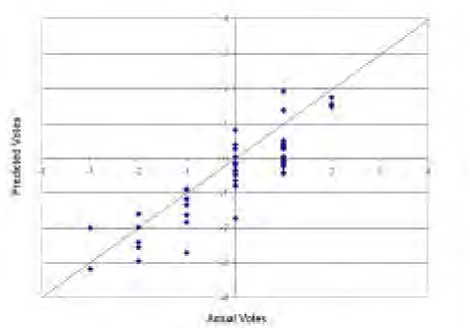

Lower arm, R^2=0.58, STDEV=0.62

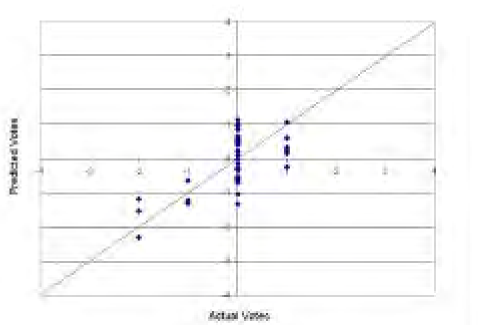

Foot, R^2=0.3, STDEV=0.65

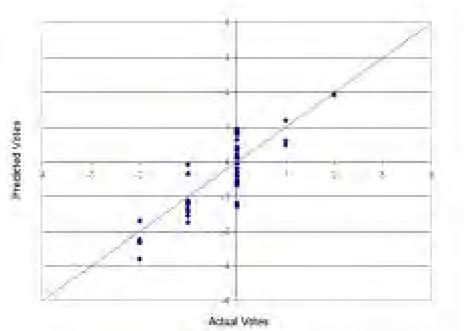

Lower leg, R^2=0.53, STDEV=0.57

Figure 6.21 Validation for Delphi Wind Tunnel winter tests (driver) (continued on next page)

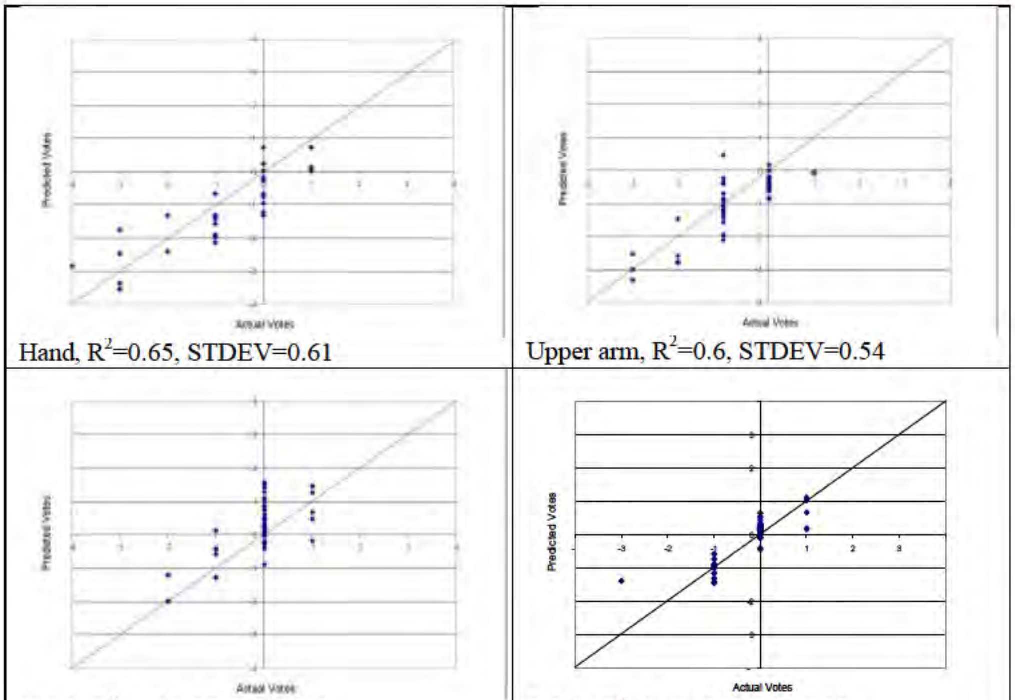

Hand, R^2=0.65, STDEV=0.61

Upper arm, R^2=0.6, STDEV=0.54

Thigh, R^2=0.36, STDEV=0.6

Pelvis, R^2=0.69, STDEV=0.38

Figure 6.21 Validation for Delphi Wind Tunnel winter tests (driver)

The prediction does not explain some actual votes well. A substantial reason is that the Delphi votes were 1-unit increment. So their actual votes were not very sensitive to physiological changes. We see this from the figures. Corresponding to one actual vote, there exist several skin temperatures and the rates of their change, which would result in different predictions.

The validation for summer is better than for winter. Some of the thermocouples were loose, not taped on the skin well. The loose thermocouples were more influenced by the environmental conditions in winter condition than in summer condition. So the thermocouple readings are less accurate in winter.

In general, the local sensation model predicts the actual votes well.

6.2.5 Use of mean skin temperature ($\overline{T}_{skin}$) and $\frac{dT_c}{dt}$

In our local sensation model, we use mean skin temperature ($\overline{T}_{skin}$) as the representative of the whole body thermal state for the static sensation portion and the derivative of core temperature ($\frac{dT_c}{dt}$) as the representative of the whole-body response for the dynamic sensation portion. The following explains why.

We found that the body core temperature is very responsive, increasing during transient local cooling especially for the most influential bodypart local cooling. When individual body parts are heated, the core temperature response is not as predictable, but it generally exhibits a decrease. We consider that Local Sensation = $Sensation_{static}$ + $Sensation_{dynamic}$ as shown in Eq. (6.4). For the dynamic local sensation, we use the derivative of core temperature and local skin temperature as independent variables. We did not use the derivative of the mean body temperature to calculate the dynamic portion, for two reasons:

- The derivative of $\overline{T}_{skin}$ is an average of several local sensations. If the sensations of some body parts grow warmer while others colder, these changes are cancelled out in the averaged derivative of mean skin temperature.
- Skin temperature measurement data inevitably show noise, which may not significantly influence the absolute skin temperature but has a huge impact when derivatives are calculated. As a result, we smoothed skin temperature data in order to get a smoothed derivative. (Smoothing of data is described in Appendix 6.4). Some estimations were introduced due to this smoothing step. In contrast, measured core temperatures show very

smooth responses during transient conditions, so these results are much cleaner; nonetheless, we went through one step to smooth core temperature data when calculating its derivative.

For the static portion of local sensation, the situation is different. The absolute values of subjects' individual core temperatures showed significant differences of about 0.4°C from morning to afternoon. Females' core temperature also changes in relation to menstrual periods. Although we made an effort to categorize core temperatures (according to subject's conditions, time of day, etc. Appendix 6.2), our model needs further development and verification with additional data. Another feature of core temperature is that during short- time cooling applications, the core temperature increases, but for long-term cooling applications (e.g., during immersion in cold water), it decreases. Our tests were not long enough to characterize this feature. Xu and Tikuisis et al. (Xu, Tikuisis et al. 2003) did a cold-water immersion test and showed that the core temperature initially increased and then, about 20 to 30 minutes later, started to decrease. The water temperature was 8°C, much colder than temperatures in our tests.

Mean skin temperature does not increase and decrease like core temperature. If there is no significant metabolic activity, core temperature and mean skin temperature correlate well. This means that, when one is hot, both core and mean skin temperatures are high, and both represent the whole-body thermal state. Core temperature and mean skin temperature behave in opposite fashion in situations such as when people exercise vigorously in cold weather; skin temperature is low because of the cold air, but core temperature is high because of the exercise. In this case, core temperature is a better predictor of overall body thermal state. Under our stable test conditions, subjects are sedentary, so we can use either of the two.

There are several other reasons that we chose mean skin temperature to represent overall body thermal state:

- mean skin temperature is more easily obtained during experiments than core temperature, so our model can be widely applied in the future.
- mean skin temperature information is readily available in the literature for use in validating or applying our model; core skin temperature is rarer in the literature.
- when we study the local sensation of extremities, mean skin temperature may better represent overall thermal status than core temperature; e.g., when a subject is cold, his/her extremities will vasoconstrict before the core temperature changes, resulting in a lower mean skin temperature.

The use of core versus mean temperature to represent whole-body thermal state is controversial. Mower (Mower 1976) suggests that sensation does not depend on internal temperature but that pleasure (comfort) does. Cabanac believes pleasure does not come from skin sensation but only from internal temperature (Cabanac 1971). However, Marks and Gonzalez argue (Marks and Gonzalez 1974) that the main goal of thermoregulation is to keep core temperature constant and that much behavior thermoregulation (e.g., putting on additional clothing) takes place at constant internal temperatures; it would be a disadvantage to wait until core temperature changes to get the signal that represents overall thermal state. Therefore, mean skin temperature is a better indicator of whole-body thermal state.

We use the seven locations proposed by Hardy (Hardy and DuBois 1938) to calculate mean skin temperature; this method is widely used by researchers, so our model can be easily applied by others. It also involves relatively few measurement points.

The limitation of our model is that it does not account for metabolic change resulting from activity. For example, as noted above, when person exercises strenuously in cold weather, s/he has a lower mean skin temperature but a higher core body temperature; this phenomenon is addressed in the Chapter 7.3.1 at the end of this thesis.

6.3 Local thermal comfort model

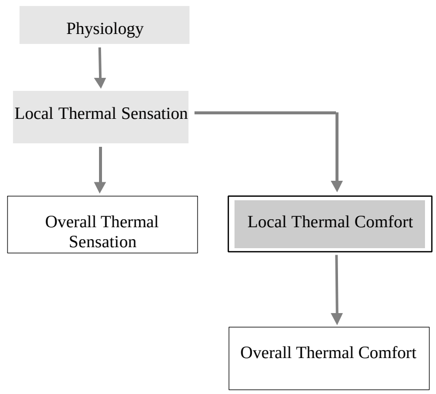

Thermal sensation probably reflects the pure response of thermoreceptors; thermal comfort describes the synthesized human feeling about the body's thermal state (McIntyre 1980). This makes thermal comfort more difficult to predict. Local comfort is influenced by local sensation and overall sensation. For example, the evaluation of a cold local body part is different when the whole body feels warm or cold,.

6.3.1 Results from literature and our tests

In a uniform environment, as the overall sensation moves away from neutral, the comfort level reduces. This relationship is presented in Figure 6.22 (transcribed from a figure by McIntyre (McIntyre 1980) using data from Gagge (Gagge, Stolwijk et al. 1967)).

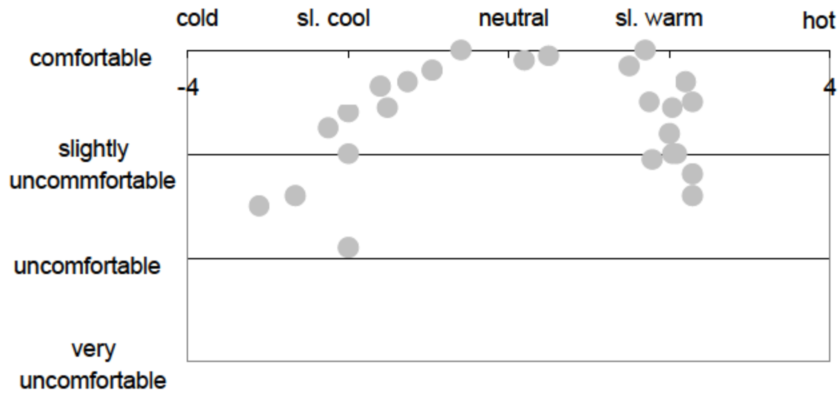

Figure 6.22 Overall sensation vs. comfort. Comfort is reduced as sensation further away from neutral (Gagge, Stolwijk et al., 1967)

When the whole body thermal state is different from a local thermal state, the comfort assessment of the local part is affected. Chatonnet and Cabanac (Chatonnet and Cabanac 1965) and Cabanac (Cabanac 1969) systematically changed the core temperature of human subjects by immersing them in baths of various temperatures (Figure 6.23). When the subjects were hypothermic, warm stimuli applied to the hand were perceived as pleasant, and cold stimuli were perceived as unpleasant. The opposite responses were observed in hyperthermic subjects. These experiments indicate that local thermal comfort is influenced by both core and skin temperatures; when the core temperature is cold, a warm hand is perceived as more comfortable than it would be if the body core temperature were not so cold, and the same applies when core temperature is warm and the hand is exposed to cool stimuli. Comfort is correlated with thermoregulatory needs. When an action satisfies a need, the action is perceived as pleasurable. Cabanac called this "sensory pleasure" (Cabanac 1992), and the process to induce the pleasure "alliesthesia", a word that he coined to describe that a given stimulus can arouse pleasure or displeasure according to the thermal state of the body. Because the primary goal of thermoregulation is to keep core temperature constant, it is clear why an action (e.g., putting a hand in warm water) can be perceived as either comfortable or uncomfortable depending on the body's thermal state.

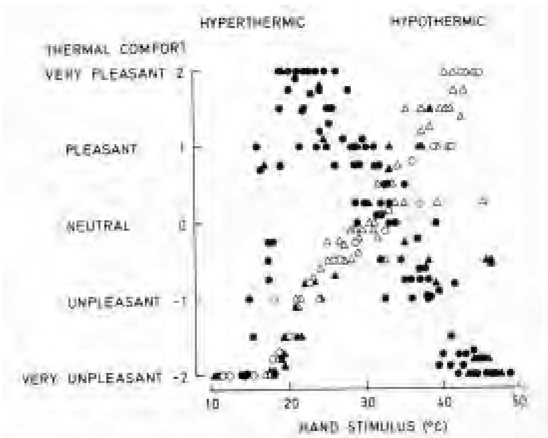

Figure 6.23 Hand comfort depends on whole body thermal status (Cabanac 1969)

Even if the body is cold, an increasingly hot local sensation will eventually be perceived as uncomfortable (Figure 6.23).

Mower (Mower 1976) (Figure 6.8) and Attia (Attia and Engel 1981, Attia 1984) (Figure 6.24) expanded Cabanac's study by adding stimuli to other body parts and including the neutral body thermal state. The observed local comfort for the body parts in that study all show a similar X-shaped pattern for hyperthermic and hypothermic thermal states. The horizontal axis is the thermode temperature, which represents the local skin temperature. Attia applied a thermode of 5 x 2.75 centimeters in size as a thermal stimulus. Mower put the entire hand into different water buckets.

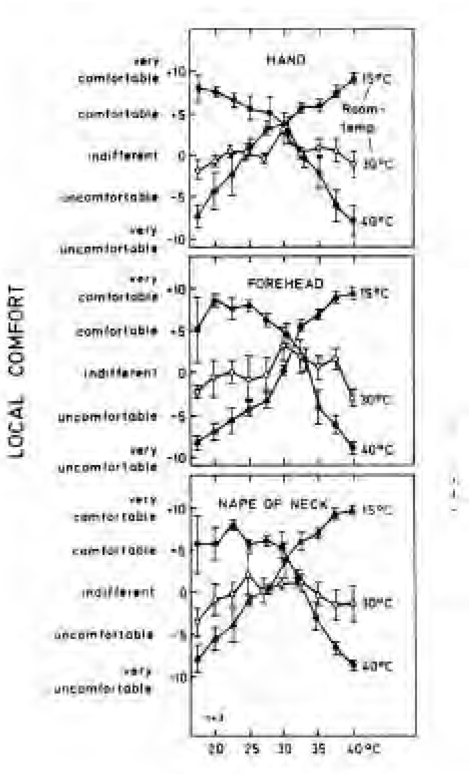

Figure 6.24 Local comfort vs. local skin temperature and whole body thermal states (Hildebrandt, Engel et al. 1981), data from Attia and Engel (Attia and Engel 1981)

An important observation of Mower and Attia's studies is that, under neutral conditions (30°C room air, 0.05 clo in Attia's study), the most comfortable vote recorded on his thermal comfort scale is close to a vote of "indifferent". Local cooling or heating produced great comfort only in hyper- and hypothermic conditions, respectively. In neutral thermal conditions, humans are less aware of the thermal environment and don't feel strong comfort/pleasure responses. Maximum pleasure is felt primarily while discomfort is being relieved or partially relieved.

Cabanac, Mower, and Attia's applied a thermal stimulus for a very short time, 3 seconds in Cabanac and Mower's studies, 10 seconds in Attia's study. The local comfort votes shown in Figure 6.8, 6.23, and 6.24 were obtained under transient conditions.

Issing and Hensel (Issing and Hensel 1981) used a constant stimulus in a gradually varying environment. They applied thermodes of 75 cm^2 to forehead, abdomen, and foot of twelve subjects. The thermodes were kept at various constant temperatures throughout the entire experiment, while the room was maintained at 12°C for 30 minutes and then continuously increased to 45°C in 45 minutes, which resulted different average skin temperatures. The local comfort was accessed in certain intervals. Their local comfort votes were obtained under relatively stable condition because the local stimulus was constant. The purpose of their study was to compare the static local thermal sensation produced by the constant local thermal stimulus with local and overall thermal comfort.

The results are shown in Figure 6.25. The horizontal axis is the thermode temperature, which is same as the local skin temperature. The skin temperatures are marked inside the figure. It is obvious that with the same thermode temperature (i.e. 38°C), the local comfort is highly depend on the average skin temperature.

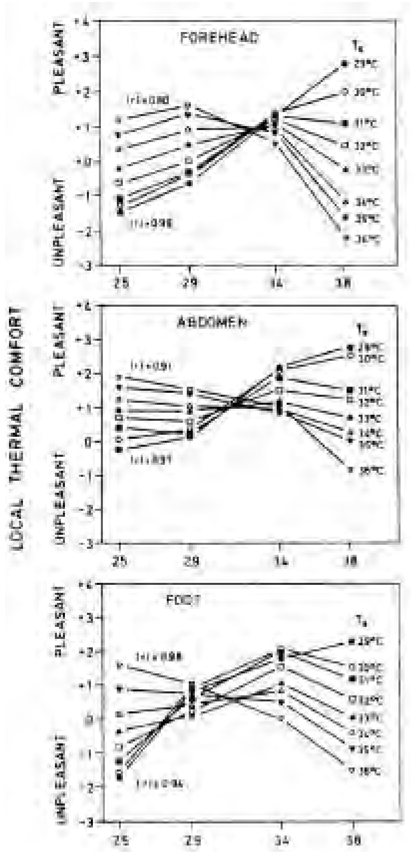

Thermode temperature (°C)

Figure 6.25 Local comfort as a function of static temperature of forehead, abdomen, and foot at various skin temperature (T_s) (Issing and Hensel 1981)

The results shown in Figure 6.25 are similar to the results by Mower (Figure 6.8) and Attia (Figure 6.24). We can assume that one of the mean skin temperatures in the middle (say T_s = 33°C represented by solid triangles) represents a neutral whole body. The maximum local comfort when applying a warm or cold thermode to the neutral whole body is lower than the maximum comfort when the body was cold or warm.

That means for both transient and stable conditions the relationships between local sensation, whole body thermal state, and local comfort are similar.

Another test by Issing and Hensel (unpublished, presented by Hensel (Hensel 1982)) put the subjects' feet into water baths from 20 – 45°C, while the subjects' whole bodies were cold, with a mean skin temperature near 29°C (room temperature at 12°C, naked subjects). Their tests show very similar results to the studies described above: for a cold whole body, the cooling of the foot was perceived as uncomfortable, while warming of the foot was perceived as very comfortable. Unlike Mower and Attia who applied the small thermode to their subjects, Issing and Hensel put the entire foot into the water bath, which is similar to Cabanac's approach of putting the subjects' entire hand into the water bath. Therefore, the results from Issing and Hensel are similar to Cabanac's hand cooling and warming tests that at very high foot temperatures the foot felt increasingly unpleasant in spite of general cold discomfort (Figure 6.26). They did not perform this test with a warm whole body.

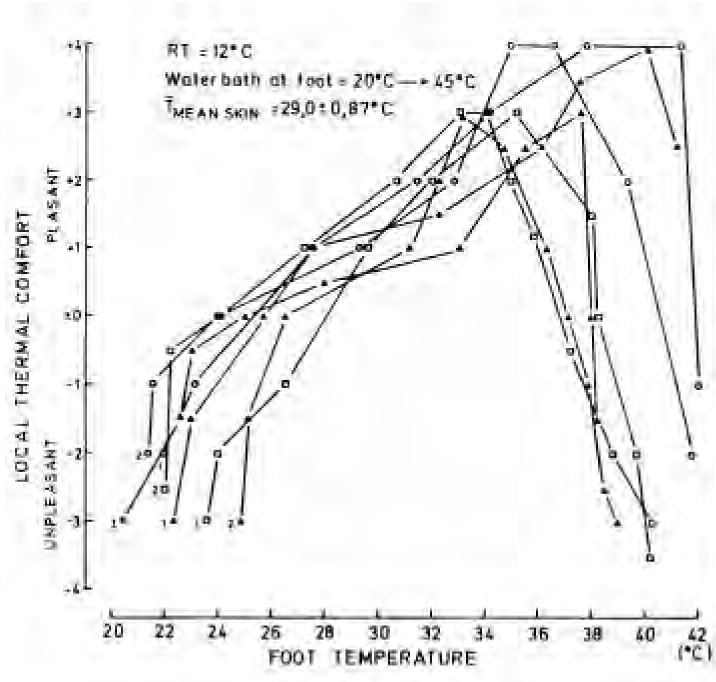

Figure 6.26 Local thermal comfort as a function of foot skin temperature as a mean skin temperature of 29°C. From Issing and Hensel, unpublished, copied from Hensel (Hensel 1982)

Figure 6.27 shows some examples from our tests in which the correlation between local sensation and comfort is similar to that found in previous studies cited above: maximum comfort shifts to the left or right based on the whole-body thermal state, maximum comfort is higher than the comfort in neutral condition (when local sensation is zero). These examples also show that when the whole body is cold, heating an individual body part creates comfort (triangles) and cooling an individual body part produces discomfort (open circles), as shown in the figures for hand and foot.

The data are taken from the last vote of one local cooling and heating applications (as described in Chapter 5.3). We consider these data as representing stable condition.

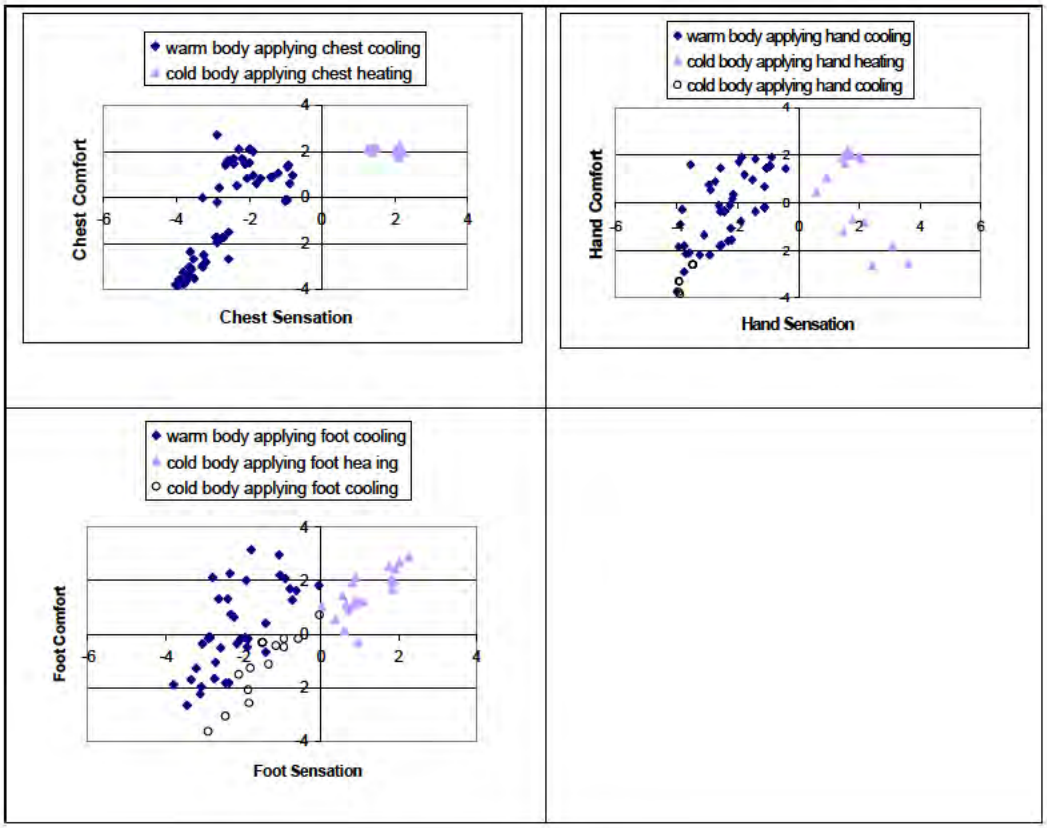

Figure 6.27 Local comfort vs. local sensation and whole body thermal states

Our test results differ from Mower's in that our subjects' comfort votes moved to the "uncomfortable" level when the sensation votes were between cool (-2) and cold (-3) or between warm (+2) and hot (+3). In Mower's study, votes never reached the uncomfortable level. For example, in our tests, when local sensation was close to –2.5 for the chest and to –3 or +3 for the hand, the local comfort vote dropped into the negative range (uncomfortable); Mower did not observe this drop in comfort. However, Cabanac's results (Figure 6.23) and Issing and Hessel (Figure 6.26) show similar drops at the extreme conditions near the ends of their scales.

Another difference between our study and both Cabanac's and Mower's is that the maximum comfort recorded in our tests is not as high as in Cabanac and Mower's studies. For the differences mentioned above, we believe the reasons are :

- We applied the cooling to entire body parts, which comprise much larger areas than the thermode-size areas (5 cm x 2.75 cm) stimulated in Mower's study. Therefore the uncomfortable feeling shown in our tests may be caused by the large stimulation areas, which produce stronger stimulations.
- We applied large volumes of air at relatively low temperature (14°C and 23 °C) to relatively large areas, so comfort levels dropped rapidly. If we had applied relatively smaller amounts of cooling, we might have seen higher peaks in comfort.
- Our subjects are not in or near extreme thermal states, i.e., hypo- or hyperthermia, so during cooling for example, our subjects likely experienced cooling as uncomfortable sooner than would have been the case of the subjects had been hypothermic as they were in Cabanac and Mover's studies. We did not experiment with applying heat to individual body parts when the entire body was hot.

Moreover, under neutral conditions, our subjects voted 2 (comfortable) but not 4 (very comfortable). This result is the same as in the Mower (Mower 1976), Issing and Hensel (Issing and Hensel 1981), and Hildebrand's (Hildebrandt, Engel et al. 1981) studies. Cabanac did not study neutral conditions.

Based our test data (Figure 6.22) and studies from Cabanac, Mower, Attain, and Issing as presented above, we propose the following hypothetical local thermal comfort model.

6.3.2 Key hypotheses for the local comfort model

1. Local thermal comfort is a piecewise linear function of local thermal sensation. As local sensation moves from neutral toward very hot (+4) and very cold (–4), local comfort moves toward very uncomfortable (–4). See Figure 6.7.

2. The local sensation at which maximum comfort is felt shifts with the overall sensation. The warmer (or cooler) the overall sensation, the cooler (or warmer) the local sensation at which the maximum local comfort is felt. See Figure 6.9.

3. Maximum comfort is a function of overall sensation. The warmer (or cooler) the overall sensation, the greater the maximum comfort in response to local cooling (or heating).

4. Maximum comfort levels are asymmetrical (see Figure 6.10) on the cool and warm sides. Some body parts feel comfortable when warmed while overall sensation is cool but do not feel comfortable when cooled while overall sensation is warm. In our tests, for example, we noticed that cooling of the breath intake air feels pleasant when subjects feel warm overall, but warming of breath intake air does not feel comfortable in any of our tests. Subjects also experience a warm pelvis region as pleasurable when the overall body is cold but do not experience a cool pelvis as pleasurable or comfortable when the overall body is warm.

5. When local sensation = 4 (very hot) or –4 (very cold), local comfort = –4 (very uncomfortable).

The proposed model is an asymmetrical saddle as shown in Figure 6.28. The five key hypothesis are marked in the figure.

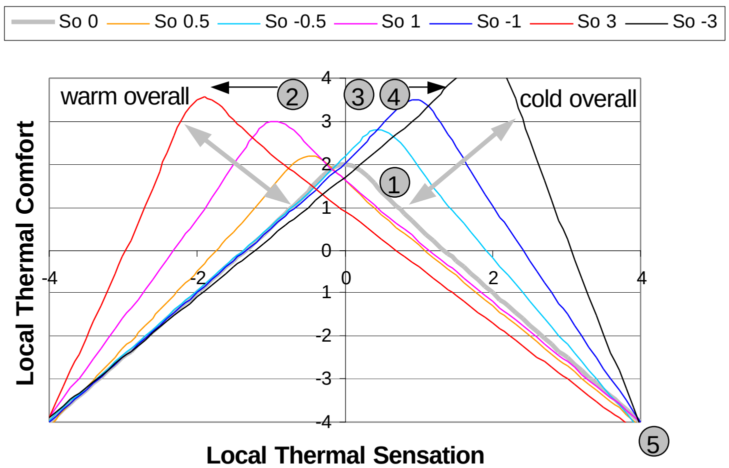

Figure 6.28 The local thermal comfort model

We spent considerable time examining the zero local sensation point, the crossover between warm and cold. We were concerned about whether the neutral overall contour (So = 0) should be above or below the contours for warm or cold overall body at this crossing point. We initially expected the neutral contour to cross below the others, but the data did not show a clear effect like this. When examining the results from other researcers (Figure 6.8, Figure 6.24), we see that at the crossing point of the hyperthermia and hypothermia body thermal states, it is unclear whether local thermal comfort is higher or lower than the local comfort under neutral condition. The study by Mower (Figure 6.8) shows that local comfort is slightly higher in the neutral condition than in hyper- or hypo-thermic states. The examples by Attia (Figure 6.24) show the local comfort in neutral condition to be slightly lower than hyper- or hypo-thermic states. In general, the local comfort contours in Mower and Attia's data at the crossing point are quite close. In our proposed model (Figure 6.28), the local comfort contours in the middle near the crossing point are also close, with some higher and some lower than the neutral condition local comfort.

The following subsection explains the mathematical definition of the model based on local and overall sensation data.

6.3.3 Mathematical description

The primary challenge is to provide a mathematical description of the two-part linear model that changes slope and magnitude at a location depending on overall sensation.

This requirement can be satisfied by a logistic function that provides two values with a transition range in between. The following example shows how the logistic function acts on the linear model.

Let us assume the following basic logistic function with arbitrary constants:

$$y = \frac{a}{e^{c(x+offset)} + 1} - b \qquad \text{Eq. (6.6)}$$

When the exponential term (x) is very large, y equals –b. The value –b is the right- hand side linear model slope. When x is negative and very small, the exponential term is near zero and y is found by: (a – b). The logistic function not only allows the sign to switch (positive vs.

negative), but also provides two different values, which correspond to the different slopes for the linear function. The exponent c controls the speed of the slope transition from –b to a – b and allows the two curves to meet in a curve rather than a sharp angle. The smaller the value, the more gradual the curve.

Thus, the proposed model is a linear model modified by a logistic function. We call it a logistic-adapted linear model. The logistic function provides two different slopes for the linear model.

$$Local\ Comfort = LogisticFunction\,(Sl + offset) + MaxComfort \qquad \text{Eq. (6.7)}$$

$$Local\ Comfort = \left(\frac{a}{e^{5(Sl+offset)}+1} + right\ slope\right)(Sl + offset) + MaxComfort \qquad \text{Eq. (6.8)}$$

When we change the ‘offset’ value, the maximum comfort shifts left or right. When we change the ‘MaxComfort’, the maximum value rises up or down. These two changes are shown in the graph in Figure 6.28. When we change the ‘right slope’ and ‘a’ values, we change the left (a - right slope) and right side slopes of local sensation. Figure 6.29 shows how the logistic function acts on the linear function in the logistic-adapted linear model.

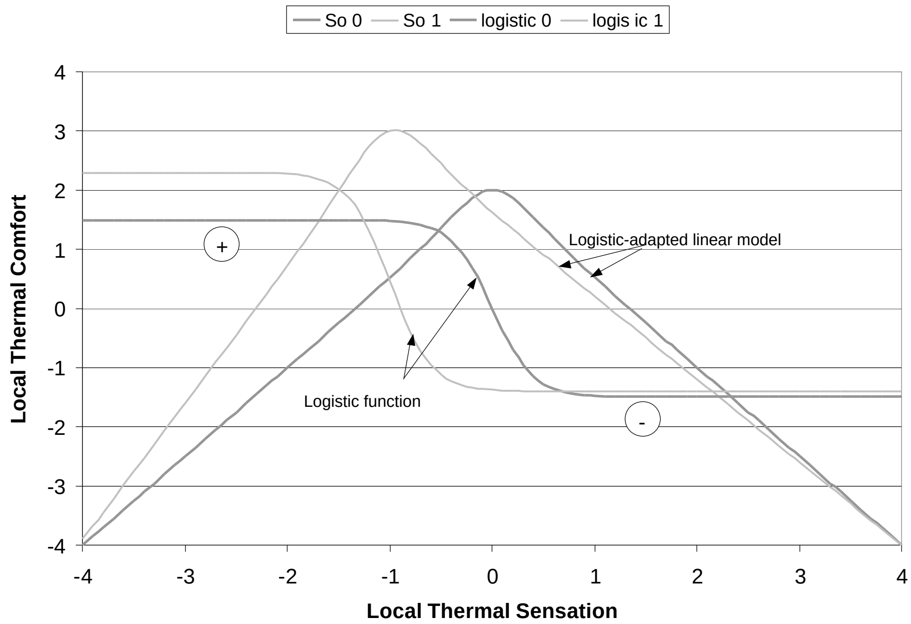

Figure 6.29 Logistic function acts on the linear function

Figure 6.30 demonstrates how the model works to create the saddle.

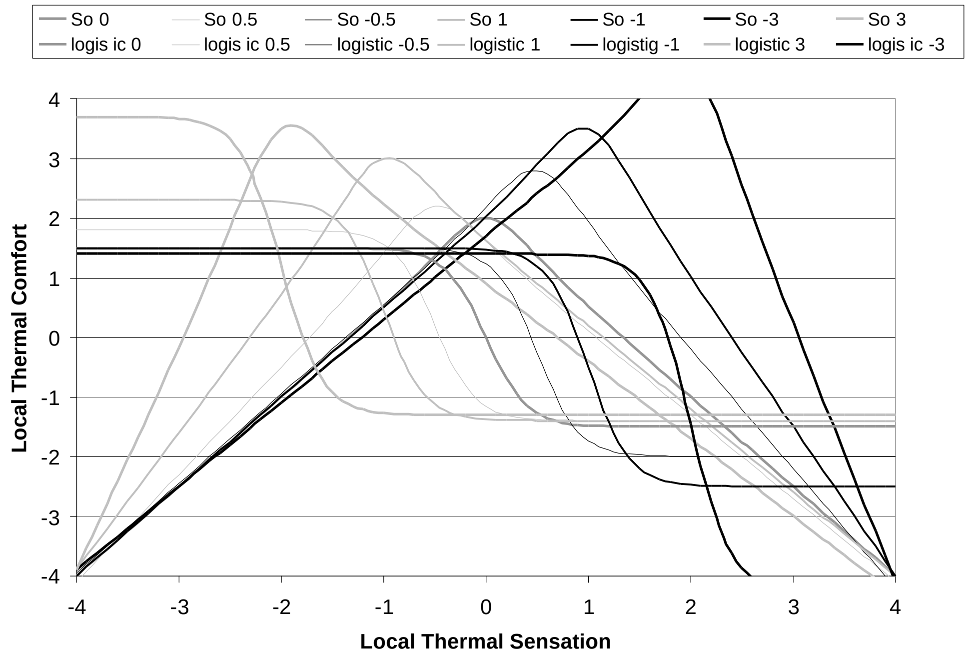

Figure 6.30 Logistic function acts on the linear function to create saddle

Offset: Based on hypothesis 2 above, local sensation at the maximum comfort point shifts based on overall sensation. Therefore, the offset is a function of overall sensation: the warmer the overall sensation, the more the shift to a cooler local sensation, and vice versa. We have assumed a simple linear model for this effect (offset = C3 x So).

MaxComfort: Based on hypothesis 3 above, maximum comfort is a function of overall sensation: the warmer (or cooler) the overall sensation, the greater the comfort produced by local cooling (or heating). We have again assumed a linear model (MaxComfort = C6 + C7 abs (So)). Based on hypothesis 4, the increases are asymmetrical for warm and cool overall sensation, so the coefficients should be separately presented, MaxComfort = C6 + C71 abs (So^-)+ C72 abs (So^+). All three coefficients (C6, C71, and C72) should be positive. This description reflects the fact that great comfort is induced by removing thermal stress.

a and right slope in the logistic function: The logistic function is responsible for the change of the slopes of the linear model. The coefficient "right slope" and the range "D1" in Eq. (6.8), which combines with the right slope to get the left slope, are the function of the overall sensation (So).

a = C1 + C2So

Right slope = C4 + C5 So

Putting the above relations into Eq. (6.8), we get:

$$Local\ Comfort = (\frac{C1 + C2So}{e^{5(Sl+C3So)} + 1} + C4 + C5So)\,(Sl + C3\,So) + C6 + C71\left|So^{-}\right| + C72\left|So^{+}\right|$$

Eq.(6.9)

There are two limits. The linear model has to pass two points (4, -4) and (-4, -4) for the local sensation and local comfort (hypothesis). The maximum comfort happens at x = shift point = -C3 So, y = MaxComfort = C6 + C71 abs (So^-)+ C72 abs (So^+).

So these limits are translated as:

$$Right\ Slope = C4 + C5\,So = \frac{C6 + C71\left|So^{-}\right| + C72\left|So^{+}\right| + 4}{-C3\,So - 4}$$

Eq. (6.10)

$$Left\ Slope = C1 + C2\ So + C4 + C5\ So = \frac{C6 + C71\left|So^-\right| + C72\left|So^+\right| + 4}{-C3\ So + 4} \quad \text{Eq. (6.11)}$$

From the above two equations, we get (C1 + C2 So) as a function of C6, C71, C72, and C3:

$$\begin{aligned} C1 + C2\ So &= \frac{C6 + C71\left|So^-\right| + C72\left|So^+\right| + 4}{-C3\ So + 4} - (C4 + C5\ So) \\ &= \frac{C6 + C71\left|So^-\right| + C72\left|So^+\right| + 4}{-C3\ So + 4} - \frac{C6 + C71\left|So^-\right| + C72\left|So^+\right| + 4}{-C3\ So - 4} \\ &= \frac{(C6 + C71\left|So^-\right| + C72\left|So^+\right| + 4)(-8)}{(-C3\ So + 4)(-C3So - 4)} \end{aligned}$$

Eq (6.12)

Putting equations 6.10 - 6.12 into the original equation 6.9, we find:

$$Local\ Comfort = \left[\frac{(C6 + C71\left|So^-\right| + C72\left|So^+\right| + 4)(-8)}{(-C3\ So + 4)(-C3\ So - 4)(e^{5(Sl + C3So)} + 1)} + \frac{C6 + C71\left|So^-\right| + C72\left|So^+\right| + 4}{-C3\ So - 4}\right] (Sl + C3\ So) + C6 + C71\left|So^-\right| + C72\left|So^+\right|$$

Eq. (6.13)

This equation is close to the final form. There are three parameters to define: C3 determines the offset of the maximum comfort (this should be a positive value, as noted above);

C6 should be a positive value because it is the maximum comfort value; and C71 and C72 should be positive values because as overall sensation moves in the direction of cooler or warmer, the maximum comfort is higher.

There are two additional adjustments, which are significant only for some body parts. When they are not significant, the regression coefficient is zero. The two adjustments are as follows:

1. The above model implies that when overall sensation is neutral, the slopes on the left and right are symmetrical; this is true for some body parts but not others. Figure 6.31 illustrates both cases; for body parts such as the hand and back, the symmetrical assumption can be met, but for other body parts, such as breathing, the foot, and the pelvis, we do not see a symmetrical pattern. Therefore, we modified Eq. (6.13) by adding a constant value to the local sensation offset portion so that when overall sensation is neutral, the local sensation can be shifted by this constant amount. The new form is shown in Eq. (6.14). In the regression, when the data are quite symmetrical, this shift is zero. That means, based on the general description of Eq. (6.13), the regression will result in one of three types of shifts: zero, toward warm (negative value, e.g., for foot), or toward cold (positive value, e.g., for breathing).

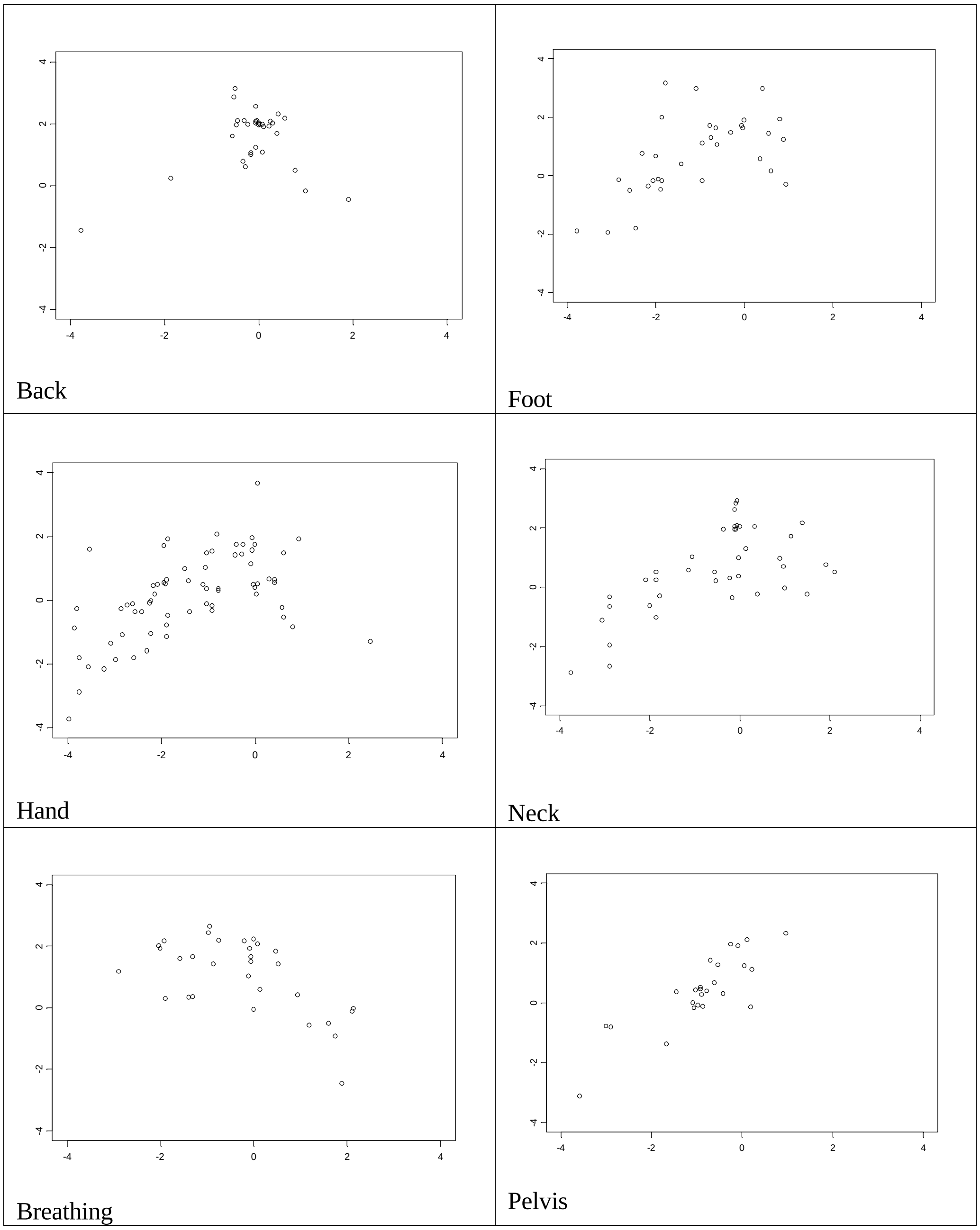

Figure 6.31 Symmetrical and asymmetrical relationships between local sensation and local comfort when the whole body is neutral. The horizontal axis represents local sensation, and the vertical axis represents local comfort.

$$Local\,Comfort = \left[\frac{(C6 + C71\left|So^{-}\right| + C72\left|So^{+}\right| + 4)(-8)}{[-(C8 + C3\,So) + 4][-(C8 + C3\,So) - 4](e^{5(Sl + C8 + C3So)} + 1)} + \frac{C6 + C71\left|So^{-}\right| + C72\left|So^{+}\right| + 4}{-(C8 + C3\,So) - 4} \right]$$
$$(Sl + C8 + C3\,So) + C6 + C71\left|So^{-}\right| + C72\left|So^{+}\right|$$

Eq. (6.14)

2. The second adjustment is in response to an observation based on the scatter plot of local sensation and comfort for different body parts, a few examples of which are shown in Figure 6.31. We don't want to limit ourselves with the linear model. For some body parts, a quadratic shape may better represent the relationship between local sensation and local comfort. We let the regression decide the order of this equation.

In sum, there are three possible models, linear-, quadratic-, 1.5 exponential (Figure 6.32).

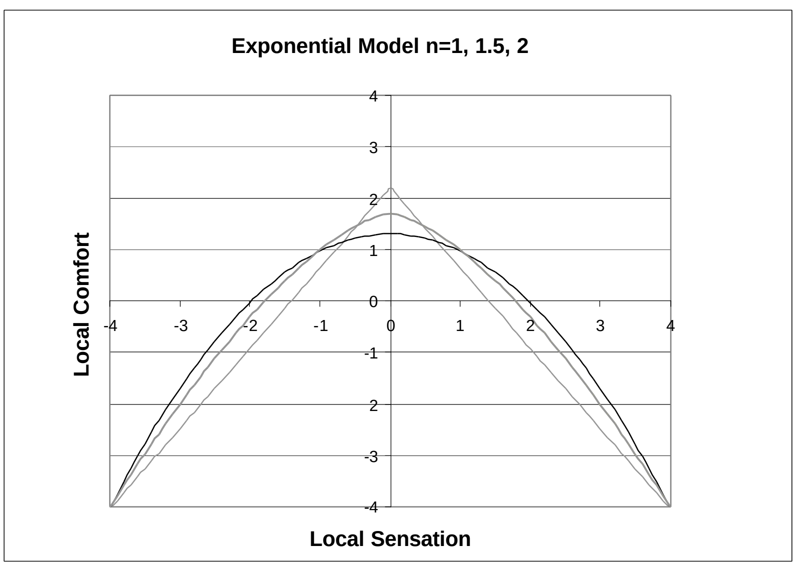

Figure 6.32 Possible three shapes to present the relationship between local sensation and local comfort

We did a regression analysis with the three values (n=1, 1.5, 2) for each body. In general, the R^2 did not change much. However, the distribution of the residual changed. By comparing R^2 and the residual distribution with the three regressions for each body part, we chose one value of n for each segment. The general regression form is presented in Eq. (6.15), and the regression results are in Table 6.3.

$$Local\,Comfort = \left[\frac{ \dfrac{-4-(C6+C71|So^-|+C72|So^+|)}{|(-4+C31|So^-|+C32|So^+|+C8)|^n} - \dfrac{-4-(C6+C71|So^-|+C72|So^+|)}{|(4+C31|So^-|+C32|So^+|+C8)|^n} }{ e^{15(Sl+C31|So^-|+C32|So|+C8)}+1 } + \frac{-4-(C6+C71|So^-|+C72|So^+|)}{|(4+C31|So^-|+C32|So^+|+C8)|^n} \right]$$
$$(Sl+C31|So^-|+C32|So^+|+C8)^n + C6 + C71|So^-| + C72|So^+|$$

Eq. (6.15)

Eq. (6.15) is the final form of local comfort model (the asymmetrical saddle). The form allows us to change the shape of the saddle (linear vs. curved), to adjust the shifts to cold or warm local sensation, and to determine maximum comfort values separately for warm and cold overall thermal states. These adjustments are functions of local and overall thermal sensation.

6.3.4 Regression results

Local comfort as a function of local and overall sensation is shown in Table 6.3.

The low R2 values, indicating that the local comfort prediction does not correlate well with local and overall sensation, are mostly for the head region. This means the ways in which people evaluate the comfort of the head region based overall sensation varies more than for other body parts.

The figures on the right side are the actual votes vs. predicted votes. The idea prediction follows the 45 degree line. The more scatter from this line, the lower the R2.

Table 6.3 Regression coefficients for the local thermal comfort model

Segment	C31	C32	C6	C71	C72	C8	n	Act vs. fit	R^2
Head	0	1.39	1.27	0.28	0.4	0.5	2	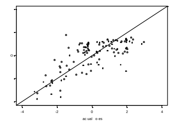	0.55
Face	-0.11	0.11	2.02	0	0.4	0.41	1.5	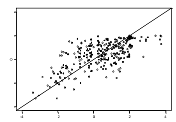	0.44
Neck	0	0	1.96	0	0	-0.19	1	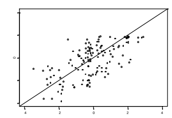	0.43
Breath	0	0.62	1.95	0	0.79	1.1	1.5	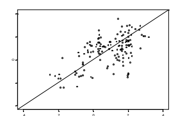	0.33
Back	-0.5	0.59	2.22	0.74	0	0	1	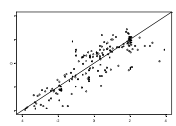	0.74
Upper Back	0	0	2.05	0	0	0	1	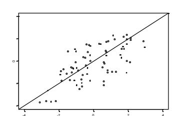	0.45
Lower Back	0	0	2.2	0	0	0	1	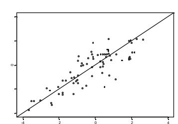	0.69
Chest	-1.15	0	1.88	0.92	0	0	1.5	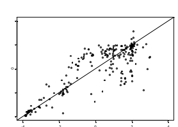	0.68

Table 6.3 (continued) Regression coefficients for local thermal comfort model

Segment	C31	C32	C6	C71	C72	C8	n	Act vs. fit	R^2
Chest	-1.07	0	1.74	0.35	0	0	2	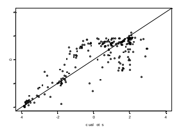	0.70
Pelvis	-1	0.38	2.7	0.83	-0.64	-0.75	1	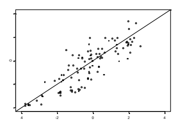	0.74
Upper Arm	-0.43	0	2.2	0	0	-0.33	1	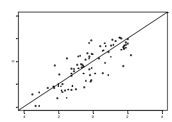	0.70
Lower Arm	-1.64	0.34	2.38	1.18	0.28	-0.41	1	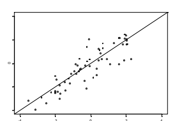	0.77
Hand	-0.8	0.8	1.99	0.48	0.48	0	1	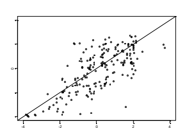	0.6
Thigh	0	0	1.98	0	0	0	1	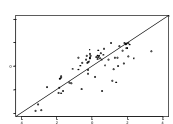	0.59
Lower Leg	-1	1.5	1.27	0.4	1.22	0.36	1.5	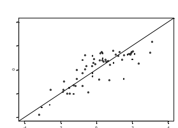	0.68
Foot	-2.31	0.21	1.62	0.5	0.3	-0.25	2	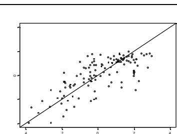	0.55

6.3.5 Analysis of the regression results

A summary of the coefficients is provided below in order to easily understand the explanation of the regression results. The coefficient C6 represents maximum local comfort with neutral overall sensation. As overall sensation gets colder or warmer, maximum local comfort is felt at warmer or colder local sensations, and rises higher than the maximum local comfort felt with neutral overall sensation. The coefficient C31 represents the shift in local sensation toward the warm direction as overall sensation gets colder, and the coefficient C32 represents the shift in local sensation toward the cold direction when overall sensation is warm. The larger the coefficients, the bigger the shifts. The coefficients C71 and C72 correspond to heightening of maximum comfort. The larger the coefficients, the higher the level of maximum comfort. The coefficient C8 reflects the preference of each body part toward cool or warm sensation under neutral condition. A positive value indicates a cool preference, and a negative value indicates a warm preference.

The regression coefficients reflect the characteristics of local comfort observed in Chapter 5. We show regression results for the breath intake air, pelvis, foot, and back below.

Our test results showed that cooling of the breathing intake air was experienced as comfortable but warming of the intake air was experienced as uncomfortable. In Table 6.3, we see a positive coefficient (1.1) for C8. This indicates that with neutral overall conditions, the maximum breathing comfort is felt at a breathing sensation near slightly cool (–1.1). This cool preference (1.1 sensation shift towards cool side) is also shown in Figure 6.27. When the overall body is warm, people feel comfortable with even cooler breathing sensations; that is, local sensation shifts toward cool (0.62, corresponding to 1 overall sensation increase), and local comfort increases (0.79, corresponding to 1 overall sensation increase). The shift to the warm side and the increase in comfort are zero (C31 = 0, C71 = 0). That indicates people don’t like breathing warm air, even when the body is cold. In our tests, the subjects show an unfavorable feeling towards breathing zone air heating (Chapter 5). Figure 6.33 shows the regression result for breathing.

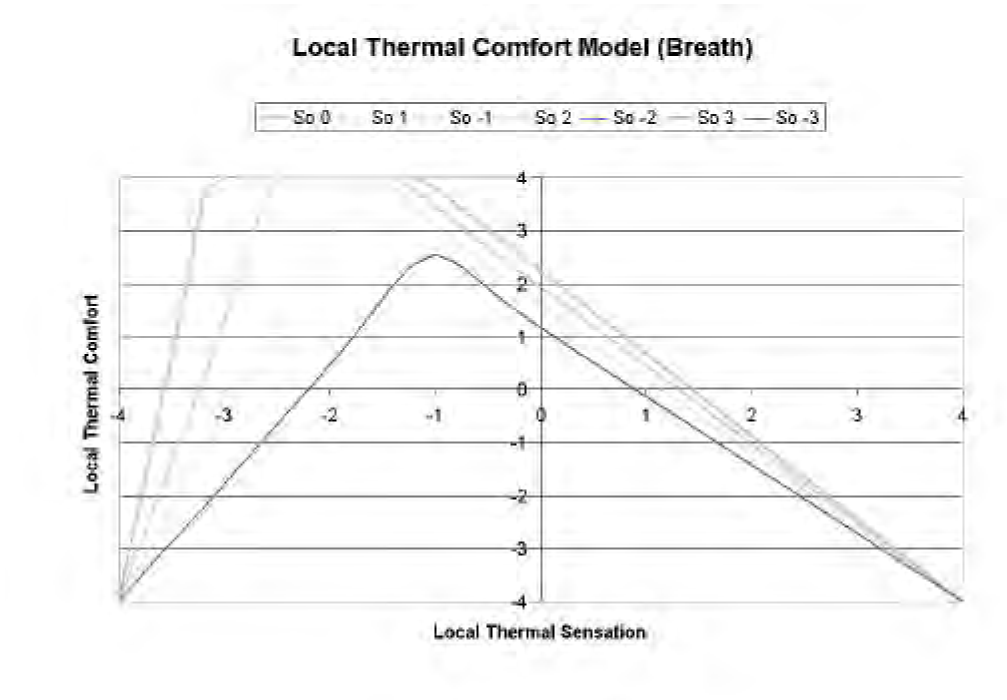

Figure 6.33 Breathing local thermal comfort model

Our test results showed that subjects were most comfortable with a cool head region and warm feet. The regression results show that three out of four coefficients of the head region (head, neck, face, breathing) for C8 are positive. The positive value indicates a negative local sensation at the maximum local comfort when overall sensation is neutral. Three out of four coefficients for C31 and C71 are zero. These zero coefficients mean that when people are colder, maximum local comfort does not shift toward the warm direction and the maximum comfort level does not increase. For the foot, there is a small preference for warm local sensation at maximum comfort (C8 = -0.25). The shift in the warm direction (C 31 = -2.31) for a cold whole body is much larger than the shift in the cold direction for a warm whole body (C32 = 0.21). The increase in maximum comfort for the warm local shift with a cold body is also higher (C71 = 0.5) than for the cold local shift with a warm body (C72 = 0.3).

Under neutral whole-body conditions, the pelvis shows a preference for a warm local sensation (C8 = -0.75). As the whole body gets colder, the shift toward the warmer local sensation in the pelvis is larger (C31 = -1) compared to the shift toward a cold local sensation when the whole body is warm (C32 = 0.38). Local maximum comfort increases (C71 = 0.83) with the shift toward warm local sensation when the overall whole body is cold. Maximum comfort does not increase as local sensation shifts toward cold (C72 = 0), when the overall body is warm.

Regression results for the upper and lower back are similar to each other but are not modified by the overall sensation. The regression for the whole back indicates a shift toward warm or cold for maximum local comfort. The level of maximum comfort increased when the back is warmed and the whole body is cold (C71 = 0.74), but there is no increase in maximum comfort when the back is cooled and the whole body is warm (C72 = 0). The exponential coefficient (n) was 1 for all three areas of the back (back, upper back, lower back). The value of n for the highly influential/dominant body parts should be equal to 1 because a linear shape rather than a curved exponential shape can indicate greater sensitivity of local thermal comfort responses as local sensation moves toward the two extremes. The more sensitive the body part, the faster the decrease in local comfort. In our regression results, n is 1 for back, upper and lower back, and pelvis.

For the chest model, the non-zero shift (C31 = -1.07) toward warm and the increased maximum comfort (C71 = 0.35) indicates that local warming of the chest feels very comfortable when the whole body is cold. There is no shift toward preference for cooling of the chest when the whole body is warm.

From the regression results above for the three dominant segments (back, chest, and pelvis), we see that local cooling does not increase maximum comfort when the body is warm. These dominant segments are sensitive to local cooling.

The hand does not show any preference in the neutral condition, so C8 =0. The hand also does not show any asymmetry during local cooling and heating when the whole body is warm or cold (for example, the study from Cabanac shown in Figure 6.23). The regression results from our data also show a symmetrical results (C31 = -C32, C71 = C72). The model for hand is shown in Figure 6.34.

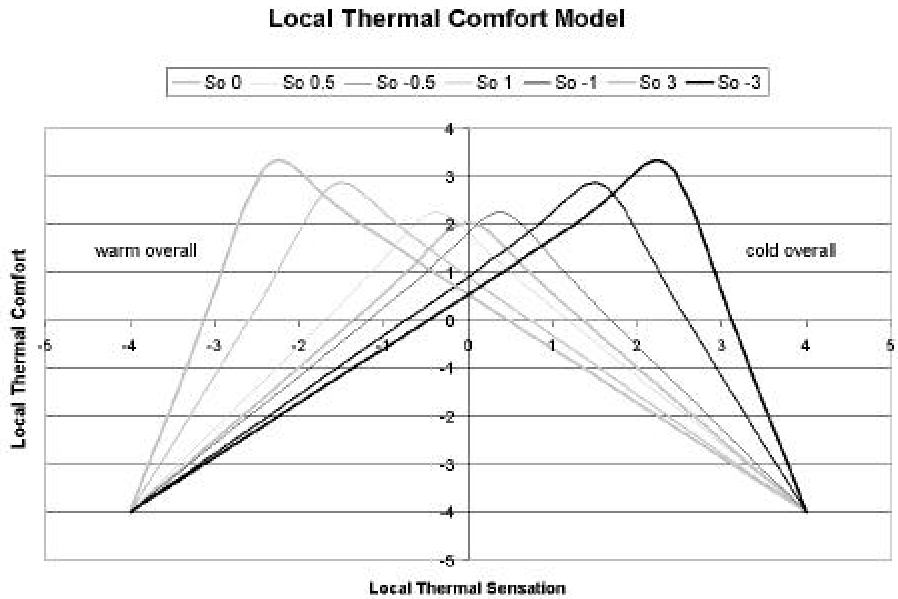

Figure 6.34 Hand local thermal comfort model

The 3-D presentation of our saddle model and the model proposed by Issing and Hensel are presented in Figure 6.35. The two figures show similar results. In our model, the x and y axis represent local and overall sensation. In Issing and Hensel's model, the x and y axes are the room (representing for the overall whole body thermal state) and the thermode (representing for the local skin) temperatures.

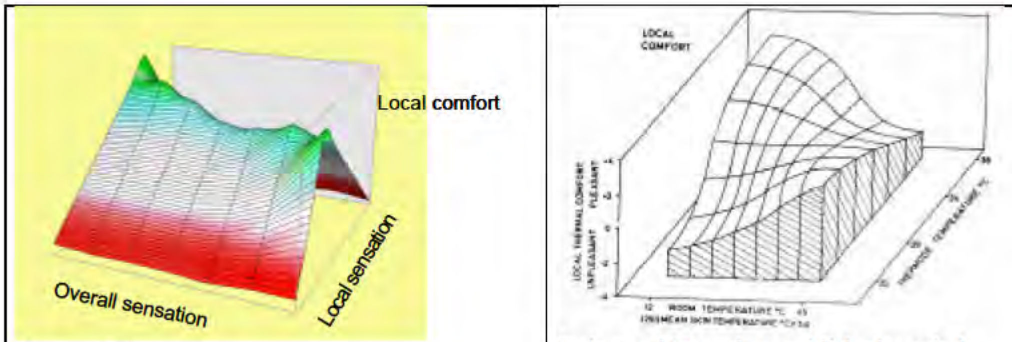

Our model

Issing and Hensel, unpublished, copied from (Hensel 1982)

Figure 6.35 3-D presentations of our saddle model and the model proposed by Issing and Hensel

The literature shows the X shape-relationship in both stable (Issing and Hensel (Issing and Hensel 1981), Figure 6.25) and transient studies (Cabanac, Mower, Attia). The data from our tests used in the regression were the last votes at the end of local cooling/heating applications. All of these data show the similar X shape for the relationship between local sensation, local comfort, and the whole body thermal state. We also tried to add a transient term in the saddle model, but the improvements were not statistically significant. Therefore we believe that the saddle model applies to both stable and transient conditions.

6.3.6 Discussion

Our approach to the regression analysis has been to use a rational model based on the literature and our test data. Our regression coefficients represent only the range of testing and test conditions in our experiments.

The gaps in our data show in places such as heating of the neck when the body is cold, which did not enhance maximum comfort in our tests. Based on real-life behavior – e.g., zipping jacket collars or wearing neck scarves when cold – we would expect a very comfortable feeling to result when the neck is warmed. However, we did only a very limited number of neck-warming tests, and our data did not support this expectation. We see a difference between our regression results and those of Attia's human subjects (Attia and Engel 1981) in response to neck cooling or warming with extremely hot and cold body. Attia's data show a local comfort increase with cooling or heating of the neck (Figure 6.4). In our regression results, there is no increase (C71 = 0, C72 = 0). This may be a result of the different sizes of areas exposed to thermal stimuli. In Attia's experiment, the area warmed or cooled is only the size of a thermode, 5 x 2.7 cm. In our test, the entire neck was heated or cooled. Subjects may welcome a small area of local heating or cooling when the overall body is cold or warm, but application of heating or cooling to an entire body part might be felt to be too much, so local comfort does not increase.

Our coefficients may also be affected because we did not explore a wide range of temperature conditions in our tests. For example, because we cooled the back using a large volume of relatively cold air, we did not see a shift toward cold local sensation and an increase in maximum comfort when the body was warm. We did not investigate the effect on local comfort of very slight cooling of the back when the overall body is warm. Had we performed this test, our results might be different.

Other examples where our data may not be sufficient include the models for the back, upper back, and lower back. The regression results for the upper and lower back are similar (C31 = 0, C32 = 0), but the results for the entire back are different from those for the upper and lower back (C31 = -0.5, C32 = 0.59). The reason may be that we did a smaller number of tests for the upper and lower back than for the whole back.

These examples show how our coefficients could be improved in the future if more data are available.

6.3.7 Validation of the local thermal comfort model – the saddle model

We applied the local thermal comfort (saddle) model to the data we gathered from tests performed in the Delphi Wind Tunnel (PRE-test data). As described in Chapter 4.4.2.6, the sensation and comfort in Delphi PRE dataset was cast after the subjects entered the car and before they started the engine and the air-conditioning. The car had been soaked in the Wind Tunnel for 60 to 90 minutes. The data can be considered as either stable or transient depending on how much difference of the environment is between the wind tunnel and inside of the soaked car. The dataset includes 67 records. Each records includes sensation and comfort for overall and all the local body parts (12 local body parts: face, chest, back, right lower arm, right foot, right calf, right hand, left upper arm, left foot, left thigh, left hand, pelvis). The validation results are shown in figures, prediction R^2, and the standard deviation of the residuals (STDEV) in Figure 6.36 for these 12 local body parts. The figures show the actual votes (x axis) vs. the prediction (y axis).

The predictions explain from 51% of the variance (right foot) to 76% of the variance (right hand), with most of the predictions around 70%. The reason that the prediction for the foot is not as good is that in the UC Berkeley chamber experiment (data used for developing the local comfort models), the subjects showed a preference towards warm feet. So the saddle is asymmetrical being more comfortable toward the warm side. However, the Delphi data did not show this preference, so the residuals are larger when evaluating foot comfort when foot is warm. We show two examples for predictions (represented by "p") vs. the actual votes (presented by open circles) in the two figures in Figure 6.37. From the two figures, we see the over-estimation of the foot local comfort on the warm side.

There is one thing that may contribute to residuals when using Delphi data to validate our models. As we described in Chapter 4.4.2.6, the Delphi sensation and comfort votes are on a one-unit discrete increment scale (sensation scale is: very cold, cold, cool, slightly cool, neutral, slightly warm, warm hot, very hot; comfort scale is from just comfortable to very comfortable and just uncomfortable to very uncomfortable). The sensation comfort scales used in the U.C. Berkeley Environmental are continuous, covering the same ranges. The one-unit increment scale resulted the Delphi votes more scattered.

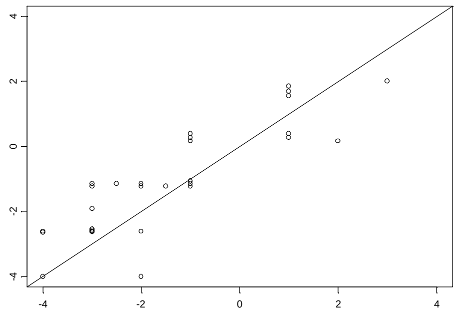

Face, R2=0.69, STDEV=0.81

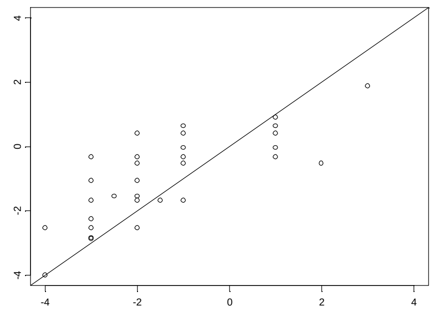

Chest, R2=0.59, STDEV=0.97

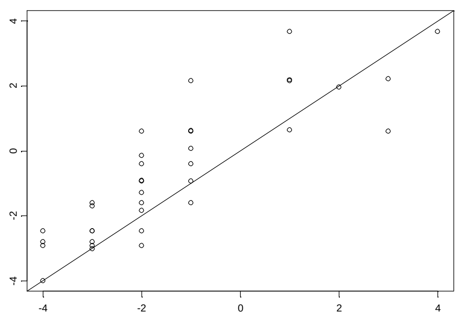

Back, R2=0.7, STDEV=1

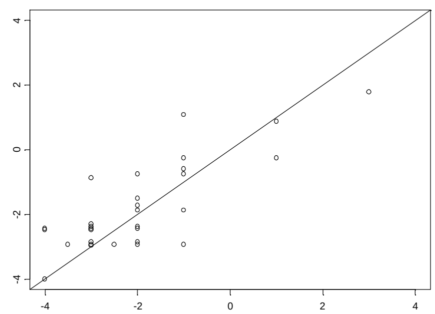

Lower arm, R2=0.67, STDEV=0.74

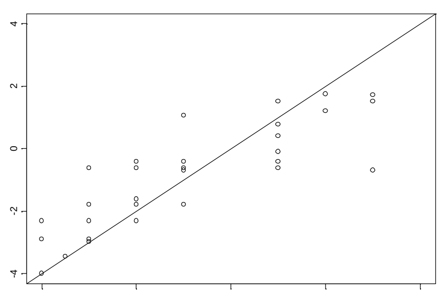

Upper arm, R2=0.68, STDEV=1.16

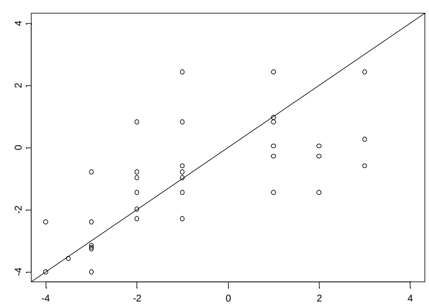

Right foot, R2=0.51, STDEV=1.4

Figure 6.36 Validation of the thermal comfort model by Delphi Wind Tunnel test data (continued on next page)

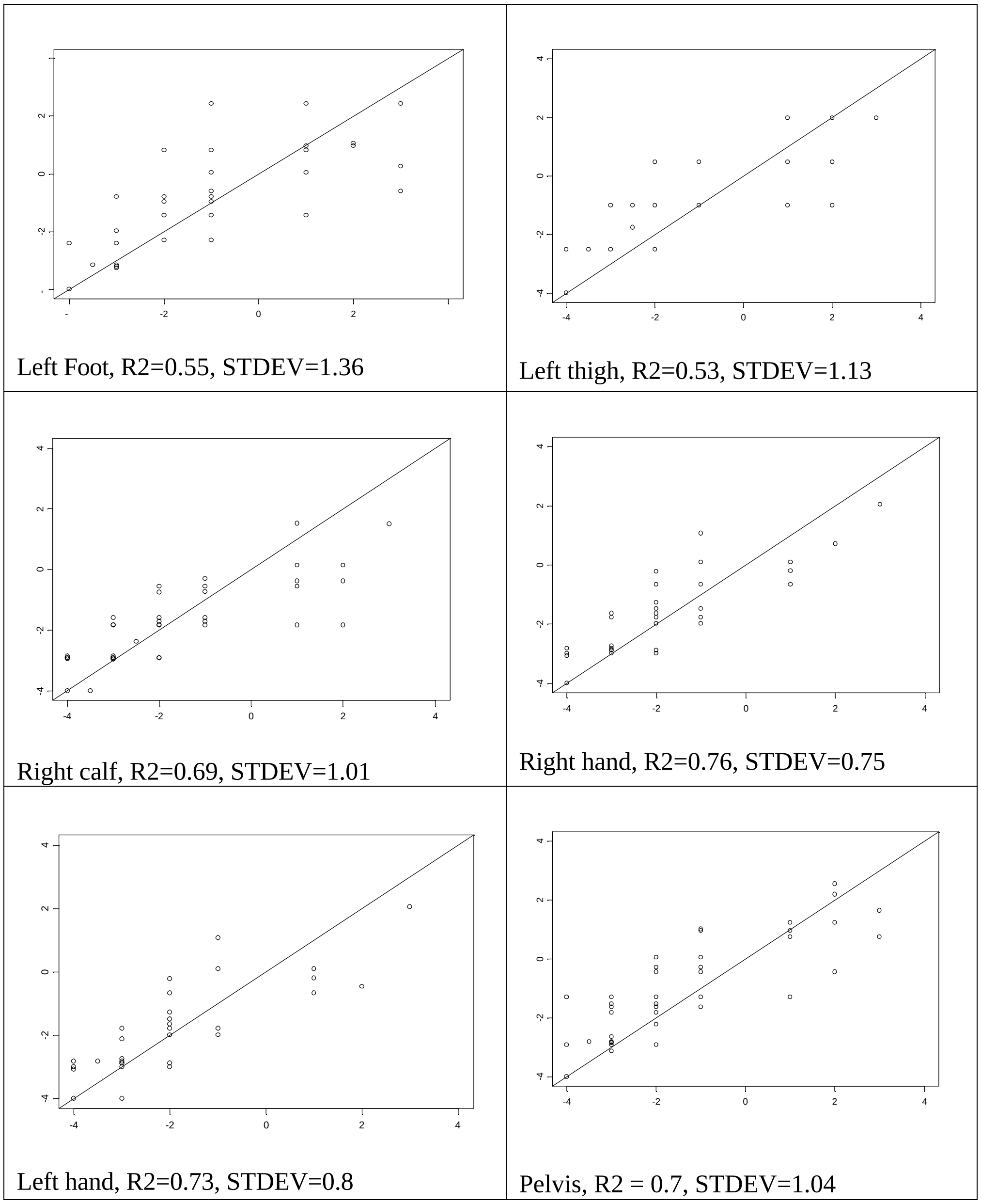

Left Foot, R2=0.55, STDEV=1.36

Left thigh, R2=0.53, STDEV=1.13

Right calf, R2=0.69, STDEV=1.01

Right hand, R2=0.76, STDEV=0.75

Left hand, R2=0.73, STDEV=0.8

Pelvis, R2 = 0.7, STDEV=1.04

Figure 6.36 Validation of the thermal comfort model by Delphi Wind Tunnel test data

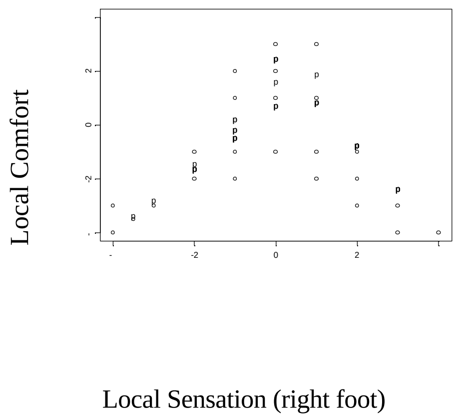

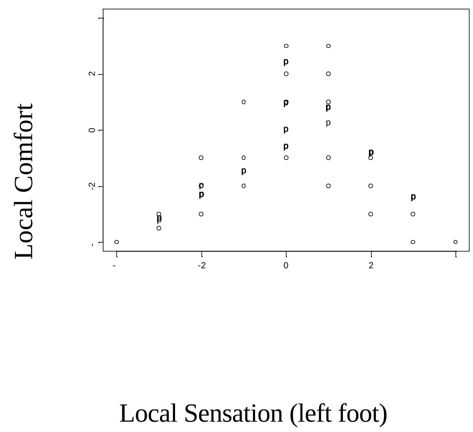

Figure 6.37 Predictions and actual votes of right and left foot (Delphi Wind Tunnel test, PRE dataset

6.4 Overall thermal sensation model

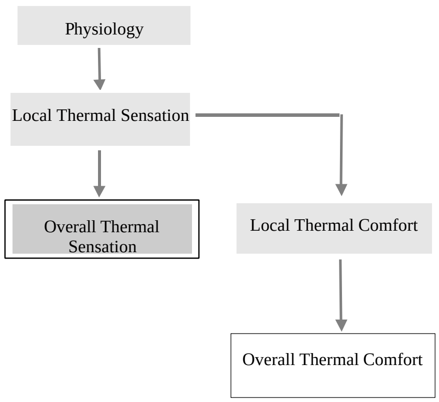

The EHT method (see Background, Chapter 2) has been the only way to quantify local sensation. However, the EHT method only provides an environmental temperature range for each body segment, within which 80% of people are said to be comfortable. The EHT evaluation method cannot assess the actual local sensations, how they interact with each other, and how the body integrates them to provide an overall impression of thermal sensation. It cannot distinguish, for example, the difference between two persons who are both within the EHT ranges, but one with EHT values for every body part on the cold side vs. a person with EHT values for every body part on the warm side. Our overall sensation model (whole body thermal sensation model) integrates the local sensations and provides an overall evaluation of the whole-body thermal state. It was developed using the measured local sensation data from our environmental chamber experiments.

The overall sensation is a weighted average of all the local sensations (Eq. (6.18)).

$$OverallSensation = \frac{\sum (weight_i \, S_{local,i})}{\sum weight_i} \qquad \text{Eq. (6.18)}$$

where $S_{local,i}$ represents for the local sensation for segment "i", and $weight_i$ is the weighting factor for that segment.

6.4.1 Proposing an integration model involving weighting factors

We know some basic things about the relationship between local and overall sensation; when our overall body is hot, putting a hand into a cool water produces a feeling of comfort. We feel the cooling hand much more strongly than the hand that remains warm, because the warm hand is registering essentially the same sensation level as the rest of the body. A similar thing happens when we are cold and put a hand into warm water. We notice the sensation of the warm hand much more strongly than the sensation of the hand that remains cold. Consider another familiar example. After a day of skiing in cold weather, we get into a car and turn on the heat, which blows warm air. All of the body quickly warms except for the very cold feet. When someone asks how we feel under those conditions, we most likely notice our cold feet rather than the sensation of the rest of the body. It appears true that the further a local sensation is from the mean sensation (ie, a simple average of the local sensations), the larger the local sensation's impact on the overall sensation, and therefore the bigger the weight.

This suggests linear or quadratic models as good candidates for predicting the weighting coefficients for each body part. Constant, linear, and quadratic models were examined (Figure 6.38).

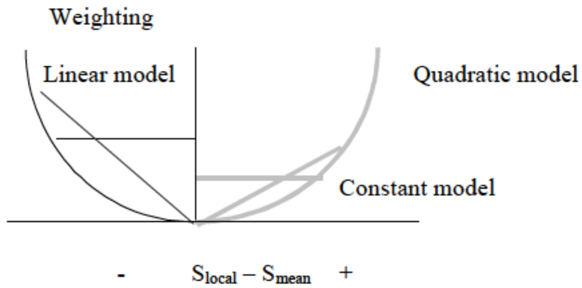

Figure 6.38 Proposed three models for predicting weights

Some of the data from our tests for a few body parts are shown in Figure 6.39. The data are from local cooling/heating tests which include data in both stable and transient conditions. In the figure, the vertical axis represents the weights, which are the ratios of overall sensation change vs. local sensation change during single-segment cooling or heating applications. The bigger the ratio, the larger the overall sensation change caused by a unit of local sensation change. The horizontal axis is the difference between local and the overall sensations. During the tests, we could not each time survey the sensation for every body part, so we could not obtain an average of the local sensations. We use instead the difference between local sensation and the overall sensation, which we did measure every time, to represent the difference between local sensation and the average of the local sensations.

The figures show test data and the linear ("sun-burst") model, which provides the best fits for most body parts. The figures on the left show the original scatter plots. The figures on the right add the linear regression results.

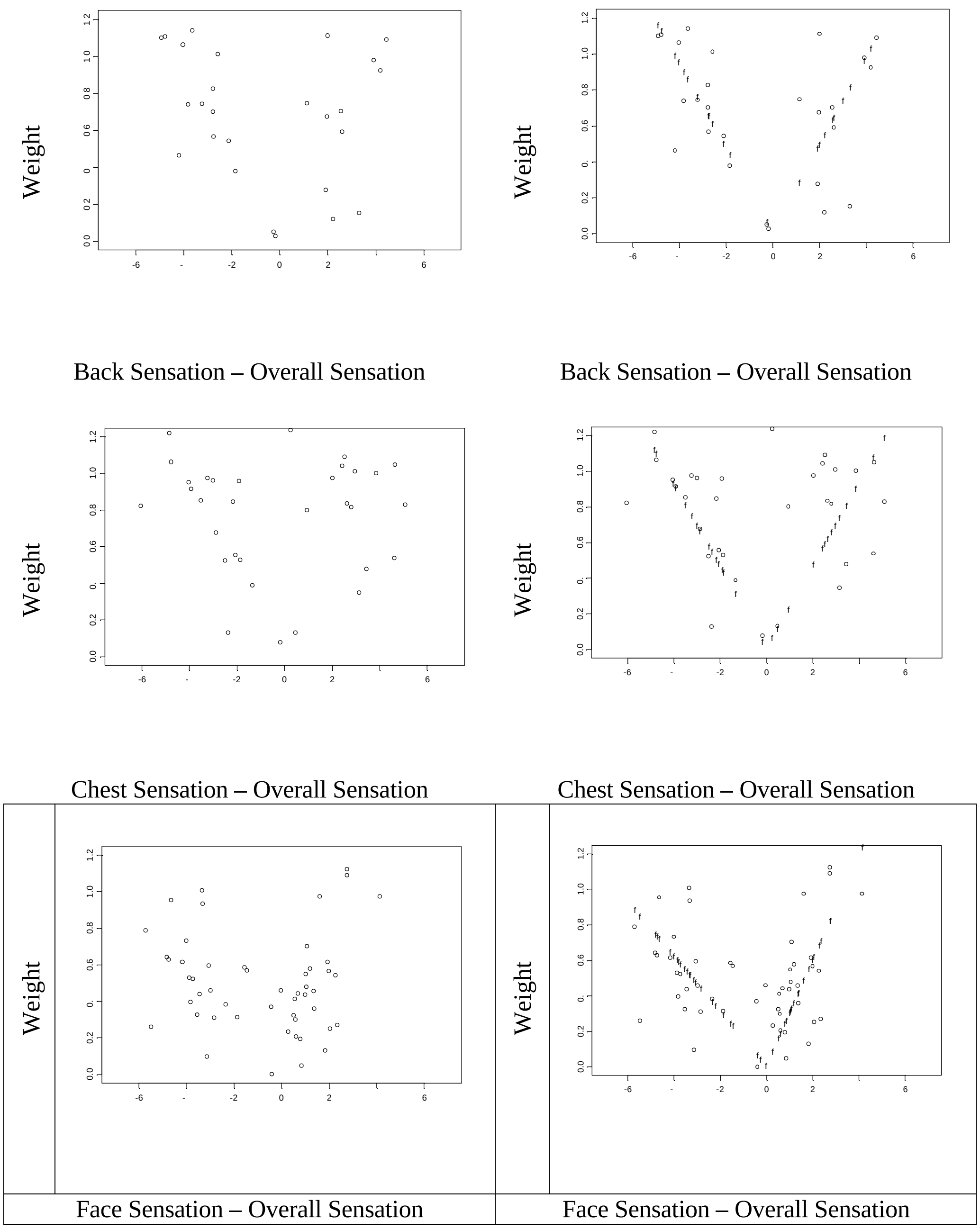

Figure 6.39 Linear relationships to calculate the weights based on the difference between local sensation and the overall sensation (continued on next page)

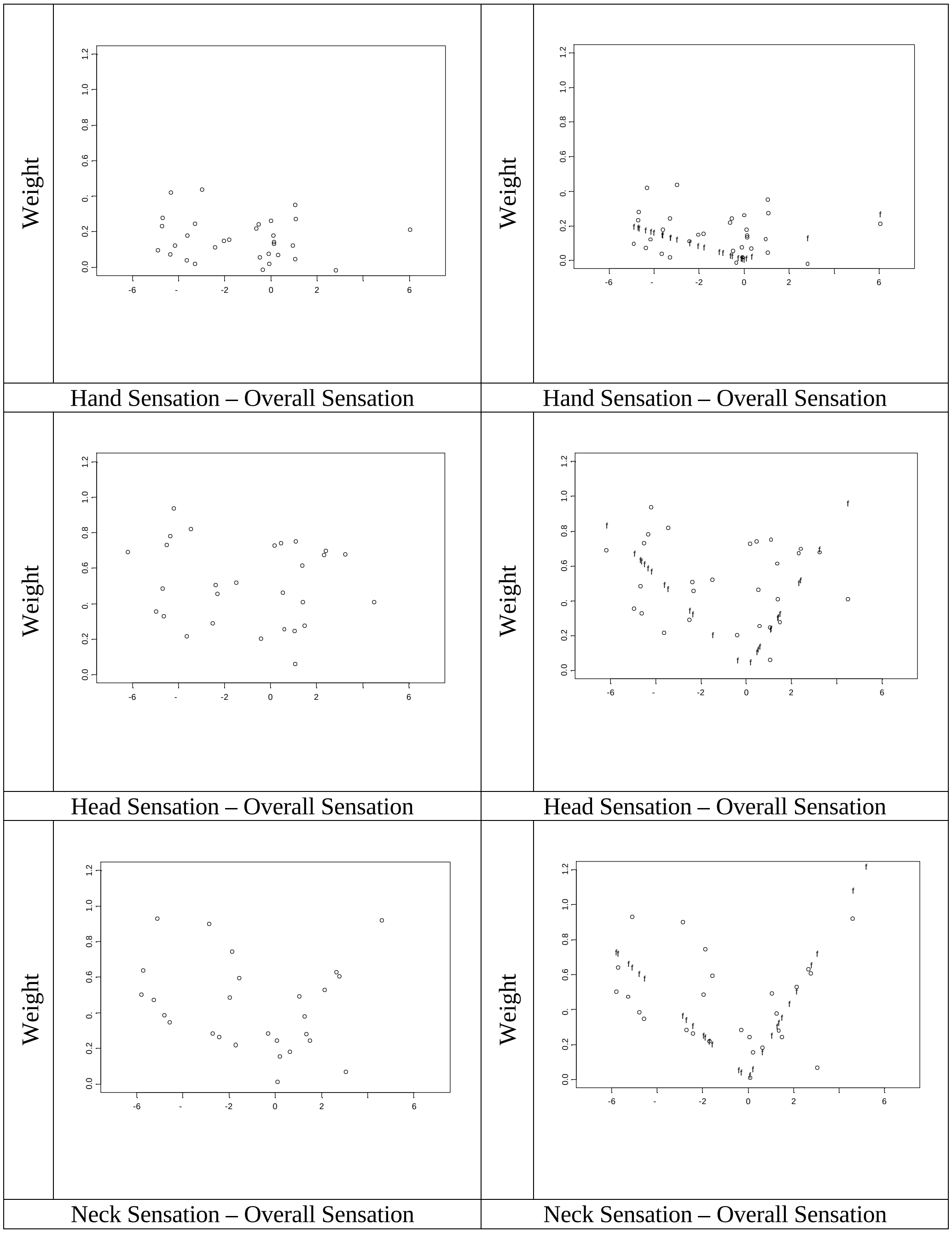

Figure 6.39 Linear relationships to calculate the weights based on the difference between local sensation and the overall sensation (continued on next page)

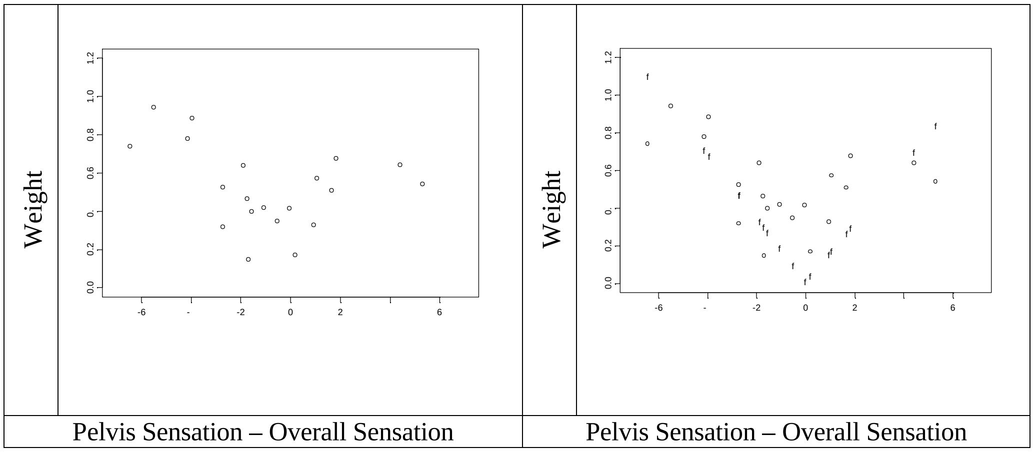

Figure 6.39 Linear relationships to calculate the weights based on the difference between local sensation and the overall sensation

6.4.2 Regression results

Table 6.4 shows the regression results for all the body parts, including the slopes of the linear models. These slopes are used to get the weights based on the differences between the local sensations and the averages of the local sensations. From the generally high values of the least square correlation, R^2, we know that the linear model predicts well. The data used for the regressions include both transient and stable condition votes, so we believe that the overall sensation model applies to both stable and transient conditions.

In the table, S_l represents the local sensation and S_o represents the overall sensation.

Table 6.4 Overall sensation model: slopes (shaded) to calculate weight, weight= a ($S_{local} - S_{mean}$) (obtained from single body part local cooling and heating tests)

Local Body Part	S_l-S_{mean} <=0	R2	S_l-S_{mean}>= 0	R2
Breathing	-0.16	0.44	0.19	0.14
Head	-0.13	0.82	0.21	0.57
Neck	-0.13	0.71	0.23	0.68
Face	-0.15	0.71	0.30	0.81
Chest	-0.23	0.90	0.23	0.70
Back	-0.23	0.81	0.24	0.80
Pelvis	-0.17	0.85	0.15	0.73
Upper arm	-0.10	0.69	0.14	0.42
Lower arm	-0.10	0.69	0.14	0.42
Hand	-0.04	0.29	0.04	0.23
Thigh	-0.13	0.38	0.26	0.30
Lower leg	-0.13	0.38	0.26	0.30
Foot	-0.09	0.10	0.24 (2 fe t)	0.37
	-0.09	0.10	0.14 (1 fc t)	0.20
Upper back	-0.16	0.86	0.26	0.88
Lower back	-0.21	0.84	0.35	0.88

6.4.3 Analysis of the regression results

As noted in Chapter 5, Results, body parts can be grouped into highly influential/dominant, moderately influential, and least influential groups. These groupings are reflected in the models. For the body parts in the dominant group, the slopes are much larger. A larger slope represents a bigger weight, and the bigger weight means a stronger impact on overall sensation. The larger slopes are found for the back, chest, and the pelvis. As mentioned, we also observed in our test results that the head is more sensitive to heating than to cooling. This is reflected in the hot/cold asymmetry in the slopes for the head region (head, face, neck, breathing zone air), and for the foot, with the warming side slopes (Sl – Smean >=0) much larger than that for the cooling side (Sl – Smean >=0). The least influential group, the hand and foot, which serve to actively adjust body heat loss, have very small slopes, so their impact on overall sensation is very small. The insignificance of the impact of these body parts on overall sensation is also reflected in their smaller least square correlation, R^2.

Figure 6.40 shows a small number of examples for back, face, and hand based on the regression results shown in Table 6.4. In these examples, we see again that the back has a strong impact on overall sensation (large weight), and the hand has the least impact. We can also see that the impacts of some body parts (i.e. face) are different on the warm side and the cold side. For the face, for example, sensation on the warm side has a stronger impact than sensation on the cold side. This means that when the face gets colder, its influence on overall sensation is not as great when it feels warmer. As the face feels warmer, its contribution to overall sensation is stronger.

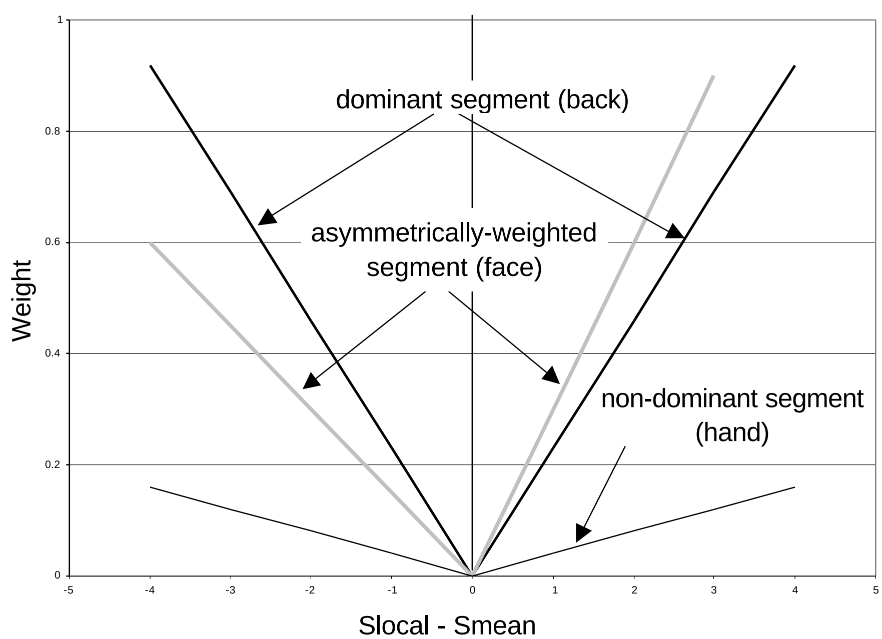

Figure 6.40 Examples of integration models for back, face, and hand

6.4.4 Overall sensation model validation

6.4.4.1 Validation using Delphi test data

To validate the overall sensation model, I applied the model to all the Delphi Wind Tunnel test data: PRE test data, datasets All1, All2, All3, and All4. In general Delphi data are good for the validation because the test conditions are complex and cover large ranges. As described in Chapter 4.4.2.6, the Delphi test range from –23.5°C to 43°C, with and without solar load. Once the air conditioning is started (datasets All1, All2, All3, All4), there are large variations in local sensation and comfort.

As described in Chapter 4.4.2.6 and 6.3.7, the sensation and comfort in the Delphi PRE dataset was obtained after the subjects entered the car and before they started the engine and the air-conditioning. Once the air-conditioning started, each time the subjects voted, they voted for only half the body parts. Based on which half of the body parts were voted on, the winter data are divided into datasets All2 and All4, and the summer data are divided into datasets All1 and All3. These datasets can be considered either as stable or transient depending on how often the subject adjusts the air conditioning. Each dataset includes about 300 records. Each record includes sensation and comfort for the overall and for half of the local body parts. Since datasets All1, All2, All3, and All4 include the data recorded after the air-conditioning was started, there exist large variations between local sensations (e.g. very cold chest (-4) vs. warm back (+2) in a summer test). Therefore, these data are valuable for validating the overall sensation model. Even the PRE data have large local sensation variations, especially in the winter tests (i.e. the overall sensation was cold (-3), while the chest was neutral (0), and the hand was cold (-3) during a cold test).

We validated our overall sensation model with these five datasets. The following figure shows the validation results for the 5 Delphi datasets (Figure 6.41). The validation R^2 and the standard deviation of the residuals (STDEV) are also included.

Overall Sensation Prediction

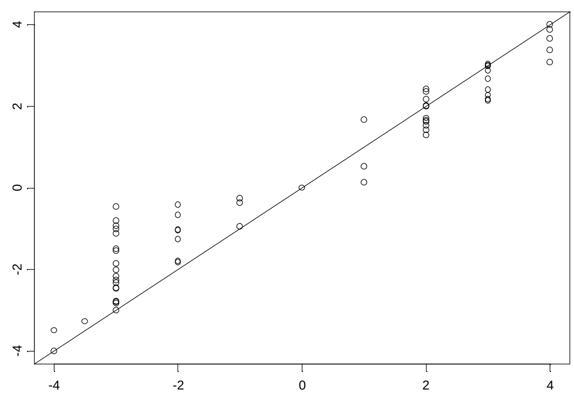

Overall Sensation Actual Votes

PRE dataset
R^2 = 0.89
STDEV = 0.87

Overall Sensation Prediction

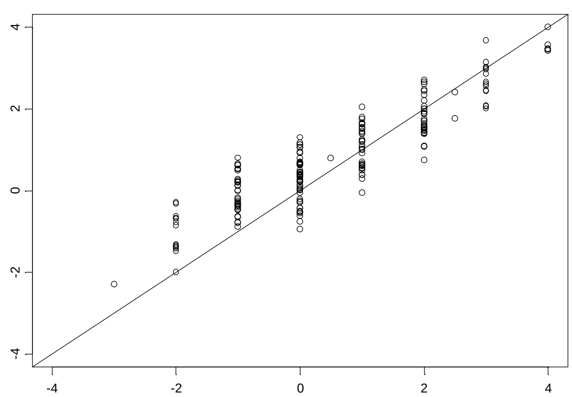

Overall Sensation Actual Votes

All1 dataset
R^2 = 0.93
STDEV = 0.61

Figure 6.41 Actual votes vs. prediction – validation of the overall sensation model (continued on next page)

Overall Sensation Prediction

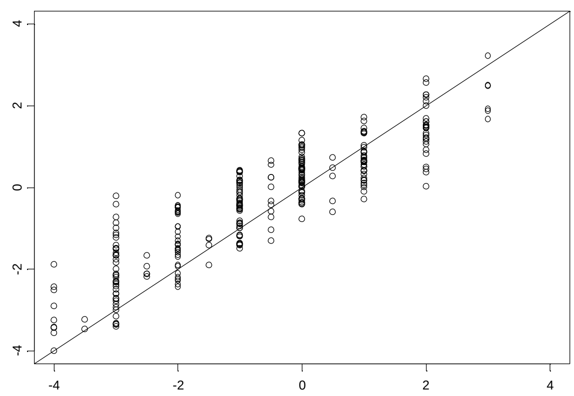

All2 dataset
$R^2 = 0.88$
STDEV = 0.77

Overall Sensation Actual Votes

Overall Sensation Prediction

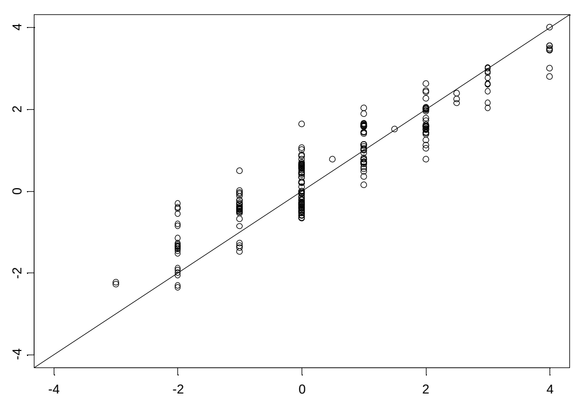

All3 dataset
$R^2 = 0.95$
STDEV = 0.54

Overall Sensation Actual Votes

Figure 6.41 Actual votes vs. prediction – validation of the overall sensation model (continued on next page)

Overall Sensation Prediction	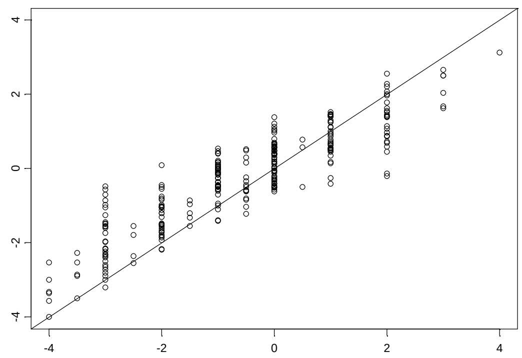	All4 dataset R^2 = 0.88 STDEV = 0.74
	Overall Sensation Actual Votes	

Figure 6.41 Actual votes vs. prediction – validation of the overall sensation model

The prediction shows that the model explains near 90% of the variance. Therefore, the integration model predicts well.

6.4.4.2 Validation using UCB stable-condition tests

Chapter 5.2 showed local sensation and comfort distributions observed in the UC Berkeley stable condition tests. The stable conditions tested were: neutral (overall sensation near 0), slightly warm (overall sensation near 1), slightly cool (overall sensation near –1), warm/hot (overall sensation between +2 and +3), cold (overall sensation near –3). This section validates the overall sensation model's predicted overall sensation using these distributions.

Figure 6.42 summarizes the six sensation distributions discussed in Chapter 5.2 There are significant local sensation variations in warm/hot and cold environments. The local sensation variations for other conditions are smaller.

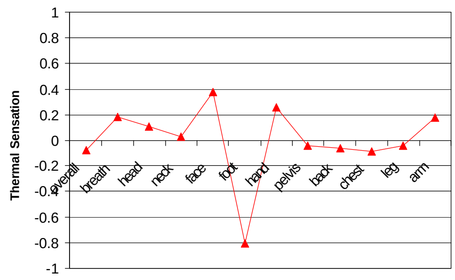

neutral 1, 8 tests

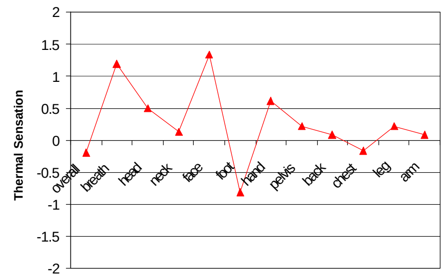

neutral 2, 07075

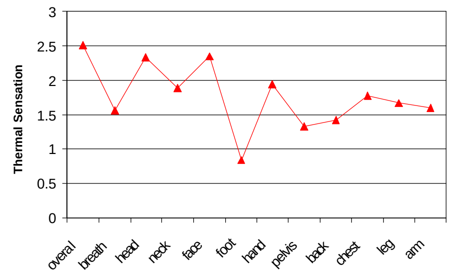

warm/hot (overall sensation between +2 and +3), 10 tests

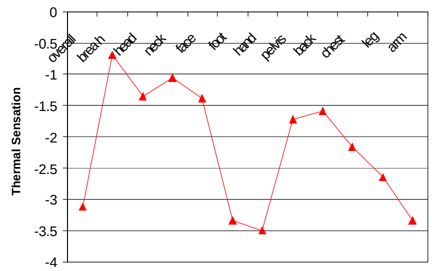

cold (overall sensation near –3), 5 tests

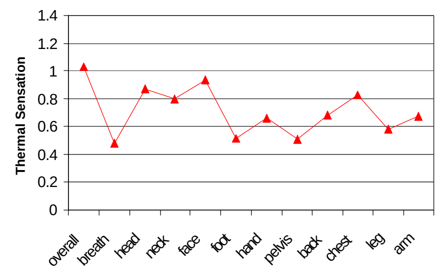

slightly warm (overall sensation near +1), 3 tests

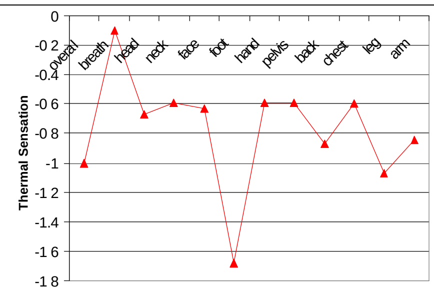

slightly cool (overall sensation near –1), 6 tests

Figure 6.42 Sensation distribution in stable conditions (UCB tests)

The validation results for the above 6 conditions are shown in Figure 6.43.

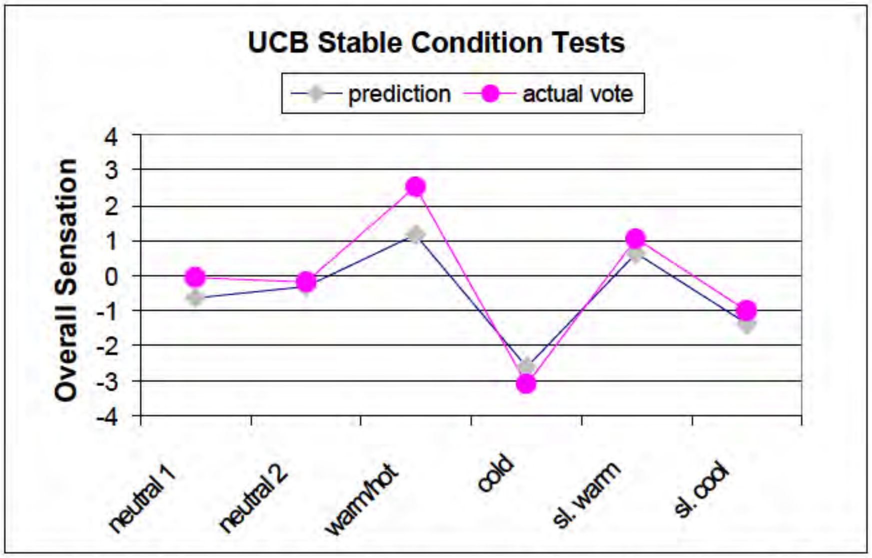

Figure 6.43 Validation of the overall sensation model in stable conditions (UCB tests)

The residuals of the prediction for the 6 conditions are presented in Table 6.5. From both Figure 6.43 and Table 6.5, we see that except for warm/hot, the residuals are near or below 0.5.

Table 6.5 Residuals of overall sensation model validation results of UCB stable condition experiment data

Test environment	Residual
neutral 1	0.5
neutral 2	0.1
warm/hot	1.3
cold	-0.5
sl. warm	0.4
sl. cool	0.4

For 'neutral 1', 'neutral 2', and 'sl. cool', the overall sensation is warmer than the coldest body part, but colder than most of the rest of the body parts. The 'sun-burst' shape of the overall sensation model assigns a larger weight for the coldest body part, so it has a bigger influence on the calculated overall sensation, and the prediction residuals are within 0.5. For 'cold', the overall sensation is not much warmer than the coldest vote. The calculated weights for the colder votes are also larger; the residual is small as well.

Observing the results in 'warm/hot' and 'sl. warm', we see that the overall sensation is closest to the head region local sensations (head, face, neck, but not the breathing zone air). This indicates that for warm conditions, the head region sensation has a bigger impact on the overall sensation than for cold conditions. That is why the overall sensation model has asymmetrical slopes for the head region, with a very large slope for the warm side. This asymmetry feature is able to make the prediction well when the whole body is not that warm (sl. cool). However, when the body is much warmer (warm/hot), the overall sensation model under predicted warmth sensation (the residual is 1.3).

6.4.5 Discussion of the overall sensation model

The analysis for warm/hot condition data suggests that the sun-burst model, although it provides large weights for the head region in warm conditions, it is still not enough to bring the predicted overall sensation close to the head region sensation when environment condition is extreme. The datasets used to develop the overall sensation model were the data from local cooling/heating tests. They are not extreme. For this warm/hot data, if bigger weights were assigned to head region, the prediction would be better. For 'cold' condition data, if bigger weights were assigned to the coldest local body parts, the prediction could also be better because we see that in Figure 6.36 the overall sensation is close to the coldest two sensations (although the current method has a residual of –0.5, not very large). These two test conditions are further from the neutral condition than the other 4 conditions. This suggests that for extreme conditions we might consider a quadratic model instead of a linear model to calculate the weights. Although our experimental data (which are not as extreme) was best represented by the linear model, in the future we may examine the quadratic model further.

The regression data are from both stable and transient conditions. The validation is also for both stable (UC Berkeley data) and transient (the five Delphi datasets may be considered to include both stable and transient data), we conclude that the overall sensation model is applicable to both stable and transient environments.

6.5 Overall thermal comfort model

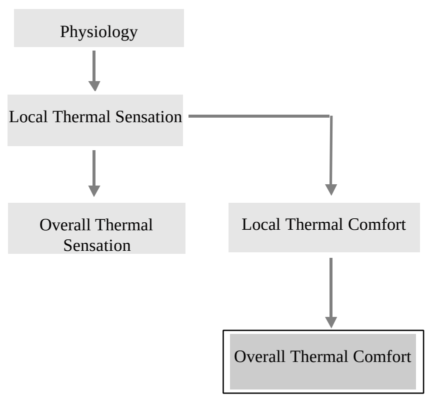

How do people determine whole-body comfort, given that different parts of the body can simultaneously feel very different, especially in asymmetrical and transient environments? There is no model in the literature addressing the complex process of determining whole-body comfort.

We have already discussed examples of the complexity of asymmetrical and transient thermal conditions, such as the following: A warm person walks into a hot car, turns on the air conditioning, and lets the cold air blow on his/her face and chest. The face becomes comfortable because the cold air eliminates the heat stress in this area. The person's back remains hot and uncomfortable, however, and the cold air on the chest creates slight discomfort there. Different levels of comfort and discomfort can exist at the same time, and the discomfort may be in response to either warm or cold. All of this sensation information is received by the person's brain and somehow integrated into an overall evaluation of the person's comfort level. The section describes how to develop a model that predicts a person's overall sense of comfort.

6.5.1 Process of developing the overall thermal comfort model

Our first attempt at developing a model to predict overall thermal comfort employed an approach similar to that used to develop the overall sensation model described in the previous section. That is, we tested a sun-burst linear model to define weights for all local comfort perceptions, and summed the local comforts using these weights to arrive at overall comfort (we called this the all-body-parts weighting method). However, when we examined the subjective comfort votes from both the U.C. Berkeley environmental chamber tests and the Delphi wind tunnel tests, we found that overall comfort is not an additive function of all local perceptions of comfort. Thermal comfort integration instead follows a “complaint” pattern; that is, the most uncomfortable body parts have the decisive impacts on the perception of overall comfort. Whenever two body parts are more uncomfortable than –2 (uncomfortable), the overall comfort vote is on the uncomfortable side no matter how comfortable the other body parts might feel. Moreover, the level of overall discomfort is similar to the level of the two local areas of discomfort.

All-body-parts weighting adds the contributions from all the local comfort perceptions; this approach overestimates overall comfort regardless of the weights applied. Figure 6.44 and Figure 6.45 show two examples of overestimates from this method. The residuals are mostly negative. (The datasets are the PRE and All4 of Delphi test data. The Delphi experimental setup and datasets are described in Chapter 4.4.2.6, and briefly summarized again in section 6.4.4.1 where Delphi data were used to validate the whole body thermal sensation model.)

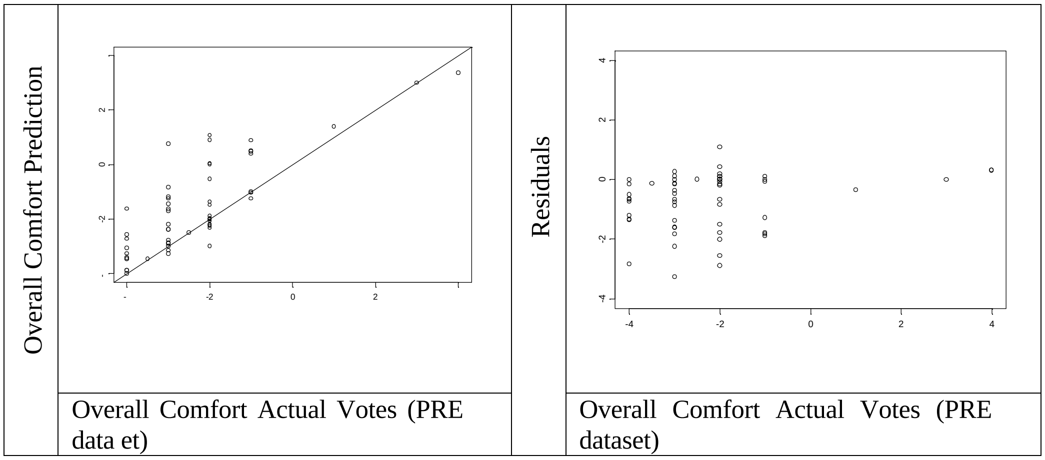

Figure 6.44 Delphi PRE dataset shows an overestimate from the all-body-part weighting method

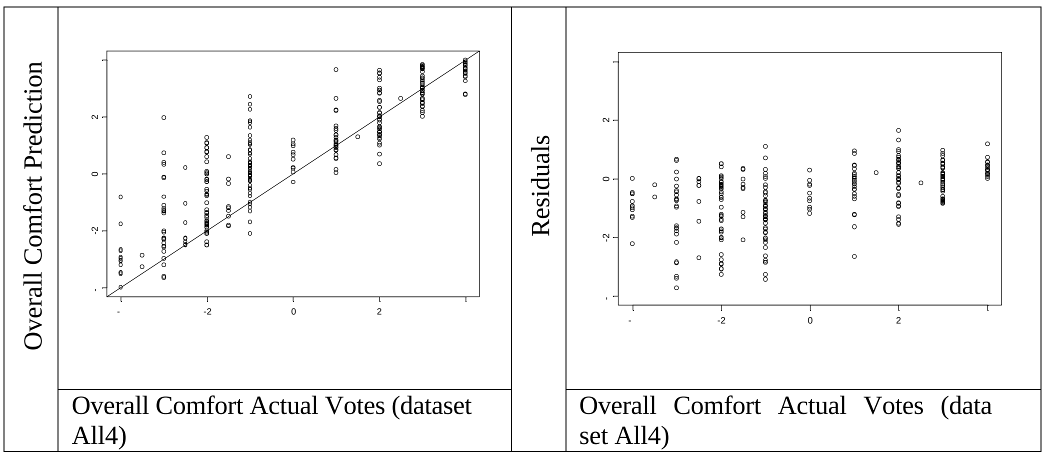

Figure 6.45 Delphi All4 dataset shows an overestimate from the all-body-part weighting method

Cabanac has been studying pleasure as a behavior motivator since the 1970s, on the premise that seeking pleasure has a central role in human life and is the key consideration in decision-making. His hypothesis is that people tend to maximize their experience of mental pleasure or minimize mental displeasure (Cabanac 1992). In one of his experiments (Cabanac, Guillaume et al. 2002), he let the subjects choose among four different behaviors in 50 situations taken from daily life. He found that the behavior selected significantly coincided with the maximizing the highest positive pleasure or minimizing the lowest negative displeasure.

Based on Cabanac's study and our comfort data, it seemed logical to give high priority to extreme feelings when modeling the brain's ranking of multiple signals. More intense signals tend to overshadow less intense ones.

Pellerin et al. (Pellerin, Deschuyteneer et al. 2003), in a study for Renault, found that whole-body comfort can be expressed as a function of the number of body parts that feel unpleasant. The important thing about this finding is that it shows that the overall comfort correlates with local discomfort, not with local comfort, supporting our observation that comfort is determined by "complaints," that is by the body parts that are most uncomfortable.

We explored more than a thousand survey records in which local and overall comfort values were entered, from the Delphi Wind Tunnel tests and the UC Berkeley chamber experiments. The best model we found for predicting overall comfort in these datasets was the following two rules:

Rule 1: Overall comfort is the average of the two minimum local comfort votes unless Rule 2 applies.

Rule 2: If the following criteria are met:

- the second lowest local comfort vote is >–2.5
- the subject has some control over his/her thermal environment

  or the thermal conditions are transient

then overall comfort is the average of the two minimum votes and the maximum comfort vote.

Note: if both hands or both feet comprise the two most uncomfortable body parts, ignore the second lowest hand or foot comfort value, and use the third lowest local comfort vote as the second lowest vote in Rule 1 and Rule 2.

The model assigns weights of 1 or 0 to the local comfort and calculates the average.

We developed this comfort model using the Delphi data as well as the UC Berkeley chamber data, because during the transient portions of the UC Berkeley cooling/heating applications, we could ask only 5 questions at a given time (normally two local sensations and one overall sensation, one local comfort and one overall comfort, as described in Chapter 4.3.3.2). The only times we could survey local comfort for all the body parts at once were in the stable period before local cooling/heating applications began. The number of UCB data points useful for the integration model is therefore small (24 records). The Delphi PRE dataset surveyed 12 local comforts and one overall comfort at a given time, and the other four datasets surveyed 7 local comforts and one overall comfort for each record. The differences in the results of the two experiments suggested the criterion in Rule 2 about transient condition and local control.

One major difference between the Delphi and the UC Berkeley chamber tests is that in the Delphi tests, the subjects had control over their environments. The subjects were allowed to adjust the car air conditioning based on their preferences. Brager et al. (Brager, G. et al. 2003a, Brager, G. et al. 2003b) have shown that when people have control over a given environment, their comfort level is higher than if they do not. In the U.C. Berkeley tests, the subjects had no control over the chamber environment, and their comfort votes were lower.

Another difference between the two experiments is that the UC Berkeley data are from stable conditions, while Delphi data involve both stable and transient conditions. The transients may create higher comfort, whether due to the overshooting from removing heat stress, or from the types of pleasurable sensation shown in Section 6.3 (Cabanac 1969, Mower 1976, Hensel 1981, and Attia 1984).

We put the second criterion in Rule 2 to account for the higher comfort levels found in the Delphi data for otherwise equal comfort combinations. Although the cause of the higher votes has not been proven to be these two effects alone, their influence can be seen to be strong. The comfort votes predictably overshoot in the positive direction as subjects manipulate the HVAC systems to restore comfort.

6.5.2 Validation of the model

We validated the model using data from both Delphi and UC Berkeley tests.

6.5.2.1 Validation using Delphi test data

First, we look at validation results for the PRE and All4 data sets. The results are improved substantially in relation to the results from the all-body-parts weighting model. The validation results are shown in Figure 6.46 and Figure 6.47.

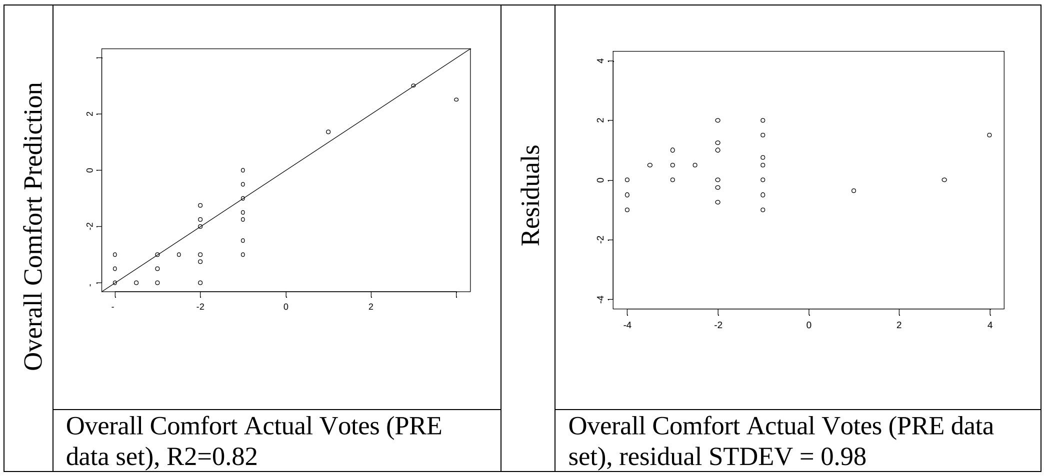

Figure 6.46 Validation of the integration comfort model for Delphi PRE dataset

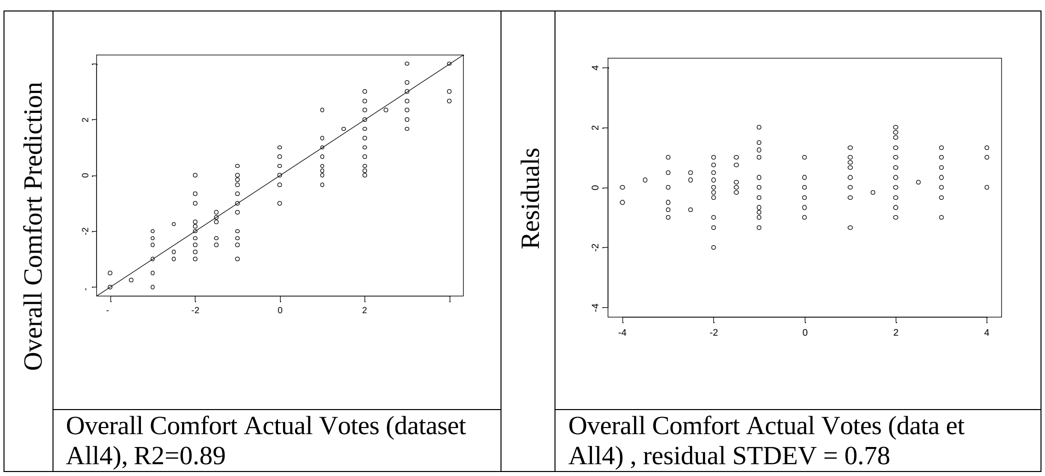

Figure 6.47 Validation of overall comfort model for Delphi All4 test dataset

Validation was also carried out for the rest of the Delphi datasets (All1, All2, All3). The results are shown in Figure 6.48, Figure 6.49, Figure 6.50.

Overall Comfort Prediction

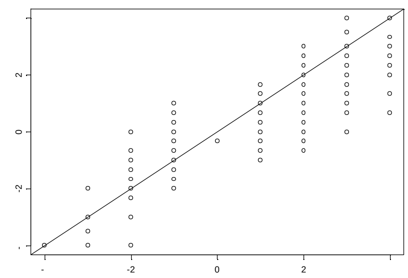

Overall Comfort Actual Votes (dataset All1), R2=0.83

Residuals

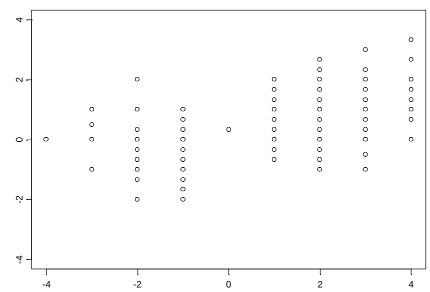

Overall Comfort Actual Votes (dataset All1), residual STDEV = 0.98

Figure 6.48 Validation of overall comfort model for Delphi All1 test dataset

Overall Comfort Prediction

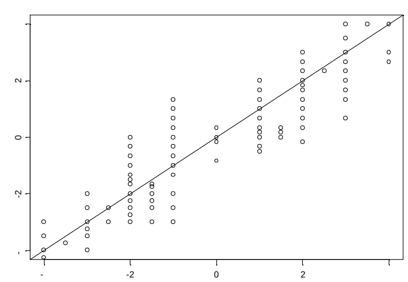

Overall Comfort Actual Votes (dataset All2), R2=0.89

Residuals

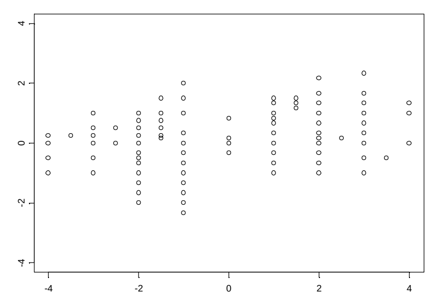

Overall Comfort Actual Votes (dataset All2), residual STDEV = 0.8

Figure 6.49 Validation of overall comfort model for Delphi All2 test dataset

Overall Comfort Prediction	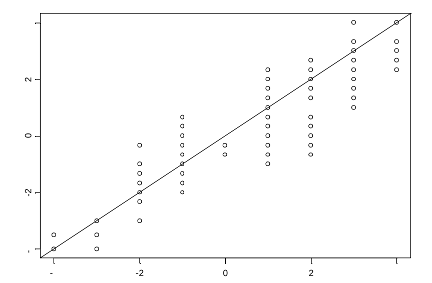	Residuals	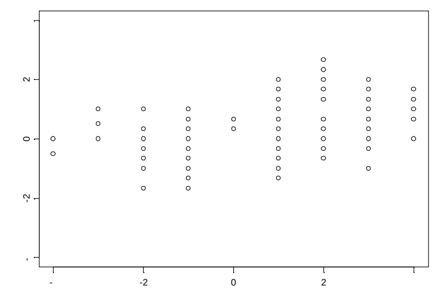
	Overall Comfort Actual Votes (dataset All3), R2=0.88		Overall Comfort Actual Votes (dataset All3), residual STDEV = 0.82

Figure 6.50 Validation of overall comfort model for Delphi All3 test dataset

The subjects in the Delphi tests experienced very complicated sets of sensations and perceptions. Some body parts were comfortable and some were uncomfortable, and the discomfort came from both warmth and cooling, i.e., an uncomfortable hot back and a slightly uncomfortable cooled chest. The validation results shown in Figure 6.40 – Figure 6.44 for the Delphi test data demonstrate that the rule-based integration comfort model gives good prediction results.

6.5.2.2 Validation using UCB steady-state-tests

As we stated in section 6.5.1, in the UCB tests, the only time we surveyed the local comfort for every body part at once was in the steady-state conditions just before local cooling/heating was applied. We validate the overall comfort model with these data.

Because the test conditions were stable and the subjects did not have control over the chamber environment, "Rule 2" is not met and "Rule 1" is applied. The UCB stable-conditions tests are grouped as cold, warm, slightly cool, and slightly warm, based on the subjects' votes.

1. Cold tests (overall sensation near -3, 5 tests)

The distributions of sensation and comfort votes from five cold tests are averaged and shown in Figure 6.51. The sensation votes are included in the figure in order to show what causes the discomfort. In this figure, we can see that local comfort covers a large range, from –3 for the hand to +1.5 for breathing. The overall comfort vote is close to the lowest two comfort votes (all three are circled). Based on our overall comfort model, prediction of overall comfort in this case is the average of –3 and –2.6, i.e., –2.8. The average of the subjects' overall comfort votes from 5 tests is also –2.8, so the predicted and actual votes are the same.

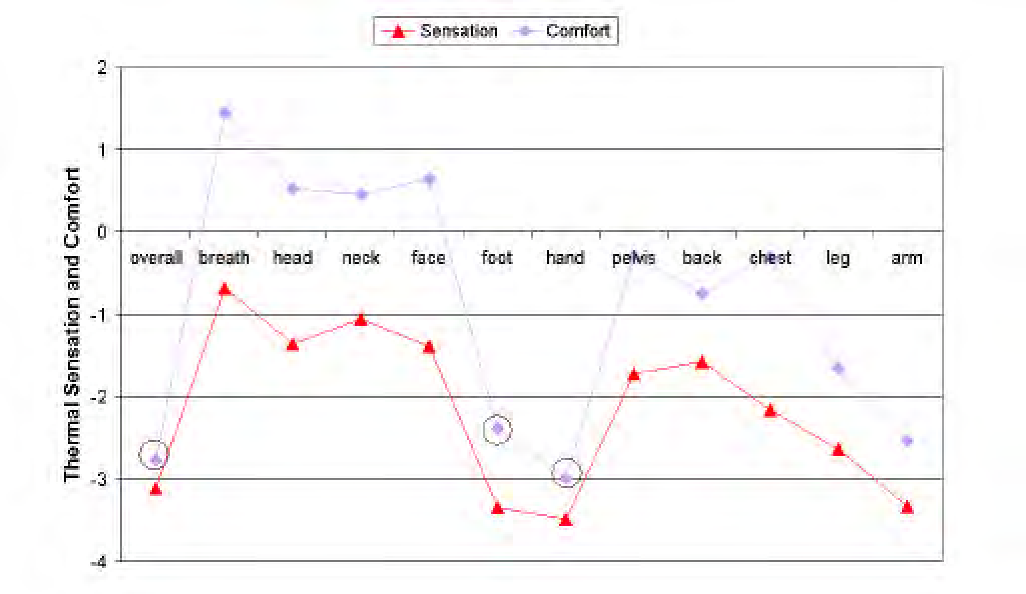

Figure 6.51 Validation of overall comfort model for UC Berkeley chamber experiment data in cold environment (overall sensation near –3, 5 tests)

2. Warm tests (overall sensation between +2 and +3, 10 tests)

The average sensation and comfort votes from 10 warm tests are shown in Figure 6.52. Local comfort varies from –0.3 to –1.7. Based on the model, the predicted overall comfort should be the average of the two least comfortable votes (-1.7 and –1.6, head and face), which is –1.65. The average of the overall comfort votes from the 10 tests–1.4, so the prediction is close to the actual vote (residual –0.25).

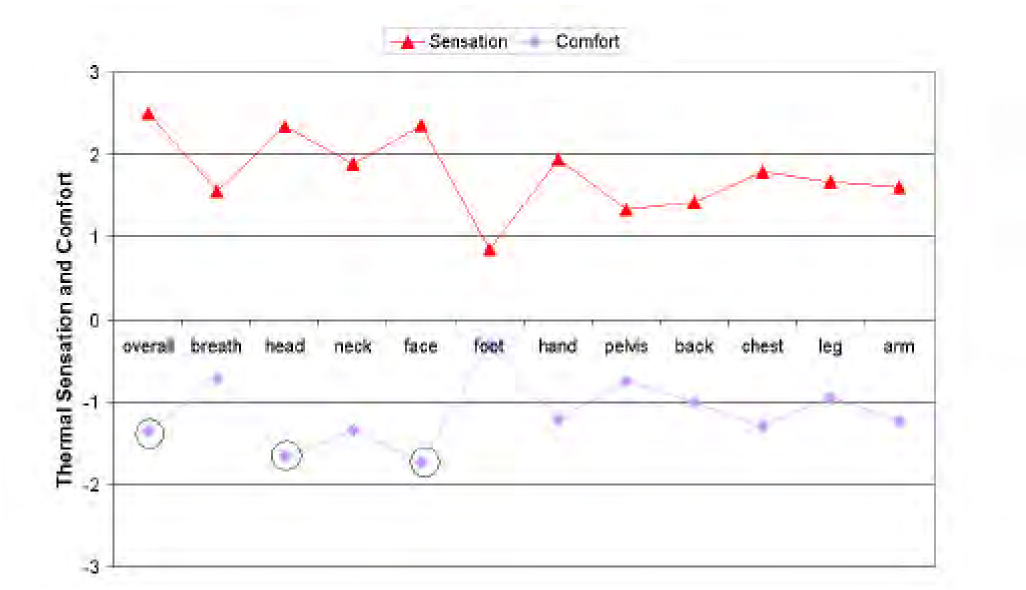

Figure 6.52 Validation of overall comfort model for UC Berkeley chamber experiment data in warm environment (overall sensation between +2 and +3, 10 tests)

3. Slightly cool tests (overall sensation near –1, 6 tests)

The average sensation and comfort votes from six slightly cold tests is shown in Figure 6.53. The prediction is the average of the two least comfortable (-0.1 and 0.2), which is 0.05. From the experiment, the average of the overall sensation votes of the six tests is –0.1. The difference between the prediction and the actual vote is 0.15.

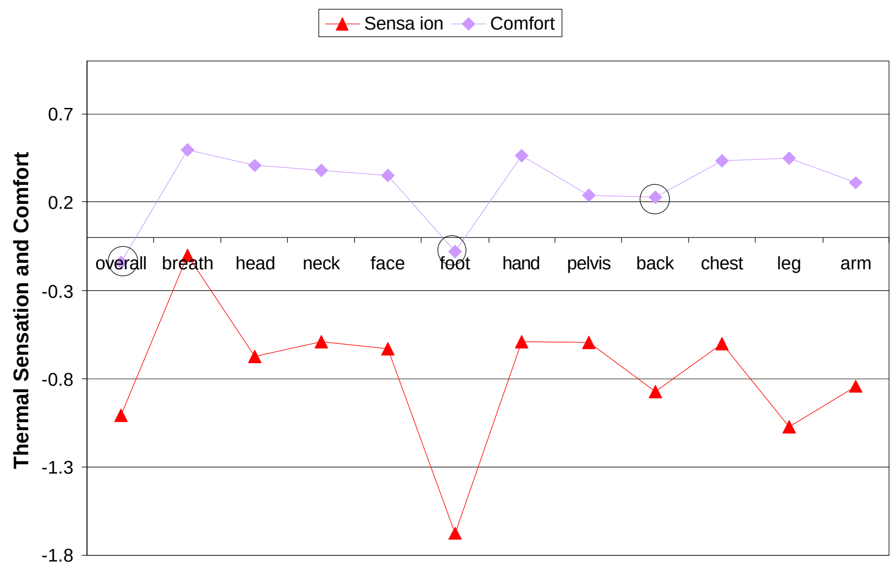

Figure 6.53 Validation of overall comfort model for UC Berkeley chamber experiment data in slightly cool environment (overall sensation near –1, 6 tests)

4. Slightly warm condition (sensation near 1)

The average sensation and comfort votes from three tests under slightly warm conditions are presented in Figure 6.54. The overall comfort (-0.44) is very close to the lowest two votes (-0.34, -0.48). The average of the two least comfortable votes is –0.41. The residual is 0.03.

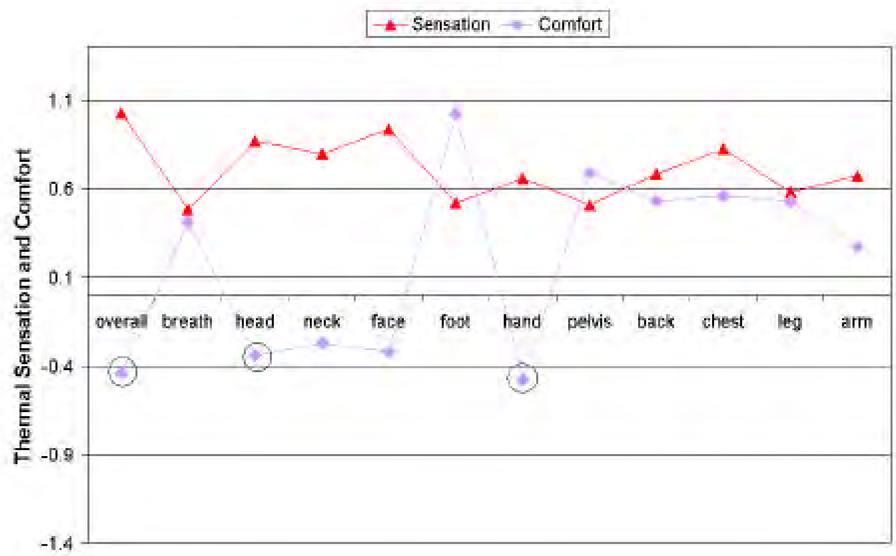

Figure 6.54 Validation of overall comfort model for UC Berkeley chamber experiment data in slightly warm environment (overall sensation near 1, 3 tests)

6.5.3 Discussion of the overall comfort model

A. Rule 1 versus rule 2; Delphi and UC Berkeley comfort data

Rule 2 in the overall comfort model raises the predicted overall comfort by adding in the maximum comfort vote when calculating the average. We tested the difference between the rules by applying Rule 1 using to the Delphi Wind Tunnel data. When we applied only Rule 1, which predicts the UC Berkeley overall comfort votes well, to all the Delphi datasets, we see a significant under-estimation of the overall comfort. Figure 6.55 presents the actual vs. predicted comfort votes (left figures) and the residuals (right figures). The under-estimation is obvious from the large amount of data below the 45° line (left figures) and the positive residuals above 0° line (right figures), and from comparison with Figures 6.46 and 6.50, which was predicted by applying Rule 2.

We also tested how Rule 2 would work with UCB data. The residuals increased for all three conditions. As shown in Figure 6.52, 6.53, 6.54, the overall comfort was close to the lowest local comfort values. Adding the maximum comfort vote into the average increased the errors. (In figure 6.51, the second minimum comfort vote was < -2.5, so Rule 2 could not be applied in any case).

Overall Comfort Prediction	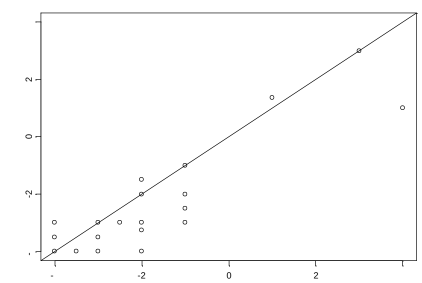	Residuals	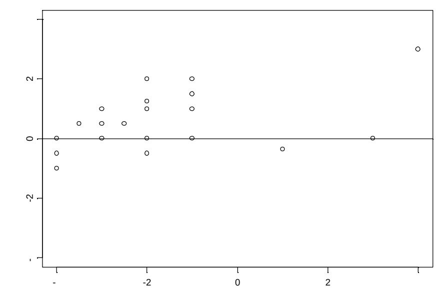
	Overall Comfort Actual Votes (dataset PRE)		Overall Comfort Actual Votes (dataset PRE)
Overall Comfort Prediction	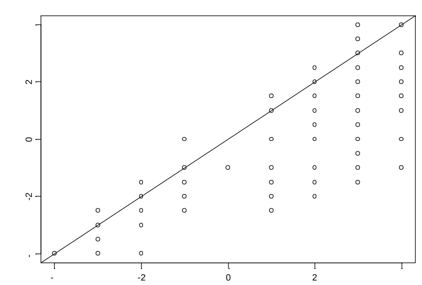	Residuals	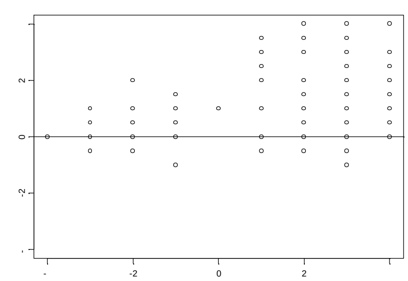
	Overall Comfort Actual Votes (dataset All1)		Overall Comfort Actual Votes (dataset All1)

Figure 6.55 Under estimation of the overall comfort Rule 1 for Delphi datasets (continued on next page)

Overall Comfort Prediction	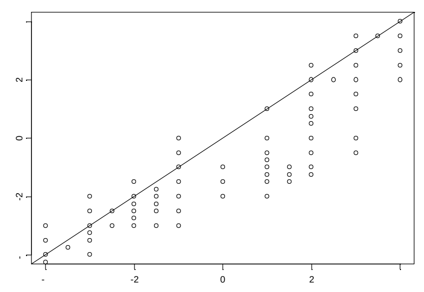	Residuals	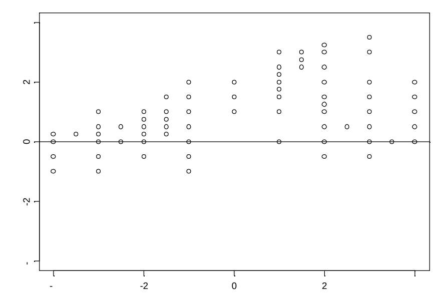
	Overall Comfort Actual Votes (dataset All2)		Overall Comfort Actual Votes (dataset All2)
Overall Comfort Prediction	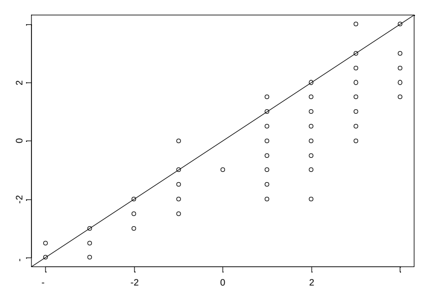	Residuals	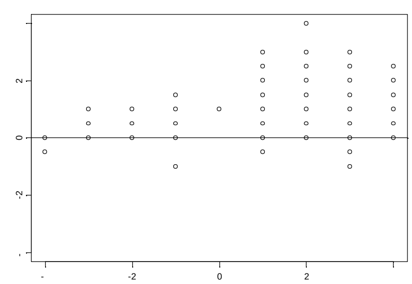
	Overall Comfort Actual Votes (dataset All3)		Overall Comfort Actual Votes (dataset All3)
Overall Comfort Prediction	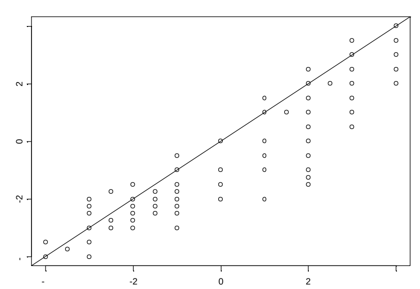	Residuals	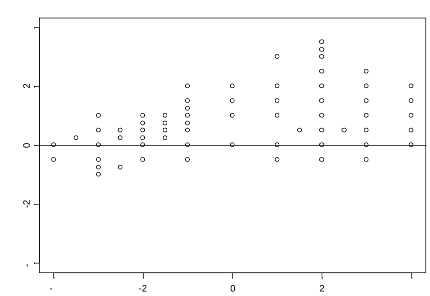
	Overall Comfort Actual Votes (dataset All4)		Overall Comfort Actual Votes (dataset All4)

Figure 6.55 Under estimation of the overall comfort of Rule 1 for Delphi datasets

B. Using the *second* minimum comfort vote in Rule 2

It is important that our Rule 2 requires the *second* lowest local comfort vote (> -2.5), rather than *a single* minimum vote. This reduces the chance of hands or feet alone becoming the decisive factor in overall comfort when either of these body parts is the only area of the body that is uncomfortable. Recall that we established above that hand and foot sensation and comfort have little impact on overall sensation and comfort. Thus, if only the hands or feet are uncomfortable, the overall state may nonetheless be perceived as comfortable, so we want the model not to determine overall comfort based on hands or feet votes alone. If the hands *and* feet are the two minimum comfort votes, the chances are good that there is discomfort in other areas of the body as well, and therefore a hand or foot could be the second minimum vote.

A summary of the four sensation and comfort prediction models has been published in "The 5th International Meeting on Thermal Manikin and Modeling" in September 2003, France (Zhang et al. 2003).

7. CONCLUSION

7.1 New sensation and comfort models

At the 10th International Conference on Environmental Ergonomics, Victor Candas stated:

> *"The interaction between temperature and sensation has not been investigated in conditions of non-uniformity or of large heterogeneity. The relationship between the various local sensations and the local sensations at various levels of body thermal state are not described. It is not even clear how the global thermal sensation is modified by changes in the local ones, a condition often observed for instance when people modify their clothing distribution." (Candas 2002)*

In discussing existing comfort models, he went on to say:

> *'Unfortunately, to our knowledge, none of the published models is effectively based on clear relationships between body temperature and sensations or pleasantness. The fact is that nobody knows exactly what these relationships are and how they interact locally to build the global judgment'.*

This thesis has examined thermal sensation and comfort in complex thermal environments and developed a series of models to predict them. The models predict: local sensation based on local thermal stimulus and the whole body thermal state (local sensation model), local thermal comfort based on local and whole body thermal sensations (local comfort model), integration of the local sensation to get a overall sensation (overall sensation model), and overall comfort based on the knowledge of local comfort (overall comfort model).

These models reflect or explain many observations found in the literature. They reflect studies of thermal sensitivities of different body parts and their different levels of influence on whole body sensation (local sensation and overall sensation models); incorporate the fact that people are more sensitive to cooling stimuli than heating stimuli; describe mathematically how a given thermal stimulus can feel pleasant or unpleasant depending on the overall thermal state of the body (local comfort model); model the observations that local sensation, with the same skin temperature, feels warmer if the whole body is colder than if the whole body is warmer (local sensation model); and propose an answer to the question of how the body integrates signals from local body parts based on their importance to the whole body, asymmetrical influences between cold vs. warm, and the higher impact of local sensations that are further away from the rest of the body.

The observations of the test results and the models answer numerous questions, such as how core temperature responds to different environment and thermal stimuli; why a sudden breeze in a slightly warm naturally ventilated house improves comfort; how repeatable subjective perception is; what influence one side of the body has on the other side when experiencing local cooling/heating; and, not least, how adaptation and transient sensation effects explain John Locke's observations of the thermal sensations of hands placed in basins of warm and cool water over 300 years ago.

This study also uncovered many interesting subjective and physiological behaviors, such as how subjective perception and thermoregulation response differs between three body groups; how the characteristics of thermoreceptors affect subjective thermal sensation and comfort in transient conditions; that local discomfort can have a decisive impact on overall comfort and therefore why a high priority in achieving comfort is to remove any local discomfort; that people do not like breathing warm air but much prefer breathing cool air; that the pelvis area always prefers to be warm; that when the body is warm, hand and finger temperature recovers very quickly after a local cooling stimulus is removed; that hand motion has a significant influence in increasing the skin temperature of a cold hand or finger.

We proposed rational models based on our test results and observations from the literature. These models are explicit in how each parameter contributes to the predicted variables. We then used the test data to statistically fit the coefficients for these models. The models are validated with Delphi wind tunnel test data and the results are satisfying.

The information provided from the test results and models will be very valuable in designing and evaluating air-conditioning systems in vehicles, personally-controllable 'task-ambient' systems in buildings, new types of glazing and solar control, perimeter zone heating and cooling, and mixed-mode naturally ventilated design.

The availability of this new model opens the door for many new interesting research areas and we provide suggestions for future study.

7.2 Limitations

7.2.1 Local sensation model during exercise

In calculating local sensation based on physiology parameters, the model uses local skin temperature to represent local thermal state, and mean skin temperature to represent the whole-body thermal state.

When people have a high metabolic rate, mean skin temperature may not represent the whole-body thermal state. Our model was developed from sedentary activity tests. How to apply it to higher metabolic activities needs further study.

Although we did not do any testing under higher metabolic rates, it is quite possible that exercise would not limit the applications of the other three models: local comfort model, overall sensation model, and the overall comfort model. These models do not directly correlate with the skin or core temperatures. Local comfort is a function of the local and overall sensations. Overall sensation integrates the local sensations, and overall comfort integrates the local comfort.

7.2.2 Skin wettedness and discomfort

Sweating serves an important purpose in thermoregulation. Heat loss through evaporation can be easily reach 75% when people are hot (the other 25% is lost through radiation and convection). When the environmental temperature is higher than core temperature, sweating becomes the only mechanism to reject heat.

Many researchers have found that thermal discomfort is correlated with skin wettedness (Gonzalez and Gagge 1973). However, our local sensation model correlates sensation only with skin and core temperatures. We also didn't design test conditions with different levels of humidity. Does that mean our models only apply to non-sweating people?

The answer is no. We believe that people feel hot or cold only through warm and cold thermoreceptors, and therefore we can correlate the local sensation with temperature. Sweating has an indirect impact on skin temperature. The skin swells when covered with sweat (Kerslake 1972, personal communication with L. Berglund). When heavy sweating is taking place, the sweat rate declines after a while because the presence of moisture on the skin inhibits local sweat secretion. When sweating is reduced, the skin temperature increases and people feel warmer. Recovery is rapid if the skin is dried (McIntyre 1980).

Skin wettedness is more closely related to the sense of discomfort or unpleasantness than to temperature sensation (ASHRAE 1993). ASHRAE *Fundamentals* terms the feeling of discomfort caused by the skin wettedness as 'moisture sensation'(ASHRAE 1997). When skin wettedness is above 0.25, people rarely feel comfortable. The stickiness of clothing caused by the increased friction between skin and the wet clothing induces an unpleasant feeling. Although our subjects did sweat in the warm and hot environment test conditions, the stickiness caused by the wet clothing may not have been sensed as much as with normal clothing, because the leotard that they wore was effective at wicking away moisture. The current study does not examine the correlation between comfort and skin wettedness.

7.3 Implications for thermal environmental control

The detailed sensation and comfort prediction models have great potential for evaluating thermal comfort in complex thermal environments and helping designing new HVAC systems in buildings and vehicles in order to provide better comfort and to use energy more efficiently.

As an example, based on the findings of this study, we propose a small step-change air temperature control strategy for task ambient HVAC systems and automobile air-conditioning. This strategy activate the high level of thermal comfort associated with the relief of discomfort during the small step-change process. This strategy and others are discussed further in Appendix 7.1.

Wireless sensors are quickly becoming more available for buildings and vehicles, and will provide the ability to inexpensively gather much more detailed information about the thermal environment than have been possible up to now. Rather than a single thermostat representing several hundred square feet of office space, we may begin to have information about the local microclimates around individual occupants. Coupled with the models developed in this study, ubiquitous wireless sensors could reshape the way we control spaces to provide comfort in an energy-efficient manner. They could enable decentralized HVAC systems to provide better control based on individual occupants' thermal comfort.

7.4 Suggestions for Future Work

7.4.1 Future studies

1. Incorporation with the UCB Physiology/Comfort Model

Over the last few years, I have been working with other researchers to develop the UCB Physiological Comfort Model (Huizenga et al. 2001). The model predicts detailed skin and core temperatures of individuals in asymmetrical and transient conditions. The subjective models described in this thesis predict sensation and comfort from skin and core temperatures. An immediate next step is to incorporate these comfort models into the UCB Physiological Comfort Model so that the model is able to predict local and overall sensation and comfort in complex environments.

2. Applications of the model

Once we have the UCB Physiological Comfort Model able to predict thermal sensation and comfort in complex environments, we will apply the model to many realistic situations to evaluate their impact on comfort. Applications areas include: glass type and window design, perimeter zones, natural ventilated buildings, local radiation, air temperature stratifications, underfloor supply systems, and different strategies for thermal environmental control in buildings and cars.

3. Additional tests in warm environments

Because of budget limitations, this project focused on cooling effects in warm environments. Although we did conduct some heating tests (applying local heating in cold environments), the number of these tests was very limited. For example, we did not do local heating tests in warm or hot conditions. We hope to be able to carry out such heating tests in the near future. The method will be similar to the local cooling tests.

Because people sweat in warm environments, when we do the heating tests, we will collect local sweating information, such as identifying sweating locations and local discomfort due to skin wettedness. We will examine the correlation between comfort (or discomfort) and local skin wettedness (moisture sensation).

4. Additional tests in cool environments

The conditions in our cooling tests were also limited. For example, we only supplied two air temperatures, 14 C and 22 C. We would like to do additional tests including more moderate air temperatures in the range of 28 to 34°C. We also need to carry out more tests of local cooling in cold environments, and tests using slower transient thermal environments.

5. Higher metabolic rate tests

The current test conditions do not include higher metabolic rates. As stated in the Limitations section above, the application of the local sensation model to higher metabolic rates needs further study. We are hoping to study the effects of increased metabolic rate on the models developed in this thesis.

6. HVAC control strategies

In Appendix 7.1, we proposed a step-change cooling pattern for air-conditioning as a means of generating higher comfort response. This idea and others like it need to be examined with human subject tests.

7. Further development of the adaptation model

This project did not focus on the study of skin thermal adaptation. During the regression analysis we realized the importance of this effect. We proposed a rational adaptation model based on a limited set our and Olesen's data. This model needs further development. One practical approach would be to create different overall thermal states by putting people in a water bath at different temperatures, then putting their hands (or other individual body parts) into a separate bath at a yet different temperature. We could then examine how quickly adaptation happens and what the adaptation ranges are for different parts of the body.

8. Further development of the overall comfort model

Currently the overall thermal comfort model is a rule-based model. Because overall comfort is complaint-driven (meaning uncomfortable local votes have a larger impact on overall comfort than comfortable votes), it might be possible to develop a comfort model as presented in Figure 7.1. In this hypothetical model, the weights for the uncomfortable segments are significantly larger than the weights for comfortable segments. How to use the existing data to develop this model needs further exploration.

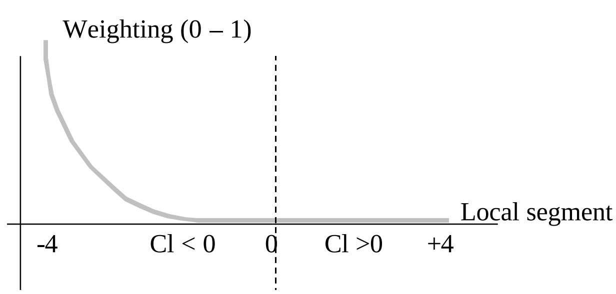

Figure 7.1 Another hypothetical overall comfort model

9. Acceptability

Our models predict thermal sensation and comfort locally and globally. It would be useful to understand the relationship between comfort and acceptability for each body part as well as the whole body. It is possible that acceptability can be expressed as a function of local and overall comfort. In order to find this relationship, we would need to do human subject tests using questionnaires for all three aspects: sensation, comfort, and acceptability.

10. Foot comfort

The relationship between sensation and comfort for the foot needs to have a separate study. People seem to have a very high preference for warm feet. There are many studies of the hand in the literature, but very few for the foot. Such a study would be useful because indoor air temperatures are often stratified, with cooler air at the feet and warmer air at the head – exactly opposite of most people's preference.

11. Breathing zone thermal sensation correlating with air temperature

In our local sensation model for the breathing zone, we correlate the sensation with the cheek skin temperature. Our purpose was to find a physiology parameter to link to the thermal sensation model. As we stated in Chapter 6.2.1.5, cheek skin temperature may not be the best to represent breathing zone air. The next regression step is to correlate the breathing zone thermal sensation directly with the air temperature, and if possible, to the relative humidity as well.

7.4.2 Recommendations for experimental methods

1. Screened human subjects

We found that for detailed human subject tests like those performed for this study, it is beneficial to use screened or trained subjects to help reduce experimental uncertainty. For example, in our tests, we found that one subject never voted above slightly warm (+1) or below slightly cool (–1) while the rest of the subjects voted ±3 or ±4 under the same test conditions. In the end we had to drop this subject from our database. Since the study was not about the use of scales, some training or pre-testing would have prevented this problem, and our data collection more efficient. Great care must be used to avoid introducing bias.

2. Effects of extremity movement on segment temperature and sensation

We found that hand motion increased finger and hand skin temperature significantly when the hand was cold. We did not provide enough instruction to our subjects about hand movement, and as a result there is more scatter in these data. It is not known whether the increased hand and finger temperatures were caused by local metabolism or by reducing vasoconstriction in hand and fingers.

3. Votes for every body part before local cooling/heating removal

During our transient heating and cooling applications, we could not survey too many body parts because the time was so limited. But at the end of local cooling/heating when steady-state had been reached, time was no longer an important issue and we should have asked sensation and comfort for every individual segment. In our tests, we asked the local sensation and comfort for the body part which had just experienced local stimulus. However, it would be useful if we had the information for the other body parts as well, even though they are less important since they had not experienced local cooling/heating.

4. Continuing core temperature measurement after cold test

During the cold tests, the subjects sat in a cold environment (16 – 20 °C) working on a computer. The activity level was around 1 to 1.1 met. The overall sensation votes were between –1 to –4 and the core temperature did not drop during the entire two hour cold exposure (Figure 5.12). There was no obvious shivering shown. After the tests, when the subjects started to walk outside, even though it was sunny and warm, they started shivering.

The reason is that their extremities had become well vasoconstricted during the cold environment tests. The hand and foot skin temperature were near 23 C (see Chapter 5.2.2). Once the subjects started to walk, the body began to deliver the blood to the working muscle, and that brought the cooler blood from the cold tissue to the core. It would be useful to have a core temperature reading during this period, but we didn't continue the readings after the chamber tests were finished. In the future, when doing the cold tests, we would recommend continuing to measure the core temperature for at least half an hour or longer, depending on how fast the core temperature recovers.

8. REFERENCES

ASHRAE (1992). ASHRAE Standard 55-1992 (Thermal Environmental Conditions for Human Occupancy). Atlanta, ASHRAE, Inc.

ASHRAE (1997). ASHRAE Handbook - Fundamentals. Atlanta, ASHRAE Inc.

Aschoff, J. (1979). Circadian Rhythms: General Features and Endocrinological Aspects. New York, Raven Press.

Attia, M. (1984). "Thermal Pleasantness and Temperature Regulation in Man." Neuroscience & Biobehavioral Reviews 8(3): 335-342.

Attia, M. and P. Engel (1981). "Thermal Alliesthesial Response in Man is Independent of Skin Location Stimulated." Physiology & Behavior 27(3): 439 - 444.

Bader, M. E. and J. Mead (1949). "The Effect of Local Cooling of the Finger and Wrist during Exposure to High Ambient Temperature (Abstract only)." Federation of American Societies of Experimental Biology, Proceedings 8: 6-7.

Baum, E., K. Bruck, et al. (1976). "Adaptive Modifications in the Thermoregulatory System of Long-distance Runners." Journal of Applied Physiology 40: 404 - 410.

Bauman, F. S., T. G. Carter, et al. (1998). "Field Study of the Impact of a Desktop Task/Ambient Conditioning System in Office Buildings." ASHRAE Transactions 104 (1).

Bauman, F. S., L. P. Johnston, et al. (1991). "Performance Testing of a Floor-Based, Occupant-Controlled Office Ventilation System." ASHRAE Transactions 97 (1).

Bazett, C. and B. McGlone (1930). "Experiments on the Mechanism of Stimulation of End-organs for Cold." America Journal of Physiology 93: 632.

Bazett, C., B. McGlone, et al. (1930). "The Temperatures in the Tissue which Accompany Temperature Sensations." Journal of Physiology (London) 69: 88 -112.

Bedford, T. (1936). "The Warmth Factor in Comfort at Work." Industr. Hlth. Res. Bd., Report No. 76, London, HMSO.

Benzinger, T. H., A. W. Pratt, et al. (1961). "The Thermostatic Control of Human Metabolic Heat Production." Proc. Natl. Acad. Sci. 47: 730.

Berg, J. V. D. (1974). "Thermal Conductivity and Heat Transfer of the Human Skin." Bibliotheca Radiologica 6: 166 - 177.

Berglund, L. G. and W. Cain (1989). Perceived Air Quality and the Thermal Environment. Indoor Air Quality 1989, San Diego: 93 - 99

Bohm, M., A. Browen, et al. (1990). Evaluation of Vehicle Climate with a Thermal Manikin - The Relationship between Human Temperature Experience and Local Heat Loss, Swedish Institute of Agricultural Engineering.

Brager, G. S. and R. de Dear (2000). "A Standard for Natural Ventilation." ASHRAE Journal: 21 - 28.

Brager, G. S., G. Paliaga, et al. (2003a). The Effect of Personal Control and Thermal Variability on Comfort and Acceptability. PR-1161 Final Reports, ASHRAE.

Brager, G. S., G. Paliaga, et al. (2003b). "Operable Windows, Personal Control & Occupant Comfort (RP-1161)." ASHRAE Transactions 110.

Brooks, G. A., T. D. Fahey, et al. (1996). Exercise Physiology - Human Bioenergetics and Its Applications. London, Mayfield Publishing Company.

Brown, J. S. and B. W. Jones (1997). "A New Transient Passenger Thermal Comfort Model." SAE: 143 - 148.

Burton, A. C. (1934). "A New Technique for the Measurement of Average Skin Temperature over Surfaces of the Body and the Changes of Skin Temperature during Exercise." The Journal of Nutrition 7(5): 481 - 496.

Cabanac, M. (1969). "Plaisir ou Deplaisir de la Sensation Thermique et Homeothermie." Physiol. Behav. 4: 359 - 364.

Cabanac, M. (1971). "The Physiological Role of Pleasure." Science 173: 1103 - 1107.

Cabanac, M. (1972). "Preferred Skin Temperature as a Function of Internal and Mean Skin Temperature." Journal of Applied Physiology 33(6): 699 - 703.

Cabanac, M., G. Hildebrandt, et al. (1976). "A Study of the Nycthemeral Cycle of Behavioral Temperature Regulation in Man." Journal of Physiology (London) 257: 275 - 291.

Cabanac, M. and B. Massonnet (1977). "Thermoregulatory Responses As a Function of Core Temperature in Humans." Journal of Physiology (London) 265: 587 - 596.

Cabanac, M. (1992). "Pleasure: The Common Currency." J. Theoret. Biol. 155: 173 - 200.

Cabanac, M. (1995). Human Selective Brain Cooling. New York, Springer-Verlag

Cabanac, M. (1997). "Heat Loss from the Upper Airways and Selective Brain Cooling in Humans." Annals of New York Academy of Science 813: 613 - 616.

Cabanac, M. (1998). "Selective Brain Cooling and Thermoregulatory Set-point." Journal of Basic and Clinical Physiology and Pharmacology 9(1): 3 - 13.

Cabanac, M., J. Guillaume, et al. (2002). "Pleasure in Decision-Making Situations." BMC Psychiatry 2(7).

Candas, V. (2002). "To Be or Not to Be Comfortable: Basis and Prediction." The 10th International Conference on Environmental Ergonomics, Fukuoka, Japan.

Chatonnet, J. and M. Cabanac (1965). "The Perception of Thermal Comfort." Int. J. Biometeorol. 9: 183 - 193.

Crawshaw, L. I., E. R. Nadel, et al. (1975). “Effect of Local Cooling on Sweating Rate and Cold Sensation.” Pflugers Arch. 354: 19 - 27.

Cunningham, D. J. and M. Cabanac (1971). "Evidence from Behavioral Thermoregulatory Responses of a Shift in Setpoint Temperature Related to the Menstrual Cycle." Journal of Physiology (Paris) 63: 236 - 238.

Cunningham, D. J., J. A. J. Stolwijk, et al. (1978). "Comparative Thermoregulatory Responses of Resting Men and Women." J. Appl. Physiol. 45: 908 - 915.

Dallenbach (1927). "The Temperature Spots and End Organs." America Journal of Psychology 39: 402 - 427.

Day, R. (1941). "Regulation of Body Temperature during Sleep." American Journal of Dis. Child 61: 734 - 746.

de Dear, R., E. Arens, et al. (1997). "Convective and Radiative Heat Transfer Coefficients for Individual Human Body Segments." International Journal of Biometeorology 40, No. 3: 145-156.

de Dear, R., J. W. Ring, et al. (1993). "Human Experience of Sudden Environmental Temperature Transients." Indoor Air 3: 181 - 192.

de Dear, R., J. W. Ring, et al. (1993). "Thermal Sensation Resulting from Sudden Ambient Temperature Changes." Indoor Air 3.

de Dear, R. and G. S. Brager (2001). "The Adaptation Model of Thermal Comfort and Energy Conservation in Built Environment." International Journal of Biometerology 45(2): 100 - 108.

DuBois, D. and E. F. DuBois (1915). “The Measurement of the Surface Area of Man.” Arch. Internal Med. 15: 868 - 881.

Fang, L., G. Clausen, et al. (1998). "Impact of Temperature and Humidity on the Perception of Indoor Air Quality." Indoor Air 8(2): 80 - 90.

Fanger, P. O. (1972). Thermal Comfort, NY, McGraw-Hill.

Fanger, P. O. and N. K. Christensen (1986). "Perception of Draught in Ventilated Spaces." Ergonomics 29: 215 - 235.

Fanger, P. O., A. K. Melikov, et al. (1988). "Air Turbulence and Sensation of Draught." Energy and Buildings 12: 21 - 39.

Fiala, D. (1998). Dynamic Simulation of Human Heat Transfer and Thermal Comfort. Ph. D. Thesis, Institute of Energy and Sustainable Development, De Montfort University, Leicester.

Fiala, D. (2002). "First Principles Modeling of Thermal Sensation Responses in Steady State and Transient Conditions." ASHRAE Transactions.

Frank, S. M., S. N. Raja, et al. (1999). "Relative Contribution of Core and Cutaneous Temperatures to Thermal Comfort and Autonomic Responses in Humans." J. Appl. Physiol. 86(5): 1588 - 1593.

Gagge, A. P., J. A. J. Stolwijk, et al. (1967). "Comfort and Thermal Sensation and Associated Physiological Responses at Various Ambient Temperatures." Environmental Research 1: 1 - 20.

Gagge, A. P., J. A. J. Stolwijk, et al. (1969). "Comfort and Thermal Sensation and Associated Responses during Exercise at Various Ambient Temperatures." Environmental Research 2: 209 - 229.

Gagge, A. P., J. A. J. Stolwijk, et al. (1970). "An Effective Temperature Scale Based on a Simple Model of Human Physiological Regulatory Response." ASHRAE Transactions 77(1): 247 - 262.

Gagge, A. P. and Y. Nishi (1977). Heat Exchange between Human Skin Surface and Thermal Environment. Bethesda, America Physiological Society.

Gonzalez, R. R. and A. P. Gagge (1973). "Magnitude Estimates of Thermal Discomfort during Transients of Humidity and Operative Temperature and Their Relation to the New ASHRAE Effective Temperature (ET*)." ASHRAE Transactions 79 (1): 88 - 96.

Gonzalez, R. R. and L. G. Berglund (1978). Efficacy of Temperature and Humidity Ramps in Energy Conservation. Connecticut, John B. Pierce Foundation, 105 - 131.

Goto, T., J. Toftum, et al. (2002). Thermal Sensation and Comfort with Transient Metabolic Rates. Proceedings of Indoor Air Conference, Monterey, USA, June 30 – July 5.

Griffiths, I. D. and D. A. McIntyre (1974). "Sensitivity to Temporal Variations in Thermal Conditions." Ergonomics 17, No. 4: 499 - 507.

Guan, Y., M. H. Hosni, et al. (2003). "Investigation of Human Thermal Comfort under Highly Transient Conditions for Automobile Applications - Part1: Experimental Design and Human Subject Testing Implementation." ASHRAE Transactions 109(2).

Guan, Y., M. H. Hosni, et al. (2003). "Investigation of Human Thermal Comfort under Highly Transient Conditions for Automobile Applications - Part2: Thermal Sensation Modeling." ASHRAE Transactions 109(2).

Guyton, C., M.D. (1971). Textbook of medical physiology. Philadelphia, London, W.B. Saunders.

Guyton, C., M.D. (2002). Textbook of medical physiology. Philadelphia, London, W.B. Saunders.

Haber, R. N. (1958). "Discrepancy from Adaptation Level as a Source of Affect." Journal of Experimental Psychology 56: 370 - 375.

Hagino, M. and J. Hara (1992). "Development of a Method for Predicting Comfortable Airflow in the Passenger Compartment." SAE Technical Paper Series 922131: 1 - 10.

Hammel, H. T., D. C. Jackson, et al. (1963). "Temperature Regulation by Hypothalamic Proportional Control with An Adjustable Set Point." Journal of Applied Physiology 18: 1146 - 1154.

DuBois, D. and E. F. DuBois (1915). “The Measurement of the Surface Area of Man.” Arch. Internal Med. 15: 868 - 881.

Hardy, J. D. and E. F. DuBois (1938). "The Technique of Measuring Radiation and Convection." Journal of Nutrition 15: 461 - 475.

Haslag, S. W. M. and A. B. Hertzman (1965). "Temperature Regulation in Young Women." Journal of Applied Physiology 20: 1283 - 1288.

Hellon, R. F. (1963). "Local Effect of Temperature." British Med. Bulletin 19: 141 - 144.

Hensel, H. (1979). Thermoreception and Human Comfort. Copenhagen, Danish Building Research Institute.

Hensel, H. (1981). Thermoreception and Temperature Regulation. London, Academic Press.

Hensel, H. (1982). Thermal Sensation and Thermoreceptors in Man. Springfield, Ill., Charles C Thomas.

Heschong, L. (1979). Thermal Delight in Architecture. Boston, MIT Press.

Hildebrandt, G., P. Engel, et al. (1981). "Temperaturegulation und Thermischer Komfort." Zeitschrift fur Physikalische Medizin 10: 49 - 61.

Hodgdon, J. A. and M. B. Beckett (1984). Prediction of Percent Body Fat for U.S. Navy Men from Body Circumferences and Height. San Diego, Naval Health Research Center.

Hodgdon, J. A. and M. B. Beckett (1984). Prediction of Percent Body Fat for U.S. Navy Women from Body Circumferences and Height. San Diego, Naval Health Research Center.

Hopkinson, R. G. (1963). Architectural Physics, Lighting. London, Her Majesty's Stationery Office.

Houdas, Y. and E. F. J. Ring (1982). Human Body Temperature: Its Measurement and Regulation. New York, London, Plenum Press.

Huizenga, C., H. Zhang, et al. (2001). "A Model of Human Physiology and Comfort for Assessing Complex Thermal Environments." Building and Environment 36(6): 691 - 699.

Ingersoll, J. G., T. G. Kalman, et al. (1992). "Automobile Passenger Compartment Thermal Comfort Model - Part II: Human Thermal Comfort Calculation." SAE Technical Paper Series 920266: 1-11.

ISO (1994). International Standard ISO 7730 - Moderate Thermal Environments - Determination of the PMV and PPD Indices and Specification of the Conditions for Thermal Comfort, International Organization for Standardization

Issing and H. Hensel (1981). "Static Thermal Sensation and Thermal Comfort." Pflugers Arch. 389:R: 39.

Ivanov, K., V. Konstantinov, et al. (1982). "Thermoreceptor Localization in the Deep and Surface Skin Layers." Journal of Thermal Biology 7: 75 - 78.

Ivanov, K., V. Konstantinov, et al. (1986). "Thermoreceptor Distribution in Different Skin Layers and its Significance for Thermoregulation." Journal of Thermal Biology 11: 25 - 29.

Jones, B. W. and Y. Ogawa (1992). "Transient Interaction between the Human and the Thermal Environment." ASHRAE Transaction 98, Pt.1.

Keller, A. D. and W. K. Hare (1932). Proceedings of Soc. Exptl. Biol. Med. 29: 1069.

Kenshalo, D. R. (1970). "Psychophysical Studies of Temperature Sensitivity." Contributions to Sensory Physiology 4: 17 - 74.

Kerslake, D. M. (1972). The Stress of Hot Environments, Cambridge University Press.

Kohri, I., T. Kataoka, et al. (1995). "Evaluation Method of Thermal Comfort in a Vehicle by SET* Using Thermal Manikin and Theoretical Thermoregulation Model in Man." IMechE C496(022): 357 - 363.

Koscheye, V. S., S. Paul, et al. (1998). "Body Surface Temperature Tuning as a Comfort Support System in Space and Other Extreme Environment." SAE Technical Paper Series 981723: 103 - 111.

Kuno, S. (1995). Comfort and Pleasantness. PAN Pacific Symposium on Building and Urban Environmental Conditioning in Asia, Nagoya, Japan.

Kuno, Y. (1956). Human Perspiration. Charles C. Thomas, Springfield, Ill.

Lewis, M. I., G. B. Meese, et al. (1983). "Effects of Moderate Cold and Heat Stress on Factory Workers in Southern Africa. 4, Skin Temperature, Oral Temperature, Heart Rate and Comfort Vote." South African Journal of Science 79: 28 - 38.

Lewis, T. (1930). "Observations Upon the Reactions of the Vessels of the Human Skin to Cold." Heart 15: 177 - 208.

Marks, L. E. and R. R. Gonzalez (1974). Skin Temperature Modifies the Pleasantness of Thermal Stimuli. Nature. 247: 473 - 475.

Matsunaga, K., F. Sudo, et al. (1993). "Evaluation and Measurement of Thermal Comfort in the Vehicles with a New Thermal Manikin." SAE Paper Series, 931958.

McIntyre, D. A. (1980). Indoor Climate. London, Applied Science Publishers LTD.

McNall, P. E., J. Jaax, et al. (1967). "Thermal Comfort (Thermally Neutral) Conditions for Three Levels of Activity." ASHRAE Trans. 73 (1): 1.3.1 - 1.3.14.

Miller, G. A. (1956). The Magical Number Seven, Plus or Minus Two. Psychological Review. 63: 81 - 97.

Mitchell, D. and C. H. Wyndham (1969). "Comparison of Weighting Formulas for Calculating Mean Skin Temperature." Journal of Applied Physiology 26(5): 616 - 622.

Mower, D. M. (1976). "Perceived Intensity of Peripheral Thermal Stimuli Is Independent of Internal Body Temperature." Journal of Comparative and Physiological Psychology 90(12): 1152 - 1155.

Nadel, E. R., J. W. Mitchell, et al. (1973). “Differential Thermal Sensitivity in the Human Skin.” Pflugers Arch. 340: 71 - 76.

Nagano, K., A. Takaki, et al. (2002). Thermal Responses to Temperature Steps in Summer. The 10th International Conference on Environmental Ergonomics, Fukuoka, Japan.

Nevins, R. G., F. G. Rohles, et al. (1966). "Temperature-humidity Chart for Thermal Comfort of Seated Persons." ASHRAE Trans. 72: 283 - 291.

Nielsen, B. and C. Jenssen (1992). “Evidence Against Brain Stem Cooling by Face Fanning in Severely Hyperthermic Humans.” Pflugers Arch 422: 168 - 172.

Nilsson, H. O. (2003). Evaluation and Visualisation of Perceived Thermal Conditions. The 5th International Meeting on Thermal Manikin and Modeling, Centre d'Etudes de Physiologie Appliquee, Strasbourg, France, September 29 – 30.

Oguro, M., E. Arens, et al. (2002). "Convective Heat Transfer Coefficients and Clothing Insulation for Each Part of the Clothed Human Body, Part 1: from 0.2 - 5.5 m/s." Architectural Institute of Japan.

Olesen, B. W. and P. O. Fanger (1973). "The Skin Temperature Distribution for Resting Man in Comfort." Arch. Sci. Physiology 27: A385 - A393.

Olesen, B. W. (1984). How Many Sites Are Necessary to Estimate a Mean Skin Temperature. New York, Raven Press.

Palmer, J. D. (1976). An Introduction to Biological Rhythms. New York, San Francisco, London, Academic Press.

Pandolf, K. B., M. N. Sawka, et al. (1988). Human Performance Physiology and Environmental Medicine at Terrestrial Extremes, Benchmark Press.

Pellerin, N., A. Deschuyteneer, et al. (2003). Local Thermal Unpleasantness and Discomfort Prediction in the Vicinity of Thermoneutrality. The 5th International Meeting on Thermal Manikin and Modeling, Centre d'Etudes de Physiologie Appliquee, Strasbourg, France, September 29 – 30.

Pittendrigh, C. S. (1974). Circadian Oscillations in Cells and Circadian Organization of Multicellular Systems. Cambridge, MA, MIT Press.

Ramanathan, N. L. (1963). “A New Weighting System for Mean Surface Temperature of the Human Body.” : 531-533.

Randall, W. C. (1946). "Quantitation and Regional Distribution of Sweat Glands in Man." Journal of Clinical Investigation 25: 761 - 767.

Randall, W. C. (1947). "Local Sweat Gland Activity Due to Direct Effect of Radiant Heat." America Journal of Physiology 150: 365 - 371.

Rapaport, S. I., E. S. Fetcher, et al. (1949). "Control of Blood Flow to the Extremities at Low Ambient Temperatures." Journal of Applied Physiology 2: 61 - 71.

Ring, J. W. and R. J. de Dear (1991). "Temperature Transients: A Model for Heat Diffusion through the Skin, Thermoreceptor Response and Thermal Sensation." Indoor Air 1(4): 448-456.

Rohles, F. H. (1970). Thermal Sensation of Sedentary Man in Moderate Temperature. Kansas, Kansas State University.

Rohles, F. H. and S. B. Wallis (1979). "Comfort Criteria for Air Conditioned Automotive Vehicles." SAE Technical Paper Series 790122.

Schiller, G. E., E. A. Arens, et al. (1988). "A field Study of Thermal Environment and Comfort in Office Buildings." ASHRAE Transactions 94(2): 280 - 308.

Segre, G. (2002). A Matter of Degrees. New York, Viking Penguin.

Shapiro, C. M., A. T. Moore, et al. (1974). "How Well Does Man Thermoregulate during Sleep." Experientia (Basel) 30: 1279 - 1281.

Stevens, J. C. (1979). "Variation of Cold Sensitivity over the Body Surface." Sensory Processes 3: 317 - 326.

Stevens, J. C. and K. K. Choo (1998). "Temperature Sensitivity of the Body Surface over the Life Span." Somatosensory & Motor Research 15(1): 13 - 28.

Stevens, J. C., L. E. Marks, et al. (1974). "Regional Sensitivity and Spatial Summation in the Warmth Sense." Physiology and Behavior 13: 825 - 836.

Stevens, J. C. and S. S. Stevens (1960). "Warmth and Cold: Dynamic of Sensory Intensity." Journal of Experimental Psychology 60(3): 183 - 192.

Stevens, J. C., L. E. Marks, et al. (1974). "Regional Sensitivity and Spatial Summation in the Warmth Sense." Physiology and Behavior 13: 825 - 836.

Stolwijk, J. A. J. (1971). NASA Contractor Report. A Mathematical Model of Physiological Temperature Regulation in Man, Yale University School of Medicine: 1-77.

Tanabe, S. (1988). Thermal Comfort Requirement in Japan, Ph. D. Thesis, Waseda University.

Taniguchi, Y., H. Aoki, et al. (1992). "Study on Car Air Conditioning System Controlled by Car Occupants' Skin Temperatures - Part 1: Research on a Method of Quantitative Evaluation of Car Occupants' Thermal Sensations by Skin Temperatures." SAE Technical Paper Series 920169: 13-19.

Teichner, W. H. (1958). “Assessment of Mean Body Surface Temperature.” Journal of Applied Physiology 12(2): 169 - 176.

Toftum, J., A. S. Jorgensen, et al. (1998). "Upper Limits for Air Humidity for Preventing Warm Respiratory Discomfort." Energy and Buildings 28(3): 15 - 23.

Toftum, J., G. Reimann, et al. (2002). Perceived Air Quality, Thermal comfort, and SBS Symptoms at Low Air Temperature and Increased Radiant Temperature. Indoor Air 2002, Monterey, California, June 30 – July 5.

Wahl, D. (1995). Rechnerische Untersuchungen Zum Thermischen Komfort in Fahrzeugkabinen.

Wang, X. L. (1994). Thermal Comfort and Sensation under Transient Conditions. Department of Energy Technology. Stockholm, The Royal Institute of Technology.

Wang, X. L. and F. K. Peterson (1992). "Estimating Thermal Transient Comfort." ASHRAE Transaction: 98, Pt. 1.

Wenger, C. B., M. F. Robert, et al. (1975). "Forearm Blood Flow during Body Temperature Transients Produced by Leg Exercise." Journal of Applied Physiology 38: 58 - 63.

Winslow, C., L. P. Herrington, et al. (1936). “A New Method of Partitional Calorimetry.” Am. Journal of Physiology 116: 641 - 655.

Wyon, D. P., S. Larsson, et al. (1989). "Standard Procedures for Assessing Vehicle Climate with a Thermal Manikin." SAE Technical Paper Series 890049: 1-11.

Xu, X. (1999). "Multi-loop Control of Liquid Cooling Garment System." Ergonomics 42(2): 282 - 298.

Xu, X., P. Tikuisis, et al. (2003). "Thermoregulatory Model for Prediction of Long-Term Cold Exposure." J. Appli. Physiol. In press.

Zhang, H., C. Huizenga, et al. (2001). "Considering Individual Physiological Differences in a Human Thermal Model." Journal of Thermal Biology 26(4-5): 401-408.

Zhang, H., C. Huizenga, et al. (2003). “Thermal Sensation and Comfort in Transient Non-uniform Thermal Environments.” The 5th International Meeting on Thermal Manikin and Modeling, Centre d'Etudes de Physiologie Appliquee, Strasbourg, France, September 29 – 30.

Zotterman, Y. (1953). "Special Senses: Thermal Receptors." Ann. Rev. Physiology 15: 357 - 372.

9. APPENDICES

9.1 Appendix 4.1 – Selection of a method to cool/heat local skin temperature

Possible alternatives

By looking at the literature and checking the products on the market, we considered four possibilities: a water suit or water blanket, phase change material, electric fabric, and air (the first three alternatives are shown in Figure A4.1.1). The two major criteria for choosing the method were to create (1) a temperature distribution over each that is as natural as possible, (2) a feeling to the wearer of the cooling/heating device that is as natural as possible. Our study is about "comfort", and so we should avoid any uncomfortable feeling produced by the experimental device used to heat and cool the body parts.

	
Commercially available tube suit	Water pads
	
Phase change gel	Electricity heating fabric

Figure A4.1.1 Possible alternatives to control local skin temperature

A commonly used method for controlling local skin temperature is the water suit. Xu (Xu, 1999) developed a liquid cooling garment to remove heat during exercise. Frank (Frank, Raja et al. 1999) applied circulating-water mattresses to control skin temperature when studying the relative contributions of core and cutaneous temperatures on thermal comfort. Our concern is that because we are conducting a thermal comfort study, the unfamiliar feeling of the heavy water suit may affect the thermal sensation. In addition, the water suit controls the skin temperature at a constant level over each body part, because the resistance from skin to the water is so low. This rarely happens in real life where our skin shows variations in temperature even on one segment. For example, the cooling of the upper arm to the same skin temperature as the lower arm probably only happens for a swimmer. Koscheye (Koscheye, Paul et al. 1998) also point out that using a water suit produces rapid skin temperature changes, which emphasizes the impact from the skin rather than from the core. That may be more proper for astronauts because they actually wear water suits in space, but less desirable for normal people. Because of the nature of our comfort study, we decided the water suit approach is not preferable.

The electric fabric has the advantage that it is a fabric and can wrap a body part (Figure A4.1.1). An electric fabric suit would not produce the unfamiliar feeling as with the water suit. However, when we checked the surface temperature of the electrical fabric with an IR camera, we realized that the surface temperature shows strong variation (Figure A4.1.2), which would cause differential heating.

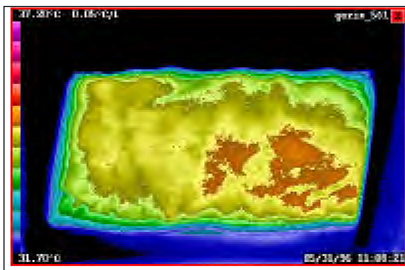	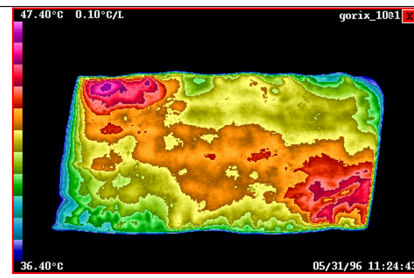
Lower power supply, surface temperature 31 – 37°C	Higher power supply, surface temperature 36 – 47°C

Figure A4.1.2 Uneven surface temperature of an electrical fabric

We intended to combine the electric fabric together with the phase change material to control the skin temperature. After measuring the phase change material surface temperature, we realized that the phase change material appears hard and rigid at the phase change temperature, which is not convenient for covering the skin; in addition, the temperature of the phase change material did continuously rise at the phase change temperature, which reduced its value as a cold sink (Figure A4.1.3).

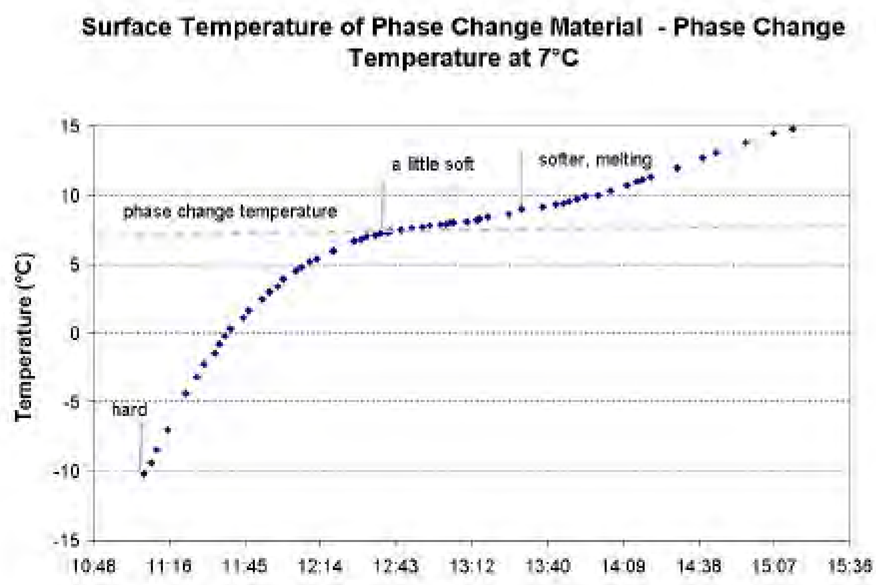

Figure A4.1.3 Phase change material surface temperature during phase change process

Local skin temperature distribution is realistic

Figure 4.4 in chapter 4 shows large skin temperature variations of the lower leg after it was cooled. Table A4.1.1 and Figure A4.1.4 shows the back skin temperature variation in a uniform environment, with a 1.5 °C variation. The middle back is warmer than the sides and the upper back is warmer than the lower back.

Table A4.1.1 Back skin temperature distribution (02004)

Location	Skin temperature (°C)
upper middle back	36.1
upper right back	35.6
upper left back	35.6
lower middle back	35.5
lower right back	34.6

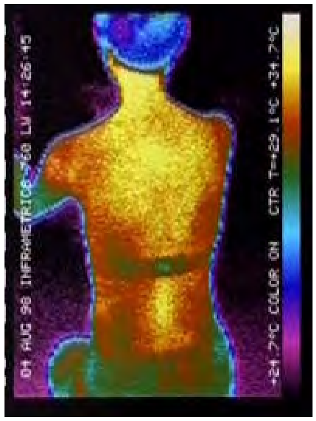

Figure A4.1.4 Back skin temperature distribution

The natural skin temperature variation implies that the contact methods (water suit and blanket, phase change material, and electrical fabric) will produce artificial skin temperature distributions. So we decided to focus on an air approach.

Early local air cooling/heating ideas

A few images showing the early designs of the air cooling/heating approach are presented in Figure A4.1.5. Judging from the effects of the two main criteria, we gradually became aware that an air-sleeve approach fitted our requirements the best.

 mock up of air sleeve	 air hood to cool head	 testing the air chair for pelvis cooling
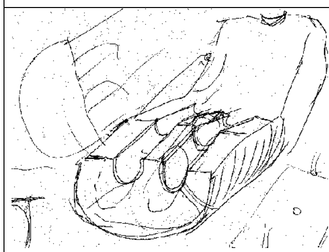 suitcase design	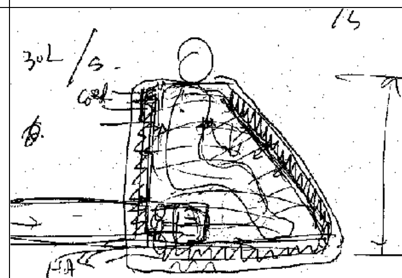 ice box	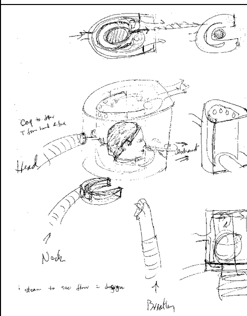 helmet for head and neck

Figure A4.1.5 Design process of local skin temperature control

9.2 Appendix 4.2 - Skin temperature measurement sites

This appendix describes how we chose the skin temperature measurement locations for our tests.

Skin temperature variation from one place to another is large in cold environment due to vasoconstriction, but much more uniform in warm environments. Figure A4.2.1 (Houdas and Ring 1982) shows skin temperature at 10 locations under 5 environmental conditions, 20 and 25°C (cold), 30°C (Neutral), 35 and 40°C (hot).

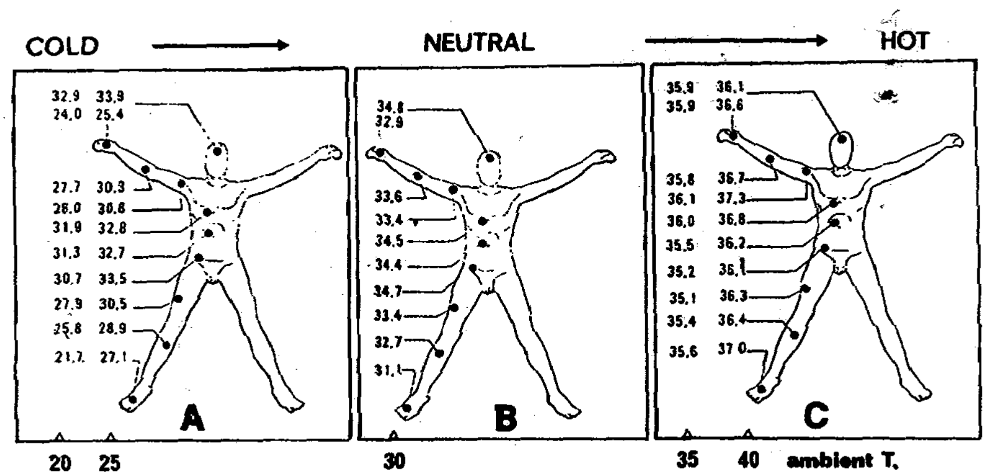

Figure A4.2.1 Skin temperature distributions under different thermal environments (Houdas and Ring, 1982)

"Mean skin temperature" is usually determined from a series of skin temperature measurements. To relate skin temperature measurements to underlying tissues, a coefficient is assigned to each of the skin temperature measurements, depending on the site and the surface characteristics of the area. If the area is large and anatomically simple, e.g., the abdomen, the thermal gradients across the surface are low and one measurement with a high coefficient can be used for the whole area. However, the extremities have complicated shapes and possess high thermal gradients. For this reason, a greater number of measurements are required and the coefficients are lower.

There are many proposals in the literature for the sets of measurement sites used to get mean skin temperature. The number of sites necessary to represent mean skin temperature depends on the level of non-uniformity of skin temperature, which is in turn determined by environmental conditions. In warm conditions when skin temperature is rather uniform and is mainly determined by vasodilation, 2 –4 sites may be enough. In neutral conditions 4 – 8 sites may be needed. In cold conditions, 8 – 12 sites may be necessary to account for local skin temperature variations (Olesen 1984). The number of sites has often been decided as a compromise between what is necessary and what is economically and technically possible. Since our experiment is about thermal comfort, we want to minimize discomfort by limiting the number of skin temperature measurement sites, because numerous cables can cause discomfort. Here I present several commonly used methods to calculate the mean skin temperature, and propose the skin temperature measurement sites for our test.

Background for mean skin temperature measurement sites

A simple method to calculate the mean skin temperature is a three-point method proposed by Burton (Burton 1934).

$$\text{Average } T_s = 0.50\ T_{chest} + 0.36\ T_{leg} + 0.14\ T_{lower\ arm} \qquad \text{Eq. (A4.2.1)}$$

Providing weights based on surface areas calculated after Dubois (Dubois and DuBois 1915), Winslow et al. proposed 15 points to get the mean skin temperature (Winslow, Herrington et al. 1936). These 15 points are shown in Figure A4.2.2. The method calculates the arithmetic mean for four anatomical segments: the head, the upper extremities, lower extremities, and trunk. Each segmental mean temperature is then weighted by the area to get the whole body mean skin temperature.

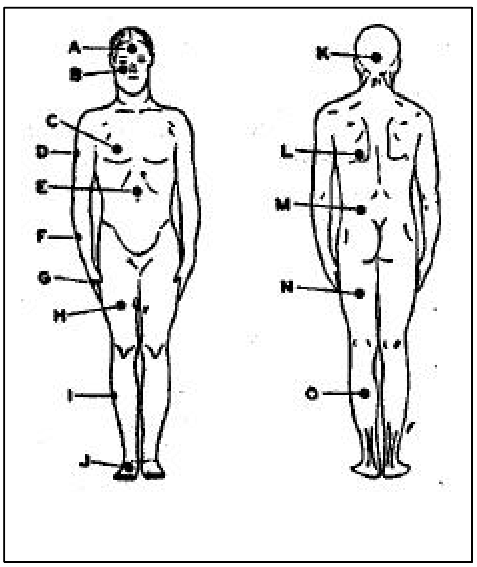

Figure A4.2.2 Fifteen locations to calculate mean skin temperature (Winslow et al. 1936)

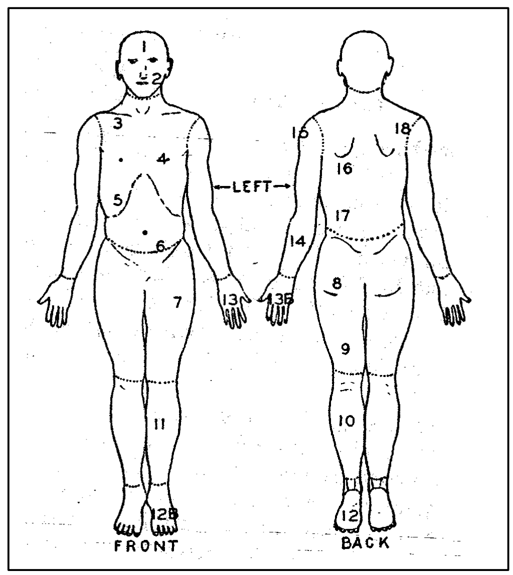

Figure A4.2.3 Twenty locations tested to get mean skin temperature by Hardy/DuBois (Hardy and DuBois 1938)

Hardy and DuBois (Hardy and DuBois 1938) produced a seven point method by modifying the 15 points of Winslow et al. They did this by switching the right front points to the left front, switching the side lower leg to the shin, and adding 5 more to provide a 20 points measurement sites (Figure A4.2.3) for which they obtained an average temperature using a radiometer. From this average skin temperature, the authors provided a mean skin temperature calculation from seven body parts as shown in equation (A4.2.2) (Hardy and DuBois 1938). The coefficients are based on area weighting. The seven-site method is widely accepted.

The letters in these two equations correspond the letters in Figure A4.2.4.

7-Site Average skin Temperature =

(0.07 x forehead (A)) +

(0.35 x left abdomen (E)) +

(0.14 x left lower arm (F)) +

(0.05 x left hand (G)) +

(0.19 x left anterior thigh (H)) +

(0.13 x left lower leg (J))+

(0.07 x left foot instep (K)) Eq. (A4.2.2)

Replacing some of the seven single point temperatures with averages of several points, Mitchell and Wyndham provided a twelve-site method in Equation (A4.2.3) (Mitchell and Wyndham 1969).

12-Site Average skin Temperature =

(0.07 x forehead (A)) +

[0.35 x [left abdomen (E)) + left upper chest (C) + left scapula (M) + left lower back (N)]+

(0.14 x left lower arm (F)) +

(0.05 x left hand (G)) +

[0.19 x ((left anterior thigh (H) + left posterior thigh (P))] +

[0.13 x ((left lower leg (J) + left calf (Q))] + (0.07 x left foot instep (15))

Eq. (A4.2.3)

The exact locations for the Hardy seven and Mitchell twelve sites are shown in Figure A4.2.4. They are a modification of the Winslow's fifteen sites so you will notice that the locations in Figure A4.2.2 and Figure A4.2.4 are very similar, except that the right front points of Winslow are switched to the left front points.

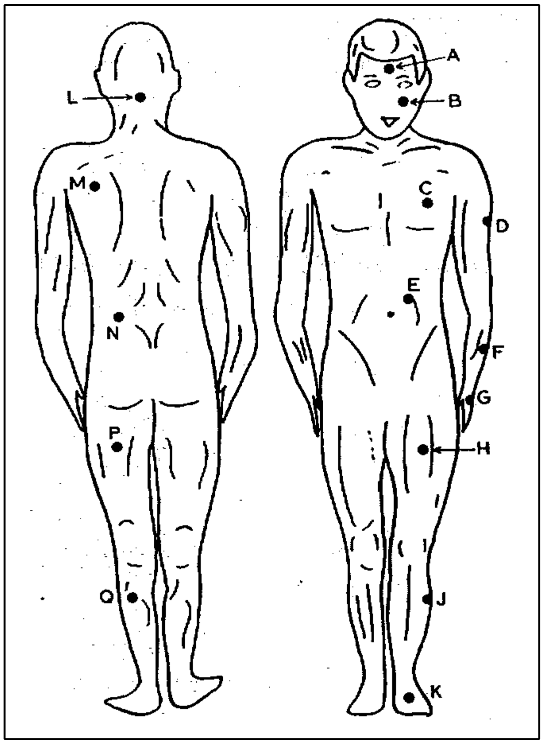

Figure A4.2.4 Seven and twelve locations to calculate mean skin temperature by Hardy and DuBios (referred from Mitchell and Wyndham 1969)

By combining the arm and hand together, thigh, lower leg, and foot together from

Hardy/DuBois seven location equation (Eq. A4.2.2), Houdas (Houdas 1982) proposed a 5-location measurement sites to get mean skin temperature. The exact locations for head and extremities are different from the original seven point method (Figure A4.2.5).

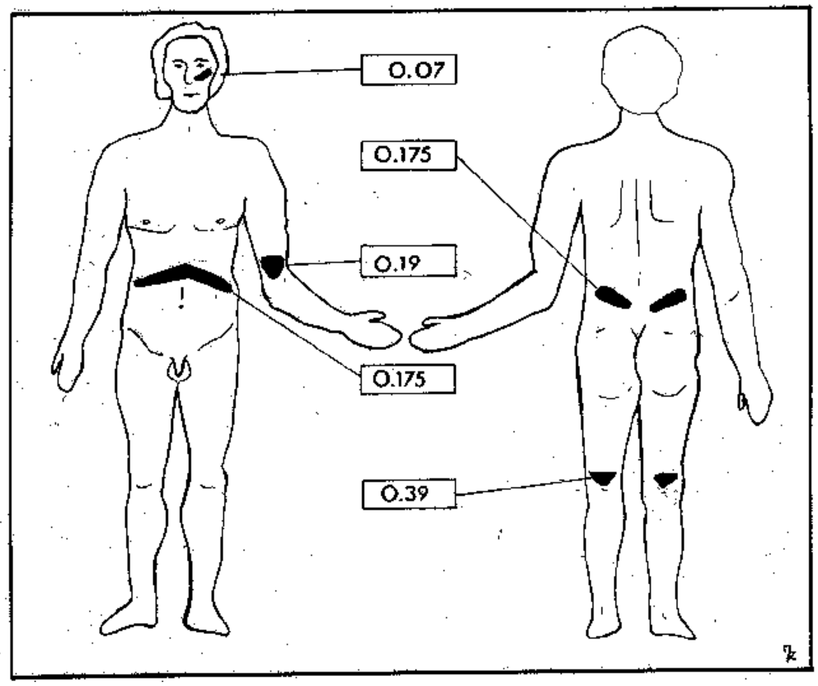

Figure A4.2.5 Five locations to calculate mean skin temperature, with weighting coefficients (Houdas 1982)

Ramanathan simplified the Hardy/DuBois seven-point method by reducing the number of measurement sites (Ramanathan 1963). For each of the seven body parts, ten observations on anterior, posterior, and either sides of the body for the extremities were taken. He found that the temperature in different body parts differed considerably on occasion (3 –4°C), but the differences of temperature from individual measurements within the same body part remained small, being less than 0.5°C. He suggested that the human body can be divided into four sections, and the corresponding mean skin temperature formula is,

$$\text{Average } T_s = 0.3\ T_{chest} + 0.3\ T_{arm} + 0.2\ T_{thigh} + 0.2\ T_{leg} \qquad \text{Eq. (A4.2.4)}$$

Gagge and Nishi (Gagge and Nishi 1977) divided the Hardy/DuBois trunk into chest and back, arm into upper arm and forearm, and combined leg and foot into leg, to create an eight-point formula for mean skin temperature. This method is still in common use.

$$\text{Average } T_s = 0.07\ T_{head} + 0.175\ T_{chest} + 0.175\ T_{back} + 0.07\ T_{upper\ arm} + 0.07\ T_{forearm} + 0.05\ T_{hand} + 0.19\ T_{thigh} + 0.20\ T_{leg} \qquad \text{Eq. (A4.2.5)}$$

Teichner (Teichner 1958) measured mean skin temperature on 10 sites on 323 soldiers and studied the possibility of the estimation from fewer points. By analyzing the relation between the 10-point mean and each of the individual points the author found that no more than six points are required to provide a good estimation. The six locations and the weightings are presented in Eq. (A4.2.6).

$$\text{Average } T_s = 0.100\ T_{cheek} + 0.125\ T_{chest} + 0.125\ T_{back} + 0.070\ T_{upper\ arm} + 0.125\ T_{lateral\ thigh} + 0.125\ T_{media\ thigh} \qquad \text{Eq. (A4.2.6)}$$

Olesen (Olesen 1984) proposed 14 sites (shown in Figure A4.2.6) to get an un-weighted mean skin temperature. He divided the whole body into 14 segments of equal body area so that the mean skin temperature is simply an average of the 14 skin temperatures. He compared 820 measurements with the results predicted by Burton, Ramanathan, Teichner, Hardy/DuBois, and Gagge/Nishi. The comparison shows that the best fits (highest R^2) are Hardy/DuBois 12 site method (0.98), Gagge/Nishi (0.91), Hardy/DuBois 7 site method (0.89), followed by Ramanathan (0.79), Burton (0.75), and Teichner (0.73).

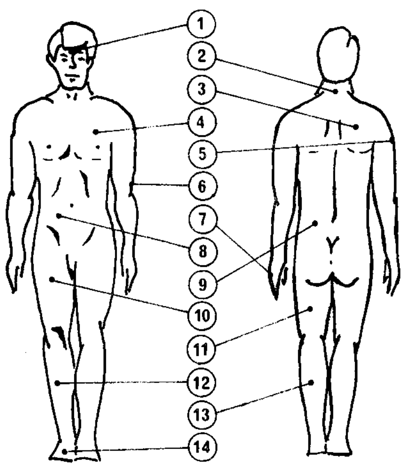

1	Forehead
2	Lower Ociput
3	Right Scapula
4	Left Upper Chest
5	Right Upper Upper Arm
6	Left Lower Upper Arm
7	Left Hand
8	Right Abdomen
9	Left Lower Back
10	Right Anterior Thigh
11	Left Posterior Thigh
12	Right Shin
13	Left Calf
14	Right Foot Instep

Figure A4.2.6 Fourteen locations used by Olesen to calculate mean skin temperature (Olesen 1984)

$$\text{Average } T_s = 0.076\ T_1 + 0.126\ T_3 + 0.094\ T_4 + 0.080\ T_5 + 0.084\ T_6 + 0.067\ T_7 + 0.095\ T_8 + 0.077\ T_{10} + 0.079\ T_{11} + 0.072\ T_{12} + 0.079\ T_{13} + 0.071\ T_{14}$$

Eq. (A4.2.7)

Our approach

The selection of skin temperature sites serve four purposes. 1. To locate thermocouples to measure the local skin temperature for each of the 19 body parts, as needed to develop the local sensation model. 2. To estimate mean skin temperature, using measurement locations that have been widely used in the literature, for the whole-body component of the local sensation model. 3. To provide more detailed measurement of the particular body parts to which local heating or cooling was being applied. 4. To add a few measurement sites which have special interests to us, such as the fingers. We wanted to keep the number of thermocouples low to avoid discomfort from having too many thermocouple wires.

The Hardy/DuBois 7-sites method provides a good fit to the 14-sites method used by Olesen to summarize previous work on measurement locations. Since it requires less measurement sites than Olesen's, and is so widely accepted in the literature, we chose it for measuring our mean skin temperatures.

In addition to the seven sites for measuring mean skin temperature, and 19 sites for the local temperatures for the 19 segments (the 19 include six of the seven Hardy/DuBois sites) , we added one more thermocouple on the neck and one on the left hand ring finger. The exact 22 measurement sites are shown in Figure 4.18 in Chapter 4.

9.3 Appendix 4.3 – Comparison of three core temperature measurements

Before the start of the human subject tests, we compared three methods of obtaining core temperatures. The CorTemp^{TM} thermometer pill from HTI Technologies, Inc. was tested against two tympanic methods: the IR thermometer (manufactured by Braun Company) and a thermocouple touching the tympanic membrane. The purpose was to see (1) how responsive the pill is to transient test conditions, (2) what the differences are between the tympanic temperature and the pill temperature, and the delay in reaching the max/min temperature, (3) what the difference is between the tympanic temperatures measured by the thermocouple and by the IR thermometer, and (4) what the difference is in measured temperature between swallowing the pill right before the test or long before the test. Swallowing the pill at different times results in it measuring different locations in the body's digestive system.

A. Test 1

In the first test we applied all three sensors - a thermocouple, an IR thermometer, and a CorTemp^{TM} pill. The thermocouple wire is very fine and is the thinnest available (28 gauge, Omega) so that it has the fastest response to the tympanic temperatures under transient conditions. The ear with the thermocouple was sealed with cotton during the measurement.

The test conditions were similar to those of our human subject tests, except that the bathtub had a high temperature (40°C) in order to show the maximal difference between the tympanic temperature and the temperature measured by the pill. First, the subject stayed in the bathtub for 25 minutes. Then she stayed in a room with an air temperature of 29.4°C for half an hour. After that the cold air (14°C) was applied to her back. This lasted about 20 minutes. After another 30-minute rest, the cold air was applied to her face for 10 minutes. After another 15-minute rest, the test was over. The results are shown in Figure A4.3.1.

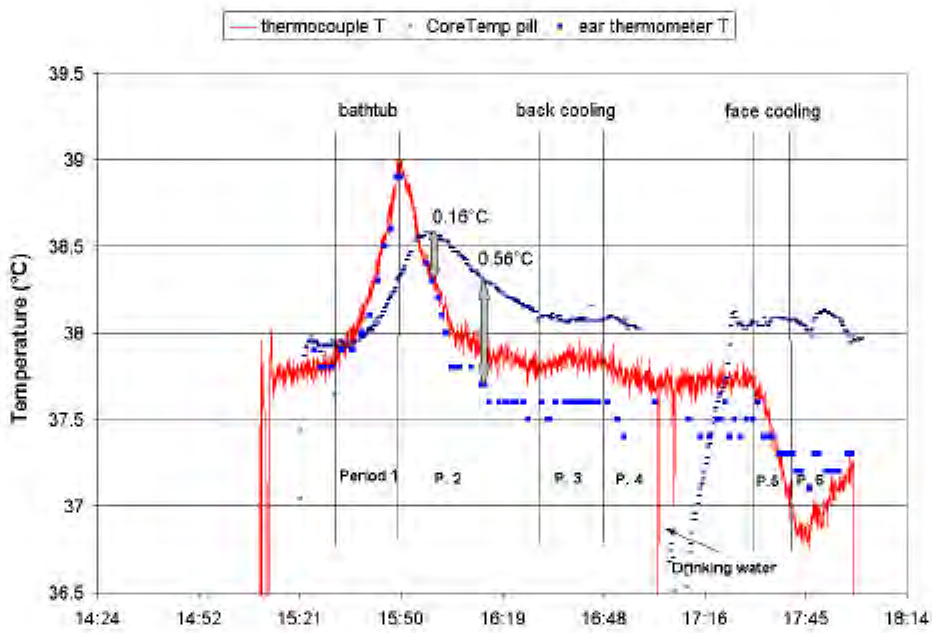

Figure A4.3.1 Comparison of tympanic temperature measured by a thermocouple and an ear thermometer, and core temperature measured by a CorTemp™ pill

These are the phenomena that we observed from the test:

(1). Tympanic temperatures measured by both the thermocouple and the IR thermometer responded to the heating in the bathtub similarly (see period 1). However, the temperature measured by the pill (CorTemp™ pill) reached the peak 8 minutes later at about 0.5°C lower. This may be due to the smaller amount of blood flowing to the stomach compared with the blood flow to the brain. A normal brain weighs 1.4 kg, receiving 15% of the body's total blood. The G.I. tract weights 2.5 kg, receiving 10% of the total blood. Per unit weight of the tissue, the G.I.

tract receives 35% as much blood as the brain. The tympanic temperature changes were dramatic right after the human subject left the bathtub.

(2). In period 2, three core measurements showed the same trends. The pill reading was higher than the other two measurements. At the end of period 2, the difference between the pill and the tympanic thermocouple was 0.4°C.

(3). In period 3, the three core temperatures stopped decreasing (the thermocouple had a very slight increase of 0.1°C) when back cooling was applied.

(4). In region 4, once the back cooling was removed, the three temperatures started to decrease again (the pill had a very brief and small increase before it decreased). This was due to the removal of the back cooling, resulting in the resumption of blood circulation to the superficial area of the back.

In period 4, when the subject drank room temperature water, it reduced the pill temperature by more than 1.5 °C. It required about 20 minutes for the pill to recover. It had been about 1.5 hours since the ingestion of the pill, and was still highly influenced by the water.

(5). A conflict between the tympanic and pill measurements occurred in period 5 during face cooling, when both tympanic sensors showed decreasing temperature, while the pill showed a slightly increasing temperature. This conflict may only happen with face cooling. We expect to see the largest difference between the tympanic and pill measurements during face cooling. This is also why we chose face cooling to examine the differences. Face cooling directly influences the tympanic temperature. However, because of the strong cooling effect from the face cooling, the body sensed the cold and started to save energy. Therefore, the pill temperature started to increase slightly. This increase is not shown in the tympanic temperatures.

Nielsen and Jessen (Nielsen and Jenssen 1992) point out that under face cooling, the tympanic temperature is not a reliable index of core temperature. The reason is that over a considerable distance, the external carotid artery is in close contact with the external jugular vein, which receives tribularies carrying cold blood from the scalp. A heat exchange across this interface must happen, and this appears to be the cause of the downward displacement of tympanic temperature in response to fanning the face with cold air. Tympanic temperature is lowered when convective heat loss from the face and the head is high. Therefore, under these conditions tympanic temperature is not a reliable index of core temperature. In this regard, the pill may be a better way to present the ”core” - hypothalamus temperature. Nielsen showed that the esophageal temperature is a better representation of the hypothalamus. However in our experiment, we didn’t do a test using esophageal measurements, so we cannot compare the readings between the pill and the esophageal temperatures.

(6). After the face cooling was removed, the tympanic temperature further decreased by about 0.2°C in 4 minutes and then started to increase. The other two measurements showed a very similar pattern.

(7). During the bathtub heating (period 1), the two tympanic readings (from the thermocouple and the IR thermometer) were very close. The readings from the IR thermometer were all about 0.2 °C lower than the thermocouple until face cooling. This may be caused by the insulation provided by the cotton in the ear which had the thermocouple. It may also indicate that the reading from the IR thermometer was contaminated by the ear canal. However, during face cooling, the thermocouple reading was lower than the IR thermometer reading. That suggests that during face cooling, the blood to the tympanic membrane was cooler than the ear canal itself.

B. Test 2

The purpose of test 2 was to compare the results when the pill was swallowed a long time before the test to the results when pill was swallowed right before the test (as described in Test 1 above).

In this test, the pill was swallowed at 7:30 AM. The test was conducted at 3:30 PM, 8 hours after the pill was swallowed. The subject first stayed in a bathtub (40°C) for about 30 minutes, then rested in a room (29.4°C) for 30 minutes before cold air (14°C) was applied to the back. After a 15-minute back cooling and another 15-minute rest, the face cooling was applied with the same cold air for 10 minutes. After removing the face cooling and taking a 20-minute rest, the test was over.

Because it is very uncomfortable to use the thin thermocouple to measure the tympanic temperature, and also because we had found in the previous test that the readings from the thermocouple and the IR thermometer were close. We only applied the IR thermometer and the pill in this test. The results are Shown in Figure A4.3.2.

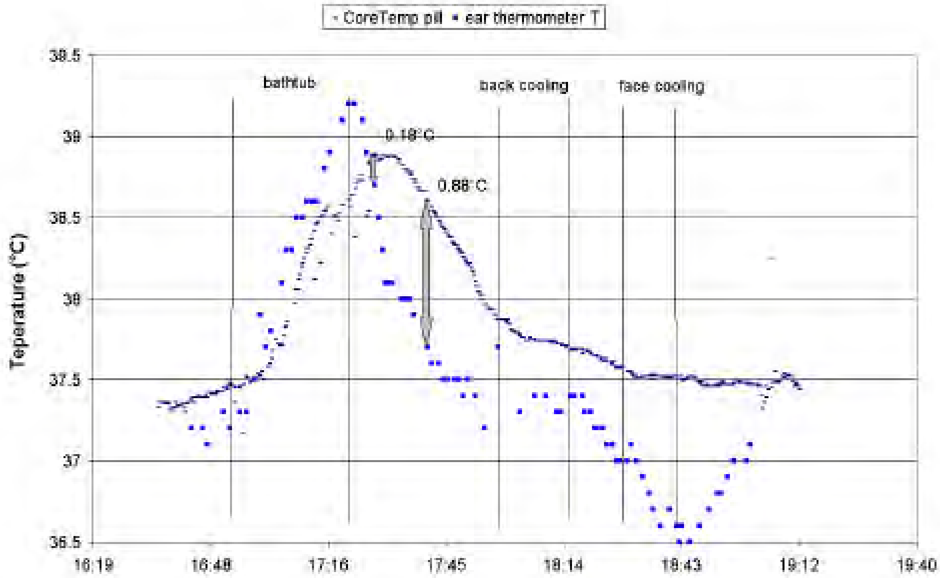

Figure A4.3.2 Comparison of tympanic temperature measured by an ear thermometer with the pill core temperature measurement

(1). The main difference between Test 1 and Test 2 occurred after the subject left the bathtub. The pill core temperature dropped much more slowly in Test 2 than in Test 1. When the pill reached the peak values, the differences between the pill and the ear thermometer temperature were 0.16°C in Test 1 and 0.18°C in Test 2, as the arrows show in the two figures. After 16 minutes, the differences were 0.59°C in Test 1 and 0.88°C in Test 2. That means the pill decreased 0.29°C less in Test 2 when it was much further down in the digestive system.

(2). Unlike in Test 1, where the pill core temperature leveled off during the back cooling, in Test 2, the pill core temperature continued decreasing. The pill was not very responsive. In general, the rectal temperature shows delay and decreased responsiveness compared with other core temperatures. By this time, the pill may be further down in the digestive system and therefore less responsive to transient changes.

From the observations described above, we believe that swallowing the pill right before the test is a better strategy. We let the subject drink warm body temperature water to swallow the pill. During the test, no drinking was allowed.

9.4 Appendix 4.4 - Test conditions

The 109 test conditions are summarized in Table A4.4.1. The five digits of the Test ID are used in this thesis to identify individual tests, as presented in several figures in Chapter 5. The first two digits are the subject ID, followed by a three-digit number which represents the test number from 1 to 109. All the tests were carried out in March and the middle of August, 2002.

The numbers under the Test type in the table correspond to:

1 local cooling

2 local heating

3 multiple cooling/heating

4 whole body step-change

5 neutral condition test

6 IR test

Table A4.4.1 Test conditions

Test ID	Subject D	Date mm/dd	Time	Test type	Room air (°C)	Supply air (°C)	Bathtub (°C)
03001	03	3/1	12:30	1	28.2	14.0	35.5
04002	04	3/5	15:30	1	26.3	14.0	35.9
05003	05	3/12	16:15	1	29.0	14.0	35.9
02004	02	3/14	14:00	1	27.0	14.0	35.9
01005	01	3/15	15:00	1	29.4	14.0	40.0
06006	06	3/19	13:00	1	28.8	14.0	35.5
07007	07	3/19	18:00	1	28.8	14.0	na*
01008	01	3/20	16:00	1	29.4	14.0	40.0
03009	03	3/26	9:30	1	28.2	14.0	36.1
08010	08	4/1	12:00	1	28.8	14.0	na
09011	09	4/2	17:45	1	28.2	14.0	35.9
10012	10	4/3	10:15	1	28.2	14.0	35.3
11013	11	4/4	14:00	1	29.0	14.0	35.9
07014	07	4/4	18:00	1	28.2	14.0	35.6
12015	12	4/5	10:00	1	28.2	14.0	35.3
13016	13	4/5	14:00	1	28.0	14.0	35.7
14017	14	4/5	18:00	1	28.0	14.0	35.3
11018	11	4/8	15:00	1	28.2	14.0	35.3
07019	07	4/9	18:30	1	28.2	14.0	35.3
07020	07	4/9	20:30	1	28.2	14.0	35.3
13021	13	4/11	14:00	1	30.0	14.0	35.3
09022	09	4/11	18:00	1	30.0	28.0	35.3
12023	12	4/12	9:30	1	30.0	14.0	35.3
15024	15	4/16	17:00	1	28.2	14.0	na
16025	16	4/17	10:00	1	30.0	14.0	35.6
12026	12	4/19	9:30	1	30.4	14.0	35.3
07027	07	4/19	14:00	1	30.4	14.0	35.8
07028	07	4/19	17:00	1	30.4	14.0	35.8
16029	16	5/1	10:00	1	30.4	14.0	35.3
13030	13	5/2	14:00	1	29.5	14.0	35.5
09031	09	5/2	18:00	1	29.2	14.0	35.5
07032	07	5/5	10:00	1	30.0	14.0	35.5
07033	07	5/5	13:00	1	30.0	14.0	35.5
06034	06	5/7	10:30	1	30.0	14.0	35.8
15035	15	5/7	16:30	1	30.0	14.0	35.5
17036	17	5/8	14:00	1	29.8	14.0	35.5
13037	13	5/9	14:00	1	29.8	14.0	35.5
09038	09	5/9	18:00	1	30.0	14.0	na
10039	10	5/10	14:00	1	30.4	14.0	35.5

Table A4.4.1 (continued) Test conditions

07040	07	5/13	10:00	1	30.0	14.0	na
07041	07	5/13	13:00	1	30.0	14.0	na
17042	17	5/15	11:30	1	30.0	14.0	35.5
18043	18	5/15	15:30	1	30.0	14.0	35.5
13044	13	5/16	14:00	1	30.5	14.0	35.5
12045	12	5/17	9:30	1	30.0	14.0	35.5
07046	07	5/20	10:00	1	30.5	14.0	35.5
07047	07	5/20	13:00	1	30.5	14.0	35.5
19048	19	5/21	14:15	1	30.5	14.0	35.6
16049	16	5/22	10:00	1	31.0	14.0	35.6
18050	18	5/23	15:00	1	31.0	14.0	35.6
16051	16	5/29	10:00	3	29.5	23 .0	35.5
17052	17	5/29	14:00	3	29.0	23 .0	35.5
19053	19	5/30	10:30	3	29.0	23 .0	35.5
12054	12	5/31	9:30	3	30.0	23 .0	35.5
19055	19	6/4	14:00	3	29.0	23 .0	35.5
12056	12	6/7	9:30	3	28.5	23 .0	35.5
13057	13	6/7	14:00	3	29.0	23 .0	35.5
16058	16	6/13	10:00	3	29.5	23 .0	35.3
13059	13	6/13	12:00	3	28.5	23 .0	35.5
10060	10	6/14	10:15	3	28.5	23 .0	35.3
20061	20	6/17	10:00	3	28.5	23 .0	35.3
16062	16	6/21	14:00	5 + 1	25.5	25 .0	34.5
10063	10	6/23	10:00	1	28.0	23 .0	35.3
21064	21	6/25	12:00	1	28.0	23 .0	35.3
22065	22	6/26	14:00	1	28.0	23 .0	35.3
18066	18	6/26	16:30	1	30.5	23 .0	35.3
01067	01	6/27	12:00	5 + 1	25.5	23 .0	34.5
12068	12	6/28	9:00	5 + 1	25.5	23 .0	34.5
10069	10	6/28	12:30	5	25.5	na	34.5
21070	21	7/3	11:00	1	26.0	23 .0	35.3
13071	13	7/3	16:00	5 + 1	25.5	23 .0	34.5
04072	04	7/8	12:00	1	28.3	23 .0	35.3
21073	21	7/9	11:00	1	29.3	23 .0	35.3
10074	10	7/10	10:30	1	22.0	14.0	32.9
07075	7	7/10	15:45	5 + 1	25.5	23 .0	35.3
19076	19	7/11	9:00	1	26.5	23 .0	35.3
09077	09	7/11	16:00	1	28.5	23 .0	35.3
22078	22	7/12	9:00	1	29.0	23 .0	35.3
18079	18	7/12	13:30	1	31.0	23 .0	35.3
24080	24	7/15	13:00	2	22.0	28.0	31.6
21081	21	7/16	9:00	2	22.0	28.0	31.6
23082	23	7/16	13:30	1	20.7	14.0	31.6

Table A4.4.1 (continued) Test conditions

21083	21	7/17	9:00	1	15.6	14.0	29.2
17084	17	7/17	13:30	1	17.0	14.0	29.2
13085	13	7/19	9:30	2	17.0	37.0	29.2
07086	07	7/19	2:00	2	19.0	36.0	29.2
25087	25	7/25	9:00	2	17.0	37.0	29.2
23088	23	7/25	13:30	2	19.5	37.0	29.2
23089	23	7/26	9:00	2	17.5	38.0	29.2
26090	26	7/26	13:30	2	20.0	35.0	29.2
27091	27	7/29	13:30	2	20.0	37.5	29.2
23092	23	7/30	14:00	2	17.5	37.0	29.2
17093	17	7/31	9:00	3	31.0	37.0/24.0	35.3
21094	21	7/31	13:30	3	31.5	37.0/24.0	35.5
21095	21	8/1	9:00	3	28.0	36.0/19.5	35.3
18096	18	8/1	15:30	3	30.0	37.0/18.0	35.3
13097	13	8/2	9:15	3	29.5	37.0/20.0	35.3
04098	04	8/2	11:30	3	30.0	38.0/20.0	38.4
23099	23	8/5	9:00	2 + 6	19.0	37.0	29.2
27100	27	8/5	13:15	5 + 6	25.5	na	34.5
27101	27	8/5	15:15	5 + 6	25.5	na	34.5
25102	25	8/6	9:00	1 + 6	28.0	14.0	35.3
26103	26	8/6	13:30	1 + 6	28.0	14.0	35.3
04104	04	8/7	9:00	4 + 6	30/22/30	na	35.5
18105	18	8/7	15:00	4 + 6	22.6/30/22.6	na	31.6
21106	21	8/8	8:30	4 + 6	23.5/32.7/23.5	na	31.6
17107	17	8/8	13:30	4 + 6	34.3/26.4/33.7	na	35.5
23108	23	8/9	8:30	3 + 6	31.5	37.0/20.0	35.5
16109	16	8/12	14:00	4 + 6	31.8/22.2/30.8	na	35.5

na* indicates that the bathtub was not used in that test.

9.5 Appendix 4.5 – A paper accepted for the SAE Technical Paper Series

A paper "Using a Driving Game to Increase the Realism of Laboratory Studies of Automobile Passenger Thermal Comfort" has been accepted for the Society of Automotive Engineers (SAE) Technical Paper Series 2003-01-2710 and to be published in 2004.

The paper examines the effect of using a computer driving game in a laboratory study on the metabolic heat production. The metabolic rates of subjects playing or watching the game are found to be very close to their rates when driving or riding in a real car. The paper is attached to the end of the thesis.

9.6 Appendix 5.1 – Database

To make all of the data accessible for analysis, we constructed a relational database. The database stores all data measured in our tests: skin temperature, core temperature, their derivatives, thermal sensation and comfort votes, the test conditions, and subjects' information. By simple operation of the database, we can construct new datasets and conduct regression analysis.

Table A5.1.1 briefly describes each file in the database. The "elapsed time" in the files assumes the start of the test at zero.

Table A5.1.1 A brief description of each file in the database

File name	information provided
skin	Test ID, elapsed time of skin temperature measurement, 28 skin temperatures
Skin der	Test ID, elapsed time of skin temperature measurement, derivatives of the 28 skin temperatures
coretemp	Test ID, elapsed time of core temperature measurement, core temperature and its rate of change
SVoteSegFix	Test ID, elapsed time of the sensation measurements, sensation votes for 19 local body parts and for the overall whole body
CVoteSegFix	Test ID, elapsed time of the comfort measurements, comfort votes for 19 local body parts and for the overall whole body
Tests	Test ID, subject ID, test category (1 – local heating/ cooling test, 2 – whole-body step-change test, 3 – neutral condition test), date of the test, elapsed time of the start and end of the test
TestPhaseWith2Number	Test ID, phase type index (0 – steady-state, 1 – cooling, 2 – cooling recovery, 3 – heating, 4 – heating recovery, 5 – multi-stimuli application, 6 – multi-stimuli removal, 7 – whole-body step to cool environment, 8 – whole-body step to warm environment, 9 – neutral test, 10 – short steady-state), elapsed time for the start and the end of each phase type
Subject	Subject ID, gender, age, height, weight, body fat, circumferences on the waist, neck and hip (women)
Segments	Body Segment ID

When we were developing the local sensation model for the back, we first put all the back cooling/heating data together by segment ID to make a new dataset for the back. The segment ID identifies the body part (e.g. back, head, hand). The new dataset includes local skin temperature, its rate of change, mean skin temperature, core temperature and its rate of change, and back sensation. From this dataset, we developed the local sensation model by regression analysis as a function of local and mean skin temperatures, as well as derivatives of skin and core temperatures.

When we were developing the local comfort model for each body part, we first constructed a new dataset which includes local sensation, overall sensation, and local comfort for the body part. Then we carried out the regression analysis to develop the local comfort model, which is a function of both local and overall sensations.

Figure A5.1.1 shows an example when constructing a new dataset based on the database.

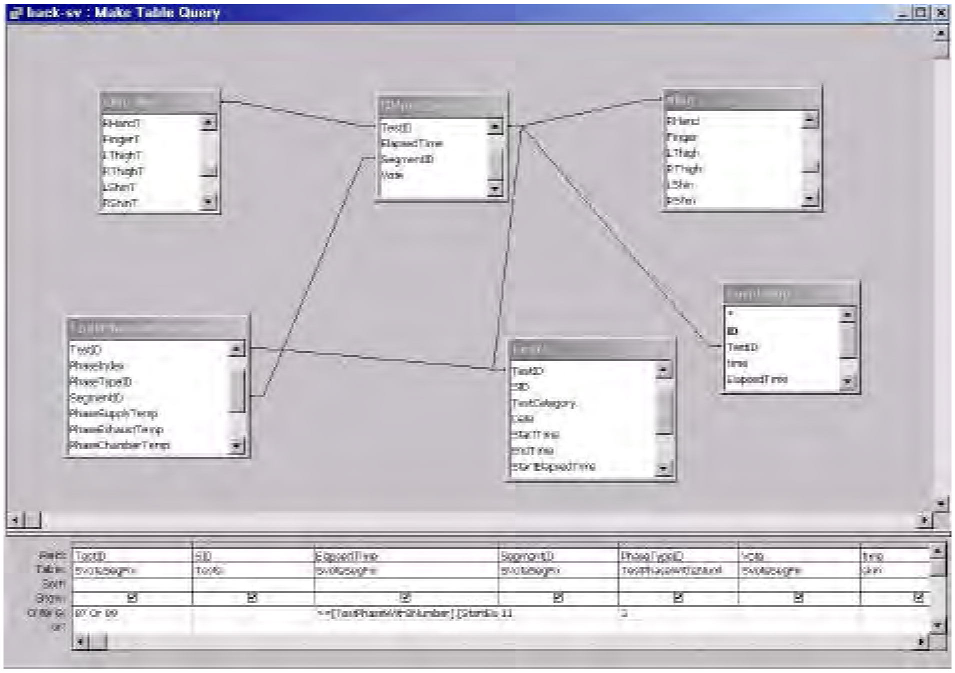

Figure A5.1.1 Constructing a new dataset based on the database

The database will be available to the public. We plan to publish the database on the Web so that people can access the data and carry out their own analyses.

9.7 Appendix 6.1 - Adaptation model

This Appendix explains how we get the coefficients for the logistic adaptation model for each individual body part. See Chapter 6.2.1.6 for the description of the proposed adaptation model.

The mathematical description is presented in Eq. (A6.1.1).

$$Adapting\,Threshold = \frac{Range}{1 + e^{slope(T_{skin,local} - T_{middle})}} - \frac{Range}{2} + Intercept \qquad \text{Eq. (A6.1.1)}$$

Eq. (A6.1.1) defines a logistic relationship between skin temperature and its adapting threshold. The center of the logistic curve is at the "Intercept", which is the average of the two skin temperatures at the ends of the neutral zone. The "T_{middle}" is the center of the logistic curve of the skin temperature, which in this case is the same as the "Intercept". The slope of the logistic has to be close to a 45° line in the middle.

The logistic curve is defined by the "Range" and the "Slope" in the equation.

The logistic curve for the warm side (the adapting threshold >= neutral zone) and for the cold side (the adapting threshold <= neutral zone) are not necessarily equal, so we are going to calculate the logistic curves for the warm side and the cold side separately.

Using the definition of the logistic function, we know that when very cold, the cold adapting threshold is constant. Therefore, I used the test data when subjects were very cold to carry out a linear regression between skin temperature and the sensation vote. Using the regression intercept and the slope, I calculated the adaptation threshold, which is a constant (minimum threshold) and is listed in the left column of Table A6.1.1 for each body part. Using the data when subjects were hot, I did another linear regression. Next, using the regression intercept and slope, I calculated the constant adapting threshold when hot (maximum threshold), which is listed in the last column of Table A6.1.1. The range of a logistic function is the difference between this constant threshold and the "Intercept", the average of the two adapting skin temperatures of the neutral zone. Figure A6.1.1 depicts the thresholds for the neutral zone (middle gray bar) visually, and the thresholds for cold and hot (the dark gray bar on the left and light bar on the right). The ends of the two bars are the two constants. The range of the logistic curve is the difference between the middle of the neutral zone (center circle) and the constant thresholds shown by the two circles at the ends of the cold and hot thresholds.

Table A6.1.1 Adapting thresholds for each body part

body part	$T_{set\text{-}ad\text{-}low\ end}$	$T_{set\text{-}ad\text{-}neut\ al\text{-}low}$	$T_{set\text{-}ad\text{-}neutral\text{-}high}$	$T_{set\text{-}ad\text{-}high\ end}$
head	33.8	34.2	35.8	35.8
breath	31.7	33	35.2	35.2
face	32	34	35.2	36.2
front neck	36.6	35.6	35.8	36
chest	33.8	34.5	35.1	35.4
back	33.8	34.4	35.3	35.8
pelvis	32.6	34.9	34.3	34.8
upper arm	31	33.5	34.2	34.6
lower arm	31	32.7	34.6	36.5
hand	30	33.5	34.4	36
thigh	31.6	33.7	34.3	34.8
lower leg	31.8	32.6	32.9	35.1
foot	30.8	32.2	33.3	35

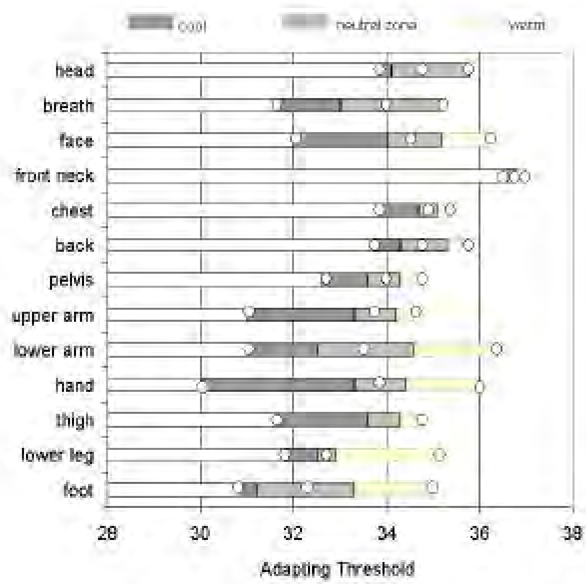

Figure A6.1.1 Skin temperature adapting threshold for each body part

Now the only variable unknown for Eq (A6.1.1) is the slope. The slope has to pass through the two ends of the neutral zone. We found the best fit and determined the slope. An example of selecting the best fit for the back is shown in Figure A6.1.2. The coefficients for Eq. A6.1.1 for each body part are provided in Table A6.1.2.

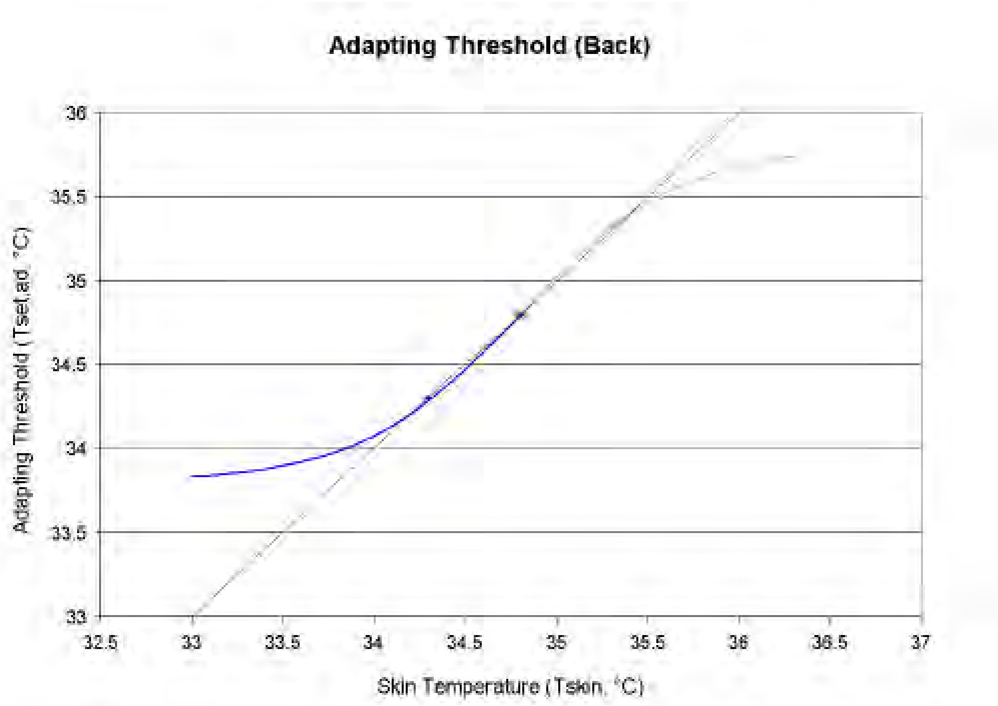

Figure A6.1.2 The adaptation model for the back

Table A6.1.2 Coefficients for the adaptation model (Eq. A6.3.1) for each body part

Body part	Cold side		Warm side		Intercept (°C)
	range	slope	range	slope	
head	2.3	-2	1.7	-3	35.0
breath	4.8	-0.9	2.2	-3	34.1
face	5.2	-0.8	3.2	-1.5	34.6
front neck	0.2	-7	0.6	-6	35.7
chest	2.2	-2	1	-4	34.8
back	2	-2.3	2	-2.3	34.8
pelvis	2.7	-1.5	1.7	-2.5	35.1
upper arm	5.5	-0.8	1.7	-3	33.8
lower arm	5.1	-0.8	5.9	-0.7	33.6
hand	7.7	-0.5	4.3	-1	33.9
thigh	4.7	-0.9	1.7	-2.5	34.0
lower leg	1.8	-1.9	4.8	-1	32.8
foot	2.9	-1.7	5.5	-0.8	32.8

There are two assumptions in determining the adaptation models:

1. We assume that the two skin temperatures under neutral conditions in our test and in Olesen and Fanger (1973) are the two end values of the neutral zone. These two values belong to the neutral zone. Whether they are the end values needs further validation.
2. In getting the constant thresholds for the cold and hot ends, we applied our cold and hot test results and assumed that the thresholds in these two conditions would reach the constant values. Whether they are the maximum and the minimum of the thresholds also needs further validation. See the suggestions for future study (Chapter 7) for a suggested method to test the adaptation model.

9.8 Appendix 6.2 - Core temperature prediction model

This appendix describes a model that we developed to calculate the core temperature set point.

The set point of the human body fluctuates follows a nyctohemeral cycle. It is caused by circadian oscillations synchronized with the earth's rotation (local time) (Hensel 1981). This change is only one of many physiological parameters subject to circadian rhythms (Pittendrigh 1974, Palmer 1976, Aschoff 1979). The magnitude of fluctuation is described differently by different authors: 0.7 – 1.5°C (Hensel 1981), 1 °C (McIntyre 1980), or 0.4°C (Pandolf, Sawka et al. 1988). The rising period starts in the morning (between 2 – 8 AM) and the falling period starts in the afternoon (between 2 – 8 PM) (Figure A6.2.1 and A6.2.2). In Figure A6.2.1, the open circles represent the esophageal temperature set point estimated when the cold and warm stimuli applied to the hand of human subjects are perceived as neither pleasant nor unpleasant (Cabanac called it the behavioral method (Cabanac et al. 1976)). Solid circles were the measured esophageal temperature at the end of a resting period. The figure shows an obvious fluctuation. Figure A6.2.2 also shows the temperature rising in the early morning and falling in the afternoon. The figure shows the resting esophageal temperature, thresholds for vasodilation and sweating (Pandolf, Sawka et al. 1988).

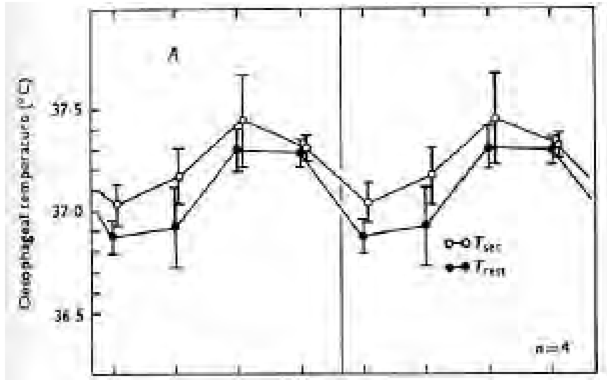

Time 2 8 14 20 2 8 14 20

Figure A6.2.1 Nyctohemeral cycling of mean esophageal temperature set point (T_{set}) estimated from the behavioral method and the resting esophageal temperature T_{rest} from human subjects tests (Hensel 1981, data from Cabanac et al. 1976)

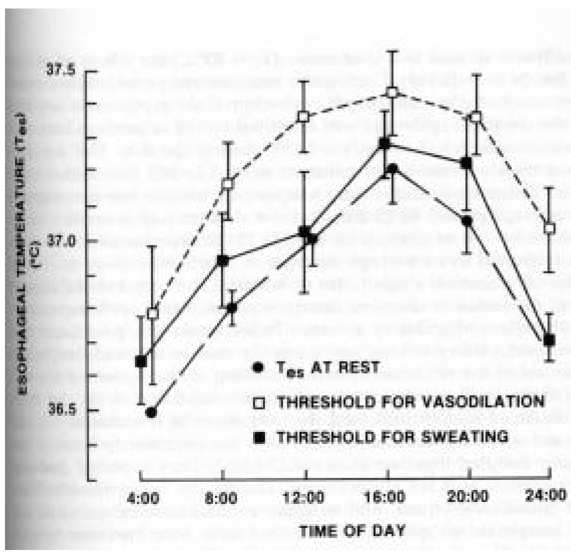

Figure A6.2.2 Changing esophageal temperature (T_{es}) at rest, T_{es} threshold for sweating and vasodilation with the circadian period (Pandolf, Sawka et al. 1988)

The shift of the set point means a shift in thermal regulation (e.g. Figure A6.2.2 shows the changes of the vasodilation and sweating thresholds). The evidence is:

(1) The onset of sweating is at a 0.4°C higher oral temperature in the luteal phase (Haslag and Hertzman 1965) of the female menstrual cycle. The luteal phase could have a core temperature as much as 0.5°C higher than the follicular phase due to the production of hormones (Hensel 1981, Pandolf, Sawka et al. 1988, McIntyre 1980). Cunningham and Cabanac found that during menstruation, when female subjects assessed thermal comfort elicited by local stimulation of the hand, the judgments change according to the shift in the set point (Cunningham and Cabanac 1971). Women in the follicular period responded as if they were regulating their core temperature 0.4 or 0.5°C lower than during the luteal phase.

(2) Sleep was associated with a burst of sweating (Day 1941, Hammel, Jackson et al. 1963) during the slow wave sleep phase in a warm environment, while during fast wave sleep, sweating was absent even in warm environments of 37 to 39°C in men (Shapiro, A. T. Moore et al. 1974). This is due to the changes in set points. Local cooling of the hypothalamus to 33°C in kangaroo rats (the normal threshold is 36°C) did not cause a metabolic heat increase during fast wave sleep (Shapiro, A. T. Moore et al. 1974).

(3) When fever is present, the set point is elevated. Therefore, unlike hyperthermia, when regulation works at the limit of its capacity, there is hardly any thermoregulatory burden during a fever.

Since signals are based on shifted set points, we need to define the set point. Figure A6.2.3 represents our 24-hour measured core temperature data during rest and sleep. The goal is to develop a formula to calculate the Tc set point.

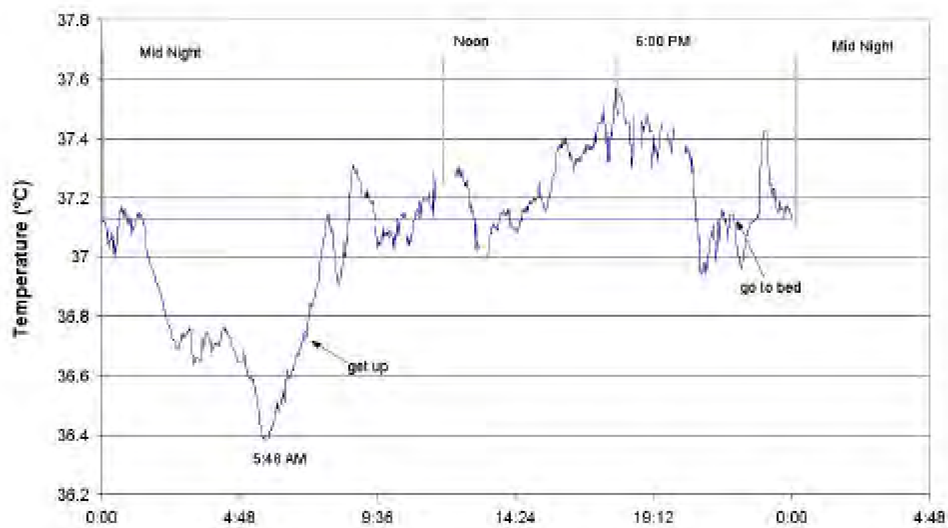

Figure A6.2.3 Measuring core temperature with a CorTemp pill in a 24-hour circle

From the data, we see that the core temperature started to rise between 2 and 6 AM, and fell in the late afternoon (around 6 PM). We did two other tests measuring the core temperature and both showed a peak core temperature in the late afternoon. Therefore, I propose a core temperature model that peaks at 5:30 PM.

This figure shows that in the morning around 9 AM, the core temperature was 37.1°C. The afternoon core temperature was around 37.3°C near 5:30 PM. The lowest core temperature was registered in the morning before waking (5:48 AM). The core temperature changed about 1°C during an entire day.

Most of our tests were conducted during the day. Observing the core temperatures during the tests (we didn't continue to measure the core temperature after the tests finished), we see that the morning core temperatures are lower than the afternoon ones. The morning core temperatures are usually located near 37.1 and the afternoon ones (2 PM) are usually located near 37.2.

Based on these data, I have proposed a hypothetical core temperature model shown in Figure A6.2.4.

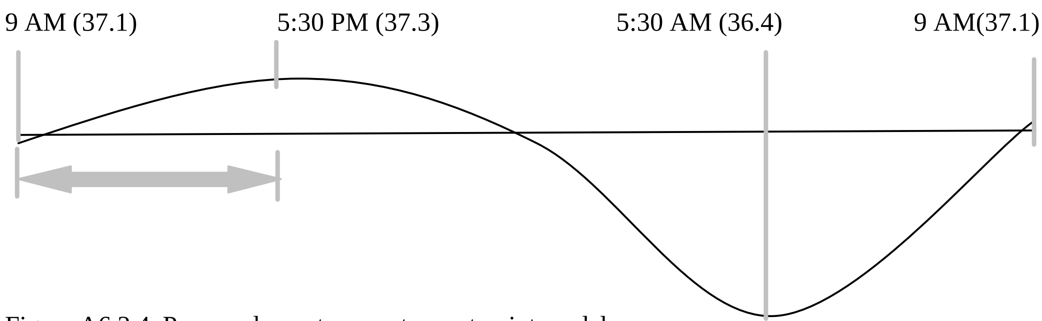

Figure A6.2.4 Proposed core temperature set point model

The region that we are interested is the daytime core temperature. We don't have enough information to propose an evening model.

The temperature from 9 AM to 5 :30 PM as a linear model is presented in Eq. A6.2.1.

$$Tc = 37.1 + (37.3 - 37.1)(\text{time} - 9)/(17.5 - 9) \ (°C) \qquad \text{Eq (A6.2.1)}$$

An example calculating the core temperature at 2 PM is:

$$Tc = 37.1 + 0.2 \times 5/8.5 = 37.22 \ (°C)$$

Considering the female menstrual cycle, the modified Eq (A6.2.1) is presented as:

$$Tc = 37.1 + (37.3 - 37.1)\,(time - 9)/(17.5 - 9) + 0.2 \times cycle\ (°C) \qquad \text{Eq (A6.2.2)}$$

where "cycle" refers to the menstrual cycle. In the luteal period, cycle = 1. During the follicular period, cycle = 0. For the period in between, we assume cycle = 0.3.

The proposed model needs further validation. From current human subject tests we don't have the data to validate the model.

9.9 Appendix 6.3 – Body composition influences on local sensation

The local thermal sensation model was derived from our test population. If we want to predict for a specific individual with human body information (body fat, gender, age), we developed a model as shown in Eq. (A6.3.1).

$$\text{Local sensation}_{body\ builder} = \text{Local sensation} + 0.025\ \text{body (fat – average fat) (\%)} - 0.12\ \text{(gender – average gender)} + 0.016\ \text{(age – average age)} \qquad \text{Eq. (A6.3.1)}$$

Local sensation in Eq. (A6.3.1) is presented in Table 6.2 in Chapter 6. Local $\text{sensation}_{body\ builder}$ is the local sensation including the body builder information. For gender, I used value 10 to represent female, 5 to represent male.

The average values in Eq. (A6.3.1) are from our tests, which is listed in Table A6.3.1.

Table A6.3.1 Average values for body builder information from our tests

Element	Age	Body fat (%)	Gender
Average value	31.8	25.4	7.78

Body fat and age are a positive influence. With the increase of body fat and age (range 20 – 51 in our tests), people tend to feel warmer. For gender influence, I used value 10 to represent female, 5 to represent male. The negative regression coefficient indicates that females tend to feel cooler.

With our human subjects, fat varies from 25 to 50%, which corresponds to 0.63 sensation difference. The subjects' ages cover a range from 20 to 51, which corresponds to a 0.5 sensation variation. The variation between male and female is 0.6, with males feeling warmer. The cold sensation goes to slim, young females, while the warmer thermal sensation goes to older, high fat level males.

9.10 Appendix 6.4 – Skin temperature data smoothing

The skin temperature measured by a thermocouple includes noise signals. The noise signals are very small. They are visible only with an enlarged skin temperature scale (from 32 – 36 °C), as shown for a three-hour test in Figure A6.4.1. The figure shows local skin temperature during a local cooling process. The vertical axis represents the skin temperature. The noise signal has little influence on measured skin temperature. The thermocouple records data every 5 seconds, and the number in the horizontal axis represents the thermocouple readings.

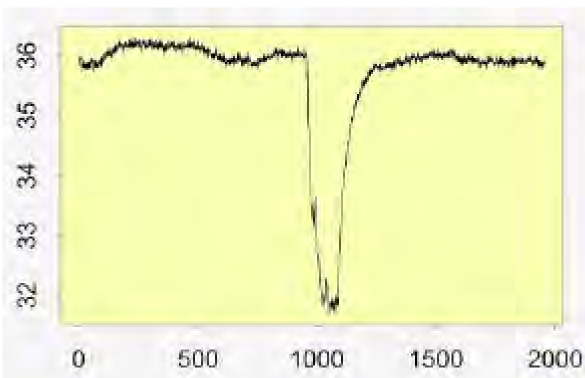

Figure A6.4.1 Small noise signal in skin temperature measurement

However, the same data, when we calculate the derivative, $\frac{dTskin}{dt}$, show that the derivative is dominated by the noise signal (Figure A6.4.2). The vertical axis represents the derivative. Since the derivative is an important part of our transient model, we need to do signal processing to remove the noise.

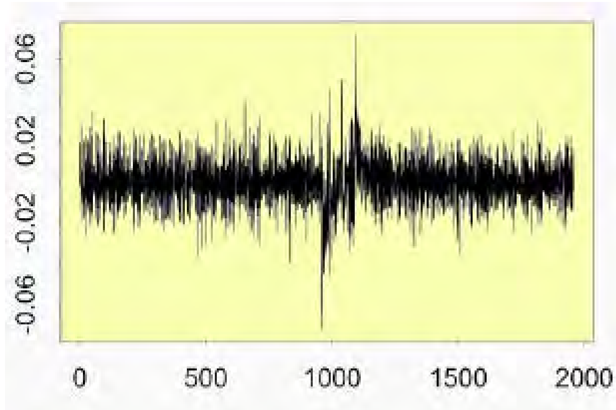

Figure A6.4.2 Dominant small noise signals in derivative of skin temperature

We used a process called wavelet smoothing, common in the signal processing industry. It filters the noise signal without losing the sharp transient resulting from the application and removal of the thermal stimulus (Figure A6.4.3).

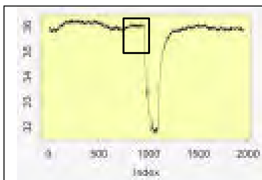 before	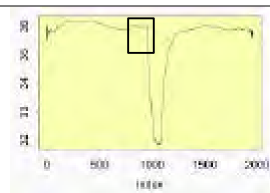 after	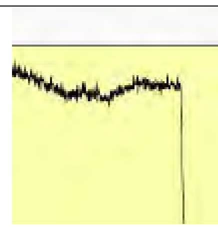 before	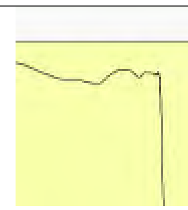 after

Figure A6.4.3 Skin temperature before and after smoothing

The influence of the noise on the derivative is significantly reduced (Figure A6.4.4).

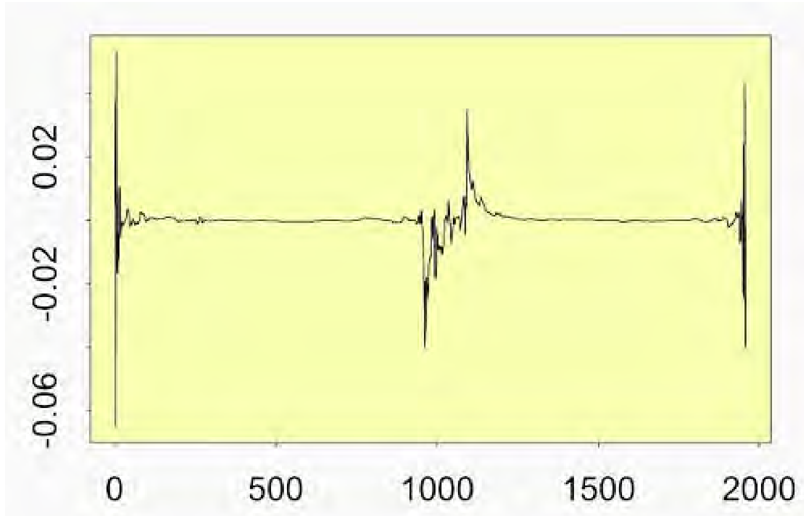

Figure A6.4.4 Derivative after wavelet smoothing

We took one more step smoothing the derivative: We used a constant time exponential function to smooth the derivative after the wavelet smoothing. The smoothed results are shown by the thick black lines in Figure A6.4.5. This derivative is used in our regression analysis.

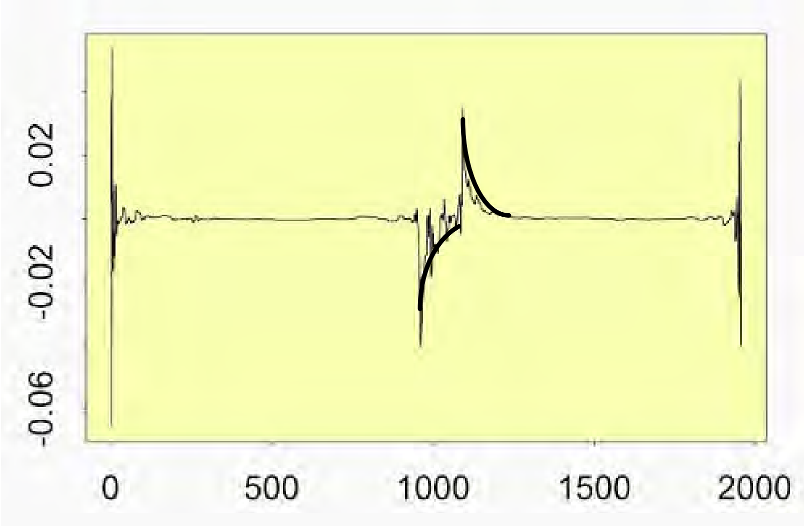

Figure A6.4.5 Smoothing of the derivative after wavelet smoothing

9.11 Appendix 6.5 – A paper for the European Journal of Applied Physiology

A summary of the predictive models (sensation and comfort for local and the whole body) will be published in the European Journal of Applied Physiology. A copy of the paper is attached to the end of the thesis.

9.12 Appendix 7.1 – Implications for air-conditioning

This appendix suggests potential implications on designing air temperature and flow rate of task ambient HVAC systems in buildings and air-conditioning in vehicles to provide better comfort.

1. Transient aspects - small step-change cycling air-conditioning

From our asymmetric and transient experiment results as well as literature studies, we know that a thermally neutral condition is not necessary to achieve the highest comfort. Thermal pleasure is associated with the removal of heat stress or the partial relief of discomfort, as seen by the saddle shape of our local comfort model. McIntyre (McIntyre 1980) recommends that engineers designing climate control and other technologies should aim to create thermal pleasure for users rather than simply for creating a state of “neutrality” or for avoiding discomfort, which is the conventional approach.

Based on this idea, it seems possible that a control strategy of small step-changes in air temperature could potentially achieve higher better comfort than the traditional constant temperature approach. By intentionally creating different temperatures, occupants would experience the removal of discomfort. The result might be similar to the pleasant feeling in a slightly warm environment with a breeze coming through an open window in a naturally ventilated building. This idea is different from the concept of ramping the air temperature slowly so that people would not feel the changes. Gonzalez and Berglund (Gonzalez and Berglund 1978) did a study of the perception of temperature and humidity drifts imposed in buildings to save energy. The study found that for sedentary persons, temperature ramps less than 0.5°C/h from a neutral comfort point were indistinguishable from constant temperature conditions.

We recommend a small, not a large, step-change supply air pattern. One of the reasons is that while we are creating high comfort when relieving thermal discomfort, people first have to experience this intentionally created discomfort. The small step-change is one way to control the level of the thermal stress that is created, so that the discomfort is not high. Another reason is that when the cooling area is large (e.g. an entire body segment as in our tests compared to the size of a thermode used in most of the literature), it might be easy to overwhelm the pleasant feeling associated with the removal of discomfort by the decreased comfort due to excessive local cooling. We know that large discrepancies from neutral conditions cause discomfort. From our overall comfort model, we also know that the most uncomfortable body part has a strong influence on overall comfort, so we have to make sure not to cause any local discomfort. For this reason, a small step-change is recommended. Haber (Haber 1958) studied the preferred water temperature when subjects put hands in different temperature water buckets. He found that smaller discrepancies (±1 °C away from the neutral water temperature) are the most preferred. Larger discrepancies caused negative feeling.

We might spend more time in transient and non-uniform environments than in uniform and stable ones. We possibly perceive these varied environments as more pleasant than the static ones. A room designed for daylighting may creates a more interesting transient, non-uniform visual environment than the flat, possibly monotonous luminance environment provided by electric lighting. From our tests results we see that under neutral condition people are comfortable, but hardly ever voted “very comfortable”. For these reasons, the small step-change air-conditioning pattern may have advantages.

This pattern could be designed for task ambient HVAC systems in buildings or the air-conditioning in a car where often the local cooling is too strong. We may have experienced this in our daily life – an uncomfortably cool hand when the air-conditioning blows cold air directly on the hand while driving a car. The strong cooling should only be applied at the beginning when the large heat load needs to be removed. After that, a small step-change may be more welcome.

A similar recommendation applies to cooling or heating of seats. Back and pelvis both belong to the highly influential sensation group. They are very sensitive to cooling. So for seat cooling, certainly a small amplitude stimulus is recommended. Again, strong cooling should only be applied at the beginning.

There are two specific things to be determined for this cycling approach.

(1). Amplitude of the small step-change cycling

Although in general we recommend a small step-change cycling for cooling air supply, for different body parts, different amplitudes need to be considered.

For the most sensitive body parts, we should apply smaller amplitude of the step-change cycling. Strong cooling is likely to cause local discomfort.

Since hand vasoconstriction is very sensitive to cooling, one should not apply strong cooling to the hand. Once the hand is vasoconstricted, it is likely to cause local discomfort, loses its ability to reject heat. However, our IR-images showed that hand skin temperature recovers very quickly when the body is warm. The warm body quickly pumps heat to the hand after the local cooling has been removed. So a small step-change cycling pattern that avoids vasoconstriction may be especially beneficial for the hand in terms of both comfort and heat regulation.

The head region in general prefers cooler conditions and the blood supply to this region is not subject to vasoconstriction. That means we can apply relatively cooler air with relatively larger amplitude to the head region. This will serve both thermal comfort and thermoregulation requirements.

(2). Frequencies of the cycling

In our tests when people voted very comfortable when a heat stress was removed, the very comfortable feeling (Kuno effect) lasted about 3 – 5 minutes before starting to decrease. In those tests the local cooling stimulus was strong. When this strong cooling stress is removed, the Kuno effect may last longer. When people use a oscillating fan to cool the body, the fan changes directions at a frequency of about 30 seconds. Tanabe (Tanabe 1988) did a test to examine the frequencies of different air supply patterns and found that 30 seconds and 60 seconds frequency sine curves took away the most heat for a given level of thermal sensation. For this reason, we recommend a frequency between 30 seconds to 3 minutes. More detailed tests would be needed to answer this question more definitively.

The same study by Tanabe also showed that a constant air supply produced less cooling effect than the fluctuating airflow pattern, and had less effect on thermal sensation.

The recommendation of small step-change airflow pattern from our tests is well supported by a study carried out by Nissan Motor Co. (Hagino and Hara 1992). The authors tested human subjective sensation by supplying four different air supply patterns (natural airflow, improved natural airflow, periodically fluctuating airflow, randomly fluctuating airflow) and they found that the improved natural airflow (small magnitude but frequent air flow fluctuation) creates the best subjective responses. They called it the *improved* natural airflow because it is similar to a natural airflow, but with more frequent air supply reduce the gaps between the maximum and minimum airflow rates found in natural wind. In the natural airflow, this gap is large, and in summer occupants feel hot and sweaty during a low velocity interval, and during the subsequent high velocity interval the sweat is evaporated and the occupants feel cold and uncomfortable. This natural fluctuation airflow was deemed unsuitable for the air-conditioning system, because the supply air is cooler than in the natural ventilation environment.

The authors also found that periodically fluctuating airflow was uncomfortable because occupants could predict the pattern of the fluctuation and they disliked the anxiety felt before the onset of the higher velocity discharge. The randomly fluctuating airflow was also found to be uncomfortable because it involved abrupt changes in velocity. Based these observations, the authors recommend a moderately fluctuating airflow with a certain degree of randomness like that of a natural wind.

Another advantage of producing a changing environment rather than a constant environment is that people are different. Even for an individual, metabolism changes with different activity levels and changes of clothing lead to differences in thermal balance. Basically it is impossible to create a single environment that will always make all people in the space comfortable. The changing feature of the environment would provide all people with a comfortable feeling at certain times, rather than a constant discomfort for some people in a stable and non-transient environment.

2. Cool head and warm feet preferred

We did a regression analysis for the uniform environment tests (warm, cold, neutral conditions) and the results show that people prefer cool head and warm feet.

The regression correlates local sensation from each body part with overall sensation. Because under a uniform environment the local body sensations in general are all correlated (i.e. when the whole body is cold, every body part is cold), the regression is done for the overall and one local sensation only. We did not use these equations in our overall sensation model because they only apply to uniform environment. Our integration model includes the situation for both uniform and asymmetrical environments. However, it is interesting to see from these regression results that all the intercepts for the head region parts are negative, and there is a large positive intercept for the foot (Table A7.1). The negative intercepts mean that when the overall sensation is zero, the head region (different parts of the head) feels warm already. The large positive intercept for the foot (0.6) means that when the overall sensation feels neutral, the foot sensation is –0.6, between neutral and slightly cool. The intercepts for the trunk are close to zero.

Table A7.1 Additional regression for whole body thermal sensation = a Local thermal sensation + b (Stable Condition)

a Local thermal tensation + b	R^2
1.34 Breathing Sensation –0.235	0.54
1.23 Head Sensation –0.4	0.86
1.30 Neck Sensation –0.283	0.72
1.20 Face Sensation –0.437	0.85
1.16 Chest Sensation –0.026	0.81
1.23 Back Sensation + 0.072	0.76
1.34 Pelvis Sensation + 0.075	0.69
1.00 Arm Sensation + 0.155	0.83
0.95 Hand Sensation + 0.039	0.85
1.14 Leg Sensation + 0.166	0.88
0.88 Foot Sensation +0.606	0.69

We need to clarify whether the positive and negative intercepts are caused by the air temperature stratification. We see that the intercepts for chest and back are near zero. Since the air temperatures for chest and back are close to the head and no positive intercepts are shown for these segments, air stratification is probably not be the reason.

Yapp, Phillip

From: Yapp, Phillip
Sent: Friday, 23 July 2021 10:27 AM
To: Morey, Teresa
Cc: Zhu, Nan
Subject: RE: HoS minute - Mitigation of COVID-19 risk in CMTEDD workplaces - building modifications
Attachments: 04-21-HVAC-Skills-Workshop.pdf

OFFICIAL

Hi Teresa

Tech data re UVGI/UVC and COVID. ASHRAE (The American Society of Heating, Refrigerating and Air-Conditioning Engineers) has the most information, research into UVC. Relevant articles and guidelines below with extracts on COVID19 and UVC/UVGI. Takeaway is it's very effective at the right dose, which would be important to specify during implementation.

https://www.ashrae.org/file%20library/about/position%20documents/filtration-and-air-cleaning-pd.pdf

> *The effectiveness of a UV-C system to inactivate microorganisms in the air and/or on surfaces has been amply demonstrated; the best results were obtained for the long-term irradiation of downstream coil surfaces to avoid fungal amplification on wet surfaces. Experience suggests that control of a moving airstream does not provide favorable killing rates because of the short dwell time. Under ideal conditions, inactivation and/or killing rates of 90% or higher can be achieved but depend on the following: the type of microbial contaminant; specific species; physical or mechanical factors such as UV-C intensity, exposure/dwell time, lamp distance and placement, and lamp life cycle and cleanliness; air movement and patterns; temperature; relative humidity; and air mixing. Airborne removal is best applied in conjunction with filtration of particles with prefilters*

https://media.ies.org/docs/standards/IES-CR-2-20-V1-6d.pdf

> *1.3 Can UV-C kill viruses as well as bacteria? Yes, UV-C kills living bacteria, but viruses are technically not living organisms; thus, we should correctly say "inactivate viruses." Individual, energetic UV-C photons photochemically interact with the RNA and DNA molecules in a virus or bacterium to render these microbes non-infectious. This all happens on the microscopic level. Viruses are less than one micrometer (μm, one-millionth of a meter) in size, and bacteria are typically 0.5 to 5 μm. 1.4 Can UV-C effectively inactivate the SARS-CoV-2 virus, responsible for COVID-19? Yes, if the virus is directly illuminated by UV-C at the effective dose level. UV-C can play an effective role with other methods of disinfection,*

https://www.ashrae.org/technical-resources/filtration-disinfection

UV-C In-Duct Air Disinfection

Perpendicular to airflow

Parallel to airflow

- Banks of UV-lamps installed inside HVAC units or associated ductwork; positioned parallel or perpendicular to airflow
- Requires increased dose of UV to inactivate microorganisms on-the-fly as they pass through the disinfection zone. Due to limited exposure time, installations should observe these guidelines:
  - Minimum target UV dose of 1,500 µW•s/cm2 (1,500 µJ/cm2)
  - Designed for 500 fpm or slower moving airstream
  - Minimum irradiance zone of two feet
  - Minimum UV exposure time of 0.25 second
- Should be coupled with mechanical filtration
  - Install the highest practical MERV filter that does not compromise system performance
  - Layering of technologies increases overall air cleaning through capture and/or viral inactivation

---

Details on the UV Dose Recommendation for SARS-CoV-2

- A minimum UV-C (254 nm) dose of 611 µJ/cm^2 should be applied for 90% inactivation of SARS-CoV-2. This extrapolates to a dose of 1222 µJ/cm^2 for 99% inactivation of SARS-CoV-2 virus in air applications.
- It is advisable to build in appropriate safety margins to account for different environmental conditions such as air flow speeds, temperature and humidity levels, number of air changes, surface soiling, lamp ageing and system configuration, etc. A conservative minimum UV-C (254 nm) dose value of 1,500 µJ/cm^2 is therefore suggested for 99% inactivation of SARS-CoV-2 in air.

Other documentation.

https://www.ashrae.org/file%20library/technical%20resources/covid-19/si_a19_ch62uvairandsurfacetreatment.pdf

https://www.ashrae.org/file%20library/technical%20resources/ashrae%20journal/2020journaldocuments/72-74_ieq_schoen.pdf

https://www.ashrae.org/File%20Library/Technical%20Resources/COVID-19/Feb2021_22-23_solving-problems_mcgowan.pdf

https://www.ashrae.org/File%20Library/Technical%20Resources/COVID-19/Filtration-and-Disinfection-FAQ.pdf

Phil Yapp | Assistant Director – Asset Strategies, Sustainability and Environment

Phone: +61 2 6207 9190 | M: 0435 655 176 | Email: phillip.yapp@act.gov.au
Infrastructure and Capital Works | Education | ACT Government
Level 4 220 London Circuit | GPO Box 158 Canberra ACT 2601 | www.det.act.gov.au

---

From: Morey, Teresa <Teresa.Morey@act.gov.au>
Sent: Thursday, 22 July 2021 5:34 PM
To: Nakkan, John <John.Nakkan@act.gov.au>
Cc: Wales, PhillipB <PhillipB.Wales@act.gov.au>; Luchetti, Christine <Christine.Luchetti@act.gov.au>; Shaw, Tania <Tania.Shaw@act.gov.au>; Parkes, Antonia <Antonia.Parkes@act.gov.au>; Cusack, Grant <Grant.Cusack@act.gov.au>; Zhu, Nan <Nan.Zhu@act.gov.au>; Yapp, Phillip <Phillip.Yapp@act.gov.au>; OConnell, Chris <Chris.OConnell@act.gov.au>
Subject: RE: HoS minute - Mitigation of COVID-19 risk in CMTEDD workplaces - building modifications

OFFICIAL

Thanks John, we'll get onto this tomorrow.

Regards,
Teresa

From: Nakkan, John <John.Nakkan@act.gov.au>
Sent: Thursday, 22 July 2021 5:28 PM
To: Morey, Teresa <Teresa.Morey@act.gov.au>
Cc: Wales, PhillipB <PhillipB.Wales@act.gov.au>; Luchetti, Christine <Christine.Luchetti@act.gov.au>; Shaw, Tania <Tania.Shaw@act.gov.au>; Parkes, Antonia <Antonia.Parkes@act.gov.au>; Cusack, Grant <Grant.Cusack@act.gov.au>; Zhu, Nan <Nan.Zhu@act.gov.au>; Yapp, Phillip <Phillip.Yapp@act.gov.au>; OConnell, Chris <Chris.OConnell@act.gov.au>
Subject: FW: HoS minute - Mitigation of COVID-19 risk in CMTEDD workplaces - building modifications

OFFICIAL

Hi Teresa,

Can you please work with the team to see what can be done about Graham's second dot point below. I think the options that end up being excluded still need to be in the body of the brief with the note that we excluded them.

Phil is chasing up ACT Health in relation to the first point.

Regards,

John Nakkan | Executive Branch Manager
Phone: +61 2 6205 2250 | Mobile: 0466 015 922 | Email: john.nakkan@act.gov.au

ACT Property Group | Chief Minister, Treasury and Economic Development Directorate | **ACT Government**
255 Canberra Avenue, Fyshwick ACT 2609 | GPO Box 777 Fyshwick ACT 2609
www.economicdevelopment.act.gov.au | www.act.gov.au

For repairs and maintenance related matters, please contact the Response Centre: actpg@act.gov.au

ACT Government

I acknowledge the traditional custodians of the ACT the Ngunnawal people, and their continuing connection to land and community. I pay my respect to them, and to the Elders both past and present.

From: Tanton, Graham <Graham.Tanton@act.gov.au>
Sent: Thursday, 22 July 2021 3:44 PM
To: Nakkan, John <John.Nakkan@act.gov.au>; Wales, PhillipB <PhillipB.Wales@act.gov.au>
Cc: Rowe, Shannon <Shannon.Rowe@act.gov.au>; Gosling, Izzie <Izzie.Gosling@act.gov.au>
Subject: HoS minute - Mitigation of COVID-19 risk in CMTEDD workplaces - building modifications

OFFICIAL

Hi John, Phil – as discussed

Stephen provided some feedback on the attached brief, I have marked up some comments.

Basically two points –

- Can we liaise with health to understand what treatment may they have in place or recommend.
- Can we look to narrow down the list of items in point two, to those we think there is evidence of benefit. And reflect in the body what that evidence is.

Shannon, can you come over the top if I have misrepresented anything.

Regards

Graham

MODULE 137
HVAC&R SKILLS WORKSHOP

PROUDLY SPONSORED BY
Opira
ENVIRONMENT RISK MANAGEMENT

ULTRAVIOLET GERMICIDAL IRRADIATION

Skills summary

What?

An introduction to ultraviolet germicidal irradiation (UVGI) as a disinfection or sterilisation method.

Who?

Relevant for HVAC&R system designers, installers, operators, and maintainers.

Ultraviolet germicidal irradiation (UVGI) is a disinfection or sterilisation method that uses ultraviolet (UV-c) light at sufficiently short wavelength to break down or degrade organic material and inactivate microorganisms. It is used in a variety of applications including food, air and water purification.

UVGI utilises the short wavelength of UV that is harmful to forms of life at the microorganic level. It is effective in destroying the nucleic acids in these microorganisms, so that their DNA is disrupted by the UV radiation. This removes their reproductive capabilities and kills them. The wavelength of UV that causes this effect is rare on Earth because the atmosphere effectively blocks it.

Introduction

Using a UVGI device in air systems creates a deadly effect on any microorganisms such as pathogens, viruses and moulds that are in these environments. The system is not a filter; inactive particles remain in the airstream and, in the case of dead fungal spores, may still cause a negative human response due to their integral mycotoxins.

Coupled with an air-filtration system, UVGI can remove harmful microorganisms from these environments. UVGI is best applied in conjunction with pre-filtration to protect lamps and filtration downstream of the system to remove the inactivated microbes.

UVGI theory

Ultraviolet light is electromagnetic radiation with wavelengths shorter than visible light.

UV can be separated into various ranges, with short-range UV-c considered "germicidal UV". At certain wavelengths UV is mutagenic to bacteria, viruses and other microorganisms. At a wavelength of 2,537 Angstroms (254nm), see Figure 1, UV will break the molecular bonds within microorganismal

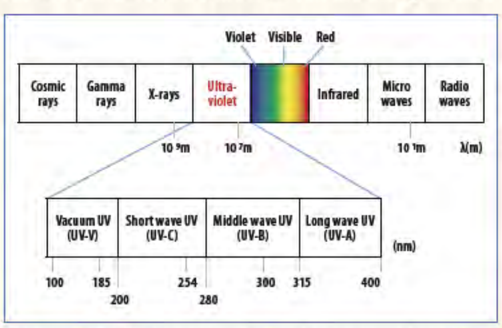

Figure 1: UV inactivates microorganisms at a wavelength of 2,537 Angstroms (254nm).

DNA, producing thymine dimers in their DNA thereby destroying them, rendering them harmless or prohibiting growth and reproduction. Ultraviolet radiation in the range of 2250 to 3020 angstroms is used in a variety of UVGI disinfection applications.

It is a process similar to the UV effect of longer wavelengths (UV-b) on humans, such as sunburn or sun glare. Microorganisms have less protection from UV-c, which does not occur naturally on Earth, and they cannot survive prolonged exposure to it.

An HVAC UVGI system is designed to expose the air stream (or surface) to germicidal UV-c shortwave radiation. Exposure comes from germicidal lamps, which emit germicidal UV-c electromagnetic radiation at the correct wavelength, irradiating the passing air or the protected surface. Lamps use a gas-filled tube with no phosphor coating and composed of fused quartz because ordinary glass absorbs UV-c. The typical source of UV-c in commercial HVAC systems is low-pressure mercury vapour lamps, which emit near optimal wavelength, see Figure 2. The lamps are designed to specifically emit 254nm ultraviolet radiation.

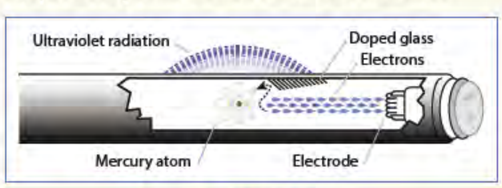

Figure 2: UV-c Lamp.

Usual UVGI lamps produce most of their output at a 254nm peak wavelength, when the optimum bacterial 'kill' is at about 265 nm (it varies with species). The optimal kill wavelength at 265nm is about 15% better than at 254nm, so the usual 254nm lamp kills with a high efficiency.

The effectiveness of germicidal UV-c in an HVAC environment depends on a number of factors including the:

- Length of time a microorganism is exposed to UV-c (exposure/dwell time)
- Presence of particles that can protect the microorganisms from UV-c
- Type of microbial contaminant (specific species) and the microorganism's inherent ability to withstand UV-c exposure
- Lamp distance and placement, air movement and patterns, temperature; relative humidity and air mixing
- Power fluctuations to the UV-c source that may impact the electromagnetic wavelength produced
- Lamp life cycle and cleanliness.

Contaminants targeted by UVGI

Given enough intensity and exposure duration UV-c kills or deactivates bacteria (including spores), fungi, DNA viruses and RNA viruses. It damages prions, but it is not proven that it permanently disables them. DNA and RNA are helical arrangements of various sequences of 4 amino acids – adenine, thymine, guanine and cytosine in the case of DNA. In RNA uracil replaces thiamine.

UV affects DNA mainly by breaking it, causing adjacent thymine amino acids to join together forming thymine dimers. DNA may self-repair after this process, so enough UV-c must be used to overwhelm any repair process. RNA is similarly affected but UV-c mainly acts on the uracil amino acid.

UVGI can control microbial growth on surfaces that are subject to moisture or high humidity; coils, ducts, filters, humidifiers. Microbial growth that can be controlled include fungi, bacteria, or even algae, but not viruses. The variety of microbes encountered by a given UVGI system is unpredictable and depends on the application (type of facility) and geographical location.

Spores, which are larger and more resistant to UVGI than most bacteria, can be controlled effectively through the use of high-efficiency filters. The coupling of filters with UVGI is the recommended practice in UVGI applications in general.

While the sterilisation of medical equipment using UVGI is a common and reliable practice, the disinfection of airstreams using UVGI has a history of varying success and unpredictable performance. A distinction exists between the terms "disinfection" and "sterilisation." Sterilisation is defined as the complete destruction of all microbial species. Disinfection is merely the reduction of microbial population. HVAC airstreams are generally disinfected, not sterilised.

Health effects of UVGI

UV radiation kills microorganisms. UV radiation damages people – for example it can cause skin cancer and damage the eyes (photokeratitis). Also, it helps vitamin D generation in the body and has minor medical uses. Disinfection is a major use.

There is limited evidence on the direct effects of UV-c on health, particularly when applied outside of healthcare settings. UVGI has been shown to be effective in reduction of microbial and endotoxin agents, which can breed and accumulate in HVAC systems, especially where condensation of water vapour occurs; however, no direct evidence of health benefits exists. UVGI for in-duct and in-room systems was named by ASHRAE as among the two highest research priorities for developing engineering controls to reduce infectious disease transmission.

Fungal contamination found in ventilation systems may contribute to fungal infections in individuals. A UVGI system is not a filter; inactive particles remain in the airstream and may still cause a negative human response. Using particulate filters in association with UVGI improves the potential health benefits.

Types of UVGI systems

The UV light germicidal effect is used in assorted medical applications (e.g. UV sterilisers). It is also used to treat potable water supplies. The types of UVGI systems developed for building and air-handling-unit (AHU) applications include:

- In-duct systems
- Microbial growth control (surface disinfection systems)
- Room recirculation systems
- Upper-air systems.

Direct UVGI exposure can sterilise any surface if given enough time.

Use of UV in for treating air in ducts or rooms (outside of the medical context) does not seem to be common in Australia, but appears to have a wider use in the USA.

The use of UVGI as a HVAC surface-disinfection system is not uncommon in Australia.

The first step in the design of an airstream – or surface-disinfection – UVGI system is to characterise the application. This includes describing the airstream (air volume, velocity, temperature and humidity), identifying the specific surfaces to be treated, and possibly targeting specific microbes (the likely air contaminants).

Performance of UVGI lamps

UVGI for HVAC application is usually generated by shortwave UV-c lamps, which use a lamp tube with no phosphor coating and composed of fused quartz. These lamps emit ultraviolet light with two peaks in the UVC band at 253.7nm and 18 5nm due to the mercury within the lamp – as well as some visible light. One type of quartz glass allows only the nominal 254nm wavelength light to pass, another allows both to pass.

254nm lamps are primarily used for germicidal use. Because this usage may be near people these lamps should not emit ozone.

ASHRAE Standard 185 establishes a test method for evaluating the efficacy of UV-c lights for their ability to inactivate airborne microorganisms. Part one covers duct or airflow irradiation and part 2 covers surface irradiation. The results of these tests can be used to directly compare UVGI equipment on a standardised basis, irrespective of their application. Results from these tests give the design engineer a basis for specifying UV devices or estimating the relative performance of UVGI for a given application.

- ASHRAE 185.1 provides a method for testing UV-c lights for use in air handling units or air ducts to inactivate airborne microorganisms
- ASHRAE 185.2 provides a method of testing ultraviolet lamps for use in HVAC units or air ducts to inactivate microorganisms on irradiated surfaces.

Applying UVGI

Chemical and mechanical cleaning of HVAC systems to control microbial growth can be costly, difficult to perform, and dangerous to maintenance staff and building occupants. System performance can begin to degrade again shortly after cleaning as organic and microbial deposits begin to reappear or reactivate.

UVGI is a way to prevent or reduce the growth of bacteria and mould on system components and keep surfaces clean continuously, rather than periodically restoring fouled surfaces. This can mean reduced maintenance cost and improved HVAC system performance.

Removing and suppressing the formation of biofilms and organic growth on coils should reduce air-side pressure drop, increase heat transfer coefficient, and reduce fan and refrigeration system energy consumption.

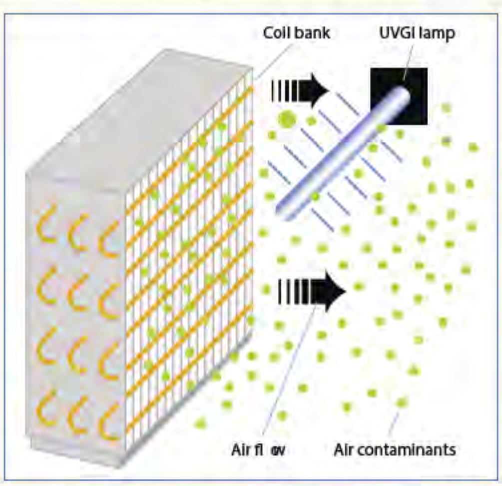

Figure 3: Coil irradiance in HVAC.

Most UVGI applied in HVAC systems is for coil irradiance to assist system maintenance and provide continuous cleaning to surfaces of coils, drain pans, filters and mixing boxes, see Figure 3. The UV light must reach the actual contamination (direct line of sight) and any light blockage by filter material or coil fins must be avoided. UV light may not adequately penetrate stagnant condensate or biofilms in corners of trays, etc.

Correctly applied UVGI coil irradiance can help maintain as-built performance and generate energy savings, improved IAQ, and comfort benefits for existing systems. In new constructions it is applied as a preventative measure to help maintain as-built conditions, in retrofit projects it is often used as a problem-solving measure.

UVGI eliminates or reduces the build-up of organic material on surfaces. This:

- Improves or maintains airflow
- Returns and/or retains design heat-transfer levels
- Reduces maintenance cleaning (inspection is still required).

The system tends to be gentler on coils than mechanical cleaning alternatives and can prolong system life.

Clean coils and HVAC surfaces will help improve indoor air quality (IAQ) by reducing mould products, pathogens and odours, which can improve comfort levels and improve productivity.

UVGI system design parameters

A number of parameters must be considered when considering UVGI products for HVAC designs. The most crucial factors are the:

- Air-flow or HVAC equipment that will be disinfected
- Lamp wattage and distance
- Ventilation system design.

The characteristics of an airstream that impact UVGI design are relative humidity (RH), temperature, and air velocity.

Increased RH is believed to decrease decay rates under ultraviolet (UV) exposure.

Air temperature has a negligible impact on microbial susceptibility to UVGI, but it can impact the power output of UVGI lamps, particularly where manufacturer design values are exceeded. Excessive lamp operating temperature can significantly degrade system performance.

Operating a UVGI system at air velocities above manufacturers' design limits can also degrade the system performance. The cooling effect of the higher air velocity on the lamp surface will cool the plasma inside of the lamp and reduce UV-c output.

Designing UVGI systems

UVGI units are commonly located in an AHU, downstream from the mixing box, typically downstream from the filter bank and upstream from the cooling coils.

UV-c output is a function of plasma temperature when power input is constant.

Data from the manufacturer should be consulted to determine the cooling effects or the limiting design air velocities and temperatures within which the lamps can be operated efficiently.

Doses are determined by the time of exposure and UVGI intensity, both of which are dependent on the velocity profile and the degree of air mixing and turbulence in the airstream.

The design velocity of a typical UVGI unit is similar to that for a filter bank.

Survival predictions for mixed- and unmixed-flow conditions differ in systems in which the lamps do not span the duct's entire width or length.

Dust, dirt or any other films coating the UV lamp surface can lower UV output. Therefore, lamps require scheduled inspection and cleaning as well as periodic replacement to ensure continued effectiveness. The lifetime of UVGI lamps varies depending on design and manufacture.

UVGI for airstream disinfection

The effectiveness of this form of disinfection is dependent on line-of-sight exposure of the microorganisms to the UV light. Environments where designs have created obstacles that block the UV light are not as effective. The placement of the UVGI lamps must achieve line of sight for disinfection to be achieved.

Removal rates depend on filtration rates, outdoor air rates, and the level of microbial contaminants in the untreated airstream (the contaminant challenge). The following design parameters must be considered when sizing a UVGI system for airstream disinfection:

- Duct height, width and length where air is exposed to UV-c
- Air velocity and temperature/humidity range
- Lamp de-rating due to cooling and fouling
- Air contaminant challenge, microorganism types and their sensitivity to UV
- Disinfection performance required
- Type and power of UV-c lamp(s)
- Reflectivity of duct materials, liner, surfaces.

Where the enclosing surfaces are highly reflective, reflectivity, can be an economical way of intensifying the UVGI field in an enclosed duct or chamber. Inter-reflected light, specular and diffuse reflection, contributes to the initial direct intensity. Note that some materials reflect visible light but not UV light. Polished aluminium for example is highly UV reflective, while copper is not.

Operating a UVGI system to disinfect a moving airstream may not provide adequate killing rates because of the short dwell time. Under ideal conditions, inactivation and/or killing rates of 90% or higher can be achieved, but performance depends on the following:

- Specific species of microbial contaminant in the air
- Air exposure/dwell time
- UV-c lamp intensity
- Lamp distance and placement
- Lamp life cycle and cleanliness
- Air movement patterns
- Temperature, relative humidity, and air mixing.

Recirculation systems deliver multiple UV-c doses to airborne microorganisms representing an effective increase in deactivation rate in comparison with the single-pass system. Redundancy in exposing microorganisms to UV is achieved by circulating the air repeatedly. Multiple passes ensures that the UV is effective against the highest number of microorganisms and will irradiate resistant microorganisms more than once, to break them down.

Airborne disinfection is best applied in conjunction with particle filtration; with pre-filtration applied in order to protect the lamps from surface contamination and downstream filtration applied to remove the inactivated microbial particles.

UVGI for coil cleaning

The effectiveness of UVGI to inactivate microorganisms on surfaces has been demonstrated. The long-term irradiation of cooling coil and other wet surfaces to avoid fungal amplification can also be applied as an effective microbial control strategy.

UVGI is commonly used in HVAC applications to help keep cooling coils clean, see Figure 4. Cooling coils have a high risk of microbiological contamination due to the presence of both moisture and nutrients. The benefits of UVGI coil cleaning can include:

- Deactivated mould, microbial growth (bio-films) and biological odours on the cooling coil
- Potential energy savings (5–30%) from a clean coil, due to improved heat-transfer efficiency
- Improved off-coil air quality
- Reduced coil maintenance tasks such as inspection and mechanical cleaning, which can damage the coil fins and impact debris into the centre of the coil
- Reduced static pressure through the coil, reducing fan energy use or increasing airflow
- Extended working life for the coil, by eliminating corrosive biofilms and reducing mechanical cleaning.

Surface irradiance levels in the order of 1μW/cm² can be effective although 50–100μW/cm² is more typical. These are minimum clean-surface values.

For practical HVAC UVGI cooling coil applications higher levels are required. An initial irradiance level of 1225μW/cm² (measured on the coil face in 2.5m/s airflow and 13°C) is recommended,

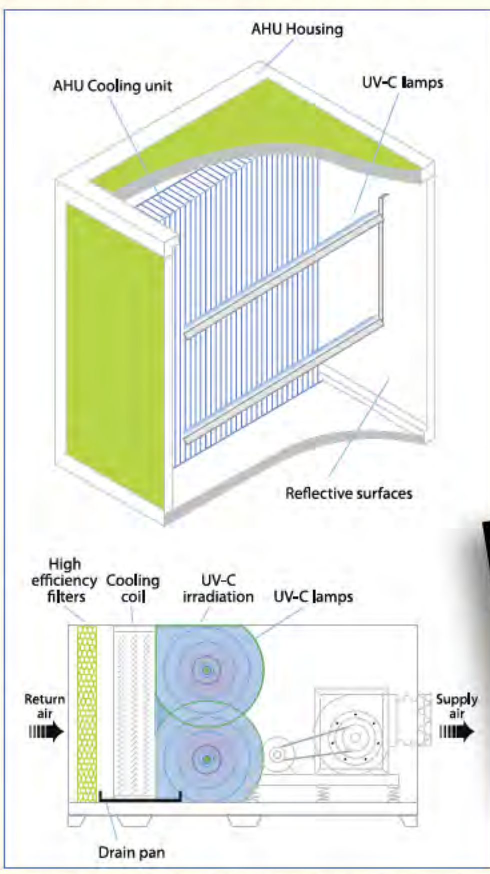

Figure 4: UVGI for AHU cooling coil cleaning.

with a minimum of 750μW/cm², after which the lamps would need replacing. This should provide the necessary penetration and ongoing coverage of microorganisms and their associated biofilms.

The use of reflectors to focus lamp output on surfaces can reduce the power required for surface treatment, but at the expense of reducing air treatment effectiveness. The UV light must have direct line of sight to the actual contamination and be assisted by reflective internal surfaces.

UVGI systems can be applied before or after the cooling coil (or both), see Figure 5, there are advantages and disadvantages to each position, see Table 1. Combining upstream and downstream irradiation provides the most comprehensive coverage.

Table 1 – Locating UVGI coil cleaning systems

UV Lamp Location	Advantages	Disadvantages
Downstream	More space to install equipment. Better irradiation of surfaces where condensation is highest. Irradiation of most contaminated part of coil and drain is achieved.	Lamp and fixtures must be rated for moist environment. Cooling effect on lamp may reduce UV output and system, performance or require additional lamps and power.
Upstream	Lamp and fixtures may be subjected to less moisture. Fewer lamps or less power may be needed.	May be space constrained for the installation. May take longer to clean coil. May not disinfect drain pan.

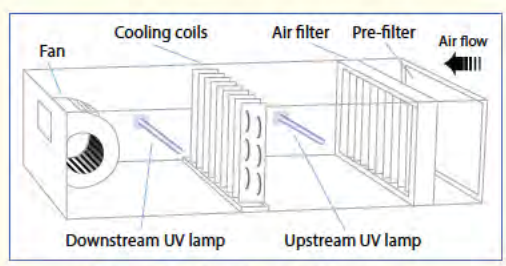

Figure 5: UVGI coil cleaning – upstream and/or downstream.

Next issue:
Needlepoint bipolar ionisation

Safe Indoor Air (Ventilation)

Recommendations

Members of the OzSAGE Safe Indoor Air Working Group (in alphabetical order)

Professor Brendan Crabb
Professor Con Doolan
Mrs Kate Cole
Professor Geoff Hanmer (chair of working group)
Professor Guy Marks (member of OzSage Executive)
Dr Andrew Miller
Professor Jason Monty
Distinguished Professor Lidia Morawska (member of OzSage Executive)
Dr Charitha de Silva

Background

VENTILATION is key to our exit strategy. Schools and businesses have immediate needs for better ventilation, and urban design needs to incorporate improved airflow in a post-COVID world. SARS-CoV-2 spreads through the air. The risk of COVID-19 infection is higher in indoor spaces, and it's even higher when those indoor spaces are poorly ventilated. In this context, ventilation means provision of safe, clean indoor air, not to be confused with ventilation (assisted breathing) of patients in ICU.

Respiratory aerosols from breathing and speaking accumulate in indoor spaces, resulting in increasing risk over time. Spending 10 minutes indoors in a poorly ventilated room is less of a risk than spending hours in there. Many studies of cluster outbreaks of COVID-19 point to airborne transmission as the most likely explanation for infections. Poor ventilation (stagnant air) in public buildings, workplace environments, schools, hospitals, and aged care homes contribute to viral spread.

Good ventilation is one of the most effective ways to reduce the risk of COVID-19 infection, in concert with other mitigations, including density limits, the use of PPE and the use of air purifying devices.

Overarching Principles

a. *High risk can be identified with*: The three V's and T (any of these is a red flag, and more than one indicates higher risk):

   Venue: Multiple people indoors, where social distancing is often harder.
   (poor) Ventilation: Staying in one place with limited fresh air.
   Vocalization: Talking, shouting or singing will increase aerosolization of the virus.
   Time: The amount of time spent in the venue in relation to the risk. Less time is better.

b. *Test*: Use a CO_2 meter to check and to monitor ventilation in the space. If it is a public space, consider making the reading visible to the public. Don't guess, test.

b. *Remediate*: Act as required to improve ventilation to the target level of less than 800 ppm. (recommendations are below)

c. *Ameliorate*: If immediate ventilation improvements are impractical, ameliorate conditions using air purifying devices. At a minimum, these should have a HEPA filter and the size of the unit should be matched to the space. Alternatively, relocate activities outside or to a better ventilated venue.

In a pandemic with a novel virus, it is important to be precautionary and to focus on minimising harm.

Naturally Ventilated Buildings – General Principles

a. Open windows and doors where safe to do so, to bring outdoor air inside and to remove contaminated air. Opening multiple windows and doors allow more outdoor air to move into the space.

b. Work to create a cross-breeze by opening windows and doors at opposite ends of the space. Where no cross-breeze exists, consider improving airflow through simple measures such as child-safe fans. Opening both the front and back doors in smaller shops can improve airflow.

c. Where airflow can't be improved, such as in lifts, stairwells and some common spaces, add localised systems such as air purifiers with a HEPA filter that are appropriately sized for the space.

d. Kitchen exhausts in many fast-food shops and restaurants often deliver good ventilation outcomes providing there is a source of fresh air. Many naturally ventilated shops are 'dead'; there is no effective air flow because openings have been blocked with signage or shop fronts have been replaced with fixed windows. These are a concern if occupancy is high.

e. Keeping exhaust fans running in toilets is recommended where the fan motors are suitable for 100 percent duty to prevent contaminated air moving outside bathrooms. A mechanical engineer or electrician can check the fans duty cycle, or you may be able to download the fan specification. *Do not operate fans continuously if they are not rated for this duty.*

f. Many of these ameliorations will increase energy consumption to maintain comfort conditions inside. Long term solutions that improve ventilation while minimising energy consumption should be considered once the pandemic has abated.

g. Common areas to many Class 2 (apartment) buildings are not ventilated. These and common lifts are a high hazard environment and there need to be urgent adaptations to provide ventilation to these spaces, or to provide air purifiers in the meantime.

Examples: Houses and apartments, motels, aged care facilities, child-care centres plus most gyms, schools, shops, pubs, medical centres and restaurants.

Mechanically Ventilated Buildings – General Principles

a. Increase the proportion of outdoor air provided into enclosed spaces. Do this through speaking with an appropriately qualified mechanical engineer and configuring the system to maximise the outdoor air intake that the Heating, Ventilation and Air Conditioning (HVAC) system can safely accommodate, without negatively impacting on key factors, including the reduction of indoor humidity. (low humidity appears to be associated with an increased risk of transmission.)

b. Consult with a mechanical engineer to disable demand-control ventilation systems so that air supply is not reduced by temperature or occupancy.

c. Consult with a mechanical engineer to increase the total airflow being supplied to maximise the air changes per hour (ACH) that the HVAC system can deliver.

d. Consult with a mechanical engineer to improve air filtration in HVAC systems to the maximum amount possible given the design of the system.

e. Ensure that mechanical ventilation systems are inspected and maintained regularly to ensure they are working as per their design. As part of this, work to understand locations of low or poor ventilation. In those locations, reduce occupancy and/or use additional measures such as localised portable HEPA air purifiers.

f. Where HVAC systems can't be improved due to design constraints, or in lifts, stairs and unventilated common spaces, add localised systems such as portable HEPA air purifiers that are appropriately sized for the space.

g. Many of these ameliorations will increase energy consumption. Long term solutions that improve ventilation while minimising energy consumption should be considered once the pandemic has abated.

Examples: Hospitals, cbd hotel quarantine, hotels, office buildings, supermarkets and shopping centres, clubs, airports, university teaching spaces, theatres, cinemas and auditoriums, some schools, medical centres, shops, pubs, gyms and restaurants.

Warnings:

a. Do not open windows or doors to improve air quality in buildings with mechanical ventilation systems unless checked with a mechanical engineer.
b. Do not operate fans outside their designed duty cycle to avoid the risk of overheating fan motors.

Buildings with wall-mounted air-conditioning systems – General Principles

Wall-mounted air-conditioning systems (split systems) without fresh-air intake will simply recirculate contaminated air. These systems need to be supplemented with an outdoor air supply (or portable air-cleaning devices). Therefore, work to bring outdoor air inside by opening windows and doors or via a mechanical fresh air system.

Always consult with a mechanical engineer when reconfiguring mechanical ventilation systems.

Differential Pressure

Using the difference in air pressure to move air from one space to another is an effective way of controlling and containing the spread of contaminated air. This is most effectively applied where confirmed or suspected COVID-19 persons are already within a confined space. Examples include healthcare and purpose designed quarantine facilities.

HVAC systems are not normally designed to achieve differential pressure and if they are, these systems need to be carefully monitored to ensure they are working properly.

Maintaining differential pressure in a room relies on a steady-state environment to be effective. If windows or doors are opened into areas that are designed to be at negative pressure, then the pressure differential can be lost and contaminated air inside the space can move outside that space. For this reason, existing buildings used for hotel quarantine must not be fitted with openable windows or balcony doors.

Ventilation Hoods for COVID patients in healthcare

These transparent polymer hoods, pioneered in the Victorian Health system and developed by Professor Jason Monty and Dr Forbes McGain are proven to reduce the transmission of SARS-CoV-2 in patient care settings. These hoods can achieve an Air Change Rate of 100 per hour, providing high quality air to patients while minimising risk to Health Care Workers (HCW) and other patients.

Carbon Dioxide Monitoring

CO_2 monitors can help assess whether there is good ventilation or poor ventilation. Measuring carbon dioxide (CO_2) is a useful and practicable surrogate indicator to assess the relative infection risk of COVID-19 indoors. Humans exhale CO_2 in addition to aerosols, which will contain SARS-CoV-2 virions if a person is infected with COVID-19. As the number of people inside a space increase, CO_2 will increase to varying degrees, depending on the ventilation effectiveness and the volume of the space.

Concentrations of CO_2 will gradually increase over time if insufficient outdoor air is delivered into the space. If persons are in poorly ventilated spaces for a prolonged time, regardless of physical distancing, then the risk of infection will increase.

There are some limitations to the use of CO_2 monitoring, because it is not representative of risk related to non-airborne transmission pathways. It doesn't account for re-circulated air that has undergone filtration and it doesn't consider other control measures, such as the use of masks as source control, nor the use of respiratory protection, nor contributions of CO_2 from other sources. Notwithstanding, if the limitations are well understood, a precautionary approach supports the use of CO_2 monitoring as a useful and relatively low-cost tool to make real-time assessments of relative infection risk, which should lead to improvements being made to improve ventilation in indoor spaces.

Outside in the open air, the ambient concentration of CO_2 is approximately 400 ppm. Humans will exhale CO_2 at approximately 8 Litres per minute, depending on the level of physical exertion.

Measurements should be taken at multiple locations within a room or space and repeated periodically during the time the room or space is occupied. A building wide system with central reporting and monitoring is desirable in all spaces with high occupancy, including healthcare, schools, aged-care and critical workplaces.

For restaurants, bars and shops, the provision of public information on CO_2 levels should be considered.

Action limits should be applied as per below:

1. Below 800 ppm - indicates a low relative risk of infection.
2. Between 800 ppm to 1,500 ppm - indicates a moderate relative risk of infection. Improvements should be made where practicable to increase the provision of fresh air into the indoor space.
3. Above 1,500 ppm - indicates a high relative risk of infection. Immediate improvements must be made to increase the provision of fresh air into the indoor space or air filters must be operational. If this is not possible, the space should be evacuated.
4. Around 600 ppm or below is best practice.

Vehicles

Shared vehicles including cars, trucks, vans, taxis and public transport are not currently subject to effective regulation of ventilation levels. National standards should be developed and implemented. Monitoring of ventilation levels and performance should be the responsibility of operators.

No vehicle transporting SCOVID or COVID patients should be operated without the fresh air intake being set to maximum. Drivers should consider lowering windows slightly where this is possible, particularly where this will encourage air to exit the vehicle at the rear. Passengers and drivers should never sit next to each other if possible, or if this is unavoidable, a minimum of fit-tested P2/N95 respiratory protection should be used.

Do not set the ventilation system to recirculate.

Short and Long-term Strategies

A key barrier to implementing ventilation strategies relates to confusion about the need to separate short-term from long-term strategies. It is recognised that there are many constraints regarding the practicality of implementing expensive large-scale ventilation modifications in the short term. Long-term strategies best implemented during design phase of new infrastructure projects or to coincide with the replacement of mechanical equipment or an interior fitout.

In contrast, there are many cost-effective short-term measures that can be practically applied to mitigate COVID infection risk focused on ventilation.

Most buildings are Deemed-to-Satisfy (DTS) naturally ventilated under the National Construction Code. Most schools, aged care facilities, small shops, restaurants, general practices, dental surgeries and so on have no mechanical systems that can be upgraded. The key here is operating manually controlled ventilation openings (mostly windows) to the extent necessary to improve ventilation to achieve target CO2 levels internally.

Hospitals are a special case; they are mostly but not all mechanically ventilated and the systems are complex. Pulling down a ceiling to upgrade the mechanical system above it may not be practical in an operating hospital, especially now. Working out whether filtration can be improved and fresh air increased without replacing components other than the filter assemblies in plant rooms is a recommended first step.

Improvement of ventilation in the built environment should be made a priority for the Australian Building Control Board (ABCB) by the Building Ministers Forum (BMF). The Regulatory Impact Statement (RIS) should consider costs and societal benefits of improved ventilation, including improved health and improvements in cognition, particularly for children in school.

The Australian Government should consider the financial support of improved ventilation through both direct budget spending and loan schemes. A benefit/cost analysis of improving ventilation across the built environment may show that benefits outweigh costs.

Air cleaners/Air purifiers

Local air cleaning (portable HEPA filters) can be an effective form of source control. This is because the air purifiers can set up a very localised air flow around them and stop infectious particles getting far from the room they were expelled in. Ventilation hoods in ICUs are proven to work and clinical settings including GP's and Dentists should consider air purifiers unless their ventilation is excellent.

In lifts, stairwells, corridors and other common spaces in buildings that have no ventilation, air purifiers are a practical option until building codes are changed to require them to be ventilated.

Operating many air purifiers in an institutional setting is complex because the operation of each unit can only be assessed locally. Devices with the capacity to be networked would be useful, but portable devices with this function are not yet generally available.

The priority in any space other than those spaces with SCOVID or COVID patients is to improve ventilation and only to introduce air purifiers if this is not possible.

Australia must set and introduce national performance standards for air cleaners and compliance should be monitored by the ACCC or another suitable body.

Re-opening Schools in High Caseload Settings

NSW is currently experiencing the highest daily infection numbers of any Australian state at any time during the pandemic. Already, over 100 schools in NSW are infection sites and the number continues to grow, therefore focussing on ventilation in schools is of utmost importance.

As approximately 5M children under 16 are unvaccinated, it is likely that this will lead to high rates of infection amongst school age children as it has in the UK, the US and Israel. All these countries have much higher rates of vaccination amongst their adult population than Australia and as a result, children in Australia will be more likely to be infected by adults or to infect them. Until vaccination is extended to young children, the 5M under 16's in Australia will be the single largest reservoir of infection, significantly outnumbering the 4M adults who will be unvaccinated at the 80 percent target adopted by the National Cabinet.

For schools to open with any degree of safety, it will be vital to consider ventilation, capacity limits, the type of activities to be allowed and the time spent together indoors. The use of outdoor facilities should be encouraged as much as possible.

Departments of Education and private providers should immediately embark on a process of measuring ventilation levels at every school and acting where required, in accordance with the recommendations contained in this document.

Yapp, Phillip

From: Mitchell, BethL
Sent: Monday, 6 September 2021 5:02 PM
To: Parkinson, Andrew; Ryan, JohnW; Blom, Dylan; Hunter, Stuart
Cc: Yapp, Phillip; Kidman, Fiona; Hooper, Richard
Subject: RE: As requested - detail of Vic plan re ventilation
Attachments: 20210906-Indoor Air Quality.docx

OFFICIAL: Sensitive

Hi Andrew, please find below and attached the information requested on colleges. Apologies that we did not get time to get the doc out to all stakeholders prior to forwarding. Took longer than we thought.

Cheers
Beth

Indoor Air Quality (IAQ) Plan

An assessment of indoor air quality is currently being undertaken across ACT Public Schools.
Colleges have been agreed as the priority school cohort for assessment of the adequacy of fresh air intake.

Ventilation

Australian Standard AS1668 provides design requirements for mechanical ventilation in buildings. The standard provides minimum outdoor airflow rate for fresh air intake per hour and per person for example 12 litres per second and a minimum floor area of $2m^2$ for children up to 16 years and 10 litres per second and a minimum floor area of $2m^2$ for children over 16 years.

C02 sensors are installed as part of a Demand Controlled Ventilation (DCV) strategies, in accordance with AS 1668.2 (for energy efficiency) in areas with highly variable and/or intermittent occupancy, such as school assembly and sports halls, libraries and lecture theatres. New schools have CO_2 sensors installed for monitoring indoor air quality (IAQ), in large learning community rooms in irrespective of whether they have DCV strategies.

Ventilation is enabled in many schools both with and without mechanical ventilation via operable windows.
Outdoor air intake and $C0^2$ are the surrogate measures used to assess ventilation. The following table provides a rapid assessment of ventilation adequacy at College sites is at Table 1.

Site	CO2 Monitoring	Other Ventilation (e.g. operable windows or manual increase to mechanical ventilation)	Comments
Canberra College	Yes	Not required	All air handling units have CO2 control of outside air / ventilation.
Gungahlin College	Yes	Not required	100% outside air in Learning Hubs and Performing Arts
Lake Tuggeranong College	Yes	Not required	All air handling units have CO2 control of outside air / ventilation.
Erindale College	TBC	TBC	
Dickson College	No	Yes	
Hawker College	No	Yes.	CO2 sensors could be installed relatively easily for a permanent solution. Temporary manual increase of economy cycle (outside air) dampers would increase fresh air up to 100%. Operable windows
Melba Copland College	No	Yes	CO2 sensors could be installed relatively easily for a permanent solution. Temporary manual increase of economy cycle (outside air) dampers would increase fresh air up to 100%.
Narrabundah College	No	TBC	

Site	CO2 Monitoring	Other Ventilation (e.g. operable windows or manual increase to mechanical ventilation)	Comments
UC Lake Ginninderra College	No	TBC	Parts of B Block have CO2 sensors, remainder of college does not.

<u>Technologies/Solutions</u>
ICW has undertaken technology investigations to assess appropriate technologies to improve indoor air quality in schools.
A preliminary review of the following technologies has been undertaken. It important to note that there is a "no one size fits all" solution.

- High Efficiency Particulate Air (HEPA) – these are particulate filters and *not* able to neutralise or remove viruses or bacteria.
- Retrofit of CO2 sensors to existing AHUs – where existing air handling units are fitted with outside air dampers, installation of CO2 sensors would allow increased ventilation rates above minimums prescribed in AS1668 to minimise COVID-19 risk.
- Energy Recovery Ventilation (ERV) – these systems remove stale air and replace it with fresh air. Expelled air and incoming are passed over a heat exchanger to recover heat from indoor air to the incoming air. The systems are used in new schools and provide an energy efficient option to improve IAQ. Retrofitting ERVs to existing schools is often difficult and high-cost option due to space constraints and equipment size.
- UV-C germicidal lights – neutralise viruses and bacteria by destroying their ability to multiply. The lights can be installed in ducting and, also in specific fan units or ERV systems.
- Fans are fitted with a Photohydroionisation (PHI) cell that emits advanced oxidation plasma (0.01 – 0.02 ppm) and is tested to neutralise 99% of the Covid 19 Virus. This technology is currently being trialled at Theodore Primary School.
- Indirect Evaporating Cooling – uses 100% outdoor air while producing low humidity (conventional direct evaporative cooling increases humidity due to the use of water in the air-cooling process). A trial is currently underway at Amaroo to assess the benefits of the indirect system. The trial has been delayed by Covid-19 restrictions.

Beth Mitchell | Director – Asset Strategies, Sustainability and Environment

Phone: +61 2 6207 8364 | Fax: +61 2 6205 9333 |Email: bethl.mitchell@act.gov.au
Infrastructure and Capital Works | Education| ACT Government
Level 4 220 London Circuit | GPO Box 158 Canberra ACT 2601 | www.det.act.gov.au

---

From: Mitchell, BethL
Sent: Monday, 6 September 2021 9:56 AM
To: Parkinson, Andrew <Andrew.Parkinson@act.gov.au>; Ryan, JohnW <JohnW.Ryan@act.gov.au>; Blom, Dylan <Dylan.Blom@act.gov.au>; Hunter, Stuart <Stuart.Hunter@act.gov.au>
Cc: Yapp, Phillip <Phillip.Yapp@act.gov.au>; Kidman, Fiona <Fiona.Kidman@act.gov.au>; Hooper, Richard <Richard.Hooper@act.gov.au>
Subject: RE: As requested - detail of Vic plan re ventilation
Importance: High

OFFICIAL: Sensitive

Indoor Air Quality in ACT Schools

<u>C02 Sensors</u>

- EDU commenced a program of installing CO2 sensors schools in 2018 through the ACTPG HVAC Maintenance Contract.
- At 2021, 200 C02 sensors with remote monitoring and management systems are installed across 30 public schools.
  - The CO2 sensors are distributed across the school ventilation systems (<u>select air handling and fan coil units as budget has allowed</u>). Sensors are commonly located in libraries, classrooms, halls and gyms.
  - The intake of outdoor air is modulated according to the reading on the sensors
  - Readings are expressed in parts per million (ppm) of CO2
  - At 600 parts per million outdoor is introduced at lower rates (in line with Australian Standards).
  - The rate of outdoor air intake increases as CO2 level increase
  - Under the National Construction Code CO2 concentrations of less than 850 ppm are considered best practice.
  - ED has remote access to this data is collated under one remote access system with the capability to report:
    - the maximum and average C02 levels in monitored spaces
    - number of hours over 850 parts per million in a school day.
- The inclusion of CO2 sensors across the public-school portfolio is a work in progress.
  - Additional sensors are required to ensure appropriate coverage across the ACT school network.
  - EDU has remote access to 65 school sites. These could be fitted with C02 sensors to increase coverage and enable improved management of ventilation fairly quickly.

<u>Research and Trials</u>

- EDU has entered into two partnerships that are currently studying CO2 levels in classrooms
  - The i-Hub for Affordable Heating and Cooling – collaboration with the University of Melbourne. The study has collected and analysed thermal comfort and Co2 levels across classrooms at Amaroo School and Fadden Primary School.
  - Sustainable Healthy Environments (SHE) – collaboration with University of Melbourne. The study has monitored a range of indoor air quality variables including C02 at Forrest Primary School. The research will review the data of the ACT school with schools in New South Wales and Victoria.
- EDU is investigating technologies that can neutralise the Covid 19 virus including
  - PureAir destratification fans are being trialled at Theodore Primary School. The fans are fitted with a Photohydroionisation (PHI) cell that emits advanced oxidation plasma (0.01 – 0.02 ppm) and is tested to neutralise 99% of the Covid 19 Virus.
  - Ultraviolet (UV-C) lights within the air distribution system, designed to neutralise 99% of the COVID-19 virus.

Schools with C02 sensors

School	Total CO2 sensors	Hall	Gym	Library	Classrooms

Neville Bonner	5				5
GC School	10				10
Amaroo School	17		6		11
Campbell High	1		1		0
Canberra College	13				13
Caroline Chisholm	18				18
CCCLarc	17				17
Charles Conder	1	1			0
Cranleigh	2				2
Fadden	2	1		1	0
Gilmore PS	1	1			0
Gordon PS	2	1	1		0
Gowrie PS	1	1			0
UC Lake Ginnenderra	3				3
Lake Tugg College	2		1		1
Lanyon High	3				3
Lyneham High	3			1	2
Lyneham Primary	3	2		1	0
Lyons ECS	1	1			0
Macquarie PS	1	1			0
Melba Copeland High	7				7
Melrose High	1			1	0
Molonglo Primary	19				19
Mt Rogers Primary	1				1
Southern Cross ECS	1	1			0
Taylor PS	12				12
Turner School	1	1			0
UC Kaleen High	11		1	1	9
Wanniassa Hills PS	11				11
Wanniassa Hills HS	30	1			29
TOTALS	**200**	**12**	**10**	**5**	**173**

Beth Mitchell | Director – Asset Strategies, Sustainability and
Environment

Phone: +61 2 6207 8364 | Fax: +61 2 6205 9333 |Email: bethl.mitchell@act.gov.au
Infrastructure and Capital Works | Education| ACT Government
Level 4 220 London Circuit | GPO Box 158 Canberra ACT 2601 | www.det.act.gov.au

From: Parkinson, Andrew <Andrew.Parkinson@act.gov.au>
Sent: Sunday, 5 September 2021 2:30 PM
To: Mitchell, BethL <BethL.Mitchell@act.gov.au>; Ryan, JohnW <JohnW.Ryan@act.gov.au>; Blom, Dylan <Dylan.Blom@act.gov.au>; Hunter, Stuart <Stuart.Hunter@act.gov.au>
Subject: Fwd: As requested - detail of Vic plan re ventilation

Here's where the ventilation conversation got to this morning between SET & Min's Office.

Can I get some quick dot points about CO2 monitors in schools (like how many have them) and ventilation / fresh air approach on our upgrades and new builds.

Have we looked at airflow as part of the building upgrade / living lab projects?

Minset will probably be on Monday morning so need some info quickly.

Regards

Andrew Parkinson | Executive Branch Manager
Infrastructure & Capital Works | Education Directorate | ACT Government
Phone 02 6205 4593 | Mobile 0478 301 085

From: Efthymiades, Deb <Deb.Efthymiades@act.gov.au>
Sent: Sunday, September 5, 2021 12:29 pm
To: Parkinson, Andrew
Cc: Oldfield, Meghan; EDUCOVID; Steele, Peter; Moore, Nicole
Subject: FW: As requested - detail of Vic plan re ventilation

OFFICIAL: Sensitive

Hey team

Per below – could we pull together what we already have in terms of ventilation pieces, especially where they connect with the Vic announcements – but also beyond where we have it?

In addition, we need a plan to do any additional assessments that would be needed to have a differentiated response for our schools (and consideration of criteria/framework that could be used by all schools/systems in the ACT

Would focus on college and high schools first (including P-10s) and then downwards from there.

This will ultimately need to feed into the pathway out work that we are doing in terms of risk mitigations for returning to schools at different points – definitely with a vaccination overlay – which leads to the order of focus.

If this could be captured appropriately in the tasking out process, that would be appreciated

Taa

d

Deb Efthymiades | Deputy Director-General System Policy & Reform
Education | ACT Government
Phone: +61 2 62059172 | Mobile : 0401 119 411| Email: Deb.Efthymiades@act.gov.au
220 London Circuit CIVIC ACT |GPO Box 158 Canberra ACT 2601
www.education.act.gov.au | Facebook | Twitter | Pinterest | LinkedIn | Google+

From: Efthymiades, Deb
Sent: Sunday, 5 September 2021 12:19 PM
To: Walker, Melanie <Melanie.Walker@act.gov.au>; Haire, Katy <Katy.Haire@act.gov.au>
Cc: EDUCOVID <EDUCOVID@act.gov.au>; Parkinson, Andrew <Andrew.Parkinson@act.gov.au>; Moore, Nicole <Nicole.Moore@act.gov.au>
Subject: RE: As requested - detail of Vic plan re ventilation

OFFICIAL: Sensitive

Hey Mel – given the announcement it is fine to share

Just as a bit of extra info – we already have CO2 monitors in a number of our schools and as we confirmed there are also 400 dyson devices.

We will be looking at some sort of similar analysis for our schools and also seeking advice from ACT Health (to test the research we have done elsewhere) on HEPA filters and ventilation. The most complicated piece would be how this applies in non-gov schools but we will have to also check that. This is all a key priority.

Will keep you up in loop of course

D

Deb Efthymiades | Deputy Director-General System Policy & Reform
Education | ACT Government
Phone: +61 2 62059172 | Mobile : 0401 119 411| Email: Deb.Efthymiades@act.gov.au
220 London Circuit CIVIC ACT |GPO Box 158 Canberra ACT 2601
www.education.act.gov.au | Facebook | Twitter | Pinterest | LinkedIn | Google+

From: Walker, Melanie <Melanie.Walker@act.gov.au>
Sent: Sunday, 5 September 2021 11:44 AM
To: Haire, Katy <Katy.Haire@act.gov.au>
Cc: Efthymiades, Deb <Deb.Efthymiades@act.gov.au>; EDUCOVID <EDUCOVID@act.gov.au>
Subject: RE: As requested - detail of Vic plan re ventilation

OFFICIAL: Sensitive

Great – thanks 😊

Are you happy for me to forward this info to CMO now or would you prefer to have a chat with Health about it and provide further info/background tomorrow?

There is great interest in this from CMO at the moment in the wake of Victoria's announcement.

Thanks in advance for your advice and best wishes, Mel.

Melanie Walker | Chief of Staff
02 6205 1638 | 0438 430 963

Office of Yvette Berry MLA | Member for Ginninderra
Deputy Chief Minister
Minister for Early Childhood Development
Minister for Education and Youth Affairs
Minister for Housing and Suburban Development
Minister for the Prevention of Domestic and Family Violence
Minister for Women
Minister for Sport and Recreation
Phone: +61 2 6205 0233 | Email: berry@act.gov.au
Facebook | Twitter | www.yvetteberry.com.au

I acknowledge the traditional custodians of the land, the Ngunnawal people, and pay my respect to their Elders past, present and emerging.

From: Haire, Katy <Katy.Haire@act.gov.au>
Sent: Sunday, 5 September 2021 11:39 AM
To: Walker, Melanie <Melanie.Walker@act.gov.au>
Cc: Efthymiades, Deb <Deb.Efthymiades@act.gov.au>; EDUCOVID <EDUCOVID@act.gov.au>
Subject: Fwd: As requested - detail of Vic plan re ventilation

OFFICIAL: Sensitive

Hi Mel.

This just in from Vic re what sits behind their announcement on Friday.

KH

Katy Haire
Director-General | Education Directorate
02 6205 9158 | Katy.Haire@act.gov.au

From: [redacted]
Sent: Sunday, September 5, 2021 10:30:41 AM
To: Haire, Katy <Katy.Haire@act.gov.au>
Subject: As requested

Hi Katy,
Quick summary re ventilation:

- A ventilation audit of a sample of 50 schools will be undertaken by the start of Term 4 to identify infrastructure characteristics that contribute to ventilation across various school building types and areas. This information will provide an indication of areas in schools with reduced scope to increase ventilation.
- CO2 monitoring across the same sample schools as above will be undertaken over a one-month timeframe as a further investigation of air flow in schools. Data will be used to provide an indication on the type of spaces within schools that may require additional ventilation and/or filtration measures.
- A ventilation assessment at 10 schools (from the sample of 50 schools above) will be undertaken early in Term 4 to measure air flow in both teaching and non-teaching spaces, including air changes per hour.
- Procurement of 2000 air purification devices will be undertaken to enable a pilot of targeted installation in rooms in schools where there is limited scope to improve ventilation or other higher COVID-19 transmission risk factors exist.

[redacted]
Department of Education and Training
2 Treasury Place, Melbourne VIC 3000
[redacted]

Indoor Air Quality (IAQ) Plan

An assessment of indoor air quality is currently being undertaken across ACT Public Schools.

Colleges have been agreed as the priority school cohort for assessment of the adequacy of fresh air intake.

<u>Ventilation</u>

Australian Standard AS1668 provides design requirements for mechanical ventilation in buildings. The standard provides minimum outdoor airflow rate for fresh air intake per hour and per person for example 12 litres per second and a minimum floor area of $2m^2$ for children up to 16 years and 10 litres per second and a minimum floor area of $2m^2$ for children over 16 years.

C02 sensors are installed as part of a Demand Controlled Ventilation (DCV) strategies, in accordance with AS 1668.2 (for energy efficiency) in areas with highly variable and/or intermittent occupancy, such as school assembly and sports halls, libraries and lecture theatres. New schools have CO_2 sensors installed for monitoring indoor air quality (IAQ), in large learning community rooms in irrespective of whether they have DCV strategies.

Ventilation is enabled in many schools both with and without mechanical ventilation via operable windows.

Outdoor air intake and $C0^2$ are the surrogate measures used to assess ventilation. The following table provides a rapid assessment of ventilation adequacy at College sites is at Table 1.

Site	CO2 Monitoring	Other Ventilation (e.g. operable windows or manual increase to mechanical ventilation)	Comments
Canberra College	Yes	Not required	All air handling units have CO2 control of outside air / ventilation.
Gungahlin College	Yes	Not required	100% outside air in Learning Hubs and Performing Arts
Lake Tuggeranong College	Yes	Not required	All air handling units have CO2 control of outside air / ventilation.
Erindale College	TBC	TBC	
Dickson College	No	Yes	
Hawker College	No	Yes.	CO2 sensors could be installed relatively easily for a permanent solution. Temporary manual increase of economy cycle (outside air) dampers would increase fresh air up to 100%. Operable windows

Site	CO2 Monitoring	Other Ventilation (e.g. operable windows or manual increase to mechanical ventilation)	Comments
Melba Copland College	No	Yes	CO2 sensors could be installed relatively easily for a permanent solution. Temporary manual increase of economy cycle (outside air) dampers would increase fresh air up to 100%.
Narrabundah College	No	TBC	
UC Lake Ginninderra College	No	TBC	Parts of B Block have CO2 sensors, remainder of college does not.

Technologies/Solutions

ICW has undertaken technology investigations to assess appropriate technologies to improve indoor air quality in schools.

A preliminary review of the following technologies has been undertaken. It important to note that there is a "no one size fits all" solution.

- High Efficiency Particulate Air (HEPA) – these are particulate filters and *not* able to neutralise or remove viruses or bacteria.
- Retrofit of CO2 sensors to existing AHUs – where existing air handling units are fitted with outside air dampers, installation of CO2 sensors would allow increased ventilation rates above minimums prescribed in AS1668 to minimise COVID-19 risk.
- Energy Recovery Ventilation (ERV) – these systems remove stale air and replace it with fresh air. Expelled air and incoming are passed over a heat exchanger to recover heat from indoor air to the incoming air. The systems are used in new schools and provide an energy efficient option to improve IAQ. Retrofitting ERVs to existing schools is often difficult and high-cost option due to space constraints and equipment size.
- UV-C germicidal lights – neutralise viruses and bacteria by destroying their ability to multiply. The lights can be installed in ducting and, also in specific fan units or ERV systems.
- Fans are fitted with a Photohydroionisation (PHI) cell that emits advanced oxidation plasma (0.01 – 0.02 ppm) and is tested to neutralise 99% of the Covid 19 Virus. This technology is currently being trialled at Theodore Primary School.
- Indirect Evaporating Cooling – uses 100% outdoor air while producing low humidity (conventional direct evaporative cooling increases humidity due to the use of water in the air-cooling process). A trial is currently underway at Amaroo to assess the benefits of the indirect system. The trial has been delayed by Covid-19 restrictions.

From:	EDU, EDBSD
To:	DGEDUoffice
Cc:	EDU, EDBSD; ICW EBM Office
Subject:	FOR URGENT CLEARANCE: FILE2021/4472 BRIEF: Ventilation status of ACT public schools
Date:	Friday, 10 September 2021 8:48:50 AM
Attachments:	PROPERTY EQUIPMENT & FLEET - Health & Safety - S G ICW BRIEF Ventilation status of ACT public schools.tr5
Importance:	High

OFFICIAL

Good morning DG Office

Please find attached REC21/52144 and REC21/52145 ready for DG clearance.

TRIM notes and workflow updated.

Thanks very much
Sarah

From: Oldfield, Meghan <Meghan.Oldfield@act.gov.au>
Sent: Thursday, 9 September 2021 7:22 PM
To: EDU, EDBSD <EDBSD.EDU@act.gov.au>
Cc: EDU, EDBSD <EDBSD.EDU@act.gov.au>; ICW EBM Office <ICWEBMOffice@act.gov.au>
Subject: Re: FOR URGENT CLEARANCE: FILE2021/4472 BRIEF: Ventilation status of ACT public schools

Cleared thanks

Get Outlook for iOS

From: EDU, EDBSD <EDBSD.EDU@act.gov.au>
Sent: Thursday, September 9, 2021 5:28:18 PM
To: Oldfield, Meghan <Meghan.Oldfield@act.gov.au>
Cc: EDU, EDBSD <EDBSD.EDU@act.gov.au>; ICW EBM Office <ICWEBMOffice@act.gov.au>
Subject: FOR URGENT CLEARANCE: FILE2021/4472 BRIEF: Ventilation status of ACT public schools

OFFICIAL

Good afternoon Meghan

Please see brief and attachment ready for your approval as soon as possible.

Thanks very much
Sarah

From: Stewart, Ell <Ell.Stewart@act.gov.au> **On Behalf Of** ICW EBM Office
Sent: Thursday, 9 September 2021 5:14 PM
To: EDU, EDBSD <EDBSD.EDU@act.gov.au>

Cc: ICW EBM Office <ICWEBMOffice@act.gov.au>; Parkinson, Andrew <Andrew.Parkinson@act.gov.au>
Subject: FOR CLEARANCE: FILE2021/4472 BRIEF: Ventilation status of ACT public schools
Importance: High

OFFICIAL

Good afternoon

Brief and attachment in TRIM for clearance to DG/MO – as soon as possible please

Thanks, Ell

From: Parkinson, Andrew <Andrew.Parkinson@act.gov.au>
Sent: Thursday, 9 September 2021 4:59 PM
To: ICW EBM Office <ICWEBMOffice@act.gov.au>
Cc: Mitchell, BethL <BethL.Mitchell@act.gov.au>; Hunter, Stuart <Stuart.Hunter@act.gov.au>; Ryan, JohnW <JohnW.Ryan@act.gov.au>
Subject: FW: Ventilation brief
Importance: High

OFFICIAL

Ell

Can you trim off to Meghan for approval?

Beth: great work – I made a few minor edits

Andrew Parkinson | Executive Branch Manager
Infrastructure & Capital Works | Education Directorate | **ACT Government**
Phone 02 6205 4593 | **Mobile 0478 301 085**
220 London Circuit, Civic | www.act.gov.au

Dhawura nguna, dhawura Ngunnawal

From: Mitchell, BethL <BethL.Mitchell@act.gov.au>
Sent: Thursday, 9 September 2021 4:35 PM
To: Parkinson, Andrew <Andrew.Parkinson@act.gov.au>
Cc: ICW EBM Office <ICWEBMOffice@act.gov.au>; Hunter, Stuart <Stuart.Hunter@act.gov.au>; Ryan, JohnW <JohnW.Ryan@act.gov.au>
Subject: RE: Ventilation brief
Importance: High

OFFICIAL

Hi Andrew,

Please find attached the brief as requested. Stuart and John have reviewed.

I have included the college assessment but not the technical assessment to keep the brief concise.

Cheers

Beth Mitchell | Director – Asset Strategies, Sustainability and Environment

Phone: +61 2 6207 8364 | Fax: +61 2 6205 9333 |Email: bethl.mitchell@act.gov.au
Infrastructure and Capital Works | Education| ACT Government
Level 4 220 London Circuit | GPO Box 158 Canberra ACT 2601 | www.det.act.gov.au

---

From: Parkinson, Andrew <Andrew.Parkinson@act.gov.au>
Sent: Thursday, 9 September 2021 8:55 AM
To: Mitchell, BethL <BethL.Mitchell@act.gov.au>
Cc: ICW EBM Office <ICWEBMOffice@act.gov.au>
Subject: Ventilation brief
Importance: High

OFFICIAL

Beth

The DG wants a brief to Min on ventilation. No idea exactly what the intent is but it needs to be today.

I've attached the content that went in a cab sub about school re-openings.

It's basically what you wrote with some feedback from Deb and Nicole.

Can you turn it into a noting brief with any other updates you want to make?

Thanks

Andrew Parkinson | Executive Branch Manager
Infrastructure & Capital Works | Education Directorate | **ACT Government**
Phone 02 6205 4593 | **Mobile 0478 301 085**
220 London Circuit, Civic | www.act.gov.au

Dhawura nguna, dhawura Ngunnawal

Portfolio/s: Education and Youth Affairs

VENTILATION IN SCHOOLS

Key Information

- An important part of ACT Public Schools return to on campus learning in Term 4, 2021 is to ensure that there is proper ventilation in line with Health advice for managing COVID-19.
- It's important to note that ventilation is part of the broader suite of controls to reduce the risk of COVID-19 transmission in school settings including vaccination, physical distancing, good hygiene, cleaning and mask use, and should not be considered in isolation of other mitigation strategies
- The CHO, AHPPC, World Health Organisation and Safe Work Australia **recommend ensuring fresh air ventilation is optimised** in all settings, including through adjusting mechanical systems to increase fresh (external) air supply and reduce air recirculation, and use of natural ventilation such as opening windows and doors.
- **Education Directorate has developed an Indoor Air Quality (IAQ) framework** to assess the IAQ of all public schools commencing with ACT Public Colleges.
- **All public school learning areas will be assessed under the IAQ framework** with immediate actions implemented to optimise fresh air flow. There are 3500 learning areas in public schools in the ACT (including approx. 3000 classrooms).
- **Every school will have an Indoor Air Quality Plan completed** by the time students go back to school for the return to on-campus learning – this includes a list of actions already undertaken by the Directorate (including increasing fresh air ventilation via HVAC systems) and actions for schools to undertake each day (including opening windows to promote natural ventilation and turning on exhaust fans). These school actions will be carried out by non-teaching staff like our Building Service Officers.
- **Site specific IAQ plans were provided to all ACT Public Colleges** on 1st of October 2021.
- From this work, the Education Directorate is confident that fresh air flow can be increased in ALL public schools to improve ventilation.
- Cooler classroom temperatures during cool weather and warmer classroom temperatures during hotter weather are expected to result from increasing fresh air to learning environments.
- **Higher energy bills** are anticipated to result from the increase in fresh air as a greater volume of air needs to be heated or cooled.
- **The Directorate is investigating technologies** to improve air quality in classrooms including modern ventilation systems for toilets and bathrooms and air purification systems.

- **The Directorate is monitoring air quality** in learning spaces to further refine the strategy to provide the best ventilation for ACT public schools including pre-schools.
- **$2 Million of additional funding has been allocated** to undertake short term actions across the public school portfolio to maximise fresh air in learning spaces.

Background Information

- ACT public schools are very well placed as there has been an extensive program of work underway to improve school ventilation since the 2019-2020 bushfires.
- The Education Directorate has been progressively upgrading building controls in 65 schools in order to have better control of the air intake sources for the Heating, Ventilation and Cooling (HVAC) systems.
- Many of our schools have building controls with CO_2 sensors which provides a proxy for ventilation in a room. CO_2 monitoring will commence once students and staff have fully returned on-site in Term 4.
- In 2018, the Education Directorate commenced a program of installing CO_2 sensors in schools. To date, more than 200 CO_2 sensors with remote monitoring and management systems have been installed across 34 public schools. An additional 80 CO_2 sensors are currently on order and will be installed at approximately 31 ACT Public Schools with suitable building control systems over the coming weeks. This will mean 73 percent (65 of 89) schools will soon have CO_2 sensors to the monitor and manage indoor air quality.
- Not all classrooms are connected to large HVAC systems with CO_2 sensors, however these rooms typically have external natural ventilation and split system air conditioning units so that fresh air can be introduced and air flow maintained.
- Longer term, the Directorate will look to introduce additional mechanical ventilation in spaces that require it. This may include installation of new building control/management systems with CO_2 sensors that can remotely control HVAC systems and windows as well as installing supplemental ventilation such as modern exhaust fans in bathrooms and toilets.

Cleared as complete and accurate:	15/09/2021	
Cleared for public release by:	Deputy Director-General	Ext:
Contact Officer name:	Nicole Moore	Ext:54999
Lead Directorate:	Education	
TRIM Ref:		